frontiers | Research Topics

Flavor chemistry of food: Mechanism, interaction, new advances

Edited by
Mingquan Huang, Gang Fan and Yanyan Zhang

Published in
Frontiers in Nutrition

ISSN 1664-8714
ISBN 978-2-8325-3032-0
DOI 10.3389/978-2-8325-3032-0

About Frontiers

Frontiers is more than just an open access publisher of scholarly articles: it is a pioneering approach to the world of academia, radically improving the way scholarly research is managed. The grand vision of Frontiers is a world where all people have an equal opportunity to seek, share and generate knowledge. Frontiers provides immediate and permanent online open access to all its publications, but this alone is not enough to realize our grand goals.

Frontiers journal series

The Frontiers journal series is a multi-tier and interdisciplinary set of open-access, online journals, promising a paradigm shift from the current review, selection and dissemination processes in academic publishing. All Frontiers journals are driven by researchers for researchers; therefore, they constitute a service to the scholarly community. At the same time, the *Frontiers journal series* operates on a revolutionary invention, the tiered publishing system, initially addressing specific communities of scholars, and gradually climbing up to broader public understanding, thus serving the interests of the lay society, too.

Dedication to quality

Each Frontiers article is a landmark of the highest quality, thanks to genuinely collaborative interactions between authors and review editors, who include some of the world's best academicians. Research must be certified by peers before entering a stream of knowledge that may eventually reach the public - and shape society; therefore, Frontiers only applies the most rigorous and unbiased reviews. Frontiers revolutionizes research publishing by freely delivering the most outstanding research, evaluated with no bias from both the academic and social point of view. By applying the most advanced information technologies, Frontiers is catapulting scholarly publishing into a new generation.

What are Frontiers Research Topics?

Frontiers Research Topics are very popular trademarks of the *Frontiers journals series*: they are collections of at least ten articles, all centered on a particular subject. With their unique mix of varied contributions from Original Research to Review Articles, Frontiers Research Topics unify the most influential researchers, the latest key findings and historical advances in a hot research area.

Find out more on how to host your own Frontiers Research Topic or contribute to one as an author by contacting the Frontiers editorial office: frontiersin.org/about/contact

Flavor chemistry of food: Mechanism, interaction, new advances

Topic editors

Mingquan Huang — Beijing Technology and Business University, China
Gang Fan — Huazhong Agricultural University, China
Yanyan Zhang — University of Hohenheim, Germany

Citation

Huang, M., Fan, G., Zhang, Y., eds. (2023). *Flavor chemistry of food: Mechanism, interaction, new advances*. Lausanne: Frontiers Media SA. doi: 10.3389/978-2-8325-3032-0

Table of contents

frontiers | Frontiers in Nutrition

TYPE Editorial
PUBLISHED 04 July 2023
DOI 10.3389/fnut.2023.1243606

OPEN ACCESS

EDITED AND REVIEWED BY
Michael Rychlik,
Technical University of Munich, Germany

*CORRESPONDENCE
Gang Fan
✉ fangang@mail.hzau.edu.cn

RECEIVED 21 June 2023
ACCEPTED 26 June 2023
PUBLISHED 04 July 2023

CITATION
Huang M, Fan G and Zhang Y (2023) Editorial: Flavor chemistry of food: mechanism, interaction, new advances.
Front. Nutr. 10:1243606.
doi: 10.3389/fnut.2023.1243606

Editorial: Flavor chemistry of food: mechanism, interaction, new advances

Mingquan Huang[1], Gang Fan[2]* and Yanyan Zhang[3]

[1]Key Laboratory of Brewing Molecular Engineering of China Light Industry, Beijing Technology & Business University (BTBU), Beijing, China, [2]Key Laboratory of Environment Correlative Dietology, Ministry of Education, College of Food Science and Technology, Huazhong Agricultural University, Wuhan, China, [3]Department of Flavor Chemistry, Institute of Food Science and Biotechnology, University of Hohenheim, Stuttgart, Germany

KEYWORDS

flavor chemistry, aroma, mechanism, interaction, volatile compounds, fermentation, storage

Editorial on the Research Topic
Flavor chemistry of food: mechanism, interaction, new advances

Flavor quality is one of the most important qualities of food, including taste and odor. The related investigations on food flavor have been widely reported during the past several decades, which includes multiple aspects, such as new methods and technologies for the analysis of flavor compounds in food; the qualitative and quantitative analysis of the flavor compound in food; the regulation and formation mechanisms of flavor compounds in food during processing and preservation; the interaction between flavor components, macromolecules, and flavor components; the interaction between flavor molecules and olfactory receptors or taste receptors. Due to the diversity and extremely low content of flavor compounds and the complexities of the formation mechanisms of flavor compounds in food, the researches on flavor compounds in food still gain worldwide attention. The goal of this special edition Research Topic was to shed light on mechanisms of metabolism, regulation or formation of key flavor components in food, the interaction between flavor components, food matrix or macromolecules and flavor components, as well as establishing new methods and technologies for the analysis of flavor compounds in food. Additionally, the effects of beer, wine, and baijiu consumption on non-alcoholic fatty liver disease, and the flavor and key influencing factors of Maillard reaction products were reviewed.

Yan et al. established a new ultraperformance liquid chromatography (UPLC) strategy that has been developed for the identification and quantification of volatile thiols in Chinese liquor (Baijiu).

The effect of different varieties on the food flavor has been investigated. Sun et al. studied the volatile constituents and odorous compounds in peach (*Prunus persica* L) fruits of different varieties. Guo F. et al. studied the sensory characteristics and aroma components of nine different fragrant rapeseed oils.

Regarding the volatile compounds in fermented food, Cao et al. investigated the effects of alcoholic fermentation on the non-volatile and volatile compounds of "Cocktail" grapefruit juice. To analyze the latter, a non-targeted metabolomics method based on UPLC-MS/MS and volatiles analysis using GC-IMS were performed. Zhou X. et al. investigated the effects of post-fermentation on the flavor compounds formation in red sour soup. Wang Ya. et al. studied the sensory characteristics of Petit Manseng wine. Its flavor was evaluated by detecting the primary organic acids, phenolic acid compounds, and volatile ester compounds. The authors found that indigenous yeast can increase the phenolic acid and volatile ester compounds in Petit Manseng wine. Pei et al. characterized the transcriptomic profiles and the change of main flavor substance of *Z. rouxii* under salt treatment. Ao et al. set up a method for the quick classification of strong-aroma types of base Baijiu using potentiometric and voltammetric electronic tongue combined with chemometric techniques.

The effect of processing and cooking on food flavor has also been investigated. Wang Yu. et al. studied the effects of four cooking methods on flavor and sensory characteristics of scallop muscle. Wang Y.-R. et al. evaluated the key aroma compounds and protein secondary structure in the roasted Tan mutton during the traditional charcoal process. Zhou M. et al. compared the changes in the quality characteristics of air-fried shrimp meat and deep-fried shrimp meat at different frying temperatures (160, 170, 180, and 190°C). Fei et al. studied the changes in volatile flavor substances during Crataegi fructus roasting using E-nose and HS-GC-MS. Xu et al. investigated the effects of different managements and shade types on the aroma and color generation of roasted coffee beans. Gao et al. investigated the changes of nucleotides, succinic acid, and free amino acids amounts in yolk and the causes leading to the changes after pickling to uncover the fundamental umami component of preserved egg yolk. Guo J. et al. studied the effects of 1% (w/v) alcohol denatured soybean protein isolates, native soybean protein isolates, as well as the thermal denaturation of soybean protein isolates on low concentration (24 μmol/L) of citral in aqueous using headspace solid-phase microextraction/gas chromatography–mass spectrometry.

Storage is an important factor affecting the flavor of food. Zhang et al. studied the effects of three antioxidants, tert-butylhydroquinone (TBHQ), tea polyphenol (TP), and L-ascorbyl palmitate (L-AP), on volatile components, physicochemical properties, and antioxidant activities of heat processed beef flavor over 168 days at different temperatures (4, 20, and 50°C). Zeng et al. studied the effects of methyl salicylate pre-treatment on the volatile profiles and key gene expressions in tomatoes stored at low temperature. Bi et al. studied the effect of high freezing rate on flavor fidelity of hand grab mutton after short-term frozen storage. Wang Z. et al. studied the flavor evolution and important aroma components during long-term storage of compressed white tea using flavor wheel, headspace gas chromatography ion mobility spectroscopy, chemometrics.

In addition, Liu N. et al. found that mild salinity improves the growth, nutrition, and flavor properties of hydroponic Chinese chive (Allium tuberosum Rottler ex Spr). Zhou Y. et al. evaluated and discussed the current human-based and laboratory-based study evidence of effects on hepatic lipid metabolism and non-alcoholic fatty liver disease from ingested ethanol, the polyphenols in beer and wine, and the bioactive flavor compounds in baijiu, and their potential mechanism. Liu S. et al. mainly reviewed the Maillard reaction-derived flavors, the main substances producing Maillard reaction-derived flavors, and the detection methods were also introduced.

In conclusion, we hope this article Research Topic can provide new information in the field of flavor chemistry of food.

Author contributions

GF wrote the initial draft of the manuscript. MH and YZ finalized the manuscript. All authors contributed to the article and approved the submitted version.

Conflict of interest

The authors declare that the research was conducted in the absence of any commercial or financial relationships that could be construed as a potential conflict of interest.

Publisher's note

frontiers | Frontiers in Nutrition

ORIGINAL RESEARCH
published: 21 July 2022
doi: 10.3389/fnut.2022.929023

Study on the Interaction Mechanism Between Soybean Protein Isolates and Lemon Flavor: Isomerization and Degradation of Citral

Jun Guo[1,2,3], *Jicheng Xu*[1,2,3]* *and Jie Chen*[3]*

[1] College of Biological and Food Engineering, Anhui Polytechnic University, Wuhu, China, [2] Department of Chemistry and Material Engineering, Chizhou University, Chizhou, China, [3] State Key Laboratory of Food Science and Technology, Jiangnan University, Wuxi, China

By headspace solid-phase microextraction/gas chromatography–mass spectrometry, the effects of 1% (w/v) alcohol denatured soybean protein isolates (L-SPI), native soybean protein isolates (N-SPI), as well as the thermal denaturation of soybean protein isolates (H-SPI) on low concentration (24 μmol/L) of citral was studied in aqueous. The results shows that the SPI could catalyze citral isomerization and yield methyl heptenone and acetaldehyde by inverse aldol condensation degradation. 3-Hydroxycitronelloal was formed as an intermediate in this reaction. The catalytic efficiency of the L-SPI was higher than that of N-SPI, whereas the catalytic efficiency of H-SPI was the lowest. Additionally, it shows that the catalytic efficiency increased as the pH increased. The catalytic efficiency of 7S (Soybean β-Conglycinin) was greater than that of 11S (Soy bean Proglycinin).

Keywords: soy protein isolate, citral, methyl heptenone, acetaldehyde, degradation

OPEN ACCESS

Edited by:
Gang Fan,
Huazhong Agricultural University, China

Reviewed by:
Yunwei Niu,
Shanghai Institute of Technology, China
Guangsen Fan,
Beijing Technology and Business University, China

***Correspondence:**
Jicheng Xu
xujicheng@ahpu.edu.cn
Jie Chen
chenjie@jiangnan.edu.cn

Specialty section:
This article was submitted to Food Chemistry, a section of the journal Frontiers in Nutrition

Received: *26 April 2022*
Accepted: *26 May 2022*
Published: *21 July 2022*

Citation:
Guo J, Xu J and Chen J (2022) Study on the Interaction Mechanism Between Soybean Protein Isolates and Lemon Flavor: Isomerization and Degradation of Citral. Front. Nutr. 9:929023. doi: 10.3389/fnut.2022.929023

INTRODUCTION

Plant protein beverage made from soybean protein isolate is cholesterol-free and has high amino acid content, resulting that plant protein beverage possess high nutritional value (1–3). However, due to the structure and properties of SPI, the flavor of vegetable beverage containing SPI is easily unbalanced (3–5). For example, when lemon juice is mixed with SPI, flavor changes occur. According to the literature (6), it is speculated that the functional groups of protein may had catalytic degradation of citral.

Citral was used in the preparation of strawberry, apple, apricot, sweet orange, and lemon flavors (7). Commercial citral usually typically contains 60% geranial and 40% neral, which are isomers (8). Geranial has a mild citrusy smell, whereas neral has a pungent grass smell (9). Lemongrass oil, lemon oil, and white lemon oil contain 70–80% citral (10). Citral can also be obtained from industrial geraniol (and nerol) by dehydrogenation using a copper catalyst. Moreover, it can be synthesized from dehydrolinalool using vanadium as a catalyst. Citral is used to manufacture citrus-based food flavors; However, as it is susceptible to oxidation, polymerization, and discoloration, it is usually used in foods that have neutral pH (11, 12); Citral is also used to synthesize iso-menthol and hydroxycitronella aldehyde and violanone, which is the raw material of vitamin A. Degradation of citral will lead to loss of the lemon-like aroma and produce off-flavor (10, 11, 13).

Citral is a terpenoid and the main flavor component of citrus foods (4, 14). Citral is an unsaturated aldehyde containing an isolated C = C double bond, C = O group, and C = C double bond conjugated with the carbonyl group that is easily degraded by other chemical components in food (15). For example, Wolken et al. (6) found that glycine and bovine serum albumin could catalyze the degradation of citral. The degradation of citral results in the loss of its unique aroma and the formation of other undesirable aroma components that lead to unpleasant alterations in the flavor of food (8).

This study to further explore the effects of SPI structures (Extracted from soybean meal) on the degradation of citral by inverse hydroxyl aldehyde condensation, and provide a theoretical reference for the flavor change in Lemon juice-SPI beverages.

MATERIALS AND METHODS

Materials

Soybean (Suyun 626) was purchased from Fengyuan Seed Co. (Lian Yungang City, China). Citral (98%), acetaldehyde (98%), methyl Heptenone (98%) were provided by J&K Chemical Ltd. (Shanghai, China). 3-hydroxycitronellal (95%) was prepared as method of Fkyerat and Tabacchi (16). Neral (containing 10% geranial and 90% neral) and geranial (containing 95% geranial and 5% neral) were prepared by separating commercial citral by Wolken et al. (6). All other chemicals (analytical grade) were purchased from Sinopharm Chemical Reagent Company (Shanghai, China). Deionized water was used in all the experiments.

Preparation of Protein Sample

Native-Soybean Protein Isolates

Native SPI was made from soybeans, by Jiang et al. (17) description, according to the alkaline pH extraction–isoelectric precipitation method. By the micro-Kjeldahl method, after solution of neutralization to pH 7.0, the protein content of SPI suspension was determined, by oven drying method (105°C overnight) and the total solid was determined. By the nitrogen conversion factor of 5.71 (18), the SPI extract was 92.1% by the calculated protein purity (dry weight basis). In deionized water, the 8% (w/v) SPI suspension was centrifuged, to remove particulates, at 10,000 × g, for 20 min. In the SPI suspension, the ionic strength, was 0.03–0.04 M, expressed as the concentration of NaCl which was determined using an S30 Seven Easy conductivity meter (Mettler Toledo GmbH Analytical, Sonnenberg strausse, Switzerland).

L-Soybean Protein Isolates

Native SPI usually has a beany smell, while use SPI as a food ingredient, it need to use ethanol to wash the defatted soybean meal, in order to remove the beany smell molecules of SPI. Broken after the soybean meal skim, skim for alcohol after wash, wash bad SPI flavor compounds in addition to further. followed by alcohol washing with anhydrous ethanol with solid/liquid ratio of 1:3 (w/v), stirring for 2 h, ethanol extraction and filtration to remove the ethanol, and alcohol washing for 2 times.

H-Soybean Protein Isolates

Preparation of fully heat-denatured protein (H-SPI, 1%, w/v): pre-heat denatured SPI at 100°C (preheat for 5 min first, and keep it for 20 min after reaching the set temperature).

7S, 11S

The soy 11S and 7S protein fractions were isolated from soy flour by using the method of Sorgentini et al. (19).

Preparation of Solutions

A stock solution containing 1,000 mg/L of citral was made up in methyl alcohol through gradient dilution, and made to give a SPI of 1% (w/v) solution of 20 mmol/L sodium phosphate/NaOH buffer, an aliquot of 24 μmol/L flavor of each 5 mL aliquots in 15 mL glass vials (AiXin Ltd., BeiJing. China). A separate solution containing a reference standard flavor was made up in a similar way. Three replications were made. The Solutions of the individual were used with small stirring bars at 37°C for 0.5 h to mixing them with the aroma compound in triplicates.

Headspace Solid-Phase Microextraction Gas Chromatography-Mass Spectrometry (SPME-GC-MS) Analysis

The SPME holder for manual sampling and the SPME fibers, 50/30 μm polydimethylsiloxane (PDMS), were purchased from AnPu (ShangHai, China). The fibers were conditioned in the gas chromatograph injector port before use at the time and temperature recommended by the manufacturer. During the development of the headspace SPME method, the following parameters were optimized: type and thickness of fiber coating; headspace extraction time text; and sample agitation during extraction. For the aroma standards and the protein-flavor solutions, 5 mL aliquots were transferred into 15 mL glass vials (AiXin Ltd., BeiJing. China). The standards and the samples containing individual SPI were prepared in triplicates. KMO-2 basic magnetic stir bar (KeYi Ltd., GuangZhou, China) was placed in each sample vial. The samples were stirred at 250 min^{-1} and keeping the temperature constant at 37°C during the SPME extraction using an RW 20 magnetic stirring plate (KeYi Ltd., GuangZhou, China) under the water bath. After equilibration, the SPME fiber was exposed into the headspace of the sample vial for 30 min and was subsequently introduced into the gas chromatograph injector port for quantification.

Gas Chromatography. A Bluker SCION SQ456 GC/MS (Bruker, Kyoto, Japan) was used throughout the study. The column used was a Supelcowax 10 fused silica capillary column, 30 m, 0.25 mm inner diameter, 0.25 μm film thickness (Agilent DB-WAX). The carrier gas was helium (linear velocity; 0.8 mL/min). The injector port (splitless mode) temperature and the detector temperature were 250°C. The oven temperature was held isothermally at 120°C. Once the SPME sampling was completed, the fiber was immediately inserted into the gas chromatograph injector for desorption. The fiber was left in the port for 5 min for purging. There was no carry-over between

samples using 7 min desorption time. Prior to the next SPME extraction, the fiber was allowed to cool to room temperature. The temperature was programmed, column temperature keeping at 40°C for 3 min, by heating the sample at a rate of 5°C /min to 90°C for the first phase and sample at a rate of 10°C /min to 230°C for the second phase, this temperature for 7 min (20).

A mass spectrometer was used to confirm the identity of volatile flavor compounds and further determine the potential volatile flavor byproducts that have been generated. The EI source for the mass spectrometer described above was operated at 70 eV.

Qualitative and Quantitative Analysis Method of the Volatile Compounds

An external standard calibration was used to calculate the extent of binding. A stock solution containing 10 mmol/L of each flavor compound was created, using propylene glycol through gradient dilution and to an SPI of 1% (w/v) solution of 20 mmol/L phosphate buffer in 18 mL hermetically closed flasks (Kebeter, Beijing, China), stock solutions contained cital in each flask with or without SPI (blanks). Four replicates were created and shaken for 24 h at 37°C for equilibration.

$$[\mathrm{L}] = \frac{[HS]_P}{[HS]_C} \times O$$

The values of [L] is the concentration of flavors in headspace, O is the flavor concentration (μmol/L) of control, $[HS]_C$ is the flavor compounds GC peak area of control, $[HS]_P$ is the flavor compounds GC peak area of sample.

Measurement of Protein Fluorescence

Fluorescence intensity was measured using a Hitachi F-2700 Fluorescence Spectrophotometer (Hitachi Ltd., Tokyo, Japan). EX WL: 280.0 nm, EX Slit: 5.0 nm, EM Slit: 5.0 nm. Stock solutions of SPI (0.02% w/v) were prepared, 10 mmol/L citric acid phosphate buffer at pH 5–10. Flavors were added to solutions of SPI by diluting, respectively, propylene glycol at the concentration of 0–0.8 mmol/L. All the samples were prepared in plastic test tubes covered with aluminum foil. And the Solutions of the individual were used with small stirring bars at 37°C for 2 h to mixing them with the Aroma Compounds, in triplicates. stored at 4°C until use.

Determination of Surface Hydrophobicity of Soybean Protein Isolates

By an 8-anilinonaphthalene-1-sulfonic acid (ANS) fluorescent probe method, in the aqueous solution, SPI hydrophobicity was determined with modifications (21). SPI was centrifuged at 12,000 × g, times is 15 min, temperature is 37°C, the supernatants were diluted in 20 mmol/L citric acid phosphate buffer (pH 5.0–pH9.0), obtain SPI concentrations ranging from 0.1 to 0.002 mg/mL. Subsequently, 20 μL of ANS (8.0 mmol/L in 0.1 M phosphate buffer, pH 7.2) was added to 2 mL of the diluted SPI solutions. Fluorescence intensity was measured using a Hitachi F-2700 Fluorescence Spectrophotometer (Hitachi Ltd., Tokyo, Japan) at 365 nm (excitation wavelength) and 520 nm (emission wavelength). The slope of the fluorescence intensity vs. protein concentration was used as an index of surface hydrophobicity (S0).

Protein Solubility

The protein solubility of the SPI solutions was obtained by the method of Sorgentini et al. (19). SPI solutions were centrifuged at 12,000 × g for 15 min. The protein concentration of the supernatant was determined by Lowry (22). The protein solubility was calculated as the percentage of the protein concentration in the supernatant over that of the original SPI solution.

Statistical Analysis

Differences between treatments were determined by analysis of variance (ANOVA) and Duncan's Multiple Range test ($p < 0.05$) using statistical package SPSS 17.0 (SPSS Inc., Chicago, IL). Data were expressed as means ± standard deviations (SD) of triplicate determinations unless specifically mentioned.

RESULTS AND DISCUSSION

Soybean Protein Isolates-Catalyzed Isomerization of Geranial and Neral

As seen in **Figure 1**, proteins and amino acid can catalyze the reverse hydroxyl aldehyde condensation reaction of citral to give methyl heptenone and acetaldehyde, with 3-hydroxycitronelloal as an intermediate (23–25). Moreover, as shown in **Figure 2**, SPI can catalyze the isomerization of geranial and neral, the two isomers of citral. Citral contains unsaturated conjugated double bonds. In the presence of polar amino acids, it is easily degraded by inverse hydroxyl aldehyde condensation to methyl heptenone and acetaldehyde.

According to the report, by X-ray diffraction method, Adachi et al. (26), Baud et al. (27), Maruyama et al. (28), and Maruyama et al. (29) determined that 7S subunit was connected to trimer through disulfide bond, and 11S peptide chain (A1aB1b, A2B1a, A1bB2, A3B4, and A5A4B3) was connected to trimer through disulfide bond, hexamer of 11S globulin is formed in face to face form by trimers. These trimers are hollow tubular structures with hydrophobic binding within or between trimers. Peptide chains of SPI contain amino acid side chains.

It is speculated that soybean protein can also catalyze the reverse hydroxyl aldehyde condensation degradation reaction of citral to produce methyl heptenone and acetaldehyde.

Figure 2 shows that SPI can catalyze the isomerization of geranial and neral. **Figure 2A1** shows that L-SPI catalyze the isomerization of geranial into neral, **Figure 2A2** shows that L-SPI catalyze the isomerization of neral into geranial. **Figure 2B1** shows that N-SPI catalyze the isomerization of geranial into neral, **Figure 2B2** shows that N-SPI catalyze the isomerization of neral into geranial. **Figure 2C1** shows that H-SPI catalyze the isomerization of geranial into neral, **Figure 2C2** shows that H-SPI catalyze the isomerization of neral into geranial.

It can be seen in **Figures 2A1,2** that the use of L-SPI led to the most rapid isomerization of citral. After 100 min, the L-SPI

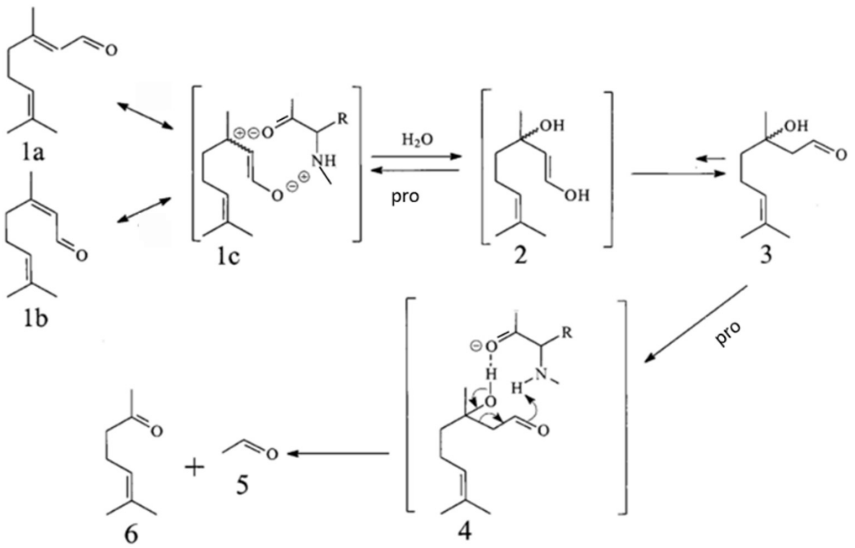

FIGURE 1 | Proposed pathway for the isomerization of geranial (1a) and neral (1b) and their conversion *via* 3-hydroxycitronellal (3) into methyl heptenone (6) and acetaldehyde (5), catalyzed by Soy Protein Isolate (SPI), in alkaline aqueous solution.

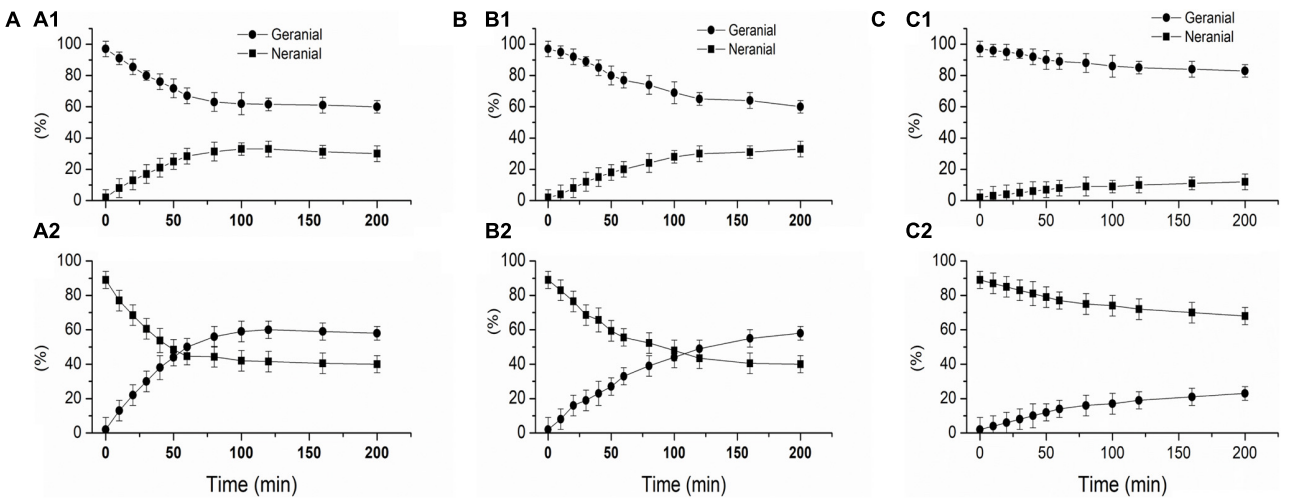

FIGURE 2 | protein-catalyzed isomerization of geranial and neral, SPI 1%, 20 mmol/L potassium phosphate buffer (pH 7.0), Geranial and neral are expressed as a percentage of total citral. **(A)** L-SPI, **(B)** N-SPI, **(C)** H-SPI.

was found to isomerize 37% of pure geranial to neral, and 60% of pure neral to geranial. It can be seen in **Figures 2B1,B2** that N-SPI has a lower efficiency in catalyzing citral isomerization, as the reaction reaches equilibrium only after 200 min. H-SPI catalyzed the isomerization of citral with the lowest efficiency (**Figures 2C1,C2**).

It has been reported (6) that glycine and bovine serum albumin can catalyze the isomerization of geranial or neral under neutral reaction conditions. In addition, Kuwahara et al. (30) have reported the enzyme-catalyzed isomerization of citral. They found that the reaction was balanced with 40% of the mixture being neral and 60% as geranial. Wolken et al. (6) have reported the isomerization of geranyl and neral at room temperature (25°C) using glycine or bovine serum albumin. Kimura et al. (31) found that geranial can also be isomerized in acidic solutions to form neral. Therefore, it can be concluded that while SPI is mixed with citral, SPI maybe catalyze the isomerization of geranial or neral.

Protein—Catalyzed Citral to Methyl Heptenone

Citral, methyl heptanone, and 3-hydroxy-citronelloal can be detected in the sample after citral and SPI exist in the aqueous solution. **Figure 3** shows the catalytic efficiency of alcohol-washed SPI (L-SPI), native SPI (N-SPI), and high-temperature denatured SPI (H-SPI) on citral degradation. Of these, L-SPI was

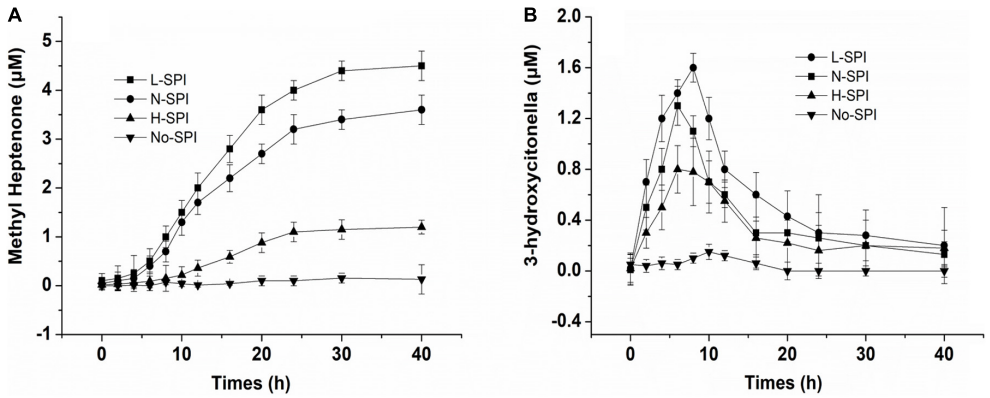

FIGURE 3 | Effect of different treated protein on the SPI—catalyzed to citral **(A,B)**, the concentration of protein is 1% (w/v), 20 mmol/L potassium phosphate buffer, citral's primary concentration is 24 μmol/L.

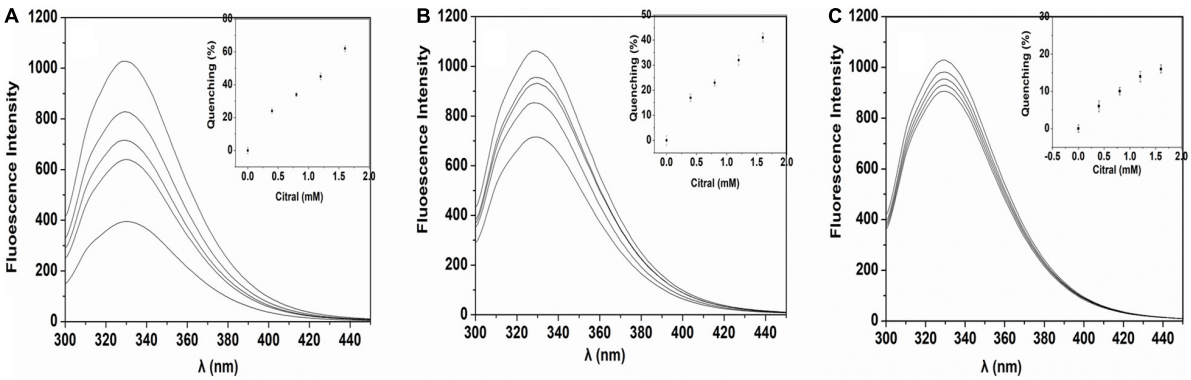

FIGURE 4 | fluorescence of SPI in citral aqueous solution. **(A)** L-SPI, **(B)** N-SPI, **(C)** H-SPI, the concentration of protein is 0.02% (w/v), 20 mM potassium phosphate buffer and, and citral's primary concentration is 0.4–1.6 mmol/L.

the most effective catalyst, followed by N-SPI and H-SPI. Methyl heptenone was not formed when only the buffer was used.

The oil and water-soluble carbohydrate moieties of the SPI were removed after alcohol treatment, and more binding sites of SPI were exposed. From **Figure 4A**, Maximum fluorescence quenching intensity was observed for L-SPI. Form the **Table 1**, L-SPI has the best solubility and the lowest surface hydrophobicity between L-SPI, N-SPI and H-SPI. It has been reported that the process of alcohol washing to obtain L-SPI results in a certain degree of SPI denaturation, thereby changing the protein conformation and altering the nature of the flavor compounds (32), The SPI structure becomes more orderly after alcohol treatment. This finding conformed to the report by Tanford, who reported the characteristic denaturation of the protein structure by organic solvents (33).

Treatment with alcohol weakens the hydrophobic forces, but strengthens the hydrogen bonding and electrostatic forces, thereby ensuring that the hydrophobic core is not damaged. Alcohol-washing treatment damages the outer structure of the soy protein and its loose and disorderly hydrophilic outer structure is transformed into the β-spiral structure. This conformation is conducive to the formation of hydrogen bonds,

TABLE 1 | Surface hydrophobicity and protein solubility of N-SPI, H-SPI, L-SPI.

	N-SPI	H-SPI	L-SPI
Solubility (%)	$83^{b} \pm 4$	$63^{c} \pm 6$	$96^{a} \pm 4$
Surface hydrophobicity (S_0)	$214^{b} \pm 8$	$365^{a} \pm 12$	$198^{c} \pm 10$

Values are means and standard deviations of three determinations, the different lower case letters (a–c) in the same row indicate significant difference among the values at the $p < 0.05$.

which results in a high degree of hydration and the protein molecules assuming a highly spiral state. Denaturation after the alcohol-washing treatment imparts more freedom to the hydrophilic chain segments in the SPI molecules, increasing its ability to move rapidly. Thus, this finding suggests that alcohol-washed soybean protein can result in the flexibility of SPI, effectively increasing its solubility (34).

According to the literature (35), It speculated that the maximum binding force was observed for the interaction of L-SPI and citral, and the most polar hydrophilic groups between L-SPI, N-SPI and H-SPI. Therefore, L-SPI had a higher probability of binding to citral and catalyzing its conversion to methyl heptenone.

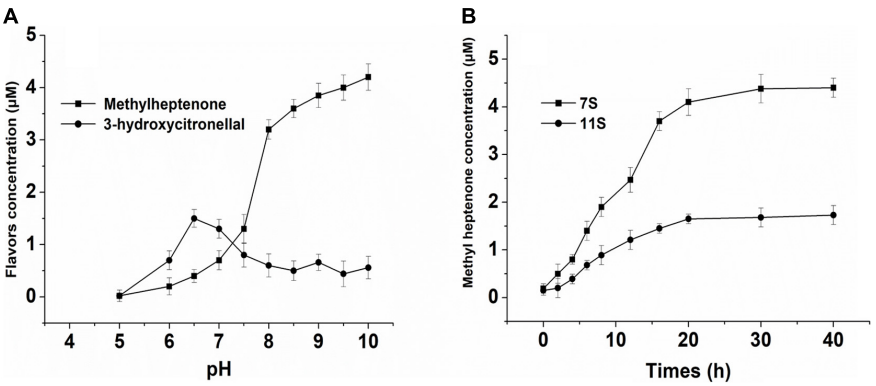

FIGURE 5 | (A) Effect of different pH solution of NSPI—catalyzed to citral. **(B)** Effect of 7S, 11S-catalyzed to citral. The concentration of protein is 1% (w/v), 20 mmol/L potassium phosphate buffer/NaOH, and primary citral's concentration is 24 μmol/L.

N-SPI is a natural protein that exists in a metastable state. The crosslinked network structure of the protein is flexible and comprises a hydrophilic peptide chain (36). Citral molecules could move into the internal spaces and bind to the polar fragment of the protein, which led to its conversion into methyl heptenone and acetaldehyde. From **Figure 4B**, Fluorescence quenching was observed for the mixture of N-SPI and citral. Form the **Table 1**, N-SPI has the more solubility and the more surface hydrophobicity than H-SPI. According to the literature (35, 37), the binding of N-SPI and citral is a possibility; thus, N-SPI could bind citral and catalyze citral to methyl heptenone. It maybe that SPI is an enzyme with conformational adaptability and participates in the reorganization of the polypeptide segments at the binding sites.

From **Figure 4C**, Minimum fluorescence quenching intensity was observed for H-SPI. Form the **Table 1**, H-SPI have the worst solubility and the highest surface hydrophobicity between L-SPI, N-SPI, and H-SPI. Thermal denaturation resulted in H-SPI losing its metastable state. The space formed within by the three-dimensional reticular structure collapsed, leading to the unfolding of the advanced structure (18). Subsequently, the orderly and compact structure of SPI was converted into an undefined peptide structure, resulting in a loss of biological and catalytic activity (1). The molecular surface structure also exhibited changes; the hydrophilic groups were relatively reduced. Moreover, the groups that were originally hidden within several groups of hydrophobic molecules were exposed to the molecular surface, resulting in the protein particles not mixing with water and losing their water film. Additionally, it was easy for the entangled molecules to collide with each other, which further resulted in the destruction of the binding sites that were likely responsible for catalytic activity. The aggregation phenomenon caused dissociation and heat accumulation in the protein solution. Heat treatment of proteins in the folding state results in a state of instability because the surface hydrophobicity is enhanced when the protein hydrophobic core is exposed. Next, the internal space of the inner hydrophilic chain participates in the catalytic reaction. The interaction of citral molecules with SPI shows that the catalytic reaction may be difficult owing to the strong surface area hydrophobicity. Thus, as the citral molecule is not within the binding pocket of the protein, the rate of the catalytic reaction is very slow. It can be inferred from the SPI catalytic reaction that citral molecules enter the sphere of the soybean protein, the catalytic site may be located on the SPI hydrophilic polar group.

Effect of pH on the Protein-Catalyzed Conversion of Citral to Methyl Heptenone

In this study, we found that SPI could catalyze the degradation of citral by reverse condensation; the end product was methyl heptenone and the intermediate was 3-hydroxycitronelloal (**Figure 5A**). No products were formed at pH 5. As the pH was increased from 5 to 7.5, the yield of 3-hydroxycitronelloal was found to be greater than that of methyl heptenone. As the pH was further increased from 7.5 to 10, the methyl heptanone yield was found to be higher than that of 3-hydroxyl citronelloal.

The study of the degradation reactions of citral mainly include those that are acid catalyzed. Kimura et al. (11) used NMR and IR to study the deacetylation and degradation of citral into terpenes in an acidic environment. In addition, it has been reported that citral is easily oxidized and that compounds such as BHT and BHA have a protective antioxidant effect on citral (8, 12, 13), however, our findings were contradictory to those reported in the literature. We found that the reverse hydroxyl aldehyde condensation degradation reaction of citral is suitable in an alkaline environment. Our findings were consistent with the results of Wolken et al. (6) who reported that glycine and bovine serum albumin catalyze the reverse hydroxyl aldehyde condensation degradation reaction of citral in neutral or dilute alkali solution to yield methyl heptenone and acetaldehyde.

7S and 11S—Catalyzed Citral to Methyl Heptenone

The effects of 7S and 11S on the SPI-catalyzed conversion of citral are shown in **Figure 5B**. The rate of conversion of citral by 7S was higher than that achieved by 11S. The deacetylation

of citral by SPI is likely attributed to the enzyme and substrate combination, both of which can change the structure of mutual induction, eventually forming a suitable complex and ensuring the completion of the catalytic process (38).

Due to the large number of hydrophobic groups on the surface of the basic subunit of 11S, spontaneous aggregation is easy to occur in the solution, so the solubility is lower in the range of pH 4.5∼8.0 (39, 40). This phenomenon may cause the 11S protein to mask part of the active site. 11S has a compact globular structure, low solubility, and low molecular flexibility when mixed with citral (41, 42). 7S is a trimer, the dissociated trimer will have more flexible mobile regions than the 11S hexamer, it maybe have more active site (26). The levels of the hydrophilic and polar amino acids in 7S are higher than in 11S (28). So 7S-catalyzed rate is also high. Based on the above analysis, we found that 7S had higher catalytic efficiency than 11S.

CONCLUSION

The results shows that the SPI could catalyze citral isomerization and yield methyl heptenone and acetaldehyde by reaction of inverse aldol condensation degradation. 3-Hydroxycitronelloal was formed as an intermediate in this reaction. The catalytic efficiency of the L-SPI was higher than that of N-SPI, whereas the catalytic efficiency of H-SPI was the lowest of L-SPI, N-SPI and H-SPI. Additionally, we found that the catalytic efficiency increased as the pH increased. The catalytic efficiency of 7S was greater than that of 11S. The catalytic site may be located on the SPI hydrophilic polar group. From this study it can be known that the reaction of SPI catalyze citral isomerization and yield methyl heptenone and acetaldehyde could change the flavor of Citrus juice-SPI beverages.

DATA AVAILABILITY STATEMENT

The original contributions presented in this study are included in the article/supplementary material, further inquiries can be directed to the corresponding author/s.

AUTHOR CONTRIBUTIONS

JG: writing the manuscript. JX: participate in experimental design and guidance. JC: guidance and others offer the materials. All authors contributed to the article and approved the submitted version.

FUNDING

This research was supported by the Excellent Young Talents Fund Program of Higher Education Institutions of Anhui Province (gxyq2021226), the Agricultural Products Processing Center of Chizhou College, the Key Nature Project of Chizhou University (CZ2020ZRZ02), and Key Discipline of Materials Science and Engineering, Chizhou University (czxyylxk03).

REFERENCES

1. Guo FX, Xiong YL, Fang Q, Jian HJ, Huang XL, Jie C. Examination of the causes of instability of soy protein isolate during storage through probing of the heat-induced aggregation. *J Am Oil Chem Soc.* (2015) 92:1075–84.
2. Arora A, Damodaran S. Removal of soy protein-bound phospholipids by a combination of sonication, β-cyclodextrin, and phospholipase A 2 treatments. *Food Chem.* (2011) 127:1007–13. doi: 10.1016/j.foodchem.2011.01.073
3. Damodaran S, Kinsella JE. Interaction of carbonyls with soy protein: conformational effects. *J Agric Food Chem.* (1981) 29:1253–7. doi: 10.3390/molecules22111893
4. Hansen AP, Heinis JJ. Benzaldehyde, citral, and d-limonene flavor perception in the presence of casein and whey proteins. *J Dairy Sci.* (1992) 75:1211–5. doi: 10.3168/jds.S0022-0302(92)77869-2
5. Aspelund TG, Wilson LA. Adsorption of off-flavor compounds onto soy protein: a thermodynamic study. *J Agric Food Chem.* (1983) 31:539–45.
6. Wolken WA, ten Have R, Van Der Werf MJ. Amino acid-catalyzed conversion of citral: cis-trans isomerization and its conversion into 6-methyl-5-hepten-2-one and acetaldehyde. *J Agric Food Chem.* (2000) 48:5401–5. doi: 10.1021/jf0007378
7. Masrat M, Aijaz Ahmad D. Inhibition of citral degradation in an acidic aqueous environment by polyoxyethylene alkylether surfactants. *Food Chem.* (2013) 138:2356–64. doi: 10.1016/j.foodchem.2012.12.031
8. Maswal M, Dar AA. Formulation challenges in encapsulation and delivery of citral for improved food quality. *Food Hydrocoll.* (2014) 37:182–95.
9. Stotz SC, Vriens J, Martyn D, Clardy J, Clapham DE. Citral sensing by transient [corrected] receptor potential channels in dorsal root ganglion neurons. *PLoS One.* (2008) 3:e2082. doi: 10.1371/journal.pone.0002082
10. Schieberle P, Grosch W. Identification of potent flavor compounds formed in an aqueous lemon oil/citric acid emulsion. *J Agric Food Chem.* (1988) 36:797–800.
11. Kimura K, Nishimura H, Iwata I, Mizutani J. Identification of acidic substances from deteriorated citral and effects of antioxidants on their formation. *J Agric Chem Soc Jpn.* (1983) 47:1661–3.
12. Kimura K, Nishimura H, Iwata I, Mizutani J. Deterioration mechanism of lemon flavor. 2. Formation mechanism of off-odor substances arising from citral. *J Agric Food Chem.* (1983) 31:801–4.
13. Xiaoqing Y, Huaixiang T, Chi-Tang H, Qingrong H. Inhibition of citral degradation by oil-in-water nanoemulsions combined with antioxidants. *J Agric Food Chem.* (2011) 59:6113–9. doi: 10.1021/jf2012375
14. Choi SJ, Decker EA, Henson L, Popplewell LM, Mcclements DJ. Inhibition of citral degradation in model beverage emulsions using micelles and reverse micelles. *Food Chem.* (2010) 122:111–6.
15. Nguyen H, Campi EM, Jackson WR, Patti AF. Effect of oxidative deterioration on flavour and aroma components of lemon oil. *Food Chem.* (2009) 112: 388–93.
16. Fkyerat A, Tabacchi R. Enantioselective preparation of 1-hydroxy neoisopulegol and 1-hydroxy neoisomenthol. *Tetrahedron Asymmetry.* (1997) 8:2231–6.
17. Jiang J, Chen J, Xiong YL. Structural and emulsifying properties of soy protein isolate subjected to acid and alkaline pH-shifting processes. *J Agric Food Chem.* (2009) 57:7576–83. doi: 10.1021/jf901585n
18. Guo F, Xiong YL, Qin F, Jian H, Huang X, Chen J. Surface properties of heat-induced soluble soy protein aggregates of different molecular masses. *J Food Sci.* (2015) 80:C279–87. doi: 10.1111/1750-3841.12761

19. Sorgentini DA, Wagner JR, Anon MC. Effects of thermal treatment of soy protein isolate on the characteristics and structure-function relationship of soluble and insoluble fractions. *J Agric Food Chem.* (1995) 43:2471–9.
20. Guo J, He Z, Wu S, Zeng M, Chen J. Binding of aroma compounds with soy protein isolate in aqueous model: effect of preheat treatment of soy protein isolate. *Food Chem.* (2019) 290:16–23. doi: 10.1016/j.foodchem.2019.03.126
21. Guo J, He Z, Wu S, Zeng M, Chen J. Binding of aromatic compounds with soy protein isolate in an aqueous model: effect of pH. *J Food Biochem.* (2019) 43:e12817. doi: 10.1111/jfbc.12817
22. Lowry OH. Protein measurement with Foli-ogenol reagent. *J Biol Chem.* (1951) 193:265–75.
23. Hagiwara H, Hamaya J, Hoshi T, Yokoyama C. Self-aldol condensation of unmodified aldehyde in supercritical carbon dioxide catalyzed by amine grafted on silica. *Tetrahedron Lett.* (2005) 46:393–5.
24. Watanabe Y, Sawada K, Hayashi M. A green method for the self-aldol condensation of aldehydes using lysine. *Green Chem.* (2010) 12:384.
25. Shimizu K-I, Hayashi E, Inokuchi T, Kodama T, Hagiwara H, Kitayama Y. Self-aldol condensation of unmodified aldehydes catalysed by secondary-amine immobilised in FSM-16 silica. *Tetrahedron Lett.* (2002) 43:9073–5.
26. Adachi M, Takenaka Y, Gidamis AB, Mikami B, Utsumi S. Crystal structure of soybean proglycinin A1aB1b homotrimer. *J Mol Biol.* (2001) 305:291–305. doi: 10.1006/jmbi.2000.4310
27. Baud F, Pebay-Peyroula E, Cohen-Addad C, Odani S, Lehmann MS. Crystal structure of hydrophobic protein from soybean; a member of a new cysteine-rich family. *J Mol Biol.* (1993) 231:877. doi: 10.1006/jmbi.1993.1334
28. Maruyama N, Adachi M, Takahashi K, Yagasaki K, Kohno M, Takenaka Y, et al. Crystal structures of recombinant and native soybean beta-conglycinin beta homotrimers. *Eur J Biochem.* (2010) 268:3595–604. doi: 10.1046/j.1432-1327.2001.02268.x
29. Maruyama Y, Maruyama N, Mikami B, Utsumi S. Structure of the core region of the soybean beta-conglycinin alpha' subunit. *Acta Crystallogr D Biol Crystallogr.* (2004) 60:289–97. doi: 10.1107/S0907444903027367
30. Kuwahara Y, Suzuki H, Mataumoto K, Wada Y. Pheromone study on acarid mites XI. Function of mite body as geometrical isomerization and reduction of citral (the alarm pheromone). *Appl Entomol Zool.* (1983) 18:30–9.
31. Kimura K, Nishimura H, Iwata I, Mizutani J. Deterioration mechanism of lemon flavor. 2 Formation of off-odor substances arising from citral. *J Agric Food Chem.* (1983) 31:57–78.
32. Hua YF, Huang AY, Liu XY. Properties of soy protein isolate prepared from aqueous alcohol washed soy flakes. *Food Res Int.* (2005) 38:273–9.
33. Eldridge AC, Wolf WJ, Nash AM, Smith AK. Protein purification, alcohol washing of soybean protein. *J Agric Food Chem.* (1963) 11:323–8.
34. Wang JM, Yang XQ, Yin SW, Zhang Y, Tang CH, Li BS, et al. Structural rearrangement of ethanol-denatured soy proteins by high hydrostatic pressure treatment. *J Agric Food Chem.* (2011) 59:7324. doi: 10.1021/jf201957r
35. Zhang J, Liu X, Subirade M, Zhou P, Liang L. A study of multi-ligand beta-lactoglobulin complex formation. *Food Chem.* (2014) 165:256–61. doi: 10.1016/j.foodchem.2014.05.109
36. Damodaran S, Parkin KL. *Fennema's Food Chemistry*. 5th ed. Boca Raton, FL: CRC Press (2016).
37. Jun G, He Z, Wu S, Zeng M, Chen J. Effects of concentration of flavor compounds on interaction between soy protein isolate and flavor compounds. *Food Hydrocoll.* (2019) 100:105388.
38. Koshland DE Jr, Neet KE. The catalytic and regulatory properties of enzymes. *Annu Rev Biochem.* (1968) 37:359.
39. Yuan D-B, Yang X-Q, Tang C-H, Zheng Z-X, Ahmad I, Yin S-W. Physicochemical and functional properties of acidic and basic polypeptides of soy glycinin. *Food Res Int.* (2009) 42:700–6. doi: 10.1021/jf801137y
40. Mo X, Zhong Z, Wang D, Sun X. Soybean glycinin subunits: characterization of physicochemical and adhesion properties. *J Agric Food Chem.* (2006) 54:7589–93. doi: 10.1021/jf060780g
41. Koshiyama I. Purification and physico-chemical properties of 11S globulin in soybean seeds. *Int J Pept Protein Res.* (1972) 4:167. doi: 10.1111/j.1399-3011.1972.tb03416.x
42. Koshland DE Jr, Némethy G, Filmer D. Comparison of experimental binding data and theoretical models in proteins containing subunits. *Biochemistry.* (1966) 5:365. doi: 10.1021/bi00865a047

Conflict of Interest: The authors declare that the research was conducted in the absence of any commercial or financial relationships that could be construed as a potential conflict of interest.

Publisher's Note: All claims expressed in this article are solely those of the authors and do not necessarily represent those of their affiliated organizations, or those of the publisher, the editors and the reviewers. Any product that may be evaluated in this article, or claim that may be made by its manufacturer, is not guaranteed or endorsed by the publisher.

frontiers | Frontiers in Nutrition

TYPE Original Research
PUBLISHED 22 July 2022
DOI 10.3389/fnut.2022.959824

OPEN ACCESS

EDITED BY
Gang Fan,
Huazhong Agricultural University, China

REVIEWED BY
Baoguo Sun,
Beijing Technology and Business University, China
Huanlu Song,
Beijing Technology and Business University, China

*CORRESPONDENCE
Rui-Ming Luo
rml9624641949@163.com

SPECIALTY SECTION
This article was submitted to Food Chemistry, a section of the journal Frontiers in Nutrition

RECEIVED 02 June 2022
ACCEPTED 01 July 2022
PUBLISHED 22 July 2022

CITATION
Bi Y, Luo Y, Luo R, Ji C, Gao S, Bai S, Wang Y, Dong F, Hu X and Guo J (2022) High freezing rate improves flavor fidelity effect of hand grab mutton after short-term frozen storage. *Front. Nutr.* 9:959824. doi: 10.3389/fnut.2022.959824

High freezing rate improves flavor fidelity effect of hand grab mutton after short-term frozen storage

Yong-Zhao Bi[1,2], Yu-Long Luo[1,2], Rui-Ming Luo[1,2]*, Chen Ji[2,3], Shuang Gao[2,3], Shuang Bai[2,3], Yong-Rui Wang[2,3], Fu-Jia Dong[1,2], Xiao-Lei Hu[1,2] and Jia-Jun Guo[1]

[1]School of Food & Wine, Ningxia University, Yinchuan, China, [2]National R & D Center for Mutton Processing, Yinchuan, China, [3]School of Agriculture, Ningxia University, Yinchuan, China

Taking the eutectic point as the final freezing temperature, the differences of flavor substances of in hand grab mutton (HGM) frozen at three rates of 0. 26 cm/h (−18°C), 0.56 cm/h (−40°C) and 2.00 cm/h (−80°C) were determined and analyzed. The results showed that the flavor of HGM decreased significantly after freezing. With the increase of freezing rate, the contents of aldehydes, alcohols, ketones, acids, esters, others, free amino acids and 5′-nucleotides were higher, and the content of specific substances was also generally increased. All samples from unfrozen and frozen HGM could be divided into four groups using an electronic nose based on different flavor characteristics. Seven common key aroma components were determined by relative odor activity value (ROAV), including hexanal, heptanal, octanal, nonanal, (*E*)-oct-2-enal, (2*E*,4*E*)-deca-2,4-dienal and oct-1-en-3-ol. The higher the freezing rate, the greater the ROAVs. Taste activity values calculated by all taste substances were far <1, and the direct contribution of the substances to the taste of HGM was not significant. The equivalent umami concentration of HGM frozen at −80°C was the highest. These findings indicated that higher freezing rate was more conducive to the retention of flavor substances in HGM, and the flavor fidelity effect of freezing at −80°C was particularly remarkable.

KEYWORDS

hand grab mutton, freezing rate, eutectic point, short-term frozen storage, flavor substance, flavor fidelity

Introduction

Tan sheep, an advantageous and characteristic breed in Ningxia of China, is famous for its meat with low "off-flavor" and good taste (1–4). In recent years, it has boarded the state banquet table many times to entertain foreign guests. With Tan sheep ribs as raw materials, hand grab mutton (HGM) is a traditional boiled meat product with national characteristics in Northwest China. At present, most of the HGM products sold in the market use the "soft can" production technology to extend the shelf life, but the

high-temperature and high-pressure sterilization has seriously damaged its flavor, which is not conducive to the development of Tan sheep meat processing industry (5, 6).

The central kitchen developed earlier in America, Japan and many developed countries in Europe (7). Some traditional Western meat foods (such as steak and roast beef) have been industrialized through the central kitchen. The construction of central kitchen started late in China. Until the continuous transformation and upgrading of China's catering industry in recent years, the "industrialized" central kitchen gradually developed rapidly, organically connected the catering industry and food industry, and gradually formed a complete industrial chain (8, 9). Freezing is one of the common ways to preserve the quality of meat products (10). There is often a cold storage in the central kitchen to store semi-finished products and finished products to be delivered. Prefabricated dishes for sale can generally be transported to the terminal after short-term freezing storage. They can be eaten only after simple processing or secondary heating, effectively maintaining the original flavor of their fresh products. However, at present, the traditional commercial freezing (−18°C) has slow freezing rate and low ice crystal nucleation rate, forming a small amount of large ice crystals, which may lose more flavor substances after thawing (11–13). Therefore, flavor is still one of the difficulties to be solved urgently in the central kitchen, and the technological innovation of low-temperature flavor fidelity of semi-finished products and finished products will become an inevitable trend.

In recent years, with the development and maturity of the cold chain industry, many enterprises of China have introduced spiral quick-freezing devices (the working temperature is generally lower than −30°C) to rapidly cool the products to below −18°C in a very short time at a high freezing rate. Through rapid freezing, high nucleation rate is promoted and small ice crystals are formed in meat products, so as to minimize the loss of flavor (14–16). Eutectic point (EP) is the temperature at which all free water in the material changes from liquid to solid (17, 18). It is located behind the maximum ice crystal generation zone of the material. It is a relatively stable state reached by the product after freezing. Through high-speed freezing, the products can be quickly cooled to the EP in a very short time, and then transported to the commercial frozen storage, so as to improve the fidelity effect of product flavor and shorten the product production cycle, which can effectively reduce the cost.

At present, most scholars focus on the effect of freezing rate on the quality of raw meat and the effect of different rates frozen raw meat on the its flavor after cooking. However, there is few reports on the effect of freezing rate on the flavor substances of meat products (19–23). Therefore, the effects of three freezing rates on the differences of flavor substances in short-term frozen storage of HGM were studied in this paper. This study provides technical guidance for the frozen storage of prefabricated dishes in the central kitchen, and increases its economic value by improving the flavor fidelity effect of quick-frozen HGM. Additionally, it can be expected to provide an effective method to solve the problem of high cost caused by maintaining high freezing rate.

Materials and methods

Chemicals

1,2-Dichlorobenzene (99.78 g/100 g) and n-alkanes (C_6-C_{26}) of chromatographic grade were bought from Dr. Ehrenstorfer GmbH (Augsburg, Germany) and Sigma-Aldrich (St. Louis, MO, USA). Adenosine monophosphate (AMP), guanosine monophosphate (GMP), inosine monophosphate (IMP), and amino acid standards of chromatographic grade were purchased from Sigma-Aldrich (Shanghai, China). Methanol and acetonitrile were of high performance liquid chromatography (HPLC) grade and purchased from Aladdin (Shanghai, China). Perchloric acid, trichloroacetic acid, sodium hydroxide, sodium dihydrogen phosphate, and hydrochloric acid were of guaranteed reagent grade. Anhydrous citric acid, triethylamine, and acetic acid were of analytical reagent grade. All the above reagents were purchased from the Guangzhou Chemical Reagent Factory (Guangzhou, China).

Preparation of samples

Fresh ribs were taken from approximately 6-month-old Tan sheep carcasses within 24 h after slaughter from a commercial meat company (Yanchi, Ningxia, China). The ribs were transported to the laboratory in the form of foam box and ice bag. With dirt on the surface removed, the ribs were diced into 10 cm length bars. 500 g ± 10 g ribs were weighed and soaked for 30 min each time. Then the ribs were taken out and drained, and put into the pot. And then 2 L purified water was poured (meat water ratio 1:4) and 3.5% salt (w/w, based on sheep ribs weight) were put into. There is no seasoning in the pot except salt. The ribs were boiled over high fire (2,200 W) for 30 min until boiling (1,500 m above sea level in Yinchuan, Ningxia, and the boiling point of water was 95.6°C), then skimmed the floating foam and adjusted to low fire (800 W) to continue cooking for 70 min. After cooking, the samples were put into polyethylene self-sealing bag. The samples were naturally cooled to room temperature and immediately frozen under different conditions. Four batches of HGM were prepared and stored separately at the following temperature: A) control group (Sampled and determined immediately without freezing); B) −80°C/−18°C group (After freezing at −80°C to EP, immediately transferred to −18°C and continued to store for 48 h); C) −40°C/−18°C group (After freezing at −40°C to EP, immediately transferred to −18°C and continued to store

for 48 h); D) −18°C/−18°C: (After freezing at −18°C to EP, immediately transferred to −18°C and continued to store for 48 h). Before analyzing, the samples were thawed at 4°C for 24 h. After thawing, bones, the visible fat and fascia of HGM were removed. The muscle was minced at 3,000 rpm for 8 s, and analysis of volatile aroma compounds, free amino acids and taste nucleotides were performed.

Eutectic point determination

The EP of the material was measured by differential scanning calorimetry (DSC) (DSC 800003061404, Perkin Elmer, USA). The test process was carried out by cooling. 2 ∼ 8 mg mutton was placed in the aluminum crucible of DSC, protected by nitrogen, and cooled from 25 to −70°C at a cooling rate of 2°C/min. The EP of the sample was determined according to the exothermic peak value during cooling, and the results were taken as the average value of three parallel times.

Measurement of temperature in freezing process and calculation of freezing rate

The TC-08 thermocouple data recorder (Pico, Britain) was used for multi-channel temperature measurement and recording. The thermocouple temperature probe was inserted into the geometric center of the HGM, and the temperature change was recorded every 1 min until the freezing temperature reached the EP. The temperature was measured for 6 times in parallel, and the freezing temperature curve was drawn. The freezing rate is calculated according to the method provided by the International Institute of Refrigeration (24). The calculation formula is as follows:

$$V = \frac{\delta_0}{\tau_0}$$

Where V represents freezing rate; δ_0 represents the shortest distance between the food surface and the heat center (cm); τ_0 represents the time required for the food surface to reach 0°C and the food center temperature to drop to 10°C lower than the food freezing point (h). In the calculation, the temperature of the central probe point of HGM was selected as the central temperature point. The determination was repeated 6 times, and δ_0 was controlled to 1 cm.

Electronic nose detection

Electronic nose (E-nose) analysis was performed using a PEN 3.5 E-nose (Airsense, Schwerin, Germany) according to the existing methods with minor modifications (25–27). The PEN3.5 system contains 10 metal oxide gas sensors (namely W1C, W5S, W3C, W6S, W5C, W1S, W1W, W2S, W2W, and W3S), which can detect olfactory cross-sensitive information (28–30). The response characteristics of each sensor are as follows: W1C (aromatic), W5S (broad range), W3C (aromatic), W6S (hydrogen), W5C (arom-aliph), W1S (broad-methane), W1W (sulphur-organic), W2S (broad-alcohol), W2W (sulph-chlor) and W3S (methane-aliph). 3 g of minced meat samples were put into 50 mL airtight vials and incubated in the water bath (HWS-12, Yiheng, Shanghai, China) at 25°C for 40 min. The chamber was flushed with clean air until the sensor signal returned to the baseline before testing new samples. Each sample was measured in triplicate, and the mean values were applied for further analysis.

Analysis of volatile compounds using headspace solid phase microextraction combined with gas chromatography-mass spectrometry

Volatile compounds in the HGM were extracted using a headspace solid phase microextraction (HS-SPME) device (Supelco, Bellefone, PA, USA) with a 50/30 μm divinylbenzene/carboxen/polydimethylsiloxane (DVB/CAR/PDMS) fibre (31–33). 3 g minced meat samples were weighed into a 20 mL headspace vial. Thereafter, 4 μL of 1,2-dichlorobenzene (0.0642 μg/μL) was added as the internal standard, and then the vial was sealed tightly with a PTFE (polytetrafluoroethylene) septum. The vials were placed in water bath at 60°C for 20 min before headspace sampling to equilibrate their headspace. Then the SPME fibre, previously conditioned for 40 min at 250°C in a gas chromatograph injection port, was exposed to the headspace of a headspace vial for extraction at 60°C for 20 min. Finally, the volatile compounds were identified and quantified using a gas chromatography-mass spectroscopy (GC-MS) (Shimadzu GC-MS 2010 plus, Kyoto, Japan). The DB-WAX (30 m × 0.25 mm × 0.25 μm, Agilent, California, USA) was selected as polar analytical column. The SPME fibre was desorbed and maintained in the GC injector for 5 min at 250°C. The injection mode was splitless. The initial temperature of the column oven was isothermal for 3 min at 40°C. Thereafter, the temperature was increased to 200°C at a rate of 5°C/min and raised to 230°C at a rate of 10°C/min and held for 3 min. Helium was used as the carrier gas with a column flow rate of 2 mL/min. The MS interface temperature was 280°C, and the MS ion source temperature was 230°C. The MS was obtained using a mass selective detector in positive electron ionization mode at 70 eV. The mass scan range of m/z was set from 50 to 350 amu. The compounds were semi-quantified by comparing their mass spectra to the NIST 14 mass spectral library and by comparison of their linear retention indices (LRI), which were calculated

by running C_6-C_{26} n-alkanes under the same chromatographic conditions. Reference RI query from https://webbook.nist.gov/chemistry/. The content of each compound was calculated by comparing its area with the internal standard. Each sample was measured in triplicate, and the mean value was applied for further analysis.

Determination of key volatile compounds

Relative odor activity value (ROAV) has been proposed to explain how to evaluate the contribution of individual volatile compounds to the overall aroma by the relative concentration of volatile compounds (34, 35). The ROAV was used to identify key volatile compounds of HGM, which range from 0 to 100. Odor thresholds in the water of volatile components were provided in the relevant literature. The calculation formula is as follows:

$$ROAV_i = \frac{C_i}{C_{\max}} \times \frac{T_{\max}}{T_i} \times 100$$

Where C_i and T_i represent the relative content of each volatile compound and the corresponding sensory threshold (μg/L); C_{max} and T_{max} represent the relative content of the components that contribute the most to the overall flavor of the sample and the corresponding sensory threshold (μg/L).

Measurement of free amino acids

Minced meat samples (0.5 g) were weighed in 50 mL centrifuge tubes, homogenized with 25 mL of 0.01 mol/L hydrochloric acid and followed by ultrasonic extraction for 30 min and centrifugation at 4,000 rpm for 5 min. 2 mL of the filtered liquid was accurately sucked into the centrifuge tube. After adding 2 mL of 8% sulfosalicylic acid, it was evenly mixed and allowed to stand for 15 min, and centrifuged at 10,000 r/min for 10 min. The lower aqueous phase was taken, and filtered through a membrane with 0.22 μm pore size for analysis. Amino acid analysis conditions: the chromatographic column was Hitachi special ion exchange resin (4.6 × 60 mm), and the detection wavelength was 440 nm; buffer flow rate was 35 mL/h; column temperature was 31 ∼ 76°C; ninhydrin solution flow rate was 25 mL/h; injection volume was 20 μL (36, 37).

Measurement of taste nucleotide

Minced meat samples (0.5 g) were weighed in 50 ml centrifuge tubes, added 25 mL ultrapure water, and then centrifuged at 10,000 r/min and 4°C for 20 min. The supernatant was taken in 50 mL centrifuge tubes and fixed to volume with ultrapure water. The resulting solution was filtered through a membrane with 0.22 μm pore size for analysis. HPLC conditions: the chromatographic column was TSK gel ods-80 TM (4.6 × 250 mm). The column temperature was 30°C. The ultraviolet detection wavelength was 254 nm, and the injection volume was 10 μL. The flow rate was 0.8 mL/min. Mobile phase: eluent A was 0.05 mol/L methanol, and eluent B was 0.05 mol/L potassium dihydrogen phosphate buffer with pH 5.4. After filtering with a membrane with 0.45 μm pore size, mobile phase was degassed with ultrasonic at room temperature for 30 min. The binary mobile phase was used for gradient elution separation and the detection time was 23 min. The ratio of potassium dihydrogen phosphate with time was 0 min: 0 ∼ 100%; 11 min: 10% ∼ 90%; 18 min: 0 ∼ 100%; 23 min: 0 ∼ 100% (38–40).

Calculation of taste activity value and equivalent umami concentration

Taste activity value (TAV) value is defined as the ratio of the relative concentration of taste substance to its taste threshold, which reflects the contribution of a taste substance to the overall taste (41, 42). The formula is as follows:

$$TAV = \frac{C}{T}$$

Where C represents the absolute concentration of taste substance (mg/kg); T represents the threshold of taste substance (mg/kg).

The EUC is the umami taste intensity produced by the synergistic action of taste nucleotide and umami amino acid mixture, which is equivalent to the amount of single monosodium glutamate required for the umami taste intensity (43, 44). The calculation formula is as follows:

$$Y = \sum \alpha_i \beta_i + 1218\left(\sum \alpha_i \beta_i\right)\left(\sum \alpha_j \beta_j\right)$$

Where Y represents EUC (g MSG/100 g); α_i represents the concentration of taste active amino acids (Asp, Glu) (g/100 g); β_i represents the relative freshness coefficients of umami amino acids (Asp is 0.077; Glu is 1; 1218 represents the synergy constant; α_j represents the concentration of taste nucleotides (5'-GMP, 5' -AMP, 5'-IMP) (g/100 g); β_j represents the relative freshness coefficients of taste nucleotides (5'-AMP is 0.18, 5'-IMP is 1, 5'-GMP is 2.3).

Sensory evaluation

The sensory evaluation gets the Ningxia University's approval in advance and is performed with 12 panelists from the students and faculty of the School of Food & Wine, Ningxia University. The panelists, 6 males and 6 females aged between

18 and 40, are considered as semi-trained as they have partaken in sensory analysis of meat products for some time and are familiar with the basics of sensory evaluation. First, the HGM were stored at 50°C for temperature equilibration, then samples were cut into 1-cm^3 pieces and mixed well before serving. Sensory analysis was undertaken in the panel booths at the university sensory laboratory (25 ± 3°C). Samples were served in plates with a glass of water and a piece of unsalted cracker to refresh the palate between samples (45). Evaluations took place in individual booths under white fluorescence light. The sensory evaluation was based on a seven-point linear scale to determine the aroma (7 = rich and strong, 1 = poor and dull), umami (7 = intense, 1 = mild), juiciness (7 = intense, 1 = mild), and overall acceptability (7 = high, 1 = low).

Statistical analysis

Analysis of variance and mean comparison were carried out using the statistical package for the social sciences (SPSS) software (version 26.0, SPSS Inc., Chicago, IL). Differences were considered significant at $P < 0.05$. The figures were generated using Origin 2021 (OriginLab, Northampton, MA).

Results and discussion

Eutectic point measurement results

At present, there are two methods to detect the EP of materials, namely DSC method and resistance method. DSC method uses the corresponding enthalpy change of materials when phase transition occurs, resulting in a certain exothermic or endothermic process of materials at this temperature. The EP is detected by recording the change of exothermic or endothermic process with time. During the cooling process of the sample, a large amount of free water inside the sample will crystallize and release a large amount of enthalpy heat. The DSC curve of the sample was detected as shown in Figure 1. There was only one prominent exothermic peak during the whole cooling process, so it was concluded that the EP of the sample was −9.66 ± 0.24°C.

Effect of freezing rate on freezing curve and thawing loss rate

The variation law of the central temperature of HGM with time under different freezing methods was revealed in Figure 2 which is in line with the trend of general food freezing curve. The two ends drop rapidly, and the middle is relatively flat, which is the maximum ice crystal generation zone. The longer the time of passing through the maximum ice crystal formation zone,

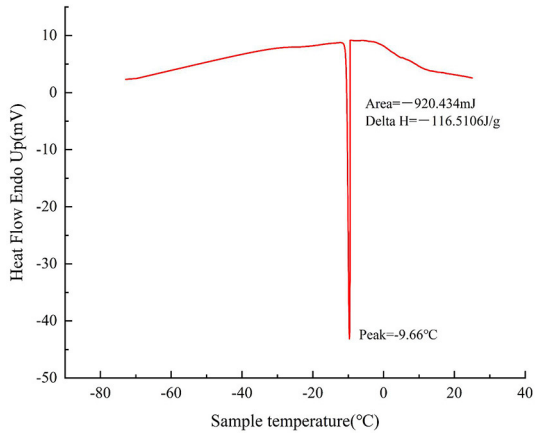

FIGURE 1
DSC cooling curve of sample.

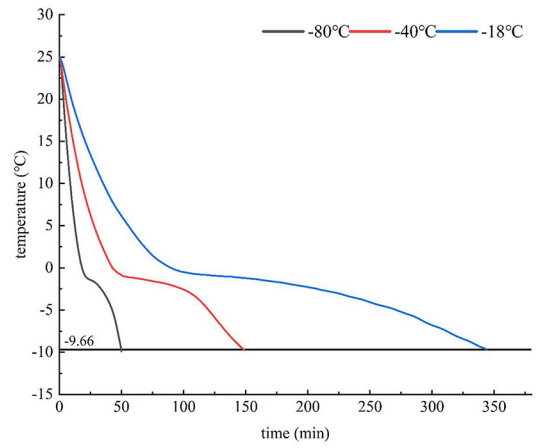

FIGURE 2
Freezing curves of different freezing temperature.

the larger the ice crystal and the more uneven the distribution, resulting in the change of cell volume, the change of colloidal properties and the mechanical damage of ice crystal, resulting in the loss of food flavor. It can be seen in the figure that the EP was located behind the maximum ice crystal generation zone. After reaching the EP, almost all the water in the mutton was coagulated into ice crystals, so that the product reached a relatively stable state after freezing. At present, in the freezing operation, we strive to pass through the maximum ice crystal generation zone as soon as possible to reduce the attenuation of product flavor. Therefore, the EP was selected as the final freezing temperature, and the samples were frozen at three rates to study the effect of freezing rate on the flavor of HGM. Jeremiah's research showed that higher freezing rate can form smaller ice crystals with large quantity and uniform distribution,

10.3389/fnut.2022.959824

TABLE 1 Freezing features of different freezing temperature.

Freezing temperature	Time to reach eutectic temperature/min	δ_0/cm	τ_0/h	v/cm·h^{-1}	Thawing loss rate (%)
−18°C	344	1.0	3.90	0.26	1.17 ± 0.09
−40°C	149	1.0	1.80	0.56	0.85 ± 0.05
−80°C	50	1.0	0.50	2.00	0.31 ± 0.02

which can well maintain the quality of food materials (46). It can be seen from Table 1 that the freezing rate increased gradually with the decrease of freezing temperature. According to the regulations of the International Institute of Refrigeration, the freezing rates of −18°C and −40°C were 0.26 cm/h and 0.56 cm/h respectively, which were slow freezing, and the freezing rate of −80°C was 2.00 cm/h, which was medium freezing. The time from room temperature to EP at −80°C was only 50 min, which was much shorter than −18°C and −40°C, and the thawing loss rate at −80°C was the lowest.

Volatile compounds profiling of hand grab mutton with different freezing rates

Volatile composition analysis of hand grab mutton using electronic nose

It can be seen from Figure 3 that the odour contour curve of E-nose radar of HGM with different freezing rates was significantly different, especially between the control group and each treatment group. The signal intensity of sensors W3S, W1C, W3C, W6S, and W5C on all samples was low, and there was no significant difference between different treatment groups, indicating that the content of some aromatic compounds, ammonia, olefins and alkanes in HGM was low, and the freezing rate had little effect on it. There was no difference in W6S odour profile curve because the hydroperoxide produced by lipid oxidation has no odour. W5S, W1S, W1W, W2S, and W2W were sensitive to the response of each group of samples. Compared with the control group, the response values of the above sensors were significantly reduced in each treatment group, indicating that freezing significantly reduced the volatile flavor substances in HGM. The changes of W1S and W2S sensors showed that freezing reduced the alcohol compounds in HGM, but there was no significant difference in signal intensity between different freezing rates. The sensor W5S was sensitive to nitrogen oxides. The retention of nitrogen oxides in the −80°C/−18°C group was higher than that in the −40°C/−18°C group, and the retention of nitrogen oxides in the −18°C/−18°C group was the lowest. Sensors W1W and W2W were sensitive to sulfur compounds, and their retention law of sulfur compounds was basically consistent with the trend of W5S to nitrogen oxides. The above changes fully showed that the volatile flavor

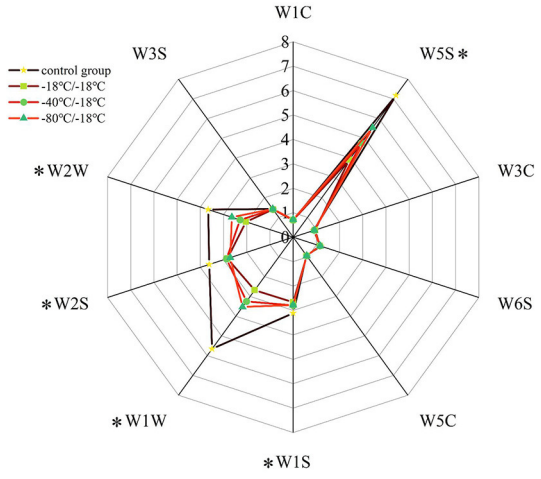

FIGURE 3
E-nose radar image of volatile flavor compounds. *Represents significant differences ($P < 0.05$).

substances of HGM were seriously attenuated after freezing, but the −80°C/−18°C group could effectively reduce the loss of flavor.

Principal component analysis (PCA) was used to analyze the detected E-nose data. The higher the contribution rate, the better the principal component reflects the original multi-index information (47, 48). As can be seen from Figure 4, the contribution rate of PC1 was 78.06%, and that of PC2 was 17.46%. The cumulative variance contribution rate of the first two principal components was 95.52% (>95%), indicating that most of the odour information of the sample was covered by the first two principal components (26). According to Figure 4, each group of samples can be easily divided into four groups. When the samples overlap or are close, it indicates that they produce similar volatile flavor substances. In the biplot, W2S, W3S, W6S, W1W, and W2W were related to the samples of the control group, W5C was related to the −18°C/−18°C group, W1C, W3C, W1S, and W5S were related to the −80°C/−18°C group, and the −40°C/−18°C group was negative on PC1 and PC2, and there was no sensor associated with it. The analysis combined with E-nose radar fingerprint showed that the nitrogen oxides, aromatic compounds and alcohol sulfur components in HGM

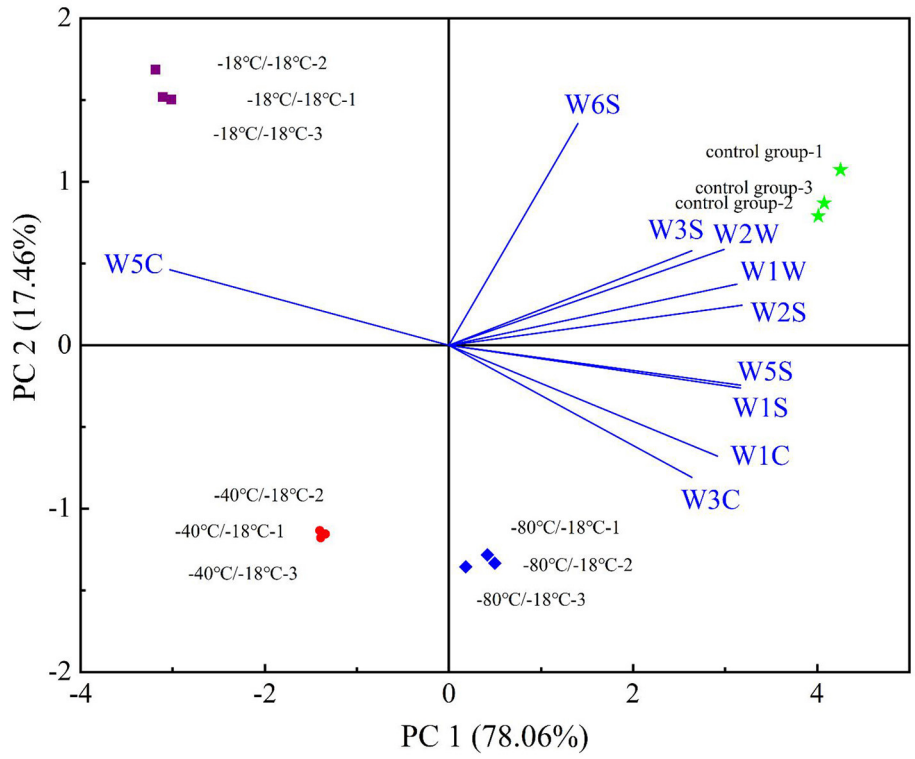

FIGURE 4
PCA biplot of E-nose.

at different freezing rates changed significantly, while alkanes, hydrides and ammonia compounds were not affected by freezing rates. Therefore, E-nose could effectively distinguish each group of HGM, but it could not characterize the change law of specific substances after freezing.

Volatile components analysis of hand grab mutton by headspace solid phase microextraction combined with gas chromatography-mass spectrometry

The volatile flavor compounds formed in the cooking process of HGM were very complex, which were mainly produced by lipid oxidation, Maillard reaction and lipid-Maillard interaction. It can be seen from Figure 5 that aldehydes, alcohols and ketones always dominated before and after frozen storage, and were the main volatile substances in HGM. The total contents of aldehydes, alcohols, ketones, acids, esters and other substances in the three treatment groups were lower than those in the control group, indicating that short-term frozen storage led to a large loss of volatile aroma components in mutton. The changes of E-nose odour contour curve (Figure 3) were corresponded to this result.

It can be seen from Table 2 that 44 kinds (control group), 43 kinds (−18°C/−18°C), 47 kinds (−40°C/−18°C) and 48 kinds (−80°C/−18°C) were detected in the four groups of samples. The contents of aldehydes, alcohols and ketones accounted for about 90% of the total volatile components of each group of samples, which were the main volatile components of HGM. Among the aldehydes, hexanal, heptanal, octanal, nonanal, benzaldehyde, (*Z*)-2-heptanal, (*E*)-oct-2-enal, (2*E*,4*E*)-deca-2,4-dienal and tetradecanal were the main aldehydes. The oxidation and degradation of fat and the Strecker degradation of amino acids were the main sources of these substances. The threshold of aldehydes was generally low, which made an important contribution to the overall characteristics of odour (49). Aldehydes in −18°C/−18°C, −40°C/−18°C and −80°C/−18°C groups decreased by 73.53, 50.75, and 29.14% respectively. The alcohols detected in the sample mainly came from fat oxidation, and most of them were saturated alcohols (50). The olfactory threshold of saturated alcohols was high, so they contribute less to the overall flavor of HGM (51). 1-octene-3-ol was the highest content of detected alcohols. It belonged to unsaturated alcohols and had a low threshold. It could be formed by eicosapentaenoic acid catalyzed by 15-lipoxygenase and arachidonic acid catalyzed by 12-lipoxygenase (52). It was an important component of mutton aroma (53, 54).

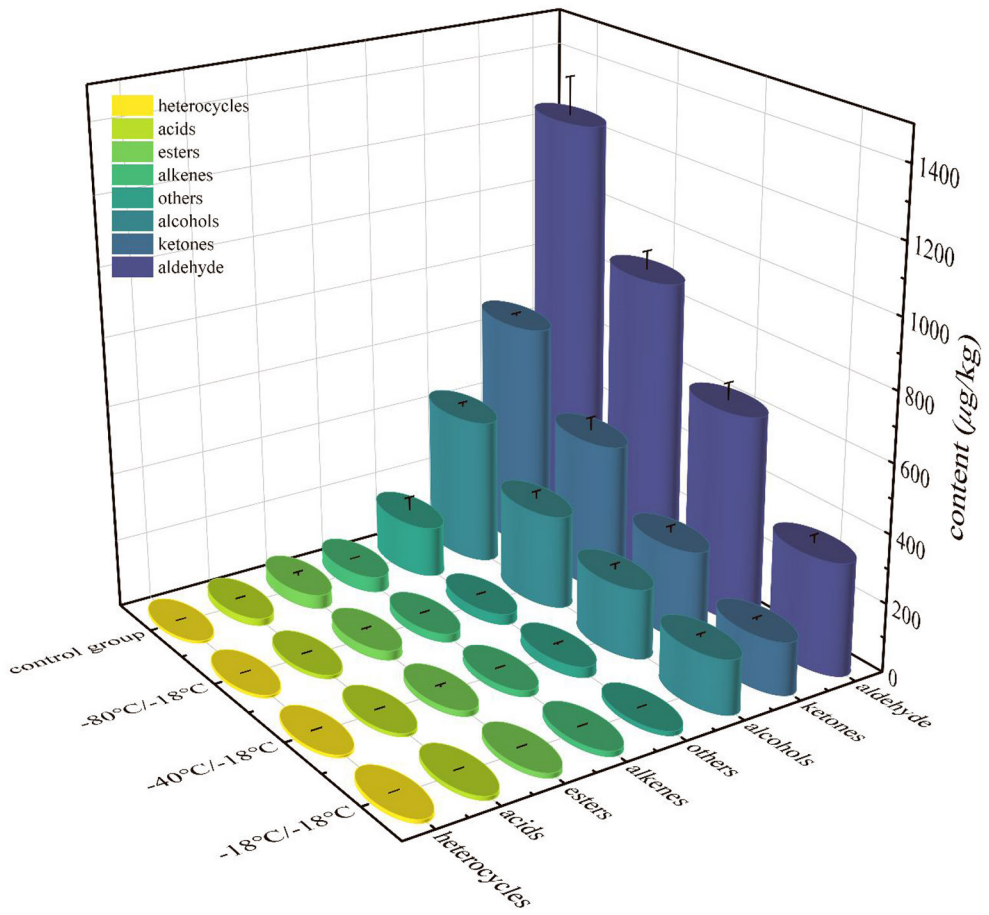

FIGURE 5
Total contents of various volatile flavor substances of HGM with different freezing rates.

Alcohol in −18°C/−18°C, −40°C/−18°C and −80°C/−18°C group decreased by 62.81, 52.28, and 35.78% respectively. Ketones were not only the product of Maillard reaction, but also the result of fat oxidation. The reaction of lysine, arginine, leucine, methionine with glucose or fructose was the main way to produce ketones (55). The highest content of ketones detected in the control group was octane-2,3-dione, followed by 3-hydroxy-2-butanone. 3-Hydroxy-2-butanone and octane-2,3-dione were common methyl ketones in the mutton. They were related to the degree of lipid oxidation. They could be produced by the decomposition of amino acids or by β-Oxidation of fatty acids produced after heat treatment of triglycerides (56, 57). Other ketone substances such as octan-3-one, pentane-2,3-dione, undecan-2-one, dihydro-5-methyl-2(3H)-furanone, 6-pentyloxan-2-one, (*Z*)-6,10-dimethyl-5,9-undediene-2-one, (3*E*,5*E*)-nona-3,5-dien-2-one, etc. had low contents or were only detected in some samples of the treatment group. The reason might be the differences of raw meat quality or the polymerization of fat cleavage products in frozen storage. The aroma threshold of ketones was high, and generally had little contribution to the overall flavor of mutton. Compared with the control group, ketones in −18°C/−18°C group, −40°C/−18°C group and −80°C/−18°C group decreased by 77.02, 60.59, and 34.56% respectively.

Acids were produced when fat was oxidized or hydrolyzed into low-grade fatty acids. Due to their low content and relatively high threshold, their contribution to the overall flavor of the sample was small (58). In the control group, only three esters were detected, including butyl prop-2-enoate, diethyl benzene-1,2-dicarboxylate and n-caproic acid vinyl ester. Protein hydrolysis, glycolysis and fat oxidation were important pathways for the formation of esters (59). 2-pentyl-furan was the only heterocyclic compound detected, which was oxygen heterocyclic compound. As an indicator of lipid oxidation in meat products, it was detected in all samples. Most furan compounds had strong meat flavor, mainly produced by thiamine degradation, caramelization and carbohydrates degradation, while 2-pentyl-furan presented fruit aroma (60,

TABLE 2 Volatile flavor compounds of HGM with different freezing rates.

Category	No.	Compounds	Threshold (43) (μg/kg)	LRI	Reference	Concentration (μg/kg)			
						Control group	−18°C/−18°C	−40°C/−18°C	−80°C/−18°C
Aldehydes (20)	1	Hexanal	7.5	1,069	1,078	648.10 ± 85.25^{d}	225.17 ± 13.82^{a}	459.34 ± 28.70^{b}	565.70 ± 42.11^{c}
	2	Heptanal	10	1,187	1,181	151.19 ± 3.98^{d}	22.13 ± 2.74^{a}	33.67 ± 5.66^{b}	73.64 ± 0.49^{c}
	3	Octanal	0.1	1,280	1,287	125.94 ± 3.56^{d}	21.54 ± 4.70^{a}	36.49 ± 3.76^{b}	55.92 ± 0.77^{c}
	4	Nonanal	3.5	1,372	1,390	250.7 ± 17.67^{d}	40.70 ± 0.83^{a}	52.05 ± 9.63^{b}	135.58 ± 7.98^{c}
	5	Decanal	5	1,485	1,498	—	0.74 ± 0.02^{a}	0.97 ± 0.25^{b}	3.32 ± 0.04^{c}
	6	Benzaldehyde	300	1,520	1,508	29.67 ± 0.11^{c}	8.15 ± 0.72^{a}	17.62 ± 1.49^{b}	17.45 ± 1.22^{b}
	7	Benzene-1,3-dicarbaldehyde	UN	1,347	2,341	—	—	0.19 ± 0.07^{a}	0.61 ± 0.27^{b}
	8	(*Z*)-Hept-2-enal	10	1,311	1,319	12.64 ± 0.22^{c}	2.09 ± 0.10^{a}	2.08 ± 0.05^{a}	6.62 ± 0.10^{b}
	9	(*E*)-Hept-2-enal	17	1,533	1,542	—	—	—	0.38 ± 0.09^{a}
	10	(*E*)-Non-2-enal	0.07	1,159	1,162	—	—	0.95 ± 0.31^{a}	—
	11	(*E*)-Oct-2-enal	0.2	1,441	1,434	16.22 ± 0.47^{c}	3.32 ± 0.19^{a}	3.41 ± 0.13^{a}	10.16 ± 0.76^{b}
	12	(*Z*)-Hept-4-enal	0.04	1,235	1,237	—	0.15 ± 0.01^{a}	—	—
	13	(*E*)-Non-4-enal	40	1,453	1,458	—	0.79 ± 0.04^{a}	0.75 ± 0.37^{a}	2.65 ± 0.23^{b}
	14	(2*E*,4*E*)-Deca-2,4-dienal	0.05	1,827	1,805	3.08 ± 0.72^{c}	1.49 ± 0.20^{a}	2.29 ± 0.15^{b}	3.15 ± 0.46^{c}
	15	(2*E*,4*E*)-Nona-2,4-dienal	0.06	1,715	1,702	—	0.95 ± 0.10^{a}	—	—
	16	(2*E*,6*Z*)-Nona-2,4-dienal	0.02	1,587	1,591	—	—	—	0.23 ± 0.00^{a}
	17	Undec-2-enal	0.14	1,747	1,755	—	—	—	0.67 ± 0.09^{a}
	18	Dodecanal	1.07	1,705	1,709	0.63 ± 0.38^{a}	—	—	—
	19	Tridecanal	10,000	1,822	1,824	—	—	0.28 ± 0.05^{a}	0.73 ± 0.39^{a}
	20	Tetradecanal	UN	1,919	1,924	3.33 ± 0.47^{c}	1.44 ± 0.92^{bd}	1.39 ± 0.37^{d}	2.92 ± 0.64^{abc}
Alcohols (22)	1	Heptan-1-ol	520	1,473	1,461	4.39 ± 0.72^{a}	—	—	—
	3	Butan-1-ol	10,000	1,138	1,150	1.35 ± 0.06^{b}	0.57 ± 0.04^{a}	—	—
	4	Pentan-1-ol	5,000	1,249	1,255	43.17 ± 0.12^{d}	17.32 ± 0.59^{a}	22.12 ± 2.16^{b}	33.84 ± 1.34^{c}
	5	Hexan-1-ol	200	1,366	1,359	42.27 ± 5.28^{d}	6.36 ± 0.13^{a}	10.91 ± 1.45^{b}	17.11 ± 0.12^{c}
	6	Octan-1-ol	54	1,565	1,554	13.18 ± 0.28^{d}	3.37 ± 0.30^{a}	5.55 ± 0.48^{b}	10.86 ± 1.34^{c}
	7	Nonan-1-ol	2	1,664	1,666	—	0.37 ± 0.06^{a}	—	—
	8	Phenylmethanol	5,500	1,870	1,877	1.07 ± 0.01^{d}	0.54 ± 0.02^{a}	0.78 ± 0.02^{b}	0.96 ± 0.07^{c}
	9	Butane-1,4-diol	2,700,000	1,868	1,861	0.76 ± 0.03^{c}	0.21 ± 0.04^{a}	0.19 ± 0.06^{a}	0.36 ± 0.01^{b}
	10	Oct-1-en-3-ol	2.00	1,427	1,456	295.00 ± 2.79^{d}	117.30 ± 5.84^{a}	153.62 ± 11.36^{b}	195.15 ± 17.86^{c}
	11	Pent-1-en-3-ol	3,000	1,144	1,157	—	4.37 ± 0.75^{a}	—	—

(Continued)

10.3389/fnut.2022.959824

TABLE 2 Continued

Category	No.	Compounds	Threshold (43) (μg/kg)	LRI	Reference	Concentration (μg/kg)			
						Control group	−18°C/−18°C	−40°C/−18°C	−80°C/−18°C
	12	Non-1-en-3-ol	UN	1,539	1,555	—	1.36 ± 0.22^{a}	1.78 ± 0.32^{ab}	2.76 ± 0.91^{b}
	13	(2*R*,3*R*)-Butane-2,3-diol	1,000,000	1,553	1,544	2.18 ± 0.06^{a}	—	—	—
	14	2-Ethylhexan-1-ol	UN	1,502	1,484	6.19 ± 2.97^{b}	3.50 ± 0.72^{a}	—	—
	15	3-Methylheptan-2-ol	UN	1,655	1,676	0.30 ± 0.02^{a}	—	—	—
	16	(*Z*)-Oct-2-en-1-ol	50	1,550	1,547	15.68 ± 0.20^{c}	4.01 ± 1.18^{a}	8.74 ± 0.88^{b}	10.79 ± 1.26^{b}
	17	Dodecan-1-ol	3	1,961	1,980	—	—	—	0.25 ± 0.15^{a}
	18	4-Methoxy-4-methylpentan-2-ol	UN	1,780	1,787	1.02 ± 0.57^{a}	—	—	—
	19	(*Z*)-3,7-Dimethylocta-2,6-dienyl	UN	1,811	1,806	0.75 ± 0.32^{a}	—	—	—
	20	Hexadecan-1-ol	UN	2,370	2,379	0.54 ± 0.24^{a}	—	—	—
	21	2,4-dimethyl-Cyclohexanol	UN	1,017	1,032	—	—	—	2.91 ± 0.15^{a}
	22	2-(dodecyloxy)-Ethanol	UN	1,138	1,135	0.38 ± 0.10^{a}	—	—	—
Ketones (10)	1	Octan-3-one	1,000	1,249	1,261	—	0.57 ± 0.02^{a}	—	—
	2	Octane-2,3-dione	UN	1,321	1,325	664.12 ± 7.50^{d}	152.59 ± 9.42^{a}	257.70 ± 20.53^{b}	425.17 ± 38.29^{c}
	3	Pentane-2,3-dione	5	1,055	1,062	—	—	4.25 ± 0.45^{a}	10.06 ± 0.85^{b}
	4	3-Hydroxy-2-butanone	10,000	1,291	1,280	5.00 ± 0.11^{a}	—	—	—
	5	Tridecan-2-one	500	1,804	1,816	0.80 ± 0.28^{b}	0.20 ± 0.03^{a}	0.66 ± 0.14^{b}	—
	6	Undecan-2-one	30	1,612	1,599	—	0.55 ± 0.17^{a}	0.63 ± 0.05^{a}	1.39 ± 0.23^{b}
	7	dihydro-5-methyl-2(3H)-Furanone	UN	1,621	1,619	—	—	—	1.97 ± 0.19^{a}
	8	6-Pentyloxan-2-one	UN	2,199	2,190	—	—	0.05 ± 0.00^{a}	—
	9	(*Z*)-6,10-dimethylundeca-5,9-dien-2-one	UN	1,810	1,813	0.28 ± 0.06^{b}	0.12 ± 0.00^{a}	0.22 ± 0.00^{b}	—
	10	(3*E*,5*E*)-nona-3,5-dien-2-one	UN	1,865	1,879	—	—	0.60 ± 0.28^{a}	—
Acids (9)	1	Acetic acid	5,500	1,473	1,452	8.66 ± 0.50^{b}	2.77 ± 0.29^{a}	2.39 ± 0.80^{a}	3.74 ± 0.82^{a}
	2	Pentanoic acid	5,000	1,765	1,744	—	—	—	1.11 ± 0.06^{a}
	3	Hexanoic acid	1,500	1,833	1,849	—	6.91 ± 0.38^{a}	5.80 ± 0.87^{a}	—
	4	Heptanoic acid	3,000	1,947	1,960	1.54 ± 0.06^{c}	0.76 ± 0.12^{a}	0.55 ± 0.09^{a}	0.94 ± 0.05^{b}
	5	Octanoic acid	800	2,065	2,070	1.25 ± 0.04^{c}	0.99 ± 0.10^{b}	0.66 ± 0.04^{a}	1.09 ± 0.05^{b}
	6	Nonanoic acid	1,500	2,180	2,169	3.81 ± 0.01^{a}	—	—	3.39 ± 0.54^{a}
	7	Decanoic acid	120,000	2,265	2,279	—	0.20 ± 0.00^{a}	—	—
	8	Dodecanoic acid	UN	2,486	2,502	0.36 ± 0.05^{a}	—	—	—

(Continued)

10.3389/fnut.2022.959824

TABLE 2 Continued

Category	No.	Compounds	Threshold (43) (μg/kg)	LRI	Reference	Concentration (μg/kg)			
						Control group	−18°C/−18°C	−40°C/−18°C	−80°C/−18°C
	9	Pentadecanoic acid	UN	2,801	2,819	4.99 ± 1.71^{a}	—	—	—
Alkenes (3)	1	3,3-Dimethylhepta-1,6-diene	UN	1,459	1,450	—	0.34 ± 0.03	—	—
	2	8-Methylundec-1-ene	UN	1,198	1,124	—	—	0.19 ± 0.03^{a}	0.38 ± 0.04^{b}
	3	Styrene	120	1,260	1,254	44.86 ± 0.34^{c}	15.21 ± 1.97^{a}	18.01 ± 1.32^{a}	23.53 ± 3.51^{b}
Esters (5)	1	Oxolan-2-one	UN	1,604	1,595	—	0.27 ± 0.01^{a}	—	—
	2	Butyl prop-2-enoate	UN	1,173	1,189	5.24 ± 0.37^{a}	—	—	—
	3	Diethyl benzene-1,2-dicarboxylate	UN	2,397	2,401	20.75 ± 10.16^{b}	4.83 ± 0.51^{a}	6.10 ± 1.25^{a}	11.18 ± 2.84^{b}
	4	n-Caproic acid vinyl ester	UN	1,258	1,244	14.12 ± 1.19^{c}	8.82 ± 2.04^{a}	9.81 ± 6.17^{abc}	14.86 ± 1.41^{b}
	5	2-oxo-Nonanoic acid, methyl ester	UN	2,274	2,290	—	—	0.59 ± 0.19^{a}	1.39 ± 0.18^{b}
Heterocycles (1)	1	2-pentyl-Furan	4.8	1,237	1,235	6.75 ± 0.32^{a}	10.79 ± 0.20^{c}	7.65 ± 1.79^{ab}	7.73 ± 0.49^{b}
Others (12)	1	Phenol	5,500	2,021	2,008	—	0.55 ± 0.02^{a}	—	—
	2	Hexanamide	280	1,113	1,135	—	—	0.24 ± 0.06^{a}	0.36 ± 0.01^{b}
	3	Toluene	500	1,059	1,043	138.10 ± 38.76^{b}	—	23.23 ± 4.75^{a}	—
	4	Ethylbenzene	2205.25	1,139	1,126	—	12.05 ± 0.79^{a}	—	19.74 ± 0.33^{b}
	5	1,4-Xylene	UN	1,156	1,164	—	—	3.01 ± 0.32^{a}	—
	6	1-Methyl-4-propan-2-ylbenzene	UN	1,259	1,272	—	—	—	1.43 ± 0.26^{a}
	7	2,6-Ditert-butyl-4-methylphenol	UN	1,880	1,902	—	—	0.58 ± 0.17^{a}	0.65 ± 0.11^{a}
	8	Nonadecane	UN	275	282	—	—	0.13 ± 0.01^{a}	—
	9	Undecane	1,170	167	180	7.44 ± 0.86^{c}	—	2.15 ± 0.72^{a}	4.08 ± 0.72^{b}
	10	Dodecane	2,040	205	200	—	—	—	2.36 ± 0.25^{a}
	11	Tridecane	2,140	227	219	—	—	1.31 ± 0.28^{a}	—
	12	Tetradecane	1,000	240	236	2.49 ± 0.95^{b}	—	0.45 ± 0.08^{a}	1.95 ± 0.59^{b}

All data are expressed as the means ± standard error of triple measurements.

$^{a-d}$Means within the same line with different uppercase letters differ significantly ($P < 0.05$).

"—" represents volatile compounds not detected.

UN, relevant threshold not found.

10.3389/fnut.2022.959824

61). Among other compounds, alkanes mainly came from lipid oxidation. The contents of undecane and tetradecane were high, but their threshold was also high. Therefore, the overall flavor contribution for HGM was small. As a harmful substance, toluene mainly presented aromatic flavor.

Among the volatile flavor substances shown in Table 2, the contents of hexanal, heptanal, octanal, nonanal, benzaldehyde, (2*E*,4*E*)-deca-2,4-dienal, pentan-1-ol, hexan-1-ol, phenylmethanol, 1-octene-3-ol, (*Z*)-oct-2-en-1-ol, 2,3-octadione and undecane showed the rule of control group > −80°C/−18°C group > −40°C/−18°C group > −18°C/−18°C group ($P < 0.05$). With the increase of freezing rate, the retention of (*Z*)-2-heptanal, (*E*)-oct-2-enal, tetradecanal, butan-1-ol, octan-1-ol, nonanoic acid, styrene, diethyl benzene-1,2-dicarboxylate and toluene increased significantly ($P < 0.05$). The contents of dodecanal, heptan-1-ol, 2-ethyl- hexan-1-ol and tetradecane decreased significantly after freezing ($P < 0.05$). In addition, (2*R*,3*R*)-butane-2,3-diol, 3-methylheptan-2-ol, 4-methoxy-4-methylpentan-2-ol, (*Z*)-3,7-dimethyl-2,6-octadiene-1-ol, hexadecan-1-ol, 2-(dodecyloxy)-ethanol, 3-hydroxy-2-butanone, dodecanoic acid, pentadecanoic acid and butyl prop-2-enoate were only present in the control group and were not detected after freezing-thawing.

Part of the reason for the above results was that the water in the mutton condensed into ice crystals during freezing, and the water lost after thawing, which took away some volatile flavor substances (62, 63). Most aroma substances had high activity in aqueous liquid phase system, so they had high relative volatility. The relative volatility of volatile flavor substances relative to water determined the relative proportion of volatile components and water (64). The size of ice crystals formed by freezing water in mutton was different with different freezing rates (65). The higher the freezing rate, the smaller, more uniform and denser ice crystals would be formed in the mutton. The larger the ice crystals formed by freezing, the greater the damage to the microstructure of the mutton, resulting in serious water loss, which was also an important reason for the different degree of water loss after thawing. The change law of the thawing loss rate mentioned above was consistent with it. The increase of freezing water loss led to the loss of more volatile flavor substances, resulting in the decline of retention. Therefore, the retention and escape of water in HGM were closely related to the embedding and release of volatile flavor substances. When HGM frozen to the EP at a high rate, it could effectively curb the loss of volatile flavor substances.

In addition, the changes in the structure and properties of macromolecules (protein and fat) in mutton might also affect the retention of volatile flavor substances (65, 66). Different protein components had been proved to have different binding affinity for flavor substances. Proteins with higher contents of lysine, arginine and cysteine may show higher flavor binding ability because they involve more covalent bonds (67). Due to the differences of physicochemical properties of flavor substances and the changes of protein structure and properties caused by freezing process, such as the exposure of protein hydrophobic groups, the adsorption and binding ability of proteins to volatile flavor substances were different after freezing (67). Additionally, freezing may also destroy the interaction between protein molecules and water and lipid molecules. In the process of meat cooking, the physical crosslinking of macromolecules formed a high-density network, which inhibited the movement of water molecules and macromolecular substances and kept the whole system stable. The formation of ice crystals in the freezing process broken the stable network structure, resulting in the loss of water diversion and the change of physical and chemical properties of macromolecular substances, which aggravated the attenuation of volatile flavor substances.

Analysis of key volatile flavor compounds

The volatile flavor compounds of HGM with different freezing rates were analyzed by ROAV method. The greater the ROAV, the greater its contribution to the mutton aroma. The components with ROAV > 1 are key flavor compounds, the components with 0.1 < ROAV < 1 are modified flavor compounds, and the components with ROAV < 0.1 are potential flavor compounds (68, 69).

It can be seen from Table 3 that there were nine key odour compounds with ROAV > 1 in the volatile flavor substances produced by each group of samples, namely: hexanal, heptanal, octanal, nonanal, (*E*)-non-2-enal, (*E*)-oct-2-enal, (2*E*,4*E*)-deca-2,4-dienal, (2*E*,4*E*)-nona-2,4-dienal and 1-octene-3-ol, which is similar with other studies on mutton products (64–66). These key odour compounds included eight aldehydes and one alcohol, indicating that aldehydes played a leading role in the overall flavor of HGM. Among them, hexanal, heptanal, octanal, nonanal, (*E*)-oct-2-enal, (*E*, *E*)-2,4-decendienal and 1-octene-3-ol were detected in the four groups of samples, and their ROAVs were the highest in the control group, and all decreased significantly after frozen storage ($P < 0.05$), indicating that the aroma loss of HGM was serious after short-term frozen storage. The ROAVs of these substances were the highest in the −80°C/−18°C group ($P < 0.05$). To sum up, the retention effects of key volatile flavor compounds in HGM at three freezing rates were −80°C/−18°C group > −40°C/−18°C group > −18°C/−18°C group.

Non-volatile compounds of hand grab mutton with different freezing rates

Free amino acids analysis of hand grab mutton

Free Amino Acid (FAA) is the final product of protein degradation. It not only promotes the production of taste, but also participates in Maillard reaction to form volatile substances

TABLE 3 Information on characteristic volatile compounds of HGM with different freezing rates.

Serial number	Compounds	Threshold (μg/kg)	Control group		−18°C/−18°C		−40°C/−18°C		−80°C/−18°C	
			Concentration (μg/kg)	ROAV	Concentration (μg/kg)	ROAV	Concentration (μg/kg)	ROAV	Concentration (μg/kg)	ROAV
1	Hexanal	7.50	648.10	6.86^{d}	225.17	2.38^{a}	459.34	4.86^{b}	565.70	5.99^{c}
2	Heptanal	10.00	151.19	1.20^{d}	22.13	0.18^{a}	33.67	0.27^{b}	73.64	0.58^{c}
3	Octanal	0.10	125.94	100^{d}	21.54	17.10^{a}	36.49	28.97^{b}	55.92	44.40^{c}
4	Nonanal	3.50	250.70	5.69^{d}	40.70	0.92^{a}	52.05	1.18^{b}	135.58	3.08^{c}
5	(*E*)-Non-2-enal	0.07	—	0.00^{a}	—	0.00^{a}	0.95	1.08^{b}	—	0.00^{a}
6	(*E*)-Oct-2-enal	0.20	16.22	6.44^{c}	3.32	1.32^{a}	3.41	1.35^{a}	10.16	4.03^{b}
7	(2*E*,4*E*)-Deca-2,4-dienal	0.05	3.08	4.89^{c}	1.49	2.37^{a}	2.29	3.64^{b}	3.15	5.00^{c}
8	(2*E*,4*E*)-Nona-2,4-dienal	0.06	—	0.00^{a}	0.95	1.26^{b}	—	0.00^{a}	—	0.00^{a}
9	Oct-1-en-3-ol	2.00	295.00	11.71^{d}	117.30	4.66^{a}	153.62	6.10^{b}	195.15	7.75^{c}

$^{a-d}$Means within the same line with different uppercase letters differ significantly ($P < 0.05$).

such as aldehydes, ketones, alcohols and esters. These substances can also react with lipid oxidation products to form unique flavor (70). The composition of FAAs is not only related to the nutritional characteristics of HGM, but also closely related to its flavor characteristics. It can be seen from Table 4 that there were 16 kinds of FAA (Asp, Thr, Ser, Glu, Gly, Ala, Cys, Val, Met, Ile, Leu, Tyr, Phe, Lys, His, Arg) and 7 kinds of essential amino acids (Val, Leu, Ile, Phe, Met, Lys, Thr) in the HGM with different freezing rates. ASP and Glu were the main umami amino acids in HGM, while Gly, Ala, Ser, and Pro were the main sweet amino acids.

The total amount of FAAs in the control group was 99.88 mg/kg, and the amount in the treatment group decreased by 21.33% (−18°C/−18°C), 12.37% (−40°C/−18°C) and 5.75% (−80°C/−18°C) respectively, indicating that the sample frozen at −80°C had the highest FAA retention degree, and there was no significant difference between −80°C/−18°C and the control group ($P > 0.05$), which was directly related to the degree of water loss after thawing. After thawing, the contents of Asp, Glu, Gly, Thr, Cys, Met, Lys, Tyr, Ile, Leu, Phe, His, and Arg decreased, but the retention of these FAAs in the −80°C/−18°C group was higher, which was due to the smaller ice crystals formed by its higher freezing rate, less mechanical damage to the tissue, less water loss and less loss of free amino acids.

5′-Nucleotide analysis of hand grab mutton

Nucleotide is composed of purine base or pyrimidine base, ribose or deoxyribose and phosphoric acid. It has important physiological functions. At the same time, it is also an important taste substance of meat products, which can give meat products good umami characteristics. Taste nucleotides and L-glutamic acid have good synergy, which can significantly improve the umami characteristics of meat products and is also an important way to improve the umami of meat products in the process of meat processing (36, 44). 5'-GMP and 5'-IMP are important umami nucleotides. When used, the two substances are generally mixed in the ratio of 1:1. When their addition amount reaches more than 5% of Glu content, the umami characteristics of food can be significantly improved. In the processing of meat products, ATP forms ADP under the action of ATPase. Under the catalysis of phosphokinase, ADP is degraded to form AMP, further dehydrogenated to form IMP, and part of IMP forms I under the action of phosphokinase, and then further hydrolyzed to form Hx (41). It can be seen from Table 5 that the contents of 5′-AMP, 5′-GMP and 5′-IMP in the control group were significantly higher than those in the freezing group ($P < 0.05$), which might be taken away some taste substances due to the water loss of HGM after thawing. The contents of 5'-AMP and 5'-IMP in −40°C/−18°C group and −80°C/−18°C group were significantly higher than those in −18°C/−18°C group ($P < 0.05$), which may be the most water loss in −18°C/−18°C group.

Taste activity value and equivalent umami concentration analysis of hand grab mutton

Compounds with TAV > 1 are considered to have taste activity and contribute to the overall taste, and the greater the value is, the greater the contribution value is. TAV < 1 means there is no taste activity and no contribution to the overall taste (37, 44).

TAV is the most classical and objective method to study the taste intensity of taste substances in food and the contribution of a single component to food taste (71). It can be seen from

TABLE 4 Free amino acids of HGM with different freezing rates.

Taste attributes	Compounds	Concentrations in HGM (mg/kg)			
		Control group	−18°C/−18°C	−40°C/−18°C	−80°C/−18°C
Umami	Asp	2.47 ± 0.05^{a}	1.62 ± 0.19^{b}	1.70 ± 0.24^{b}	2.35 ± 0.12^{a}
	Glu	12.86 ± 0.55^{ab}	12.16 ± 0.30^{ab}	11.82 ± 0.97^{b}	14.13 ± 1.81^{a}
TUAA		15.33 ± 0.49^{ab}	13.78 ± 0.4^{b}	13.52 ± 0.99^{b}	16.48 ± 1.58^{a}
Sweetness	Ser	1.08 ± 0.14^{a}	0.85 ± 0.18^{a}	0.91 ± 0.09^{a}	1.10 ± 0.12^{a}
	Ala	2.82 ± 0.10^{a}	2.71 ± 0.28^{a}	2.93 ± 0.34^{a}	2.65 ± 0.06^{a}
	Gly	9.37 ± 0.05^{a}	7.92 ± 0.14^{c}	8.75 ± 0.09^{b}	9.27 ± 0.14^{a}
	Thr*	3.16 ± 0.30^{a}	1.59 ± 0.17^{b}	1.57 ± 0.05^{b}	1.82 ± 0.08^{b}
TSAA		16.43 ± 0.48^{a}	13.07 ± 0.63^{c}	14.16 ± 0.47^{bc}	14.84 ± 0.33^{b}
Bitterness	Cys	7.80 ± 0.11^{a}	5.79 ± 0.09^{b}	7.82 ± 0.15^{a}	7.87 ± 0.10^{a}
	Met*	6.83 ± 0.10^{a}	6.19 ± 0.21^{b}	6.49 ± 0.35^{ab}	6.24 ± 0.34^{b}
	Val*	5.92 ± 0.45^{a}	5.44 ± 0.21^{a}	5.72 ± 0.32^{a}	5.87 ± 0.15^{a}
	Lys*	7.49 ± 0.26^{a}	5.20 ± 0.42^{c}	5.56 ± 0.26^{c}	6.72 ± 0.27^{b}
	Tyr	11.66 ± 0.21^{a}	7.70 ± 0.13^{b}	11.95 ± 0.74^{a}	11.76 ± 0.36^{a}
	Ile*	4.77 ± 0.91^{a}	3.73 ± 0.22^{a}	4.02 ± 0.35^{a}	4.25 ± 0.17^{a}
	Leu*	5.31 ± 0.14^{a}	3.29 ± 0.07^{d}	3.76 ± 0.24^{c}	4.28 ± 0.32^{b}
	Phe*	10.74 ± 0.35^{a}	8.55 ± 0.46^{b}	8.52 ± 0.79^{b}	9.01 ± 0.16^{b}
	His	5.73 ± 0.25^{a}	4.61 ± 0.11^{b}	4.74 ± 0.19^{b}	5.40 ± 0.32^{a}
	Arg	1.87 ± 0.15^{a}	1.23 ± 0.18^{b}	1.26 ± 0.18^{b}	1.42 ± 0.20^{b}
TBAA		68.12 ± 2.39^{a}	51.73 ± 1.71^{c}	59.84 ± 2.91^{b}	62.82 ± 1.95^{ab}
EAA		44.22 ± 2.05^{a}	33.99 ± 1.44^{c}	35.64 ± 1.93^{bc}	38.19 ± 1.22^{b}
TFAA		99.88 ± 3.36^{a}	78.58 ± 2.74^{c}	87.52 ± 4.37^{b}	94.14 ± 3.85^{ab}

$^{a-d}$Means within the same line with different uppercase letters differ significantly ($P < 0.05$).

*Represents essential amino acid.

TUAA, total umami amino acid; TSAA, total sweet amino acid; TBAA, total bitter amino acid; EAA, essential amino acid; TFAA, total free amino acid; Asp, aspartic acid; Glu, glutamic acid; Ser, Serine; Ala, Alanine; Gly, glycine; Thr, threonine; Cys, cysteine; Met, methionine; Val, valine; Lys, lysine; Tyr, tyrosine; Ile, isoleucine; Leu, leucine; Phe, phenylalanine; His, hlstidine; Arg, argnine.

TABLE 5 Taste nucleotides of HGM with different freezing rates.

Taste substances	Taste attributes	Control group	−18°C/−18°C	−40°C/−18°C	−80°C/−18°C
5′-AMP	Umami	13.22 ± 0.34^{a}	10.77 ± 0.34^{c}	11.99 ± 0.66^{b}	12.19 ± 0.44^{b}
5′-GMP		16.01 ± 0.77^{a}	14.83 ± 0.23^{b}	15.06 ± 0.27^{ab}	15.18 ± 0.49^{ab}
5′-IMP		39.54 ± 0.37^{a}	24.80 ± 0.39^{d}	36.56 ± 0.09^{c}	37.78 ± 0.07^{b}
Total		68.77 ± 1.21^{a}	50.40 ± 0.78^{c}	63.61 ± 0.83^{b}	65.15 ± 0.82^{b}

$^{a-d}$Means within the same line with different uppercase letters differ significantly ($P < 0.05$).

Table 6 that the TAVs calculated by all taste substances in HGM with different freezing rates were far <1. Therefore, the direct contribution of these substances to the taste of HGM was not significant. However, these taste substances can contribute to the overall flavor of HGM through synergistic effect. For example, 5'-IMP could cooperate with other free amino acids and taste nucleotides. Misako et al. (72) found that although the TAVs of amino acids and other nucleotides were <1, they could cooperate with 5'-IMP to give food strong umami. Lioe et al. (73) found that bitter amino acids below the taste threshold could enhance the freshness and sweetness of other amino acids. For example, Arg could work synergistically with NaCl and Glu to provide a pleasant overall taste. Phe and Tyr were aromatic amino acids with bitter taste, but they had been found to be important flavor components in soy sauce except Glu. Additionally, studies have shown that ASP can also act in synergy with NaCl alone (74). Chen et al. (75) studied the non-volatile taste active substances in Chinese mitten crab

TABLE 6 TAVs of HGM with different freezing rates.

Taste substances	Threshold (mg/kg)	Control group		−18°C/-18°C		−40°C/-18°C		−80°C/-18°C	
		Content	TAV	Content	TAV	Content	TAV	Content	TAV
Asp	1,000	2.47	< 0.01	1.62	< 0.01	1.70	<0.01	2.35	<0.01
Glu	300	12.86	0.04	12.16	0.04	11.82	0.04	14.13	0.05
Ser	1,500	1.08	< 0.01	0.85	<0.01	0.91	<0.01	1.10	<0.01
Ala	600	2.82	< 0.01	2.71	<0.01	2.93	<0.01	2.65	<0.01
Gly	1,300	9.37	< 0.01	7.92	<0.01	8.75	<0.01	9.27	<0.01
Thr	2,600	3.16	< 0.01	1.59	<0.01	1.57	<0.01	1.82	<0.01
Cys	N	7.80	-	5.79	-	7.82	-	7.87	-
Met	300	6.83	0.02	6.19	0.02	6.49	0.02	6.24	0.02
Val	400	5.92	0.01	5.44	0.01	5.72	0.01	5.87	0.01
Lys	500	7.49	0.01	5.20	0.01	5.56	<0.01	6.72	0.01
Tyr	910	11.66	0.01	7.70	0.01	11.95	0.01	11.76	0.01
Ile	900	4.77	0.01	3.73	<0.01	4.02	<0.01	4.25	<0.01
Leu	1,900	5.31	<0.01	3.29	<0.01	3.76	<0.01	4.28	<0.01
Phe	900	10.74	0.01	8.55	0.01	8.52	0.01	9.01	0.01
His	200	5.73	0.03	4.61	0.02	4.74	0.02	5.40	0.03
Arg	500	1.87	<0.01	1.23	<0.01	1.26	< 0.01	1.42	<0.01
5′-AMP	500	13.22	0.03	10.77	0.02	11.99	0.02	12.19	0.02
5′-GMP	125	16.01	0.13	14.83	0.12	15.06	0.12	15.18	0.12
5′-IMP	140	39.54	0.28	24.80	0.18	36.56	0.26	37.78	0.27

TABLE 7 EUC of HGM with different freezing rates.

Sample	Control group	−18°C/-18°C	−40°C/-18°C	−80°C/-18°C
EUC (g MSG/100 g)	4.80	3.19	3.94	4.22

meat. Because the concentrations of other amino acids in crab meat were significantly lower than the corresponding taste detection threshold, it was speculated that some amino acids interacted with each other at their sub-threshold concentration to enhance the freshness and sweetness. Due to the loss of taste substances after freezing and thawing, the TAVs of the treatment groups also showed a general downward trend, and the TAVs of taste substances in samples with high freezing rate was also high.

As shown in Table 7, the EUC of the four groups of samples was between 3.19 and 4.80 g MSG/100 g, which was much higher than the freshness threshold of MSG (30 mg/100 g). The EUC of the control group was higher than that of each treatment group. In the treatment group, the EUC of −80°C/−18°C group was the highest and the EUC value of −18°C/−18°C group was the lowest, which was jointly determined by the content of umami substances left in the mutton after thawing. Because taste nucleotides could play a synergistic role in enhancing freshness at a very low content, after thawing, the content of fresh substances in HGM was significantly reduced, and the EUC of the product was significantly reduced, which was also the reason why the EUC of the control group was significantly higher than that of the freezing group.

Most researchers focused on umami taste in the research of meat products, free amino acids and nucleotides are important taste related compounds in meat products (76, 77). In this study, the calculation of EUC only covered the influence of umami amino acids and 5'-nucleotides on the umami of the samples. In recent years, a series of structurally diverse umami compounds have been discovered and identified, including free L-amino acids, purine nucleotides, peptides, organic acids, amides, and their derivatives (78). Umami peptides can supplement and enhance the overall taste of food, making it more harmonious, soft, and full-bodied (79, 80). In meat products, many small molecular umami peptides have been characterized and identified recently, and they also played a significant role in the overall umami of meat products (76, 77).

TABLE 8 Sensory evaluation of HGM with different freezing rates.

Sample	Aroma	Umami	Juiciness	Overall acceptability
Control group	6.37 ± 0.52^{a}	5.22 ± 0.25^{a}	5.19 ± 0.41^{a}	5.95 ± 0.63^{a}
−18°C/−18°C	2.42 ± 0.85^{c}	1.97 ± 0.49^{d}	3.89 ± 0.98^{b}	2.63 ± 0.59^{b}
−40°C/−18°C	3.06 ± 0.54^{c}	3.60 ± 0.12^{c}	4.87 ± 0.75^{a}	3.41 ± 0.20^{b}
−80°C/−18°C	4.90 ± 0.81^{b}	4.33 ± 0.40^{b}	4.74 ± 0.26^{a}	4.80 ± 0.92^{a}

$^{a-d}$Means within the same raw with different uppercase letters differ significantly ($P < 0.05$).

In particular, the raw material of HGM was ribs. As one of the main components of rib, the bones might release small molecular peptides into muscle during cooking, thus affecting the umami of the samples (77).

Sensory evaluation

The sensory panel analysis of the HGM is shown in Table 8. The control group had the highest sensory evaluation scores. The −80°C/−18°C sample had higher aroma scores than the other samples ($P < 0.05$). The sensory evaluation results for aroma were in accordance with the results of volatile flavor compound concentrations and the ROAVs of key volatile flavor compounds. The umami scores of the samples showed −80°C/−18°C > −40°C/−18°C > −18°C/−18°C ($P < 0.05$). The −80°C/−18°C sample was more acceptable than lower rate frozen samples ($P < 0.05$). The −18°C/−18°C sample had lower juiciness scores than the other samples ($P < 0.05$). The results of juiciness scores were in accordance with the results of thawing loss. Notably, the −80°C/−18°C sample had the highest overall acceptability ($P < 0.05$), which indicates that the sample with higher freezing rate had higher sensory acceptability.

Conclusion

In this study, the contents of volatile compounds in high-speed frozen HGM (−80°C/−18°C group) were significantly higher than that in low-speed frozen HGM (−40°C/−18°C and −18°C/−18°C group), especially aldehydes, alcohols and ketones. For the −80°C/−18°C group, most key odor compounds had the highest ROAVs, indicating that the high freezing rate retained the typical aroma of HGM to the greatest extent. HGM samples were clearly divided into four groups, which indicated that there were significant differences in volatile composition of four groups of HGM samples. The contents of TFAAs, TSAAs, TBAAs and 5'-nucleotides in −80°C/−18°C group were significantly higher than those in −40°C/−18°C group and −18°C/−18°C group. At the same time, −80°C/−18°C group had the highest freshness due to the highest EUC. It can be concluded that the HGM frozen at a high rate (−80°C/−18°C) had the best flavor fidelity effect after short-term freezing, which was closest to fresh HGM and conducive to the fidelity of HGM flavor.

Data availability statement

The original contributions presented in the study are included in the article/supplementary material, further inquiries can be directed to the corresponding author.

Author contributions

Y-ZB: conceptualization, formal analysis, investigation, and writing–original draft preparation. Y-LL: validation and supervision. R-ML: supervision, project administration, and funding acquisition. CJ: writing–review and editing. SG: investigation and formal analysis. SB: methodology and resources. Y-RW: methodology and resources. F-JD: writing–review and editing. X-LH: visualization, software, and data curation. J-JG: investigation and formal analysis. All authors contributed to the article and approved the submitted version.

Funding

This study was financially supported by the State Key Research and Development Plan Modern Food Processing and Food Storage and Transportation Technology and Equipment (2018YFD0400101).

Conflict of interest

The authors declare that the research was conducted in the absence of any commercial or financial relationships that could be construed as a potential conflict of interest.

Publisher's note

References

1. Wang B, Zhao XG, Zhang BY, Cui YM, Nueraihemaiti M, Kou QF, et al. Assessment of components related to flavor and taste in Tan-lamb meat under different silage-feeding regimens using integrative metabolomics. *Food Chem X.* (2022) 14:100269. doi: 10.1016/j.fochx.2022.100269

2. Jia W, Wu XX, Li RT, Liu SX, Shi L. Effect of Nisin and potassium sorbate additions on lipids and nutritional quality of Tan sheep meat. *Food Chem.* (2021) 365:130535. doi: 10.1016/j.foodchem.2021.130535

3. Jia XT, Li J, Li S, Zhao QY, Zhang K, Tang CH, et al. Effects of dietary supplementation with different levels of selenium yeast on growth performance, carcass characteristics, antioxidant capacity, and meat quality of Tan sheep. *Livest Sci.* (2021) 255:104783. doi: 10.1016/j.livsci.2021.104783

4. Gao XG, Wang ZY, Miao J, Xie L, Dai Y, Li XM, et al. Influence of different production strategies on the stability of color, oxygen consumption and metmyoglobin reducing activity of meat from Ningxia Tan sheep. *Meat Sci.* (2014) 96(2pt.A):769–74. doi: 10.1016/j.meatsci.2013.09.026

5. Gustavo VC, Ilce MM, Kezban C, Daniela BA. Advanced retorting, microwave assisted thermal sterilization (mats), and pressure assisted thermal sterilization (pats) to process meat products. *Meat Sci.* (2014) 98:420–34. doi: 10.1016/j.meatsci.2014.06.027

6. Wang QB, Zhang M, Adhikari B, Cao P, Yang CH. Effects of various thermal processing methods on the shelf-life and product quality of vacuum-packaged braised beef. *J Food Process Eng.* (2019) 42:e13035. doi: 10.1111/jfpe.13035

7. Luan CN, Zhang M, Fan K, Devahastin S. Effective pretreatment technologies for fresh foods aimed for use in central kitchen processing. *J Sci Food Agr.* (2021) 101:347–63. doi: 10.1002/jsfa.10602

8. Liu B, Zhang M, Sun YN, Wang YC. Current intelligent segmentation and cooking technology in the central kitchen food processing. *J Food Process Eng.* (2019) 42:e13149. doi: 10.1111/jfpe.13149

9. Qi CH. Establish central kitchen under HACCP control in food and beverage industry to ensure food safety and hygiene. *S Web Con.* (2014) 6:8. doi: 10.1051/shsconf/20140603005

10. Lun N, Ma J, Sun DW. Enhancing physical and chemical quality attributes of frozen meat and meat products: mechanisms, techniques and applications. *Trends Food Sci Tech.* (2022) 124:63–85. doi: 10.1016/j.tifs.2022.04.004

11. Leygonie C, Britz TJ, Hoffman LC. Impact of freezing and thawing on the quality of meat: review. *Meat Sci.* (2012) 91:93–8. doi: 10.1016/j.meatsci.2012.01.013

12. Sanz PD, Otero L. High-pressure freezing. *Emerg Technol Food Process.* (2005) 627–52. doi: 10.1016/B978-012676757-5/50026-8

13. Cheng LN, Sun DW, Zhu ZW, Zhang Z. Emerging techniques for assisting and accelerating food freezing processes-a review of recent research progresses. *Crit Rev Food Sci.* (2015) 57:769–81. doi: 10.1080/10408398.2015.1004569

14. Zhan XM, Sun DW, Zhu ZW, Wang QJ. Improving the quality and safety of frozen muscle foods by emerging freezing technologies: a review. *Crit Rev Food Sci.* (2018) 58:2925–38. doi: 10.1080/10408398.2017.1345854

15. Mohsen DI, Nasser H, Epameinondas X, Alain LB. Review on the control of ice nucleation by ultrasound waves, electric and magnetic fields. *J Food Eng.* (2017) 195:222–34. doi: 10.1016/j.jfoodeng.2016.10.001

16. Zaritzky NE. 20-Chemical and physical deterioration of frozen foods. *Chem Deteriorat Phys Instab Food Beverages.* (2010) 561–607. doi: 10.1533/9781845699260.3.561

17. Ma Y, Wu S, Meng XJ, Liu WW. Manufacturing research with key applied technology in vacuum freeze-drying leisure meat processing. *Adv Material Res.* (2014) 1056:88–91. doi: 10.4028/www.scientific.net/AMR.1056.88

18. Ma Y, Wu XZ, Zhang Q, Giovanni V, Meng XJ. Key composition optimization of meat processed protein source by vacuum freeze-drying technology. *Saudi J Biol Sci.* (2018) 25:724–32. doi: 10.1016/j.sjbs.2017.09.013

19. Tuell JR, Seo JK, Kim YHB. Combined impacts of initial freezing rate of pork leg muscles (*M. biceps femoris* and *M. semitendinosus*) and subsequent freezing on quality characteristics of pork patties. *Meat Sci.* (2020) 170:108248. doi: 10.1016/j.meatsci.2020.108248

20. Kim YHB, Liesse C, Kemp R, Balan P. Evaluation of combined effects of ageing period and freezing rate on quality attributes of beef loins. *Meat Sci.* (2015) 110:40–5. doi: 10.1016/j.meatsci.2015.06.015

21. Kim HW, Kim JH, Seo JK, Setyabrata D, Kim YHB. Effects of aging/freezing sequence and freezing rate on meat quality and oxidative stability of pork loins. *Meat Sci.* (2018) 139:162–70. doi: 10.1016/j.meatsci.2018.01.024

22. Zhang MC, Niu HL, Chen Q, Xia XF, Kong BH. Influence of ultrasound-assisted immersion freezing on the freezing rate and quality of porcine longissimus muscles. *Meat Sci.* (2018) 136:1–8. doi: 10.1016/j.meatsci.2017.10.005

23. Bueno M, Resconi VC, Campo MM, Cacho J, Ferreira V, Escudero A. Effect of freezing method and frozen storage duration on odor-active compounds and sensory perception of lamb. *Food Res Int.* (2013) 54:772–80. doi: 10.1016/j.foodres.2013.08.003

24. Seetapan N, Limparyoon N, Gamonpilas C, Methacanon P, Fuongfuchat A. Effect of cryogenic freezing on textural properties and microstructure of rice flour/tapioca starch blend gel. *J Food Eng.* (2015) 151:51–9. doi: 10.1016/j.jfoodeng.2014.11.025

25. Gao LH, Liu T, An XJ, Zhang JL, Ma XR, Cui JM. Analysis of volatile flavor compounds influencing Chinese-type soy sauces using GC–MS combined with HS-SPME and discrimination with electronic nose. *J Food Sci Technol.* (2017) 54:130–43. doi: 10.1007/s13197-016-2444-0

26. Shi J, Nian YQ, Da DD, Xu XL, Zhou GH, Zhao D, et al. Characterization of flavor volatile compounds in sauce spareribs by gas chromatography–mass spectrometry and electronic nose. *LWT-Food Sci Technol.* (2020) 124:109182. doi: 10.1016/j.lwt.2020.109182

27. Zhang JH, Cao J, Pei ZS, Wei PY, Xiang D, Cao XY, et al. Volatile flavour components and the mechanisms underlying their production in golden pompano (*Trachinotus blochii*) fillets subjected to different drying methods: a comparative study using an electronic nose, an electronic tongue and SDE-GC-MS. *Food Res Int.* (2019) 123:217–25. doi: 10.1016/j.foodres.2019.04.069

28. Men H, Shi Y, Fu SL, Jiao YN, Qiao Y, Liu JJ. Discrimination of beer based on E-tongue and E-nose combined with SVM: comparison of different variable selection methods by PCA, GA-PLS and VIP. (2017). doi: 10.20944/preprints201705.0054.v1

29. Zhang L, Hu YY, Wang Y, Kong BH, Chen Q. Evaluation of the flavour properties of cooked chicken drumsticks as affected by sugar smoking times using an electronic nose, electronic tongue, and HS-SPME/GC-MS. *LWT-Food Sci Technol.* (2020) 140:110764. doi: 10.1016/j.lwt.2020.110764

30. Yin XY, Lv YC, Wen RX, Wang Y, Chen Q, Kong BH. Characterization of selected Harbin red sausages on the basis of their flavour profiles using HS-SPME-GC/MS combined with electronic nose and electronic tongue. *Meat Sci.* (2021) 172:108345. doi: 10.1016/j.meatsci.2020.108345

31. Marušić N, Petrović M, Vidaček S, Petrak T, Medić H. Characterization of traditional Istrian dry-cured ham by means of physical and chemical analyses and volatile compounds. *Meat Sci.* (2011) 88:786–90. doi: 10.1016/j.meatsci.2011.02.033

32. Jin GF, He LC, Li CL, Zhao YH, Chen C, Zhang YH, et al. Effect of pulsed pressure-assisted brining on lipid oxidation and volatiles development in pork bacon during salting and drying-ripening. *LWT-Food Sci Technol.* (2015) 64:1099–106. doi: 10.1016/j.lwt.2015.07.016

33. Wen RX, Hu YY, Zhang L, Wang Y, Chen Q, Kong BH. Effect of NaCl substitutes on lipid and protein oxidation and flavor development of Harbin dry sausage. *Meat Sci.* (2019) 156:33–43. doi: 10.1016/j.meatsci.2019.05.011

34. Zhuang KJ, Wu N, Wang XC, Wu XG, Wang S, Long XW, et al. Effects of 3 feeding modes on the volatile and nonvolatile compounds in the edible tissues of female Chinese mitten crab (*Eriocheir sinensis*). *J Food Sci.* (2016) 81:S968–81. doi: 10.1111/1750-3841.13229

35. Su D, He JJ, Zhou YZ, Li YL, Zhou HJ. Aroma effects of key volatile compounds in Keemun black tea at different grades: HS-SPME-GC-MS, sensory evaluation, and chemometrics. *Food Chem.* (2021) 373(pt.B):131587. doi: 10.1016/j.foodchem.2021.131587

36. Li H, Li X, Zhang CH, Wang JZ, Tang CH, Chen LL. Flavor compounds and sensory profiles of a novel Chinese marinated chicken. *J Sci Food Agr.* (2016) 96:1618–26. doi: 10.1002/jsfa.7263

37. Li R, Sun ZL, Zhao YQ, Li LH, Yang XQ, Chen SJ, et al. Effect of different thermal processing methods on water-soluble taste substances of tilapia fillets. *J Food Compos Anal.* (2022) 106:104298. doi: 10.1016/j.jfca.2021.104298

38. Liu DY, Li SJ, Wang N, Deng YJ, Sha L, Gai SM, et al. Evolution of taste compounds of Dezhou-braised chicken during cooking evaluated by chemical analysis and an electronic tongue system. *J Food Sci.* (2017) 82:1076–82. doi: 10.1111/1750-3841.13693

39. Liu TT, Xia N, Wang QZ, Chen DW. Identification of the non-volatile taste-active components in crab sauce. *Foods.* (2019) 8:324. doi: 10.3390/foods8080324

40. Liu Y, Xu XL, Zhou GH. Changes in taste compounds of duck during processing. *Food Chem.* (2007) 102:22–6. doi: 10.1016/j.foodchem.2006.03.034

41. Zhu WH, Luan HW, Bu Y, Li JR, Li XP, Zhang YY, et al. Changes in taste substances during fermentation of fish sauce and the correlation with

protease activity. *Food Res Int.* (2021) 144:110349. doi: 10.1016/j.foodres.2021.110349

42. Zhou CY, Bai Y, Wang C, Li CB, Xu XL, Zhou GH, et al. 1H NMR-based metabolomics and sensory evaluation characterize taste substances of Jinhua ham with traditional and modern processing procedures. *Food Control.* (2021) 126:107873. doi: 10.1016/j.foodcont.2021.107873

43. Han D, Zhang CH, Fauconnier ML, Jia W, Wang JF, Hu FF, et al. Characterization and comparison of flavor compounds in stewed pork with different processing methods credit authorship contribution statement. *LWT-Food Sci Technol.* (2021) 144:111229. doi: 10.1016/j.lwt.2021.111229

44. Zou YH, Kang DC, Liu R, Qi J, Zhou GH, Zhang WG. Effects of ultrasonic assisted cooking on the chemical profiles of taste and flavor of spiced beef. *Ultrason Sonochem.* (2018) 46:36–45. doi: 10.1016/j.ultsonch.2018.04.005

45. Bai S, Wang YR, Luo RM, Shen F, Ding D, Bai H. Formation of flavor volatile compounds at different processing stages of household stir-frying mutton sao zi in the northwest of China. *LWT.* (2021) 139:110735. doi: 10.1016/j.lwt.2020.110735

46. Jeremiah LE. Freezing effects of food quality. *Ciencia Techol Alime.* (1996) 72:520.

47. Karabasanavar NS, Singh SP, Kumar D, Shebannavar SN. Development and application of highly specific PCR for detection of chicken (*Gallus gallus*) meat adulteration. *Eur Food Res Technol.* (2013) 236:129–34. doi: 10.1007/s00217-012-1868-7

48. Huang XH, Qi LB, Fu BS, Chen ZH, Zhang YY, Du M, et al. Flavor formation in different production steps during the processing of cold-smoked Spanish mackerel. *Food Chem.* (2019) 286:241–9. doi: 10.1016/j.foodchem.2019.01.211

49. Suleman R, Wang ZY, Aadil RM, Hui T, Hopkins DL, Zhang DQ. Effect of cooking on the nutritive quality, sensory properties and safety of lamb meat: current challenges and future prospects. *Meat Sci.* (2020) 167:108172. doi: 10.1016/j.meatsci.2020.108172

50. Thakeow P, Sergio A, Bernhard W, Schütz S. Antennal and behavioral responses of *cis boleti* to fungal odor of *Trametes gibbosa*. *Chem Senses.* (2008) 33:379–87. doi: 10.1093/chemse/bjn005

51. Liu H, Hui T, Fang F, Li SB, Wang ZY, Zhang DQ. The formation of key aroma compounds in roasted mutton during the traditional charcoal process. *Meat Sci.* (2021) 184:108689. doi: 10.1016/j.meatsci.2021.108689

52. Giri A, Osako K, Ohshima T. Identification and characterisation of headspace volatiles of fish *miso*, a Japanese fish meat based fermented paste, with special emphasis on effect of fish species and meat washing. *Food Chem.* (2010) 120:621–31. doi: 10.1016/j.foodchem.2009.10.036

53. Wang Q, Li L, Ding W, Zhang DQ, Wang JY, Reed K, et al. Adulterant identification in mutton by electronic nose and gas chromatography-mass spectrometer. *Food Control.* (2018) 98:431–8. doi: 10.1016/j.foodcont.2018.11.038

54. Bueno M, Campo MM, Cacho J, Ferreira V, Escudero A. A model explaining and predicting lamb flavour from the aroma-active chemical compounds released upon grilling light lamb loins. *Meat Sci.* (2014) 98:622–8. doi: 10.1016/j.meatsci.2014.06.019

55. Zhang M, Chen X, Hayat K, Duhoranimana E, Zhang XM, Xia SQ, et al. Characterization of odor-active compounds of chicken broth and improved flavor by thermal modulation in electrical stewpots. *Food Res Int.* (2018) 109:72–81. doi: 10.1016/j.foodres.2018.04.036

56. Timón ML, Ventanas J, Carrapiso AI. Subcutaneous and intermuscular fat characterisation of dry-cured Iberian hams. *Meat Sci.* (2001) 58:85–91. doi: 10.1016/S0309-1740(00)00136-4

57. Andres AI, Cava R, Ventanas S, Muriel E, Ruiz J. Effect of salt content and processing conditions on volatile compounds formation throughout the ripening of Iberian ham. *Eur Food Res Technol.* (2007) 225:677–84. doi: 10.1007/s00217-006-0465-z

58. Song SP, Zhang XM, Hayat K, Liu P, Jia CS, Xia SP, et al. Formation of the beef flavour precursors and their correlation with chemical parameters during the controlled thermal oxidation of tallow. *Food Chem.* (2011) 124:203–9. doi: 10.1016/j.foodchem.2010.06.010

59. Casaburi A, Filippis F D, Villani F, Ercolini D. Activities of strains of *Brochothrix thermosphacta in vitro* and in meat. *Food Res Int.* (2014) 62:366–74. doi: 10.1016/j.foodres.2014.03.019

60. Boekel MV. Formation of flavour compounds in the Maillard reaction. *Biotechnol Adv.* (2006) 24:230–3. doi: 10.1016/j.biotechadv.2005.11.004

61. Martín A, Córdoba JJ, Aranda E, Córdoba MG, Asensio MA. Contribution of a selected fungal population to the volatile compounds on dry-cured ham. *Int J Food Michobiol.* (2006) 110:8–18. doi: 10.1016/j.ijfoodmicro.2006.01.031

62. Zhang MC, Xia XF, Liu Q, Chen Q, Kong, B. Changes in microstructure, quality and water distribution of porcine longissimus muscles subjected to ultrasound-assisted immersion freezing during frozen storage. *Meat Sci.* (2019) 151:24–32. doi: 10.1016/j.meatsci.2019.01.002

63. Roos KB. Effect of texture and microstructure on flavour retention and release. *Int Dairy J.* (2003) 13:593–605. doi: 10.1016/S0958-6946(03)00108-0

64. Kluth IK, Teuteberg V, Ploetz M, Krischek C. Effects of freezing temperatures and storage times on the quality and safety of raw turkey meat and sausage products. *Poultry Sci.* (2021) 100:101305. doi: 10.1016/j.psj.2021.101305

65. Guichard E. Flavour retention and release from protein solutions. *Biotechnol Adv.* (2006) 24:226–9. doi: 10.1016/j.biotechadv.2005.11.003

66. Xiang XL, Liu YY, Liu Y, Wang XY, Jin YG. Changes in structure and flavor of egg yolk gel induced by lipid migration under heating. *Food Hydrocolloid.* (2019) 98:105257. doi: 10.1016/j.foodhyd.2019.105257

67. Guo ZW, Teng F, Huang ZX, Lv B, Lv XQ, Babich O, et al. Effects of material characteristics on the structural characteristics and flavor substances retention of meat analogs. *Food Hydrocolloid.* (2020) 105:105752. doi: 10.1016/j.foodhyd.2020.105752

68. Zhang HY, Huang D, Pu DD, Zhang YY, Chen HT Sun BG, et al. Multivariate relationships among sensory attributes and volatile components in commercial dry porcini mushrooms (*Boletus edulis*). *Food Res Int.* (2020) 133:109112. doi: 10.1016/j.foodres.2020.109112

69. Fan Y, Liu W, Xu F, Huang YJ, Zhang NN, Li K, et al. Comparative flavor analysis of eight varieties of Xinjiang flatbreads from the Xinjiang region of China. *Cereal Chem.* (2019) 96:1022–35. doi: 10.1002/cche.10207

70. Guo J, Wang Q, Chen CG, Yu H, Xu BC. Effects of different smoking methods on sensory properties, free amino acids and volatile compounds in bacon. *J Sci Food Agr.* (2020) 101:2984–93. doi: 10.1002/jsfa.10931

71. Bertram HC, Purslow PP, Andersen HJ. Relationship between meat structure, water mobility, and distribution: a low-field nuclear magnetic resonance study. *J Agr Food Chem.* (2002) 50:824–9. doi: 10.1021/jf010738f

72. Kawai M, Okiyama A, Ueda Y. Taste enhancements between various amino acids and IMP. *Chem Senses.* (2002) 27:739–45. doi: 10.1093/chemse/27.8.739

73. Lioe HN, Apriyantono A, Takara K, Wada K, Yasuda M. Umami taste enhancement of MSG/NaCl mixtures by subthreshold L-α-aromatic amino acids. *J Food Sci.* (2006) 70:s401–5. doi: 10.1111/j.1365-2621.2005.tb11483.x

74. Huang Y, Pu DD, Hao ZL, Liang L, Zhao J, Tang YZ, et al. Characterization of taste compounds and sensory evaluation of soup cooked with sheep tail fat and prickly ash. *Food Chem.* (2022) 11:896. doi: 10.3390/foods11070896

75. Chen DW, Zhang M. Non-volatile taste active compounds in the meat of Chinese mitten crab (*Eriocheir sinensis*). *Food Chem.* (2007) 104:1200–5. doi: 10.1016/j.foodchem.2007.01.042

76. Liang L, Duan W, Zhang JC, Huang Y, Zhang YY, Sun BG. Characterization and molecular docking study of taste peptides from chicken soup by sensory analysis combined with nano-LC-Q-TOF-MS/MS. *Food Chem.* (2022) 383:132455. doi: 10.1016/j.foodchem.2022.132455

77. Liang L, Zhou CC, Zhang JC, Huang Y, Zhao J, Sun BG, et al. Characteristics of umami peptides identified from porcine bone soup and molecular docking to the taste receptor T1R1/T1R3. *Food Chem.* (2022) 387:132870. doi: 10.1016/j.foodchem.2022.132870

78. Zhu WH, Luan HW, Bu Y, Li XP, Li JR, Zhang YY. Identification, taste characterization and molecular docking study of novel umami peptides from the Chinese Anchovy Sauce. *J Sci Food Agr.* (2021) 101:3140–55. doi: 10.1002/jsfa.10943

79. Zhang LL, Duan W, Huang Y, Zhang YY, Sun BG, Pu DD, et al. Sensory taste properties of chicken (Hy-Line brown) soup as prepared with five different parts of the chicken. *Int J Food Prop.* (2020) 23:1804–24. doi: 10.1080/10942912.2020.1828455

80. Wang WL, Zhou XR, Liu Y. Characterization and evaluation of umami taste: a review. *Trac-Trend Anal Chem.* (2020) 127:115876. doi: 10.1016/j.trac.2020.115876

81. Qi SS, Wang P, Zhan P, Tian HL. Characterization of key aroma compounds in stewed mutton (goat meat) added with thyme (*Thymus vulgaris* L.) based on the combination of instrumental analysis and sensory verification. *Food Chem.* (2022) 371:131111. doi: 10.1016/j.foodchem.2021.131111

82. Liu H, Hui T, Fang F, Ma QL, Li SB, Zhang DQ, et al. Characterization and discrimination of key aroma compounds in pre- and postrigor roasted mutton by GC-O-MS, GC E-nose and aroma recombination experiments. *Foods.* (2021) 10:2387. doi: 10.3390/foods10102387

83. Gemert L. *Compilations of Flavour Threshold Values in Water and Other Media (Second Enlarged and Revised Edition)*. Oliemans, punter and Partners BV (2015).

84. Kong Y, Zhang LL, Sun Y, Zhang YY, Sun BG, Chen HT. Determination of the free amino acid, organic acid, and nucleotide in commercial vinegars. *J of Food Sci.* (2017) 82:1116–23. doi: 10.1111/1750-3841.13696

frontiers | Frontiers in Nutrition

TYPE Original Research
PUBLISHED 03 August 2022
DOI 10.3389/fnut.2022.945144

OPEN ACCESS

EDITED BY
Yanyan Zhang,
University of Hohenheim, Germany

REVIEWED BY
Ashu Gulati,
Council of Scientific and Industrial Research (CSIR), India
Baocai Xu,
Hefei University of Technology, China
Mustafa Kiralan,
Balıkesir University, Turkey

*CORRESPONDENCE
Xiaoxia Su
suxiaoxia@cofco.com
Jihong Wu
wjhcau@hotmail.com

SPECIALTY SECTION
This article was submitted to Food Chemistry, a section of the journal Frontiers in Nutrition

RECEIVED 16 May 2022
ACCEPTED 01 July 2022
PUBLISHED 03 August 2022

CITATION
Guo F, Ma M, Yu M, Bian Q, Hui J, Pan X, Su X and Wu J (2022) Classification of chinese fragrant rapeseed oil based on sensory evaluation and gas chromatography-olfactometry. *Front. Nutr.* 9:945144. doi: 10.3389/fnut.2022.945144

Classification of chinese fragrant rapeseed oil based on sensory evaluation and gas chromatography-olfactometry

Fei Guo[1,2], Mingjuan Ma[2,3,4], Miao Yu[2,3,4], Qi Bian[2,3,4], Ju Hui[2,3,4], Xin Pan[1], Xiaoxia Su[2,3,4]* and Jihong Wu[1,5,6,7]*

[1]College of Food Science and Nutritional Engineering, China Agricultural University, Beijing, China, [2]COFCO Nutrition and Health Research Institute Co., Ltd., Beijing, China, [3]Beijing Key Laboratory of Nutrition & Health and Food Safety, Beijing, China, [4]Beijing Engineering Laboratory for Geriatric Nutrition Food Research, Beijing, China, [5]National Engineering Research Center for Fruit and Vegetable Processing, Beijing, China, [6]Key Laboratory of Fruit and Vegetable Processing, Ministry of Agriculture, Beijing, China, [7]Beijing Key Laboratory for Food Non-thermal Processing, Beijing, China

Fragrant rapeseed oils and traditional pressed oils are increasingly popular in China owing to their sensory advantages. Many fragrant rapeseed oils are labeled by different fragrance types; however, the scientific basis for these differences is lacking. To identify the distinctive aroma and achieve fragrance classification, the sensory characteristics and aroma components of nine different fragrant rapeseed oils were analyzed *via* sensory evaluation and gas-chromatography-mass spectrometry-olfactometry. A total of 35 aroma compounds were found to contribute to the overall aroma. By using chemometrics methods, rapeseed oils were categorized into three fragrance styles: "strong fragrance," "umami fragrance," and "delicate fragrance." In total, 10 aroma compounds were predicted to be the most effective compounds for distinguishing sensory characteristics of fragrant rapeseed oil. According to our results, this approach has excellent potential for the fragrance classification and quality control of rapeseed oil.

KEYWORDS

fragrant rapeseed oil, fragrance styles, sensory evaluation, gas chromatography-olfactometry, chemometrics methods

Introduction

Rapeseed, a traditional cash crop, is usually processed through roasting, screw pressing, and filtration to obtain edible oil in China. Fragrant rapeseed oil is a traditional pressing oil employed in China. According to the Chinese standard, pressing rapeseed oil is defined as a fragrant-pressing rapeseed oil that is prepared by roasting and squeezing rapeseed without the addition of other spices. The traditional processing of fragrant-pressing rapeseed oil is shown in Supplementary Figure S1. The consumption of fragrant rapeseed oil reached ~1.5 million tons (amounting to ~US 1.6 billion dollars) and has continued to increase (1). The aroma characteristics are the main driving factors of consumption, in terms of consumer preferences. Therefore, numerous products are being labeled with specific aroma advantages. However, a scientific basis is lacking to support these labels, ultimately creating chaos.

Sensory evaluation can be performed to quantify the intensity of a product's sensory characteristics. In fact, a sensory evaluation can effectively reflect the final aroma presented by a combination of aroma substances (2, 3), ultimately playing an essential role in fragrance classification (4, 5). Mao et al. explored changes in six flavor attributes of the rapeseed oil at different roasting temperatures using quantitative descriptive analysis (QDA) (6). As a result, the sensory evaluation results were found to always correlate with the aroma compound content of the rapeseed oil.

Several scholars have recently analyzed the aroma components of fragrant rapeseed oil. Wagner et al. identified 29 volatile components of virgin cold-pressed rapeseed oil during storage by gas-chromatography–mass spectrometry (GC–MS); however, all the components were not identified as aroma compounds (7). Zhou et al. identified six important aroma compounds in commercial rapeseed oil through gas chromatography–olfactometry (GC–O) (8). Of note, these studies have mainly focused on the volatile and aromatic compounds of rapeseed oils. Accordingly, there is a lack of systematic studies on fragrance classification, the identification of aroma components, and the correlation between sensory attributes and aroma compounds of fragrant rapeseed oil.

Chemometrics significantly contribute to the development of food sensory and aroma compounds. Correlation analysis between the parameters plays an important role in bridging the connection between the chemical and sensory data. Principal component analysis (PCA), hierarchical cluster analysis (HCA), and partial least squares regression (PLSR) have been successfully applied to explore the relationship between physical, chemical, and sensory data (9–11). According to the results of such studies, PLSR is confirmed as a highly effective tool for sensory quality control of mango (12) and commercial boletus (13).

In this study, nine fragrant rapeseed oils from the main production areas in China were selected as representative samples. The sensory characteristics of these oils were then evaluated using sensory analysis and the aroma compounds were identified using headspace solid–phase microextraction gas chromatography–mass spectrometry/olfactometry (HS–SPME–GC–MS/O). Based on the principal component analysis (PCA) and partial least squares regression (PLSR) analysis, the relationship between the sensory characteristics and aroma compounds was established, and the fragrance types of these different products were classified, which would be meaningful for quality control and the marketing strategies employed for industrial production.

Materials and methods

Fragrant rapeseed oils

In total, 9 samples were purchased from different rapeseed oil-producing areas in China, including the upper Yangtze River (Sichuan), lower Yangtze River (Jiangsu, Shanghai), and the plateau region (Yunnan) (details in Supplementary Table S4). In total, 9 samples of rapeseed oil are popular among local consumers. All the samples were produced using the traditional Chinese hot-pressing technology. Samples were stored at 4°C until further analysis.

Chemicals

Acetaldehyde (95%), propanal (96%), 2-heptanone (97%), heptanal (98%), 2,5-dimethyl pyrazine (95%), 2,6-dimethyl pyrazine (95%), and 2-ethyl pyrazine (96%) were purchased from Sigma-Aldrich Co. Ltd (Shanghai, China). 5-Hepten-2-one, 6-methyl-(97%), dimethyl trisulfide (95%), 2-ethyl-3-methyl pyrazine (93%), 2-ethyl-6-methyl pyrazine (95%), furfural (97%), 2-ethyl-5-methyl pyrazine (98%), 2-ethyl-3,5-dimethyl pyrazine (96%), acetic acid (99%), benzaldehyde (97%), 1-butene, 4-isothiocyanato (94%), (E,E)-2,4-heptadienal (99%), (E)-2-nonenal (98%), dimethyl sulfoxide (97%), and 5-methyl-2-furancarboxaldehyde (97%) were supplied by CNW Technologies GmbH Co. Ltd (Shanghai, China). (E,Z)-2,6-Nonadienal (97%), butanoic acid (98%), (E)-2-decenal (99%), 2-furanmethanol (98%), (E,E)-2,4-nonadienal (99%), 2(5H)-furanone (97%), (E,E)-2,4-decadienal (96%), hexanoic acid (97%), benzyl nitrile (96%), heptanoic acid (99%), and benzenepropanenitrile (97%) were from Alfa Aesar reagent company (Shanghai, China).

Sensory analysis

The sensory panel was composed of 10 experts with more than 2 years of experience in the sensory evaluation. The experts were recruited to comply with ISO standards and were selected based on their ability to identify and describe differences among oil samples (14). Quantitative descriptive analysis (QDA) was used to analyze the sensory characteristic intensity of fragrant rapeseed oils. The expert panel completed eight sessions in the sensory room. The first three sessions involved term generation based on the fragrant rapeseed oil samples. Subsequently, standardized evaluation skills were required. To formulate the scoring standards, the following sessions focused on the panelist training, including attribute learning, difference recognition,

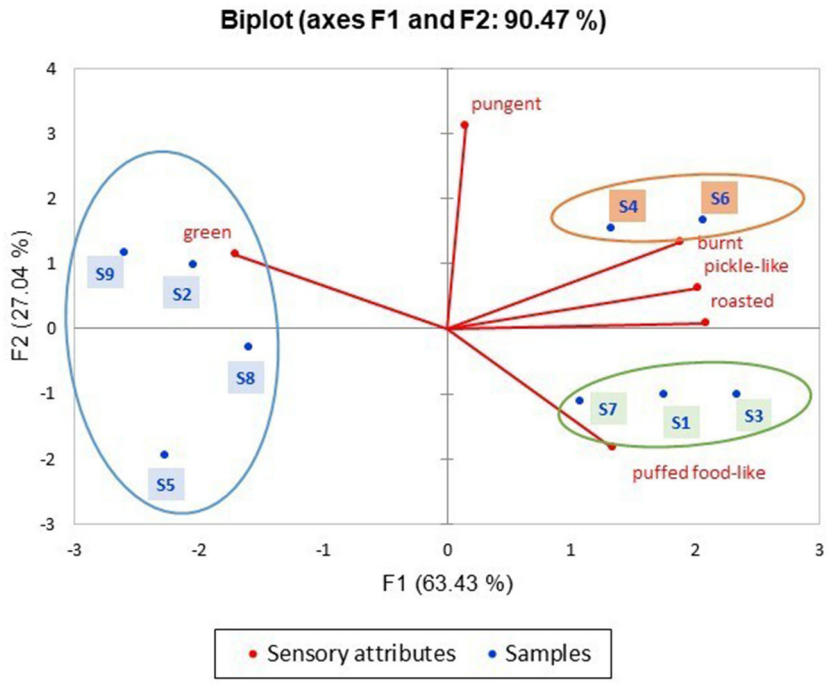

FIGURE 1
Principal component analysis diagrams of the nine fragrant rapeseed oils.

and intensity ranking. A proficiency test was then employed to check the evaluation ability of the experts to ensure the accuracy and consistency of the obtained data. The sensory attributes of fragrant rapeseed oil include roasted, pickle-like, burnt, green, pungent, and puffed food-like characteristics, the definitions of which are listed in Supplementary Table S5. The aforementioned six attributes were evaluated using a linear scale of 15 cm, where 0 indicates that the attribute was not detected and 15 indicates the strongest detection of a particular sensory characteristic. To ensure the consistency and repeatability of the evaluation results, blind samples were inserted into each test for verification. The oil samples were presented in random order during the sensory evaluation and served at 25°C in odorless cups with an effective volume of 10 ml. For each sensory evaluation test, the panelists assessed a maximum of five samples in separate compartments. Each panelist took a 1-min break between each sample to enable restoration of their sensory ability and prevent fatigue. The panelists drew a line on a 15-cm line scale, which indicated their perception of the sensory characteristics.

Shield light was applied during the complete sensory evaluation to alleviate the color interference of the testing samples. Boiled water and plain crackers were available for palate cleansing, and the final result was the average value of three replicates.

Volatile compound analysis

According (HS–SPME–GC–MS) was used to measure the volatile compounds in the oil (8, 15). An oil sample of 5.00 ± 0.10 g and an internal standard material were added to a 20 ml vial, balanced at 60°C for 20 min, and extracted with a 2 cm 50/30 μm DVB/CAR/PDMS fiber (Supelco Ltd., Bellefonte, PA) for 40 min. After extraction, the fiber was desorbed in a split-less inlet at 250°C for 5 min.

An Agilent 7890B/5977A GC–MS instrument (Agilent Technologies Inc., Santa Clara, CA) was used for GC–MS analysis, with HP−5MS and DB–WAX chromatographic columns (30 m × 0.25 mm i.d., 0.25 μm film thickness, J&W Scientific, Folsom, CA). Helium was used as the carrier gas at a constant current of 1.20 ml/min. For the DB–WAX column, the internal standard, 2-octanol (50 μl; 0.819 mg/L, caprylic/capric triglyceride) was added. The initial oven temperature was 45°C, which was increased to 180°C at rate was 4°C /min; this temperature was held for 2 min, increased to 230°C at a rate of 10°C/min, and held for 6 min. For the HP−5MS column, the internal standard, 2-methyl-3-heptanone (10 μl; 0.816 mg/L, caprylic/capric triglyceride), was added. The initial oven temperature was 45°C, which was increased to 180°C at a rate of 4°C /min; this temperature was held for 5 min, increased to 250°C at a rate of 10°C /min, and held for 5 min. The electron energy of the MS was 70 eV, the temperature of the

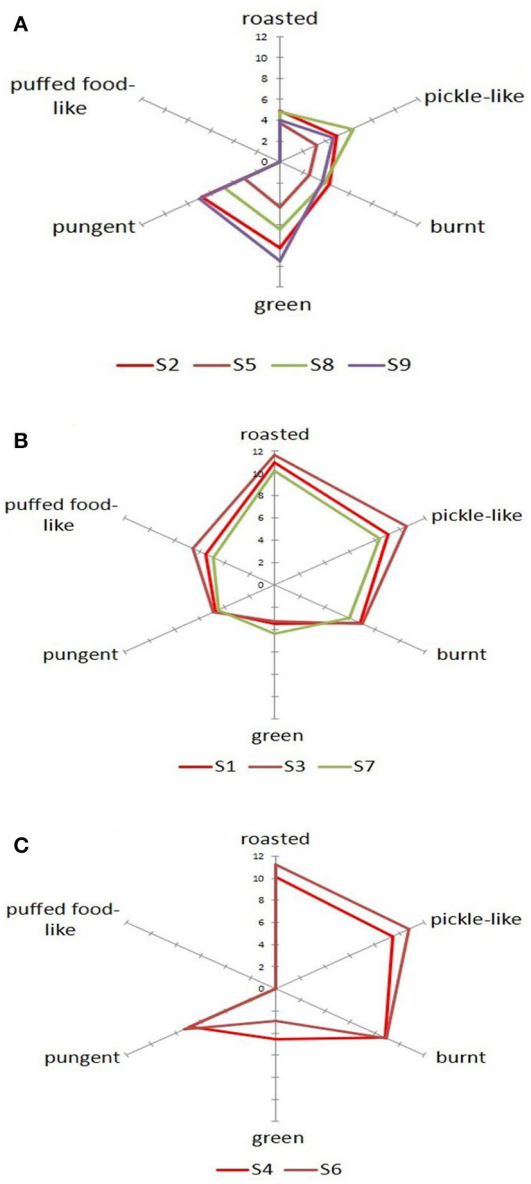

FIGURE 2
Distribution diagrams of the sensory characteristics of the nine fragrant rapeseed oils. **(A)** Delicate fragrance. **(B)** Umami fragrance. **(C)** Strong fragrance.

ion source was 250°C, and the scanning range was 40–500 *m/z*. By comparing their RI values relative to the C6–C23 n-alkanes, the volatile components were identified and obtained from the columns, retention times, standard substances, and NIST 2014 (National Institute of Standards and Technology, Gaithersburg, MD, USA). The relative content of each volatile component was calculated according to the normalized scanning total ion current peak area using the internal standard, and the final result was the average value of three replicates.

Identification of the aroma compounds

The aromatic components in the oil samples were identified using an Agilent 7890B/5977A GC–MS coupled with a Sniffer (Sniffer 9000, Brechbuhler AG, Switzerland). The analysis conditions were the same as those employed for GC–MS. The DB–WAX column was employed, and the sniffing port was set at 230°C. In total, 5 well-trained panelists were selected for the GC–O analysis. In GC operation, the nose must be close to the sniffer port to record the aroma characteristics. Compounds identified by more than three panelists were selected as aroma compounds for further analysis.

Relative odor activity value analysis

Relative odor activity value, which ranges from 0 to 100, was used to evaluate the contribution of the individual compounds to the entire aroma. To identify key odorous compounds in foods, the ROAV was calculated according to a method published by Zhang et al. (13). If the ROAV value of the aroma component was >1, the component could be considered the main contributor to the aroma of the sample (16). If the ROAV value was between 0.1 and 1, the component could be considered to have a specific effect on the overall aroma (17). Of note, the contributions of other compounds were considered minimal. The greater the ROAV value, the greater the aroma component that influences the overall aroma of the sample.

Statistical analysis

Multivariate statistical analysis, including PCA, PLSR, and variable importance in projection (VIP) score analysis, was performed using the sensory and aroma component data on XLSTAT v.2016 (Microsoft Corporation, Redmond, Washington). Tukey's HSD *post-hoc* test ($p < 0.05$) was conducted to assess the statistical significance between aroma compounds *via* SPSS 22.0 statistical software (Chicago, Armonk, NY, USA). R 3.6.0 software (R Foundation for Statistical Computing, Vienna, Austria) was used to conduct Pearson correlation coefficient (r) analysis of the sensory data to identify correlations among the variables. The heatmap was visualized using Hemel (version 1.0, The Cuckoo Workgroup, Wuhan, China). Panel performance was monitored using Panel Check Software (Version 1.3.2, www.panelcheck.com).

Results and discussion

Sensory analysis

Quantitative descriptive analysis is a commonly applied descriptive sensory analysis for measuring the intensity of the

TABLE 1 Aroma compounds and their contents in fragrant rapeseed oils with significant differences ($p < 0.05$) analysis.

No.	CAS	Compounds	Retention index		Aroma descriptors[1]	Concentration (mg/kg)[2]								
			DB-WAX	HP-5MS		S1	S2	S3	S4	S5	S6	S7	S8	S9
V1	74-93-1	methanethiol	694	464	Cabbage-like	0.14^{a}	ND^{e}	0.05^{c}	ND^{e}	ND^{e}	0.04^{d}	0.12^{b}	ND^{e}	ND^{e}
V2	75-07-0	Acetaldehyde[3]	713	412	Green	0.37^{c}	ND^{f}	0.36^{c}	0.42^{b}	0.08^{e}	0.32^{d}	0.46^{a}	0.08^{e}	ND^{f}
V3	123-38-6	Propanal[3]	801	506	Grass-like	ND^{b}	ND^{b}	ND^{b}	ND^{b}	ND^{b}	ND^{b}	ND^{b}	ND^{b}	0.58^{a}
V4	96-17-3	2-methyl butanal	915	659	Cocoa-like	ND^{e}	ND^{e}	0.12^{d}	0.14^{b}	ND^{e}	0.15^{a}	0.13^{c}	ND^{e}	ND^{e}
V5	600-14-6	2,3-Pentanedione	1,071	700	Nutty	0.08^{a}	ND^{d}	0.07^{b}	ND^{d}	ND^{d}	ND^{d}	0.04^{c}	ND^{d}	ND^{d}
V6	624-92-0	dimethyl disulfide	1,072	740	Cabbage-like	0.08^{d}	0.04^{f}	0.06^{e}	0.11^{b}	0.02^{h}	0.06^{e}	0.09^{c}	0.16^{a}	0.03^{g}
V7	110-43-0	2-heptanone[3]	1,187	900	Herbal	ND^{d}	0.09^{b}	ND^{d}	ND^{d}	0.03^{c}	ND^{d}	ND^{d}	0.03^{c}	0.17^{a}
V8	111-71-7	Heptanal[3]	1,188	903	Green	ND^{e}	0.24^{b}	ND^{e}	ND^{e}	0.06^{d}	ND^{e}	ND^{e}	0.16^{c}	0.58^{a}
V9	123-32-0	2,5-dimethyl pyrazine[3]	1,318	913	Cocoa-like	0.77^{f}	1.00^{e}	1.87^{c}	6.47^{a}	ND^{g}	3.57^{b}	0.78^{f}	0.77^{f}	1.23^{d}
V10	108-50-9	2,6-dimethyl pyrazine[3]	1,325	912	Coffee-like	0.60^{c}	0.18^{e}	0.57^{c}	0.93^{b}	0.01^{g}	1.47^{a}	0.48^{d}	0.11^{f}	0.18^{e}
V11	13925-00-3	2-ethyl pyrazine[3]	1,334	917	Nutty	0.54^{c}	ND^{d}	0.96^{a}	ND^{d}	ND^{d}	ND^{d}	0.74^{b}	ND^{d}	ND^{d}
V12	110-93-0	5-hepten-2-one, 6-methyl-[3]	1,341	980	Green	ND^{e}	0.95^{c}	ND^{e}	2.31^{a}	0.46^{d}	1.49^{b}	ND^{e}	0.80^{c}	2.36^{a}
V13	3658-80-8	dimethyl trisulfide[3]	1,383	963	Sulfur	ND^{e}	0.04^{c}	0.04^{c}	ND^{e}	ND^{e}	0.01^{d}	ND^{e}	0.22^{a}	0.07^{b}
V14	15707-23-0	2-ethyl-3-methyl pyrazine[3]	1,397	999	Nutty	0.23^{cd}	0.14^{d}	0.30^{c}	0.82^{b}	ND^{e}	0.95^{a}	0.15^{d}	0.12^{d}	ND^{e}
V15	13925-03-6	2-ethyl-6-methyl pyrazine[3]	1,402	992	Roasted potato	0.25^{c}	0.20^{d}	0.30^{a}	ND^{g}	ND^{g}	ND^{g}	0.16^{e}	0.09^{f}	0.27^{b}

(Continued)

10.3389/fnut.2022.945144

TABLE 1 Continued

No.	CAS	Compounds	Retention index		Aroma descriptors[1]	Concentration (mg/kg)[2]								
			DB-WAX	HP-5MS		S1	S2	S3	S4	S5	S6	S7	S8	S9
V16	13360-64-0	2-ethyl-5-methyl pyrazine[3]	1,415	1,001	Nutty	0.03^{d}	0.16^{c}	0.32^{b}	0.84^{a}	ND^{d}	0.87^{a}	ND^{d}	0.13^{c}	0.15^{c}
V17	13925-07-0	2-ethyl-3,5-dimethyl pyrazine[3]	1,443	1,088	Nutty	ND^{e}	0.37^{d}	ND^{e}	2.27^{a}	ND^{e}	ND^{e}	ND^{e}	0.48^{c}	0.57^{b}
V18	3386-97-8	1-butene, 4-isothiocyanato[3]	1,452	1,006	Pungent	0.75^{f}	0.97^{e}	2.41^{c}	9.35^{b}	ND^{h}	10.40^{a}	0.59^{g}	0.66^{fg}	2.11^{d}
V19	98-01-1	furfural[3]	1,473	830	Baked bread	4.78^{e}	2.97^{f}	12.83^{c}	16.09^{b}	0.10^{i}	23.86^{a}	6.21^{d}	0.87^{h}	1.84^{g}
V20	64-19-7	acetic acid[3]	1,480	600	Sour	14.50^{b}	3.15^{e}	12.74^{c}	8.23^{d}	0.71^{f}	19.90^{a}	14.76^{b}	1.15^{f}	3.23^{e}
V21	4313-03-5	(*E,E*)-2,4-heptadienal[3]	1,494	1,007	Fatty	ND^{e}	0.20^{c}	0.17^{c}	ND^{e}	ND^{e}	0.27^{b}	ND^{e}	0.11^{d}	1.26^{a}
V22	100-52-7	benzaldehyde[3]	1,534	921	Bitter	0.19^{d}	0.19^{d}	0.26^{c}	0.56^{a}	ND^{f}	0.45^{b}	0.14^{d}	0.07^{e}	0.41^{b}
V23	18829-56-6	(*E*)-2-nonenal[3]	1,543	1,171	Green	ND^{b}	ND^{b}	ND^{b}	ND^{b}	ND^{b}	ND^{b}	ND^{b}	ND^{b}	0.42^{a}
V24	67-68-5	dimethyl sulfoxide[3]	1,574	827	Garlic-like	0.49^{e}	0.22^{f}	0.86^{c}	1.32^{a}	ND^{i}	1.09^{b}	0.57^{d}	0.06^{h}	0.14^{g}
V25	620-02-0	5-methyl-2-furancarboxaldehyde[3]	1,591	964	Spicy	2.79^{d}	0.87^{e}	4.71^{b}	3.69^{c}	0.04^{f}	11.03^{a}	2.72^{d}	0.19^{f}	0.66^{e}
V26	557-48-2	(*E,Z*)-2,6-nonadienal[3]	1,595	1,156	Green	ND^{b}	ND^{b}	ND^{b}	ND^{b}	ND^{b}	ND^{b}	ND^{b}	ND^{b}	0.08^{a}
V27	107-92-6	butanoic acid[3]	1,630	850	Cheese-like	ND^{d}	ND^{d}	ND^{d}	ND^{d}	0.06^{c}	ND^{d}	ND^{c}	0.11^{b}	0.59^{a}
V28	3913-81-3	(*E*)-2-decenal[3]	1,630	1,234	Fatty	ND^{e}	0.02^{c}	ND^{e}	ND^{e}	ND^{e}	ND^{e}	0.01^{d}	0.09^{a}	0.08^{b}
V29	98-00-0	2-furanmethanol[3]	1,678	864	Baked bread	1.43^{a}	0.20^{d}	0.36^{c}	ND^{e}	ND^{e}	0.57^{b}	0.30^{c}	0.01^{e}	0.04^{e}

(Continued)

10.3389/fnut.2022.945144

TABLE 1 Continued

No.	CAS	Compounds	Retention index		Aroma descriptors[1]	Concentration (mg/kg)[2]								
			DB-WAX	HP-5MS		S1	S2	S3	S4	S5	S6	S7	S8	S9
V30	5910-87-2	(*E,E*)-2,4-nonadienal[3]	1,704	1,204	Green	ND^{b}	ND^{b}	ND^{b}	ND^{b}	ND^{b}	ND^{b}	ND^{b}	ND^{b}	0.07^{a}
V31	497-23-4	2(5H)-furanone[3]	1,767	915	Buttery	0.70^{b}	0.09^{e}	ND^{g}	0.50^{d}	ND^{g}	0.88^{a}	0.62^{c}	0.03^{f}	ND^{g}
V32	2363-88-4	2,4-decadienal	1,767	1,284	Green	ND^{b}	ND^{b}	ND^{b}	ND^{b}	ND^{b}	ND^{b}	ND^{b}	ND^{b}	0.08^{a}
V33	25152-84-5	(*E,E*)-2,4-decadienal[3]	1,826	1,326	Oily	ND^{b}	ND^{b}	ND^{b}	ND^{b}	ND^{b}	ND^{b}	ND^{b}	ND^{b}	0.28^{a}
V34	142-62-1	hexanoic acid[3]	1,854	1,008	Sour	0.36^{c}	0.17^{de}	0.29^{cd}	1.57^{a}	0.10^{e}	0.62^{b}	0.24^{cd}	0.16^{de}	0.71^{b}
V35	140-29-4	benzyl nitrile[3]	1,931	1,140	Pungent	ND^{e}	0.02^{d}	0.03^{d}	0.17^{b}	ND^{e}	0.22^{a}	ND^{e}	ND^{e}	0.08^{c}
V36	111-14-8	heptanoic acid[3]	1,960	1,080	Sour	ND^{d}	0.10^{b}	ND^{d}	ND^{d}	ND^{d}	ND^{d}	0.06^{c}	ND^{d}	0.19^{a}
V37	2785-89-9	4-ethyl-2-methoxy phenol	2,033	1,243	Smoky	ND^{b}	ND^{b}	ND^{b}	ND^{b}	ND^{b}	ND^{b}	ND^{b}	ND^{b}	0.08^{a}
V38	645-59-0	benzenepropanenitrile[3]	2,048	1,244	Spicy	0.60^{f}	0.84^{e}	1.96^{c}	6.34^{b}	0.17^{g}	7.05^{a}	0.43^{f}	1.16^{d}	2.02^{c}

"ND" Not detected.

[1] Odor perceived at sniffing port.

[2] Aroma compounds were identified by DB–Wax column. Values in the same row followed by the same letter were not significantly different by Tukey's HSD post-hoc testing ($p < 0.05$).

[3] Identification using the authentic standards.

10.3389/fnut.2022.945144

sensory characteristics of fragrant rapeseed oil. By applying PCA to the sensory results of the nine samples to clarify their fragrance classification (Supplementary Table S1, Figure 1), the nine samples could be classified into three groups. Radar plots were used to illustrate the sensory characteristic distribution of each sample by determining the sensory characteristics of the three groups (Figure 2). The two figures show that the nine rapeseed oils had obvious differences in their fragrance styles. In total, 4 of the samples, namely, S2, S5, S8, and S9, were similar, with lower intensity of roast, pickled-like, and burnt odor, and higher intensity of the green odor. As a result, these samples were assigned to the "delicate fragrance" category. Samples S1, S3, and S7 were also similar, with a prominent puffed food-like structure, and were assigned to the "umami fragrance" category. The two remaining samples, S4 and S6, were similar as their four sensory characteristics of pickle-like, roasted, burnt, and pungent were relatively prominent. Accordingly, these samples were assigned to the "strong fragrance" category. Different fragrant rapeseed oils exhibit different sensory characteristics. Grass, nutty, roasted, and burnt were the main aromas from virgin rapeseed oil (18). The pungent attribute is the key characteristic used to differentiate between rapeseed oil samples (19).

To analyze the correlations between the sensory characteristics of fragrant rapeseed oil, the Pearson's correlation was used to measure the direct statistical relationship or association between two continuous variables (Supplementary Figure S2). Roasted food was found to be positively correlated with pickle-like ($r = 0.95$, $sig < 0.0001$) and burnt ($r = 0.89$, $sig = 0.001$) attributes, but negatively correlated with green ($r = -0.77$, $sig = 0.014$), and less correlated with pungent and puffed food-like. Pickle-like was positively correlated with burnt ($r = 0.94$, $sig = 0.0002$) and negatively correlated with green ($r = -0.69$, $sig = 0.038$) attributes. Therefore, strong positive correlations were found between roasted, burnt, and pickle-like attributes, which negatively correlated with green.

Analysis of the volatile compounds

The volatile compounds in the nine fragrant rapeseed oils were identified by HS–SPME–GC–MS. A total of 158 volatile components were identified using the DB–WAX column and HP−5MS column, including 15 nitriles, 17 sulfides, 10 alcohols, 3 phenols, 31 N-heterocycles, 4 O-heterocycles, 30 aldehydes, 15 acids, 27 ketones, 2 olefins, and 4 esters (Supplementary Table S2). The volatile components in fragrant rapeseed oil are produced mainly through complex reactions, such as the Maillard reaction, glucosinolate (GLS) degradation, lipid peroxidation, and amino acid degradation (19). GLS degradation widely occurs in the metabolites of cruciferous plants, mainly producing sulfides and nitriles, which is the main reason for the pungent aroma of cold-pressed rapeseed oils (20). Differences in the nitriles and sulfides in the samples may be linked to the GLS composition and content of the different rapeseed varieties (6). The nitrile and sulfide contents of the "strong fragrance" rapeseed oil samples were higher than those of other samples, such as S4 (112.87 mg/kg) and S6 (108.89 mg/kg), but were little difference in the other two fragrance types. During seed roasting, GLS degradation tends to produce low-carbon nitriles and sulfide compounds, such as 4-isothiocyanato-1-butene and 2-isothiocyanato-butane (6). Among the samples, "strong fragrance" rapeseed oil had the highest amount of 4-isothiocyanato-1-butene. Some sulfide compounds can be further hydrolyzed to form low-molecular sulfides and disulfides (21). Low-molecular-weight sulfides and disulfides, such as carbon disulfide, dimethyl disulfide, dimethyl sulfoxide, and dimethyl trisulfide, were detected in nine fragrant rapeseed oils.

During the heating process in which the rapeseeds are roasted, many N-heterocycle and O-heterocycle compounds are produced by the Maillard reaction and amino acid degradation, such as pyrazine, pyridine, and furanone (22). Studies have shown that pyrazines are essential compounds in edible vegetable oils (15). A total of 16 pyrazines were identified in the nine fragrant rapeseed oils, with most of these compounds found in "umami fragrance" rapeseed oils (S1 and S7). 2,6-dimethylpyrazine was detected in all nine oils, which is similar to the results of Zhou, who identified two compounds in the commercial fragrant rapeseed oil (8). Aldehydes, alcohols, ketones, acids, and esters are mainly involved in the lipid oxidation, Strecker degradation, and amino acid degradation (23). Hexanal, (E)-2-octenal, and nonanal were identified in nine fragrant rapeseed oils. Ren et al. (24) also found hexanal and nonanal in the rapeseed oil. Of note, acetic acid had the highest content of all acids; however, its contents in the different types of fragrant rapeseed oils were found to markedly vary. Furaneol and 2,3-pentanedione were only found in the "umami fragrance" rapeseed oils (S1, S3, and S7) and have not been reported in the previous studies on rapeseed oils (6, 8, 24, 25).

Analysis of the aroma compounds

The aroma compounds were identified by GC–O analysis. As shown in Table 1 and Supplementary Figure S3, 38 aroma compounds were detected in nine rapeseed oils, including two nitriles, four sulfides, two alcohols, one phenol, seven N-heterocycles, two O-heterocycles, 13 aldehydes, four acids, and three ketones. Tukey's HSD *post-hoc* test ($p < 0.05$) was employed to determine whether the 38 aroma compounds were significantly different between the rapeseed oils and could serve as critical markers for distinguishing between fragrant rapeseed oils (Table 1).

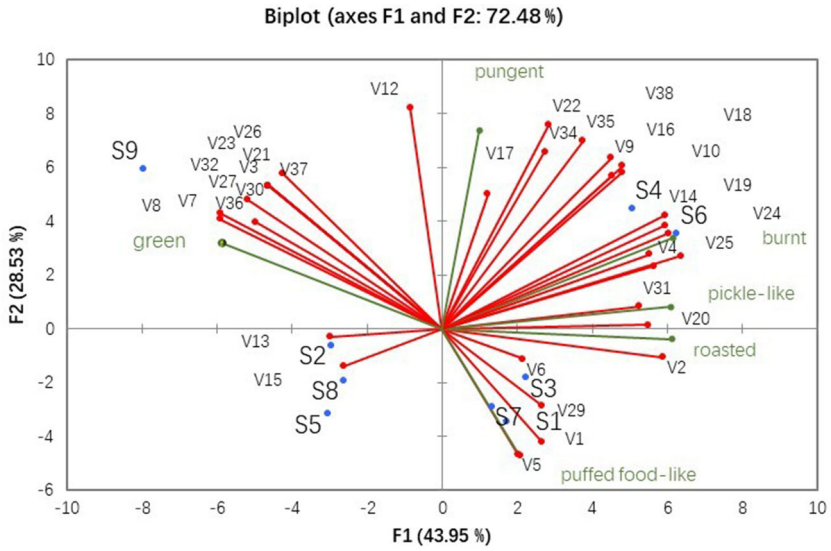

FIGURE 3
PCA analysis of nine fragrant rapeseed oils based on aroma compounds and sensory characteristics.

The ROAV is increasingly applied to evaluate the contribution of aroma compounds to the entire odor of samples (16, 17, 26). In this study, 35 aroma compounds contributing to the overall aroma of fragrant rapeseed oils (*ROAV* > 0.1) were selected for further analysis, as shown in Supplementary Table S3.

In total, 2 nitrile and 4 sulfide aroma compounds were identified from the GLS degradation products, including dimethyl disulfide (cabbage-like), dimethyl trisulfide (sulfur), 4-isothiocyanato-1-butene (pungent), dimethyl sulfoxide (garlic-like), benzyl nitrile (pungent), and benzenepropanenitrile (spicy). Dimethyl disulfide and dimethyl trisulfide were also detected in cold-pressed rapeseed oil (25). Zhou et al. discovered that benzyl nitrile provides pungency in the commercial rapeseed oils (8). Furthermore, 4-isothiocyanato-1-butene was reported to be the main contributor to the pungent aroma of rapeseed oils (24).

Heterocyclic compounds play an important role in roasted, baked, and nutty aroma (15). Pyrazine compounds are intermediate products of the Maillard reaction that have a nutty and roasted aroma. These compounds include 2,5-dimethyl pyrazine (cocoa-like), 2,6-dimethyl pyrazine (coffee-like), 2-ethyl pyrazine (nutty), 2-ethyl-3-methyl pyrazine (nutty), 2-ethyl-6-methyl pyrazine (roasted potato), 2-ethyl-5-methyl pyrazine (nutty), and 2-ethyl-3,5-dimethyl pyrazine (nutty). The "strong fragrance" and "umami fragrance" rapeseed oils had a higher content of pyrazine aroma compounds and a stronger roast intensity than the "delicate fragrance" rapeseed oils. S4, a "strong fragrance" rapeseed oil, had the highest content of pyrazine aroma compounds (11.33 mg/kg), S5, a "delicate fragrance" rapeseed oil, had the lowest content (0.01 mg/kg). According to Wei et al. (22), 2,5-dimethyl pyrazine exists in different varieties of rapeseed oils. Herein, 2-ethyl pyrazine was only detected in "umami fragrance" rapeseed oils (S1, S3, and S7), with concentrations of 0.54, 0.96, and 0.74 mg/kg, respectively.

Methanethiol (cabbage-like) was mainly found in the "umami flavor" oils, such as S1, S3, and S7. Methanethiol is produced *via* the degradation of sulfur amino acids, such as cysteine, methionine, and s-methylmethionine, in the Maillard reaction (27). Herein, 2-furanmethanol (baked bread) was not detected in S4 or S5. Furthermore, the highest content of 2-furanmethanol was found in S1 (1.43 mg/kg). Ren et al. (24) also found 2-furanmethanol in microwave-pretreated rapeseed oils.

The aldehyde compounds in rapeseed oil mainly provide green and tallow aromas, such as acetaldehyde (green), propanal (grass-like), heptanal (green), and (E)-2-nonenal (green). Zhou et al. (8) identified heptanal as an aroma-active compound in commercial rapeseed oil. (E,E)-2,4-heptadienal (fatty), (E)-2-decenal (fatty), and (E,E)-2,4-decadienal (oily) were found in S8, with relatively higher contents than those found in "delicate fragrance" rapeseed oil.

Only one phenolic aroma compound was found among the aroma components. This compound, 4-ethyl-2-methoxy phenol, provided a smoky aroma in S9. According to previous studies, 4-ethyl-2-methoxy phenol is prominent in the roasted mustard seeds and may be produced during the rapeseed roasting process (28).

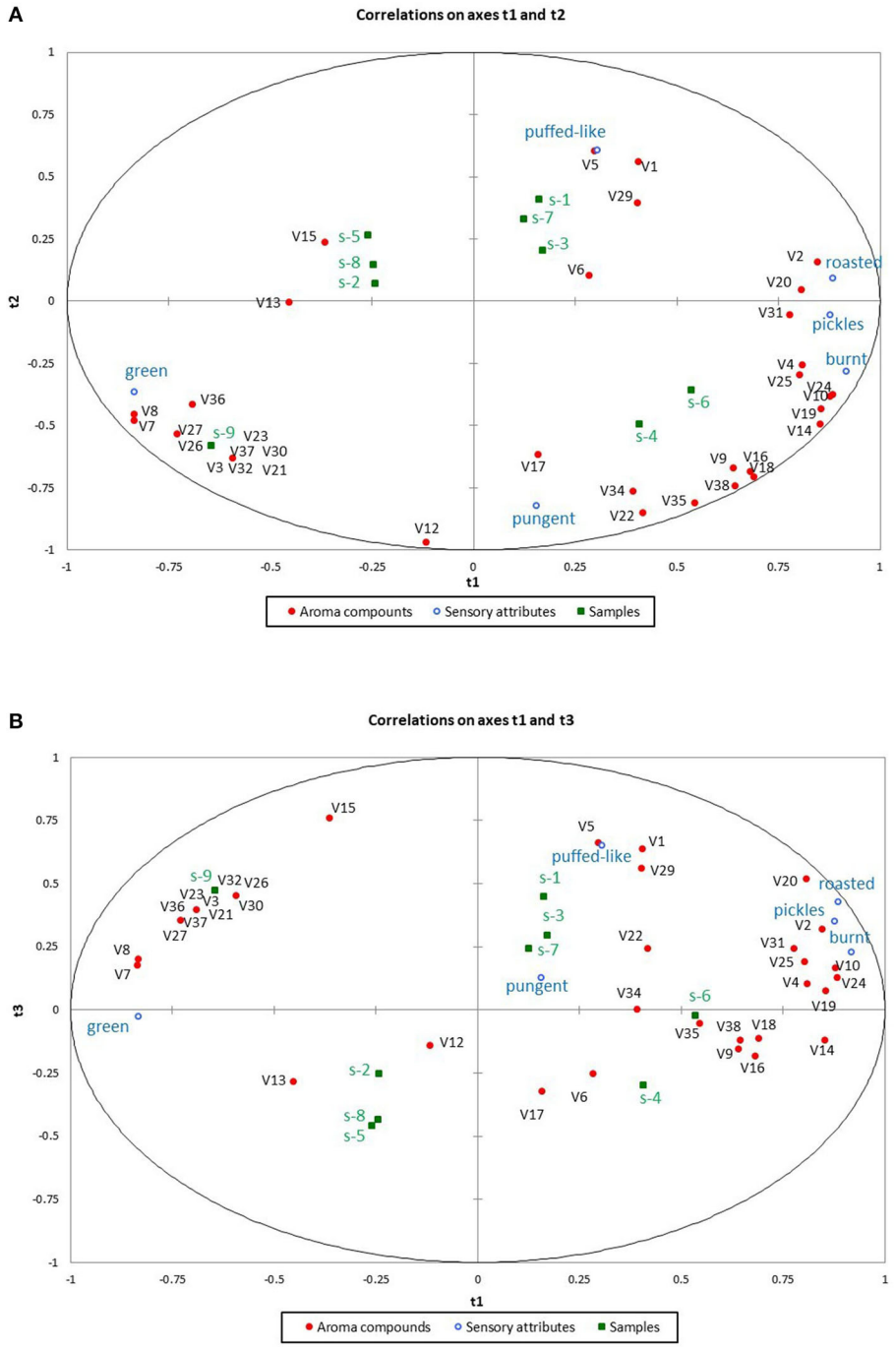

FIGURE 4
Partial least squares correlation model analysis of aroma compounds and sensory characteristics **(A)** axes t1 and t2. **(B)** axes t1 and t3.

Correlation analysis of the sensory characteristics and aroma components

Principal component analysis was used to evaluate the correlation between the aroma compounds (Supplementary Table S3, $ROAV > 0.1$) and sensory characteristics (Figure 2) of the nine fragrant rapeseed oils (Figure 3). The first two principal components accounted for 72.48% of the total variance, with the first principal component accounting for 43.95% and the second principal component accounting for 28.53% of the total.

As shown in Figure 3, S4 and S6 were located in the first quadrant, where roasted, burnt, and pickle-like sensory characteristics were surrounded by acetic acid (sour), 2(5H)-furanone (buttery), 5-methyl-2-furancarboxaldehyde (spicy), 2-methyl butanal (cocoa-like), dimethyl sulfoxide (garlic-like), furfural (baked bread), 2-ethyl-3-methyl pyrazine (nutty), 2-ethyl-5-methyl pyrazine (nutty), and 2,5-dimethyl pyrazine (cocoa-like). The left side of Figure 3 contains the S9, S2, S8, S5, and S6 samples (green). Few aroma compounds, such as 2-heptanone (herbal), heptanal (green), heptanoic acid (sour), butanoic acid (cheese-like), 2,4-decadienal (green), and (E,E)-2,4-nonadienal (green), were observed in this quadrant. Samples S1, S3, and S7 and puffed food-like were positioned in the fourth quadrant, which had dimethyl disulfide (cabbage-like), methanethiol (cabbage-like), 2,3-pentanedione (nutty), and 2-furanmethanol (baked bread). The pungent compound was positioned on the left side of the first quadrant. According to the Pearson's correlation analysis (Supplementary Figure S2) of the sensory characteristics, the pungent compound was correlated with burnt, roasted, pickle-like, and green, which may be produced by combining multiple compounds. PCA was also employed to identify the relationships between the nine fragrant rapeseed oils, which led to the same classification as the QDA. Notably, aroma compounds can explain the sensory characteristics of rapeseed oil.

To confirm the aforementioned findings, PLSR was used to determine the correlation between aroma compounds (Supplementary Table S3, $ROAV > 0.1$) and sensory characteristics (Figure 2). PLSR is a multivariate statistical analysis method that is applied to small sample sizes with many variables (29). The quality of the PLSR model was determined using cross-validation parameters. R^2 and Q^2 represent the variance and predictive capability, respectively. As shown in Figure 4, the x variables ($R^2X = 0.879$) explain the variation in the y variables ($R^2Y = 0.841$) according to the first three factors ($p < 0.05$, $Q^2 = 0.701$). The circle indicates a 100% explanation. Most variables were located around the circle, and no variables were collected in the center, indicating the reliability of the PLSR prediction model.

As shown in Figure 4, the umami fragrances of rapeseed oil samples (S1, S3, and S7) and puffed food-like were located on the upper right side of the chart. Meanwhile, 2, 3-pentanedione (nutty) and 2-ethyl pyrazine (nutty) were only detected in "umami fragrance" rapeseed oil samples. The "strong fragrance" rapeseed oil samples (S4 and S6) and the burnt, pickle-like and pungent aroma were located on the lower right side with many aroma components that promoted the burnt, pickle-like, and pungent aroma. The "delicate fragrance" rapeseed oil samples (S2, S5, S8, and S9) were located on the left side, close to the green aroma. Meanwhile, 2-heptanone (herbal) and heptanal (green) were only found in the "delicate fragrance" rapeseed oil samples. These results are consistent those of PCA and could be used to further categorize the nine rapeseed oils into three fragrance styles.

Aroma compounds with VIP values ($p < 0.05$) greater than one are considered the main reasons for the differences in the sensory characteristics. The VIP values for the 35 aroma compounds were > 1, including those of acetaldehyde (green), 2-methyl butanal (cocoa-like), 2-heptanone (herbal), heptanal (green), 2,6-dimethyl pyrazine (coffee-like), 2-ethyl-3-methyl pyrazine (nutty), furfural (baked bread), acetic acid (sour), dimethyl sulfoxide (garlic), and 5-methyl-2-furancarboxaldehyde (spicy). The SD was low (<0.35) and the results were statistically significant ($p < 0.05$). Thus, the 10 aroma compounds were significantly correlated with roasted, burnt, pickle-like, green, and puffed food-like compounds, which can be considered the main contributors for distinguishing the sensory characteristics of the nine fragrant rapeseed oils. A heat map was used to visualize the relationship between the nine fragrant rapeseed oil samples from the three fragrance styles and the 10 aroma compounds to derive the correlation, as shown in Supplementary Figure S4. Our findings indicate that the nine oils can be classified into three groups. Thus, the 10 aroma compounds play a vital role in the sensory characteristics of fragrant rapeseed oil.

Conclusion

In conclusion, the findings of the present study revealed that roasted, pickle-like, burnt, green, pungent, and puffed food-like are the sensory characteristics of the fragrant rapeseed oil. Furthermore, 10 aroma compounds can be considered to be mainly responsible for the differences in the sensory characteristics. On the basis of the sensory and aroma compound analyses, the fragrant rapeseed oil can be classified into three different fragrance styles: "strong fragrance," "umami fragrance," and "delicate fragrance." Our findings indicate that this approach has potential for application in the flavor classification and sensory quality control of fragrant rapeseed oil and could be used to establish an important basis for the market positioning, fragrance grading, and process improvement of fragrant edible oils in the future.

Data availability statement

The original contributions presented in the study are included in the article/Supplementary materials, further inquiries can be directed to the corresponding authors.

Author contributions

FG, XS, and JW designed the study. FG, MM, MY, and XP collected the data and participated in the design of the

experimental. FG lead the data analysis, with the participation of QB and JH. All authors participated in manuscript preparation and revised the final version of the manuscript. All authors contributed to the article and approved the submitted version.

Funding

This work was supported by the National Key Research and Development Program, China (Grant Number: 2017YFD0400106).

Conflict of interest

The authors declare that the research was conducted in the absence of any commercial or financial relationships that could be construed as a potential conflict of interest.

Publisher's note

Supplementary material

The Supplementary Material for this article can be found online at: https://www.frontiersin.org/articles/10.3389/fnut.2022.945144/full#supplementary-material

References

1. Zhang Y, Zhu Y, Shi L, Guo Y, Wei L, Zhang H, et al. Physicochemical properties and health risk assessment of polycyclic aromatic hydrocarbons of fragrant rapeseed oils in China. *J Sci Food Agric.* (2020) 100:3351–9. doi: 10.1002/jsfa.10368

2. Escuderos ME, Uceda M, Sánchez S, Jiménez A. Instrumental technique evolution for olive oil sensory analysis. *Eur J Lipid Sci Technol.* (2007) 109:536–46. doi: 10.1002/ejlt.200600239

3. Lukić I, Horvat L, Godena S, Krapac M, Lukić M, Vrhovsek U, et al. Towards understanding the varietal typicity of virgin olive oil by correlating sensory and compositional analysis data: a case study. *Food Res Int.* (2018) 112:78–89. doi: 10.1016/j.foodres.2018.06.022

4. De Santis D, Frangipane MT. Sensory perceptions of virgin olive oil: new panel evaluation method and the chemical compounds responsible. *Nat Sci.* (2015) 7:132. doi: 10.4236/ns.2015.73015

5. Borràs E, Ferré J, Boqué R, Mestres M, Aceña L, Calvo A, et al. Prediction of olive oil sensory descriptors using instrumental data fusion and partial least squares (PLS) regression. *Talanta.* (2016) 155:116–23. doi: 10.1016/j.talanta.2016.04.040

6. Mao X, Zhao X, Huyan Z, Liu T, Yu X. Relationship of glucosinolate thermal degradation and roasted rapeseed oil volatile odor. *J Agric Food Chem.* (2019) 67:11187–97. doi: 10.1021/acs.jafc.9b04952

7. Wagner C, Bonte A, Brühl L, Niehaus K, Bednarz H, Matthäus B. Micro-organisms growing on rapeseed during storage affect the profile of volatile compounds of virgin rapeseed oil. *J Sci Food Agric.* (2018) 98:2147–55. doi: 10.1002/jsfa.8699

8. Zhou Q, Xiao J, Yao Y, Wang B, Wei C, Zhang M, et al. Characterization of the aroma-active compounds in commercial fragrant rapeseed oils via monolithic material sorptive extraction. *J Agric Food Chem.* (2019) 67:11454–63. doi: 10.1021/acs.jafc.9b05691

9. Cheng K, Peng B, Yuan F. Volatile composition of eight blueberry cultivars and their relationship with sensory attributes. *Flavour Fragr J.* (2020) 35:443–53. doi: 10.1002/ffj.3583

10. Pu D, Zhang Y., Sun B, Ren F, Zhang H, Chen H, et al. Characterization of the key taste compounds during bread oral processing by instrumental analysis and dynamic sensory evaluation. *LWT.* (2021) 138:110641. doi: 10.1016/j.lwt.2020.110641

11. Zielinski AA, Haminiuk CW, Nunes CA, Schnitzler E, Ruth SM, Granato D. Chemical composition, sensory properties, provenance, and bioactivity of fruit juices as assessed by chemometrics: a critical review and guideline. *Comprehens Rev Food Sci Food Safety.* (2014) 13:300–16. doi: 10.1111/1541-4337.12060

12. Sung J, Suh JH, Chambers AH, Crane J, Wang Y. Relationship between sensory attributes and chemical composition of different mango cultivars. *J Agric Food Chem.* (2019) 67:5177–88. doi: 10.1021/acs.jafc.9b01018

13. Zhang H, Huang D, Pu D, Zhang Y, Chen H, Sun B, et al. Multivariate relationships among sensory attributes and volatile components in commercial dry porcini mushrooms (*Boletus edulis*). *Food Res Int.* (2020) 133:109112. doi: 10.1016/j.foodres.2020.109112

14. ISO. International Standard 8586. *Sensory Analysis—General Guidelines for the Selection, Training and Monitoring of Selected Assessors and Expert Sensory Assessors* (2014).

15. Diez-Simon C, Mumm R, Hall RD. Mass spectrometry-based metabolomics of volatiles as a new tool for understanding aroma and flavour chemistry in processed food products. *Metabolomics.* (2019) 15:1–20. doi: 10.1007/s11306-019-1493-6

16. Wei J, Zhang Y, Wang Y, Ju H, Niu C, Song Z, et al. Assessment of chemical composition and sensorial properties of ciders fermented with different non-Saccharomyces yeasts in pure and mixed fermentations. *Int J Food Microbiol.* (2020) 318:108471. doi: 10.1016/j.ijfoodmicro.2019.108471

17. Fan Y, Liu W, Xu F, Huang Y, Zhang H. Comparative flavor analysis of eight varieties of Xinjiang flatbreads from the Xinjiang Region of China. *Cereal Chem.* (2019) 96:1022–35. doi: 10.1002/cche.10207

18. Jing B, Guo R, Wang M, Zhang L, Yu X. Influence of seed roasting on the quality of glucosinolate content and flavor in virgin rapeseed oil. *LWT.* (2020) 126:109301. doi: 10.1016/j.lwt.2020.109301

19. Zhou Q, Tang H, Jia X, Zheng C, Huang F, Zhang M, et al. Distribution of glucosinolate and pungent odors in rapeseed oils from raw and microwaved seeds. *Int J Food Properties.* (2018) 21:2296–308. doi: 10.1080/10942912.2018.1514632

20. Kushad MM, Brown AF, Kurilich AC, Juvik JA, Klein BP, Wallig MA, et al. Variation of glucosinolates in vegetable crops of Brassica o leracea. *J Agric Food Chem.* (1999) 47:1541–8. doi: 10.1021/jf980985s

21. Pechacek R, Velíšek J, Hrabcová H. Decomposition products of allyl isothiocyanate in aqueous solutions. *J Agric Food Chem.* (1997) 45:4584–8. doi: 10.1021/jf970316z

22. Wei F, Yang M, Zhou Q, Zheng C, Peng J, Liu C, et al. Varietal and processing effects on the volatile profile of rapeseed oils. *LWT Food Sci Technol.* (2012) 48:323–9. doi: 10.1016/j.lwt.2012.04.007

23. Xu L, Yu X, Li M, Chen J, Wang X. Monitoring oxidative stability and changes in key volatile compounds in edible oils during ambient storage through HS-SPME/GC–MS. *Int J Food Properties.* (2018) 20:1–13. doi: 10.1080/10942912.2017.1382510

24. Ren X, Wang L, Xu B, Wei B, Liu Y, Zhou C, et al. Influence of microwave pretreatment on the flavor attributes and oxidative stability of cold-pressed rapeseed oil. *Drying Technol.* (2019) 37:397–408. doi: 10.1080/07373937.2018.1459682

25. Zhou Q, Mei Y, Huang F, Zhang C, Deng Q. Effect of pretreatment with dehulling and microwaving on the flavor characteristics of cold-pressed rapeseed oil by GC-MS-PCA and electronic nose discrimination. *J Food Sci.* (2013) 78:C961–70. doi: 10.1111/1750-3841.12161

26. Wang M, Zhang J, Chen J, Jing B, Zhang L, Yu X, et al. Characterization of differences in flavor in virgin rapeseed oils by using gas chromatography–mass spectrometry, electronic nose, and sensory analysis. *Eur J Lipid Sci Technol.* (2020) 122:1900205. doi: 10.1002/ejlt.201900205

27. Zhang Y, Liu Y, Yang W, Huang J, Liu Y, Huang M, et al. Characterization of potent aroma compounds in preserved egg yolk by gas chromatography–olfactometry, quantitative measurements, and odor activity value. *J Agric Food Chem.* (2018) 66:6132–41. doi: 10.1021/acs.jafc.8b01378

28. Ortner E, Granvogl M, Schieberle M. Elucidation of thermally induced changes in key odorants of white mustard seeds (*Sinapis alba* L.) and rapeseeds (*Brassica napus* L.) using molecular sensory science. *J Agric Food Chem.* (2016) 64:8179–90. doi: 10.1021/acs.jafc.6b03625

29. Mehmood T, Liland KH, Snipen L, Sæbø S. A review of variable selection methods in partial least squares regression. *Chemom Intell Lab Syst.* (2012) 118:62–9. doi: 10.1016/j.chemolab.2012.07.010

frontiers | Frontiers in Nutrition

TYPE Original Research
PUBLISHED 04 August 2022
DOI 10.3389/fnut.2022.968783

OPEN ACCESS

EDITED BY
Mingquan Huang,
Beijing Technology and Business University, China

REVIEWED BY
Ye Liu,
Beijing Technology and Business University, China
Meigui Huang,
Nanjing Forestry University, China

*CORRESPONDENCE
Su Xu
xs8515@126.com

SPECIALTY SECTION
This article was submitted to Food Chemistry, a section of the journal Frontiers in Nutrition

RECEIVED 14 June 2022
ACCEPTED 12 July 2022
PUBLISHED 04 August 2022

CITATION
Xu S, Liu Y, Ma F, Yang N, Virginio Filho EdM and Fisk ID (2022) Impact of agro-forestry systems on the aroma generation of coffee beans. *Front. Nutr.* 9:968783. doi: 10.3389/fnut.2022.968783

Impact of agro-forestry systems on the aroma generation of coffee beans

Su Xu[1,2]*, Yuze Liu[1], Fengwei Ma[1], Ni Yang[2], Elias de Melo Virginio Filho[3] and Ian Denis Fisk[2]

[1]Food and Pharmaceutical Engineering Institute, Guiyang University, Guiyang, China, [2]Division of Food Sciences, University of Nottingham, Nottingham, United Kingdom, [3]Centro Agronómico Tropical de Investigación y Enseñanza, CATIE, Turrialba, Costa Rica

A long experiment has been established since 2000 at CATIE (Tropical Agricultural Research and Higher Education Center), Turrialba, Costa Rica. Twenty agro-forestry systems with different shade types and managements (organic and non-organic) consisting of an incomplete randomized block-design with shade tree as main effect and subplots represented by management were set up. The effects of different managements and shade types on the aroma and color generation of roasted coffee beans were investigated. The total protein content was significantly higher ($P < 0.05$) under the intensive conventional (IC) (168 g/Kg) and intensive organic (IO) (167 g/Kg) managements than under the moderate conventional (MC) (153 g/Kg in IC vs. MC group, 157 g/Kg in MC vs. IO group). Comparing with the moderate conventional (MC) management, the intensive organic (IO) management had a stronger ability to generate more flavor and color. The total protein content was significantly higher ($P < 0.05$) under the full sun system (172 g/Kg) than under the shaded (159 g/Kg) and *Erythrina* system (155 g/Kg), under the service system (165 g/Kg) than under the timber system (146 g/Kg), under the legume timber system (170 g/Kg) than under the non-legume timber system (152 g/Kg). The full sun system had a greater flavor generation and color after roasting. Comparing with the timber system, the service system produced roasted beans with the more flavor and color. Comparing with the non-legume shade tree, the legume shade tree improved the performance of flavor and color in the roasted coffee beans.

KEYWORDS

agro-forestry systems, shade trees, organic management, coffee color, aroma generation

Introduction

Coffee is widely appreciated and consumed due to its pleasant flavor generated during the roasting process (1). In addition, expert coffee tasters assess the quality of coffee, to a greater extent, by its aroma and taste, and the highest quality coffee beans can obtain a considerable price premium (2). A large number of investigations, therefore, have been carried out to evaluate the types and quantities of volatile compounds as well as its formation principals in the roasted coffee beans. Most volatile compounds

formed during roasting are derived from a range of chemical precursors in the green coffee beans, these include sugars, amino acids, organic acids and phenolic compounds, and these react through many complex reactions including the Maillard reaction, degradation of sugars and lipid oxidation (3–7). Nine specific pathways to generate the volatile compounds during roasting of coffee have been outlined by Dart and Nursten (2) in 1985. There were the Maillard reaction, Strecker degradation, trigonelline degradation, phenolic acids degradation, lipid degradation, sugar degradation, breakdown of sulphur amino acid, breakdown of hydroxyl amino acids and proline, and hydroxyproline degradation. Moreover, the dominating volatile compounds, according to their functional groups, have been divided into ten classes by Dart and Nursten (2). They included sulphur compounds, pyrazines, pyridines, pyrroles, oxazoles, furans, aldehydes, ketones, phenols, and other heterocyclic compounds.

There are many sourcess affecting the aroma generation of roasted coffee beans: the origin of coffee beans (i.e., Arabica, Robusta) may contribute to the differences (8); seasonal variation may also play an essential role in differences (9, 10); additionally, differences in geographical locations (11), differences in post-harvest processing (wet or dry processing) and aging before roasting also affect the final aroma generation (1). Furthermore, roasting profile (time-temperature) and the roaster models are aslo significant contributors to the differences of final coffee flavor (12, 13).

Coffee roasting plays an essential role in the formation of organoleptic properties including flavor and color. During the roasting process, moisture content decreases and many chemical reactions occur, along with crucial variations in terms of flavor, color, volume, weight, bean pop, pH, density and presence of volatile compounds (14).

Gas chromatograph is widely used to analyse the coffee volatile composition followed by mass spectrometer (15) or other specific detectors [flame ionization detectors (16), nitrogen-phosphorous detectors, photo-ionization detectors] due to its sensitivity and operability. It can separate and identify a complex mixture of aromas in one operation as well as quantify the volatiles at extremely low concentrations (2).

Numerous researches have been carried to identify the volatile compounds of coffee, explore the formation mechanisms of these pleasant aromas and investigate the relationship between the composition of green coffee beans and aroma generation of roasted coffee beans (17–21), but only a limited number of studies have actually connected these to the growth conditions, levels and types of fertilizers, the species of shade trees. As a result, it is necessary for coffee scientists to explore the interactions and detail the specific effects of fertilizer levels and shade types on aroma generation of roasted coffee beans. The aim of this research was to investigate the impact of agro-forestry systems including fertilizer levels and shade types on the aroma generation of roasted coffee bean.

TABLE 1 Agroforestry systems with main plot (Shade type) and subplot (Management) treatments.

Shade types*	E	T	C	C+T	E+T	C+E	Full Sun
Managements**	IC	IC				IC	IC
	MC	MC	MC	MC	MC	MC	MC
	IO	IO	IO	IO	IO	IO	
	LO	LO				LO	

*E, Erythrina poepiggiana; C, Chloroleucon eurycyclum; T, Terminalia amazonia.
**IC, Intensive conventional; MC, Moderate conventional; IO, Intensive organic, LO, Low organic; (n = 3).

TABLE 2 Characteristics of shade trees (22).

Species	Phenology	Canopy	N-fixer	Use
Erythrina poepiggiana (E)	Evergreen	Low compact	Yes	Service
Chloroleucon eurycyclum (C)	Deciduous*	High spreading	Yes	Timber
Terminalia amazonia (T)	Deciduous*	High compact	No	Timber

* Deciduous for about 20–30 days per year.

Materials and methods

Agro-forestry methodologies

The experiment was established in 2000 at CATIE (Tropical Agricultural Research and Higher Education Center), Turrialba, Costa Rica (9°53'44" N, 83°40'7" W, CATIE, Turrialba, Costa Rica), which is defined as a low altitude (600 m above sea level), wet coffee zone without a marked dry season. Average annual rainfall, temperature, relative humidity and solar radiation was 2,915 mm/year, 22°C, 90.2%, and 15.9 MJ/m^2/year (2000–2013).

Twenty agroforestry systems with different shade types and managements consisting of an incomplete randomized block-design with shade tree as main effect and subplots represented by management were set up (Table 1). For each system, three replicates were established. Shade type [initially 417 trees per ha-1 (6 × 4 m^2 spacing)] consisted of timber and service tree species with contrasting characteristics (Table 2). Trees were progressively thinned to maintain a reasonable shade environment for coffee production (Table 3).

Intensive conventional (IC) *Erythrina* trees were biannually pollarded to a 1.8–2.0 m main trunk. Whilst this is normal practice in Costa Rica, Muschler (24) found that coffee quality benefited from increased *Erythrina* shade levels, therefore, for all the other treatments with *Erythrina*, trees were pollarded to 4 m leaving three branches for partial shade. Temporary shade was planted in the form of *Ricinus* in organic treatments. This took place 1 year after the coffee plants, to improve coffee plant

TABLE 3 Mean shade tree density after thinning.

Agroforestry system		Tree density per ha^{-1}		
System	**Tree species**	**2008**	**2011**	**2013**
Monocultures				
E	E	360	285	241
C	C	381	154	65
T	T	317	167	73
Polycultures				
C+E	C	183	100	45
	E	181	134	115
C+T	C	166	77	39
	T	170	77	34
E+T	E	147	143	109
	T	158	81	34

E, Erythrina poepiggiana; C, Chloroleucon eurycyclum; T, Terminalia Amazonia.

TABLE 4 Mean input levels of fertilizers (Kg ha^{-1}year^{-1}) and weed/disease control since 2006, adapted from Haggar et al. (23) and Noponen et al. (25).

Management	Fertilization N:P:K **	Weed control	Disease/Pest control
IC	287:20:150	Six* herbicides	3–4* Fungicides/ insecticides
MC	150:10:75	Five herbicides four manual	1–4 Fungicides/ insecticides as required
IO	248:205:326	Four Manual	Organic substances as required
LO	66:2:44	Four Manual	No

IC, Intensive conventional, MC, Moderate conventional, IO, Intensive organic, LO, Low organic. IO fertilization: Chicken manure 10 t ha^{-1}year^{-1}and K-Mag (fertilizer)100 kg ha^{-1}year^{-1}; LO fertilization: Coffee pulp 5 t ha^{-1}year^{-1}.

*Number of treatments applied per year.

**Fertilization levels (Kg ha^{-1}year^{-1}) are 7 years means (2003–2009), from the second to fourth year LO systems received the same fertilization as IO ones, due to the site limitations that did not allow organic coffee to establish effectively with lower inputs.

survival and impede weed growth. Lower branches of the timber trees were pruned annually (year 1–7) to improve stem quality. In all pruning scenarios, pruning residuals from coffee trees and shade trees were left on the ground (trunks were removed). Management consisted of fertilization, weed, disease and pest control, detailed in Table 4.

Coffea Arabica L. var. *Caturra,* was planted at 5000 holes ha^{-1} with dead plants replaced each year. Two plants per planting hole were planted (local practice) but were treated as one plant in every analysis. The distance between rows and holes were 2 m and 1 m. Sub-plots were 500–600 m^2 of which the central 225–300 m^2 was studied (100 coffee plants and 24 shade trees).

Coffee plants were manually pruned from 2004 leaving 1–4 resprouts per stump, according to the productive potential of each coffee resprout in the next harvest. Every coffee planting hole thus comprised 1–2 stumps and a total of 1–4 resprouts per stump.

Coffee roasting

All green coffee beans harvested in different agro-forestry systems from CATIE, Costa Rica in both 2013 and 2014 were sent to Edgehill Coffee Company (Warwick, UK) for roasting. The coffee roaster (Roastilino, Fracino) with a small fluidized bed and a nominal capacity of about 200 g of green coffee beans was used and 50 g of green coffee beans were prepared and roasted. The air outlet temperature and roasting time were 166°C and 1 min 50 s, respectively. All coffee beans were taken past first crack and roasted to medium roasting. After roasting, 30 g of different roasted coffee beans were ground into powders using a mini chopper (CH180 mini chopper, 300 W, Kenwood) and a 710 μm sieve was used to obtain even coffee powder samples. All coffee beans and powders were stored at −20°C.

Measurement of color

The colorimeter (ColorQuest XE, HunterLab Inc.) was used to measure the color of the coffee bean (25). The colorimeter was calibrated using the white plate and packed coffee powder was added to a transparent preservative film and then placed on the detection port to obtain data. Results were calculated by the equipment using the Hunter Lab color scale. In this scale, L ranges from 0 (black) to 100 (white), a indicates degree of greenness (for negative a values) and degree of redness (for positive a results), b axis also ranges from negative to positive values indicating, respectively, degree of blueness to yellowness.

Measurement of total protein content

A bicinchoninic acid (BCA) assay kit (23225/23227, Thermo Scientific) was used to measure the total protein content (26).

0.1 g of coffee powders (wet basis, 11% water content) was weighed and 2 mL of chloroform was used to extract lipid with three replicates. After lipid extraction, the solid phase was dried at 60°C for 30 min and placed in a 15 mL centrifuge tube. After that, 1 mL of 2% sodium dodecyl sulfate (SDS) solution was added into the tube to eliminate interference from lipids and the tube was heated at 60°C in a water bath for 30 min. The

TABLE 5 Principal contrasts used in the analysis of shade type and management effects.

Contrast	Treatments compared
Management	
IC vs. MC	IC(FS, E, T, CE) vs. MC(FS, E, T, CE)
MC vs. IO	MC(E, T, C, CE, CT, ET) vs. IO(E, T, C, CE, CT, ET)
IO vs. LO	IO(E, CE) vs. LO(E, CE)
IC vs. IO	IC(E, T, CE) vs. IO(E, T, CE)
Shade type	
FS vs. shaded	FS(IC, MC) vs. E(IC, MC) + T(IC, MC) + CE(IC, MC)
Erythrina vs. FS*	E(IC, MC) vs. FS(IC, MC)
Service vs. timber trees	E(MC, IO) vs. T(MC, IO) + C(MC, IO) + TC(MC, IO)
Legume timber vs. non-legume timber	C(MC, IO) vs. T(MC, IO)

IC, Intensive conventional; MC, Moderate conventional; IO, Intensive organic; LO, Low organic; FS, Full sun. E, Erythrina poepiggiana; C, Chloroleucon eurycyclum; T, Terminalia Amazonia; CE, Chloroleucon eurycyclum and Erythrina poepiggiana; CT, Chloroleucon eurycyclum and Terminalia Amazonia; ET, Erythrina poepiggiana and Terminalia Amazonia.
*Erythrina was regarded as a low canopy tree with low shade cover and compared with full sun.

sample was then vortexed for 1 min and centrifuged at 13,000 g for 3 min. And then, samples were filtered and diluted 100 times using 2% SDS.

According to the instructions of BCA protein assay kit, 0.1 mL of each standard and sample replicate was added into test tubes. 2.0 mL of the working reagent containing 50 parts of BCA Reagent A (sodium carbonate, sodium bicarbonate, bicinchoninic acid and sodium tartrate in 0.1 mol/L sodium hydroxide) and 1 part of BCA Reagent B (4% cupric sulfate) was added to each tube and mixed well. All tubes were covered and incubated at 37°C for 30 min, after incubation, tubes were cooled to room temperature. The absorbance of the samples was measured at 562 nm by the ultraviolet spectrophotometer (Evolution 350, Thermo Scientific) and subtracted the average 562 nm absorbance measurement of the Blank standard replicates. A standard curve was prepared by plotting the average blank-corrected 562 nm measurements for each bovin serum albumin (BSA) standard vs. its concentration in μg/mL. Finally, the standard curve was used to determine the protein concentration of each sample.

Measurement of sucrose

The sucrose standard was prepared at a concentration of 10, 20, 40, and 50 mg/L. 0.1 g of coffee powder was placed in a 50 mL centrifuge tube with 20 mL of boiling water and vortexed for 5 min. Samples then were centrifuged at 1,600 g for 10 min at room temperature. After centrifugation, the liquid phase was transferred into a new glass vial. The above processes were repeated three times for extracting sucrose completely. The mixture was cooled to room temperature and then filtered using a syringe filter (0.45 μm, hydrophilic nylon syringe filter, Millipore Corporation). The final extract was diluted with water (1:1) prior to Liquid chromatography-mass spectrometry (LC/MS) analysis [the method was modified from Ky et al. (27), Mccusker et al. (28), Perrone et al. (29)].

The LC equipment (1,100 Series, Agilent) consisted of a degasser (G1322A, Agilent), a pump (G1312A, Agilent), an auto-sampler (G1313A, Agilent). This LC system was interfaced with a Quattro Ultima mass spectrometer (Micromass, UK Ltd.) fitted with an electrospray ion source.

The Kromasil 5 ODS (C18) column (250 × 3.20 mm, 5 μm, Phenomenex) was used to separate sucrose and the column was maintained at room temperature. The mobile phase consisted of 0.3% aqueous formic acid (eluent A) and methanol (eluent B) which was delivered at a flow rate of 0.4 ml/min. Initially the solvent was 25% B. After the injection, this proportion was changed immediately to 60% B until the end of the run at 8 min. Between injections, the column was re-equilibrated with 25% B for 4 min.

The electrospray ionization source was operated in the negative mode (3.5 KV) from 0.0 to 4.0 min to generate the formic acid adduct of sucrose $(M+HCOO)^-$ and in the positive mode (3.5 KV) from 4.0 to 8.0 min to generate caffeine $(M+H)^+$ ions. Desolvation gas (N_2) flow rate was 500 L/h and desolvation temperature was 400°C. The mass spectrometer was operated in the selected ion recording (SIR) model to measure sucrose. Identification of compounds was performed by comparing retention time and molecular weight of the respective standards. Quantification was achieved by comparing peak areas of samples and standards using Masslynx software (version 4.0, Waters) (the method was modified from 24 and 25).

Measurement of volatile compounds

2 g of each coffee sample powders and 2.5 μL of 1% heptanone (internal standard) were placed GC vials for analysis (30).

A GC-ISQ (Thermo Electron Corporation Inc.) was used to detect the volatile compounds of coffee in full scan mode over the mass range 20–200 m/z (ion source 200°C). The sample was incubated at 55°C for 5 min with shaking using the autosampler. A 50/30 μm DVB/CAR/PDMS (Divinylbenzene/Carboxen/Polydimethylsiloxane) was the fiber sampled the volatiles for 3.5 min followed by a 1.5 min desorption (inlet temperature 200°C). A splitless mode was used and the constant carrier pressure was at 103 kPa.

10.3389/fnut.2022.968783

TABLE 6 Contrast results for total protein and sucrose contents (g/Kg) by dry weight of green coffee beans.

Contrast	Total protein (g/Kg)			Sucrose (g/Kg)		
Managements	**Mean**	**S.E.$_D$**	***p*-value**	**Mean**	**S.E.$_D$**	***p*-value**
IC vs. MC	167.62	17.25	**0.001**	91.52	9.12	0.544
	152.53			90.09		
MC vs. IO	157.11	21.31	**0.01**	88.12	11.25	0.053
	166.51			92.25		
IO vs. LO	162.39	12.18	0.94	86.97	6.91	0.915
	161.92			87.33		
IC vs. IO	166.92	14.73	0.414	89.89	8.21	0.328
	162.79			87.22		
Shade types						
FS vs. S	171.88	29.87	**0.011**	91.73	16.05	0.647
	159.05			90.49		
E vs. FS	155.36	12.11	**<0.001**	90.36	7.36	0.68
	171.78			91.73		
Ser. vs. Tim.	165.33	30.24	**<0.001**	88.50	16.18	0.984
	146.29			88.56		
LT vs. NLT	170.33	12.21	**<0.001**	84.21	6.87	0.077
	152.26			90.14		

Values were presented as mean, standard error of the contrast difference (S.E.D), and significance of the difference (P-value), P-values < 0.05 were shown in bold. IC, Intensive conventional; MC, Moderate conventional; IO, Intensive organic; LO, Low organic; FS, Full sun; S, Shaded; E, Erythrina poepiggiana; Ser., Service, Tim, Timber; LT, Legume timber; NLT, Non-legume timber.

The GC oven was held at 40°C for 5 min, and then increased from 40 to 240°C at a rate of 5°C/min, and held at 240°C for 2 min. Separation was carried out on a ZB-WAX Capillary GC Column (Length 30 m, inner diameter 0.25 mm, and film thickness 0.25 μm; Phenomenex Inc., Macclesfield, UK). The identity and quantity of volatile compounds was determined using Thermo Xcalibur software. The mass spectrum was used to identify the volatile compounds by comparing with the library (NIST/EPA/NIH Mass Spectral Library. Version 2.0, Faircom Corporation, U.S.) in Xcalibur software. The peak areas of compounds and the internal standard were determined using Thermo Xcalibur software (30). The following formula could be used to calculate the concentration of volatile compounds:

$$\begin{aligned} &\textit{The concentration of volatile compounds } (mg/kg) \\ &= \frac{\textit{Peak area of volatile compound} \times \textit{Amount of internal standard}(mg)}{\textit{Peak area of internal standard} \times \textit{Dry weight of coffee powder}(kg)} \end{aligned}$$

Statistical analysis

The experimental design consisted of shade types as main plot and subplots represented by managements but with an unbalanced structure since not all managements were represented under all Shade types (Table 1). Therefore, the specific pre-planned contrast models (Modified from 19) (Table 5) were used to compare the differences between different managements and shade types.

Data was analyzed using One-Way ANOVA contrasts model with SPSS statistics software (Version 22nd, IBM), treatment as contrast factor to analyze eight contrast groups as shown in Table 5. Significant value ($P < 0.05$) in contrast tests was used to decide if there was a significant difference in each contrast model and the standard error of each contrast could be obtained from contrast tests table. In addition, the mean value of every management and shade type under each contrast model was calculated.

Results and discussion

Impact of fertilizer levels and shade types on the total protein and sucrose contents of green coffee bean

During the coffee roasting progress, carbohydrates especially sucrose are degraded, dehydrated and interacted with protein to generate a large number of volatile compounds (31, 32), which contributes to the formation of organoleptic properties of roasted coffee beans including flavor, aroma and color (14). As

10.3389/fnut.2022.968783

TABLE 7 Detection of sixty-four volatile aroma compounds in the roasted coffee beans in the different agricultural treatments.

	Aroma compound	ID	KI	Literature KI	Odor description	Functional group
1	2,5-Dimethylfuran	m, r	721	706	Ethereal	Furan
2	2-Methylfuran	m, r	893	888	Chocolate	Furan
3	2-Methylbutanal	m, r	918	930	Malty	Aldehyde
4	3-Methylbutanal	m, r	950	934	Malty	Aldehyde
5	2,3-Butanedione	m, r	983	1,000	Buttery, cheesy	Ketone
6	Dimethyl-Disulphide	m, r	1,053	1,050	Onion	Sulphide
7	Hexanal	m, r	1,063	1,064	Grassy, green oily	Aldehyde
8	2,3-Pentanedione	m, r	1,078	1,072	Oily buttery	Ketone
9	2-Vinylfuran	m, r	1,112	1,096	Ethereal, rum, cocoa note	Furan
10	2,3-Hexanedione	m, r	1,154	1,138	Buttery, cheesy, sweet, creamy	Ketone
11	1-Methylpyrrole	m, r	1,171	1,168	White bread, woody	Pyrrole
12	2,4,5-Trimethyloxazole	m, r	1,219	1,200	Green, woody, musty	Heterocyclic N
13	Pyridine	m, r	1,225	1,213	Bitter, astringent, roasted, burnt	Pyridine
14	2-Pentylfuran	m, r	1,239	1,235	Fruity, green	Fruan
15	Furfuryl methyl ether	m, r	1,262	1,243	Nutty, rich, phenolic	Ether
16	Dihydro-2-methyl-3-furanone	m, r	1,267	1,246	Sweet, roasted	Ketone
17	2-Methylpyrazine	m, r	1,282	1,297	Nutty, roasted, chocolate	Pyrazine
18	4-Methylthiazole	m, r	1,335	1,312	Nutty, green	Heterocyclic N
19	Acetoin	m, r	1,348	-	Buttery, creamy	Ketone
20	2,5-Dimethylpyrazine	m, r	1,370	1,357	Nutty, roasted, grassy, corn	Pyrazine
21	2,6-Dimethylpyrazine	m, r	1,375	1,362	Nutty, sweet, fried	Pyrazine
22	2-Ethyl-3-methylpyrazine	m, r	1,382	1,363	Nutty	Pyrazine
23	2-Methyl-2-cyclopentenone	m, r	1,388	1,366	Fruity	Ketone
24	2-Ethylpyrazine	m, r	1,391	1,370	Nutty, roasted	Pyrazine
25	2,3-Dimethylpyrazine	m,r	1,395	1,383	Nutty, roasted, green	Pyrazine
26	2,3,5-Trimethylpyrazine	m, r	1,410	1,395	Nutty, roasted	Pyrazine
27	2-Ethyl-5-methylpyrazine	m, r	1,416	1,397	Nutty, roasted	Pyrazine
28	2-Ethyl-6-methylpyrazine	m, r	1,426	1,420	Roasted, hazelnut-like	Pyrazine
29	Propyl pyrazine	m, r	1,437	1,428	Green	Pyrazine
30	Vinyl pyrazine	m, r	1,446	1,434	Nutty, green	Pyrazine
31	2,6-Diethylpyrazine	m, r	1,458	1,444	Nutty, roasted	Pyrazine
32	Acetic acid	m, r	1,471	1,454	Sour	Acid
33	Furfural	m, r	1,479	1,462	Bread, almond, sweet	Aldehyde
34	2-Ethyl-3,5-dimethylpyrazine	m, r	1,483	1,464	Nutty	Pyrazine
35	Acetoxy acetone	m, r	1,491	1,469	Buttery	Ketone
36	2-Ethyl-3,6-dimethylpyrazine	m, r	1,498	1,480	Nutty, roasted	Pyrazine
37	2-Fufurylmethylsulfide	m, r	1,506	-	Alliaceous, sulfurous	Sulphide
38	2-Acetylfuran	m, r	1,514	1,500	Balsamic-sweet	Furan
39	Pyrrole	m, r	1,518	1,512	Nutty, hay-like, herbaceous	Pyrrole
40	2,3-Dimethyl-2-cyclopentenone	m, r	1,523	1,524	Grassy, bitter	Ketone
41	Propionic acid	m, r	1,536	1,527	Sour	Acid
42	Acetoxy-2-butanone	m, r	1,546	-	Sour	Ketone
43	2-Furfurylacetate	m, r	1,552	1,566	Fruity, green	Ester
44	5-Methylfurfural	m, r	1,562	1,566	Sweet, caramel, bready	Furan
45	3-Methylpyrrole	m, r	1,574	1,569	Woody	Pyrrole
46	2-Acetylpyridine	m, r	1,588	1,602	Popcorn type, corn type	Pyridine
47	1-Methyl-2-formylpyrrole	m, r	1,593	1,626	Bread, burnt, caramel	Pyrrole

(Continued)

TABLE 7 Continued

	Aroma compound	ID	KI	Literature KI	Odor description	Functional group
48	2-Furfuryl-5-methylfuran	m, r	1,647	1,659	Chocolate	Furan
49	g-Butyrolactone	m, r	1,658	-	Creamy, milky	Ester
50	Furfuryl alcohol	m, r	1,671	1,662	Burnt	Alcohol
51	Isovaleric acid	m, r	1,681	1,682	Cheesy	Acid
52	2,5-Dihydrofuranone	m, r	1,749	1,767	Caramel	Ketone
53	1-Furfurylpyrrole	m, r	1,814	1,822	Vegetable	Pyrrole
54	Guaiacol	m, r	1,843	1,855	Phenolic, woody	Phenolic
55	2-Thiophenemethanol	m,r	1,872	1,890	savory	Alcohol
56	Phenylethyl alcohol	m, r	1,902	1,896	Floral	Alcohol
57	2-Acetylpyrrole	m, r	1,953	1,949	White bread	Pyrrole
58	Difurfuryl ether	m,r	1,991	1,977	Coffee-like, toasted odour	Ether
59	Phenol	m, r	2,011	-	Smoky	Phenolic
60	4-Ethylguaiacol	m,r	2,042	2,034	Phenolic	Phenolic
61	2-Formylpyrrole	m, r	2,048	2,036	White bread, jasmine rice	Pyrrole
62	Furaneol	m, r	2,053	2,037	Fruity	Ketone
63	p-Cresol	m, r	2,091	2,078	Phenolic-type	Phenolic
64	2-Methoxy-4-vinylguaiacol	m, r	2,112	-	Woody, smoky	Phenolic

ID, Identification method; m, mass spectrum based on Mass library - NIST/EPA/NIH Mass Spectral Library. Version 2.0, Faircom Corporation, U.S.; r, identified by retention index; KI, Kovats index calculated by n-alkanes on the ZB-WAX Capillary GC Column (Length 30 m, inner diameter 0.25 mm, and film thickness 0.25 μm; Phenomenex Inc., Macclesfield, UK); Literature KI was collected from NIST database: webbook.nist.gov; Odor Description: data was collected from odor database: www.flavornet.org; origin-scifinder.cas.org).

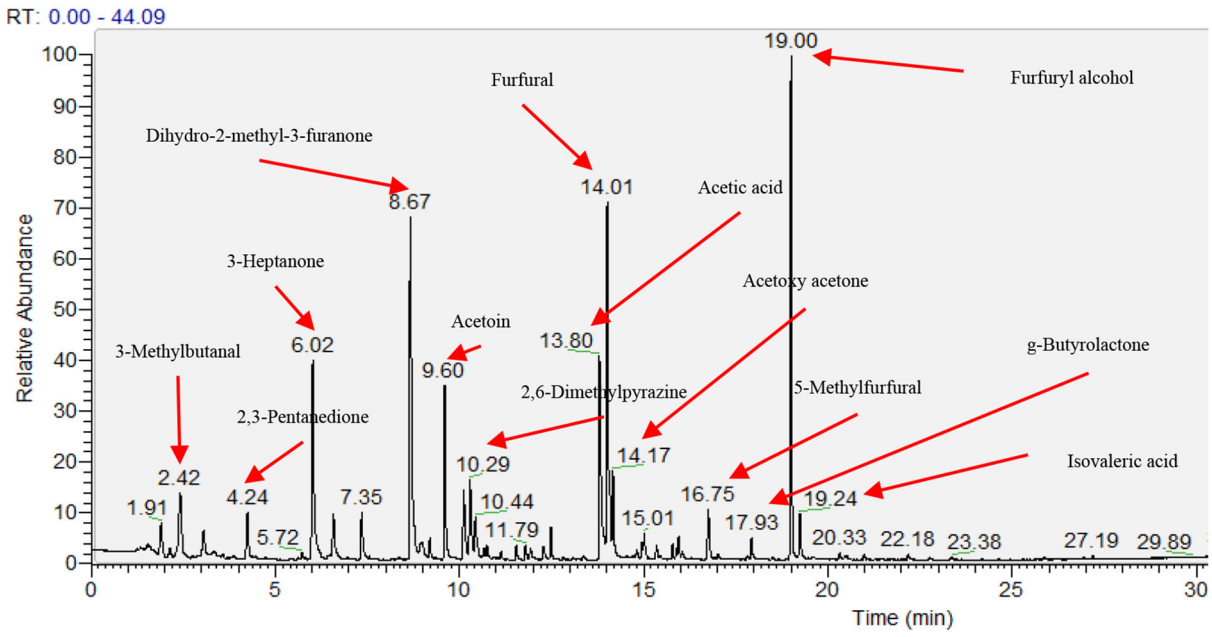

FIGURE 1
Gas chromatogram of head space of roasted coffee powders on ZB-WAX capillary column. The results showed the coffee beans from the intensive conventional management combined with the shade tree *Erythrina poepiggiana*.

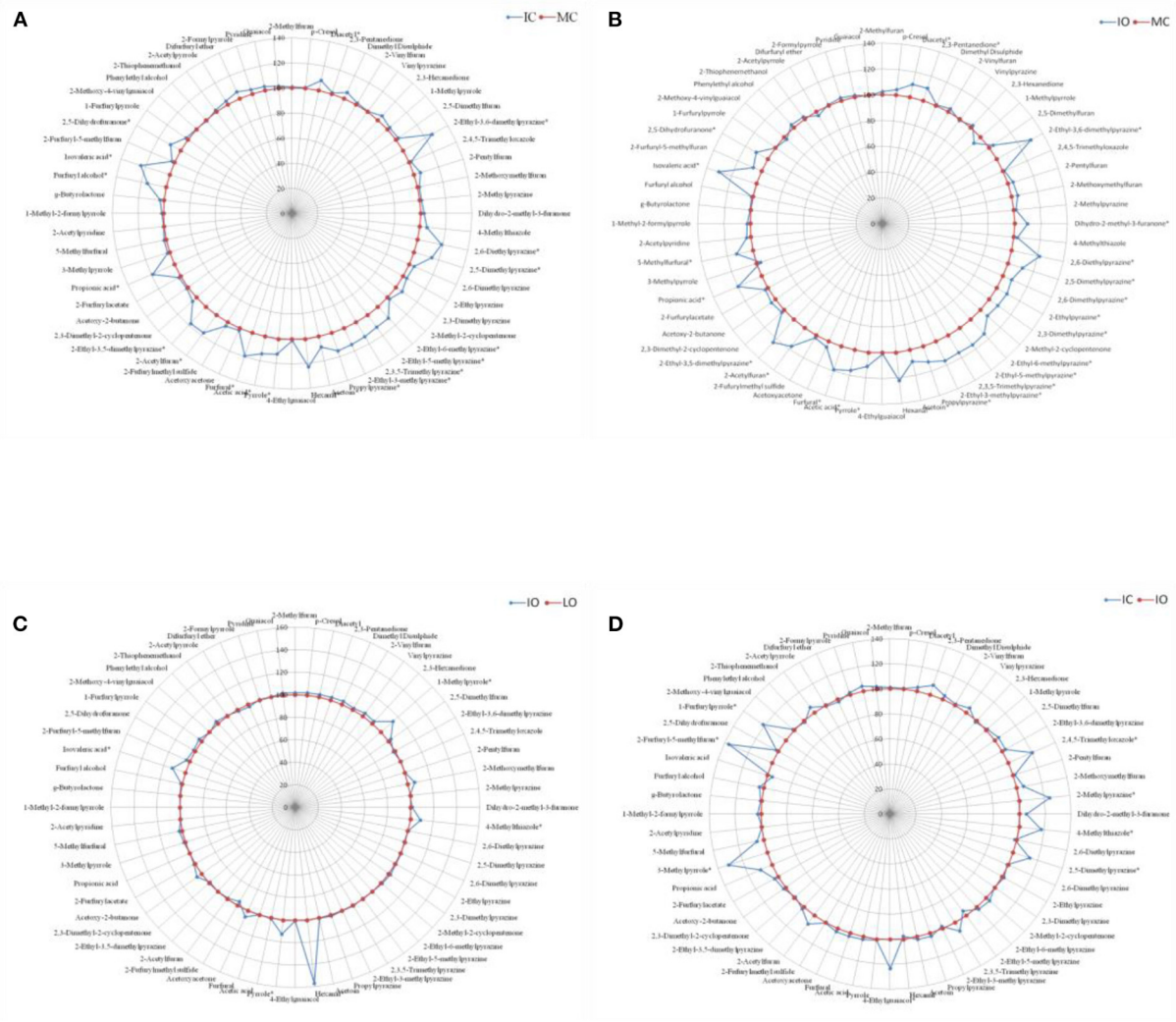

FIGURE 2
Comparison of volatile aroma compounds generation in roasted coffee beans between the different managements, results were presented as the mean value of three replicates. **(A)** Intensive conventional (IC) vs. moderate conventional (MC). **(B)** Intensive organic (IO) vs. moderate conventional (MC). **(C)** Intensive organic (IO) vs. low organic (LO). **(D)** Intensive conventional (IC) vs. intensive organic (IO). *represented significant differences ($P < 0.05$) of volatile compounds between different groups.

a result, the sucrose and protein were analyzed due to the main contribution to the generation of volatile compounds.

The results of total protein content were shown in Table 6. The total protein content was significantly lower ($P < 0.05$) under the MC (153, 11.3 g/Kg) than under the IC (168, 12.2 g/Kg). Furthermore, the total protein content was significantly higher ($P < 0.05$) under the IO (167, 12.4 g/Kg) than under the MC (157, 11.8 g/Kg). Nevertheless, no significant differences ($P > 0.05$) were detected in the total protein content between the IO and LO, and the IC and IO.

For the different shade types, the total protein content of green coffee beans was significantly higher ($P < 0.05$) under the full sun system (172 g/Kg) than under the shaded system (159 g/Kg) and the *Erythrina* system (155 g/Kg). In addition, the total protein content of green coffee beans was significantly higher ($P < 0.05$) under the service system (165 g/Kg) than under the timber system (146 g/Kg), while it was significantly lower ($P < 0.05$) under the non-legume timber system (152 g/Kg) than under the legume timber system (170 g/Kg).

The sucrose content was shown in the Table 6. There were no significant differences ($P > 0.05$) detected between the different managements and shade types.

The total protein content was significantly higher ($P < 0.05$) under the IC and IO managements than under the MC due to the higher input amount of fertilizers especially the nitrogen. After a long period management (about 13 years), the IO management had a similar total protein content in the green coffee beans to the IC management and even a

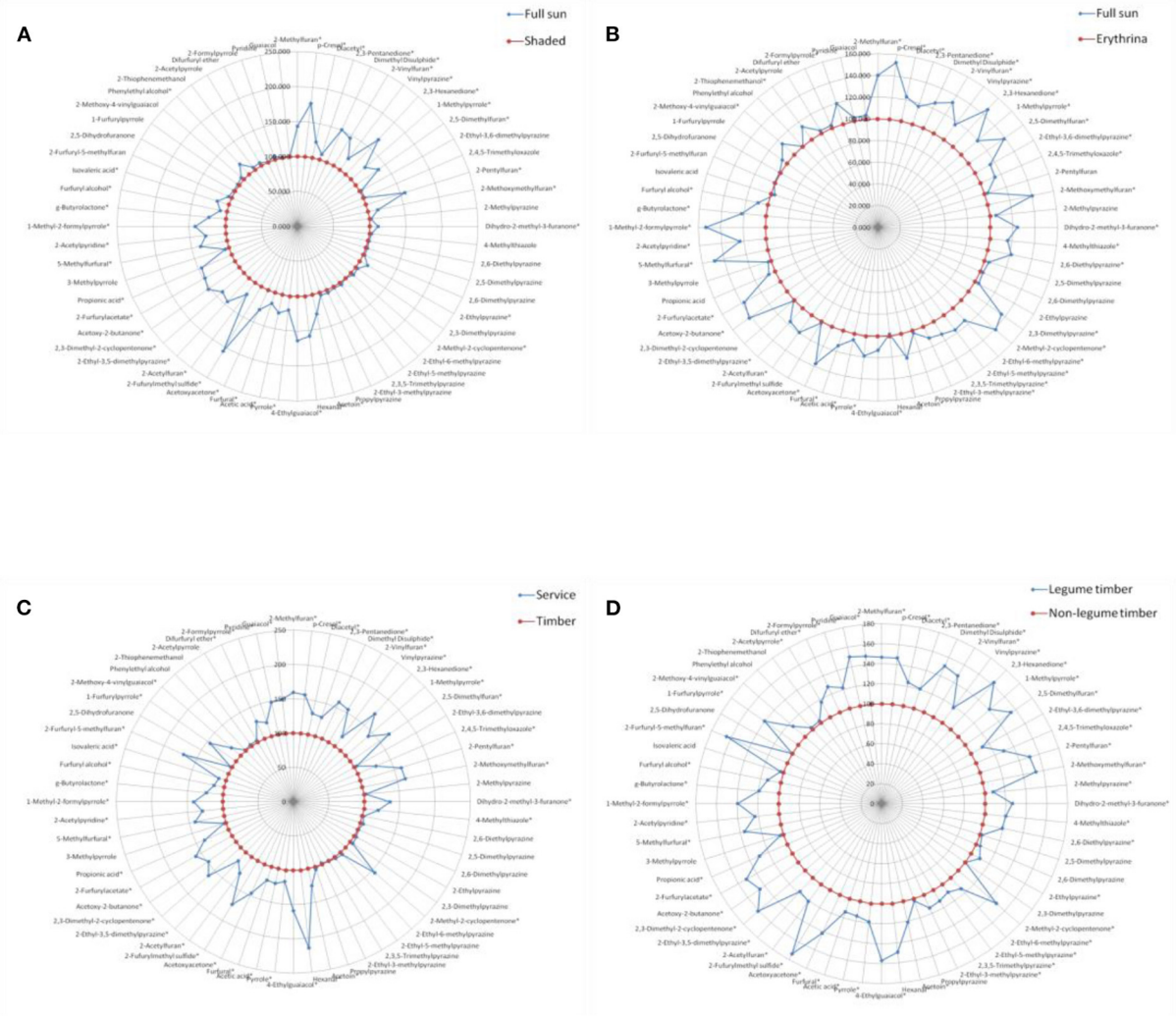

FIGURE 3
Comparison of volatile aroma compounds generation in roasted coffee beans between the different shade types, results were presented as the mean value of three replicates. **(A)** Full sun vs. shaded. **(B)** Full sun vs. *Erythrina*. **(C)** Service vs. timber. **(D)** Legume timber vs. non-legume timber. *represented significant differences ($P < 0.05$) of volatile compounds between different groups.

significantly higher ($P < 0.05$) value than the MC management. Nonetheless, there was no significant difference ($P > 0.05$) in the total protein content between the IO and LO system. When compared with the IO management, the LO management was combined with the legume species *Erythrina* and *Chloroleucon*. On the one hand, the legume species can replenish the lack of N_2 due to the low input level by N_2 fixation (33); on the other hand, the high pruning intensity like *Erythrina* may compensate the lower external inputs, as the leaves and branches pruned from the *Erythrina* shade tree were left on the field (22, 34).

The result of the effect of different shade types on the total protein content suggested that light intensity was the main factor to drive the protein generation in the green coffee beans in our experiment, as the protein biosynthesis in the ribosome is adenosine triphosphate (ATP) dependent (35). As a result, the total protein content was significantly higher ($P < 0.05$) under the full sun system than under the shaded and *Erythrina* system due to the higher shade cover and lower light intensity in the shaded and *Erythrina* systems, moreover, it was also significantly higher ($P < 0.05$) under the service system than under the timber system due to the lower shade cover and higher light intensity in the service system (the *Erythrina* was the only service tree in our experiment). Additionally, the total protein content in the green coffee beans was significantly higher ($P < 0.05$) under the legume timber system than under the non-legume timber system due to the N_2 fixation of the legume species to supply the organic N_2 for the coffee plant to synthesize the amino acids and protein.

10.3389/fnut.2022.968783

TABLE 8 Contrast results for the color of roasted coffee beans.

Contrast	*L*-value		
	Mean	S.E.$_D$	*p*-value
Managements			
IC vs. MC	50.77	2.01	**0.042**
	53.96		
MC vs. IO	54.02	2.21	**0.006**
	50.26		
IO vs. LO	53.04	1.33	0.085
	54.52		
IC vs. IO	53.16	2.21	0.102
	54.03		
Shade types			
FS vs. S	52.97	3.05	**0.016**
	56.82		
E vs. FS	57.70	1.21	**<0.001**
	52.97		
Ser.v. Tim.	50.53	3.11	**<0.001**
	56.98		
LT vs. NLT	52.09	1.27	**<0.001**
	59.48		

Values were presented as mean, standard error of the contrast difference (S.E.$_D$) and significance of the difference (P-value), P-values <0.05 were shown in bold. IC, Intensive conventional; MC, Moderate conventional; IO, Intensive organic; LO, Low Organic; FS, Full sun; S, Shaded; E, Erythrina poepiggiana; Ser., Service; Tim, Timber; LT, Legume timber; NLT, Non-legume timber.

It is well-known that the inorganic carbon is converted to the organic carbon in the plant mainly through photosynthesis, and also, the plant can also absorb the organic carbon fixed by fungi as well as from organic matters on the field (36, 37). In addition, photosynthesis is affected by light intensity, carbon dioxide concentration, water availability, temperature (38, 39). For each contrast group of different managements in our experiment, the shade types have been fixed. Thus, it could be assumed that light intensity and temperature were the same when comparing the different managements in each contrast group. Different managements had no effect on the carbon dioxide concentration due to the same atmospheric conditions. Furthermore, Costa Rica site was considered as the wet coffee zone, which had the adequate water resource. Therefore, no significant differences ($P > 0.05$) were detected in the sucrose content between the different managements.

In our experiment, there were no significant differences ($P > 0.05$) found in the sucrose content between the full sun and shaded system, service and timber, and the legume timber and non-legume timber system, which demonstrated that the light intensity, shaded cover and the N_2 fixation of shade tree were not the main factors to affect the sucrose content of green coffee beans.

Impact of different fertilizer levels and shade types on the aroma and the color generation of roasted coffee beans

Sixty-four volatile aroma compounds, which had previously been identified in coffee, were detected in the roasted coffee beans (30, 40). These aroma compounds were classified into thirteen groups based on their chemical attributes (three alcohols, four aldehydes, 11 ketones, three acids, one ether, two esters, 14 pyrazines, two pyridines, seven pyrroles, two sulfides, eight furans, five phenolic compounds, and 2 N-containing heterocyclic compounds), and their odors and functional group were described (Table 7). Figure 1 showed the gas chromatogram of roasted coffee beans and identified some main peaks of volatile aroma compounds based on the library (NIST/EPA/NIH Mass Spectral Library. Version 2.0, Faircom Corporation, U.S.). The quantitative data sets of the volatile aroma compounds measured in the current work can be found in Supporting Information.

For each contrast model, the fertilizer level with the relatively lower amount of volatile compounds generation was assumed as the control group and the other one with the relatively higher amount of volatile compounds generation was supposed to be the non-control group. The values of these volatile compounds in the control group were defined as 100. The ratio of the non-control group to the control group were calculated, and then, the final values of these volatile compounds in the non-control group were expressed as the ratio multiplied by 100. For example, in the Figure 2A, the MC with the relatively lower volatile compounds generation was assumed as the control group and showed as the circle with round markers at 100%, while the IC with the relatively higher abundance of volatile compounds was defined as the non-control group and showed as the spider diagram with diamond markers. Although sixty-four volatile compounds were detected in our experiment, only sixty volatile compounds were displayed in Figures 2, 3, as there were sno significant differences ($P > 0.05$) in the amounts of these four volatile compounds (2-Methylbutanal, Isovaleraldehyde, Phenol and Furaneol) between the different fertilizer levels and shade types.

Figure 2 showed the effect of different managements on the aroma generation of roasted coffee beans. The relative abundance of twenty volatile compounds were significantly higher ($P < 0.05$) in the roasted coffee beans under the IC management than in those roasted coffee beans under the MC management (Figure 2A, more details see Table 1 in supplementary). The amounts of twenty-five volatile compounds were significantly higher ($P < 0.05$) in the roasted coffee beans under the IO management than in those roasted coffee beans under the MC management (Figure 2B, more details see Table 2 in supplementary file). Nevertheless, only five volatile compounds had significantly higher ($P < 0.05$) amounts in the roasted coffee beans under the IO management

than in those roasted coffee beans under the LO management (Figure 2C, more details see Table 3 in supplementary file). Moreover, there were eight volatile compounds with a significantly higher ($P < 0.05$) amount in the roasted coffee beans under the IC management than in those roasted coffee beans under the IO management (Figure 2D, more details see Table 4 in supplementary file).

Similarly, for each contrast model, the shade type with the relatively lower volatile compounds generation was assumed as the control group and the other one with the relatively higher volatile compounds generation was supposed to be the non-control group. The values of these volatile compounds in the control group were defined as 100. The ratio of the non-control group to the control group was calculated, and then, the final values of these volatile compounds in the non-control group were expressed as the ratio multiplied by 100.

Figure 3 showed the effect of different shade types on the aroma generation of roasted coffee beans. Thirty-six volatile compounds had a significantly higher ($P < 0.05$) amounts in the roasted coffee beans under the full sun system than in those roasted coffee beans under the shaded system (Figure 3A, more details see Table 5 in supplementary file). The amounts of forty volatile compounds were significantly higher ($P < 0.05$) in the roasted coffee beans under the full sun system than in those roasted coffee beans under the Erythrina system (Figure 3B, more details see Table 6 in supplementary file). Additionally, there were forty-three volatile compounds with a significantly higher ($P < 0.05$) amount in the roasted coffee beans under the service shade tree system than in those roasted coffee beans under the timber shade tree system (Figure 3C, more details see Table 7 in supplementary file). The amounts of fifty-one volatile compounds were significantly higher ($P < 0.05$) in the roasted coffee beans under the legume timber shade tree system than in those roasted coffee beans under the non-legume timber shade tree system (Figure 3D, more details see Table 8 in supplementary file).

As mentioned in the methods, L value ranges from 0 to 100, which represents the relevant color is from black (0) to white (100). As a result, the color turns darker with the decreasing of L value. Table 8 showed the effects of fertilizer levels and shade tree types on the color of roasted coffee beans.

With regards to the different fertilizer levels, *L*-values of roasted coffee beans were significantly lower ($P < 0.05$) under the IC (51) and the IO (50) management than under the MC (54) management. As a result, the color of roasted coffee beans was significantly darker ($P < 0.05$) under the IC and the IO management than under the MC management. Nevertheless, no significant differences ($P > 0.05$) were detected in the L values between the IO and LO, and the IC and IO.

In terms of shade types, the roasted coffee beans under the full sun system (53) had a significantly lower ($P < 0.05$) L-value than under the shaded (57) and *Erythrina* (58) systems. Thus, the color of roasted coffee beans was significantly darker ($P < 0.05$) under the full sun system than under the shaded and *Erythrina* systems. Furthermore, the L value of roasted coffee beans was significantly lower ($P < 0.05$) under the service shade tree system (51) than under the timber shade tree system (57), while there was a significantly higher ($P < 0.05$) L value detected in the roasted coffee beans under the non-legume timber shade tree system (59) than under the legume timber shade tree system (52). Therefore, the color of roasted coffee beans was significantly darker ($P < 0.05$) under the service shade tree system than under the timber shade tree system, whilst the roasted coffee beans under the non-legume timber shade tree system had a significantly lighter ($P < 0.05$) color than under the legume shade tree system.

Although many complex chemical reactions such as the degradation of sugar and acids occur during coffee bean roasting progress, Maillard reaction is obviously one of the most important chemical reactions to promote the formation of coffee flavor and color (2, 41). Maillard reaction is related to the interactions between reducing sugars and amino acids (42). Even though there is a large number of polysaccharides present in the green coffee beans (43), most carbohydrates are relatively stable to roasting (44, 45) and therefore it is the relative abundance of free or available sugars drives the thermal flavor generation. Moreover, on roasting, sucrose is rapidly degraded and its content dramatically decreases by about 97% (46). As a result, during coffee bean roasting, the reducing sugars and amino acids, as the main precursors of Maillard reaction, are mainly derived from the decomposition of sucrose and protein in the green coffee beans, respectively. Furthermore, the melanoidins, which contributes to the color formation of roasted coffee beans, are derived from Maillard reaction and dehydration of sucrose (47). Therefore, it is proposed that the contents of sucrose and total protein in the green coffee beans are responsible for the formation of coffee flavor and color.

There were no significant differences ($P > 0.05$) detected in the sucrose content of green coffee beans among the different fertilizer levels and shade types (see Table 6). Nonetheless, significant differences ($P < 0.05$) were found in the total protein content of green coffee beans among the different fertilizer levels and shade types (see Table 6).

In terms of the different fertilizer levels, the total protein content of green coffee beans was significantly lower ($P < 0.05$) under the MC management than under the IC and IO management. This explains why the roasted coffee beans under MC management presented a significantly lower ($P < 0.05$) number of volatile compounds and lighter color than those roasted coffee beans under the IC and IO management.

With regards to the different shade types, the amounts of volatile compounds in the roasted coffee beans were significantly higher ($P < 0.05$) and the color of roasted coffee beans was significantly darker ($P < 0.05$) under the full sun system than under the shaded and *Erythrina* system due to a significantly higher ($P < 0.05$) total protein content of green coffee beans in the full sun system. Similarly, due to the significantly higher ($P < 0.05$) total protein content of green coffee beans under

the service and legume timber shade tree system, the roasted coffee beans under the service and legume timber shade tree system had a significantly higher ($P < 0.05$) number of volatile compounds and significantly darker ($P < 0.05$) color than those roasted coffee beans under the timber and non-legume timber shade tree system, respectively.

Conclusion

To sum up, in our experiment, the total protein content of green coffee beans was significantly affected by the fertilizer levels and shade types, while there was no significant effect on the sucrose content of green coffee beans. As a result, the total protein content was the main factor to drive the formation of aroma and color of roasted coffee beans. As has been discussed, the green coffee beans under the intensive conventional (IC) and intensive organic (IO) management had a significantly higher ($P < 0.05$) total protein content than those under the moderate conventional (MC) management due to the higher fertilizer input amount, especially the nitrogen. Thus, the higher N input amount could increase the protein generation in the green coffee beans and further improve the formation of final flavor and color of roasted coffee beans. Furthermore, the legume shade tree could improve the protein generation in the green coffee beans by fixing more N_2 and further promote the formation of final flavor and color of roasted coffee beans. Compared with shaded system, the light intensity of full sun system was significant higher, which improved the protein biosynthesis in the ribosome, and finally, promoted the formation of flavor and color of roasted coffee beans.

Data availability statement

The original contributions presented in the study are included in the article/Supplementary material, further inquiries can be directed to the corresponding author.

Author contributions

SX, IF, and EV conceived the experiments. SX, YL, and FM drafted the manuscript. SX conducted all the experiments. NY helped to discuss the results and perfected the language assisted with the structure elucidation and manuscript revision. IF and EV designed and supervised the research and revised the manuscript. All authors have read and agreed to the published version of the manuscript.

Funding

This research was financially supported by Science and Technology Fund Project of Guizhou (Qian Ke He Zhicheng [2022] Zhongdian No. 015), Youth Science and Technology Talent Development Project of Education Department of Guizhou Province (Qian Jiao He KY Zi [2018]303), the Special Funding of Guiyang Science, and Technology Bureau and Guiyang University (GYU-KY-[2021]).

Conflict of interest

The authors declare that the research was conducted in the absence of any commercial or financial relationships that could be construed as a potential conflict of interest.

Publisher's note

All claims expressed in this article are solely those of the authors and do not necessarily represent those of their affiliated organizations, or those of the publisher, the editors and the reviewers. Any product that may be evaluated in this article, or claim that may be made by its manufacturer, is not guaranteed or endorsed by the publisher.

Supplementary material

The Supplementary Material for this article can be found online at: https://www.frontiersin.org/articles/10.3389/fnut.2022.968783/full#supplementary-material

References

1. Fisk ID, Kettle A, Hofmeister S, Virdie A, Kenny JS. Discrimination of roast and ground coffee aroma. *Flavour*. (2012) 1:14. doi: 10.1186/2044-7248-1-14

2. Dart S, Nursten H. *Volatile Components Coffee*. Dordrecht: Springer (1985).

3. Tressl R. Formation of flavor components in roasted coffee. *ACS Publications*. (1989) 9:27. doi: 10.1021./bk-1989-0409.ch027

4. Ho C, Hwang H, Yu T, Zhang J. An overview of the Maillard reactions related to aroma generation in coffee. *COLLOQUE Scientifique International sur le Café*. (1993) 15:6–11.

5. Holscher W, Steinhart H. Formation pathways for primary roasted coffee aroma compounds. *ACS Publications*. (1994) 3:16. doi: 10.1021./bk-1994-0543.ch016

6. Holscher W, Steinhart H. Aroma compounds in green coffee. *Develop Food Sci*. (1995) 37:785–803.

7. Reineccius G. The Maillard reaction and coffee flavor. *16th International Scientific Colloquium on Coffee*, Kyoto (1995) 9–14.

8. Semmelroch P, Grosch W. Studies on character impact odorants of coffee brews. *J Agric Food Chem*. (1996) 44:537–43.

9. Agresti PDM, Franca AS, Oliveira LS, Augusti R. Discrimination between defective and non-defective Brazilian coffee beans by their volatile profile. *Food Chem*. (2008) 106:787–96.doi: 10.1016/j.foodchem.06019

10. Silva EAD, Mazzafera P, Brunini O, Sakai E, Arruda FB, Mattoso LHC, et al. The influence of water management and environmental conditions on the chemical composition and beverage quality of coffee beans. *Br J Plant Physiol*. (2005) 17:229–38. doi: 10.1590/S1677-04202005000200006

11. Risticevic S, Carasek E, Pawliszyn J. Headspace solid-phase microextraction–gas chromatographic–time-of-flight mass spectrometric methodology for geographical origin verification of coffee. *Analytica Chimica Acta*. (2008) 617:72–84. doi: 10.1016/j.aca.2008.04.009

12. Franca AS, Oliveira LS, Oliveira RC, Agresti PCM, Augusti R. A preliminary evaluation of the effect of processing temperature on coffee roasting degree assessment. *J Food Enginee*. (2009) 92:345–52. doi: 10.1016/j.jfoodeng.2008.12.012

13. Bhumiratana N, Adhikari K, Chambers E. Evolution of sensory aroma attributes from coffee beans to brewed coffee. *LWT-Food Sci Technol*. (2011) 44:2185–92. doi: 10.1016/j.lwt.2011.07.001

14. Bottazzi D, Farina S, Milani M, Montorsi L. A numerical approach for the analysis of the coffee roasting process. *J Food Enginee*. (2012) 112:243–52. doi: 10.1016/j.jfoodeng.2012.04.009

15. Yeretzian C, Jordan A, Lindinger W. Analysing the headspace of coffee by proton-transfer-reaction mass-spectrometry. *Int J Mass Spectromet*. (2003) 223:115–39. doi: 10.1016/S1387-3806(02)00785-6

16. Freitas AC, Mosca A. Coffee geographic origin—an aid to coffee differentiation. *Food Res Int*. (1999) 32:565–73.

17. Aeschbacher H, Wolleb U, Löliger J, Spadone J, Liardon R. Contribution of coffee aroma constituents to the mutagenicity of coffee. *Food Chem Toxicol*. (1989) 27:227–32. doi: 10.1016/0278-6915(89)90160-9

18. Bade-Wegner H, Holscher W, Vitzthum O. Quantification of 2-methylisoborneol in roasted coffee by, GCMSCOLLOQUE. *Scientifique International Sur Le, Cafe Asic Association Scientifique Internationale*. (1993). 56:537.

19. Amrani-Hemaimi M, Cerny C, Fay LB. Mechanisms of formation of alkylpyrazines in the Maillard reaction. *J Agri Food Chem*. (1995) 43:2818–22. doi: 10.1021/jf00059a009

20. Blank I, Devaud S, Fay LB. Study on the formation and decomposition of the amadori compound. *Maillard Rea Foods Med*. (1998) 223:43.

21. Czerny M, Grosch W. Potent odorants of raw Arabica coffee. Their changes during roasting. *J Agricul Food Chem*. (2000) 48:868–72.

22. Haggar J, Barrios M, Bolaños M, Merlo M, Moraga P, Munguia R, et al. Coffee agroecosystem performance under full sun, shade, conventional, and organic management regimes in Central America. *Agrofor Sys*. (2011) 82:285–301. doi: 10.1007/s10457-011-9392-5

23. Noponen MR, Edwards-Jones G, Haggar JP, Soto G, Attarzadeh N, Healey. Greenhouse gas emissions in coffee grown with differing input levels under conventional and organic management. *Agri Ecosys Environ*. (2012) 151:6–15. 01, 019.

24. Muschler RG. Shade improves coffee quality in a sub-optimal coffee-zone of Costa Rica. *Agrofor Sys*. (2001) 51:131–9.

25. Baggenstoss J, Poisson L, Luethi R, Perren R, Escher F. Influence of water quench cooling on degassing and aroma stability of roasted coffee. *J Agri Food Chem*. (2007) 55:6685–91. doi: 10.1021/JF070338D

26. Fisk ID, Gkatzionis K, Lad M, Dodd CER, Gray DA. Gamma-irradiation as a method of microbiological control, and its impact on the oxidative labile lipid component of Cannabis sativa and Helianthus annus. *Eu Food Res Technol*. (2009) 228:613–21. doi: 10.1007/s00217-008-0970-3

27. Ky CL, Doulbeau S, Guyot B, Akaffou S, Charrier A, Hamon S, et al. Inheritance of coffee bean sucrose content in the interspecific cross Coffea pseudozanguebariae^{x} Coffea liberica 'dewevrei'. *Plant Breeding*. (2000) 119:165–8. doi: 10.1046/j.1439-0523.2000.00464.x

28. Mccusker RR, Goldberger BA, Cone EJ. Caffeine content of specialty coffees. *J Anal Toxicol*. (2003) 27, 520–522. doi: 10.1093/jat/27.7.520

29. Perrone D, Donangelo CM, Farah A. Fast simultaneous analysis of caffeine, trigonelline, nicotinic acid and sucrose in coffee by liquid chromatography–mass spectrometry. *Food Chem*. (2008) 110:1030–5. doi: 10.1016/j.foodchem.2008.03.012

30. Yang N, Liu C, Liu X, Degn TK, Munchow M, Fisk I. Determination of volatile marker compounds of common coffee roast defects. *Food Chem*. (2016) 211:206–14. doi: 10.1016/j.foodchem.2016.04.124

31. Tressl R, Wondrak GT, Garbe LA, Krüger RP, Rewicki D. Pentoses and hexoses as sources of new melanoidin-like Maillard polymers. *J Agri Food Chem*. (1998) 46:1765–6.

32. Ginz M, Balzer HH, Bradbury AG, Maier HG. Formation of aliphatic acids by carbohydrate degradation during roasting of coffee. *Eu Food Res Technol*. (2000) 211:404–10.

33. Nygren P, Fernández MP, Harmand JM, Leblanc HA. Symbiotic dinitrogen fixation by trees: an underestimated resource in agroforestry systems? *Nutrient Cycl Agroecosys*. (2012) 94:123–160. doi: 10.1007/s10705-012-9542-9

34. Boreux V, Vaast P, Madappa LP, Cheppudira KG, Garcia C, Ghazoul J. Agroforestry coffee production increased by native shade trees, irrigation, and liming. *Agronomy Sustain Develop*. Paris (2016) 36:1–9. doi: 10.1007/s13593-016-0377-7

35. Boulter D. Protein synthesis in plants. *Annu Rev Plant Physiol*. (1970) 21:91–114.

36. Kucey R, Paul EA. Carbon flow in plant microbial associations. *Science*. (1981) 6:473. doi: 10.1126./science.213.4506.473

37. Stumpf W, Conn PM, Preiss J. *The Biochemistry of Plants: Carbohydrates*: Academic Press (2012). doi: 10.1016/C2009-0-02820-7

38. Boardman NT. Comparative photosynthesis of sun and shade plants. *Annu Rev Plant Physiol*. (1977) 28:355–77.

39. Robarts RD, Zohary T. Temperature effects on photosynthetic capacity, respiration, and growth rates of bloom-forming cyanobacteria. *N Z J Mar Freshwater Res*. (1987) 21:391–9.

40. Liu, Yang N, Yang Q, Ayed C, Linforth R, Fisk ID, et al. Enhancing Robusta coffee aroma by modifying flavour precursors in the green coffee bean. *Food Chem*. (2019). 281:8–17.

41. Grosch W. (2001). Chemistry III: volatile compounds. *Coffee: recent Develop* 68–89. doi: 10.1002./9780470690499.ch3

42. Maillard LC. Action des acidesamines sur les sucres: formation des melanoidines par voie methodique. *CR Acad Sci(Paris)*. Paris (1912) 154:66–8.

43. Bradbury AGW, Halliday DJ. *Polysaccharides in Green Coffee Beans*. Paris: ASIC (1987).

44. Bradbury AGW, Halliday DJ. Chemical structures of green coffee bean polysaccharides. *J Agric Food Chem*. (1990) 38:389–92.

45. Wilson A, Petracco M, Illy E. Some preliminary investigations of oil biosynthesis in the coffee fruit and its subsequent re-distribution within green and roasted beans. *Proceedings of the 17th International Conference on Coffee, Science*. (1997) 92.

46. Trugo LC, Macrae R. *The Use of the Mass Detector for Sugar Analysis of Coffee Products*. Paris, France: ASIC (1985).

47. Bradbury, AGW. LA Carbohydrates. In: Clarke RJ, Vitzthum OG (eds.) *Coffee: Recent Development*. Cornwall: Blackwell Science Ltd (2001).

frontiers | Frontiers in Nutrition

TYPE Original Research
PUBLISHED 15 August 2022
DOI 10.3389/fnut.2022.965796

OPEN ACCESS

EDITED BY
Mingquan Huang,
Beijing Technology and Business University, China

REVIEWED BY
Tingting Zou,
Beijing Technology and Business University, China
Shuang Chen,
Jiangnan University, China

*CORRESPONDENCE
Jiansheng Shen
sjszjnky@163.com
Tao Feng
fengtao@sit.edu.cn

SPECIALTY SECTION
This article was submitted to Food Chemistry, a section of the journal Frontiers in Nutrition

RECEIVED 10 June 2022
ACCEPTED 18 July 2022
PUBLISHED 15 August 2022

CITATION
Sun P, Xu B, Wang Y, Lin X, Chen C, Zhu J, Jia H, Wang X, Shen J and Feng T (2022) Characterization of volatile constituents and odorous compounds in peach (*Prunus persica L*) fruits of different varieties by gas chromatography–ion mobility spectrometry, gas chromatography–mass spectrometry, and relative odor activity value. *Front. Nutr.* 9:965796. doi: 10.3389/fnut.2022.965796

Characterization of volatile constituents and odorous compounds in peach (*Prunus persica L*) fruits of different varieties by gas chromatography–ion mobility spectrometry, gas chromatography–mass spectrometry, and relative odor activity value

Ping Sun[1,2], Bing Xu[1,2], Yi Wang[1,2], Xianrui Lin[1,2], Chenfei Chen[1,2], Jianxi Zhu[1,2], Huijuan Jia[3], Xinwei Wang[4], Jiansheng Shen[1,2]* and Tao Feng[1,2]*

[1]Jinhua Academy of Agricultural Sciences (Zhejiang Institute of Agricultural Machinery), Jinhua, China, [2]School of Perfume and Aroma Technology, Shanghai Institute of Technology, Shanghai, China, [3]The College of Agriculture and Biotechnology, Zhejiang University, Hangzhou, China, [4]Zhengzhou Fruit Research Institute, Chinese Academy of Agricultural Sciences, Zhengzhou, China

The aim of this study is to acquire information for future breeding efforts aimed at improving fruit quality *via* effects on aroma by comparing the diversity of Chinese local peach cultivars across 10 samples of three varieties (honey peach, yellow peach, and flat peach). The volatile components of peach fruits were analyzed and identified by gas chromatography–ion mobility spectrometry (GC-IMS) combined with gas chromatography–mass spectrometry (GC-MS), and the main flavor components of peach fruit were determined by relative odor activity value (ROAV) and principal component analysis (PCA). A total number of 57 volatile components were detected by GC-IMS, including eight aldehydes, nine alcohols, eight ketones, 22 esters, two acids, two phenols, two pyrazines, one thiophene, one benzene, and two furans. The proportion of esters was up to 38.6%. A total of 88 volatile components were detected by GC-MS, among which 40 were key aroma compounds, with an ROAV $\geq$ 1. The analysis results showed that alcohols, ketones, esters, and aldehydes contributed the most to the aroma of peach fruit. PCA demonstrated that (E,E)-2, 6-non-adienal, γ-decalactone, β-ionone, and hexyl hexanoate were the key contributors to the fruit aroma. A reference

for future directional cultivation and breeding could be provided by this study through evaluating the aroma quality of the peach at the cultivar level. The possible reasonable application of these peach fruits pulp will be guided through these research.

KEYWORDS

gas chromatography–ion mobility spectrometry (GC-IMS), peach, odorous compounds, gas chromatography–mass spectrometry (GC-MS), relative odor activity value (ROAV)

Introduction

Peach (*Prunus persica L.*) is a small deciduous tree with edible fruit belonging to the Rosaceae genus *Amycdalus L.* (1). The flowers can be ornamental, the fruit is juicy and can be eaten raw or canned, etc., and the kernels can also be eaten. Peaches with white and yellow flesh are referred to as "longevity peaches" and "immortal peaches." It is also known as the "first fruit in the world" because of its delicious pulp (2). Its history dates back 4000 years. It originated in China and is widely cultivated in the latitude range of 23 to 45° north (3). Thanks to a long planting history and a vast planting area, diligent and intelligent laborers of China have cultivated a variety of colorful peach trees almost everywhere from the southern provinces of Jiangsu and Zhejiang to the northern province of Jilin (4). According to statistics, China is the origin of thousands of peach tree varieties (5).

Due to their thick, juicy flesh, rich aroma and high nutritional value, peaches are a popular fruit on the market (6). Currently, most research on the aroma of peach fruit focuses on the analysis and identification of aroma components of a single variety. However, there are few studies evaluating the aroma quality of peach fruit of different varieties. Therefore, it is necessary to establish and implement an objective method and system for evaluating the aroma of peach fruit. Currently, gas chromatography–ion migration spectrometry, headspace solid-phase microextraction–gas chromatography–mass spectrometry, gas chromatography–olfactometry, electronic nose, etc. are the primary analytical methods for volatile components of aroma (7).

Gas chromatography–ion mobility spectrometry (GC-IMS) is a detection technique that combines gas chromatography and ion mobility spectrometry. This technology overcomes the limitation of the poor separation degree in ion migration technology so that the ion migration signal response in gas chromatography can be identified by the difference in the ion migration rate in the electric field after gas-phase pre-separation, resulting in more chemical information from GC separation (8, 9). The technology is simple and sensitive and requires no pretreatment. It has a wide range of applications, including food flavor analysis and quality detection. Headspace solid-phase microextraction is a common method for the extraction of aroma substances from peach fruit, with the benefits of easy operation, less loss of aroma components, and high sensitivity (10, 11). The purpose of principle component analysis (PCA) is to recombine multiple indicators into several new comprehensive indicators by reducing the data dimensions in order to conduct a comprehensive evaluation (12). This method has been applied to evaluate the aroma quality of Dongbei suancai (13), Tricholoma matsutake Singer (14), and soybean whey tofu (15).

Therefore, in this study, GC-IMS technology was combined with HS-SPME-GC-MS technology and the PCA method to detect and analyze volatile substances in 10 kinds of peach samples of three varieties. Meanwhile, the ROAV method was used to identify key flavor substances in peach fruits. Numerous studies, such as Keemun black tea (16), orange juice (17), and faba bean (18) studies, had used this method for their aroma quality evaluation. In order to provide a theoretical basis for peach fruit variety differentiation, peach fruit aroma detection, and quality evaluation, the principal component comprehensive score model was developed to analyze the similarities and differences of aroma of 10 peach samples using the principal component analysis method. In addition, this study can aid in the selection of peach varieties suitable for public taste and breeding efforts aimed at genetically enhancing peach flavor.

Materials and methods

Experimental materials and reagents

The volatile compounds of honey peach ("Yuanmeng," "Yihe," "Yuandong," "Baifeng," "Wanhujing"), yellow peach ("Huangguifei," "Jinxiu," "Jinyuan"), and flat peach ("Ruipan-19," "Yulu") were studied. Because early August is the best maturation period for peach, we collected the samples from a local commercial orchard in Jinhua city, Zhejiang Province, on 1 August 2021. At maturity, ripe fruits free of physical damage and fungal infection were selected based on color, firmness, and aroma of the peaches by the local farmer. Ripe peaches were brought back to the laboratory in Shanghai on the same day, pureed, sealed, and stored in a −18°C freezer for analysis (within

24 h). A homologous series of alkanes (C_8–C_{30}) were purchased from Sigma Aldrich (St. Louis, MO, United States). Purified water was obtained using a Milli-Q purification system (Model Milli-Q Advantage A10, Millipore, Bedford, MA, United States).

Methods

Gas chromatography sample pretreatment

In order to ensure the reliability of the carboxen polydimethyl siloxane (CAR-PDMS) fiber, it should be aged for 15 min at 250°C. In tandem with the description by Zhu and Xiao (4) and many pre-experiments, the best operational procedure was selected as follows: 5 g peach puree taken in 20-mL screw capped vials fitted with PTEE silicone septa. Then, 75 μm carboxen polydimethyl siloxane (CAR-PDMS) fiber was exposed to the headspace of the sample in a water bath at 60°C for 30 min. Thereafter, SPME fiber was directly introduced into the GC injector for desorption and analysis at 250°C for 5 min. All the experiments were performed in triplicate.

Conditions of gas chromatography–mass spectrometry

The samples were analyzed using the HP-5MS column (30 m × 0.25 mm × 0.25 μm, Agilent, Santa Clara, CA, United States), with purified helium as the carrier gas, at a constant flow rate of 1 ml/min. The oven temperature was maintained at 40°C for 5 min, then increased to 100°C at a rate of 3°C/min, increased to 230°C at a rate of 3°C/min, and finally held at 230°C for 5 min. The injector and FID temperatures were set to 250°C and 280°C, respectively. The injection port was set at 250°C with splitless mode. For mass spectrometry analysis, electron ionization (EI) at 70 eV was used, and the MS scanning was undertaken from 40 to 450 m/z. The ion source temperature was 230°C. The mass spectrometer was operated in the full scan mode, and ChemStation software (Agilent Technologies) was used to determine the area of each peak. Identification of volatile compounds was achieved by comparing the mass spectra with the data system library (NIST 20) and retention index. The experiments were performed in triplicate.

Conditions of gas chromatography–ion mobility spectrometry

Volatile fingerprint analysis of Jinhua peaches was performed using a GC-IMS composed of an Agilent 490 gas chromatograph (Agilent Technologies, United States) and an IMS instrument (FlavourSpec®, Gesellschaft für Analytische Sensorsysteme mbH, Dortmund, Germany). The GC apparatus was equipped with an autosampler (CTC Analytics AG, Zwingen, Switzerland) device that connected to a headspace sampling unit. Before GC-IMS analysis, each peach sample (5 mL) was transferred into the headspace sampling vial (20 mL) and incubated at 40°C for 20 min of equilibration. Thereafter, 200 μL of headspace gas was extracted using a heated (50°C) syringe and automatically injected by the autosampler (in the splitless mode). For GC analysis, volatile compounds were separated by using an FS-SE-54-CB-1 capillary column (15 m × 0.53 mm, 1 μm film thickness) at 40°C with nitrogen (> 99.95% purity) used as carrier gas using the programmed procedure: 2 mL/min for 2 min, increased to 10 mL/min within 10 min, and further increased to 150 mL/min within 10 min. The IMS instrument was programmed at 45°C with a constant drift gas (nitrogen, > 99.95% purity) flow in a drift tube under a flow rate of 150 mL/min. The retention index (RI) of each compound was calculated using n-ketones C_4–C_{12} (Sinopharm Chemical Reagent Beijing Co., Ltd., China) as external references (19).

Qualitative and quantitative analyses of aroma components

Data processing of the gas chromatography–mass spectrometry

Matching retention times of authentic standards, retention indices (RIs), and mass spectra in the NIST20 database identified the compounds. RIs were determined by injecting the homologous series of alkanes (C_8 - C_{30}) (6). The retention index was calculated as shown in Equation 1:

$$\text{Retention index} = 100\,n + 100\,(t_a - t_n)/(t_{n+1} - t_n) \quad (1)$$

In the formula, t_a is the retention time of the chromatographic peak a and t_n,t_{n+1} is the retention time of Cn_n and C_{n+1} in orthoalkanes.

The relative content of each volatile compound in peach fruit was calculated by peak area normalization:

$$\text{Relative amount}(\%) = M/N \times 100 \quad (2)$$

In the formula, M is the peak area of individual component aroma substances and N is the overall peak area.

Data processing of the gas chromatography–ion mobility spectrometry

The qualitative analysis of volatile compounds was determined by the RI value and drift time of standards in the GC-IMS library (Gesellschaft für Analytische Sensorsysteme mbH, Dortmund, Germany). The quantitative analysis of volatile compounds was determined by the signal intensity of each compound obtained using Laboratory Analytical Viewer (LAV, G.A.S., Dortmund, Germany). In addition, the fingerprints and the difference profiles of volatile molecules in peaches were obtained by Reporter and Gallery plug-ins. All analyses were performed in triplicate.

Determination of main flavor compounds in peach fruit by the relative odor activity value method

With reference to the ROAV method, the contribution of volatile flavor substances in peach fruit was evaluated, and then the main flavor substances were determined. The threshold in ROAV calculation was selected by olfactory thresholds in water taken from the literature (20). Compounds with ROAVs equal to or greater than 1 were actually the main flavor components of the analyzed samples, and compounds with ROAVs greater than 0.1 and less than 1 play a embellish role in aroma (21). The components that contribute most to the total flavor of a solid peach sample were defined as follows:

$ROAV_{max}$ = 100, then other components (a):

$$ROAV_a \approx 100 \times C_a/C_{max} \times T_{max}/T_a \quad (3)$$

In the formula, C_a is the relative content of the volatile components (%), T_a is the sensory threshold for the volatile components (ppb), and C_{max},T_{max} is the relative contents of volatile components with the largest contribution to the total aroma of samples (%) and their sensory threshold (ppb).

Statistical analysis

GC × IMS Library Search V 2.2.1 analysis software, built-in NIST database, and IMS database were used for qualitative analysis of volatile flavor substances in the samples. The Reporter, Gallery Plot, and Dynamic PCA plug-ins were combined with Laboratory Analytical Viewer (LAV, G.A.S., Dortmund, Germany) to establish standard curves of samples for quantitative analysis, and then the differences of volatile organic compounds among samples of honey peach, yellow peach, and flat peach were compared intuitively. The data from GC-MS were standardized using TBtools (Toolbox for Biologists) v1.098696 software for heat map, and principal components analysis (PCA) was used to evaluate similarity and difference using Origin 2022 software.

Results and discussion

Fingerprints of volatile compounds in peaches by HS-gas chromatography–ion mobility spectrometry analysis

The background of the two-dimensional top view generated by the Reporter plug-in is blue, and the vertical red line at abscissa 1.0 represents the RIP peak (reaction ion peak, normalized). According to the presence or shade of a peak (color point), differences in composition and concentration between different samples can be visualized. The vertical axis represents the gas chromatography retention time (s), while the horizontal axis represents the ion migration time (normalized treatment). Each point on either side of the RIP peak represents a volatile organic compound. The color represents the concentration of the substance; white indicates a low concentration, and red indicates a high concentration; the darker the color, the higher the concentration. Diffferentiation spectrum is a method to analyze the difference of GC-IMS spectrum (top view). It uses a particular sample as a reference and compares all volatile substances in different samples to determine their differences. Red indicates that the concentration of volatile substances in the sample is greater than that in the reference sample, whereas blue indicates that the concentration of volatile substances in the sample is less than that in the reference sample. **Figure 1A** demonstrates that the volatile organic compounds of "Baifeng," "Yihe," and "Yuandong" peaches were similar, whereas the volatile organic compounds of "Yuanmeng" and "Wanhujing" peaches were vastly dissimilar from the other three peach samples. **Figure 1C** shows that the volatile organic compounds of "Jinxiu" and "Huangguifei" yellow peaches were similar, whereas the differences between "Jinyuan" and the other two samples were obvious. **Figure 1B** found that the volatile organic compounds of "Ruipan- 19" and "Yulu" flat peaches were similar, but the volatile compounds of "Yulu" were demonstrably greater than those of "Ruipan-19".

In HS-GC-IMS, volatile compounds with varying retention times were ionized separately by the ion source to form molecular ion groups (15). **Table 1** presents the volatile component information obtained *via* GC-IMS analysis. By comparing the relative retention index (RI) and the drift time (Dt) of the standard in the GC-IMS library, volatile compounds were identified (22). As shown in **Table 1**, the GC-IMS profiles of the 10 samples revealed that the C chains of 57 volatile organic compounds were all within the range of $C_4 \sim C_{12}$; these included eight aldehydes, nine alcohols, eight ketones, 22 esters, two acids, two phenols, two pyrazines, one thiophene, one benzene, and two furans. The majority of the 57 known volatile components qualitatively identified were prevalent aroma components in peach fruit. Rarely reported in the study of peach fruit volatile components were neryl acetate, citronellyl acetate, geranyl formate, bread thiophene, methyl ortho-anisate, 2-ethylpyrazine, 2-pentylfuran, diethyl malonate, cumin aldehyde, and other volatile components. These substances typically had unique aromas, such as neryl acetate, which had a rose-like odor; citronellyl acetate, which had pear and apple aromas; diethyl malonate, which had apple and pineapple aromas; bread thiophene, which had sweet, almond, fruity, heliotrope, and nutty flavors; and 2-ethylpyrazine, which smelled like nuts, fish, meat, potatoes, and coco.

Figure 2 depicts the volatile organic compound (VOC) fingerprints of various peaches, including honey peaches, yellow

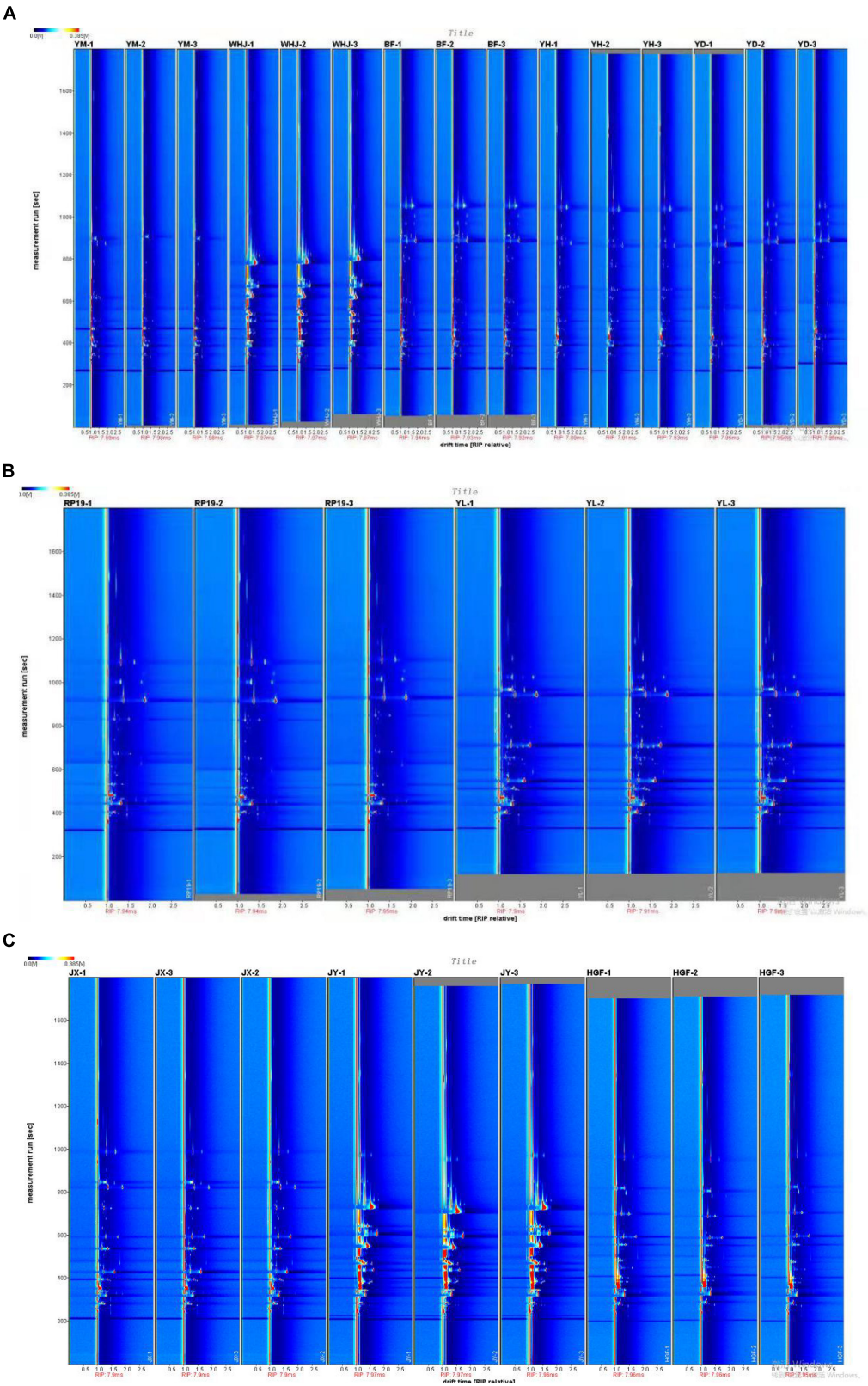

FIGURE 1
Gas-phase ion migration spectrum of peach samples [**(A)**-honey peach, **(B)**-flat peach, **(C)**-yellow peach].

TABLE 1 Qualitative results for all volatile components on the basis of gas chromatography–ion mobility spectrometry (GC-IMS).

No.	Name	CAS	Molecular formula	Molecular weight	RI[a]			RT[b](s)			DT[c](ms)			Aroma description
					Honey	Flat	Yellow	Honey	Flat	Yellow	Honey	Flat	Yellow	
1	p-Anisaldehyde	123-11-5	$C_8H_8O_2$	136.15	1268.2	—	—	898.55994	—	—	1.231	—	—	sweet floral balsam
2	Phenylacetaldehyde	122-78-1	C_8H_8O	120.15	1054.1	—	—	614.445	—	—	1.554	—	—	green sweet floral
3	Tetrahydrothiophene	1003-04-9	C_4H_6OS	102.15	809.5	—	—	387.65997	—	—	1.327	—	—	garlic meaty green
4	allyl isothiocyanate	57-06-7	C_4H_5NS	99.15	918.2	912	—	472.68	467.41498	—	1.11	1.395	—	strong pungent mustard
5	*cis*-dihydrocarvone	3792-53-8	$C_{10}H_{16}O$	152.23344	1183	—	—	772.98	—	—	1.313	—	—	herbal warm
6	Isophorone	78-59-1	$C_9H_{14}O$	138.21	1132.5	—	—	711.94495	—	—	1.263	—	—	woody sweet green
7	2-non-anone	821-55-6	$C_9H_{18}O$	142.24	1122.5	—	—	700.44	—	—	1.4	—	—	cheesy green fruity,
8	isoamyl butyrate	106-27-4	$C_9H_{18}O_2$	158.24	1091.4	—	—	663.975	—	—	1.401	—	—	fruity green apricot
9	2-Octanol	123-96-6	$C_8H_{18}O$	130.23	1005.6	—	—	555.555	—	—	1.446	—	—	fresh spicy green
10	ethyl 3-methylbutyrate	108-64-5	$C_7H_{14}O_2$	130.18	885.6	—	—	445.37997	—	—	1.255	—	—	fruity sweet apple
11	2-Methylbutanal	96-17-3	$C_5H_{10}O$	86.13	729.8	—	—	335.205	—	—	1.16	—	—	musty cocoa phenolic
12	4-ketoisophorone	1125-21-9	$C_9H_{12}O_2$	152.19	1108.7	—	—	684.83997	—	—	1.326	—	—	citrus floral musty
13	Hexan-2-one	591-78-6	$C_6H_{12}O$	100.16	848.6	—	—	416.32498	—	—	1.202	—	—	fruity fungal meaty buttery
14	geranyl formate	105-86-2	$C_{11}H_{18}O_2$	182.26	1326.3	—	—	1006.98	—	—	1.853	—	—	green floral citrus
15	Methyl anisate	121-98-2	$C_9H_{10}O_3$	166.17	1308.5	1334.5	—	970.12494	1024.5299	—	1.808	1.814	—	herbal anise sweet
16	Neryl acetate	141-12-8	$C_{12}H_{20}O_2$	196.29	1380.6	—	—	1128.6599	—	—	1.239	—	—	floral rose soapy citrus
17	citronellyl acetate	150-84-5	$C_{12}H_{22}O_2$	198.3	1408.8	—	—	1197.2999	—	—	1.482	—	—	floral green rose fruity
18	Isobornyl acetate	125-12-2	$C_{12}H_{20}O_2$	196.29	1294.2	—	—	941.45996	—	—	1.385	—	—	herbal woody sweet

(Continued)

10.3389/fnut.2022.965796

TABLE 1 Continued

No.	Name	CAS	Molecular formula	Molecular weight	RI[a]			RT[b](s)			DT[c](ms)			Aroma description
					Honey	Flat	Yellow	Honey	Flat	Yellow	Honey	Flat	Yellow	
19	Isopulegyl acetate	89-49-6	$C_{12}H_{20}O_2$	196.286	—	1290.4	—	—	934.82996	—	—	1.386	—	minty leafy
20	2-Hexen-1-ol	2305-21-7	$C_6H_{12}O$	100.16	—	916.8	—	—	471.50998	—	—	1.183	—	fruity green leafy
21	Isopentyl formate	110-45-2	$C_6H_{12}O_2$	116.16	—	824.7	830.1	—	398.58	402.47998	—	1.277	1.267	fruit green
22	2-Methyl-1-butanol	137-32-6	$C_5H_{12}O$	88.15	824.7	817.5	829.3	398.58	393.31497	401.895	1.24	1.471	1.47	ethereal fusel alcoholic fatty
23	Aniline	62-53-3	C_6H_7N	93.13	—	959.3	—	—	509.53497	—	—	1.423	—	unknown
24	2-formyl-5-methylthiophene	13679-70-4	C_6H_6OS	126.18	1065.7	1086	1156	629.45996	656.565	739.6395	1.169	1.173	1.176	sweet almond cherry
25	Methyl benzoate	93-58-3	$C_8H_8O_2$	136.15	—	1105.9	—	—	681.72	—	—	1.206	—	wintergreen almond floral
26	Ethyl benzoate	93-89-0	$C_9H_{10}O_2$	150.17	1218.1	1209	—	821.73	808.47	—	1.248	1.262	1218.1	fruity dry musty sweet
27	p-Methyl guaiacol	93-51-6	$C_8H_{10}O_2$	138.16	1214.3	1230.2	—	816.07495	839.67	—	1.179	1.179	1214.3	spicy clove woody leathery
28	Methyl 2-methoxybenzoate	606-45-1	$C_9H_{10}O_3$	166.17	—	1307.2	—	—	967.39496	—	—	1.234	—	herbal floral fruity
29	Geranyl acetate	105-87-3	$C_{12}H_{20}O_2$	196.29	—	1427.7	—	—	1245.855	—	—	1.224	—	floral rose lavender green
30	Thymol	89-83-8	$C_{10}H_{14}O$	150.22	1241.8	1255.7	—	857.22	878.67	—	1.253	1.25	—	herbal thyme phenolic
31	2-Methylpropanal	78-84-2	C_4H_8O	72.11	—	—	635.1	—	—	281.97	—	—	1.112	fresh aldehydic floral green
32	2-Pentanone	107-87-9	$C_5H_{10}O$	86.13	—	—	761.7	—	—	355.28998	—	—	1.137	sweet fruity ethereal
33	Pentanal	110-62-3	$C_5H_{10}O$	86.13	756.9	—	735.6	352.16998	—	338.715	1.187	—	1.171	bready fruity nutty berry
34	Isopentanal	590-86-3	$C_5H_{10}O$	86.13	—	—	734.6	—	—	338.12997	—	—	1.395	chocolate peach fatty
35	3-Methyl-2-butenal	107-86-8	C_5H_8O	84.12	845.8	—	819.6	414.18	—	394.875	1.088	—	1.364	sweet fruity pungent
36	Butyl acetate	123-86-4	$C_6H_{12}O_2$	116.16	—	—	865	—	—	428.99997	—	—	1.609	fruity sweet banana
37	2-Methylbutanol	616-16-0	$C_5H_{12}O$	88.15	—	—	809	—	—	387.27	—	—	1.473	fermented fatty
38	Methional	3268-49-3	C_4H_8OS	104.17	—	—	988.7	—	—	537.615	—	—	1.391	musty potato tomato
39	Methyl 2-furoate	611-13-2	$C_6H_6O_3$	126.11	—	956.4	991.9	—	506.805	540.735	—	1.477	1.171	fruity mushroom sweet
40	Ethyl 2-hydroxy-4-methylpentanoate	10348-47-7	$C_8H_{16}O_3$	160.2108	—	—	1037	—	—	592.995	—	—	1.299	fresh black berry[d]

(Continued)

10.3389/fnut.2022.965796

TABLE 1 Continued

No.	Name	CAS	Molecular formula	Molecular weight	RI[a]			RT[b](s)			DT[c](ms)			Aroma description
					Honey	Flat	Yellow	Honey	Flat	Yellow	Honey	Flat	Yellow	
41	Octen-3-ol	3391-86-4	$C_8H_{16}O$	128.21	—	—	1035.4	—	—	591.045	—	—	1.738	mushroom earthy green
42	2-formyl-5-methylthiophene	13925-00-3	$C_6H_8N_2$	108.14	—	—	1068.5	—	—	633.165	—	—	1.179	peanut butter musty
43	3-isopropyl-2-methoxypyrazine	25773-40-4	$C_8H_{12}N_2O$	152.19	—	—	1143.4	—	—	724.62	—	—	1.24	pea earthy beany
44	Cumin aldehyde	122-03-2	$C_{10}H_{12}O$	148.20	—	—	1219.1	—	—	823.095	—	—	1.891	spicy cumin green herbal
45	p-Cymen-7-ol	536-60-7	$C_{10}H_{14}O$	150.22	1265.2	1307.8	1334	893.685	968.75995	1023.36	1.887	1.33	1.326	harsh plastic acrylate fruity
46	Methyl chavicol	140-67-0	$C_{10}H_{12}O$	148.2	1198.4	—	1234.7	793.25995	—	846.3	1.239	—	1.231	sweet spice green
47	ethyl acrylate	140-88-5	$C_5H_8O_2$	100.12	—	—	744.9	—	—	344.565	—	—	1.401	harsh plastic acrylate fruity
48	2-pentyl furan	3777-69-3	$C_9H_{14}O$	138.21	—	—	1025.8	—	—	579.345	—	—	1.252	fruity green earthy
49	3-Methyl valeric acid	105-43-1	$C_6H_{12}O_2$	116.16	955.5	—	994.4	506.025	—	543.26996	1.605	—	1.253	cheesy green fruity sweaty
50	diethyl malonate	105-53-3	$C_7H_{12}O_4$	160.17	1079.7	—	1078.9	647.985	—	647.00995	1.252	—	1.257	sweet fruity green apple
51	Propyl butanoate	557-00-6	$C_8H_{16}O_2$	144.21	—	—	929.1	—	—	482.235	—	—	1.252	bitter sweet apple fruity
52	2-Butylfuran	4466-24-4	$C_8H_{12}O$	124.18	—	—	932	—	—	484.77	—	—	1.191	fruity wine sweet spicy
53	3-Octanol	589-98-0	$C_8H_{18}O$	130.2279	—	—	1005.6	—	—	555.555	—	—	1.385	earthy mushroom herbal melon
54	1-Phenylethyl acetate	93-92-5	$C_{10}H_{12}O_2$	164.2	—	—	1218.1	—	—	821.73	—	—	1.067	fruity berry green
55	Benzyl acetate	140-11-4	$C_9H_{10}O_2$	150.17	1197.5	1201.8	1216.7	792.08997	798.13495	819.58496	1.313	1.312	1.323	sweet floral fruity jasmin
56	Isopulegol	89-79-2	$C_{10}H_{18}O$	154.2493	—	—	1191.7	—	—	783.89996	—	—	1.381	minty cooling medicinal woody
57	6-Methyl-5-hepten-2-one	110-93-0	$C_8H_{14}O$	126.2	—	—	1008.2	—	—	558.48	—	—	1.168	citrus green musty lemongrass

[a] RI, retention index;[b] RT, retention time;[c] DT, migration time; [d] G Lytra, S Tempere, G De Revel, JC Lytra et al. (23); "–" indicates not detected.

10.3389/fnut.2022.965796

10.3389/fnut.2022.965796

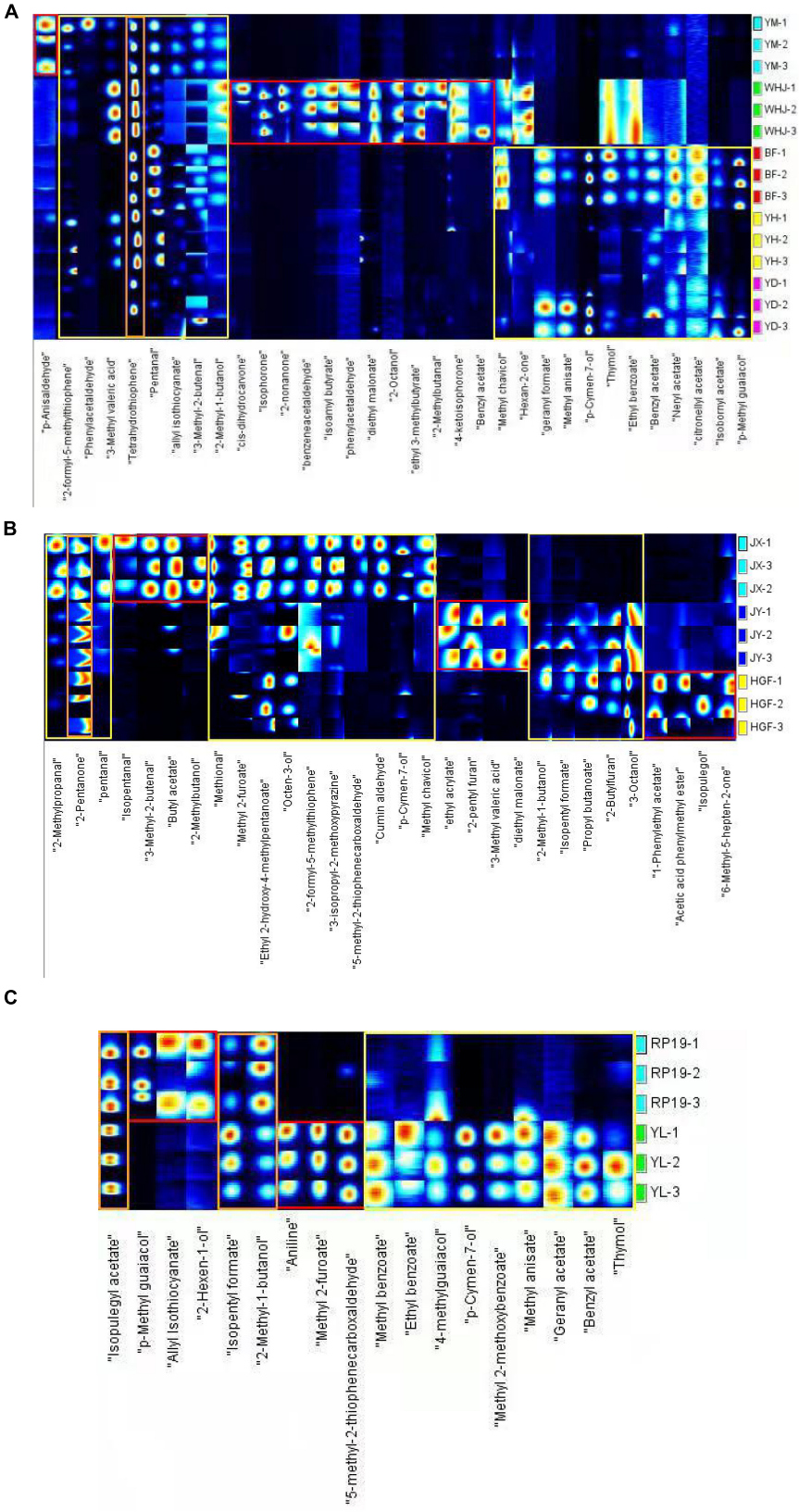

FIGURE 2
Gallery Plot of volatile organic compounds in peach samples [**(A)**-honey peach; **(B)**-yellow peach; **(C)**-flat peach].

peaches, and flat peaches. Each row represents the signal peaks extracted from a single sample, while each column represents the signal peaks of the same volatile organic compounds extracted from multiple samples. Figure 2 also shows the complete VOC information of each sample and the differences between the peach samples. The fingerprint spectrum of Gallery Plot revealed the variation of flavoring substances in various samples more clearly. Each column represents a flavor substance in various samples, with the color intensity representing the concentration level. Through longitudinal comparison, the concentration of various flavoring substances revealed a very intuitive rule. The fingerprints of volatile organic compounds collected from peach fruits were roughly divided into three distinct color regions, with the red region indicating that the volatile organic compounds in this region were unique to certain peach fruits, or that their concentration was significantly higher than that in other regions. The yellow area indicates that the volatile organic compound content of various peach fruits varied greatly in this region, whereas the orange area indicates that there were less differences between large peach samples in this region. Figure 2A demonstrates that "Yuanmeng," "Wanhujing," "Baifeng," "Yihe," and "Yuandong" peaches had a high concentration of 3-tetrahydrothiophenone and possessed special aromas such as green vegetables and butter. A total of five honey peach samples had significantly different levels of volatile organic compounds, namely, 3-methylpentanoic acid, valeraldehyde, allyl isothiocyanate, 3-methyl-2-butenal, and 2-methyl-1-butanol, and the odor of these compounds was predominantly fruity. "Wanhujing" and "Yihe" contained significantly more 3-methyl-pentanoic acid than the other three varieties. "Baifeng" and "Yihe" contained more valeraldehyde, while "Yuandong" and "Baifeng" contained more geranyl formate. Anisaldehyde was a special flavoring component in "Yuanmeng," whereas cis-dihydrocarvone, isophorone, 2-non-one, and diethyl malonate were special ingredients in "Wanhujing". Figure 2B demonstrates that the 2-pentanone content of "Jinxiu," "Jinyuan," and "Huangguifei" yellow peaches were relatively high, exhibiting a sweet fruit and banana flavor with a slight variation in fermentation. The distinctive components of "Jinxiu" were iso-valeraldehyde, 3-methyl-2-butenal, and (R)-2-methyl-1-butanol. Specific volatile organic compounds of "Jinyuan" were ethyl acrylate, 2-pentylfuran, 3-methylpentanoic acid, and diethyl malonate. The distinctive constituents of "Huangguifei" included sulfenyl acetate, benzyl acetate, methyl heptenone, and isopropyl alcohol. Jinxiu contained higher levels of methyl 2-furoate, cumin aldehyde, and pyrazine than "Jinyuan" and "Huangguifei," while "Huangguifei" contained more 3-octanol. As shown in Figure 2C, the content levels of iso-humenthol acetate, iso-amyl formate, and 2-methyl butanol in "Ruipan-19" and "Yulu" flat peach were high, indicating the flavor of fruit and fragrance. The specific volatile organic compounds of Ruipan-19 included 4-methylguaiacol, 2-hexenol, and allyl isothiocyanate, whereas "Yulu" had aminobenzene, bread thiophene, and methyl 2-furoate. "Yulu" contained more volatile organic compounds, such as methyl benzoate, benzyl acetate, and geranyl acetate, than "Ruipan-19."

Distinction of different peach samples by principal component analysis

Based on volatile components of peach fruits identified through GC-IMS, PCA statistics were used to analyze different honey peaches (such as the "Yuanmeng," "Wanhujing," "Baifeng", "Yihe" and "Yuandong"), yellow peaches (such as "Jinxiu," "Jinyuan," "Huangguifei"), and flat peaches (such as "Ruipan-19" and "Yulu"). Figure 3 depicts the results of Dynamic PCA plug-in analysis. Figure 3A demonstrates that PC-1 and PC-2 had variance contribution rates of 59% and 12%, respectively, and a cumulative variance contribution of 71%, which is greater than the trusted value of 60%. Consequently, PC-1 and PC-2 are adequate to reflect the distinctions between various peach samples. In the PCA diagram, a close distance between samples indicates a small difference, whereas a far distance indicates a significant difference. As shown in Figure 3A, the differences between the three parallel groups of the same sample were negligible, whereas the volatile organic compounds in the peach fruits of different peaches were significantly diverse. The "Wanhujing" peach, which was the most special among the five kinds of honey peaches, was distinct from the other four varieties. The close distance between "Yuanmeng" and "Yihe" honey peaches indicated that their volatile composition and flavor were similar. Figure 3B reveals that the cumulative variance contribution rate of PC-1 and PC-2 was 88%, which can reflect the difference between the three yellow peach samples. It was evident from that the distance between different kinds of yellow peaches was quite large, indicating that the similarity of volatile organic compounds in these three yellow peach varieties was low. Similarly, Figure 3C demonstrates that the composition of volatile organic compounds in "Ruipan-19" and "Yulu" flat peach was relatively not identical. Consequently, GC-IMS results combined with PCA can quickly and easily differentiate between various peach samples. In addition, this method can be served as a guide for distinguishing peach fruit from different producing regions, harvesting stages, and storage methods.

Gas chromatography–mass spectrometry analysis of peach fruit in different peach varieties

Names and relative contents of volatile flavor compounds in peach fruits of different varieties are shown in Table 2. A total of 88 kinds of volatile flavor compounds were detected in 10

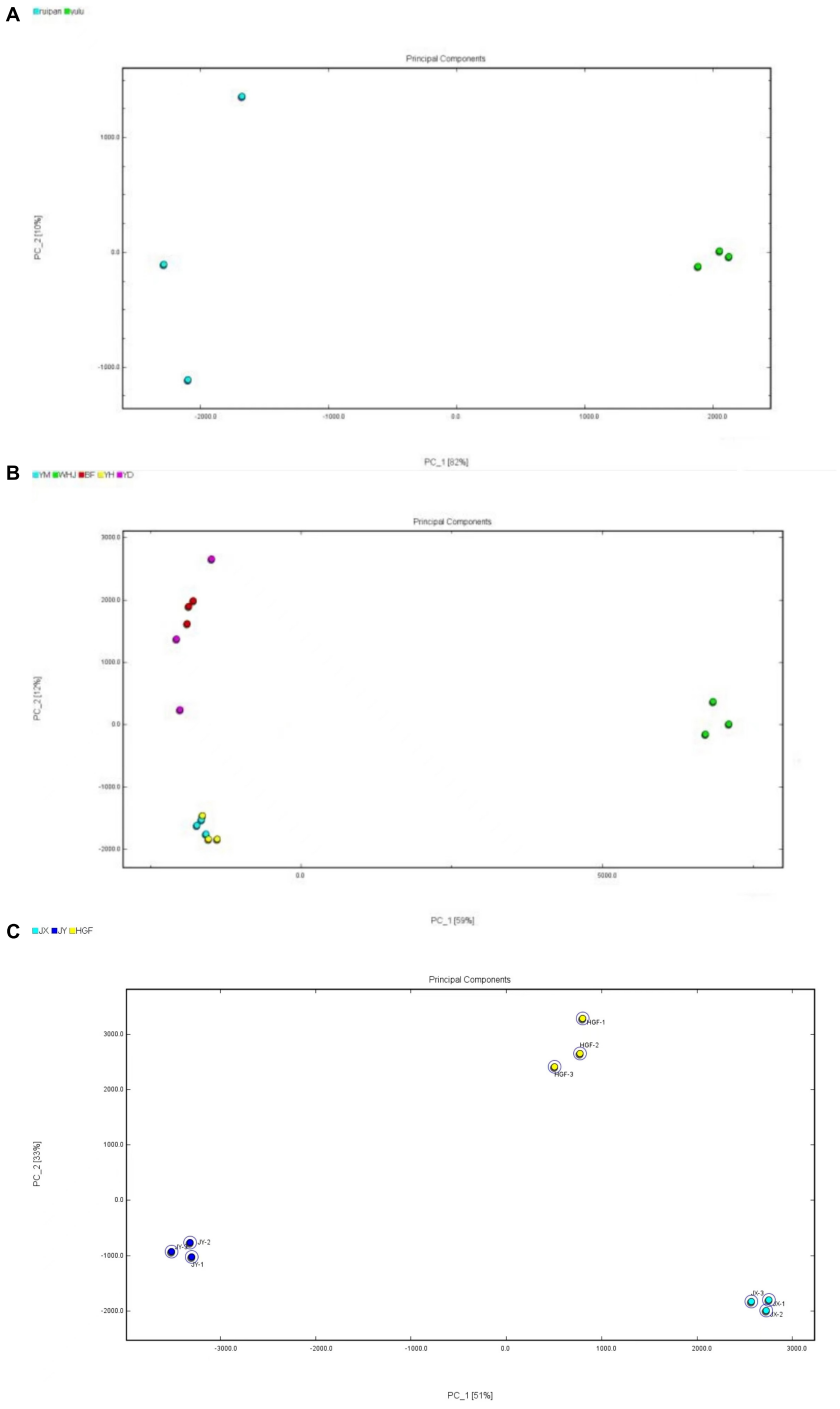

FIGURE 3
Principal component analysis (PCA) diagrams of peach samples [**(A)**-honey peach; **(B)**-yellow peach; **(C)**-flat peach].

peaches. The quantity and relative content of volatile flavor compounds in peach samples were different.

Esters are considered major contributors to fruity and floral aromas, and high levels of esters should give peaches a pleasant flavor (24). A total of eight esters were found in peach samples, namely, ethyl palmitate (17), (E,E)-farnesyl acetate (32), (E)-2-hexen-1-yl hexanoate (38), hexyl hexanoate (42), bornyl acetate (47), eugenyl acetate (57), hexyl acetate (64), and ethyl valerate (78), contributing to 9.09% of the total volatiles (**Table 2**). Among the three groups, the sum of the esters was highest in

honey peach and lower in the yellow peach group. Moreover, a significantly higher content of total esters was found in "Wanhujing" and "Yuandong" than in "Yuanmeng," "Yihe," and "Baifeng" (Table 2). Regarding individual ester contents, the most abundant content of hexyl acetate (64) was found in "Wanhujing." High hexyl hexanoate (42) levels were observed in "Yulu," with contents of about 0.525% (Table 2). For the other six esters, the levels were generally lower than 0.1%; therefore, it is not meaningful to be discussed.

There were five lactones found in groups, namely, γ-hexalactone (11), δ-tridecalactone (24), γ-decalactone (26), γ-octalactone (34), and γ-dodecalactone (49), and these accounted for 5.68% of the total volatiles. The most abundant content of compounds is γ-decalactone (26) in honey peach of "Baifeng" and "Yuandong," except "Yuanmeng" and "Wanhujing," and high γ-dodecalactone (49) levels were observed in "Yihe." Flat peach had not been detected any lactones. In yellow peach, "Huangguifei" had very high levels of γ-dodecalactone (49), with 0.13%. The other three lactones were found only in individual peaches, for example, γ-octalactone (34) was higher in "Yuandong," with 0.235%. Lactones, particularly γ-decalactone and -decalactone, have been reported as "character-affecting" compounds in peach and nectarine aromas. In this study, honey peaches had significantly a higher content of γ-decalactone (26) than yellow peaches and flat peaches. However, Wang et al. (25) concluded that flat peaches contain significantly higher amounts of γ-decalactone (26) than other peaches. There was significant differences between honey peaches and other two peaches.

In total, 11 aldehydes were detected, and benzaldehyde (1) and (E)-2-hexenal (2) were dominant, with contents ranging from 0 to 2.288% and 0 to 1.206%, respectively (Table 2). "Yuanmeng" had the highest benzaldehyde content, with 2.288%, and "Yuandong" had the most abundant content of (E)-2-hexenal among all the taxa, with 1.206%. In all samples, only "Huangguifei" was not detected with aldehydes. Several taxa, "Yihe," "Baifeng," and "Yulu," had high levels of hexanal (53), ranging from 0 to 0.258%. For the other eight aldehydes, the levels were generally lower, except "Yuanmeng" and "Yuandong," where (E,E)-2,4-heptadienal (5) was abundant, with 0.385% and 0.167%, respectively; high β-cyclocitral (36) levels were observed in "Yuandong," with 0.206%; and "Jinyuani" had very high levels of (E,E)-2,4-hexadienal (80), with 0.296%.

The total content of terpenoids accounted for 18.18% of total volatiles. The sum of terpenoids in "Yuandong" and "Wanhujing" was significantly higher than in other samples, and it was also significantly higher in yellow peaches. Of 16 terpenoids found, dextro-limonene (33) was the major compound. There was no terpenoid detected in "Yulu," but dextro-limonene was high in some cultivars with honey peach and yellow peach: "Yuandong," "Yihe," "Wanhujing," and "Jinxiu." The second abundant terpenoid was styrene (13). Levels of dextro-limonene tended to be positively correlated with the styrene content, with high levels in "Yuandong," "Yihe," and "Jinxiu." High (+)-aromadendrene (82) levels were observed in "Jinyuan," with 6.799%. "Huangguifei" had the most abundant content of α-pinene (73), with 3.827%.

In this research, 12 ketones were found, including (E)-geranyl acetone (27), β-ionone (28), 2-octanone (30), dihydro-β-ionone (44), (E)-β-ionone (52), and watermelon ketone (79), contributing to 13.64% of the total volatiles. The sum of ketones in "Wanhujing" was significantly higher than that in "Baifeng," "Huanguifei," "Jinyuan," and "Yulu." Dihydro-β-ionone (44) and (E)-geranyl acetone (27) were dominant, with contents ranging from 0 to 1.488% and 0 to 1.526%, respectively (Table 3). "Wanhujing" had the most abundant content of dihydro-β-ionone among all the taxa (44), with 1.488%, and highest (E)-geranyl acetone (27) levels were observed in "Yuandong," with contents of about 1.526%. The lowest dihydro-β-ionone (44) and (E)-geranyl acetone (27) levels were detected in "Ruipan-19," with 0.104% and 0.068%, respectively. Almost all samples were detected with ketones, and the contents of ketones in peaches were relatively high, with about 0.1% or more, but there was no found in "Baifeng."

A total of 15 alcohols were only found in honey peach, accounting for 17.05% of top compounds. Among them, "Wanhujing" contained the largest number of alcohols, while the content of each alcohol had high rates. High hexanol (29) levels were observed in "Jinyuan," "Wanhujing," and "Baifeng," with contents of 1.152%, 3.304%, and 1.173%, respectively. As results showed, the difference between honey peaches and other kinds of peaches was definitely significant. A total of six acids were found in this work, namely, benzoic acid (2), (E)-2-hexenoic acid (50), hexanoic acid (51), butyric acid (85), hexanoic acid, 5-methyl- (86), and heptanoic acid (87). For the six acids, the levels were generally lower, except in "Yulu" where heptanoic acid (87) and (E)-2-hexenoic acid (50) were abundant, with 1.351% and 2.251%, respectively. Also high (E)-2-hexenoic acid (50) levels were detected in "Yihe," with a content of 1.297%. In general, the content of acid substances in flat peaches was higher than that in honey peaches and yellow peaches.

Because of the number of rest compounds detected in peaches was much lower, we did not discuss in detail. But there was something interesting that we found: "Baifeng" and "Yulu" had high phenol levels, such as eugenol (88) and phenol (22), with contents of 1.505% and 1.152%, respectively, and 1-pentylpyrrole (83) and γ-selinene (84) were dominant, with contents of 4.922% and 16.389%, respectively, in "Jinyuan."

In combination with Table 2, honey peach contained an abundance of volatile components, whereas volatile components of yellow peach and flat peach contained were relatively lower. The relative content of terpenes in all peach species was relatively lower, whereas the relative content of alcohols, esters, ketones, and aldehydes was significantly higher, and this result was generally consistent with the fingerprints of

10.3389/fnut.2022.965796

TABLE 2 Relative content of volatile compounds in peach samples based on gas chromatography–mass spectrometry (GC-MS).

No.	Name	CAS	Aroma description	Relative content (%)									
				Honey peach					Yellow peach			Flat peach	
				YM	YD	YH	WHJ	BF	HGF	JX	JY	RP19	YL
1	benzaldehyde	100-52-7	sweet bitter almond cherry	2.288	1.988	0.622	0.800	1.044	—	0.369	0.069	0.140	0.629
2	(E)-2-hexenal	6728-26-3	green banana fatty cheesy	0.751	1.206	1.383	0.622	0.544	—	0.080	0.018	0.092	0.851
3	benzoic acid	65-85-0	faint balsam urine	0.531	0.370	—	—	—	—	—	—	—	—
4	para-cymene	99-87-6	fresh citrus terpene woody	0.390	0.101	—	—	—	0.443	—	—	—	—
5	(E,E)-2,4-heptadienal	4313-03-5	fatty green oily	0.385	0.167	—	—	—	—	—	—	—	—
6	4-carvomenthenol	562-74-3	pepper woody earth musty sweet	0.378	—	—	—	—	—	—	—	—	—
7	camphene	79-92-5	woody herbal fir	0.238	—	—	0.093	—	—	—	—	—	—
8	isoquinoline	119-65-3	sweet balsam herbal	0.237	—	—	—	—	—	—	—	—	—
9	(E)-2-octenal	2548-87-0	fresh cucumber fatty green	0.210	—	—	—	—	—	—	—	—	—
10	cyclohexanol	108-93-0	camphor menthol phenol	0.194	—	—	2.020	—	—	—	—	—	—
11	γ-hexalactone	695-06-7	herbal coconut sweet creamy	0.177	—	—	—	—	—	—	—	—	—
12	non-anal	124-19-6	waxy aldehydic rose fresh	0.152	—	—	0.055	—	—	—	—	—	—
13	styrene	100-42-5	sweet balsam floral	0.141	0.091	0.100	—	—	—	0.063	—	—	—
14	geranyl acetone	689-67-8	floral fruity rose	0.130	—	—	—	—	—	—	—	—	—
15	dihydro-β-ionol	3293-47-8	woody floral amber	0.114	—	—	—	0.245	—	—	—	—	—
16	acetophenone	98-86-2	sweet pungent hawthorn	0.112	—	—	—	—	—	—	0.039	—	—
17	ethyl palmitate	628-97-7	waxy fruity creamy	0.111	—	—	—	—	—	—	—	—	—
18	3,5-octadien-2-one	38284-27-4	fruity fatty mushroom	0.100	—	—	—	—	—	—	—	—	—
19	meta-tolualdehyde	620-23-5	sweet fruity cherry	0.084	—	—	—	—	—	—	0.000	—	—
20	(E,E)-2,6-non-adienal	17587-33-6	fresh citrus green	0.083	—	—	—	—	—	—	—	—	—
21	cedrol	77-53-2	woody amber floral sweet	0.073	—	—	—	0.828	—	—	—	—	—
22	phenol	108-95-2	phenolic plastic rubber	0.072	—	—	—	1.505	—	—	—	—	—
23	2-ethyl-1-hexanol	104-76-7	sweet fatty fruity	0.068	—	—	—	—	—	—	—	—	—
24	δ-tridecalactone	7370-92-5	creamy coconut dairy	0.028	—	—	—	—	—	—	—	—	—
25	para-anisyl nitrile	874-90-8	sweet floral hawthorn	0.028	—	—	—	—	—	—	—	—	—
26	γ-decalactone	706-14-9	fruity creamy peach	—	2.111	—	1.359	2.936	—	—	—	—	—
27	(E)-geranyl acetone	3796-70-1	floral fruity green	—	1.526	0.382	0.556	—	—	—	—	0.104	—
28	β-ionone	14901-07-6	floral woody sweet fruity	—	1.310	—	0.474	—	—	—	—	—	—
29	hexanol	111-27-3	green fruity sweet	—	1.152	—	3.304	1.173	—	—	—	—	—
30	2-octanone	111-13-7	earthy weedy natural woody herbal	—	0.702	—	—	—	—	—	—	—	—
31	amber naphthofuran	3738-00-9	dry woody amber sweet	—	0.672	—	—	—	—	—	—	—	—
32	(E,E)-farnesyl acetate	4128-17-0	oily waxy	—	0.351	—	—	—	—	—	—	—	—

(Continued)

TABLE 2 Continued

No.	Name	CAS	Aroma description	Relative content (%)									
				Honey peach					Yellow peach			Flat peach	
				YM	YD	YH	WHJ	BF	HGF	JX	JY	RP19	YL
33	dextro-limonene	5989-27-5	citrus orange fresh sweet	—	0.277	0.184	0.070	—	—	0.087	—	—	—
34	γ-octalactone	104-50-7	sweet coconut peach	—	0.235	—	—	—	—	—	—	—	—
35	ipsdienol	35628-00-3	pine balsamic	—	0.218	—	0.237	—	—	—	—	—	—
36	β-cyclocitral	432-25-7	tropical saffron herbal fruity	—	0.206	—	—	—	—	—	—	—	—
37	linalool	78-70-6	citrus floral sweet rose	—	0.200	—	—	—	—	—	—	—	—
38	(E)-2-hexen-1-yl hexanoate	53398-86-0	green natural cognac herbal	—	0.195	—	0.038	—	—	—	—	—	—
39	(E)-2-tridecenal	7069-41-2	waxy fatty citrus creamy	—	0.132	—	—	—	—	—	—	—	—
40	(E)-3-hexen-1-ol	928-97-2	fruity green cortex floral	—	0.131	—	0.243	—	—	—	—	—	—
41	myrcene	123-35-3	peppery terpene spicy	—	0.128	—	—	—	0.289	—	—	—	—
42	hexyl hexanoate	6378-65-0	herbal fresh sweet fruity	—	0.114	0.314	0.122	—	—	—	—	0.064	0.525
43	β-ocimene	13877-91-3	citrus tropical green	—	0.101	—	—	—	—	—	—	—	—
44	dihydro-β-ionone	17283-81-7	earthy woody mahogany	—	0.067	0.240	1.488	—	—	—	—	0.068	0.328
45	non-adecane	629-92-5	bland	—	0.056	—	—	—	—	—	—	—	—
46	anethol	104-46-1	sweet anise licorice	—	0.049	—	—	—	—	—	—	—	—
47	bornyl acetate	76-49-3	woody pine herbal	—	0.049	—	0.091	—	—	—	—	—	—
48	cis-allocimene	7216-56-0	grass floral	—	0.034	—	—	—	—	—	—	—	—
49	γ-dodecalactone	2305-05-7	fatty peach sweet fruity	—	—	2.500	—	—	0.130	—	—	—	—
50	(E)-2-hexenoic acid	13419-69-7	fruity sweet	—	—	1.297	—	—	—	—	—	—	2.251
51	hexanoic acid	142-62-1	sour fatty sweat cheese	—	—	0.399	—	—	—	—	—	—	—
52	(E)-β-ionone	79-77-6	powdery floral woody berry	—	—	0.293	—	—	—	1.428	—	—	—
53	hexanal	66-25-1	fresh green fatty fruity	—	—	0.224	—	0.068	—	—	—	—	0.258
54	(E)-4-hexen-1-ol	928-92-7	green herbal musty	—	—	0.194	—	—	—	—	—	—	—
55	Costol	515-20-8	—	—	—	—	1.952	—	—	—	—	—	—
56	alloaromadendrene	25246-27-9	woody	—	—	—	0.874	—	—	—	0.397	—	—
57	eugenyl acetate	93-28-7	fresh sweet woody	—	—	—	0.840	—	—	—	—	—	—
58	(-)-spathulenol	77171-55-2	honey	—	—	—	0.739	—	—	—	—	—	—
59	β-irone	79-70-9	fresh sweet violet fruity	—	—	—	0.595	—	—	—	—	—	—
60	theaspirane	36431-72-8	tea herbal green	—	—	—	0.249	—	—	—	—	—	—
61	beta-santalol	77-42-9	woody	—	—	—	0.196	—	—	—	—	—	—
62	valencene	4630-07-3	sweet fresh citrus grapefruit	—	—	—	0.195	—	—	—	—	—	—
63	ethyl benzene	100-41-4	—	—	—	—	0.147	—	—	—	—	—	—
64	hexyl acetate	142-92-7	fruity green apple banana	—	—	—	0.127	—	—	—	—	0.026	—
65	3,7-dimethyl-1-octene	4984-01-4	woody, piney, herbaceous	—	—	—	0.126	—	—	—	—	—	—
66	hexahydrofarnesyl acetone	502-69-2	oily sweet green melon	—	—	—	0.039	—	—	—	—	—	—
67	β-caryophyllene	87-44-5	sweet woody spice	—	—	—	—	0.904	—	—	—	—	—

(Continued)

TABLE 2 Continued

No.	Name	CAS	Aroma description	Relative content (%)									
				Honey peach					Yellow peach			Flat peach	
				YM	YD	YH	WHJ	BF	HGF	JX	JY	RP19	YL
68	(E)-2-hexen-1-ol	928-95-0	fresh green leafy fruity	—	—	—	—	0.229	—	—	—	—	—
69	(Z)-3-hexen-1-ol	928-96-1	fresh green cut grass	—	—	—	—	0.138	—	—	—	—	—
70	isocaryophyllene	118-65-0	woody spicy	—	—	—	—	0.061	—	—	—	—	—
71	α-guaiene	3691-12-1	sweet woody balsam peppery	—	—	—	—	0.033	—	—	—	—	—
72	meta-dimethyl hydroquinone	151-10-0	acid fruity nutmeg neroli	—	—	—	—	0.025	—	—	—	—	—
73	α-pinene	80-56-8	fresh camphor sweet	—	—	—	—	—	3.827	—	—	—	—
74	(E)-β-ocimene	3779-61-1	sweet herbal	—	—	—	—	—	0.267	—	—	—	—
75	para-methyl acetophenone	122-00-9	sweet creamy fruity	—	—	—	—	—	0.163	—	—	—	—
76	2-pentyl furan	3777-69-3	fruity green earthy	—	—	—	—	—	0.088	—	—	—	—
77	tetradecane	629-59-4	mild waxy	—	—	—	—	—	—	0.045	—	—	—
78	ethyl valerate	539-82-2	sweet fruity apple	—	—	—	—	—	—	0.060	—	—	—
79	watermelon ketone	28940-11-6	fresh watery clean melon	—	—	—	—	—	—	0.662	—	—	—
80	(E,E)-2,4-hexadienal	142-83-6	sweet green spicy floral	—	—	—	—	—	—	—	0.296	—	—
81	dipentene	138-86-3	citrus herbal terpene	—	—	—	—	—	—	—	0.019	0.100	—
82	(+)-aromadendrene	489-39-4	wood	—	—	—	—	—	—	—	6.799	—	—
83	1-pentylpyrrole	699-22-9	green fatty	—	—	—	—	—	—	—	4.922	—	—
84	γ-Selinene	515-17-3	woody	—	—	—	—	—	—	—	16.38	—	—
85	Butyric acid	107-92-6	sour chessy fruity	—	—	—	—	—	—	—	—	0.048	—
86	Hexanoic acid,5-methyl-	628-46-6	fatty chessy oily fruity	—	—	—	—	—	—	—	—	0.128	—
87	Heptanoic acid	111-14-8	waxy chessy fruity	—	—	—	—	—	—	—	—	—	1.351
88	Eugenol	97-53-0	sweet spicy woody	—	—	—	—	—	—	—	—	—	1.152

"–" indicates not detected.

volatile components detected by GC-IMS (Figure 2). The relative content analysis suggested that alcohols, esters, and aldehydes were likely the primary sources of the distinctive aroma substances in peach fruit.

Heat map analysis of the content of volatile components in peach fruit of different varieties

Figure 4 shows that the components and contents of volatile substances in 10 kinds of peach fruits were significantly different. According to the cluster analysis of volatile compounds in the heat map, except for "Huangguifei," "Jinxiu," "Jinyuan," and "Ruipan-19," the red and pink regions of volatile compounds in the heat map of other varieties were mainly benzaldehyde (1) and (E)-2-hexenal (2). The heat maps of volatile substances of "Jinyuan" and "Ruipan-19" were concentrated at limonene (81). The volatile substances of "Jinxiu," "Yuandong," and "Yihe" heat maps in the red region were concentrated in styrene (13). In addition, the red part of heat maps of "Yuandong," "Wanhujing," and "Baifeng" also concentrated on prodecalactone (26), while the red part of the heat maps of "Yulu" and "Yihe" concentrated in (E)-2-hexenoic acid (50) and hexanal (53).

Relative odor activity value analysis of volatile flavor compounds in peach fruits of different varieties

A variety of volatile flavor compounds were detected in different varieties of peach fruit, but only some of them contributed to the overall flavor of peach fruit, and the rest only played a role in modifying and synergizing the flavor of

TABLE 3 Volatile components of ROAV ≥ 1 in peach samples and their thresholds and aroma notes.

No.	Name	CAS	Threshold[a](ppb)	ROAV									Note
				YM	YD	YH	WHJ	BF	HGF	JX	JY	RP19	YL	
1	Benzaldehyde	100-52-7	750.9	100.0	1.439	–	–	–	–	–	1.857	100.0	70.67	sweet
2	(E)-2-hexenal	6728-26-3	88.7	277.9	—	—	1.191	—	—	—	4.105	559.1	811.3	green
3	benzoic acid	65-85-0	568	30.68	—	—	—	—	—	—	—	—	—	fatty
4	para-cymene	99-87-6	5.01	2554	1.051	—	—	—	32.34	—	—	—	—	citrus
5	4-carvomenthenol	562-74-3	1200	10.34	—	—	—	—	—	—	—	—	—	spicy
6	(E)-2-octenal	2548-87-0	3	2300	—	—	—	—	—	—	—	—	—	green
7	cyclohexanol	108-93-0	470	13.52	—	—	—	—	—	—	—	—	—	green
8	γ-hexalactone	695-06-7	260	22.37	—	—	—	—	—	—	—	—	—	sweet
9	non-anal	124-19-6	1.1	1978	—	—	8.463	—	—	—	—	—	—	aldehydic
10	styrene	100-42-5	3.6	1281	1.310	—	—	—	—	—	—	—	—	sweet
11	geranyl acetone	689-67-8	60	71.17	—	—	—	—	—	—	—	—	—	floral
12	acetophenone	98-86-2	65	56.35	—	—	—	—	—	—	12.24	—	—	sweet
13	ethyl palmitate	628-97-7	2000	1.815	—	—	—	—	—	—	—	—	—	fruity
14	(E,E)-2,6-non-adienal	17587-33-6	0.5	5422	—	—	—	—	—	—	—	—	—	citrus
15	γ-decalactone	706-14-9	1.1	—	100.0	—	209.4	100	—	—	—	—	—	peach
16	(E)-geranyl acetone	3796-70-1	60	—	1.325	—	1.570	—	—	—	—	927.8	—	floral
17	β-ionone	14901-07-6	3.5	—	19.50	—	22.96	—	—	—	—	—	—	sweet
18	hexanol	111-27-3	5.6	—	10.72	—	100	7.850	—	—	—	—	—	fruity
19	γ-octalactone	104-50-7	12	—	1.018	—	—	—	—	—	—	—	—	peach
20	β-cyclocitral	432-25-7	5	—	2.148	—	—	—	—	—	—	—	—	fruity
21	linalool	78-70-6	0.22	—	47.40	—	—	—	—	—	—	—	—	green
22	myrcene	123-35-3	1.2	—	5.548	—	—	—	87.94	—	—	—	—	spicy
23	γ-dodecalactone	2305-05-7	0.43	—	—	100.0	—	—	110.1	—	—	—	—	peach
24	(E)-β-ionone	79-77-6	0.007	—	—	720.1	—	—	—	100.0	—	—	—	floral
25	dihydro-β-ionone	17283-81-7	3.6	—	—	1.148	70.05	—	—	—	—	10145	7685	woody
26	(Z)-3-hexen-1-ol	928-96-1	3.9	—	—	—	—	1.325	—	—	—	—	—	green
27	α-pinene	80-56-8	14	—	—	—	—	—	100.0	—	—	—	—	green
28	(E)-β-ocimene	3779-61-1	34	—	—	—	—	—	2.868	—	—	—	—	herbal
29	para-methyl acetophenone	122-00-9	21	—	—	—	—	—	2.834	—	—	—	—	sweet
30	2-pentyl furan	3777-69-3	5.8	—	—	—	—	—	5.518	—	—	—	—	fruity
31	(E,E)-2,4-hexadienal	142-83-6	60	—	—	—	—	—	—	—	100.0	—	—	green
32	dipentene	138-86-3	200	—	—	—	—	—	—	—	1.888	267.8	—	citrus
33	hexyl acetate	142-92-7	115	—	—	—	—	—	—	—	—	119.2	—	fruity
34	Butyric acid	107-92-6	2400	—	—	—	—	—	—	—	—	10.78	—	sour
35	hexyl hexanoate	6378-65-0	6400	—	—	—	—	—	—	—	—	5.345	6.926	fruity
36	Hexanoic acid,5-methyl-	628-46-6	4600	—	—	—	—	—	—	—	—	14.92	—	fatty
37	(E)-2-hexenoic acid	13419-69-7	1900	—	—	—	—	—	—	—	—	—	100.0	sour
38	Heptanoic acid	111-14-8	640	—	—	—	—	—	—	—	—	—	178.1	fruity
39	Eugenol	97-53-0	0.71	—	—	—	—	—	—	—	—	—	136930	spicy
40	hexanal	66-25-1	5	—	—	—	—	—	—	—	—	—	4358	fruity

[a]Olfactory thresholds in water taken from the literature (20). "–" indicates not detected.

peach fruit. The contribution of volatile flavor substances to the flavor characteristics of peach fruit is determined by their relative content and aroma threshold. The aroma threshold is a minimum olfactory value of odor. Therefore, the relative content of flavor substances cannot explain their contribution to the flavor of peach fruit. As a result, ROAV analysis was carried out based on the threshold value of each flavor substance. The compounds with an ROAV ≥ 1 had a greater contribution to the aroma of the sample and were the key aroma compounds. The components with a higher ROAV value had a greater contribution to the overall flavor of the peach sample.

As can be seen from Table 3, 14 key aroma substances were detected in "Yuanmeng," among which (E,E)-2, 6-non-adienal (14) and para-cymene (4) had a great influence on its overall flavor. There were three compounds with an ROAV ≥ 1 of "Yihe," and (E)-β-ionone (24) had a great effect on its flavor.

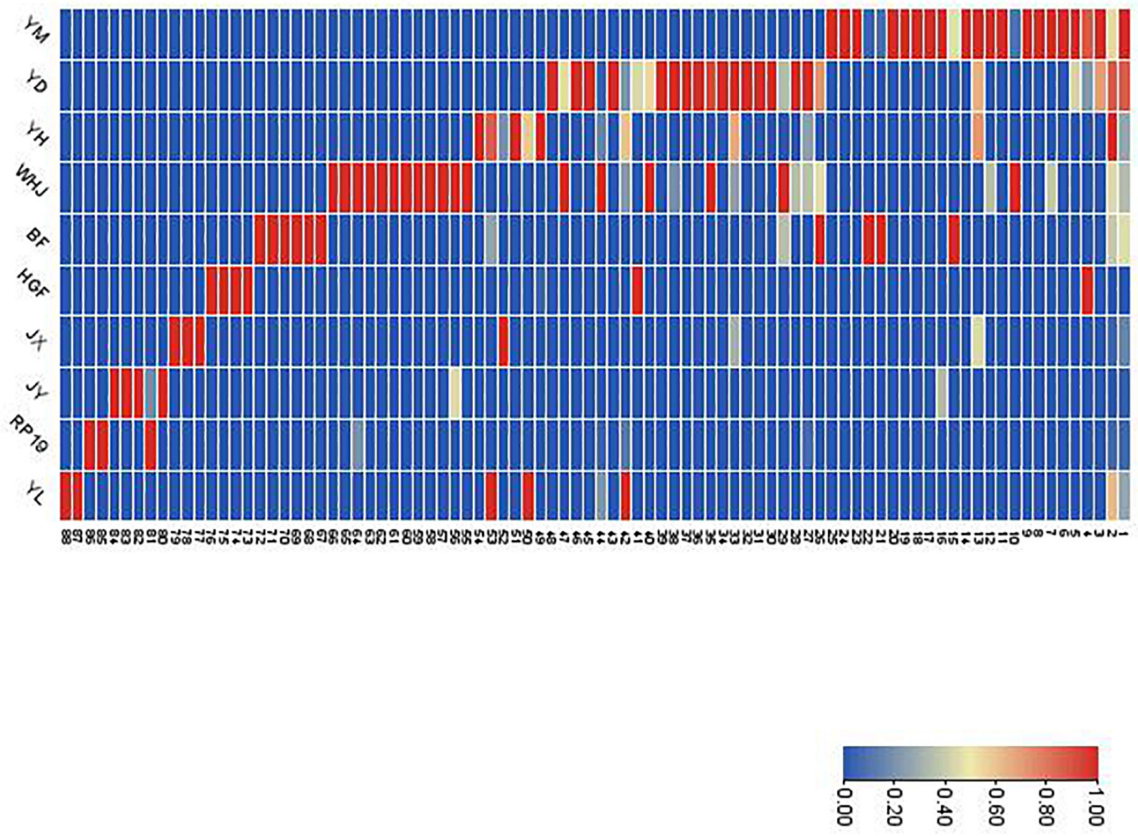

FIGURE 4
Relative contents (as shown by heat map) of all volatile compounds in the fruits of 10 peach samples. The codes in this figure correspond to the codes of cultivars in Table 2.

There were 11 kinds of peach in "Yuandong," and γ-decalactone (15) and linalool (21) had a great influence on its flavor. There were seven species of "Wanhujing," and γ-decalactone (15) and hexanol (18) had a great influence on its flavor. There were three kinds of "Baifeng," and the influence of γ-decalactone (15) on its flavor was great. There were seven kinds of "Huangguifei," and γ-dodecalactone (23) and α-pinene (27) had a great influence on its overall flavor. There were five kinds of "Jinyuan," and (E,E)-2, 4-hexadienal had a great influence on its overall flavor. "Jinxiu" only had one kind of compound with an ROAV $\geq$ 1, which was (E)-β-ionone (24). There were nine kinds of key flavor compounds in Ruipan-19, and dihydro-β-ionone (25) had a great influence on its overall flavor. There are eight kinds of "Yulu," and dihydro-β-ionone (25) and eugenol (39) had a great influence on its overall flavor.

According to the volatile components and aroma of ROAV $\geq$ 1, a radar map was made. As no more than three key aroma substances were detected in "Jinxiu" yellow peach, the map could not be made. According to the analysis of ROAV $\geq$ 1 components of "Jinxiu" yellow peach, the overall flavor of "Jinxiu" yellow peach was floral fragrance. It can be seen from Figure 5 that the main odor of different peach fruits was citrus flavor. "Huangguifei," "Yuandong," "Wanhujing," and "Baifeng" peach had the main flavor was peach. The main flavor of "Yulu" was spicy, and that of "Ruipan-19" peach was woody.

Principal component analysis based on gas chromatography–mass spectrometry

In order to further study the effect of volatile flavor substances on peach fruit flavor, principal component analysis (PCA) was carried out on the compounds contributing to peach fruit flavor, and Figure 6 is made by the volatile substance with an ROAV $\geq$ 1 in peach fruit. The accumulative variance contribution rate of PC1 (30.1%) and PC2 (16.9%) was 47.0%. Results are shown in Figure 6, and the chart can be divided into four quadrants, as we can see "Yuandong," "Baifeng," "Wanhujing," and "Huang Guifei" split throughout the second, and "Yihe," "Jinxiu," "Jinyuan," "Yulu," and "Ruipan-19" split throughout the third quadrant had good aggregation, which meant that the fruit flavor characteristics of these 10 peach samples were similar. "Yuanmeng" was located in the fourth

10.3389/fnut.2022.965796

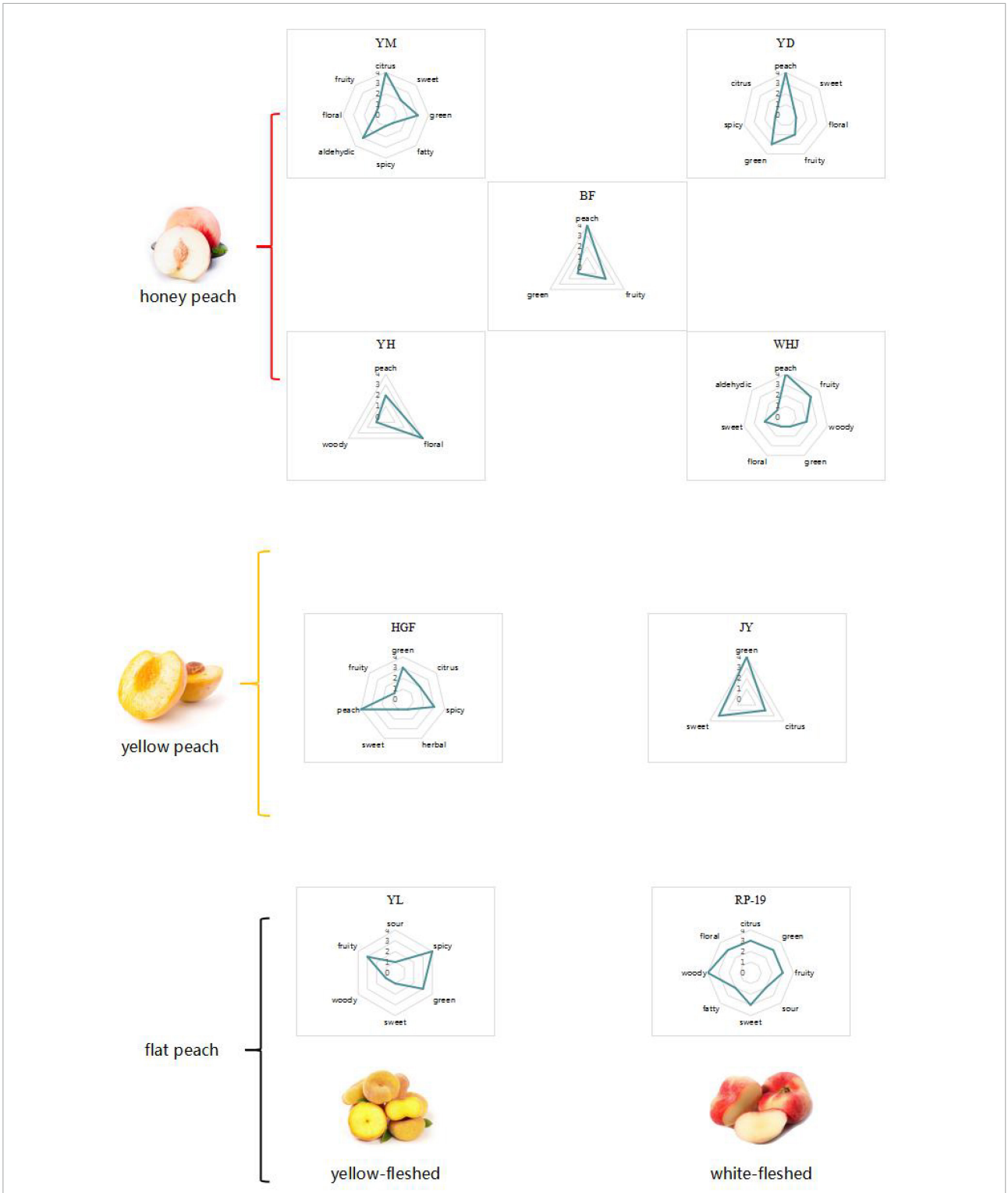

FIGURE 5
Flavor profile of each peach sample.

quadrant, which was very different from the other nine kinds, indicating that there were certain differences in the flavor characteristics of different peach fruits.

The load values of each principal component represented the reaction degree of the principal component to such substances, which can be used for flavor data analysis, as shown

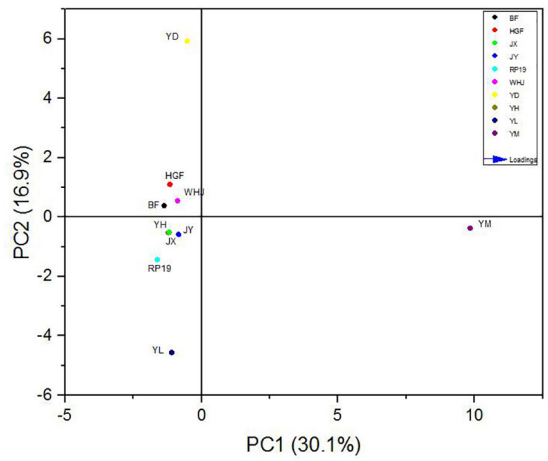

FIGURE 6
Scatter plot of principal component analysis (PCA) of 10 peach samples.

in Figure 7. In PC1, (E,E)-2, 6-non-adienal (14) had the highest positive load and γ-decalactone (15) had the highest negative load, while in PC2, the substance with the highest positive load was β-ionone (17) and the highest negative load was hexyl hexanoate (35). The results showed that (E,E)-2, 6-non-adienal (14), γ-decalactone (15), β-ionone (17), and hexyl hexanoate (35) contributed the most to the overall aroma of peach fruit, which constituted the main aroma of different varieties of peach fruit, and could distinguish different peach fruits well.

In the PCA model, 10 peach samples were clustered into four different groups; their characteristic aroma volatiles were included in each group (Figure 7). "Yuanmeng" clustered in one group with (E)-2-octenal (6), non-anal (9), and (E,E)-2,6-non-adienal (14). "Yulu" clustered with heptanoic acid (38), eugenol (39), and hexanal (40) individually, and also "Yuandong" clustered with β-ionone (17) and linalool (21). The remaining seven peaches "Baifeng," "Wanhujing," "Yihe," "Jinxiu," "Jinyuan," "Huangguifei," and "Ruipan-19" were clustered with γ-dodecalactone (23), (E)-β-ionone (24), dihydro-β-ionone (25), etc.

According to the preceding classification, we can apply these three varieties of 10 peach samples to various application directions, as depicted in Figure 8. For instance, the aroma of "Yuanmeng" was predominantly sweet, with a trace of aldehyde, and it is a honey peach; therefore, it can be processed into peach by-products such as juice, fruit wine, and jam (26, 27). "Yulu" is a type of flat peach whose aroma characteristics were more reflective of its spicy and fruity aroma, making it an excellent candidate for preserved fruit (6, 28). "Yuandong"

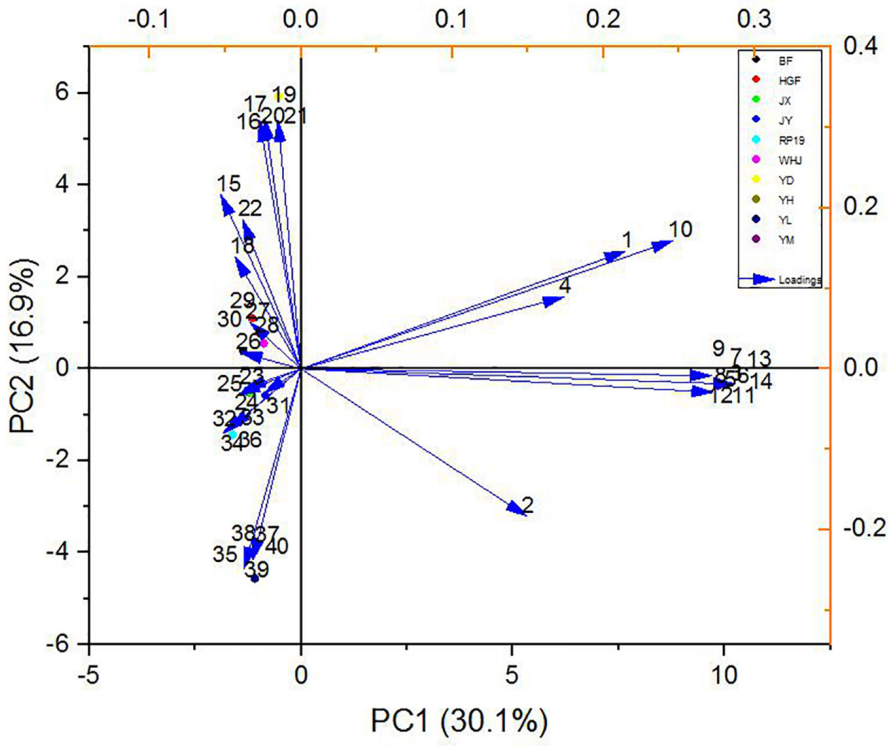

FIGURE 7
Principal component loading diagram of key flavor compounds in peach samples. The codes correspond to the codes of volatiles in Table 3.

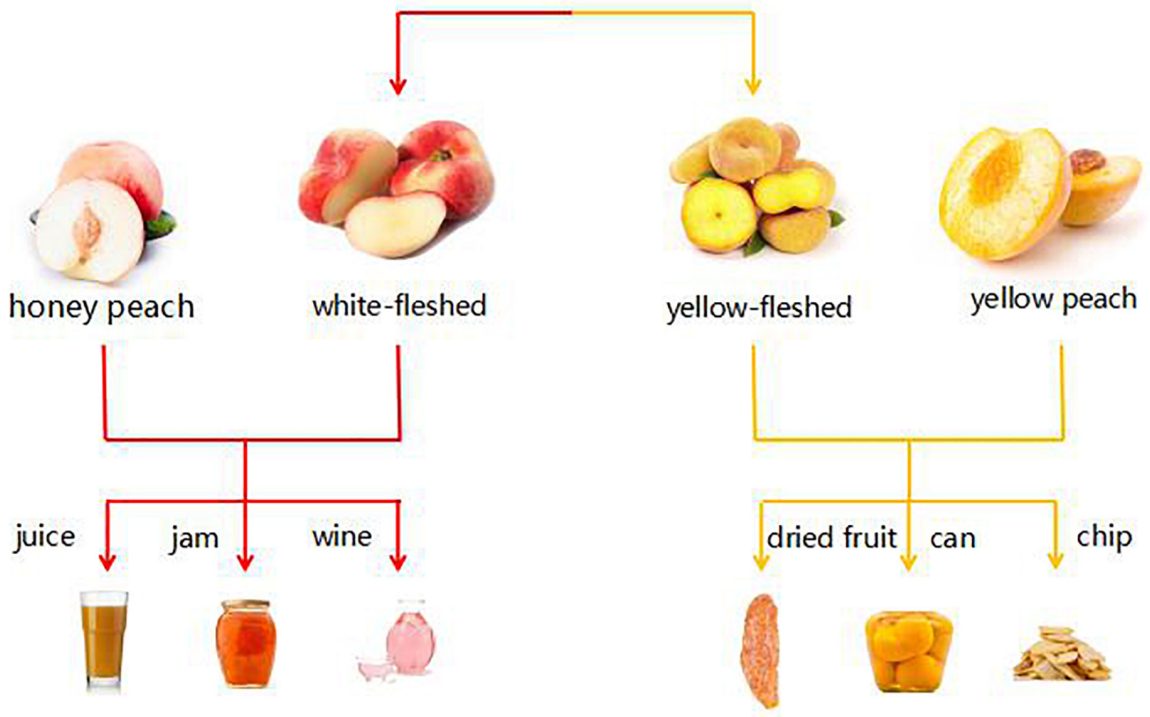

FIGURE 8
Sketch of possible application of three varieties of peach (honey peach, yellow peach, and flat peach).

is also a honey peach variety, but unlike "Yuanmeng," its aroma was predominantly green, making it more suitable for dried fruit (29). Among the remaining seven varieties, there were three yellow peach varieties, three honey peach varieties, and one flat peach variety. Despite being of different varieties, their characteristic aroma volatiles were relatively similar, with a predominant peach flavor and a hint of flower. Among the remaining seven varieties, there were three kinds of yellow peach, three kinds of honey peach, and one kind of flat peach. Although they were of different varieties, the characteristic aroma volatiles of them were comparatively similar, mainly peach flavor, with a slight hint of flower. According to Da Rosa Louzada et al. (30); Joshi et al. (31), these peaches were better suited for canning or making wine. If it is not necessary to extend the shelf life of peaches, eating them fresh is the optimal strategy. Honey peaches were more suitable for consumption as juice, jam, etc., or extraction of aroma components for use in daily cosmetics, whereas yellow peaches, due to their hardness and slight green flavor, were more suitable for canned or crispy foods (32–36). But flat peach differs between yellow-fleshed and white-fleshed varieties; if it is white-fleshed, it tends to be similar to the method of honey peach by-products, whereas if it is yellow-fleshed, it tends to be similar to the method of yellow peach.

Conclusion

In this study, gas chromatography–ion mobility spectrometry was used in conjunction with headspace solid-phase microextraction–gas chromatography–mass spectrometry to analyze and identify the volatile constituents of 10 distinct peach fruit samples. GC-IMS detected a total of 57 volatile compounds, the most volatile of which were esters, which primarily exhibited the aroma characteristics of fruit and flower. The majority of volatile components detected by GC-IMS were small, low-concentration molecules. Although the concentration of these small-molecule organic compounds was low, their molecular weight was small and volatile, making them the easiest to "capture" using sensory or instrumental analysis (37). The composition of volatile components in peach fruits of different kinds can be visualized based on ion migration, despite the fact that the volatiles detected by this method were difficult to be quantified or relatively quantified. The majority of the 88 types of volatile components detected by GC-MS had a high concentration and molecular weight, making them more suitable for headspace solid-phase microextraction technology but insensitive to low-concentration substances. These two technologies enabled the content investigation-related amplification of volatile components in the sample. It demonstrated that the two techniques can be combined to

compensate for their respective limitations. Ketones, esters, alcohols, and aldehydes made up a large proportion of various peach fruits as determined by the two techniques. The results of ROAV analysis revealed that the primary flavor substances of 10 peach samples varied. Through principal component analysis of the components, the components with an ROAV ≥ 1 in the aroma components of peach fruits, the cluster analysis of peach fruits revealed that except "Yuanmeng," the other nine kinds of peach fruits clustered together. The results demonstrated that the volatile substance compositions of "Yuandong," "Yihe," "Wanhujing," "Baifeng," "Huangguifei," "Jinxiu," "Jinyuan," "Ruipan-19," and "Yulu" were similar, whereas those of "Yuanmeng" and other varieties were distinct. It was determined that (E,E)-2, 6-non-adienal, γ-decalactone, β-ionone, and hexyl hexanoate contributed the most to the overall aroma of peach fruit and were the primary flavoring substances in three varieties of 10 peach samples, allowing for a good distinction between different peach fruit samples.

Due to its low concentration, GC-MS and GC-IMS are difficult to detect because the relative quantitative method cannot fully explain the composition of volatile flavor compounds in peach fruit and the sulfur compounds in peach fruit, which have a certain effect on the aroma of peach fruit. Therefore, in the next step of this study, the internal standard method and flame photometric detection (FPD) will be used to determine the volatile flavor compounds in peach fruit. Then, aroma recombination and omission experiments are performed to determine the contributions of the selected key aroma compounds. Finally, on the basis of principal component analysis, the partial least squares method (PLS) is applied to analyze the differences between various peach fruits.

Data availability statement

The original contributions presented in this study are included in the article/supplementary material, further inquiries can be directed to the corresponding authors.

Author contributions

PS contributed to the conception of the study. YW, XL, CC, and JZ performed the experiment. HJ, XW, and SJS contributed significantly to analysis and manuscript preparation. BX performed the data analyses and wrote the manuscript. TF helped perform the analysis with constructive discussions. All authors contributed to the article and approved the submitted version.

Funding

This work was supported by the major science and technology project for new variety breeding of agriculture (forest) of Zhejiang province (2021C02066-4), the Major Agricultural Technology Collaborative Promotion project of Zhejiang Province (2020xttggp02-03), and the biological seed industry and Jinhua Modern Agricultural Machinery Laboratory cooperation project (ydhz2020ky03).

Conflict of interest

The authors declare that the research was conducted in the absence of any commercial or financial relationships that could be construed as a potential conflict of interest.

Publisher's note

References

1. Xingrong WU, Xuan WU. Exploration on the innovation of peach cultivation and management technology. *Theory Pract Innov Entrep.* (2019) 2:163–4. doi: 10.12677/HJAS.2018.84044

2. Zhu GY, Xiao ZB, Zhou RJ, Zhu YL, Niu YW. Study on development of a fresh peach flavor. *Adv Mater Res.* (2013) 781–4:1570–3. doi: 10.4028/www.scientific.net/AMR.781-784.1570

3. Smykov AV, Mesyats NV. State analysis of horticulture and peach culture in the world. *Plant Biol Hortic Theory Innov.* (2020) 155:130–7. doi: 10.36305/2712-7788-2020-2-155-130-137

4. Zhu JC, Xiao ZB. Characterization of the key aroma compounds in peach by gas chromatography–olfactometry, quantitative measurements and sensory analysis. *Eur Food Res Technol.* (2019) 245:129–41. doi: 10.1007/s00217-018-3145-x

5. Xie R, Li X, Chai M, Song L, Jia H, Wu D, et al. Evaluation of the genetic diversity of Asian peach accessions using a selected set of SSR markers. *Sci Hortic.* (2010) 125:622–9. doi: 10.1016/j.scienta.2010.05.015

6. Niu Y, Deng J, Xiao Z, Zhu J. Characterization of the major aroma-active compounds in peach (*Prunus persica* L. Batsch) by gas chromatography-olfactometry, flame photometric detection and molecular sensory science approaches. *Food Res Int.* (2021) 147:110457. doi: 10.1016/j.foodres.2021.110457

7. Zhang T, Ni H, Qiu XJ, Li T, Zhang LZ, Li LJ, et al. suppressive interaction approach for masking stale note of instant ripened Pu-Erh tea products. *Molecules.* (2019) 24:4473. doi: 10.3390/molecules24244473

8. Yang Y, Qian MC, Deng Y, Yuan H, Jiang Y. Insight into aroma dynamic changes during the whole manufacturing process of chestnut-like aroma green tea

by combining GC-E-Nose, GC-IMS, and GC× GC-TOFMS. *Food Chem.* (2022) 387:132813. doi: 10.1016/j.foodchem.2022.132813

9. Wang S, Chen H, Sun B. Recent progress in food flavor analysis using gas chromatography–ion mobility spectrometry (GC–IMS). *Food Chem.* (2020) 315:126158. doi: 10.1016/j.foodchem.2019.126158

10. Bi S, Xu X, Luo D, Lao F, Pang X, Shen Q, et al. Characterization of key aroma compounds in raw and roasted peas (*Pisum sativum* L.) by application of instrumental and sensory techniques. *J Agric Food Chem.* (2020) 68:2718–27. doi: 10.1021/acs.jafc.9b07711

11. Shi J, Wu H, Xiong M, Chen Y, Chen J, Zhou B, et al. Comparative analysis of volatile compounds in thirty nine melon cultivars by headspace solid-phase microextraction and gas chromatography-mass spectrometry. *Food Chem.* (2020) 316:126342. doi: 10.1016/j.foodchem.2020.126342

12. Bi J, Li Y, Yang Z, Lin Z, Chen F, Liu S, et al. Effect of different cooking times on the fat flavor compounds of pork belly. *J Biochem.* (2022) 46:e14184. doi: 10.1111/jfbc.14184

13. Han Y, Wang C, Zhang X, Li X, Gao Y. Characteristic volatiles analysis of *Dongbei Suancai* across different fermentation stages based on HS-GC-IMS with PCA. *J Food Sci.* (2022) 87:612–22. doi: 10.1111/1750-3841.16045

14. Li M, Yang R, Zhang H, Wang S, Chen D, Lin S. Development of a flavor fingerprint by HS-GC-IMS with PCA for volatile compounds of *Tricholoma matsutake* Singer. *Food Chem.* (2019) 290:32–9. doi: 10.1016/j.foodchem.2019.03.124

15. Yang Y, Wang B, Fu Y, Shi Y, Chen F, Guan H, et al. HS-GC-IMS with PCA to analyze volatile flavor compounds across different production stages of fermented soybean whey tofu. *Food Chem.* (2021) 346:128880. doi: 10.1016/j.foodchem.2020.128880

16. Su D, He JJ, Zhou YZ, Li YL, Zhou HJ. Aroma effects of key volatile compounds in Keemun black tea at different grades: HS-SPME-GC-MS, sensory evaluation, and chemometrics. *Food Chem.* (2022) 373:131587. doi: 10.1016/j.foodchem.2021.131587

17. Sun R, Xing R, Zhang J, Wei L, Ge Y, Deng T, et al. Authentication and quality evaluation of not from concentrate and from concentrate orange juice by HS-SPME-GC-MS coupled with chemometrics. *LWT.* (2022) 162:113504. doi: 10.1016/j.lwt.2022.113504

18. Akkad R, Buchko A, Johnston SP, Han J, House JD, Curtis JM. Sprouting improves the flavour quality of faba bean flours. *Food Chem.* (2021) 364:130355. doi: 10.1016/j.foodchem.2021.130355

19. Yi C, Li P, Liao L, Qin Y, Jiang L, Yang L. Characteristic fingerprints and volatile flavor compound variations in Liuyang *Douchi* during fermentation via HS-GC-IMS and HS-SPME-GC-MS – ScienceDirect. *Food Chem.* (2021) 361:130055. doi: 10.1016/j.foodchem.2021.130055

20. Van Gemert LJ. . *Odour Thresholds: Compilations of Odour Threshold Values in air, Water and Other Media*. Utrecht: Oliemans Punter (2011).

21. Bi J, Lin Z, Li Y, Chen F, Liu S, Li C, et al. Effects of different cooking methods on volatile flavor compounds of chicken breast. *J Food Biochem.* (2021) 45:e13770. doi: 10.1111/jfbc.13770

22. Guo S, Zhao X, Ma Y, Wang Y, Wang D. Fingerprints and changes analysis of volatile compounds in fresh-cut yam during yellowing process by using HS-GC-IMS. *Food Chem.* (2022) 369:130939. doi: 10.1016/j.foodchem.2021.130939

23. Lytra G, Tempere S, Le Floch A, De Revel G, Barbe J. Study of sensory interactions among red wine fruity esters in a model solution. *J Agric Food Chem.* (2013) 61:8504–13. doi: 10.1021/jf4018405

24. Li Q, Yang S, Zhang R, Liu S, Zhang C, Li Y, et al. Characterization of honey peach (*Prunus persica* (L.) Batsch) aroma variation and unraveling the potential aroma metabolism mechanism through proteomics analysis under abiotic stress. *Food Chem.* (2022) 386:132720. doi: 10.1016/j.foodchem.2022.132720

25. Wang Y, Yang C, Li S, Yang L, Wang Y, Zhao J, et al. Volatile characteristics of 50 peaches and nectarines evaluated by HP-SPME with GC-MS. *Food Chem.* (2009) 116:356–64. doi: 10.1016/j.foodchem.2009.02.004

26. Liu Q, Weng P, Wu Z. Quality and aroma characteristics of honey peach wines as influenced by different maturity. *Int J Food Properties.* (2020) 23:445–58. doi: 10.1080/10942912.2020.1736094

27. Medeiros A, Tavares E, Bolini HMA. Descriptive sensory profile and consumer study impact of different nutritive and non-nutritive sweeteners on the descriptive, temporal profile, and consumer acceptance in a peach juice matrix. *Foods.* (2022) 11:244. doi: 10.3390/foods11020244

28. Tan F, Wang P, Zhan P, Tian H. Characterization of key aroma compounds in flat peach juice based on gas chromatography-mass spectrometry-olfactometry (GC-MS-O), odor activity value (OAV), aroma recombination, and omission experiments. *Food Chem.* (2022) 366:130604. doi: 10.1016/j.foodchem.2021.130604

29. Huang H, Chen B, Wang C. Comparison of high pressure and high temperature short time processing on quality of carambola juice during cold storage. *J Food Sci Technol.* (2018) 55:1716–25. doi: 10.1007/s13197-018-3084-3

30. Da Rosa Louzada AR, De Oliveira Oliz L, Gomes CG, Bonemann DH, Scherdien SH, Ribeiro AS, et al. Assessment of total concentration and bioaccessible fraction of minerals in peaches from different cultivars by MIP OES. *Food Chem.* (2022) 391:133228. doi: 10.1016/j.foodchem.2022.133228

31. Joshi VK, Panesar PS, Rana VS, Kaur S. Chapter 1 – Science and technology of fruit wines: an overview. In: Kosseva MR, Joshi VK, Panesar PS editors. *Science and Technology of Fruit Wine Production*. Cambridge, MA: Academic Press (2017). p. 1–72. doi: 10.1016/B978-0-12-800850-8.00001-6

32. Tzouros NE, Arvanitoyannis IS. Agricultural produces: Synopsis of employed quality control methods for the authentication of foods and application of chemometrics for the classification of foods according to their variety or geographical origin. *Crit Rev Food Sci Nutr.* (2001) 41:287–319. doi: 10.1080/20014091091823

33. Kelley KM, Primrose R, Crassweller R, Hayes JE, Marini R. Consumer peach preferences and purchasing behavior: A mixed methods study. *J Sci Food Agric.* (2016) 96:2451–61. doi: 10.1002/jsfa.7365

34. Budak NH, Özdemir N, Gökırmaklı Ç. The changes of physicochemical properties, antioxidants, organic, and key volatile compounds associated with the flavor of peach (*Prunus cerasus* L. Batsch) vinegar during the fermentation process. *J Food Biochem.* (2021) 46:e13978. doi: 10.1111/jfbc.13978

35. Florkowski WJ, Takács I. What mining the text tells about minding the consumer: the changing fruit and vegetable consumption patterns and shifting research focus. 4th ed. In: Florkowski WJ, Banks NH, Shewfelt RL, Prussia SE editors. *Postharvest Handling*. Cambridge, MA: Academic Press (2022). p. 517–64. doi: 10.1016/B978-0-12-822845-6.00018-X

36. Dar AH, Kumar N, Shah S, Shams R, Aga MB. Processing of fruits and vegetables. In: Sharma HK, Kumar N editors. *Agro-Processing and Food Engineering*. Singapore: Springer (2022). p. 535–79. doi: 10.1007/978-981-16-7289-7_13

37. Xiao Z, Xiang P, Zhu J, Zhu Q, Liu Y, Niu Y. Evaluation of the perceptual interaction among sulfur compounds in mango by feller's additive model, odor activity value and vector model. *J Agric Food Chem.* (2019) 67:8926–37. doi: 10.1021/acs.jafc.9b03156

frontiers | Frontiers in Nutrition

TYPE Original Research
PUBLISHED 24 August 2022
DOI 10.3389/fnut.2022.990380

OPEN ACCESS

EDITED BY
Mingquan Huang,
Beijing Technology and Business University, China

REVIEWED BY
Georgi Kostov,
University of Food Technologies, Bulgaria
Chongde Wu,
Sichuan University, China

*CORRESPONDENCE
Mingqiang Ai
amq1983@qq.com
Bin He
hebin.li@foxmail.com
Runlan Wan
wanrunlan@swmu.edu.cn

†These authors have contributed equally to this work

SPECIALTY SECTION
This article was submitted to Food Chemistry, a section of the journal Frontiers in Nutrition

RECEIVED 09 July 2022
ACCEPTED 01 August 2022
PUBLISHED 24 August 2022

CITATION
Pei R, Lv G, Guo B, Li Y, Ai M, He B and Wan R (2022) Physiological and transcriptomic analyses revealed the change of main flavor substance of *Zygosaccharomyces rouxii* under salt treatment.
Front. Nutr. 9:990380.
doi: 10.3389/fnut.2022.990380

Physiological and transcriptomic analyses revealed the change of main flavor substance of *Zygosaccharomyces rouxii* under salt treatment

Rongqiang Pei[1†], Gongbo Lv[1†], Binrong Guo[1], Yuan Li[1], Mingqiang Ai[1*], Bin He[1*] and Runlan Wan[2*]

[1]Jiangxi Key Laboratory of Bioprocess Engineering, College of Life Sciences, Jiangxi Science and Technology Normal University, Nanchang, China, [2]Department of Oncology, The Affiliated Hospital of Southwest Medical University, Luzhou, China

Zygosaccharomyces rouxii was a highly salt-tolerant yeast, playing an important role in soy sauce fermentation. Previous studies reported that *Z. rouxii* under salt treatment produces better fermented food. However, the detailed change of main flavor substance was not clear. In this study, the physiological and transcriptomic analyses of *Z. rouxii* under salt treatment was investigated. The results revealed the high salt tolerance of *Z. rouxii*. Analysis of physiological data showed that the proportion of unsaturated fatty acids was significantly increased with the increment of salt concentrations. The analysis of organic acids showed that the content of succinic acid was significantly higher in the salt-treated *Z. rouxii* while oxalic acid was only identified at the 18% salt concentration-treated group. Results of volatile substances analysis showed that concentrations of 3-methyl-1-butanol and phenylethyl alcohol were significantly increased with the increment of salt concentrations. A comparison of transcriptome data showed that the genes involved in the TCA cycle and the linoleic acid synthesis process exhibited different expressions, which is consistent with the results of physiological data. This study helps to understand the change of main flavor substance of *Z. rouxii* under salt treatment and guide their applications in the high salt liquid state fermentation of the soy sauce.

KEYWORDS

***Zygosaccharomyces rouxii*, salt treatment, transcriptomics, flavor substance, physiological**

Introduction

Zygosaccharomyces rouxii belongs to the genus *Zygosaccharomyces*, which plays an important part in the manufacture of traditional fermented foods, such as soy sauce and miso. It mainly participates in consuming the sugars and amino acids of the soybeans and wheat during soy sauce fermentation. Apart from catalyzing the glucose conversion into ethanol, *Z. rouxii* is also capable of releasing higher alcohols from free amino acids *via* the Ehrlich pathway and produces a sweet and caramel type of flavor (1). The main flavor substances are two 4-hydroxyfuranones derivatives, 4-hydroxy-2,5-dimethyl-3(2H)-furanone (HDMF) and 4-hydroxy-2(or 5)-ethyl-5(or 2)-methyl-3(2H)-furanone (HEMF), the latter is also a potent antioxidant and has anticarcinogenic effects (2–4). In addition, it was also reported that the quality of fermented foods was improved and the fermentation process could be accelerated by the addition of *Z. rouxii* as a starter culture (5).

The volatile and non-volatile substances, such as organic acids, alcohols, and amino acids, contribute to the nutrition, unique taste, and aroma of fermented foods. Organic acids are one of the crucial compounds present in fermented products that not only have a huge effect on the sour taste but several of which also have other flavor attributes including a bitter or salty taste (6). Additionally, organic acids also affect the pH of the fermented products, which further affects the product quality, such as flavor stability (7, 8). Succinic acid, derived from the fermentation of glucose, is generally found in various fermented foods such as soy sauce, seasonings, and miso. All of these fermentation products have very distinct and marked flavors, which might attribute in part to a flavor enhancement by the small amounts of succinic acid. This would imply that succinic acid may have vital effects on various flavors that cannot be replicated with other food organic acids (9). As a major inhibitory and volatile compound, acetic acid can cause intracellular acidification or cell death and inhibit cell metabolism that acts to stress microbiota, finally leading to the reduction of yeast fermentative performance (10, 11). Intriguingly, acetic acid is generally used in foods as a flavor enhancer and flavoring agent. In addition to ethanol, alcohols, and organic acids, aldehydes, the main aroma-active compounds, ketones, esters, furans, phenols, and pyrazines were known as critical characteristic flavor substances of fermented foods produced *via Z. rouxii* (12).

Zygosaccharomyces rouxii inevitably suffer from multiple abiotic stresses covering osmotic, acidic, oxidative, temperature, and alcohol stresses during the process of fermented food production. Especially the high salt concentration triggers osmotic stress resulting in structural and physiological damage of cells, and thus negatively affects the growth and survival of organisms (13, 14). Previous studies have reported that *Z. rouxii* harbor a good tolerance toward high concentrations of salt, and the related physiological, transcriptomic, and metabolomics analysis of the salt tolerance mechanism of *Z. rouxii* have been comprehensively elucidated (5, 15, 16). Even though the high salinity environment leads to the injury cell and the low metabolic activity of *Z. rouxii*, on the other hand, a characteristic of *Z. rouxii* fermentation under that condition was also observed in the past several decades, accelerating and enhancing the flavor formation of fermented foods (17, 18). In addition, *Z. rouxii* is capable of slowly fermenting the sugars and amino acids present in high salty, typically in 18–20% NaCl environment, releasing flavors vital to the quality during soy sauce fermentation (19). Considerable investigations have been made regarding the enhancing and accelerating flavor formation of fermented foods by *Z. rouxii* under the high salinity environment in the last several decades. Nevertheless, to the best of our knowledge, little progress has been made on the detailed mechanism of enhancing and accelerating flavor formation by *Z. rouxii* under the above-mentioned abiotic stress. In the post-genomic era, with the advance of the omics approaches such as metabolomics, genomics, transcriptomics, and proteomics for flavor materials component and ratio analyses, a comprehensive understanding of the mechanisms, processes and environmental stress responses might obtain about the functions of *Z. rouxii* on fermented foods (15, 16, 20). These may also help to understand the genetic, biochemical, and physiological constraints on the metabolic processes of *Z. rouxii* in a high salinity environment.

High-salt condition is the main environmental factor in the high salt liquid state fermentation of the soy sauce (18–20% salt concentration), and *Z. Rouxii* would inevitably be subject to high-salinity stress. The present study aims to delineate the related mechanism of flavor formation by *Z. rouxii* under a high salinity environment. Based on physiological and transcriptome analysis, the salt tolerance response of *Z. rouxii* including growth performance, changes in organic acids content, intracellular fatty acid, and volatile substances, as well as the overall transcription levels of key genes were investigated. Results of this study not only contribute to further completing the mechanism of flavor formation of *Z. rouxii* under high salt stress, but also might be beneficial to enhance and accelerate flavor formation, and thus ultimately improve its fermentation characteristics and guide their applications in the production of traditional fermented foods.

Materials and methods

Fungal strain and cultivation

The *Z. rouxii* CICC 32899 strain, purchased from China Center of Industrial Culture Collection, was used in this study. It was grown statically in a YPD medium (yeast paste 10 g/L, protein 20 g/L, glucose 20 g/L, pH 6.0) at 30°C for 24 h for activating strain. To observe the growth of *Z. rouxii* at different salt concentrations, the activated *Z. rouxii* was

inoculated in an YPD medium treated with different salt concentrations (0, 6, 12, and 18%) for 3 days, each sample was performed in triplicate.

Determination of OD values in *Zygosaccharomyces rouxii* under salt stress

The growth of *Z. rouxii* was mainly reflected by the OD values of *Z. rouxii*. *Z. rouxii* had a maximum absorption at 600 nm, thus this wavelength was chosen to determine the OD values. All samples were collected for 12, 24, 48, 60, and 72 h, and then the bacterial broth was diluted in a ratio of 1:3 for determination the OD values. It was determined by the UV spectrophotometer with a wavelength of 600 nm, deionized water as a control and the diluted bacteria solution as samples. The OD values are equal to the OD read multiplied by the dilution multiple. Each sample was performed in triplicate.

Determination of intracellular fatty acid and volatile substances

Lipids were extracted from cell homogenates and methylated by following previously described methods (21). Specifically, *Z. rouxii* mycelia were filtered, collected, washed with distilled water, and freeze dried. After that, the mycelia of each group were powdered and weighed. The same weight of mycelia powder was subjected to lipid extraction. The lipid extracts were incubated in chloroform with 2% H_2SO_4–MeOH solution at 70°C for 2 h to obtain fatty acid methyl esters (FAMEs). The FAME components were separated and analyzed by QP2010 gas chromatography-mass spectrometry (GC-MS) (Shimazjin, Kyoto, Japan). The system was equipped with Supelco SP-2340 fused silica capillary column (30 m × 0.25 mm i.d., with a film thickness of 0.2 μm; Bellefonte, PA, United States). FAMEs were identified by comparing their mass spectra with a spectrum database. FA peaks were identified based on comparisons of their retention times to the external standards or similarity search. The relative amounts of individual FA components were performed by using the peak area of the most intensive ion of each peak, and the percentage of UFAs was also calculated (21).

Same treated samples were also used to determine the volatile substances *via* GC-MS based on Benucci et al. method with some changes (22). It analyzed by QP2010 gas chromatography-mass spectrometry (GC-MS) (Shimazjin, Kyoto, Japan). The system was equipped with Supelco SP-2340 fused silica capillary column (30 m × 0.25 mm i.d., with a film thickness of 0.25 μm; Bellefonte, PA, United States).

Determination of organic acids content

After 3 days of liquid culture, *Z. rouxii* mycelium was filtered with a 0.45 μm membrane, and then the content of organic acids was determined for the following analysis. Briefly, the mycelia were lyophilized, vacuum freeze dried to a constant weight, and ground to powder. Two grams of dry powder were weighted from each sample was used to perform High Performance Liquid Chromatography (HPLC) detection. HPLC assay was conducted on Waters Alliance e2695 HPLC (Milford, MA, United States) using a UV detector set at 210 nm equipped with Aminex HPX-87H (Bio-Rad, CA, United States) column (300 × 7.8 mm, 9 μm). The analysis conditions were as follows: the mobile phase was 0.065% H_3PO_4 with isocratic elution at flow rate of 0.6 ml min^{-1}, and 10 μl injection sample volume. A standard organic acids curve was generated using tartaric acid, propanedioic acid, acetic acid, citric acid, succinic acid, malic acid, and oxalic acid standard (Sigma-Aldrich, Burlington, MA, United States). These yield of organic acids was calculated using the detected peak area according to the standard curve.

Preparation of cDNA libraries and RNA sequencing

After obtaining the cell samples, RNA extraction was performed using the fungal RNA kit (Omega Bio-Tek, Norcross, GA, United States). The RNA concentrations were detected by using a NanoDrop ND-1000 spectrophotometer (Thermo Scientific, Wilmington, DE, United States), and the RNA integrity values were analyzed with a Bioanalyzer 2100 (Agilent Technologies, Palo Alto, CA, United States). To ensure reliability and reproducibility, equal quantities of RNA of each pool from three individual cultures were used for cDNA library construction. Afterward, the mRNA was enriched from pooled total RNA using oligo (dT) magnetic beads and then digested into short pieces with fragmentation buffer at 94°C for 5 min and then reversely transcripted into cDNA using random hexamer primers. Using these mRNA fragments as templates, the first-strand cDNA was synthesized, followed by second-strand cDNA synthesis by DNA polymerase I and RNase H (23). The cDNA fragments were purified using QIAquick PCR extraction kit, end repaired, and ligated to Illumina sequencing adapters to create the cDNA library. After that the libraries were sequenced by the Illumina HiSeq 2500 platform (Illumina, San Diego, CA, United States). The obtained raw reads containing adapters or low-quality bases will be further filtered by our previous criterion to get clean reads, and thus, removed (21). Moreover, the Bowtie2 software was used to remove reads that mapped to ribosome RNA (rRNA) database to get the final clean reads, which were further employed for assembly and transcriptome analysis (24). RNA-seq data of *Z. rouxii* under distinct salt stress were deposited

in the NCBI/SRA database, under the BioProject accession number PRJNA837122.

Identification and KEGG enrichment of differentially expressed genes

The obtained clean-read datasets were aligned to *Z. rouxii* reference genome using HISAT2 (25). The RSEM software was used to quantify gene abundances, and the quantification of gene expression level was normalized using the FPKM (Fragments Per Kilobase of transcript perMillion mapped reads) method (26, 27). Differentially expressed genes (DEGs) across samples were identified using DESeq2 v1.18.1 on R package (version 3.4.2). The $\log_2$ (fold change) over 1 and false discovery rate (FDR) within 0.05 were set as the threshold for significant DEGs (28). Besides, the identified DEGs were carried out into hierarchical clustering, with the KEGG pathway enrichment analysis (29).

Quantitative real-time PCR analysis

To validate the transcriptional level results from RNA-seq data analysis, six genes including elongase 1–4, D9D, and D12D genes which are involved in the linoleic acid biosynthesis in *Z. rouxii*, were selected for real-time RT-PCR validation. Total RNA was extracted with E.Z.N.A. Fungal RNA Kit (Omega Bio-Tek, Norcross, GA, United States) according to the protocols of the manufacturer. Real-time RT-PCR was performed according to our previous work (30). GAPDH served as the reference gene for the normalization of the target gene expression and to correct for variation between samples. Primers used for the candidate genes were designed based on the Illumina sequencing data by using Primer Premier 5 and listed in **Supplementary Table 1**. The comparative $2^{-\Delta\Delta CT}$ method was employed to calculate the relative expression between the target genes.

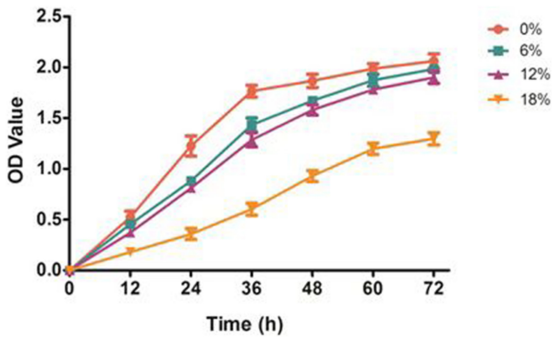

FIGURE 1
Effect of salt stress on the growth of *Z. rouxii*. 0, 6, 12, and 18% represent different salt concentrations, respectively.

Statistical analysis

All the data obtained in this experiment are presented as the mean of three replicates. Data from the same period were evaluated by two-way nested analysis of variance (ANOVA), followed by the least significant difference test (LSD) for mean comparison. All statistical analysis was performed with SAS 9.20 software (SAS Institute Inc., Cary, NC, United States) at a $p < 0.05$.

Results

Effect of salt stress on the growth performance of *Zygosaccharomyces rouxii*

To investigate the effects of salt stress on the growth performance of *Z. rouxii*, a preliminary study of different concentrations of salt treatments was conducted (**Figure 1**). *Z. rouxii* grew well in the control condition, and the maximum biomass yield (OD 600) reached to 2.1. With the salt concentrations increasing from 0 to 18%, the growth of *Z. rouxii* was gradually inhibited, and the highest OD 600 decreased from 2.1 to 1.2. This result suggested a great effect of salt stress on the growth performance of *Z. rouxii*. Of note, the similar growth performance of *Z. rouxii* was detected at 6 and 12% salt concentration, which illustrated both of these salt concentrations harbor the analogous effect on *Z. rouxii* growth. Moreover, the almost same maximum OD 600 was identified at 0, 6, and 12% salt concentrations, elucidating the high salt tolerance of *Z. rouxii*. The *Z. rouxii* grew slowly and almost stagnant during the period from 60 to 72 h, the samples thus cultured for 72 h were selected for the follow-up analysis.

Analysis of intracellular fatty acid of *Zygosaccharomyces rouxii* under salt stress

Previous studies have documented that changes of the membrane lipid composition have impacts on the membrane fluidity and then affect the stress resistance of yeast (31, 32). *Z. rouxii* inevitably encountered salt stress in the manufacture of high salty foods. However, the effect of salt stress on the fermented food produced by *Z. rouxii* is poorly understood. In the present study, the fatty acid content profiles of *Z. rouxii* grown under salt stress and control conditions were

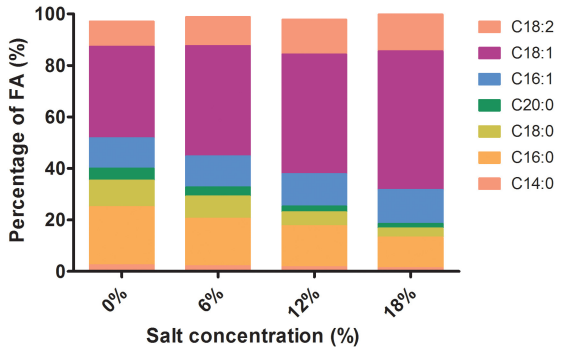

FIGURE 2
The main intracellular fatty acids content in *Z. rouxii* under salt stress.

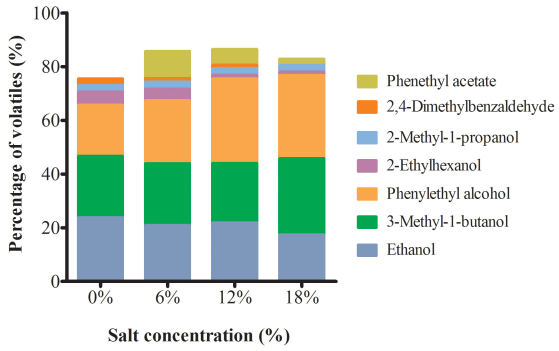

FIGURE 3
The main volatile substances content in *Z. rouxii* under salt stress.

qualitative and quantitative determinations by GC-MS. Our results revealed that the unsaturation of *Z. rouxii* increases with increasing salt concentrations (**Supplementary Figure 1**). In addition, the main composition of unsaturated and saturated fatty acid was also present on the **Figure 2**. The composition of fatty acid in *Z. rouxii* cells was dominated by C18 and C16, of them, the proportion of oleic acid (C18:1) was significantly increased with the increment of salt concentrations. Moreover, the proportion of linoleic acid was slightly increased, while palmitoleic acid was hardly increased at different salt concentrations. As for saturated fatty acid, palmitic acid and stearic acid were decreased significantly, while myristic acid and arachidic acid was slightly decreased (**Figure 2**).

Analysis of volatile substances of *Zygosaccharomyces rouxii* under salt stress

Volatile substances are essential compositions of flavor in fermented food (33). Here, GC-MS was applied to determine the volatile compounds present in the extracts of *Z. rouxii*. A total of 98, 91, 94, and, 90 volatile compounds was identified at 0, 6, 12, and 18% salt-treated group, of which, 33 volatiles were found commonly to all *Z. rouxii* (**Supplementary Table 2**). Alcohols and acids made more contributions to the total volatiles in comparison with esters, furans, aldehydes, phenols, and pyrazines. Furthermore, the main seven volatile compounds were identified as the major volatile compounds in *Z. rouxii* due to their higher concentration, such as ethanol, 3-methyl-1-butanol, and phenylethyl alcohol (**Figure 3**). Among them, the relative contents of ethanol, 2-ethylhexanol, and 2, 4-dimethylbenzaldehyde were decreased with the increment of salt concentration. In contrast, the relative contents of two edible spices, 3-methyl-1-butanol and phenylethyl alcohol were increased, whereas 2-methyl-1-propanol was kept steady under distinct salt stress. Noteworthily, phenethyl acetate, a food flavoring agent, was not detected in the control group.

Changes in organic acids content of *Zygosaccharomyces rouxii* under salt stress

Yeast bacteria can produce a greater diversity of organic acids during their metabolisms, such as lactic acid, lemon acid, malic acid, and succinic acid (29). Here, the profile of organic acids produced by *Z. rouxii* during fermentation at different salt concentrations was determined. The content of seven main organic acids has distinct degree changes under salt stress compared with the control group (**Figure 4**). Among them, the content of tartaric acid, acetic acid, and citrate acid was decreased significantly with the increment of salt concentrations. In contrast, no significantly increased content of malonic acid and D-malic acid was identified with the salt treatment, with the exception of 18% salt concentration, of which the content of malonic acid was decreased significantly. In addition, succinic acid was not detected in the control group and its content significantly increased with the increment of salt concentrations while oxalic acid was only identified in the 18% salt concentration-treated group.

Overview of transcriptome sequencing

To investigate the environmental stress response of *Z. rouxii* induced by salt, a transcriptome analysis based on RNA sequencing of *Z. rouxii* that was subjected to distinct salt concentrations were performed. This resulted into the generation of 43.84, 43.16, 45.05, and 45.66 million clean reads per library, respectively (**Table 1**). The GC content for all treatments was approximately 43%, and the % ≥Q30 (99.9% accuracy of bases) was greater than 94.4% for all samples,

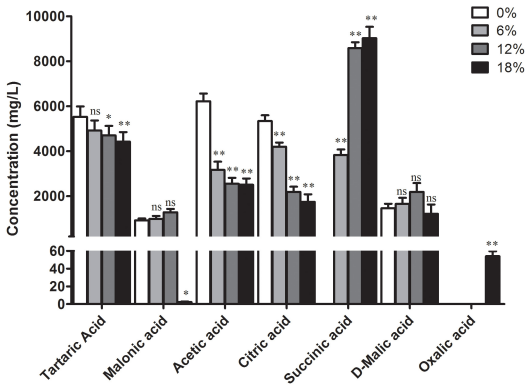

FIGURE 4
Intracellular content of seven organic acids in *Z. rouxii* under different salt concentrations, 0, 6, 12, and 18% represent different salt concentrations, respectively. The bars represent the average (±SE) of biological repeats. ^{ns}No significant difference; $^{*}p < 0.05$; $^{**}p < 0.01$.

elucidating a good quality of the sequencing data. Moreover, the clean reads were aligned to *Z. rouxii* genome sequence, and more than 83% of the clean reads for each sample were uniquely mapped to the genome. A summary of the RNA-seq sequencing was shown in **Table 1**.

Differentially expressed genes analysis of *Zygosaccharomyces rouxii* transcriptome under salt concentrations

To search genes with altered expression levels treated by different salt concentrations, the overall transcription levels of genes was quantified by RPKM metrics. Based on the global transcriptional changes from normalizing the DEG data, a total of 2,575 genes showed altered expression levels in the three salinity treatment groups, as compared to the control. There were 543, 659, and 1,373 DEGs that was identified in the control group and three salinity treatment groups, respectively (**Figure 5A**). Among them, 232, 173, and 685 genes expression being up-regulated at three salt concentrations compared to control groups, separately, whereas 311, 486, and 688 genes were down-regulated. To better present the effect of salt stress on *Z. rouxii*, a Venn diagram of DEG distribution at these groups was constructed for follow-up analysis due to their significant differences (**Figure 5B**). It was observed that only 153 DEGs were commonly shared among the distinct salt concentrations. It is noteworthy that the number of specific DEGs between WT-vs-NaCl-18 groups was significantly higher than that of the other two groups, revealing the involvement of complex developmental events of *Z. rouxii* cells under 18% salinity treatments (**Figure 5B**).

Differentially expressed genes involved in the citrate cycle

The citrate cycle (TCA cycle, Krebs cycle) is a crucial aerobic pathway involved in for the final steps of the oxidation of carbohydrates and fatty acids. Hence, differentially expressed genes involved in the TCA cycle was investigated according to the KEGG enrichment analysis. A total of 42 DEGs encodings 10 enzymes were identified to be involved in different steps in carbohydrate metabolism (**Figure 6**). In addition to phosphoenol-pyruvate carboxykinase, fumarase, and aconitase, both of which are encoded by two DEGs, the remaining enzymes responsible for TCA cycle are encoded by four to eight DEGs, such as succinate dehydrogenase (eight DEGs). The expression level of a majority of these DEGs was up-regulated obviously under 6% salt concentration treatment, and only a partly of DEGs was up-regulated at 12%, while the remaining DEGs were down-regulated or harbor no remarkable change. Intriguingly, almost all of the enzyme-encoding genes identified in the TCA cycle was significantly down-regulated under 18% salinity treatment, for example, succinate dehydrogenase and aconitase gene, and with special attention paid to several malate dehydrogenase and pyruvate dehydrogenase gene, which possessed a high expression level.

Expression analysis of linoleic acid biosynthesis genes under salt stress

Linoleic acid, a principal essential fatty acid, is also a critical structural component of cell membranes and has effect on cell membrane properties like fluidity, flexibility and permeability. These are six crucial enzymes involved in linoleic acid biosynthesis pathway, including elongase 1–4, two rate-limiting enzymes delta 9 fatty acid desaturases (D9D) and delta 12 fatty acid desaturases (D12D). According to the KEGG pathway analysis, 14 genes responsible for linoleic acid biosynthesis in *Z. rouxii* under salt stress were identified (**Figure 7**). Just three genes were up-regulated under 6% salinity treatment, the remaining gene were down-regulated or hardly changed, and the same number up-regulated and down-regulated genes were observed under 12% salinity treatment. Additionally, the great majority of genes encoding linoleic acid biosynthesis-related key enzymes were up-regulated under 18% salinity treatment. It has to be noted that four D9D and D12D genes were significant up-regulated under 6 and 18% salinity treatments. This result illustrated that high salt stress is beneficial to unsaturated fatty acid accumulation, which was consistent to the result of the proportion of unsaturated fatty acid determined before. Given that these six genes with notable expression levels in the distinct salt stress, the activity of D9D and D12D genes was enhanced at periods corresponding to linoleic acid production, implying a close correlation between

TABLE 1 Summary of the sequencing data of *Z. rouxii* under salt stress.

Samples	Clean reads	GC content	≥Q30	Mapped reads	Unique mapped	Multiple mapped
Control	43,842,750	43.44%	94.48%	39,983,819 (91.20%)	39,273,892 (89.58%)	709,927 (1.62%)
6%	43,164,604	42.61%	94.55%	36,394,985 (84.32%)	35,909,796 (83.19%)	485,189 (1.12%)
12%	45,056,174	43.71%	94.79%	40,484,678 (89.85%)	39,832,104 (88.41%)	652,574 (1.45%)
18%	45,667,748	43.70%	94.54%	41,373,537 (90.60%)	40,587,615 (88.88%)	785,922 (1.72%)

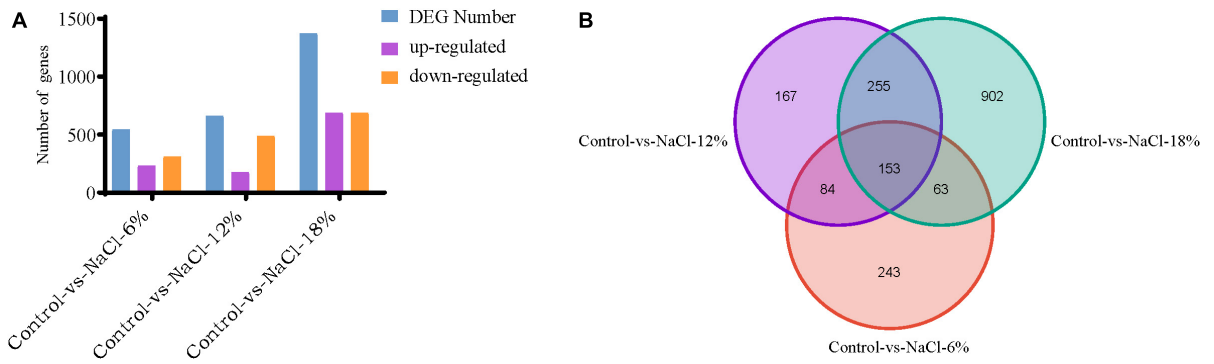

FIGURE 5
Distribution of differently expressed genes (DEGs) identified in the three samples. **(A)** Distribution of DEGs in the control group as compared to the salt-treated group. **(B)** Venn diagram exhibiting DEG distribution in three samples. NaCl-6%, -12%, and -18% represent the salt concentration of 6, 12 and 18% group, respectively.

salt stress and transcriptional regulation. This result was further supported by the relative expression levels of gene encoding elongase and D12D using qRT-PCR (**Supplementary Figure 2**).

Discussion

Accelerating and enhancing the flavor formation of fermented foods was a paramount pursuit of industrial production. The industrial important microbes, *Z. rouxii*, was observed this characteristic of fermentation under high salinity condition over the past few decades, and related molecular mechanism was being explored. Nevertheless, no convincing evidence or strongly explanation was obtained regarding the related molecular mechanism of accelerating and enhancing the flavor formation by *Z. rouxii* fermentation under high salinity condition. Herein, we performed a physiological and transcriptomic analysis to reveal the main flavor substance of *Z. rouxii* during fermentation under high-salt treatment conditions.

High salinity environment represents a stress induced high osmotic perturbation to fungi cells due to the excess salt disturbs osmotic potential and results in metabolic toxicity. In the present study, the growth performance of *Z. rouxii* was significantly decreased by salt stress, especially in high salt concentration (**Figure 1**), and this result was analogous to the study of Wang et al. (15). Meanwhile, the number of DEGs reached a peak in the 18% salt treatment group (1,373) while the number was reduced at 6 and 12% salinity (543 and 659), indicating a larger degree of change in gene expressions in the high salt group than that in the low salt treatment (**Figure 5**). The similar change of gene expressions was also observed in our previous studies on *Aspergillus oryzae* (21). Further more, the characteristic of *Z. rouxii* fermentation under hyper-osmotic condition, accelerating and enhancing the flavor formation of fermented foods, thus require a strong salt tolerance of *Z. rouxii* cells for the long-term fermentation. Previous researches pointed out that several compatible solutes such as carbohydrates, intracellular glycerol, amino acids, and trehalose were accumulated under salt stress, which can be used as osmotic protectants against stress-induced perturbations (15, 34). Aside from the accumulation of these osmotic protectants, changes in the membrane composition and properties represent an essential factor in the adaptation to high salinity environment (35). It is reported that *Z. rouxii* cells responded to the changes in lipid composition in the high NaCl condition, especially the increment of phospholipids with high oleic acid contents and decreases in triacylglycerol and linoleic acid (36). Moreover, this change can also affect the leakage of glycerol, and keep from the influx of sodium ions under that conditions (37). Herein, the unsaturation of fatty acids in *Z. rouxii* has a positive correlation with salt concentrations, and the main composition of unsaturated fatty acids was palmitoleic acid, oleic acid, and linoleic acid (**Figure 2** and **Supplementary Figure 1**). These results suggested that *Z. rouxii* produces more unsaturated fatty acids under salt stress, keeps the structure and function of

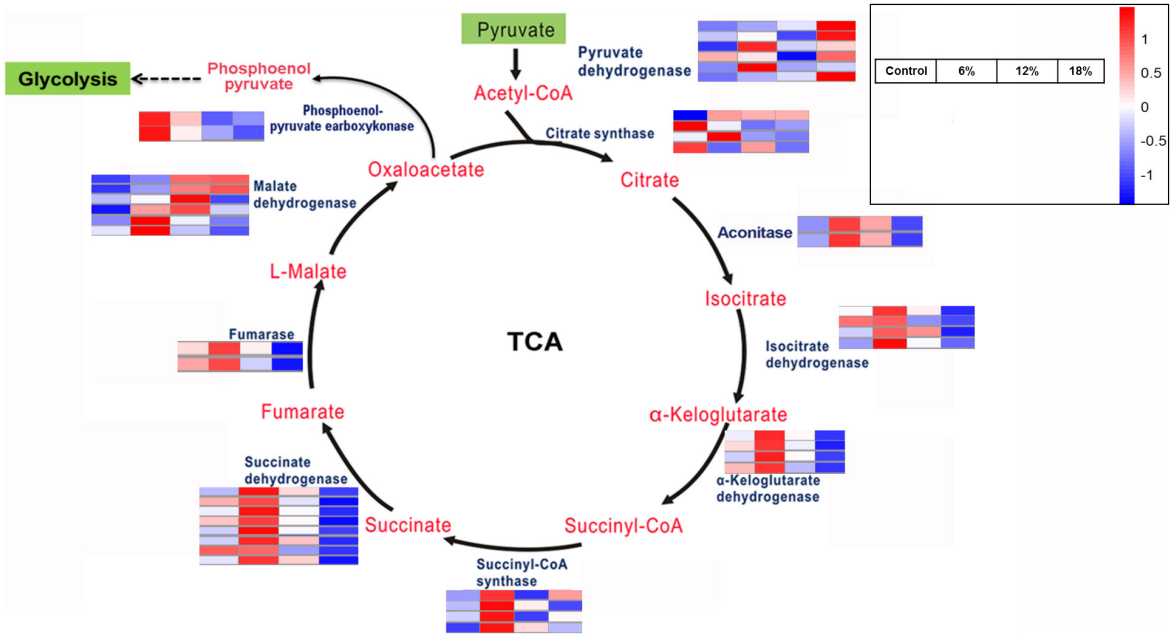

FIGURE 6
Key enzymes encoded by the DEGs involved in the citrate cycle.

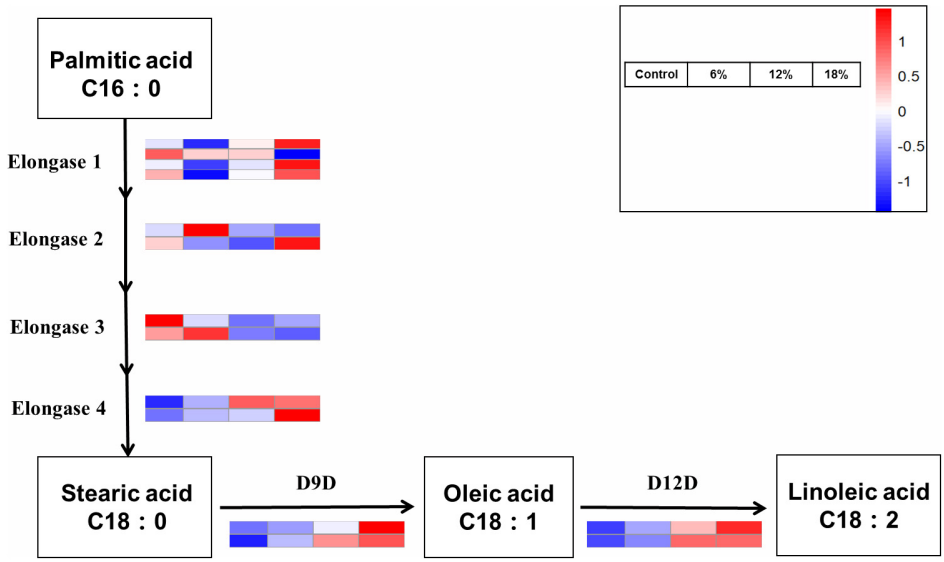

FIGURE 7
Differentially expressed genes involved in the linoleic acid biosynthesis pathways.

the cells and helps them adapt to the hypertonic environment. Similar results were also found in *Frankia* strains, *A. oryzae*, and halophilic yeast-like melanized fungi (23, 38, 39). Additionally, the relative expression levels of genes related to linoleic acid biosynthesis in *Z. rouxii* under salt stress further supported the conclusion that salinity stress led to an increase in fatty acid unsaturation to maintain the osmotic balance of cells with this condition. In fact, in the case of exposure of *Z. rouxii* cells to salinity stress, 7 genes encoding elongase 1, 2, and 4 (from C16:0 to C18:0) were up-regulated (Figure 7). However, the content of C16:0 and C18:0 were both decreased under salt stress. According to the expression level of D9D and D12D, we may know that large amounts of C18:0 were biosynthesized into oleic acid and linoleic acid. Noteworthily, the potential health benefits

of unsaturated fatty acids have attracted attention recently, and evidence is mounting on the role that several unsaturated fatty acids might play in the primary and secondary prevention of cardiovascular disease (40).

The volatile and non-volatile substances, such as organic acids, alcohols, and amino acids, have a considerable contribution to the main aroma of fermented foods. Through the analysis of volatile substances of *Z. rouxii* under salt stress, it is observed that 3-methyl-1-butanol and phenylethyl alcohol were increased with the increment of salt concentrations (**Figure 3**). 3-Methyl-1-butanol has apple brandy aroma and spicy flavor and is usually use as food spices, mainly for the preparation of apple and banana flavor. It is reported found in over 230 natural sources including apple, apricot, banana, sour cherry, cheese and so on (41). Phenylethyl alcohol usually existed in rose, carnation, hyacinth, Aleppo pine, orange blossom, and other organisms. It has a pleasant floral odor and used as an additive in cigarettes and also used as a preservative in soaps (42). Additionally, it is observed that phenethyl acetate was specially observed in the salt-treat Z. *rouxii*. Phenethyl acetate occurs in a number of essential oils and is a volatile aroma component of many fruits and alcoholic beverages. Phenylethyl acetate is a colorless liquid with a fine rose scent and a secondary, sweet, honey note. It is used in perfumery as a modifier of phenylethyl alcohol, for example, in rose and lilac compositions. In addition, it is used in a large number of aromas, in keeping with its natural occurrence (43). Hence, we speculate that these volatile substances are the main substance enhancing the flavor formation in *Z. rouxii* fermentation under salinity environment.

Further more, distinct degree changes of organic acids content in *Z. rouxii* was observed under salt treatment (**Figure 4**). The influence of salinity on the content of organic acids varies according to the microorganism and fermented production. The total levels of organic acids were elevated by salinity during the grapevine fermentation, which increased the production of tartaric and malic acids (44). In the less salt-sensitive cv. Korona, the concentration of total organic acids remained fairly constant under salinity environment. In the salt-sensitive cv. Elsanta, the contents of total organic acids, especially citric acid, increased significantly due to salt stress (45). The majority of organic acids were derived from glucose through the citrate cycle. Transcriptome analysis revealed that the pathway of the citrate cycle was activated corresponding to the content of organic acids, of which a majority of related DEGs were significantly up-regulated under salt treatment (**Figure 6**). The decrease of some organic acids, such as citric acid, may be due to the more conversion of downstream product. From the results, the content of succinic acid was significant higher in the salt-treated *Z. rouxii* while oxalic acid was only identified at the 18% salt concentration-treated group. Accordingly, we speculate that the content of glucose would be decreased under salt treatment, which need to be confirmed by experiment. Succinic acid is used as a dietary supplement for symptoms related to menopause such as hot flashes and irritability and also used as a flavoring agent for food and beverages (46). The FDA has granted succinic acid with the GRAS status (Generally Recognized as Safe Substance). These results suggested that succinic acid and oxalic acid may endow *Z. rouxii* under salt concentrations with special flavor.

Conclusion

In summary, we successfully characterized the transcriptomic profiles and the change of main flavor substance of *Z. rouxii* under salt treatment. *Z. rouxii* exhibited a good tolerance toward high concentrations of salt. Analysis of physiological data showed a accumulation of unsaturated fatty acids, succinic acid and oxalic acid. In addition, volatile substances analysis showed that concentrations of 3-methyl-1-butanol and phenylethyl alcohol were significantly increased with the increment of salt concentrations. Transcriptomic analysis showed an up-regulated expression of the genes related to TCA cycle and the linoleic acid synthesis. This study helps to understand the change of main flavor substance of *Z. rouxii* under salt treatment and guide their applications in the high salt liquid state fermentation of the soy sauce.

Data availability statement

The RNA-seq data presented in the study are deposited in the NCBI/SRA repository (www.ncbi.nlm.nih.gov/sra), accession number: PRJNA837122.

Author contributions

BH and MA conceived and designed the experiments. BG and RP performed the experiments. GL and YL analyzed the data. RW contributed to reagents, materials, analysis tools, and revised the manuscript. GL and RP wrote the manuscript. All authors contributed to the article and approved the submitted version.

Funding

This research was funded by the Natural Science Foundation of Jiangxi Province (Grant Nos. 20202BABL203043 and

20212BAB215005) and Graduate Education Reform Project (KSDYJG-2021-21).

Acknowledgments

Thank to Yayi Tu and Bin Zeng for the critical review of this manuscript.

Conflict of interest

The authors declare that the research was conducted in the absence of any commercial or financial relationships that could be construed as a potential conflict of interest.

Publisher's note

All claims expressed in this article are solely those of the authors and do not necessarily represent those of their affiliated organizations, or those of the publisher, the editors and the reviewers. Any product that may be evaluated in this article, or claim that may be made by its manufacturer, is not guaranteed or endorsed by the publisher.

Supplementary material

The Supplementary Material for this article can be found online at: https://www.frontiersin.org/articles/10.3389/fnut.2022.990380/full#supplementary-material

SUPPLEMENTARY FIGURE 1
Proportion of unsaturated and saturated fatty acids content in *Z. rouxii* at different salt concentrations.

SUPPLEMENTARY FIGURE 2
Relative expression level of six genes encoding crucial enzymes involved in linoleic acid biosynthesis pathway in *Z. rouxii* under different salt concentrations, 0, 6, 12, and 18% represent different salt concentrations, respectively. Gene 10103, 5047, 217, and 5506 are encoding elongase and gene 5111 and 1576 are encoding D12D, separately. The bars represent the average (±SE) of biological repeats. ^{ns}, *, **, and *** indicate statistically significant differences between the control and salt-treated groups (the least significant difference test): ns, no significant difference; $*p < 0.05$; $**p < 0.01$; $***p < 0.001$.

SUPPLEMENTARY TABLE 1
qRT-PCR primers used in this study.

SUPPLEMENTARY TABLE 2
Volatile compounds identified in this study.

References

1. van der Sluis C, Wolken WA, Giuseppin ML, Tramper J, Wijffels RH. Effect of threonine, cystathionine, and the branched-chain amino acids on the metabolism of *Zygosaccharomyces rouxii**. *Enzyme Microb Technol.* (2000) 26:292–300. doi: 10.1016/s0141-0229(99)00165-9

2. Sasaki M, Nunomura N, Matsudo T. Biosynthesis of 4-hydroxy-2(or 5)-ethyl-5(or 2)-methyl-3(2H)-furanone by yeasts. *J Agric Food Chem.* (1991) 39:934–8. doi: 10.1021/jf00005a027

3. Hecquet L, Sancelme M, Bolte J, Demuynck C. Biosynthesis of 4-hydroxy-2,5-dimethyl-3(2H)-furanone by *Zygosaccharomyces rouxii*. *J Agric Food Chem.* (1996) 44:1357–60. doi: 10.1021/jf950435j

4. Kataoka S. Functional effects of Japanese style fermented soy sauce (shoyu) and its components. *J Biosci Bioeng.* (2005) 100:227–34. doi: 10.1263/jbb.100.227

5. Dakal TC, Solieri L, Giudici P. Adaptive response and tolerance to sugar and salt stress in the food yeast *Zygosaccharomyces rouxii*. *Int J Food Microbiol.* (2014) 185:140–57. doi: 10.1016/j.ijfoodmicro.2014.05.015

6. Whiting GC. Organic acid metabolism of yeasts during fermentation of alcoholic beverages-a review. *J Inst Brew.* (1976) 82:84–92. doi: 10.1002/j.2050-0416.1976.tb03731.x

7. Kaneda H, Takashio M, Tamaki T, Osawa T. Influence of PH on flavour staling during beer storage. *J Inst Brew.* (1997) 103:21–3. doi: 10.1002/j.2050-0416.1997.tb00932.x

8. Li G, Liu F. Changes in organic acids during beer fermentation. *J Am Soc Brew Chem.* (2015) 73:275–9. doi: 10.1094/ASBCJ-2015-0509-01

9. Featherstone S. Ingredients used in the preparation of canned foods. In: Featherstone S editor. *A Complete Course in Canning and Related Processes*. Oxford: Woodhead Publishing (2015). p. 147–211.

10. Sousa MJ, Ludovico P, Rodrigues F, Leão C, Côrte-Real M. "Stress and cell death in yeast induced by acetic acid," In: Bubulya P Editor. *Cell Metabolism – Cell Homeostasis and Stress Response*. Princes Gate Court: InTech (2012). doi: 10.5772/27726

11. Chaves SR, Rego A, Martins VM, Santos-Pereira C, Sousa MJ, Côrte-Real M. Regulation of cell death induced by acetic acid in yeasts. *Front Cell Dev Biol.* (2021) 9:642375. doi: 10.3389/fcell.2021.642375

12. Wah TT, Walaisri S, Assavanig A, Niamsiri N, Lertsiri S. Co-culturing of *Pichia guilliermondii* enhanced volatile flavor compound formation by *Zygosaccharomyces rouxii* in the model system of Thai soy sauce fermentation. *Int J Food Microbiol.* (2013) 160:282–9. doi: 10.1016/j.ijfoodmicro.2012.10.022

13. Csonka LN. Physiological and genetic responses of bacteria to osmotic stress. *Microbiol Rev.* (1989) 53:121–47. doi: 10.1128/mr.53.1.121-147.1989

14. Prasad J, McJarrow P, Gopal P. Heat and osmotic stress responses of probiotic *Lactobacillus rhamnosus* HN001 (DR20) in relation to viability after drying. *Appl Environ Microbiol.* (2003) 69:917–25. doi: 10.1128/aem.69.2.917-925.2003

15. Wang D, Hao Z, Zhao J, Jin Y, Huang J, Zhou R, et al. Comparative physiological and transcriptomic analyses reveal salt tolerance mechanisms of *Zygosaccharomyces rouxii*. *Process Biochem.* (2019) 82:59–67. doi: 10.1016/j.procbio.2019.04.009

16. Wang D, Mi T, Huang J, Zhou R, Jin Y, Wu C. Metabolomics analysis of salt tolerance of *Zygosaccharomyces rouxii* and guided exogenous fatty acid addition for improved salt tolerance. *J Sci Food Agric.* (2022) 5:11975. doi: 10.1002/jsfa.11975

17. van der Sluis C, Tramper J, Wijffels RH. Enhancing and accelerating flavour formation by salt-tolerant yeasts in Japanese soy-sauce processes. *Trends Food Sci Technol.* (2001) 12:322–7. doi: 10.1016/S0924-2244(01)00094-2

18. Liu B, Wang X, Zhao J, Qin L, Shi L, Zhou T, et al. Effects of salinity on the synthesis of 3-methylthiopropanol, 2-phenylethanol, and isoamyl acetate in *Zygosaccharomyces rouxii* and *Z. rouxii* 3-2. *Bioprocess Biosyst Eng.* (2020) 43:831–8. doi: 10.1007/s00449-019-02279-3

19. Hayashida Y, Nishimura K, Slaughter JC. The influence of mash pre-aging on the development of the flavour-active compound, 4-hydroxy-2(or5)-ethyl-5(or2)-methyl-3(2H)-furanone (HEMF), during soy sauce fermentation. *Int J Food Sci Technol.* (2003) 32:11–4. doi: 10.1046/j.1365-2621.1997.00378.x

20. Solieri L, Vezzani V, Cassanelli S, Dakal TC, Pazzini J, Giudici P. Differential hypersaline stress response in *Zygosaccharomyces rouxii* complex yeasts: a physiological and transcriptional study. *FEMS Yeast Res.* (2016) 16:fow063. doi: 10.1093/femsyr/fow063

21. He B, Hu Z, Ma L, Li H, Ai M, Han J, et al. Transcriptome analysis of different growth stages of *Aspergillus oryzae* reveals dynamic changes of distinct classes of genes during growth. *BMC Microbiol.* (2018) 18:12. doi: 10.1186/s12866-018-1158-z

22. Benucci I, Cecchi T, Lombardelli C, Maresca D, Mauriello G, Esti M. Novel microencapsulated yeast for the primary fermentation of green beer: kinetic behavior, volatiles and sensory profile. *Food Chem.* (2021) 340:127900. doi: 10.1016/j.foodchem.2020.127900

23. He B, Ma L, Hu Z, Li H, Ai M, Long C, et al. Deep sequencing analysis of transcriptomes in *Aspergillus oryzae* in response to salinity stress. *Appl Microbiol Biotechnol.* (2018) 102:897–906. doi: 10.1007/s00253-017-8603-z

24. Langmead B, Salzberg SL. Fast gapped-read alignment with Bowtie 2. *Nat Methods.* (2012) 9:357–9. doi: 10.1038/nmeth.1923

25. Kim D, Langmead B, Salzberg SL. HISAT: a fast spliced aligner with low memory requirements. *Nat Methods.* (2015) 12:357–60. doi: 10.1038/nmeth.3317

26. Mortazavi A, Williams BA, McCue K, Schaeffer L, Wold B. Mapping and quantifying mammalian transcriptomes by RNA-Seq. *Nat Methods.* (2008) 5:621–8. doi: 10.1038/nmeth.1226

27. Dewey CN, Bo L. RSEM: accurate transcript quantification from RNA-Seq data with or without a reference genome. *BMC Bioinformatics.* (2011) 12:323–323.

28. Wang D, Chen H, Yang H, Yao S, Wu C. Incorporation of exogenous fatty acids enhances the salt tolerance of food yeast *Zygosaccharomyces rouxii*. *J Agric Food Chem.* (2021) 69:10301–10. doi: 10.1021/acs.jafc.1c03896

29. Zou M, Zhu X, Li X, Zeng X. Changes in lipids distribution and fatty acid composition during soy sauce production. *Food Sci Nutr.* (2019) 7:764–72. doi: 10.1002/fsn3.922

30. Lv G, Xu Y, Tu Y, Cheng X, Zeng B, Huang J, et al. Effects of nitrogen and phosphorus limitation on fatty acid contents in *Aspergillus oryzae*. *Front Microbiol.* (2021) 12:739569. doi: 10.3389/fmicb.2021.739569

31. Rodríguez-Vargas S, Sánchez-García A, Martínez-Rivas JM, Prieto JA, Randez-Gil F. Fluidization of membrane lipids enhances the tolerance of *Saccharomyces cerevisiae* to freezing and salt stress. *Appl Environ Microbiol.* (2007) 73:110–6. doi: 10.1128/aem.01360-06

32. Vázquez J, Grillitsch K, Daum G, Mas A, Beltran G, Torija MJ. The role of the membrane lipid composition in the oxidative stress tolerance of different wine yeasts. *Food Microbiol.* (2019) 78:143–54. doi: 10.1016/j.fm.2018.10.001

33. Shukla S, Choi TB, Park HK, Kim M, Lee IK, Kim JK. Determination of non-volatile and volatile organic acids in Korean traditional fermented soybean paste (Doenjang). *Food Chem Toxicol.* (2010) 48:2005–10. doi: 10.1016/j.fct.2010.04.034

34. Wood JM, Bremer E, Csonka LN, Kraemer R, Poolman B, van der Heide T, et al. Osmosensing and osmoregulatory compatible solute accumulation by bacteria. *Comp Biochem Physiol A Mol Integr Physiol.* (2001) 130:437–60. doi: 10.1016/S1095-6433(01)00442-1

35. Russell NJ, Evans RI, ter Steeg PF, Hellemons J, Verheul A, Abee T. Membranes as a target for stress adaptation. *Int J Food Microbiol.* (1995) 28:255–61. doi: 10.1016/0168-1605(95)00061-5

36. Watanabe Y, Takakuwa M. Change of lipid composition of *Zygosaccharomyces rouxii* after transfer to high sodium chloride culture medium. *J Ferment Technol.* (1987) 65:365–9. doi: 10.1016/0385-6380(87)90131-2

37. Yoshikawa S, Mitsui N, Chikara K-I, Hashimoto H, Shimosaka M, Okazaki M. Effect of salt stress on plasma membrane permeability and lipid saturation in the salt-tolerant yeast *Zygosaccharomyces rouxii*. *J Ferment Bioeng.* (1995) 80:131–5. doi: 10.1016/0922-338X(95)93207-Z

38. Turk M, Méjanelle L, Šentjurc M, Grimalt JO, Gunde-Cimerman N, Plemenitaš A. Salt-induced changes in lipid composition and membrane fluidity of halophilic yeast-like melanized fungi. *Extremophiles.* (2004) 8:53–61. doi: 10.1007/s00792-003-0360-5

39. Srivastava A, Singh SS, Mishra AK. Modulation in fatty acid composition influences salinity stress tolerance in Frankia strains. *Ann Microbiol.* (2014) 64:1315–23. doi: 10.1007/s13213-013-0775-x

40. Abdelhamid AS, Brown TJ, Brainard JS, Biswas P, Thorpe GC, Moore HJ, et al. Omega-3 fatty acids for the primary and secondary prevention of cardiovascular disease. *Cochrane Database Syst Rev.* (2020) 3:CD003177. doi: 10.1002/14651858.CD003177.pub5

41. Kaminarides S, Stamou P, Massouras T. Changes of organic acids, volatile aroma compounds and sensory characteristics of Halloumi cheese kept in brine. *Food Chem.* (2007) 100:219–25. doi: 10.1016/j.foodchem.2005.09.039

42. Ghosh S, Kebaara BW, Atkin AL, Nickerson KW. Regulation of aromatic alcohol production in Candida albicans. *Appl Environ Microbiol.* (2008) 74:7211–8. doi: 10.1128/aem.01614-08

43. Trindade de Carvalho B, Holt S, Souffriau B, Lopes Brandão R, Foulquié-Moreno MR, Thevelein JM. Identification of novel alleles conferring superior production of rose flavor phenylethyl acetate using polygenic analysis in yeast. *mBio.* (2017) 8:e01173–7. doi: 10.1128/mBio.01173-17

44. Li X, Wang C, Li X, Yao Y, Hao Y. Modifications of Kyoho grape berry quality under long-term NaCl treatment. *Food Chem.* (2013) 139:931–7. doi: 10.1016/j.foodchem.2013.02.038

45. Keutgen A, Pawelzik E. Quality and nutritional value of strawberry fruit under long term salt stress. *Food Chem.* (2008) 107:1413–20.

46. Dessie W, Wang Z, Luo X, Wang M, Qin Z. Insights on the advancements of in Silico metabolic studies of succinic acid producing microorganisms: a review with emphasis on *Actinobacillus succinogenes*. *Fermentation.* (2021) 7:220. doi: 10.3390/fermentation7040220

frontiers | Frontiers in Nutrition

TYPE Original Research
PUBLISHED 30 August 2022
DOI 10.3389/fnut.2022.966697

OPEN ACCESS

EDITED BY
Yanyan Zhang,
University of Hohenheim, Germany

REVIEWED BY
Oluwaseun Bamidele,
University of Mpumalanga,
South Africa
Xiufang Dong,
Qingdao University of Science
and Technology, China

*CORRESPONDENCE
Bei Wang
wangbei@th.btbu.edu.cn
Yanping Cao
caoyp@th.btbu.edu.cn

SPECIALTY SECTION
This article was submitted to
Food Chemistry,
a section of the journal
Frontiers in Nutrition

RECEIVED 11 June 2022
ACCEPTED 11 August 2022
PUBLISHED 30 August 2022

CITATION
Zhang Z, Meng F, Wang B and Cao Y
(2022) Effects of antioxidants on
physicochemical properties
and odorants in heat processed beef
flavor and their antioxidant activity
under different storage conditions.
Front. Nutr. 9:966697.
doi: 10.3389/fnut.2022.966697

Effects of antioxidants on physicochemical properties and odorants in heat processed beef flavor and their antioxidant activity under different storage conditions

Zeyu Zhang, Fanyu Meng, Bei Wang* and Yanping Cao*

Beijing Advanced Innovation Center for Food Nutrition and Human Health, School of Food and Health, Beijing Higher Institution Engineering Research Center of Food Additives and Ingredients, Beijing Technology and Business University, Beijing, China

Heat processed beef flavor (HPBF) is a common thermal process flavoring, whose flavor properties can be affected by lipid oxidation during storage. Addition of antioxidants is an option to avoid the changes of HPBF induced by lipid oxidation. In this study, the effects of three antioxidants, tert-butylhydroquinone (TBHQ), tea polyphenol (TP), and L-ascorbyl palmitate (L-AP), on volatile components, physicochemical properties, and antioxidant activities of HPBF were studied over 168 days at different temperatures (4, 20, and 50°C). Although all three antioxidants had little effect on browning, acidity, water activity, and secondary lipid oxidation products, L-AP and TBHQ showed greater capabilities to prevent the formation of primary lipid oxidation products than TP. According to the results of oxidation reduction potential and DPPH radical scavenging experiments, TBHQ had better antioxidant ability compared to L-AP and TP during the storage. Of note, TBHQ affected the flavor profiles of HPBF, mainly on volatile odorants produced by lipid degradation. TBHQ could mitigate the development of unfavorable odorants. This study indicated TBHQ would enhance lipid oxidation stability and maintain physicochemical properties and flavor profiles of HPBF during storage. It suggested that TBHQ could be applied as an alternative additive to improve the quality of HPBF related thermal process flavorings.

KEYWORDS

heat processed beef flavor, antioxidant, odorant, physicochemical, lipid oxidation

Introduction

Heat processed beef flavor (HPBF) is known as one of the "thermal process" flavorings produced by heating a mixture of two or more precursor materials (1). A major purpose of "thermal process" flavorings is to enhance the characteristic meaty note of foods (2, 3). However, the negative changes in quality during storage might be affected by storage time and temperature. It is well-known that the Maillard reaction and lipid oxidation are of the utmost importance for the development of meaty note, which occur as the main processes during thermal treatment and storage (4). Lipids determine the flavor properties of products with a meaty note (5, 6). Lipid oxidation products give generally fatty and meaty notes which determines the aroma differences between meats from different species (7). Lipid-derived compounds, such as certain aldehydes with higher odor detection threshold values, generally have a higher contribution to overall favor profiles than the sulfur or nitrogen heterocyclic compounds formed through the Maillard reaction (5, 8).

The quality changes caused by lipid oxidation reactions are more prominent than those caused by reactions with other precursors (9, 10). All lipid-containing products, even those with minimal unsaturated fatty acid contents, have essentially the potential ability to undergo lipid oxidation in highly processing or during prolonged storage (11). Fatty acids presented in animal meats, especially polyunsaturated fatty acids increase the risk of oxidation reaction, leading to undesirable flavors (12). Radical species produced by lipid oxidation may have an unfavorable effect on the physicochemical properties, such as browning (13). Thus, appropriate evaluation and control of lipid oxidation are controversial issues.

Antioxidants have been employed to improve food quality by preventing lipid oxidation (14). Tert-butylhydroquinone (TBHQ), L-ascorbyl palmitate (L-AP), and tea polyphenol (TP) are the most commonly used antioxidants in the current relevant Chinese national standard GB-2760 (15). These antioxidants have the potential ability to prevent lipid oxidation in meat-based products and maintain the flavor stability of food (16). Lipid-soluble TBHQ as one of the synthetic antioxidants has been widely utilized to prevent lipid oxidation (17). Even the addition of TP, a water-soluble antioxidant, could inhibit the lipid oxidation of sausages made of meat (18), which has shown antioxidant performance comparable to TBHQ (19). L-AP as one of the intermediate polarity antioxidants provided antioxidant protection comparable to TBHQ during a long-term storage of flaxseed oil (20).

However, the effects of antioxidants with different solubility on the performance and flavor properties of the water-oil mixtures are controversial (21, 22). Frankel et al. (23) reported that the antioxidant activity of TBHQ was higher than that of L-AP in the emulsion system, which could mitigate flavor deterioration. This finding by Frankel et al. (23) is consistent with the results obtained by Gordon and Kourkimskå (24) in deep-fried rapeseed oil (as with bulk oils). This could be due to the fact that lipophilic antioxidants are more potent in emulsions than in bulk oils (considered water-in-oil nanoemulsions) (25). In contrast, Wanasundara and Shahidi (26) found that TBHQ and butylated hydroxyanisole (BHA) were not as effective as catechins (the primary component of TP) in preventing the oxidation of seal blubber or menhaden oil, as well as the odor and flavor of lipid-containing foods. Zhang et al. (27) reported that polyphenolic antioxidants (e.g., TP) can effectively alleviate lipid oxidation while also enhancing unpleasant odors due to their astringency. Consequently, it is still challengeable to control lipid oxidation and improve aroma profiles in parallel.

Hence, it is necessary to obtain the optimum antioxidant to control lipid oxidation and mitigate flavor deterioration of HPBF within a water-oil mixture during the storage. To achieve this purpose, TBHQ, TP, and L-AP were added into HPBF as lipid soluble, water soluble, and intermediate polarity antioxidants respectively. A potential antioxidant was determined by evaluating the effects of three antioxidants on lipid oxidative stability, physicochemical properties, and volatile components of HPBF. The purpose of this study was to provide a basis for the development of thermal process flavorings with high quality.

Materials and methods

Materials and reagents

Amino acids (glycine, cysteine), monosaccharide (glucose, xylose), Protamex (120 U/mg), and Flavourzyme (20 U/mg) were obtained from Shanghai Yuanye Biotechnology Co., Ltd. (Shanghai, China). Yeast extract was purchased by Beijing Aoboxing Biotech Co., Ltd. (Beijing, China). Spices (including clove, cinnamon, and fennel), fresh beef lean meat, fresh onion, garlic, and ginger were purchased from the local supermarket.

Reagents used in the study are listed as follows: isooctane, isopropyl alcohol, potassium thiocyanate, ferrous chloride

Abbreviations: HPBF, heat processed beef flavor; TBHQ, tert-butylhydroquinone; TP, tea polyphenol; L-AP, L-ascorbyl palmitate; BHA, butylated hydroxyanisole; ORP, oxidation reduction potential; PV, peroxide value; TBARS, thiobarbituric acid reactive substances; a_w, water activity; SPME-GC/MS, solid phase microextraction-gas chromatography/mass spectrometry.

anhydrous, ethanol, and butanol were purchased from Fuchen Chemical Reagent Co., Ltd. (Tianjin, China). Trichloroacetic acid (TCA) and 2-thiobarbituric acid (TBA, biochemical reagent, purity ≥ 98.5%) were obtained from Sinopharm Chemical Reagent Co., Ltd. (Beijing, China). Ethylene diamine tetraacetic acid (EDTA) was provided by Beijing Biotopped Science and Technology Co., Ltd. (Beijing, China). 1,1-Diphenyl-2-picrylhydrazyl (DPPH) was purchased from Shanghai Yuanye Biotechnology Co., Ltd. (Shanghai, China). Tert-butylhydroquinone (TBHQ), tea polyphenols (TP), L-ascorbyl palmitate (L-AP), and 1,1,3,3-tetraethoxy propane were purchased from Shanghai Macklin Biochemistry Co., Ltd. (Shanghai, China). 2-Methyl-3-heptanone and n-alkane were purchased by Sigma-Aldrich (Shanghai, China). Methanol [purity ≥ 99.9%, Mreda Technology Inc. (United States)], and ammonium acetate (purity ≥ 98.7%, Thermo Fisher Scientific, Inc.) were of HPLC grade. In addition, n-hexane (purity ≥ 99.9%) of GC grade was purchased from Mreda Technology Inc. (United States). Distilled-deionized water used in all experiments was purified using a Milli-Q Gradient (Millipore, Bedford, MA, United States). Helium gas (99.9992% purity) was provided by Beijing Tianlirenhe Material Trade Co. Ltd. (Beijing, China).

Samples preparation

The HPBF samples (control) was prepared by mixing of an enzymatic hydrolysate and other ingredients. To prepare the enzymatic hydrolysate, the fresh beef lean meat was trimmed of its fat and connective tissue and then crushed prior to the experiment. The meat paste was hydrolyzed by 0.21 g of Protamex (120 U/mg) and 0.42 g of Flavourzyme (20 U/mg) for 60 and 240 min, respectively. After cooling of the above enzymatic hydrolysate, the ingredients of HPBF were weighed according to the proportion of ingredients including 21.0% bovine bone, 2.7% yeast extract, 0.3% glycine, 0.3% cysteine, 0.9% glucose, 0.3% xylose, 4.8% fresh onion, 1.9% garlic, 0.9% ginger, and 0.076% spice powder. Those ingredients of HPBF were completely mixed with the enzymatic hydrolysate before being placed in a steam sterilization pot at 115°C for 60 min. In the treatment group, TBHQ, TP, and L-AP were added at a level of 0.02% based on fat content.

The sterilized HPBF was filtered and filled into 40 mL glass vials (Supelco, United States) sealed with screwed top PTFE/silicone septa. The HPBF samples were stored at 4, 20 and 50°C, respectively. Among them, 4°C represents low temperature and 20°C represents room temperature. In addition to accelerate the storage, the temperature of 50°C also applied and represents the high temperature conditions. The relevant physicochemical characteristics and odorants were determined for 168 days including a total of 17 sets (1, 7, 14, 21, 28, and so on up to 168 days).

Oxidative stability

Oxidation reduction potential

Oxidation reduction potential (ORP) was measured using a calibrated hand-held ORP Electrode LE501 [Mettler Toledo International Trading (Shanghai) Co., Ltd., Shanghai, China]. The ORP readings (mV) was determined by the method described in Capuani et al. (28) with minor modifications. The redox electrode was inserted into the HPBF immediately after leaving the electrolyte solution of 3 M KCl in order to minimize the effect of air. The redox electrode was checked using a redox buffer solution of 220 mV/pH 7 from Mettler Toledo before each use.

Peroxide value

Lipid peroxides were quantitated using a modified method by Chaiyasit et al. (29). The original sample (1 mL) and 5 mL of isooctane-isopropyl alcohol (2:1, v/v) solution were stirred by eddy current for 30 s, and then centrifugation at 9000 rpm for 5 min. The clear upper layer (2 mL) was mixed thoroughly with 20 μL of potassium thiocyanate solution and 20 μL of ferrous chloride solution (0.144 M). The mixture was mixed with butanol-methanol (v/v, 2:1) solution to obtain a 5 mL mixed solution. Absorbance was measured at 510 nm after incubation away from light for 20 min at room temperature. A standard curve made up of diluted ferrous chloride solutions was used to calculate lipid peroxide concentrations in the HPBF. The results of PV value were expressed as the uptake of mEq of active oxygen per kg of lipid (mEq/kg).

Thiobarbituric acid reactive substances

The TBARS assay was performed according to a previously method described by Papastergiadis et al. (30) with slight adjustments. Briefly, 1 g HPBF was mixed with a total of 5 mL of 7.5% TCA (w/v) with 0.02% (w/v) of EDTA. The mixed solution was homogenized with a refrigerated centrifuge (Hunan Herexi Instrument and Equipment Co., Ltd., Changsha, China) for 10 min at 8000 rpm. The homogenate was treated with 5 mL TBA reagent (20 mM) at 90°C for 30 min, and then filtered through a 0.22 Millipore membrane filter (MREDA Technology Inc., Beijing, China) after cooled using running water. Ten μL mixture solution was separated by Waters 2695 HPLC on a Waters SunFireTM C18 column (4.6 × 250 mm, 5 μm) using a mobile phase of 10 mM ammonium acetate and methanol (7:3, v/v). The column temperature was 30°C. The detection wavelength was 532 nm using Waters 2996 photodiode array detector (PAD). A standard curve made up of diluted 1,1,3,3-tetraethoxy propane solutions was used to calculate the amount of TBARS. The results were given in milligrams of MDA equivalents per kilogram of the sample (mg MAD/kg).

1,1-Diphenyl-2-picrylhydrazyl radical scavenging activity

The antioxidant activity in the DPPH assay was performed in the manner of the descriptions given by previous reports (31) with minor modifications. A dilution of 1 mL HPBF (diluted 500 times with deionized water) was thoroughly mixed with 3 mL of DPPH ethanol solution (0.1 mM). The mixture was incubated at room temperature for 30 min in the dark. The ethanol control group was added as a blank for DPPH. An ultraviolet-visible spectrophotometer (UV-1240, Shimadzu, Co., Ltd., Tokyo, Japan) was used to measure the absorbance at 517 nm to estimate the radical scavenging capacity of antioxidant samples at each storage time.

Physicochemical characteristics evaluation

Browning determination

Browning degree was linked with the absorbance at 420 nm (32). Non-enzymatic browning was monitored using the ultraviolet-visible spectrophotometer (UV-1240, Shimadzu, Co., Ltd., Tokyo, Japan) against water at 420 nm.

pH level determination

The pH was measured by using a calibrated hand-held pH meter [TB-214, Mettler Toledo International Trading (Shanghai) Co., Ltd., Shanghai, China]. The pH was calibrated using pH 4, pH 6.86, and pH 9.18 calibration buffers.

Water activity (a_w) determination

The water activity (a_w) was measured using an AquaLab 4TEV water activity meter in capacitance mode after samples reached equilibrium at 25°C.

Volatile compounds analysis

Extraction of volatiles by HS-SPME

Volatile compounds of HPBF were analyzed by means of solid-phase microextraction-Gas chromatography/Mass spectrometry (SPME-GC/MS) with a DB-WAX column (30 m, 0.25 mm i.d., 0.25 μm film thickness, Agilent). For each sample, 10 mL of HPBF were added to a 40 mL headspace bottle (Supelco, United States) containing 1 μL of 2-methyl-3-heptanone (diluted by a factor of 1000 in hexane) as the internal standard, and allowed to stand for 30 min at 45°C. The DVB/carboxen/PDMS fiber (Supelco, United States) was then exposed to the headspace of HPBF for 30 min while the vial was maintained at 45°C, and desorbed at 250°C for 5 min in the injection port after headspace collection. The experiments were performed in triplicate.

GC-MS analysis

GC-MS analyses were performed on an Agilent 7890B gas chromatography coupled to an Agilent 5977A mass spectrometer. The DVB/carboxen/PDMS fiber was desorbed in splitless mode with a splitless inlet liner of 0.75 mm inlet diameter (Agilent) suitable at 250°C for SPME analysis. The mass spectrometer was operated in electron impact mode with the electron energy set at 70 eV to obtain the mass spectra. A mass scan from *m/z* 35 to *m/z* 400 was performed with the ion source at 230°C. Helium was used as the carrier gas at a rate of 1 mL/min. The oven program started at 40°C for 2 min, then increased at 4°C/min to 190°C, and subsequently to 240°C at 8°C/min.

Isolation and identification of the volatiles

Volatile compounds were identified by comparing mass spectrometry patterns from the NIST14 database with linear retention indices (RI) based on a homologous series of even numbered n-alkanes (C7-C40). A semi-quantitative analysis of the detected volatile compounds was performed based upon comparison of their GC-MS peak regions to the internal standard (2-methyl-3-heptanone).

An Agilent 7890B gas chromatography coupled to a sniffing port ODP-3 from Gerstel was employed to analyze HPBF under the same analytical conditions. Volatile odorants were sniffed by trained panelists (two females and one male) on the top of the sniffing port and were used for the PCA analysis.

Statistical analysis

The least significant difference among different samples was analyzed using the one-way analysis of variance (ANOVA) with SPSS Statistics 22.0 (IBM Corporation, New York, NY, United States). All analyses for significant differences set at a 5% significance level. Statistical analysis each experiment was independently triplicated to derive an average and standard deviation. The data were subjected to principal component analysis (PCA) and illustrated using Origin 2021b (OriginLab Corporation, Northampton, MA, United States).

Results and discussion

Oxidative stability analysis

Oxidation reduction potential

Oxidation reduction potential is a measure of a chemical species to acquire electrons and thereby be reduced. As shown in **Supplementary Figures 1A–C**, the ORP values increased steadily in all treatments (TBHQ, TP, and L-AP) with the increasing storage time. The results showed that lipids in HPBF were continuously oxidized during storage. Besides, three

antioxidants (TBHQ, TP, and L-AP) had only a small effect on the potential redox of HPBF during storage. There was no significant difference ($p > 0.05$) between the treatment groups (TP or L-AP) and control. An addition of TBHQ in HPBF decreased potential redox values after 98 days compared to the control at a lower temperature (4°C). This suggested that the antioxidant effect of TBHQ in HPBF was superior to that of TP and L-AP at 4°C. As a results, TBHQ may be a potent antioxidant that produce an additive protective effect during storage, inhibiting the oxidative degradation of lipids.

Peroxide value

Peroxide value (PV) was quantified by measuring the concentration of lipid peroxides, which is normally considered as the product of primary lipid oxidation (33). As shown in Figure 1, the three antioxidants (TBHQ, TP, L-AP), as well as storage period, have a significant ($p < 0.05$) effect on the PV of HPBF. PV increased significantly ($p < 0.05$) both in the control and treated samples during the storage. The increased PV value suggested that the number of lipid peroxides produced by lipid oxidative processes increased gradually with time. A distinct drop before 28 days may be due to the unstable decomposition of primary lipid oxidation products into shorter chain hydrocarbon (34).

In the initial stage of storage, the PV of the L-AP treatment group was lower than that of the control group at any storage temperatures, followed by the TBHQ treatment group and TP treatment group. There was no clear distinction between the control group and the TP treatment group. The results indicated that TBHQ, followed by L-AP, had an antioxidant effect on primary lipid oxidation products for HPBF during storage. According to the findings of Wang et al. (35), both TBHQ and L-AP showed a significant ($p < 0.05$) antioxidant effect, which effectively retarded the oxidative degradation of polyunsaturated fatty acids. However, the antioxidant activity of TBHQ was better than that of L-AP in oil and fat, which was different from our results. This could be as a consequence that L-AP with compatible properties had a better antioxidant activity than TBHQ for a water-oil mixture of the HPBF. Besides, the antioxidant effect of TP was lower than TBHQ. A similar effect of TBHQ and TP was observed by Rababah et al. (36) who confirmed that TBHQ was the most effective

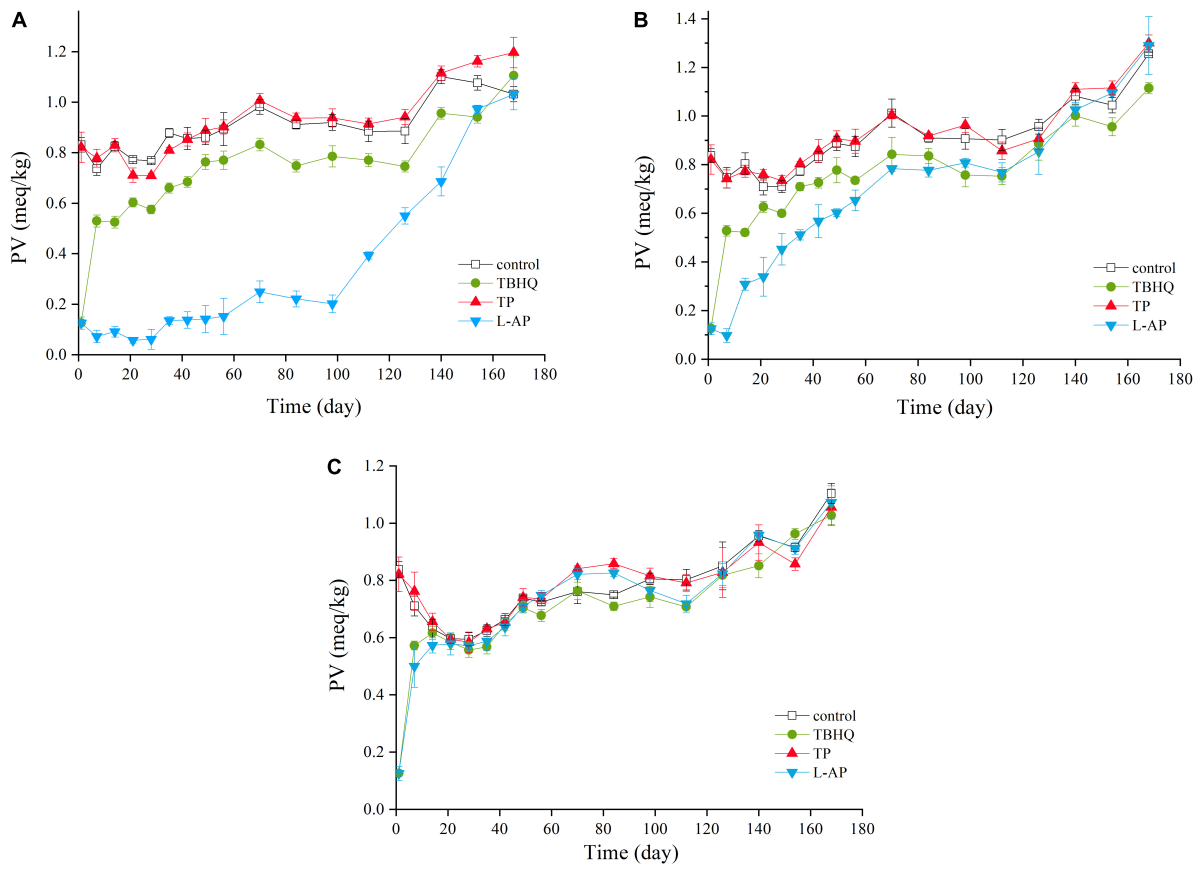

FIGURE 1
PV values of HPBF with the addition of TBHQ, TP, and L-AP during the storage display at different temperature [**(A)** 4°C; **(B)** 20°C; **(C)** 50°C]. The color discrimination is to distinguish four groups including control test, TBHQ, TP, and L-AP.

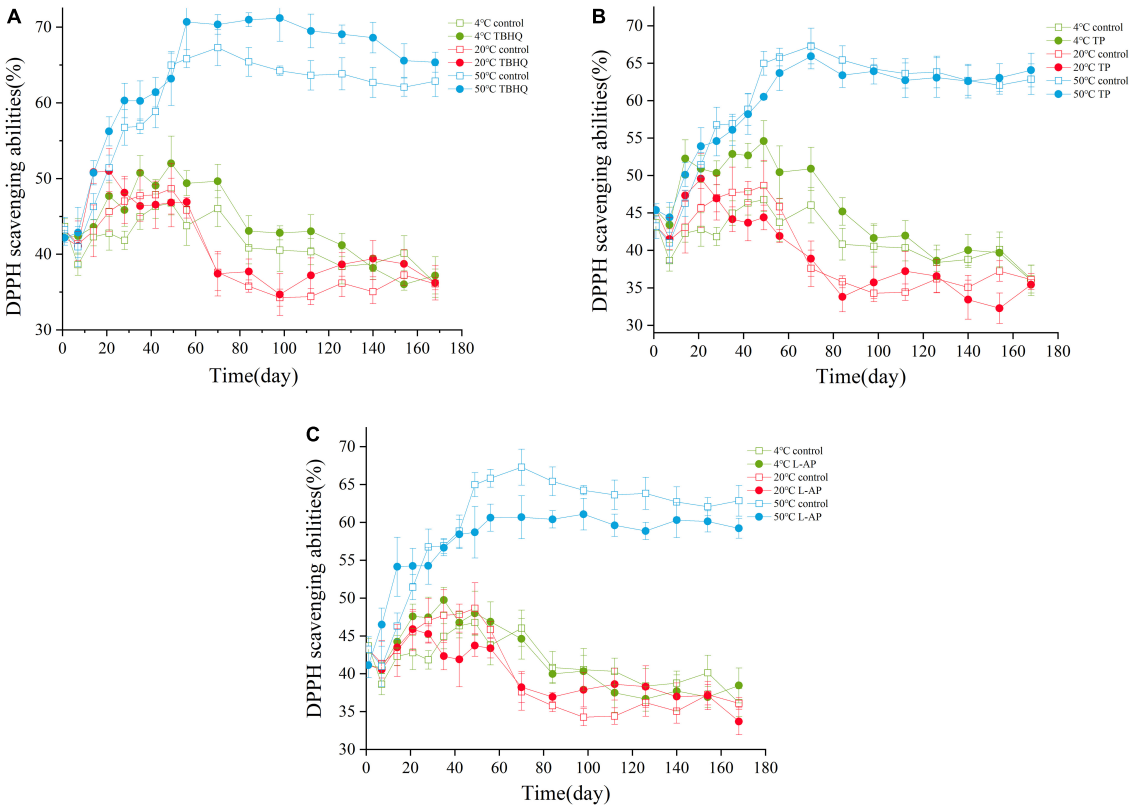

FIGURE 2
Levels of DPPH during the storage of HPBF with the addition of TBHQ **(A)**, TP **(B)**, and L-AP **(C)**. The discrimination of the shape is shown to distinguish the control group and the treatment groups. The color discrimination represents various temperature (4, 20, and 50°C).

in preventing lipid oxidation in cooked chicken, followed by TP. Although TBHQ had a higher lipid solubility than TP and L-AP, it was clear that L-AP had the best antioxidant impact on primary oxidation products of HPBF among three antioxidants in the study, followed by TBHQ.

Thiobarbituric acid reactive substance value

Thiobarbituric acid reactive substance are used as an estimate of the concentration of secondary lipid oxidation products and the results of TBARS are shown in **Supplementary Figures 1D–F** for HPBF with different treatments (TBHQ, TP, L-AP). As shown in **Supplementary Figures 1D–F**, TBARS values of HPBF are significantly different between storage temperatures during storage. TBARS values increased faster at a higher temperature (50°C) compared to that at lower temperature (4 and 20°C), which was consistent with the production of primary lipid oxidation (PV value) as mentioned above. Interestingly, TBARS values gradually increased during the first 14 days at 50°C and then decreased during the following stages. The decrease of TBARS values with time was attributed to the advanced reactions of secondary lipid oxidation products with protein residues (33). The result of TBARS increased and then decreased during storage, which have previously been reported by Koutina et al. (33) who explained that interesting observations were a consequence of secondary lipid oxidation products being consumed by proteins to produce oxidized modified proteins.

In contrast to our suspicion, there were no variations in lipid oxidation ($p > 0.05$) among the three control treatments at any storage temperatures. It demonstrated that the three antioxidants had a limited ability to inhibit secondary lipid oxidation products in HPBF during the storage. A similar finding was reported by Jin et al. (37) who affirmed that TBHQ or L-AP alone did not show many protective properties on heat-treated corn oil with the TBARS assay.

1,1-Diphenyl-2-picrylhydrazyl scavenging activity

The assay of DPPH scavenging activity is a simple method to assess the ability of antioxidants to trap free radicals (38). The DPPH scavenging activity is related to the delocalization of the unpaired electron throughout the molecule, such as peroxide-free radical, hydroxyl radicals and reactive oxygen species (38). The antioxidant effectiveness of TBHQ, TP, and L-AP evaluated

in HPBF during the storage are shown in **Figure 2**. Based on the results in **Figure 2**, the DPPH scavenging ability increased first and then decreased during storage. One unanticipated discovery was that the values of DPPH scavenging ability were always the largest in the storage condition of 50°C. This was mainly owing to the ease with the Maillard reaction that occurs as the temperature rises. The Maillard reaction products had an effective antioxidant effect, which resulted in enhanced DPPH scavenging ability through the conversion of DPPH into a stable DPPH-H form (39, 40). The values gradually decreased and tended to be flat as storage time increased indicating that the oxidation reaction of HPBF was caused by the consumption of antioxidants. These findings would be confirmed by the results of oxidative stability analysis.

Compared with the control group, the addition of TBHQ, TP, and L-AP in HPBF could efficiently scavenge DPPH radicals and inhibit oil oxidation after being stored at a low temperature (4°C) for a short period. There was no significant difference in free radical scavenging between the three treatment groups at room temperature (20°C). TBHQ had an effective DPPH scavenging ability at higher temperatures (50°C), which indicted that its antioxidant impact was substantially greater than that of TP and L-AP. The results were consistent with previous research findings reported by Jin (41). TBHQ as one outstanding synthetic antioxidant reported by Liang et al. (42) who found that TBHQ can effectively inhibit the formation of free radicals and hence contributes to the stabilization of lipids. More unexpectedly, HPBF with the addition of L-AP (as another synthetic antioxidant), exhibited a lower DPPH scavenging activity than that of the control group at a higher storage temperature (50°C). This could be associated with the initial acidity of HPBF or the stability and structure of L-AP. Under acidic conditions, L-AP could be entirely hydrolyzed to ascorbic acid and their respective fatty acids in the reporter of EFSA and ANS (43), which affect its own free radical scavenging ability. Comparatively, TBHQ had a noticeable effect on scavenging free radicals terminating the free radical chain reaction, which could be attributed to its molecular structure, high thermal resistance and stability.

Evaluation of physicochemical profiles

Browning

Browning is one of the most common natural phenomena during the processing and storage of food (44). As shown in **Supplementary Figures 1G–I**, the brown color (A420) of samples increased over time, particularly when stored at 50°C; A420 values of samples stored at 50°C were higher compared to that of samples stored at 4 and 20°C at each time point during storage. The results suggested that Maillard browning depended greatly on temperature and time. However, it was worth noting that the growing trend of browning in the three treatment groups (TBHQ, TP, and L-AP) did not differ substantially. The similarity of A420 values between TBHQ, TP, and L-AP groups indicated that the addition of antioxidants had little effect on the browning of HPBF during storage. In fact, products of the Maillard browning reaction during storage were also regarded as antioxidants and could interfere with the antioxidant effect from TBHQ, TP, and L-AP (45, 46). For example, Mshayisa (47) revealed that Maillard reaction products showed higher antioxidant capacity than TBHQ (0.02% w/w) according to the TBARs assay in a glucose-casein model system. As also demonstrated by Kirigaya et al. (48), melanoidin pigment, a component of Maillard browning, played an important role in the antioxidant activity. Accordingly, it may be suspected that the impact of three antioxidants on browning was much lower than that of Maillard reaction products during the storage.

pH

An examination of the acidity of HPBF with three antioxidants (TBHQ, TP, L-AP) treatment during storage (**Supplementary Figures 2A–C**) indicated that TBHQ, TP and L-AP did not alter ($p > 0.05$) the acidity values, except after 112 days during the low temperature (4°C) storage. TBHQ, TP, and L-AP may be able to limit the hydrolytic and oxidative rancidity of lipid to a certain extent in the long term at low temperatures. However, the activities of three antioxidants to control the change of acidity value was not significantly different ($p > 0.05$).

Water activity

Water activity (a_w) is another important parameter to evaluate the physicochemical quality that governs storage stability (49). The effects of three antioxidants (TBHQ, TP, L-AP) on HPBF are shown in **Supplementary Figures 2D–F**. Based on the results, the a_w values of the TBHQ and L-AP groups were similar at all temperatures. The a_w of the HPBF samples in either TBHQ group or L-AP group equilibrated to the control indicating that the addition TBHQ or L-AP had little effect on the a_w of HPBF during storage. However, the TP group exhibited higher a_w values than other treatment groups and the control at both low (4°C) and room (20°C) temperature after 14 days of storage. No distinguished difference in a_w was found between the three treatment groups and the control at 50°C. The HPBF samples with the addition of TP or stored at 50°C may increase the value of a_w, which may adversely affect the physicochemical profiles and stability of the HPBF samples.

Analysis of volatility odorants

Lipid oxidation rancidity affects flavor quality. It was attributed to the results that TBHQ had a better effect on controlling lipid oxidation than TP and L-AP, based on the evaluation of lipid oxidation stability and physicochemical

TABLE 1 Volatile odorants of HPBF identified by SPME-GC-MS/GC-O stored for 168 days.

No.	Compounds	Formula	CAS#[a]	RI[b] (DB-WAX)	Identification[c]
Alcohols					
1	Allyl alcohol	C_3H_6O	107-18-6	1109	RI,MS,O
2	1-Butanol	$C_4H_{10}O$	71-36-3	1142	RI,MS
3	Eucalyptol	$C_{10}H_{18}O$	470-82-6	1196	RI,MS,O
4	2-Methyl-1-butanol	$C_5H_{12}O$	137-32-6	1208	RI,MS
5	Hydroxyacetone	$C_3H_6O_2$	116-09-6	1289	RI,MS,O
6	Linalool	$C_{10}H_{18}O$	78-70-6	1552	RI,MS,O
7	Propylene Glycol	$C_3H_8O_2$	57-55-6	1593	RI,MS
8	(-)-Terpinen-4-ol	$C_{10}H_{18}O$	20126-76-5	1597	RI,MS
9	β-Acorenol	$C_{15}H_{26}O$	28400-11-5	1690	RI,MS
10	L-α-Terpineol	$C_{10}H_{18}O$	10482-56-1	1694	RI,MS
11	Phenylethyl Alcohol	$C_8H_{10}O$	60-12-8	1901	RI,MS,O
12	Maltol	$C_6H_6O_3$	118-71-8	1950	RI,MS,O
13	α-Cadinol	$C_{15}H_{26}O$	481-34-5	2175	RI,MS
Aldehydes					
14	2-Methylbutanal	$C_5H_{10}O$	96-17-3	859	RI,MS,O
15	3-Hydroxybutanal	$C_4H_8O_2$	107-89-1	1027	MS
16	Octanal	$C_8H_{16}O$	124-13-0	1282	RI,MS,O
17	2-Isopropyl-5-methylhex-2-enal	$C_{10}H_{18}O$	35158-25-9	1352	RI,MS
18	Non-anal	$C_9H_{18}O$	124-19-6	1388	RI,MS,O
19	Furfural	$C_5H_4O_2$	98-01-1	1454	RI,MS,O
20	Benzaldehyde	C_7H_6O	100-52-7	1506	RI,MS,O
21	5-Methyl furfural	$C_6H_6O_2$	620-02-0	1560	RI,MS,O
22	4-(1-Methylethyl)-benzaldehyde	$C_{10}H_{12}O$	122-03-2	1762	RI,MS
23	Tetradecanal	$C_{14}H_{28}O$	124-25-4	1867	RI,MS,O
24	10-Octadecenal	$C_{18}H_{34}O$	56554-92-8	1872	RI,MS
Acids					
25	Acetic acid	$C_2H_4O_2$	64-19-7	1440	RI,MS,O
26	Propanoic acid	$C_3H_6O_2$	79-09-4	1534	RI,MS,O
27	Butanoic acid	$C_4H_8O_2$	107-92-6	1623	RI,MS,O
28	4-Methyl-pentanoic acid	$C_6H_{12}O_2$	646-07-1	1800	RI,MS,O
29	Octanoic acid	$C_8H_{16}O_2$	124-07-2	2058	RI,MS,O
30	Decanoic acid	$C_{10}H_{20}O_2$	334-48-5	2271	RI,MS,O
31	4-oxo-Pentanoic acid	$C_5H_8O_3$	123-76-2	2311	RI,MS
32	Sorbic Acid	C6H8O2	110-44-1	2120	RI,MS
Ketones					
33	4-Methyl-3-penten-2-one	$C_6H_{10}O$	141-79-7	1118	RI,MS
34	6-Methyl-5-hepten-2-one	$C_8H_{14}O$	110-93-0	1332	RI,MS,O
35	2(5H)-Furanone	$C_4H_4O_2$	497-23-4	1730	RI,MS
36	Isosafrole	$C_{10}H_{10}O_2$	120-58-1	1861	MS
37	Furaneol	$C_6H_8O_3$	3658-77-3	2025	RI,MS,O
Terpenes and terpenoids					
38	(+)-α-Pinene	$C_{10}H_{16}$	7785-70-8	1016	RI,MS
39	D-Limonene	$C_{10}H_{16}$	5989-27-5	1186	MS
40	*trans*-β-Ocimene	$C_{10}H_{16}$	3779-61-1	1229	RI,MS
41	γ-Terpinene	$C_{10}H_{16}$	99-85-4	1236	RI,MS
42	3-Carene	$C_{10}H_{16}$	13466-78-9	1246	RI,MS
43	Terpinolene	$C_{10}H_{16}$	586-62-9	1272	RI,MS
44	α-Copaene	$C_{15}H_{24}$	3856-25-5	1480	RI,MS,O

(Continued)

TABLE 1 (Continued)

No.	Compounds	Formula	CAS#[a]	RI[b] (DB-WAX)	Identification[c]
45	1-Caryophyllene	$C_{15}H_{24}$	87-44-5	1582	RI,MS
46	Humulene	$C_{15}H_{24}$	6753-98-6	1653	RI,MS
47	Estragole	$C_{10}H_{12}O$	140-67-0	1661	RI,MS,O
48	γ-Muurolene	$C_{15}H_{24}$	30021-74-0	1680	RI,MS
49	α-Amorphene	$C_{15}H_{24}$	483-75-0	1717	RI,MS
50	Di-epi-α-cedrene	$C_{15}H_{24}$	50894-66-1	1718	MS
51	β-Bisabolene	$C_{15}H_{24}$	495-61-4	1724	RI,MS
52	δ-Cadinene	$C_{15}H_{24}$	483-76-1	1752	RI,MS
53	α-Curcumene	$C_{15}H_{22}$	644-30-4	1772	RI,MS
54	Anethole	$C_{10}H_{12}O$	104-46-1	1825	RI,MS,O
55	Calamenene	$C_{15}H_{22}$	483-77-2	1830	RI,MS
56	Elemicin	$C_{12}H_{16}O_3$	487-11-6	2221	RI,MS,O
57	Myristicin	$C_{11}H_{12}O_3$	607-91-0	2247	RI,MS
Phenols					
58	Phenol	C_6H_6O	108-95-2	1996	RI,MS
59	Methyleugenol	$C_{11}H_{14}O_2$	93-15-2	2006	RI,MS
60	4-Ethyl-2-methoxy-phenol	$C_9H_{12}O_2$	2785-89-9	2018	RI,MS
61	Eugenol	$C_{10}H_{12}O_2$	97-53-0	2156	RI,MS,O
62	Isoeugenol	$C_{10}H_{12}O_2$	97-54-1	2243	RI,MS
63	*trans*-Isoeugenol	$C_{10}H_{12}O_2$	5932-68-3	2332	RI,MS
64	4-(2-Propenyl)-phenol	$C_9H_{10}O$	501-92-8	2328	RI,MS
Thiophenes					
65	3-Methylthiophene	C_5H_6S	616-44-4	1067	RI,MS
66	2-Methylthiophene	C_5H_6S	554-14-3	1068	RI,MS
67	2-Thiophenemethanol	C_5H_6OS	636-72-6	1934	RI,MS,O
Thiazoles					
68	2-Acetylthiazole	C_5H_5NOS	24295-03-2	1633	RI,MS
69	4-Methyl-5-thiazoleethanol	C_6H_9NOS	137-00-8	2296	RI,MS,O
Pyrazines					
70	2-Methylpyrazine	$C_5H_6N_2$	109-08-0	1256	RI,MS
71	2,5-Dimethylpyrazine	$C_6H_8N_2$	123-32-0	1314	RI,MS,O
72	2,6-Dimethylpyrazine	$C_6H_8N_2$	108-50-9	1321	RI,MS,O
73	2-Ethylpyrazine	$C_6H_8N_2$	13925-00-3	1326	RI,MS
74	2,3-Dimethylpyrazine	$C_6H_8N_2$	5910-89-4	1338	RI,MS,O
75	2-Ethyl-6-methylpyrazine	$C_7H_{10}N_2$	13925-03-6	1379	RI,MS,O
76	2,3,5-Trimethylpyrazine	$C_7H_{10}N_2$	14667-55-1	1397	RI,MS,O
77	2-Methyl-3-propylpyrazine	$C_8H_{12}N_2$	15986-80-8	1460	RI,MS
78	Acetylpyrazine	$C_6H_6N_2O$	22047-25-2	1612	RI,MS,O
Pyrrole					
79	2-Acetyl pyrrole	C_6H_7NO	1072-83-9	1959	RI,MS,O
Pyrimidines					
80	2-Methylpyrimidine	$C_5H_6N_2$	5053-43-0	1256	RI,MS
81	4-Methylpyrimidine	$C_5H_6N_2$	3438-46-8	1256	RI,MS
Furans					
82	2-Pentylfuran	$C_9H_{14}O$	3777-69-3	1225	RI,MS
83	2-Acetylfuran	$C_6H_6O_2$	1192-62-7	1494	RI,MS,O
Sulfur compounds					
84	Dimethyl disulfide	$C_2H_6S_2$	624-92-0	1049	RI,MS,O
85	Diallyl sulfide	$C_6H_{10}S$	592-88-1	1131	RI,MS,O

(Continued)

TABLE 1 (Continued)

No.	Compounds	Formula	CAS#[a]	RI[b] (DB-WAX)	Identification[c]
86	Methyl propyl disulfide	$C_4H_{10}S_2$	2179-60-4	1220	RI,MS,O
87	Allyl methyl disulfide	$C_4H_8S_2$	2179-58-0	1270	RI,MS,O
88	2-Methyl-3-furanthiol	C_5H_6OS	28588-74-1	1304	RI,MS,O
89	Dimethyl trisulfide	$C_2H_6S_3$	3658-80-8	1363	RI,MS,O
90	Dipropyl disulfide	$C_6H_{14}S_2$	629-19-6	1369	RI,MS,O
91	2-Furfurylthiol	C_5H_6OS	98-02-2	1426	RI,MS,O
92	Diallyl disulfide	$C_6H_{10}S_2$	2179-57-9	1470	RI,MS,O
93	Methyl allyl trisulfide	$C_4H_8S_3$	34135-85-8	1574	RI,MS,O
94	Tropical trithiane	$C_9H_{18}S_3$	828-26-2	1712	RI,MS,O
95	Methyl furfuryl disulfide	$C_6H_8OS_2$	57500-00-2	1791	RI,MS,O
96	Furfuryl sulfide	$C_{10}H_{10}O_2S$	13678-67-6	2045	RI,MS,O
97	Difurfuryl disulfide	$C_{10}H_{10}O_2S_2$	4437-20-1	2546	RI,MS,O
Esters					
98	Ethyl octanoate	$C_{10}H_{20}O_2$	106-32-1	1435	RI,MS
99	Linalyl acetate	$C_{12}H_{20}O_2$	115-95-7	1556	RI,MS,O
100	Ethyl decanoate	$C_{12}H_{24}O_2$	110-38-3	1643	RI,MS
101	Terpinyl acetate	$C_{12}H_{20}O_2$	80-26-2	1690	RI,MS
102	Methyl salicylate	$C_8H_8O_3$	119-36-8	1756	RI,MS
103	Eugenyl acetate	$C_{12}H_{14}O_3$	93-28-7	2246	RI,MS
Other					
104	*o*-Cymene	$C_{10}H_{14}$	527-84-4	1259	RI,MS
105	1-Methyl-3-(1-methylethyl)-benzene	$C_{10}H_{14}$	535-77-3	1257	RI,MS
106	2,2′-Methylenebis furan	$C_9H_8O_2$	1197-40-6	1603	RI,MS
107	Butylated hydroxytoluene	$C_{15}H_{24}O$	128-37-0	1902	RI,MS

[a]CAS, Chemical Abstract Service registration number.
[b]RI, Retention indices calculated using the n-alkanes of C7-C40 on DB-WAX column.
[c]MS, mass spectrometry; O, reference standard odor description.

profiles. The results of volatile odorants detected by SPME-GC-MS only discussed the effect of TBHQ on flavor profiles during storage. Volatile flavor compounds in HPBF were detected during storage (**Table 1**). As shown in **Table 1**, alcohols, terpenes, and terpenoids, nitrogenous heterocyclic compounds (thiophenes, thiazoles, pyrazines, pyrrole, and pyrimidines) and sulfur compounds accounted for a large percentage of volatility odorants. The concentration and amount of volatile odorants in HPBF altered with the storage environment, which was depicted in **Figures 3A–D**. The concentration of volatile components in HPBF did not exhibit significant changes at different temperatures (4 and 20°C). All of alcohols, acids, and sulfur compounds were significantly decreasing, when HPBF is held at 50°C. The accelerate experiment at the high temperature could give a negative impact on the total concentration of volatile chemicals. Interestingly, the concentration of aldehydes and furans in HPBF, and the number of pyrazines and sulfur compounds increased slightly with the storage time.

The decrease of alcohols and the increase of aldehydes were reported to be due to oxidation reactions under high temperature conditions, which promoted the conversion of alcohols to aldehydes, or the generation of aldehydes attributed to lipid oxidation or thermal degradation of amino acids (50). As reported by Frank et al. (51), the increase of 2-methylbutanal was produced through thermal Strecker degradation of isoleucine. The protein oxidation and Maillard reaction were responsible for Strecker aldehydes have been reported by Zhou et al. (52) and Wen et al. (53). However, alcohols and aldehydes in the TBHQ treatment group were higher than those in the control group as storage time went on, indicating that the antioxidant impact of TBHQ was able to stabilize their reaction activity throughout storage.

Pyrazines are usually produced at higher temperatures and contribute to the roast and nutty aroma of overall flavor attributes (54). Changes in concentration and amount during storage may due to the decomposition of proteins and amino acids (55) or the generation of Maillard reaction *via* sugar dehydration or fragmentation (56), instead of lipid oxidation. This confirmed that TBHQ had no significant effect on pyrazines.

Sulfur compounds are considered to be essential volatile aroma active compounds due to their lower odor threshold (57). The decrease or increase of sulfur compounds had a direct effect on the overall flavor profiles of HPBF during storage. Some

sulfur compounds include 2-methyl-3-furanthiol, dipropyl disulfide, 2-furfurylthiol, diallyl disulfide, tropical trithiane, methyl furfuryl disulfide, and difurfuryl disulfide decreased over the time. The reaction of lipid oxidation degradation products with H_2S produced by Strecker degradation of cysteine, interfering with the reaction pathway and reducing the reactants of sulfur compounds, which resulted in a large reduction in the overall content of sulfur compounds (54). Thiols and other sulfur compounds with oxygen heterocycles were extremely reactive, susceptible to oxidation, and easily affected by the environment (58). They can degrade thermally to produce a variety of carbonyl and hydroxyl carbonyl components (59). However, an addition of TBHQ increased the total concentration of sulfur compounds during storage, which could attribute to that TBHQ was more effective in inhibiting lipid oxidation and maintaining greater oxidation stability of HPBF than control group. Notably, in the TBHQ treatment group and the control group, dimethyl disulfide and dimethyl trisulfide increased in the later stage of storage and accounted for a large proportion. These volatiles had been previously linked to meat spoilage and strong objectionable odors (51, 60).

Furans as oxygen-containing heterocyclics are major intermediate products of the Maillard reaction, mostly from sugar degradation (61). It had little correlation with fat oxidation during storage. The concentration of 2-acetylfuran (one of the oxygenated heterocyclic compounds) gradually increased with storage time. However, this odorant with a high odor threshold had little effect on the flavor profiles (62).

Generally speaking, only a few volatile components were important aroma active compounds, which contributed effectively to the overall flavor properties. A total of 51 odorants were sniffed and semi-quantified from the headspace of the HPBF during the storage (**Table 1**). In order to more accurately and intuitively analyze the influence of the TBHQ treatment group on volatile aroma components in HPBF, PCA applied to reveal patterns in the dataset was shown in **Figures 3E–G**. At 4, 20, and 50°C, the Bi-plot of the sum of first two principal components accounted for 91.5, 94.6, and 96.8% of the total

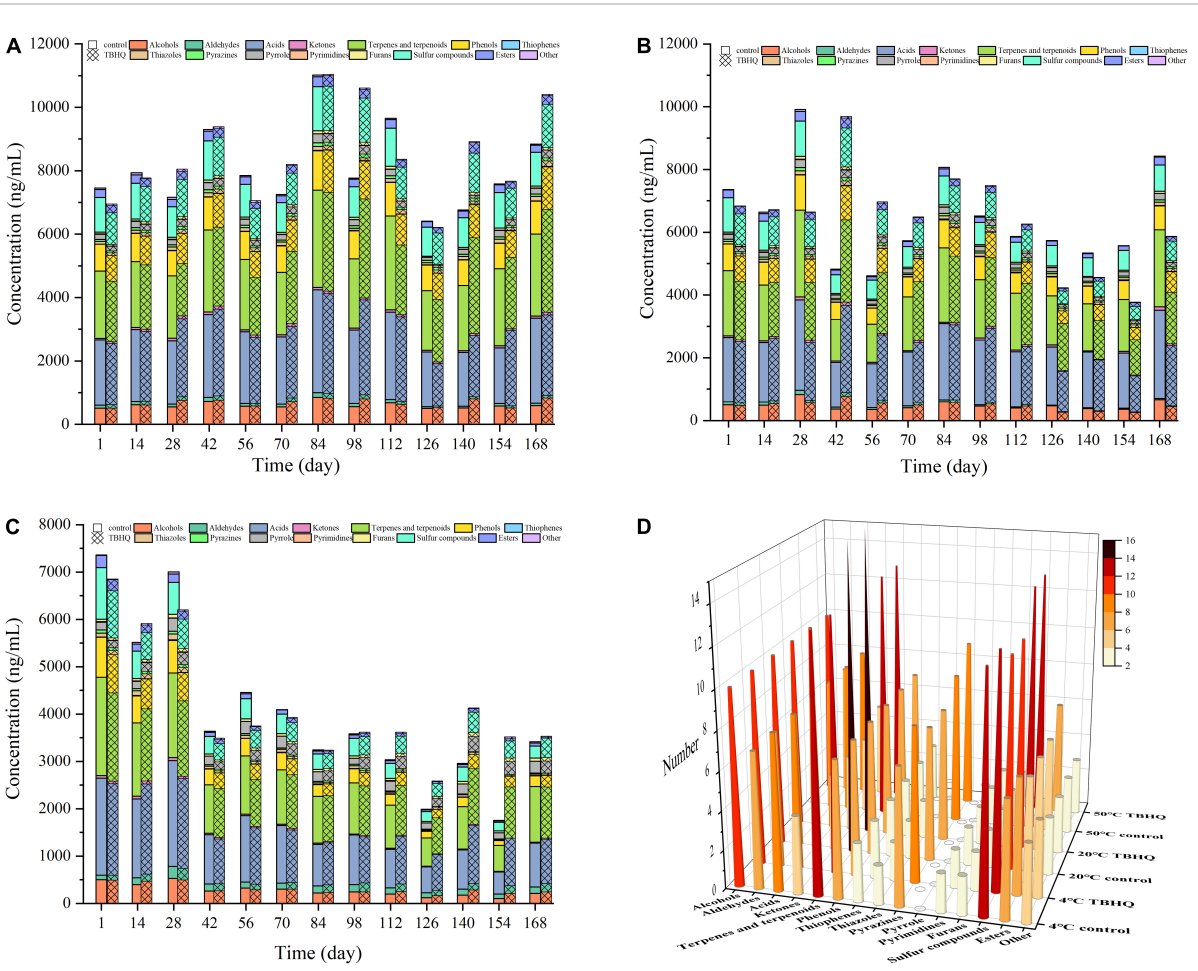

FIGURE 3
(Continued)

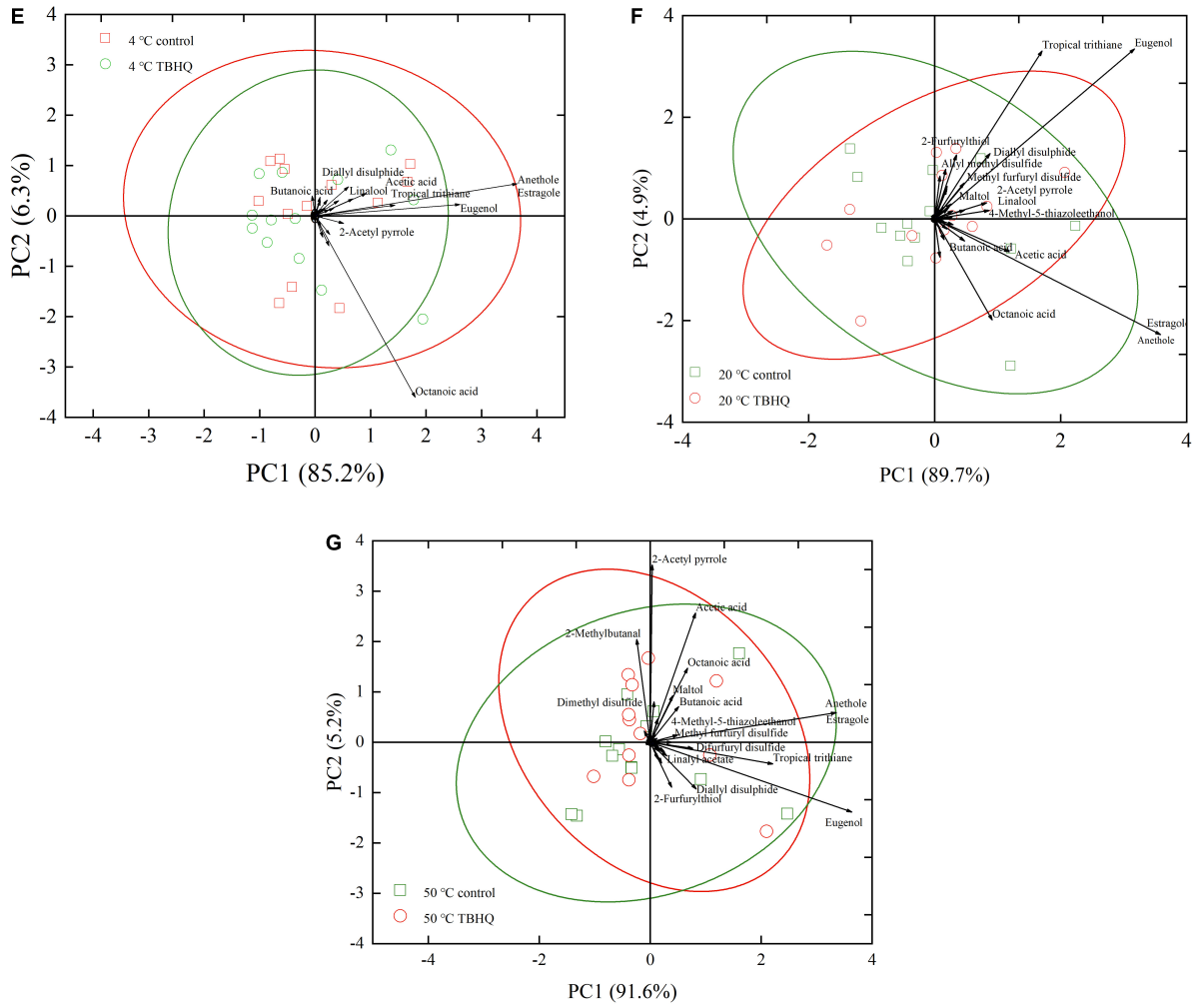

FIGURE 3
Effect of TBHQ on the quantity [**(A)** 4°C; **(B)** 20°C; **(C)** 50°C] and concentration **(D)** of volatile odorants in HPBF during storage. PCA diagram shows the difference of volatile odorants between TBHQ group and control test group [**(E)** 4°C; **(F)** 20°C; **(G)** 50°C].

variance in raw data, respectively, which explained fully the variation trend of the volatile odorants. The data points with distinct markers belonged to different treatments, according to the distribution of data mapped on the principal components. There was a hazy demarcation between HPBF samples from the blank and TBHQ treatment groups during the storage at any temperature. The importance of different volatile odorants to HPBF with different treatments could be distinguished by the visual loading matrix (the black lines). Closer inspection of Figures 3E–G revealed that clove-smelling eugenol, anise-smelling anethole, and estragole had a higher contribution value to the overall flavor attribute of HPFB during storage due to their positions far from the coordinate origin. The loading matrix of 2-furfurylthiol, diallyl disulfide, tropical trithiane, and methyl furfuryl disulfide increased were larger than that of control group with the increasing of temperature at 4 and 20°C, implying that these odorants have a higher contribution to the flavor profiles of TBHQ treatment group. 2-Methylbutanal, 2-acetyl pyrrole, and difurfuryl disulfide were more prominent in the TBHQ treatment group at 50°C. This was possible because TBHQ could maintain the oxidation stability of HPBF during the storage, owing to the antioxidant effect. The loss of some active aroma components (2-methylbutanal, 2-methyl-3-furanthiol, 2-furfurylthiol, diallyl disulfide, tropical trithiane, methyl furfuryl disulfide, and difurfuryl disulfide) in HPBF during storage was minimized in the TBHQ treatment group. It was interesting to find that the contribution value of octanoic acid gradually decreases, indicating that it was oxidized due to the influence of storage temperature and time. In short, these findings provide vital information about that several volatile odorants were affected by TBHQ contributing to the overall flavor qualities during storage. Meanwhile, these odorants were the main differences between the blank and TBHQ treatment group.

Conclusion

The effect of three antioxidants (TBHQ, TP, and L-AP) on the flavor profiles, oxidative stability and the physicochemical profiles in HPBF at different temperatures during the storage was analyzed. The results indicated that TBHQ, TP, and L-AP had a little influence on the browning, a_w, and acidity of HPBF. Based on the results of an oxidative stability assessment, L-AP had a better ability to limit the production of primary oxidation products than TBHQ, although both L-AP and TBHQ exhibited poor control over secondary lipid oxidation products regardless of storage temperature. In particular, TBHQ performed better in the DPPH radical scavenging assays, inhibiting lipid oxidation during storage with a higher DPPH radical scavenging ability. According to the results of oxidative stability and physicochemical profiles, HPBF with the addition of TBHQ exhibited greater lipid stability than L-AP, followed by TP. In addition, TBHQ could inhibit high-activity compounds from being oxidized and forming other objectionable odorants. However, an addition antioxidant (i.e., TBHQ) had a lower impact on flavor qualities during storage than storage temperature and storage time. It was undeniable that TBHQ may play an antioxidant role in HPBF during storage. The developed compound additive containing TBHQ had the potential to be employed as an effective additive in a complex system of beef flavor with the capacity to postpone oxidation reactions thereby enhancing flavor quality.

Data availability statement

The original contributions presented in this study are included in the article/**Supplementary material**, further inquiries can be directed to the corresponding authors.

Author contributions

ZZ: data curation, methodology, writing – original draft preparation, investigation, and validation. FM: writing – review and editing and funding acquisition. BW: writing – review and editing, project administration, and funding acquisition. YC: conceptualization, supervision, and project administration. All authors contributed to the article and approved the submitted version.

Funding

This work was supported by National Natural Science Foundation of China (project no. 32072345; Beijing) and Young Teachers Scientific Research Start-up Fund of Beijing Technology and Business University (Project No: QNJJ2022-04).

Conflict of interest

The authors declare that the research was conducted in the absence of any commercial or financial relationships that could be construed as a potential conflict of interest.

Publisher's note

Supplementary material

The Supplementary Material for this article can be found online at: https://www.frontiersin.org/articles/10.3389/fnut.2022.966697/full#supplementary-material

References

1. Lotfy SN, Fadel HH, El-Ghorab AH, Shaheen MS. Stability of encapsulated beef-like flavourings prepared from enzymatically hydrolysed mushroom proteins with other precursors under conventional and microwave heating. *Food Chem.* (2015) 187:7–13. doi: 10.1016/j.foodchem.2015.04.027

2. Song S, Zhang X, Hayat K, Huang M, Liu P, Karangwa E, et al. Contribution of beef base to aroma characteristics of beeflike process flavour assessed by descriptive sensory analysis and gas chromatography olfactometry and partial least squares regression. *J Chromatogr A.* (2010) 1217:7788–99.

3. Cui H, Yu J, Xia S, Duhoranimana E, Huang Q, Zhang X. Improved controlled flavor formation during heat-treatment with a stable maillard reaction intermediate derived from xylose-phenylalanine. *Food Chem.* (2019) 271:47–53. doi: 10.1016/j.foodchem.2018.07.161

4. Wellner A, Huettl C, Henle T. Formation of maillard reaction products during heat treatment of carrots. *J Agric Food Chem.* (2011) 59:7992–8. doi: 10.1021/jf2013293

5. Mottram DS. Flavour formation in meat and meat products: a review. *Food Chem.* (1998) 62:415–24. doi: 10.1016/S0308-8146(98)00076-4

6. Flores M. *The Eating Quality of Meat: III—Flavor. Lawrie' S Meat Science.* Duxford: Elsevier (2017). p. 383–417.

7. Van Ba H, Hwang I, Jeong D, Touseef A. Principle of meat aroma flavors and future prospect. *Latest Res Qual Control.* (2012) 2:145–76. doi: 10.5772/51110

8. Khan MI, Jo C, Tariq MR. Meat flavor precursors and factors influencing flavor precursors-a systematic review. *Meat Sci.* (2015) 110:278–84. doi: 10.1016/j.meatsci.2015.08.002

9. Frankel EN. *Lipid Oxidation*. Amsterdam: Elsevier (2014).

10. Gray J, Gomaa E, Buckley D. Oxidative quality and shelf life of meats. *Meat Sci.* (1996) 43:111–23. doi: 10.1016/0309-1740(96)00059-9

11. Vieira SA, Zhang G, Decker EA. Biological implications of lipid oxidation products. *J Am Oil Chem Soc.* (2017) 94:339–51. doi: 10.1007/s11746-017-2958-2

12. Wood J, Richardson R, Nute G, Fisher A, Campo M, Kasapidou E, et al. Effects of fatty acids on meat quality: a review. *Meat Sci.* (2004) 66:21–32. doi: 10.1016/S0309-1740(03)00022-6

13. Huang X, Ahn DU. Lipid oxidation and its implications to meat quality and human health. *Food Sci Biotechnol.* (2019) 28:1275–85. doi: 10.1007/s10068-019-00631-7

14. Tao L. Oxidation of polyunsaturated fatty acids and its impact on food quality and human health. *Adv Food Technol Nutr Sci.* (2015) 1:135–42.

15. Huali W, Jiyue Z, Jianbo Z. Revision on the "National food safety standard-standards for uses of food additives" (GB 2760–2011). *China Food Addit.* (2013) 67–71.

16. Min DB, Wen J. Qualitative and quantitative effects of antioxidants on the flavor stability of oil. *J Food Sci.* (1983) 48:1172–4. doi: 10.1111/j.1365-2621.1983.tb09185.x

17. Sohaib M, Anjum FM, Sahar A, Arshad MS, Rahman UU, Imran A, et al. Antioxidant proteins and peptides to enhance the oxidative stability of meat and meat products: a comprehensive review. *Int J Food Prop.* (2017) 20:2581–93. doi: 10.1080/10942912.2016.1246456

18. Meng FB, Lei YT, Zhang Q, Li YC, Chen WJ, Liu DY. Encapsulation of *Zanthoxylum bungeanum* essential oil to enhance flavor stability and inhibit lipid oxidation of Chinese-style sausage. *J Sci Food Agric.* (2022) 102:4035–45. doi: 10.1002/jsfa.11752

19. Cisneros-Yupanqui M, Lante A. Tea from the food science perspective: an overview. *Open Biotechnol J.* (2020) 14:78–83. doi: 10.2174/1874070702014010078

20. Mohanan A, Nickerson MT, Ghosh S. Oxidative stability of flaxseed oil: effect of hydrophilic, hydrophobic and intermediate polarity antioxidants. *Food Chem.* (2018) 266:524–33. doi: 10.1016/j.foodchem.2018.05.117

21. Chen B, McClements DJ, Decker EA. Minor components in food oils: a critical review of their roles on lipid oxidation chemistry in bulk oils and emulsions. *Crit Rev Food Sci Nutr.* (2011) 51:901–16. doi: 10.1080/10408398.2011.606379

22. Chastain M, Huffman D, Hsieh W, Cordray J. Antioxidants in restructured beef/pork steaks. *J Food Sci.* (1982) 47:1779–82. doi: 10.1111/j.1365-2621.1982.tb12881.x

23. Frankel EN, Huang S-W, Kanner J, German JB. Interfacial phenomena in the evaluation of antioxidants: bulk oils vs emulsions. *J Agric Food Chem.* (1994) 42:1054–9. doi: 10.1021/jf00041a001

24. Gordon MH, Kourkimskå L. The effects of antioxidants on changes in oils during heating and deep frying. *J Sci Food Agric.* (1995) 68:347–53. doi: 10.1002/jsfa.2740680314

25. Budilarto ES, Kamal-Eldin A. The supramolecular chemistry of lipid oxidation and antioxidation in bulk oils. *Eur J Lipid Sci Technol.* (2015) 117:1095–137. doi: 10.1002/ejlt.201400200

26. Wanasundara U, Shahidi F. Stabilization of seal blubber and menhaden oils with green tea catechins. *J Am Oil Chem Soc.* (1996) 73:1183–90. doi: 10.1007/BF02523382

27. Zhang L, McClements DJ, Wei Z, Wang G, Liu X, Liu F. Delivery of synergistic polyphenol combinations using biopolymer-based systems: advances in physicochemical properties, stability and bioavailability. *Crit Rev Food Sci Nutr.* (2020) 60:2083–97. doi: 10.1080/10408398.2019.1630358

28. Capuani A, Behr J, Vogel RF. Influence of lactic acid bacteria on the oxidation–reduction potential of buckwheat (*Fagopyrum esculentum* Moench) sourdoughs. *Eur Food Res Technol.* (2012) 235:1063–9. doi: 10.1007/s00217-012-1834-4

29. Chaiyasit W, Silvestre MPC, McClements DJ, Decker EA. Ability of surfactant hydrophobic tail group size to alter lipid oxidation in oil-in-water emulsions. *J Agric Food Chem.* (2000) 48:3077–80. doi: 10.1021/jf000323e

30. Papastergiadis A, Mubiru E, Van Langenhove H, De Meulenaer B. Malondialdehyde measurement in oxidized foods: evaluation of the spectrophotometric thiobarbituric acid reactive substances (Tbars) test in various foods. *J Agric Food Chem.* (2012) 60:9589–94. doi: 10.1021/jf302451c

31. Zhang YY, Zhang F, Thakur K, Ci AT, Wang H, Zhang JG, et al. Effect of natural polyphenol on the oxidative stability of pecan oil. *Food Chem Toxicol.* (2018) 119:489–95. doi: 10.1016/j.fct.2017.10.001

32. Chen XM, Kitts DD. Correlating changes that occur in chemical properties with the generation of antioxidant capacity in different sugar-amino acid maillard reaction models. *J Food Sci.* (2011) 76:C831–7. doi: 10.1111/j.1750-3841.2011.02215.x

33. Koutina G, Jongberg S, Skibsted LH. Protein and lipid oxidation in Parma ham during production. *J Agric Food Chem.* (2012) 60:9737–45. doi: 10.1021/jf3026887

34. Farajzadeh F, Motamedzadegan A, Shahidi S-A, Hamzeh S. The effect of chitosan-gelatin coating on the quality of shrimp (*Litopenaeus vannamei*) under refrigerated condition. *Food Control.* (2016) 67:163–70. doi: 10.1016/j.foodcont.2016.02.040

35. Wang L, Liu G, Cao L-X. Optimization of L-ascorbate oleate production using response surface methodology and its properties. *Sci Technol Food Industry.* (2016) 11:226–31.

36. Rababah TM, Ereifej KI, Al-Mahasneh MA, Al-Rababah MA. Effect of plant extracts on physicochemical properties of chicken breast meat cooked using conventional electric oven or microwave. *Poult Sci.* (2006) 85:148–54. doi: 10.1093/ps/85.1.148

37. Jin W, Shoeman DW, Shukla VKS, Csallany AS. Retardation of 4-hydroxy-2-transnonenal (Hne), a toxic aldehyde formation by antioxidants in heat-treated corn oil at frying temperature. *Food Nutr Sci.* (2020) 11:869–83. doi: 10.4236/fns.2020.117048

38. Shanmugapriya K, Saravana P, Payal H, Mohammed SP, Binnie W. Antioxidant activity, total phenolic and flavonoid contents of *Artocarpus heterophyllus* and *Manilkara zapota* seeds and its reduction potential. *Int J Pharm Pharmaceut Sci.* (2011) 3:256–60.

39. Benjakul S, Lertittikul W, Bauer F. Antioxidant activity of maillard reaction products from a porcine plasma protein–sugar model system. *Food Chem.* (2005) 93:189–96. doi: 10.1016/j.foodchem.2004.10.019

40. Phisut N, Jiraporn B. Characteristics and antioxidant activity of maillard reaction products derived from chitosan-sugar solution. *Int Food Res J.* (2013) 20:1077.

41. Jin Q. *Effects of Antioxidants on the Oxidative Stability of Gardenia Fruit Oil*. Hangzhou: Zhejiang A&F University (2018).

42. Liang Y, May C, Foon C, Ngan M, Hock C, Basiron Y. The effect of natural and synthetic antioxidants on the oxidative stability of palm diesel. *Fuel.* (2006) 85:867–70. doi: 10.1016/j.fuel.2005.09.003

43. EFSA. Scientific opinion on the re-evaluation of ascorbyl palmitate (E 304 (I)) and ascorbyl stearate (E 304 (II)) as food additives. *EFSA J.* (2015) 13:4289. doi: 10.2903/j.efsa.2015.4289

44. Manzocco L, Calligaris S, Mastrocola D, Nicoli MC, Lerici CR. Review of non-enzymatic browning and antioxidant capacity in processed foods. *Trends Food Sci Technol.* (2000) 11:340–6. doi: 10.1016/S0924-2244(01)00014-0

45. Yu X, Zhao M, Liu F, Zeng S, Hu J. Antioxidants in volatile maillard reaction products: identification and interaction. *LWT Food Sci Technol.* (2013) 53:22–8. doi: 10.1016/j.lwt.2013.01.024

46. Alfawaz M, Smith JS, Jeon IJ. Maillard reaction products as antioxidants in pre-cooked ground beef. *Food Chem.* (1994) 51:311–8. doi: 10.1016/0308-8146(94)90032-9

47. Mshayisa VV. *Antioxidant Effects of Maillard Reaction Products (MRPS) Derived from Glucose-Casein Model Systems*. Cape Town: Cape Peninsula University of Technology (2016).

48. Kirigaya N, Kato H, Fujimaki M. Studies on antioxidant activity of nonenzymic browning reaction products part I. Relations of color intensity and reductones with antioxidant activity of browning reaction products. *Agric Biol Chem.* (1968) 32:287–90. doi: 10.1271/bbb1961.32.287

49. Kek SP, Chin NL, Yusof YA, Tan SW, Chua LS. Classification of entomological origin of honey based on its physicochemical and antioxidant properties. *Int J Food Prop.* (2018) 20(Suppl. 3):S2723–38. doi: 10.1080/10942912.2017.1359185

50. Zamora R, Hidalgo FJ. Coordinate contribution of lipid oxidation and maillard reaction to the nonenzymatic food browning. *Crit Rev Food Sci Nutr.* (2005) 45:49–59. doi: 10.1080/10408690590900117

51. Frank D, Hughes J, Piyasiri U, Zhang Y, Kaur M, Li Y, et al. Volatile and non-volatile metabolite changes in 140-day stored vacuum packaged chilled beef and potential shelf life markers. *Meat Sci.* (2020) 161:108016.

52. Zhou Y, Wang Y, Pan Q, Wang XX, Li PJ, Cai KZ, et al. Effect of salt mixture on flavor of reduced-sodium restructured bacon with ultrasound treatment. *Food Sci Nutr.* (2020) 8:3857–71. doi: 10.1002/fsn3.1679

53. Wen R, Hu Y, Zhang L, Wang Y, Chen Q, Kong B. Effect of Nacl substitutes on lipid and protein oxidation and flavor development of Harbin dry sausage. *Meat Sci.* (2019) 156:33–43. doi: 10.1016/j.meatsci.2019.05.011

54. Wei CK, Ni ZJ, Thakur K, Liao AM, Huang JH, Wei ZJ. Aromatic effects of immobilized enzymatic oxidation of chicken fat on flaxseed (*Linum usitatissimum* L.) derived maillard reaction products. *Food Chem.* (2020) 306:125560. doi: 10.1016/j.foodchem.2019.125560

55. Li X, Wang K, Yang R, Dong Y, Lin S. Mechanism of aroma compounds changes from sea cucumber peptide powders (Scpps) under different storage conditions. *Food Res Int.* (2020) 128:108757. doi: 10.1016/j.foodres.2019.108757

56. Gao X, Feng T, Sheng M, Wang B, Wang Z, Shan P, et al. Characterization of the aroma-active compounds in black soybean sauce, a distinctive soy sauce. *Food Chem.* (2021) 364:130334. doi: 10.1016/j.foodchem.2021.130334

57. McGorrin RJ. The significance of volatile sulfur compounds in food flavors: An overview. In: Qian M, Xuetong F, Kanjana M editors. *Volatile Sulfur Compounds in Food*. Washington, DC: ACS Publications (2011). p. 3–31. doi: 10.1080/10408398.2010.536918

58. Dulsat-Serra N, Quintanilla-Casas B, Vichi S. Volatile thiols in coffee: a review on their formation, degradation, assessment and influence on coffee sensory quality. *Food Res Int.* (2016) 89:982–8. doi: 10.1016/j.foodres.2016.02.008

59. Weerawatanakorn M, Wu JC, Pan MH, Ho CT. Reactivity and stability of selected flavor compounds. *J Food Drug Anal.* (2015) 23:176–90. doi: 10.1016/j.jfda.2015.02.001

60. Casaburi A, Piombino P, Nychas GJ, Villani F, Ercolini D. Bacterial populations and the volatilome associated to meat spoilage. *Food Microbiol.* (2015) 45(Pt A):83–102. doi: 10.1016/j.fm.2014.02.002

61. Jousse F, Jongen T, Agterof W, Russell S, Braat P. Simplified kinetic scheme of flavor formation by the maillard reaction. *J Food Sci.* (2002) 67:2534–42. doi: 10.1111/j.1365-2621.2002.tb08772.x

62. Diez-Simon C, Mumm R, Hall RD. Mass spectrometry-based metabolomics of volatiles as a new tool for understanding aroma and flavour chemistry in processed food products. *Metabolomics.* (2019) 15:41. doi: 10.1007/s11306-019-1493-6

frontiers | Frontiers in Nutrition

TYPE Original Research
PUBLISHED 12 September 2022
DOI 10.3389/fnut.2022.977929

OPEN ACCESS

EDITED BY
Gang Fan,
Huazhong Agricultural University, China

REVIEWED BY
Zhou Qi,
Chinese Academy of Agricultural Sciences (CAAS), China
Honglei Tian,
Shaanxi Normal University, China

*CORRESPONDENCE
Wei Dong
20200812@btbu.edu.cn
Jinyuan Sun
sunjinyuan@btbu.edu.cn

SPECIALTY SECTION
This article was submitted to Food Chemistry, a section of the journal Frontiers in Nutrition

RECEIVED 25 June 2022
ACCEPTED 18 August 2022
PUBLISHED 12 September 2022

CITATION
Ao L, Guo K, Dai X, Dong W, Sun X, Sun B, Sun J, Liu G, Li A, Li H and Zheng F (2022) Quick classification of strong-aroma types of base Baijiu using potentiometric and voltammetric electronic tongue combined with chemometric techniques. *Front. Nutr.* 9:977929. doi: 10.3389/fnut.2022.977929

Quick classification of strong-aroma types of base Baijiu using potentiometric and voltammetric electronic tongue combined with chemometric techniques

Ling Ao[1,2], Kai Guo[1,2], Xinran Dai[1,2], Wei Dong[1,2]*, Xiaotao Sun[1,2], Baoguo Sun[1,2], Jinyuan Sun[1,2]*, Guoying Liu[3], Anjun Li[3], Hehe Li[1,2] and Fuping Zheng[1,2]

[1]Beijing Laboratory of Food Quality and Safety, Beijing Technology and Business University, Beijing, China, [2]Key Laboratory of Brewing Molecular Engineering of China Light Industry, School of Light Industry, Beijing, China, [3]Center for Solid-state Fermentation Engineering of Anhui Province, Bozhou, China

Nowadays, the classification of strong-aroma types of base Baijiu (base SAB) is mainly achieved by human sensory evaluation. However, prolonged tasting brings difficulties for sommeliers in guaranteeing the consistency of results, and may even cause health problems. Herein, an electronic tongue (E-Tongue) combined with a gas chromatography-mass spectrometry (GC-MS) method was successfully developed to grade high-alcoholic base SAB. The E-tongue was capable of identifying base SAB samples into four grades by a discriminant function analysis (DFA) model based on human sensory evaluation results. More importantly, it could effectively and rapidly predict the quality grade of unknown base SAB with an average accuracy up to 95%. The differences of chemical components between base SAB samples were studied by the GC-MS analysis and 52 aroma compounds were identified. The qualitative and quantitative results showed that with the increase of base SAB grade, the varieties and contents of aroma compounds increased. Overall, the comprehensive analysis of E-tongue data and GC-MS results could be in good agreement with human sensory evaluation results, which also proved that the newly developed method has a potential to be a useful alternative to the overall quality grading of base Baijiu.

KEYWORDS

strong-aroma types of base Baijiu, electronic tongue, principal component analysis, discriminant function analysis, GC-MS

Introduction

Baijiu, also called as Chinese liquor or spirit, is one of the most popular alcoholic beverages in China, with the annual production of about 7.156 billion liters in 2021 (1). Baijiu is mainly composed of water, ethanol, and other trace flavor compounds, in which the mass fraction of flavor compounds account for approximately 1–2% of the total mass of Baijiu. Although the proportion of the aforementioned flavor substances in Baijiu is relatively low, the quantitative blending of these flavor substances will play the most important role in the overall aroma. In decades, on the basis of its aroma characteristics, Baijiu are generally classified into twelve categories, such as strong, soy sauce, light, sesame, Chi, complex (Jian), herblike, Feng, rice, Fuyu, Te, and Laobaigan aroma-types (2). With the largest production among them, strong-aroma types of Baijiu (SAB) have gained popularity due to their sensory characterization, such as rich mellow, sweet, and pure, particularly the fragrant after drinking and aftertaste (3).

Based on the characteristics of SAB production, the fresh distillates (base SAB) and the finished product (commercial SAB) are both called SAB (4). In general, during SAB production, freshly distilled base SAB usually has undesirable characteristics and is not preferable for drinking (5). It needs to go through a long aging process, ranging from months to years, to develop a well-balanced "matured" Baijiu (6). Finally, the aforementioned base Baijiu is blended by sommeliers to obtain commercial SAB with standardized flavor and taste. Until now, the classification of base SAB is conventionally graded according to the human sensory evaluation (7). Moreover, coupled with multivariate data analysis (MVDA), the correlation between the chemical profiles and sensory evaluation of samples could be also demonstrated successfully (8). Recently, the contributions of many key aroma compounds to the overall flavor of Baijiu have been identified in this way, such as the "mud-like" aromas in base SAB (9), retronasal "burnt" flavor in soy sauce aroma-types of Baijiu (10), and the sweetness perception of Baijiu (11). However, the method mentioned above is susceptible to environmental impacts and subjective factors, making it difficult to ensure the results during a prolonged tasting in the busy season. More importantly, long-term and abundant base Baijiu tasting does harm to the sommelier because of the high alcohol content (generally at 60–70% alcohol by volume, ABV). Hence, developing a rapid and efficient method for the base SAB classification is of great value and demand.

The electronic tongue (E-tongue) is a kind of human sensory simulating system, which consists of a number of low-selective sensors and uses advanced mathematical procedures for signal processing based on pattern recognition and multivariate data analysis (12). In recent years, E-tongue has been widely used for the analysis of wines, fruit juices, coffee, milk, and beverages, in addition to the detection of trace amounts of impurities or pollutants in waters (13, 14). Moreover, it also has been extensively used for the discrimination of alcoholic beverages by their variety, age, taste, and geographical origin, and it can eliminate panelist bias for taste evaluation of liquor products (15, 16). For instance, an exploratory study was conducted by Schmidtke et al. whose results indicated that bitterness and astringency could be predicted from wines with good precision by using E-tongue and sensory evaluation (17). Legin et al. evaluated 56 Italian wines by recognition and quantitative analysis of E-tongue and concluded that E-tongue was capable of discriminating Barbera d'Asti and Gutturnio wines (18). However, the sensitivity of sensors is easily reduced or lost in high alcohol content.

Due to the high alcohol content of base SAB, the ability of alcohol tolerance of sensors determines whether they are suitable for the analysis of base SAB. Currently, it has been proved by numerous researchers that E-tongue based on inert metal electrodes or modified epoxy-composite sensors could be a good instrument for the distilling spirits analysis (19, 20). Among them, the Smartongue is a kind of E-tongue based on multifrequency large amplitude pulse voltammetry (MLAPV). More importantly, based on a combination of pulse applied relaxation techniques combined with the specific pattern recognition system and multivariate statistical analysis, a lot of signals could be processed more accurately and effectively by MLAPV compared with other sensors (16, 20). In 2007, Tian et al. discriminated six Baijiu samples successfully by using an electronic tongue based on MLAPV coupled with a series of metal electrodes at different frequency segments (21). However, to the best of our knowledge, only a few studies have been reported dealing with the application of E-tongue based on inert metal electrode sensors for the classification of base SAB. Moreover, they simply focused on the differences in statistics without considering the chemical composition.

Therefore, the main objectives of this work were to (i) grade the quality attributes of base SAB by the electronic tongue combined with gas chromatography-mass spectrometry (GC-MS), (ii) establish prediction models by principal component analysis (PCA) or discriminant function analysis (DFA) according to sensory evaluation results, and (iii) better elucidate the differences of aroma compounds from each grade of base SAB using the GC-MS analysis and compared with the national standard of GB/T 10781.1-2021. These results will be useful for the quick quality grading of SAB from the Baijiu industry.

Materials and methods

Chemicals

Authentic standards, including twenty-seven kinds of esters (ethyl acetate, ethyl butanoate, ethyl pentanoate, ethyl

TABLE 1 Aroma compounds identified by gas chromatography-mass spectrometry (GC-MS) in four grades of strong-aroma types of base Baijiu (base SAB).

No	Aroma compounds	[a]Identification	DB-WAX		TG-5MS		Monitored ions m/z
			RI	[b]LRI	RI	[b]LRI	
1	Ethyl acetate	MS, RI, S	881	884	614	613	43, 61, 70, 88
2	Diethyl acetal	MS, RI, S	906	900	726	725	45, 73, 103, 118
3	Ethyl butanoate	MS, RI, S	1035	1032	803	803	43, 71, 88, 116
4	2-butanol	MS, RI, S	1038	1041	604	598	45,59,74
5	1-propanol	MS, RI, S	1046	1049	539	532	59, 60
6	2-methylpropanol	MS, RI, S	1105	1094	624	622	43, 74
7	Ethyl pentanoate	MS, RI, S	1121	1120	903	900	57, 85, 101, 130
8	2-pentanol	MS, RI, S	1132	1124	701	706	45, 55, 73, 88
9	1-butanol	MS, RI, S	1156	1150	658	656	43, 56, 74
10	Ethyl 4-methylpentanoate	MS, RI, S	1180	1180	970	969	88, 99, 101, 144
11	2-methylbutanol	MS, RI, S	1206	1208	734	736	56, 70, 88
12	3-methylbutanol	MS, RI, S	1208	1211	732	730	43, 55, 88
13	Ethyl hexanoate	MS, RI, S	1218	1220	1009	1002	88, 99, 101, 144
14	1-pentanol	MS, RI, S	1246	1255	763	764	55, 70, 88
15	Hexyl acetate	MS, RI, S	1262	1265	1016	1014	56, 69, 84, 144
16	Propyl hexanoate	MS, RI, S	1305	1300	1097	1094	61, 99, 117, 158
17	Ethyl heptanoate	MS, RI, S	1314	1317	1100	1095	88, 101, 113, 158
18	Ethyl lactate	MS, RI, S	1337	1340	817	815	45, 75, 118
19	1-hexanol	MS, RI, S	1343	1345	868	867	55, 56, 69, 102
20	Butyl hexanoate	MS, RI, S	1396	1392	1193	1188	56, 99, 117, 172
21	Ethyl octanoate	MS, RI, S	1419	1420	1199	1195	88, 101, 127, 172
22	Isopentyl hexanoate	MS, RI, S	1438	1450	1253	1250	70, 71, 99, 186
23	Acetic acid	MS, RI, S	1442	1441	620	625	43, 45, 60
24	1-octanol	MS, RI, S	1542	1546	1079	1070	56, 70, 84, 130
25	2-methylpropanoic acid	MS, RI, S	1556	1564	789	785	43, 73, 88
26	2,3-butanediol	MS, RI, S	1567	1576	–	–	45, 57, 90
27	Hexyl hexanoate	MS, RI, S	1593	1593	1386	1385	84, 99, 117, 200
28	Butanoic acid	MS, RI, S	1615	1610	793	793	45, 60, 73, 88
29	Ethyl decanoate	MS, RI, S	1622	1629	1395	1392	88, 101, 155, 200
30	Isoamyl octanoate	MS, RI, S	1643	1651	1447	1450	70, 127, 145, 214
31	Ethyl benzoate	MS, RI, S	1655	1652	1172	1170	105, 122, 150
32	3-methylbutanoic acid	MS, RI, S	1658	1660	864	866	60, 87, 102
33	Diethyl butanedioate	MS, RI, S	1666	1667	1185	1181	101, 128, 129, 174
34	Pentanoic acid	MS, RI, S	1726	1729	–	–	60, 73, 102
35	Ethyl phenylacetate	MS, RI, S	1775	1785	1247	1252	65, 91, 164
36	4-methylpentanoic acid	MS, RI, S	1791	1792	–	–	73, 74, 83, 116
37	Hexyl octanoate	MS, RI, S	1795	1795	1583	1582	84, 127, 145, 228
38	Ethyl dodecanoate	MS, RI, S	1829	1828	1595	1597	88, 101, 183, 228
39	Hexanoic acid	MS, RI, S	1833	1827	–	–	60, 73, 87, 116
40	ethyl 3-phenylpropionate	MS, RI, S	1874	1872	1350	1350	91, 104, 178
41	Phenylethyl alcohol	MS, RI, S	1903	1901	1112	1116	91, 92, 122
42	Heptanoic acid	MS, RI, S	1940	1943	1070	1071	60, 73, 87, 130
43	4-methylguaiacol	MS, RI, S	1951	1956	1192	1192	95, 123, 138
44	4-ethylguaiacol	MS, RI, S	2023	2032	1280	1280	122, 137, 152
45	Ethyl tetradecanoate	MS, RI, S	2034	2040	1794	1793	88, 101, 256
46	Octanoic acid	MS, RI, S	2045	2050	1190	1191	60, 73, 101, 144

(Continued)

TABLE 1 (Continued)

No	Aroma compounds	[a]Identification	DB-WAX		TG-5MS		Monitored ions m/z
			RI	[b]LRI	RI	[b]LRI	
47	4-methylphenol	MS, RI, S	2075	2079	1082	1084	77, 107, 108
48	Ethyl hexadecanoate	MS, RI, S	2240	2246	1995	1994	88, 101, 284
49	Ethyl octadecanoate	MS, RI, S	2441	2455	2194	2194	88, 101, 312
50	Ethyl oleate	MS, RI, S	2461	2461	2168	2169	68, 88, 264, 310
51	Ethyl linoleate	MS, RI, S	2508	2510	2163	2163	81, 95, 109, 308
52	Ethyl linolenate	MS, RI, S	2575	2578	2169	2173	79, 95, 108, 306

[a]MS, compounds were identified by MS spectra; RI, the retention index of compounds were identified on FFAP and TG-5MS by comparison to reference standards; S, compounds were identified by standards.
[b]LRI, Literature RI.

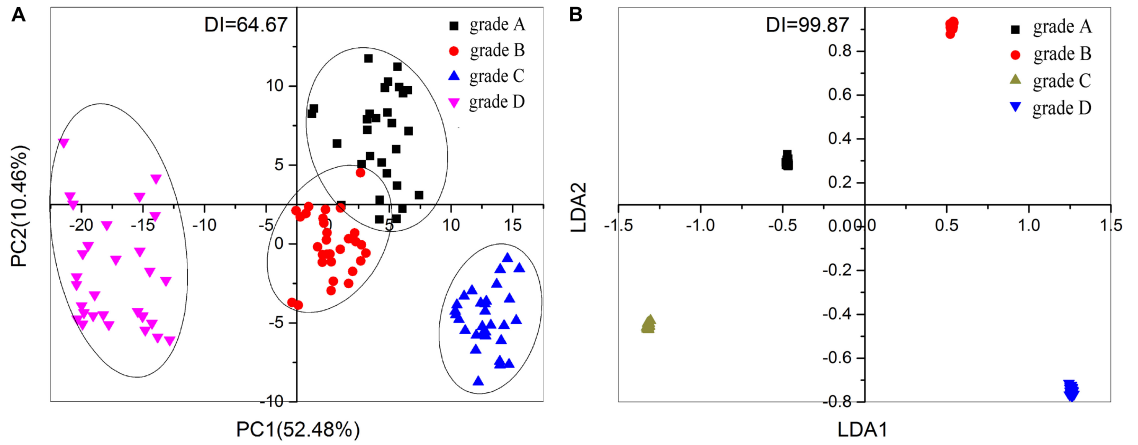

FIGURE 1
Multivariate statistical analysis based on the result of the Smartongue analysis: loading plot of **(A)** principal component analysis (PCA) and **(B)** discriminant function analysis (DFA) for the classification of 120 strong-aroma types of base Baijiu (base SAB) samples from four different grades.

4-methylpentanoate, ethyl hexanoate, hexyl acetate, propyl hexanoate, ethyl lactate, ethyl heptanoate, butyl hexanoate, ethyl octanoate, isopentyl hexanoate, hexyl hexanoate, ethyl decanoate, isoamyl octanoate, ethyl benzoate, diethyl butanedioate, ethyl phenylacetate, hexyl octanoate, ethyl dodecanoate, ethyl 3-phenylpropionate, ethyl tetradecanoate, ethyl hexadecanoate, ethyl octadecanoate, ethyl oleate, ethyl linoleate, and ethyl linolenate), twelve types of alcohols (1-propanol, 1-butanol, 2-butanol, 2-methylpropanol, 1-pentanol, 2-pentanol, 2-methylbutanol, 3-methylbutanol, 1-hexanol, 1-octanol, 2,3-butanediol, and phenylethyl alcohol), nine kinds of acids (acetic acid, 2-methylpropanoic acid, butanoic acid, 3-methylbutanoic acid, pentanoic acid, 4-methylpentanoic acid, hexanoic acid, heptanoic acid, and octanoic acid), three kinds of phenols (4-methylguaiacol, 4-ethylguaiacol, and 4-methylphenol), and one kind of acetal (diethyl acetal), were all purchased from Sigma-Aldrich (Beijing, China). Compounds, such as 4-octanol (internal standard, IS1), 4-hydroxy-2-butanone (IS2), n-pentyl acetate (IS3), and 2-ethylbutyric acid (IS4), used as internal standards in this study, were purchased from Sigma-Aldrich (Beijing, China). A C5-C30 n-alkane mixture (Sigma-Aldrich, Beijing, China) was employed for the determination of linear retention indices (RIs). Sodium chloride, anhydrous sodium sulfate, dichloromethane, kalium chloratum, and absolute ethanol were purchased from Sinopharm Chemical Reagent Co., Ltd. (Beijing, China). All the chemicals used above were of analytical reagent grade, with at least 97% purity.

Sampling and sample preparation

Sampling

A total of 140 base SAB samples from 140 different pits were obtained from Anhui Gujing Distillery Co., Ltd., (Anhui, China), with alcohol content ranging from 55 to 70% ABV. All samples (125 ml from each bottle) were stored at 4°C until analysis.

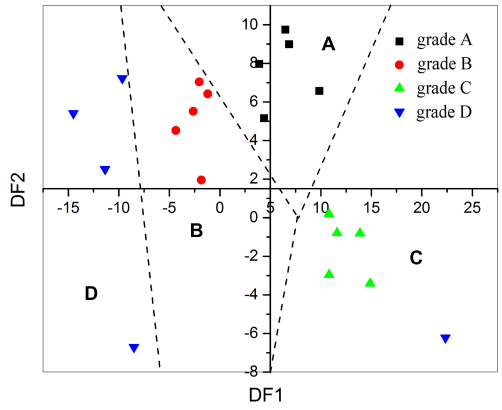

FIGURE 2
The established DFA model map was verified by 20 real SAB samples.

Sample preparation of base SAB for liquid-liquid extraction

According to the method reported by Zheng, and associated with some modifications (22), a total of 25 ml of base SAB sample was diluted to 10% ABV with Milli-Q water (Millipore, Bedford, MA, United States). Before being used, the water was boiled for 5 min, and then cooled to 20°C in a 1.0 L flask. The diluted base SAB sample was saturated with NaCl, and extracted 3 times with freshly distilled dichloromethane (50.0 ml each time). The dichloromethane extracts (about 150.0 ml) were dried with plenty of anhydrous Na_2SO_4 overnight, concentrated to a final volume of 1.0 ml under a gentle stream of nitrogen, and then the concentrated extracts were stored at −20°C before GC-MS analysis.

Sensory evaluation

Each base SAB sample (20 ml) was subjected to sensory descriptive judgment by the sommeliers at 20°C after it was poured into a glass cup. The procedure was conducted in a sensory laboratory following the national standard of GB/T 10345-2007 (23). There were eight panelists (4 men and 4 women, composed of a team, including 4 junior sommeliers, 2 intermediate sommeliers, 2 senior sommeliers, and age range 25–40 years) participating in the sensory evaluation session with a weighted score in this research. The weights of junior sommeliers, intermediate sommeliers, and senior sommeliers were 0.8, 1.0, and 1.2, respectively. The panelists were required to rinse their mouth thoroughly with purified water and rest for 1.0 min at least between two-samples-tasting and rest 10.0 min or more per four-samples-tasting. Each sample, randomly marked with a three-digit number, was presented randomly.

Smartongue analysis

In total, 140 target base SAB samples were analyzed by Smartongue (RuiFen International Trading Co., Ltd., Shanghai, China). The sensor of Smartongue should be preheated successively with 20.0 ml of 0.01 mol/L KCl solution and 20.0 ml SAB samples after each start of Smartongue. The programmed parameters of Smartongue were set as follows: the step voltage was set at 0.2 V, and 6 sensors were all chosen at 10^{-4} sensitivity. Each base SAB (20.0 ml) was subjected to test by the Smartongue at 20°C in a glass cup. Between each measurement, the sensors were rinsed with 25.0 ml of deionized water. Three replicate measurements were conducted for each base SAB sample.

GC-MS analysis

Qualitative analysis

The aroma compounds in the base SAB samples were detected by both direct injection and liquid–liquid extraction coupled with GC-MS method (3). The GC-MS analysis of base SAB samples was performed on an Agilent 7890 gas chromatograph equipped with an Agilent 5977A mass-selective detector (MSD) and a DB-WAX column (60 m × 0.25 mm i.d., 0.25 μm film thickness, J&W Scientific). The column carrier gas was helium at a constant flow rate of 1.0 ml/min and the direct injection volume was 1.0 μl with a split ratio of 5:1. The injector temperature was set at 250°C. The oven temperature was held at 40°C for 0.5 min, then programmed to 50°C at a rate of 10°C/min and held for 8 min and then, programmed to 70°C at a rate of 3°C/min and held for 5 min afterward. Next, it was programmed to 187°C at a rate of 3°C/min and held for 1 min, and finally programmed to 230°C at a rate of 5°C/min and held for 4 min. The temperature of the mass-selective detector transfer line was kept at 240°C. Mass spectra in the electron ionization mode (EI) were recorded at 70 eV. The temperature of the ion source was 230°C, and the mass range was from 40 to 500 amu at full-scan mode. Peak identifications of the odorants were performed by comparison of mass spectra with those of the NIST 19.0 database (Agilent Technologies Inc., Santa Clara, CA, United States). Positive identification was achieved by comparison of their retention indices (RIs) and mass spectra with those of pure standards. The RIs of the odorants were calculated from the retention times of n-alkanes (C5–C30), according to a modified Kovats method (24).

To confirm the identification of these aroma compounds, the analytical procedures were also performed on a TG-5MS non-polar capillary column (5% phenyl methylpolysiloxane, 30 m × 0.25 mm × 0.25 μm, Thermo Fisher Scientific). The GC-MS analysis of extracts was implemented by a Thermo Trace 1300 gas chromatograph equipped with a Thermo ISQ

TABLE 2 Standard curves and concentrations of 52 aroma compounds in four grades of base SAB.

No	Aroma compound	Standard curve			A		B		C		D	
		Slope	Intercept	R^2	[a]av ± SD (mg/L)	[b]RSD (%)	av ± SD (mg/L)	RSD (%)	av ± SD (mg/L)	RSD (%)	av ± SD (mg/L)	RSD (%)
13	Ethyl hexanoate	31.302	−2.048	0.9994	2712.98 ± 21.16	0.78	2245.57 ± 11.00	0.49	2047.17 ± 7.98	0.39	288.41 ± 6.81	2.36
1	Ethyl acetate	307.67	−1.382	0.9957	1556.69 ± 69.90	4.49	1167.78 ± 6.66	0.57	1000.94 ± 16.92	1.69	979.83 ± 15.58	1.59
18	Ethyl lactate	41.556	−1.2471	0.9991	1038.02 ± 11.31	1.09	1457.65 ± 2.19	0.15	1542.16 ± 4.78	0.31	1570.86 ± 24.51	1.56
39	Hexanoic acid	22.832	−0.0237	0.9996	909.14 ± 4.18	0.46	808.67 ± 19.25	2.38	490.83 ± 1.23	0.25	59.62 ± 1.08	1.81
23	Acetic acid	161.78	−0.912	0.9945	778.56 ± 14.87	1.91	649.30 ± 7.34	1.13	491.79 ± 17.61	3.58	528.11 ± 12.67	2.40
5	1-propanol	76.956	−0.9049	0.9992	596.94 ± 12.37	2.07	320.97 ± 4.01	1.25	238.34 ± 0.60	0.25	183.97 ± 4.10	2.23
2	Diethyl acetal	78.695	−0.7763	0.9976	513.49 ± 18.13	3.53	434.37 ± 2.91	0.67	361.09 ± 5.81	1.61	250.17 ± 3.40	1.36
12	3-methylbutanol	96.038	−1.0605	0.9993	288.68 ± 4.85	1.68	239.98 ± 0.05	0.02	278.47 ± 28.49	10.23	23.37 ± 0.50	2.15
3	Ethyl butanoate	81.061	−1.6081	0.9994	269.31 ± 7.57	2.81	226.02 ± 1.83	0.81	200.45 ± 2.16	1.08	107.12 ± 4.17	3.89
28	Butanoic acid	18.57	1.8407	0.9965	267.51 ± 5.11	1.91	238.30 ± 2.91	1.22	151.17 ± 0.33	0.22	46.88 ± 2.97	6.34
6	2-methylpropanol	42.383	−1.6759	0.9995	173.46 ± 3.02	1.74	168.29 ± 1.06	0.63	172.85 ± 0.02	0.01	126.89 ± 3.45	2.72
21	Ethyl octanoate	40.712	−3.3363	0.9941	165.24 ± 0.78	0.47	168.38 ± 1.40	0.83	182.95 ± 0.20	0.11	7.00 ± 0.22	3.13
4	2-butanol	202.58	−0.873	0.9996	165.17 ± 2.68	1.62	28.18 ± 0.48	1.69	20.91 ± 0.16	0.77	13.33 ± 0.09	0.65
9	1-butanol	93.41	−0.9313	0.9993	163.19 ± 0.39	0.24	143.04 ± 5.38	3.76	179.70 ± 2.61	1.45	152.63 ± 3.04	1.99
11	2-methylbutanol	81.863	−1.1663	0.9993	119.46 ± 1.04	0.87	107.30 ± 0.26	0.24	112.69 ± 0.36	0.32	74.35 ± 1.10	1.48
19	1-hexanol	36.08	−0.9008	0.9992	96.74 ± 0.52	0.54	110.04 ± 0.57	0.52	84.21 ± 0.08	0.09	25.30 ± 1.17	4.61
7	Ethyl pentanoate	30.692	−1.6759	0.9994	57.18 ± 1.36	2.37	39.24 ± 0.27	0.68	40.16 ± 0.17	0.43	10.25 ± 0.48	4.65
17	Ethyl heptanoate	25.251	−1.8775	0.9995	56.53 ± 0.03	0.05	51.13 ± 0.21	0.42	58.86 ± 0.21	0.36	2.20 ± 0.01	0.31
48	Ethyl hexadecanoate	12.978	−0.7642	0.9994	40.91 ± 0.36	0.87	35.61 ± 0.32	0.91	41.04 ± 0.02	0.05	7.91 ± 0.15	1.85
8	2-pentanol	25.355	−1.3041	0.9992	40.83 ± 0.61	1.49	9.18 ± 0.75	8.16	6.13 ± 0.06	1.03	1.76 ± 0.06	3.66
34	pentanoic acid	18.131	1.6381	0.9963	39.89 ± 0.71	1.79	25.65 ± 0.44	1.70	18.19 ± 0.002	0.01	3.86 ± 0.14	3.66
25	2-methylpropanoic acid	22.565	0.9897	0.9965	34.45 ± 0.54	1.58	35.52 ± 0.32	0.91	31.74 ± 0.13	0.42	32.38 ± 2.92	9.02
46	Octanoic acid	26.695	1.127	0.9981	27.72 ± 0.05	0.19	39.17 ± 0.02	0.05	18.36 ± 0.06	0.34	[c]nd	
22	Isopentyl hexanoate	40.267	−3.0078	0.9934	26.20 ± 0.05	0.19	21.25 ± 0.32	1.52	18.79 ± 0.38	2.00	nd	
32	3-methylbutanoic acid	28.585	1.4284	0.997	22.83 ± 0.47	2.04	21.49 ± 0.31	1.45	12.97 ± 0.01	0.06	4.75 ± 0.14	2.85
51	Ethyl linoleate	22.675	−0.4406	0.9996	21.85 ± 0.04	0.18	23.22 ± 0.19	0.80	22.09 ± 0.10	0.47	29.06 ± 0.55	1.89
27	Hexyl hexanoate	11.53	−0.0939	0.9973	21.31 ± 0.80	3.75	22.55 ± 0.07	0.32	12.91 ± 0.13	1.04	0.21 ± 0.01	3.12
40	Ethyl 3-phenylpropionate	11.602	−0.6449	0.9993	18.84 ± 0.16	0.85	16.29 ± 0.14	0.86	7.91 ± 0.03	0.43	1.62 ± 0.05	3.09
50	Ethyl oleate	42.673	−0.2761	0.9997	15.17 ± 0.09	0.57	16.54 ± 0.11	0.64	17.79 ± 0.09	0.50	22.94 ± 0.05	0.22
42	Heptanoic acid	21.417	1.9262	0.9988	13.92 ± 0.02	0.12	13.97 ± 0.16	1.13	8.06 ± 0.03	0.34	nd	

(Continued)

10.3389/fnut.2022.977929

TABLE 2 (Continued)

No	Aroma compound	Standard curve			A		B		C		D	
		Slope	Intercept	R^2	[a]av ± SD (mg/L)	[b]RSD (%)	av ± SD (mg/L)	RSD (%)	av ± SD (mg/L)	RSD (%)	av ± SD (mg/L)	RSD (%)
14	1-pentanol	39.533	−1.5388	0.9993	13.64 ± 0.09	0.64	11.21 ± 0.73	6.49	11.21 ± 0.02	0.16	3.90 ± 0.11	2.84
16	Propyl hexanoate	26.416	−1.5796	0.9992	13.01 ± 0.001	0.01	6.69 ± 0.06	0.95	3.03 ± 0.02	0.55	nd	
20	Butyl hexanoate	20.406	−3.014	0.9932	12.27 ± 0.006	0.05	13.81 ± 0.14	1.01	10.93 ± 0.02	0.17	nd	
29	Ethyl decanoate	9.6506	−0.0487	0.9974	7.75 ± 0.73	9.43	7.74 ± 0.08	0.97	7.24 ± 0.08	1.10	3.50 ± 0.24	6.98
33	Eiethyl butanedioate	8.6862	−0.3331	0.9972	7.07 ± 0.20	2.84	14.49 ± 0.21	1.44	9.36 ± 0.04	0.43	25.74 ± 2.33	9.04
10	Ethyl 4-methylpentanoate	27.917	−1.9502	0.9994	4.20 ± 0.08	1.83	3.42 ± 0.01	0.33	1.23 ± 0.02	1.53	nd	
26	2,3-butanediol	24.525	0.5784	0.9968	4.15 ± 0.10	2.49	6.48 ± 0.05	0.79	8.51 ± 0.11	1.33	8.24 ± 0.54	6.58
41	Phenylethyl alcohol	9.2004	−0.5347	0.9993	$3.48 \pm 3.0 \times 10^{-4}$	0.01	3.50 ± 0.04	1.04	3.94 ± 0.01	0.16	5.65 ± 0.47	8.31
36	4-methylpentanoic acid	37.98	1.4439	0.9989	3.14 ± 0.01	0.47	3.09 ± 0.01	0.32	1.85 ± 0.01	0.37	nd	
47	4-methylphenol	10.291	−0.5812	0.9992	2.61 ± 0.01	0.34	2.83 ± 0.02	0.74	$1.10 \pm 7.70 \times 10^{-4}$	0.07	nd	
49	Ethyl octadecanoate	36.649	−0.5657	0.9995	2.09 ± 0.02	1.15	1.82 ± 0.18	9.66	1.80 ± 0.01	0.49	nd	
52	Ethyl linolenate	46.229	0.0968	0.9998	2.08 ± 0.01	0.43	$2.46 \pm 3.69 \times 10^{-3}$	0.15	2.18 ± 0.01	0.60	2.92 ± 0.13	4.43
45	Ethyl tetradecanoate	13.849	−0.5317	0.9994	2.03 ± 0.04	1.91	1.93 ± 0.01	0.62	2.11 ± 0.01	0.27	1.75 ± 0.05	2.85
35	Ethyl phenylacetate	9.0471	−0.585	0.9993	1.90 ± 0.02	1.10	1.93 ± 0.02	0.97	3.07 ± 0.02	0.71	0.79 ± 0.03	4.00
15	Hexyl acetate	35.685	−1.4155	0.9992	1.79 ± 0.04	1.96	2.30 ± 0.02	0.70	$0.56 \pm 2.74 \times 10^{-3}$	0.49	nd	
31	Ethyl benzoate	11.114	−0.6108	0.9975	1.71 ± 0.08	4.52	0.54 ± 0.02	2.94	0.48 ± 0.01	1.66	nd	
43	4-methylguaiacol	11.703	−0.5721	0.9993	1.66 ± 0.04	2.59	$2.68 \pm 5.36 \times 10^{-4}$	0.02	$1.37 \pm 2.74 \times 10^{-3}$	0.20	1.42 ± 0.03	2.13
38	Ethyl dodecanoate	11.096	−0.097	0.9988	1.63 ± 0.04	2.32	1.32 ± 0.01	0.79	1.54 ± 0.01	0.42	0.89 ± 0.01	1.09
24	1-octanol	22.072	0.3593	0.9977	1.45 ± 0.03	2.26	2.42 ± 0.02	0.67	1.46 ± 0.01	0.39	nd	
44	4-ethylguaiacol	9.3486	−0.2911	0.9991	1.38 ± 0.01	0.74	$1.5 \pm 3.00 \times 10^{-3}$	0.20	$0.87 \pm 8.70 \times 10^{-4}$	0.10	1.74 ± 0.03	1.71
30	Isoamyl octanoate	10.48	−0.0887	0.9975	0.67 ± 0.03	4.73	0.64 ± 0.01	1.38	0.61 ± 0.01	1.01	nd	
37	Hexyl octanoate	13.831	−0.507	0.9993	0.55 ± 0.001	0.23	1.16 ± 0.01	0.82	$0.32 \pm 3.52 \times 10^{-3}$	1.10	nd	

[a]av ± SD (n = 3), average concentration of triplicates; [b]RSD, relative standard deviation of the average concentration; [c]nd, not detected.

10.3389/fnut.2022.977929

TABLE 3 Physicochemical indexes comparison of 4 grades of base SAB samples.

Item	[a]First grade	A	B	C	D
Total acid (of acetic acid count)/(g/L)	≥ 0.30	✓	✓	✓	✓
Total ester (of ethyl acetate count) /(g/L)	≥ 1.50	✓	✘	✘	✘
Ethyl hexanoate/(g/L)	0.60–2.50	✓	✓	✓	✘

[a]First grade, the physicochemical standard of SAB with high alcohol content (41–68% ABV) following the national standard of GB/T 10781.1-2021.

LT mass selective detector system (Thermo Fisher Scientific). Helium (> 99.999%) was applied as the carrier gas at a flow rate of 1.0 ml/min. The temperature of the injector was set at 250°C. The oven temperature was programmed as follows: 40°C for 2 min, 1°C/min up to 50°C and held for 2 min, 3°C/min up to 70°C and held for 3 min, 6°C/min up to 230°C and held for 2 min, and 20°C/min up to 320°C and held for 4 min. All injections were set in split mode, and the split ratio was 30:1. The mass spectrometer was operated in the electron ionization mode with electron energy set as 70 eV and the mass range was from 43 to 500 amu at full-scan mode. The transfer line and ion source temperatures were both set to 300°C. Most aroma compounds were identified by comparing their retention indices (RIs) and mass spectra with those of pure standards.

Quantitative analysis

Quantitative analyses were routinely performed following the IS method, and the internal standard compounds were n-pentyl acetate, 4-octanol, 4-hydroxy-2-butanone, and 2-ethylbutyric acid. The selected ion monitoring (SIM) mode was adopted, and each analyte was quantified on the basis of the peak area using one quantitative fragment and two qualitative fragments (Table 1). The selected quantitative ions of the four IS were m/z 70, 69, 43, and 73, respectively. Moreover, standard calibration curves were used to quantify the target aroma compounds using a suitable capillary column based on the ratio of the peak area of the compound relative to the peak area of the internal standard to determine the concentration of the analyte.

Statistical analysis

All chemical analyses in this work were carried out in triplicate, and the concentrations of each aroma compound acquired from GC-MS analysis were expressed as the means ± standard deviation (SD). The raw data obtained from the Smartongue were analyzed by both PCA and DFA pattern recognition techniques. PCA is mainly used to model, compress, and visualize multivariate data by setting a new coordinate system in which Euclidean distances between the objects remain the same. As a well-known unsupervised method, PCA allows the reduction of multidimensional data and simplifies the interpretation of the data by a few principal components (25). DFA is used to examine differences between or among groups by using a discriminant prediction equation, which allows for the rejection of variables that are little related to group distinctions (26). Among them, 120 types of base SAB samples were used to establish a quality grading model through PCA and DFA by the Smartongue system version 3.0 as a calibration set. The rest 20 base SAB samples were used to verify these models as validation set.

Results and discussion

Sensory evaluation

A total of 140 base SAB samples were classified into 4 grades (A, B, C, and D) through their taste characteristics by the eight sommeliers, and 35 types of base SAB samples of each grade were included. Among the sensory evaluation of these four grades, the base SAB from grades A, B, and C all showed strong cellar fragrance, pure, long aftertaste, and no peculiar smell with a tendency to decrease; however, grade D showed fermented grains flavor, less cellar fragrance, and short aftertaste. These results suggest that the rank of four grades from good to bad were successively A, B, C, and D according to the sensory requirements of national standard of GB/T 10781.1-2021 (27).

Smartongue analysis

In this study, 120 types of base SAB samples of 4 different grades (30 samples of each grade) were tested by the Smartongue and the map of its PCA and DFA are shown in Figure 1. As shown in Figure 1A, base SAB samples of grade C and grade D could be classified apparently by PCA; however, base SAB from grade A and grade B can be only discriminated with a little overlap. Moreover, Figure 1A also shows the score plot relative to the first and second principal components (PC1 and PC2) were 52.48 and 10.46%, respectively. The total principal component score (62.94%) indicated that base SAB samples could only be discriminated by PCA roughly. The discrimination index (DI, a number to evaluate the separation level for the above non-linear multivariate data analysis methods and its maximum DI value is 100%, indicating the best separation of the samples) value of PCA is 64.67, which also means base SAB samples could be discriminated reluctantly. As can be observed in Figure 1B, the four grades base SAB samples of A, B, C, and D could be discriminated obviously

by the DFA. It could be seen that DFA had a good separation ability among these four grades (A, B, C, and D) base SAB samples with a DI value of 99.87. The analysis above showed that DFA was more applicable to grade base SAB samples than PCA. Therefore, the DFA was used to establish a quality grading prediction model.

On the basis of the DFA prediction model, the predicted quality grade result of the validation set is shown in Figure 2. As shown in Figure 2, 20 validations set base SAB samples from four grades could be classified obviously by the DFA model except for one base SAB sample from grade D. Hence, all the results above revealed that the Smartongue system was capable of classifying the base SAB and quality grade predicting results with an average accuracy up to 95%.

Qualitative analysis

A total of 52 aroma compounds, including 27 esters, 12 alcohols, 9 acids, 3 phenols, and 1 acetal, were determined in base SAB samples by direct injection and liquid-liquid extraction (LLE) coupled with GC-MS analysis (Table 1). As exhibited in Table 1, all aroma compounds could be successfully identified in grades A, B, and C base SAB samples while only 38 aroma compounds were identified in grade D, which suggested that the component is more abundant in higher grade samples. Main volatile compounds of SAB, such as ethyl acetate, ethyl lactate, ethyl butanoate, ethyl hexanoate, 1-butanol, 3-methylbutanol, butanoic acid, and hexanoic acid have been determined in previous literature (3, 28). Among them, ethyl hexanoate, hexyl hexanoate, ethyl pentanoate, and hexanoic acid were regarded as odor-active compounds and contribute greatly to the odors of SAB (29). Besides, most of these compounds have been earlier identified as aroma compounds in other aroma types of Baijiu (30). Hence, the qualitative method used in this study turned out to be appropriate and reliable.

Quantitative analysis

To gain a deeper insight into the characterization and relevance of base SAB samples, a total of 52 aroma compounds were quantitated in these four grades. As shown in Table 2, the obtained standard curves were observed to have a good linearity with a correlation coefficient (R^2) $\geq$ 0.99 and the RSDs in triplicate of samples were $\leq$ 10%, which illustrated the good precision of the quantitative methods. Based on these result, ethyl hexanoate were present in the highest concentrations in grades A, B, C, and D (2,712.98, 2,245.57, 2,047.17, and 288.41 mg/L, respectively), followed by ethyl acetate (1,556.69 mg/L-A, 1,167.78 mg/L-B, 1,000.94 mg/L-C, and 979.83 mg/L-D), ethyl lactate (1,038.02 mg/L-A, 1,457.65 mg/L-B, 1,542.16 mg/L-C, and 1,570.86 mg/L-D), and ethyl butanoate (269.31 mg/L-A, 226.02 mg/L-B, 200.45 mg/L-C, and 107.12 mg/L-D). These 4 compounds were all present at levels above 100 mg/L, and they were taken as the key volatile components of SAB. Additionally, hexanoic acid (909.14 mg/L-A, 808.67 mg/L-B, 490.83 mg/L-C, and 59.62 mg/L-D), acetic acid (778.56 mg/L-A, 649.30 mg/L-B, 491.79 mg/L-C, and 528.11 mg/L-D), 1-propanol (596.94 mg/L-A, 320.97 mg/L-B, 238.34 mg/L-C, and 183.97 mg/L-D), and diethyl acetal (513.49 mg/L-A, 434.37 mg/L-B, 361.09 mg/L-C, and 250.17 mg/L-D) were also presented in high concentrations. Moreover, as shown in Table 3, the content of ethyl hexanoate, total acid, and total ester in grade A had reached the first grade standard of high alcohol content Chinese strong flavor Baijiu following the national standard of GB/T 10781.1-2021, but partly achieved in grades B, C, and D. These findings indicated that a high-grade base SAB sample (e.g., grade A) was superior to a low-grade base SAB sample (e.g., grade D). Besides, most of the concentrations of aroma compounds in grades A, B, C, and D presented a sequentially decreasing trend. Overall, the aforementioned results demonstrated that the quality ranks of four grades of base SAB samples from good to bad were A, B, C, and D, successively, which is consistent with the grading result acquired from the electronic tongue and human sensory evaluations.

Conclusion

In the present study, an electronic tongue combined with the GC-MS method was developed to grade high-alcoholic base SAB for the first time. The E-tongue showed a good prediction in different grades of base SAB when models were established using DFA, which suggests that the E-tongue combined with data modeling is promising for flavor quantification and quality grading. Moreover, to gain a deeper insight into the characterization and relevance of base SAB samples, a total of 52 aroma compounds were identified in four grades of base SAB and differences in the composition of volatile components from four grades were observed by GC-MS analysis. In general, the variety and concentration of high-grade base SAB were more than that of low grade, which showed a good agreement with human sensory evaluation results. These findings provide a guide for Baijiu industries to select the proper method to the overall quality grading for base Baijiu. Nonetheless, we still question the applicability of E-tongue in quantifying the overall quality of base Baijiu from other aroma types. Further research on the quality classification by using more base Baijiu varieties will confirm and improve our findings.

Data availability statement

The original contributions presented in this study are included in the article/supplementary material, further inquiries can be directed to the corresponding authors.

Author contributions

LA: investigation, formal analysis, and writing—original draft. KG: methodology, validation, data curation, and writing—original draft. XD: investigation and visualization. WD: writing—review and editing and funding acquisition. XS: data curation and writing—review and editing. BS: editing, supervision, and funding. JS: writing—review and editing and visualization. GL: methodology and validation. AL: supervision and funding. HL: methodology and software. FZ: supervision and validation. All authors have read and approved the submitted version.

Funding

This work was supported by the National Natural Science Foundation of China (32102122), Department of Science and Technology of Sichuan Province (2019YFS0520 and 2021ZYD0102), and Beijing Outstanding Young Scientist Program (BJJWZYJH01201910011025).

Acknowledgments

Many thanks to the RuiFen International Trading Co., Ltd., for providing the experimental conditions.

Conflict of interest

The authors declare that the research was conducted in the absence of any commercial or financial relationships that could be construed as a potential conflict of interest.

Publisher's note

All claims expressed in this article are solely those of the authors and do not necessarily represent those of their affiliated organizations, or those of the publisher, the editors and the reviewers. Any product that may be evaluated in this article, or claim that may be made by its manufacturer, is not guaranteed or endorsed by the publisher.

References

1. Wang J, Chen H, Wu Y, Zhao D. Uncover the flavor code of strong-aroma baijiu: Research progress on the revelation of aroma compounds in strong-aroma baijiu by means of modern separation technology and molecular sensory evaluation. *J Food Compos Anal.* (2022) 109:104499. doi: 10.1016/j.jfca.2022.104499

2. Du J, Li Y, Xu J, Huang M, Wang J, Chao J, et al. Characterization of key odorants in Langyatai Baijiu with Jian flavour by sensory-directed analysis. *Food Chem.* (2021) 352:129363. doi: 10.1016/j.foodchem.2021.129363

3. Dong W, Guo R, Liu M, Shen C, Sun X, Zhao M, et al. Characterization of key odorants causing the roasted and mud-like aromas in strong-aroma types of base Baijiu. *Food Res Int.* (2019) 125:108546. doi: 10.1016/j.foodres.2019.108546

4. Xu Y, Zhao J, Liu X, Zhang C, Zhao Z, Li X, et al. Flavor mystery of Chinese traditional fermented baijiu: The great contribution of ester compounds. *Food Chem.* (2022) 369:130920. doi: 10.1016/j.foodchem.2021.130920

5. Fan W, Qian MC. Headspace solid phase microextraction and gas chromatography-olfactometry dilution analysis of young and aged Chinese "Yanghe Daqu" liquors. *J Agric Food Chem.* (2005) 53:7931–8. doi: 10.1021/jf051011k

6. Huang Z, Zeng Y, Sun Q, Zhang W, Wang S, Shen C, et al. Insights into the mechanism of flavor compound changes in strong flavor baijiu during storage by using the density functional theory and molecular dynamics simulation. *Food Chem.* (2022) 373:131522. doi: 10.1016/j.foodchem.2021.131522

7. Jia W, Li Y, Du A, Fan Z, Zhang R, Shi L, et al. Foodomics analysis of natural aging and gamma irradiation maturation in Chinese distilled Baijiu by UPLC-Orbitrap-MS/MS. *Food Chem.* (2020) 315:126308. doi: 10.1016/j.foodchem.2020.126308

8. Ronningen IG, Peterson DA-O. Identification of aging-associated food quality changes in citrus products using untargeted chemical profiling. *J Agric Food Chem.* (2018) 66:682–8. doi: 10.1021/acs.jafc.7b04450

9. Dong W, Shi K, Liu M, Shen C, Li A, Sun X, et al. Characterization of 3-methylindole as a source of a "Mud"-like off-odor in strong-aroma types of base baijiu. *J Agric Food Chem.* (2018) 66:12765–72. doi: 10.1021/acs.jafc.8b04734

10. Zhao T, Chen S, Li H, Xu Y. Identification of 2-Hydroxymethyl-3,6-diethyl-5-methylpyrazine as a key retronasal burnt flavor compound in soy sauce aroma type baijiu using sensory-guided isolation assisted by multivariate data analysis. *J Agric Food Chem.* (2018) 66:10496–505. doi: 10.1021/acs.jafc.8b03980

11. Sun Y, Ma Y, Chen S, Xu Y, Tang K. Exploring the mystery of the sweetness of baijiu by sensory evaluation, compositional analysis and multivariate data analysis. *Foods.* (2021) 10:1–13. doi: 10.3390/foods10112843

12. Sierra-Padilla A, García-Guzmán JJ, López-Iglesias D, Palacios-Santander JM, Cubillana-Aguilera L. E-Tongues/Noses based on conducting polymers and composite materials: Expanding the possibilities in complex analytical sensing. *Sensors.* (2021) 21:4976. doi: 10.3390/s21154976

13. Zhu Y, Zhou X, Chen YP, Liu Z, Jiang S, Chen G, et al. Exploring the relationships between perceived umami intensity, umami components and electronic tongue responses in food matrices. *Food Chem.* (2022) 368:130849. doi: 10.1016/j.foodchem.2021.130849

14. Skládal P. Smart bioelectronic tongues for food and drinks control. *TrAC Trends Anal Chem.* (2020) 127:115887. doi: 10.1016/j.trac.2020.115887

15. Zhang H, Shao W, Qiu S, Wang J, Wei Z. Collaborative analysis on the marked ages of rice wines by electronic tongue and nose based on different feature data sets. *Sensors.* (2020) 20:1065. doi: 10.3390/s20041065

16. Han F, Zhang D, Aheto JH, Feng F, Duan T. Integration of a low-cost electronic nose and a voltammetric electronic tongue for red

wines identification. *Food Sci Nutr.* (2020) 8:4330–9. doi: 10.1002/fsn3.1730

17. Schmidtke LM, Rudnitskaya A, Saliba AJ, Blackman JW, Scollary GR, Clark AC, et al. Sensory, chemical, and electronic tongue assessment of micro-oxygenated wines and oak chip maceration: Assessing the commonality of analytical techniques. *J Agric Food Chem.* (2010) 58:5026–33. doi: 10.1021/jf904104f

18. Legin A, Rudnitskaya A, Lvova L, Vlasov Y, Di Natale C, D'Amico A. Evaluation of Italian wine by the electronic tongue: Recognition, quantitative analysis and correlation with human sensory perception. *Anal Chim Acta.* (2003) 484:33–44. doi: 10.1016/S0003-2670(03)00301-5

19. Cetó X, Llobet M, Marco J, Valle MD. Application of an electronic tongue towards the analysis of brandies. *Anal Methods.* (2013) 5:1120–9. doi: 10.1039/C2AY26066B

20. Geană E-I, Ciucure CT, Apetrei C. Electrochemical sensors coupled with multivariate statistical analysis as screening tools for wine authentication issues: A review. *Chemosensors.* (2020) 8:59. doi: 10.3390/chemosensors8030059

21. Tian S-Y, Deng S-P, Chen Z-X. Multifrequency large amplitude pulse voltammetry: A novel electrochemical method for electronic tongue. *Sensor Actuat B Chem.* (2007) 123:1049–56. doi: 10.1016/j.snb.2006.11.011

22. Zheng Y, Sun B, Zhao M, Zheng F, Huang M, Sun J, et al. Characterization of the key odorants in Chinese zhima aroma-type baijiu by gas chromatography–olfactometry, quantitative measurements, aroma recombination, and omission studies. *J Agric Food Chem.* (2016) 64:5367–74. doi: 10.1021/acs.jafc.6b01390

23. General Administration of Quality Supervision, Inspection and Quarantine [AQSIQ], SAC,. *Method of analysis for Chinese spirits*. Beijing: AQSIQ (2007).

24. Kovats E. Gas-chromatographische charakterisierung organischer verbindungen. Teil 1: Retentions indices aliphatischer halogenide, alkohole, aldehyde und ketone. *Helv Chim Acta.* (1958) 41:1915–32. doi: 10.1002/hlca.19580410703

25. Yang S, Li C, Mei Y, Liu W, Liu R, Chen W, et al. Determination of the geographical origin of coffee beans using terahertz spectroscopy combined with machine learning methods. *Front Nutr.* (2021) 8:680627. doi: 10.3389/fnut.2021.680627

26. Śliwińska M, Wiśniewska P, Dymerski T, Namieśnik J, Wardencki W. Food analysis using artificial senses. *J Agric Food Chem.* (2014) 62:1423–48. doi: 10.1021/jf403215y

27. General Administration of Quality Supervision, Inspection and Quarantine [AQSIQ], SAC. *Strong flavour Chinese spirits*. Beijing: AQSIQ (2021).

28. Zhao D, Shi D, Sun J, Li A, Sun B, Zhao M, et al. Characterization of key aroma compounds in Gujinggong Chinese Baijiu by gas chromatography–olfactometry, quantitative measurements, and sensory evaluation. *Food Res Int.* (2018) 105:616–27. doi: 10.1016/j.foodres.2017.11.074

29. Liu H, Sun B. Effect of fermentation processing on the flavor of baijiu. *J Agric Food Chem.* (2018) 66:5425–32. doi: 10.1021/acs.jafc.8b00692

30. Li H, Qin D, Wu Z, Sun B, Sun X, Huang M, et al. Characterization of key aroma compounds in Chinese Guojing sesame-flavor baijiu by means of molecular sensory science. *Food Chem.* (2019) 284:100–7. doi: 10.1016/j.foodchem.2019.01.102

frontiers | Frontiers in Nutrition

TYPE Review
PUBLISHED 12 September 2022
DOI 10.3389/fnut.2022.973677

OPEN ACCESS

EDITED BY
Yanyan Zhang,
University of Hohenheim, Germany

REVIEWED BY
Majid Nooshkam,
Ferdowsi University of Mashhad, Iran
Chao-Kun Wei,
Ningxia University, China

*CORRESPONDENCE
Hanju Sun
sunhanjv@163.com

SPECIALTY SECTION
This article was submitted to Food Chemistry, a section of the journal Frontiers in Nutrition

RECEIVED 20 June 2022
ACCEPTED 11 August 2022
PUBLISHED 12 September 2022

CITATION
Liu S, Sun H, Ma G, Zhang T, Wang L, Pei H, Li X and Gao L (2022) Insights into flavor and key influencing factors of Maillard reaction products: A recent update. *Front. Nutr.* 9:973677. doi: 10.3389/fnut.2022.973677

Insights into flavor and key influencing factors of Maillard reaction products: A recent update

Shuyun Liu, Hanju Sun*, Gang Ma, Tao Zhang, Lei Wang, Hui Pei, Xiao Li and Lingyan Gao

School of Food and Biological Engineering, Hefei University of Technology, Hefei, China

During food processing, especially heating, the flavor and color of food change to a great extent due to Maillard reaction (MR). MR is a natural process for improving the flavor in various model systems and food products. Maillard reaction Products (MRPs) serve as ideal materials for the production of diverse flavors, which ultimately improve the flavor or reduce the odor of raw materials. Due to the complexity of the reaction, MR is affected by various factors, such as protein source, hydrolysis conditions, polypeptide molecular weight, temperature, and pH. In the recent years, much emphasis is given on conditional MR that could be used in producing of flavor-enhancing peptides and other compounds to increase the consumer preference and acceptability of processed foods. Recent reviews have highlighted the effects of MR on the functional and biological properties, without elaborating the flavor compounds obtained by the MR. In this review, we have mainly introduced the Maillard reaction-derived flavors (MF), the main substances producing MF, and detection methods. Subsequently, the main factors influencing MF, from the selection of materials (sugar sources, protein sources, enzymatic hydrolysis methods, molecular weights of peptides) to the reaction conditions (temperature, pH), are also described. In addition, the existing adverse effects of MR on the biological properties of protein are also pointed out.

KEYWORDS

Maillard reaction, Maillard reaction products, flavor, flavor mechanism, potential application

Highlights

- Implicating the efficiency of MR as natural method for improving flavor in different food model systems and resulting food products.
- Introducing the different Maillard reaction-derived flavors, with an emphasis on the flavor substances.
- A well-controlled MR may be useful in the production of flavor-enhancing peptides and other compounds to increase the consumer preference and acceptability of processed foods.
- The negative effects of Maillard reaction and its solutions are proposed.
- Highlighting the recent application trend of MRPs as flavor agents.

Introduction

The Maillard reaction (MR) is a non-enzymatic reaction that occurs when the carbonyl group of reducing sugars reacts with the amino group of amino acids, polypeptides, or proteins, resulting in the natural production of Maillard reaction products (MRPs), a class of compounds with a wide range of sensory properties (1). Due to the heteroatoms in amino acids, the resultant scents are heterocyclic compounds with ring structures including an atom of N, O, S, or mixtures of these. In food industry, different flavor and color are produced during the MR, especially as food is heated. This is known not only to alter the food properties (flavor, color, and odor), but also to enhance the functional properties (antioxidant and bacteriostasis) of amino acids, peptides, and proteins (2, 3). Chiang et al. (4) explored how heat treatment affected the volatile profiles of beef bone hydrolysates, and found that MR can be used to alter the flavor characteristics of beef bone hydrolysates as a natural meat flavor product. Song et al. (5) detected the flavor substances in pepper powder and revealed that adding exogenous MR substrate can offer a mechanism to improve BPP flavor quality. In another study, sensory evaluation revealed that soybean protein-derived MRPs have higher umami and caramel traits than soybean protein controls (6). The bitter taste and off-flavor of peptides are regarded as serious challenges to their use in the food industry. The most frequent method for removing or reducing beany flavor components is heating (7). Chen et al. (8) modified the *Cucumaria frondosa* hydrolysate with glucose/xylooligosaccharide by MR which largely increased desirable aroma compounds and reduced off-flavor compounds, improving the overall flavor. These studies implicit the efficiency of MR as natural method for improving flavor in different food model systems and resulting food products.

In MR, flavor relates to peptides of various molecular weights present in amine group substrates. After the reaction, the content of flavor precursors in the resulting products increased significantly, and their umami and strong taste were also improved (9). Until now, over 100 umami peptides (with 2–11 amino acids) responsible for umami or kokumi taste from different sources have been distinguished, such as pea protein hydrolysates (10), sweet potato protein hydrolysates (11), edible mushrooms (12), peanut protein (13), and *Takifugu rubripes* (14). It has been evident that different MR conditions result in different flavor products. Since the open-chain concentrations of sugars and active forms of amino reactants depend on pH (15). Lotfy et al. (16) heated the Quinoa protein hydrolysates at varying initial pH values and increased the pH from 5 to 9 to change the sensory attributes from caramel to burnt-coffee. Furthermore, MR is made up of a chain of complex reactions, in which the sensitivity of each reaction and reactant to temperature are different. At higher temperatures, bitter and umami FAAs were present in higher concentrations (17). Thus, a well-controlled MR may be useful in the production of flavor-enhancing peptides and other compounds to increase the consumer preference and acceptability of processed foods.

Recent reviews on this research area have mainly focused on the MR during processing (18, 19), or their effects on functional and biological properties (2, 20), without elaborating the flavor compounds obtained by the MR. To bridge the knowledge gap, we aim to introduce the MR and different MF, with an emphasis on the flavor substances. The influencing factors, flavor formation mechanism of MRPs, and widely used flavor detection methods are also analyzed. Besides, we highlight the recent application trend of MRPs as flavor agents. The development direction and trend are comprehensively discussed, to provide theoretical support for expanding the existing application standing of MRPs.

Maillard reaction-derived flavors

As the foods containing proteins/peptides and carbohydrates are heated, MR (formation of covalent bonds between carbonyl groups and free amino groups) is a common reaction (17). It started in 1912 with French chemist Louis Camille Maillard, who studied the interaction between glucose and glycine and labeled the resultant dark pigment melanin. Generally, in MR there are three steps, namely primary stage, medium stage, and final stage, as shown in Figure 1.

Amadori products of the primary stage are often used as an indicator of food processing degree (21). In a simple model of cysteine and xylose, relatively stable cyclic 2-3-thiazolidine-4-carboxylic acid (TTCA) and the Amadori rearrangement product of cysteine are formed at the early stage. Gly-Amadori reacts fastest, followed by Cys-Amadori and TTCA. Free glycine accelerates the reaction of TTCA, whereas cysteine inhibits that of Gly-Amadori due to forming relatively stable thiazolidines. Cys-Amadori/Gly has the highest efficiency in developing both meaty flavors and brown products. TTCA/Gly is conducive to yield meaty flavors, whereas Gly-Amadori/Cys is conducive to generate brown products (22). Conclusively, initial formation of initial intermediates/pathways could be regulated for the maximal formation of related flavors.

In the medium stage, the ketone aldehydes and other compounds produced in this process are the flavor precursors and flavor substances of foods. For example, amino ketones could be converted to enol-amines through isomerization. Strecker aldehydes and acids, which have strong aromatic potential, produce different aroma characteristics according to the types of amino acids and act as precursors. Various special aldehydes could be generated by the MR of different α-amino acids and reducing sugars as Strecker degradation

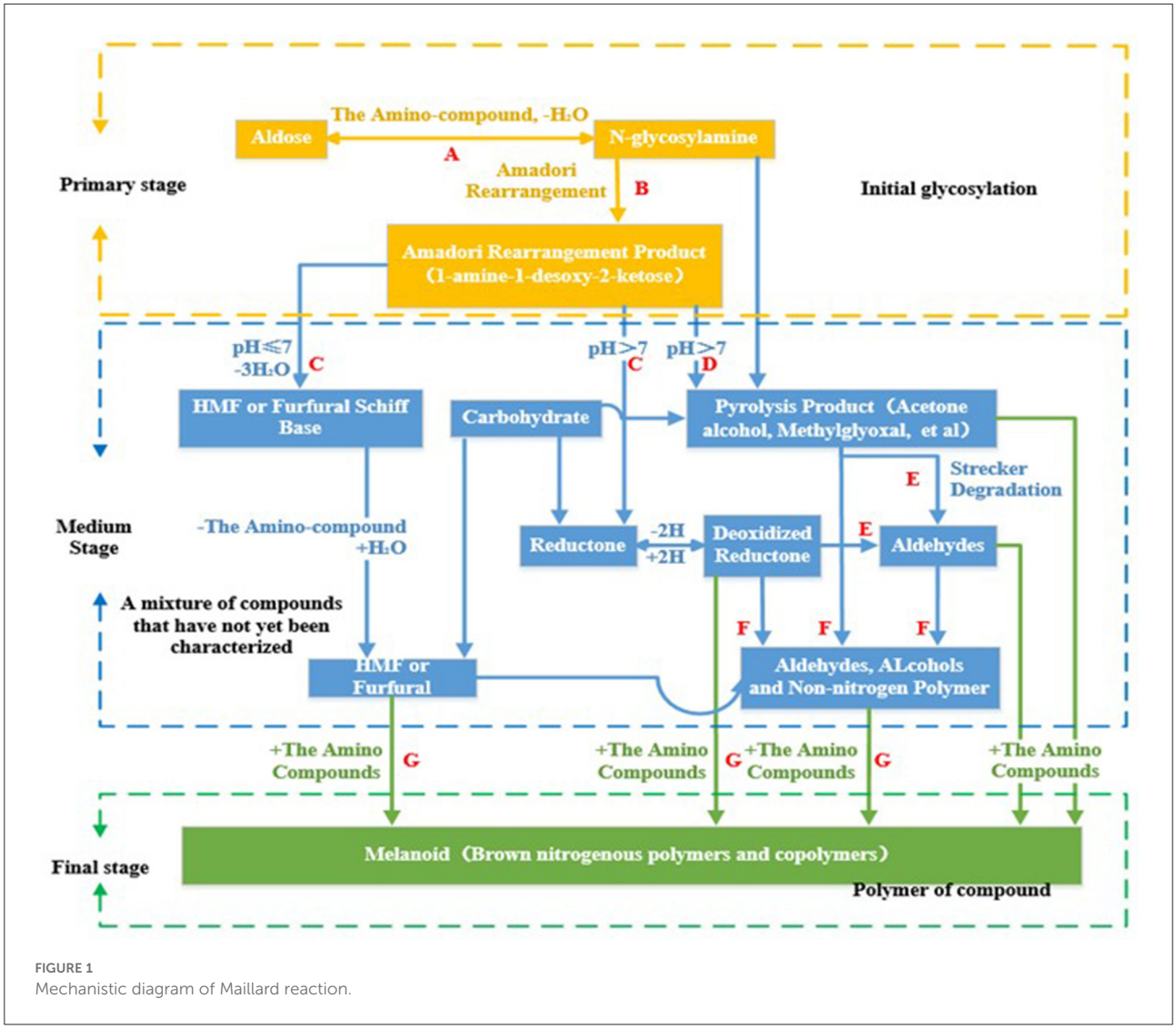

FIGURE 1
Mechanistic diagram of Maillard reaction.

(23). Therefore, Strecker degradation is related to browning and aroma production. For example, Val reacts with glucose, chocolate aroma is produced (24). The reaction of Lys and Pro with glucose produces the aroma of toasted bread (25).

The final stage mainly includes dehydrogenation, cyclization, retro-Aldol reaction, isomerization, rearrangement and condensation. Nitrogen-containing dark compounds, namely melanoidins, are formed eventually. In addition, the carbohydrate in MR also is cracked after heating. Ketones, keto alcohols, ketoaldehydes and other crackates react with amino compounds, before the final MRPs are further formed (26).

MF refers to characteristic flavor formed by MR during food processing and storage. The flavor characteristics could be pleasant floral, nutty, caramel, attractive meat, or even spicy (5, 27, 28), depending on the types, composition or reaction pathways of aminos and carbonyls. In 1960, Morton prepared meat flavor by using reducing sugar and cysteine, and applied for the first patent on MF in the UK. Since then, the research on MFs have been continuously progressing. MF is caused by MR that produces compounds, such as aldehydes, ketones, furans, thiophenes, pyrazines, pyrrols, etc. These compounds (MRPs) contribute to the overall flavor perception in foods during the processing. Due to the edible safety of MRPs and the high efficiency of flavor enhancement, the preparation of MFs through thermal reaction has gained an immense focus from researchers engaged in flavor industry and food processing ingredients (8, 16). At present, the key technologies for thermal reaction flavors have been developed, which are composed of adipo-regulated oxidation (28), targeted biocatalysis (28), and temperature-controlled (17).

Flavor ingredients of MRPs and detection methods

Flavor ingredients of MRPs

Flavor components in MR

Flavor is an important characteristic of MRPs and flavor substances are initially formed in the middle stage of MR. The structure, formation process, and flavor characteristics of some representative flavor substances are summarized in Table 1. Most of MRPs are furans and their derivatives, and the precursors of other condiments (such as thiazole and furan mercaptan). Linoleic acid and other n-6 including 2-pentylfuran, which is a non-carboxylated molecule (28). 1-Octen-3-ol was degraded from lipids and had a mushroom and baking aroma (36), as well as antibacterial efficacy against spoilage and opportunistic microorganisms (37). The MR generated furan compounds, which are a key odor group for hibiscus flowers (38); 3-methylbutanal provides a malty scent, while pyrazines (typical MRPs) contribute a barbeque taste to food, with higher pyrazine levels owing to the possibility of lipid-derived active carbonyl and ammonia reactions (39). MR is known to significantly contribute to baked red pepper powder flavor due to these compounds (5). Meat flavor is characterized by sulfur-containing volatile compounds with sulfury and meaty aromas. Meaty tastes described with high odor in model MR containing cysteine including 2-methyl-3-furanthiol, 2-furfurylthiol, 3-thiophenethiol, 3-mercapto-2-pentanone, bis(2-methyl-3-furyl)disulfide, and 2-methylthiophene (40).

Furfural, 5-methyl furfural, 2-acetyl furan, maltol, isomaltol, and other substances have strong caramel and fruit aroma. 2, 5-Dimethyl-4-hydroxy-3-furanone and its 5-methyl homolog have a pleasant caramel taste and roasted pineapple smell. Dicarbonyl compounds (such as butanedione) with buttery aroma are obtained by deoxyglucone rearrangement and dehydration. Aldehydes, such as 3-methyl-butyraldehyde, are formed through Strecker degradation by dicarbonyl compounds, and present a refreshing malt aroma. Pyrazines, which are a kind of flavor compound with pleasant mood and nutty aroma, have attracted much attention from flavor chemistry researchers since the 1960s. They're generally produced by condensation of -aminoketone, which is formed through Strecker degradation. Similarly, pyrrole and its derivatives formed by dehydration and cyclization of 3-deoxyketone with amino compounds are also important flavor substances. When proteins react with methylglyoxal or dihydroxyacetone, 2-acetyl-1-pyrroline with bread aroma is produced. The sulfur-containing flavor substances formed directly relate to sulfur-containing amino acids in the reaction system. Hydrogen sulfide and ammonia are easily produced by cysteine hydrolyzation or Strecker degradation. Similarly, thiophenes are formed by hydrogen sulfide\deoxyglucose after dehydration and oxidation. Recently, MRPs derived from protein hydrolysates/peptides and carbs have been shown in numerous researches to impact the flavor properties of food (8, 28, 41). Table 2 summarizes the flavor attributes of MRPs generated from different protein hydrolysates/peptides and carbs.

In the heated cysteine-xylic-glycine system, the possible processes of different compounds are summarized in Figure 2. 2-Methyltetrahydrothiophene-3-ketone could be formed from 1-deoxypentanone through reduction. Furfural may be generated from 3-deoxypentosone *via* cyclization and dehydration, while 2-furfurylthiol could be formed from the reaction of ffurfural and H_2S. Besides, 2-methylfuran could be formed after the reduction of furfural. After 2,3-pentadione reacting with H_2S, 3-mercapto-2-pentanone may be generated. Analogously, after cyclization and dehydration with hydrogen sulfide, 3-thiophene mercaptan is formed. Subsequently, 2-ethylthiophene is formed through dehydration and reduction. As aromatization occurs, 2,5-dimethylthiophene is formed (40).

Flavor components in foods associated with MR

In heat processed foods, such as coffee, cocoa, bread, peanuts, pork, beef, chicken, fish and potatoes, most aromatic substances are produced by MR. Over 400 volatile compounds including pyrazines, thiazoles, oxazoles, pyrrole derivatives, furans, and pyridine derivatives have been identified in roasted cocoa. Furthermore, the pattern of alkyl pyrazines generation depends on oligopeptides and free amino acids presented in the particular foods before roasting (46). Kocadagli et al. (32) selected precursors to add to potato dough before baking for improving the baked flavor of low-acrylamide potato products. Due to the reactive complexities of tea, noticeable changes such as pigment destruction, oxidative polymerization of catechin, and oxidative degradation of amino acids have been recorded following high-temperature esterification and long-term storage. Compared with the roasted spring and autumn tea leaves, the color, stewing aroma, taste and chemical composition of pan-fired spring tea leaves changed to least, indicating that baking enhanced the flavor stability of tea drinks (47).

In addition to improving the food taste, MR is also used to improve the food smell. For example, shellfish hydrolysates usually produce strong unpleasant odors (such as fishy odors), which is the key reason for their limited application (47). After MR, the number of volatile components detected in the enzymatic hydrolysate of clams was changed insignificantly. Nevertheless, there were differences in the types, and the contents of aldehydes, ketones and esters were also increased. After enzymatic hydrolysis, MR eliminated the unpleasant smell of oyster, and a pleasant smell of milk, nut and meat was generated at the same time (48).

TABLE 1 Flavor characteristics and forming pathway of flavor products.

Substance	System	Forming pathway	Flavor	References
Sulfur-containing compounds				
Thiophene				
3-methyl-2-thiophenecarboxaldehyde	a) Peony seed-derived, chicken fat, and L-cysteine b) Camellia seed meal hydrolysates, ribose or xylose or glucose or fructose, and L-cysteine	Derived from thermal degradation of cysteine and carbonyl compounds from lipid oxidation	Cooked meat-like odor	(28, 29)
3-methyl-2-thiophene carboxaldehyde	Bacon and woodchips		Similar flavor of cooked meat and sulfur	(30)
2-methyltetrahydrothiophen-3-one	Tilapia fish head hydrolysate, xylose, and cysteine		Sulfurous, fruity and berry odor notes	(31)
Thiols				
2-furfurylthiol	Peony seed-derived, chicken fat, and L-cysteine	\	Strong aroma of baked products, coffee, and fleshy odors	(28)
Thiazoles				
2-acetylthiazole	Peony seed-derived, chicken fat, and L-cysteine	Oxidized lipids react with the MRPs	The aroma of nuts, cereals, and popcorn, with a low odor threshold	(28)
Benzothiazole	Potato and glycine		Caramel characteristic, and its threshold is low	(32)
2-Acetylthiazole	Tilapia fish head hydrolysate, xylose, and cysteine	The reciprocity of sulfur-containing amino acids with carbohydrates or carbonyls	Nutty, popcorn, peanut, roasted and hazelnut odor notes	(31)
Other sulfur-containing compounds				
Dimethyl trisulfide	Bacon and woodchips	\	An ideal onion-like odor at low concentration and an undesirable sulfur odor at high concentration	(30)
Nitrogen containing compounds				
Pyridine	a) Peony seed-derived, chicken fat, and L-cysteine b) Sesame seed hydrolysate, d-xylose, and L-cysteine or L-methionine or thiamine	Trigonelline degradation and MR	Unique roasted, nutty, meaty, earthy, and popcorn-like aroma	(27, 28)
Pyrazine	Potato and glycine	Oxidized lipids react with the MRPs	Sweet	(32)
Pyrrole	Coffee	The carbonyl compounds could either react with amino acids or the sugar degradation products	Nutty, hay-like, and herb aroma	(33)
Oxygen containing compounds				
Ketones				
3-methyl-1,2-cyclopentanedione	Bacon and woodchips	The degradation of amino acid, oxidation or degradation of unsaturated fatty acids, carbohydrate metabolism, and β-keto acid oxidation	Unique fragrance, fruity, woody aroma, and mushroom-like flavor	(30)
Furanones	Quinoa protein and xylose	Sugar degradation products and can undergo condensation reaction via Maillard reaction	Mainly described to have caramel-like, sweety, nutty and burnt notes	(16)

(Continued)

10.3389/fnut.2022.973677

TABLE 1 (Continued)

Substance	System	Forming pathway	Flavor	References
Cyclopentenones			Caramel and burnt odors	
Furan				
2-Methylfuran	Quinoa protein and xylose	Obtain by xylose cyclization	Contributes to the fresh taste of roasted coffee	(16)
2-Pentylfuran	Pork hydrolysate and xylose	Form from the oxidation of linoleic acid	Fruity, floral, buttery, green and beany notes	(34)
Alcohols				
Furfuryl alcohol	Bacon and woodchips	\	The warm "burnt" odor and cooked sugar taste	(30)
1-octen-3-ol	Clam hydrolysate	Enzymatic peroxidation of polyunsaturated fatty acids	Strong grassy and fatty odors	(35)
Methanethiol	Tilapia fish head hydrolysate, xylose, and cysteine	The oxidation products of methanethiol derived from the degradation of methionine via the Strecker degradation	Sulfurous, alliaceous and eggy odor notes	(31)
2-furanmethanethiol	Pork hydrolysate and xylose	Furfural reacts with the hydrogen sulfide, which is formed from the cysteine breakdown	A strong and distant "roasted meat" aroma	(34)
Esters				
Methyl ester	Bacon and woodchips	The hydroxy acids' intramolecular esterification	Contribute a fruity odor to meat products	(30)
Butanoic acid ethyl ester	Clam hydrolysate	Esterification of an alcohol with a carboxylic acid	Sweet and fruity aroma	(35)
Aldehydes				
2-methylbutanal	a) Peony seed-derived, chicken fat, and L-cysteine	Strecker degradation of isoleucine	Malty and chocolate	(28)
Furfural		\	Sweet	
Benzaldehyde		Originates from the oxidation of benzyl alcohol catalyzed by dehydrogenases	Almond-like	
Benzeneacetaldehyde		\	Honey, sweet, and floral	
Hexanal	Bacon and woodchips	Linoleic acid and other unsaturated fatty acid oxidation	A rancid odor in high concentration, a fruity and broth-like odor at low concentration	(30)
Nonanal		Lipid oxidation	A greasy and sweet orange flavor	
Octanal	Potato and glycine	\	Beef aroma	(32)
2-Furfural		Xylose cyclization in the second later stage of the MR	Almond-like aroma	
Phenols				
Guaiacol	Bacon and woodchips	Pyrolysis of lignin	A smoky flavor	(30)
Hydroxybenzol		Mainly derived from the thermal pyrolysis of lignin or hemicellulose of woodchips	A pungent, smoky aroma	
Hydrocarbons				
α-Pinene and β-pinene	Peony seed-derived, chicken fat, and L-cysteine	\	Unique turpentine aroma	(28)

TABLE 2 Summary of the recent studies on flavor properties of Maillard reaction products generated from various protein/ protein hydrolysates/peptides and carbohydrate sources.

Protein/protein hydrolysates/peptides	Carbohydrate	Maillard reaction conditions	Flavor properties	References
Camellia seed meal	Ribose	110°C, 90 min	Meaty and umami taste	(29)
Sesame seed meal	d-xylose	120°C, 2 h	Strong meat flavor	(27)
Takifugu obscurus by-products hydrolysates	Xylose	pH 7.4, 120°C, 2 h	Umami taste, volatile aroma, and overall acceptance ascension, bitterness and fishy smell reduce	(42)
C. frondosa hydrolysate	Xylooligosaccharide	115°C, 20 min	Stronger sweety, baked, and caramel notes, weaker seafood and fishy odors	(8)
Pork hydrolysate	Xylose	pH 4.5, 100°C, 1 h	Roasted and sweety taste	(34)
Large-leaf yellow tea	\	145–155°C, 3.5 h	Strong roasted, nutty, woody odors and weak fatty, fruity odors	(43)
Grass carp hydrolysate	Glucose	120 °C, 1 h	Caramel and bitterness reduce, and overall acceptance ascension	(44)
Clam (Aloididae aloidi) hydrolysate	\	70°C, 10 min	Stronger pleasant flavors, less green, grassy and fishy odors	(35)
Agaricus bisporus mushrooms	\	176.7°C, 4–6 min	Dark meat, roasted, and fried notes, and portobello increased. Woody, and earthy notes decreased.	(30)
Oyster meat hydrolysate	Glucose	pH 7.0, 115°C, 35 min	Overall acceptance ascension	(45)

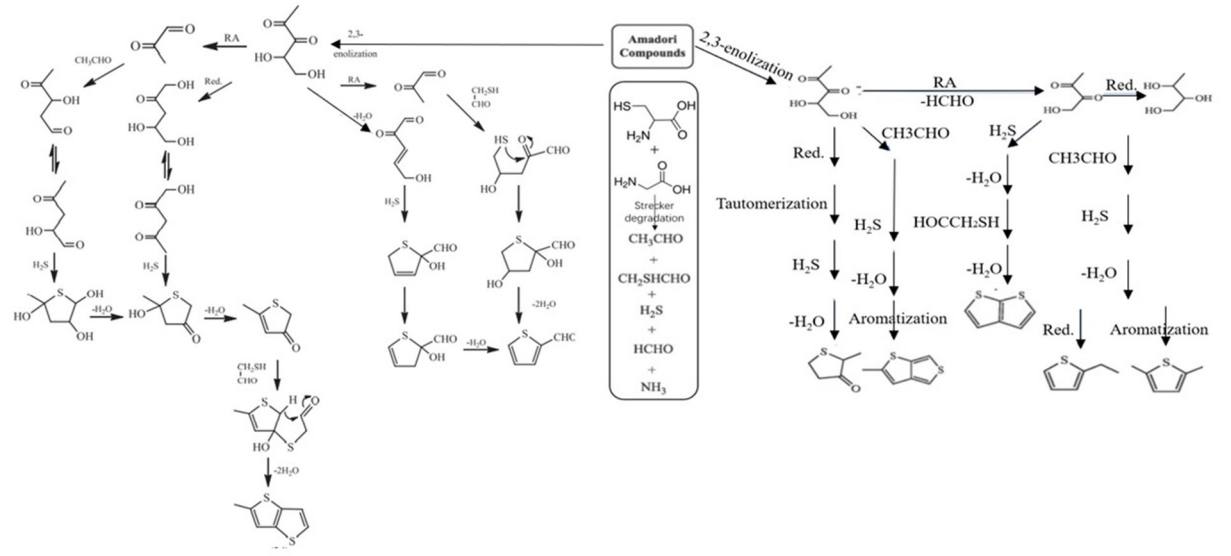

FIGURE 2
Possible formation pathways for compounds in the Gly-Cys reaction systems (Red., reduction reaction; RA, retro-aldol reaction) (40).

Extraction and detection methods of MRPs

Extraction and analysis are important technical strategies to study the food flavor components. Flavor components are mainly composed of many volatile substances with complex structures and different chemical properties. They act on olfactory organs to transmit information, and their contents are usually below the nanogram level. Therefore, it is relatively difficult to analyze their chemical composition by conventional chemical methods. Analysis of the chemical composition usually includes separation, enrichment, desorption, and identification of volatile components. All the processes should avoid oxidation, thermal degradation and other biochemical reactions, which

are the prerequisites for pretreatment of volatile compounds. Common methods for samples pretreatments include solvent extraction (SE), simultaneous distillation extraction (SDE), headspace extraction (HS), solvent assisted flavor evaporation (SAFE), super-critical fluid extraction (SFE), purge and trap method (PT), solid phase microextraction (SPME), etc. The commonly used analytical instruments for the identification of volatile aroma compounds in food systems include electronic nose (E-nose), gas chromatography (GC), and high-performance liquid chromatography (HPLC).

E-nose is a rapid detection system suitable for detecting large number of samples, without the need to separate the volatiles. Using E-nose as a human sensory simulator, sensory evaluation could be conducted conveniently and sensitively. Currently, E-nose is used to analyze the overall level of aroma components for MR conditions optimization (49). However, the electronic nose cannot detect the quantity and content of each substance in MRPs. An useful analytical technique for identifying MRPs is HPLC or anion-exchange chromatography in combination with a diode array detector (DAD) and an evaporative light scattering detector (ELSD) (50). The majority of these approaches, nonetheless, did not succeed in clearly identifying each MRP with good peak shape and resolution. The high polarity of MRPs, which results in early elution with many compounds in the reversed phase (RP) column and substantial retention in the normal phase (NP) column, is attributed as one major cause. Satisfactory separation of polar substances is now possible thanks to the recent invention of the hydrophilic interaction liquid chromatography (HILIC) column, which strikes a fair compromise between RP and NP columns. Its use concurrently separates the amino acids glycine, diglycine, and triglycine as well as the associated MR intermediate (51).

These analytical techniques have limitations, such as low selectivity, especially when compared to cutting-edge analytical techniques utilizing mass spectrometry (MS) and nuclear magnetic resonance (NMR) spectroscopy (52). For the analysis of both tiny and large organic compounds, MS is regarded as one of the fundamental methods (53). Sensory assessment, GC-MS and E-nose were used to investigate the flavor differences of five sections of the Chinese blanched chicken (CBC): skin, breast, thigh, head, and butt. This examination of several aspects of CBC might give guidance on how to cater consumers' preferences and forecast the quality changes that may occur. Additionally, using a combination of GC-MS and E-nose, the volatile and taste components of foods (such as golden pompano filets, roasted coffee beans, apple fruits, and so on) were evaluated to gain complete information on flavor profiles. Nowadays, GC-MS is a popular approach for analyzing aroma that has been widely applied in meat science. For example, the investigation of volatile profiles of fermented sausages, dry-cured hams, and bacons (54, 55). It provides an accurate approach to qualitatively and quantitatively analyze the volatile and semi-volatile compounds (56). GC-MS, on the other hand, requires extra derivatization and is not appropriate for large-scale detection (57).

MS is a standard mass detector that detects ionized chemicals and delivers mass spectra and compound structures at each location. MS/MS or even MS^3 approaches improved selectivity and structure identification by analyzing each ion fragment of a molecular ion (58). In a recent investigation, the standards of glycine-glucose and proline-glucose-Schiff bases, Amadori, and Heyns compounds were well separated by ESI-MS/MS (59). Additionally, techniques utilizing LC-MS/MS and stable isotope dilution assay were proposed (60). The identification of tiny molecules like ARPs in a complex matrix becomes feasible and reliable, which is favorable and has a wide range of applications, despite certain hurdles brought by the high cost of MS detection and onerous technique.

A key component of MS approach is the MS Library; flavor analysis, for instance, benefits from the NIST library (61). A dedicated library for Maillard reaction chemicals does not exist, though. On the basis of ion fragments, researchers must infer the molecule and/or further confirmed by NMR. Only a few attempts have been made to create tiny libraries of sulfur-methyl thioesters so far, and they haven't been put into too much use. Therefore, the creation of a thorough library of MRPs would be a significant addition.

Influencing factors of MF

Influencing factors of MF

The sort of amino acids and reducing sugars, as well as the reaction circumstances (such as temperature, time and pH), play a big role in flavor development *via* MR. The sugar has only a limited influence on flavor character, while the amino acid has a major impact. Rather than altering the flavor character, sugars have a significant impact on the reaction rate. The influence of different influencing factors of MRPs is showed in Table 3.

Reducing sugar

The MR refers to the reaction between an amino group (e.g., amino acids) and a carbonyl group (e.g., reducing sugars), a non-enzymatic modification of proteins with reducing sugars. Therefore, sugars were a key participant of MR, and the content and structure of reducing sugars have an important effect on the MR and the structure and flavor of MRPs. The level of the reducing sugars inside the beans has a potential impact on coffee aroma, flavor and color during roasting process (64). In the searing-cooked steak, the reducing sugar was lower and MRPs were higher than oven-cooked steak, which had higher scores for overall flavor and roasted meat flavor (65).

TABLE 3 The influence of different influencing factors of Maillard reaction products (MRPs).

System	Maillard reaction conditions					Influencing factor	Observations	References
	pH	Time (min)	Temperature (°C)	Protein: sugar ratio	Heating method			
Camellia seed meal hydrolysates and ribose/xylose/glucose/fructose and L-cysteine	\	90	110	2:1	Wet	Sugar species	Ribose-MRPs and Xylose-MRPs were more common in meat and umami flavors than other MRPs. There was no greater diversity between MRPs in taste, saltiness and continuity strength.	(29)
Sesame seed meal hydrolysates and d-xylose and l-cysteine/l-methionine/thiamine	7.5	120	120	10:3	Wet	Amino acid species	The MRPs with cysteine showed the strongest flavor. The MRPs with thiamine showed the highest meat flavor, followed by Cys-MRPs. All of the MRPs have lower bitterness and stronger caramel flavor.	(27)
Beef bone hydrolysates and d-ribose	6.5	10	113	1:0.068	Wet	Protease species	When comparing Flavourzyme -MRP in single hydrolysis treatment with both Protamex + Flavourzyme -MRP and Bromelain + Flavourzyme -MRP in simultaneous hydrolysis treatment, there were no significant differences on those major volatile compounds for the three MRPs. This showed that Flavourzyme® is effective in generating major volatile compounds during MR, without the need for addition of other enzymes.	(4)
Rapeseed peptide, d-xylose, and L-cysteine	7.4	120	80/100/120/140	5:1.4	Wet	Reaction temperature	The sample reacted at 80°C had a significant effect on mercaptan content, the 100°C sample showed a significant effect on aliphatic sulfur compounds, indole, indazole, esters and Tyr, showing more umamy and saltier taste. While the 140°C sample was rich in nitrogen oxides. They are closely related to thiophene, furan, pyrrole, pyrimidine, pyrazole, pyran, aldehydes, Thr, Met and Leu.	(17)
Duck legs	\	45	85/95/121	\	Wet	Reaction temperature	Thermal treatment caused further Maillard reaction in the water-boiled salted duck, although the degree of this change was small	(62)
Pork, d-xylose, and L-cysteine	\	5 min at 120 and 90°C for 25 min		200:1	Dry	Thermal way	High-temperature stewed pork had the significant effect on the formation of furans, N- and S-containing compounds, the processing technology of traditional stewed pork was more sensitive to aromatic compounds.	(63)

10.3389/fnut.2022.973677

TABLE 4 The latest studies on the role of the Maillard reaction in the production of flavor.

System	Application	Effect	References
Sesame seed meal protein hydrolysate (SSH)-Cys/Thi	Low sodium seasoning salts	The Cys-MRPs salt had the smallest angle of repose, the highest bulk density, and the highest sensory score. The seasoning salt with SSH-MRPs had appreciable hygroscopicity and thermal stability. The seasoning salt with Thi-MRPs had the highest solubility.	(105)
Glutathione-xylose	Meaty food	Significantly improve and stabilize the flavor quality of the meaty food	(106)
Pea protein hydrolysates- Arabinose	Seasoning salt	Greater umami-enhancing and saltiness enhancement abilities	(10)
Beer yeast, chicken meal, chicken liver, and soybean meal- xylose	Dog foods	Improve palatability of dog food	(107)
Oyster meat hydrolysate- glucose	Oyster meat	The flavor and antioxidative activity of oyster meat hydrolysate MRPs was significantly improved	(45)
Characterized flavor peptides from beef enzymatic hydrolysates- xylose	Beef broth	Stronger meaty delicious flavor and flavor enhancement ability	(108)
Wheat bran	Wheat flavor additive	Added to flour products to enhance flavor and acceptability	(109)
Bovine meat/heart hydrolysates -Glucosamine	Savory applications	Higher in umami, and thereby good candidates for savory applications	(110)
Porcine plasma hydrolysate-Glucosamine	Meat products where liver flavor is desirable	Higher in umami and liver flavor	
Peony seed meal protein hydrolysates-xylose-cysteine-chicken fat	Thermal processing meat flavor	Improve meat flavor and bioactivity	(28)

Nevertheless, one of the limitations of these studies is that they only studied the effect of the total reducing sugar content in the system on the flavor produced by the Maillard reaction. It is not explained which reducing sugar plays the key role. Deng et al. (66) found reducing sugars such as glucose and ribose could react with α-amino acids *via* the Maillard reaction and promote the formation of the cooked meat aroma compound. Furan is a necessary intermediate in some chemical systems and composed of pentose and generated by Amadori intermediate 1, 2-enolization. In the Maillard reaction with xylose, the content of furfural and meat related volatile flavor substances was higher than that with ribose and glucose (29). Furthermore, the addition of reducing sugars could induce protein glycation and facilitate the solubilization of myosin, which in turn might increase the water holding capacity of meat (66). However, only the sensory evaluation of the products after adding different sugars is not enough. According to the current research, it can only be confirmed that the addition of reducing sugar is beneficial to the formation of flavor, and xylose is relatively widely used. These studies would be more relevant if the effects of sugars on the flavor orientation produced by the MR were explored more broadly.

Source of proteins

Proteins of different sources react with sugars and further produce different flavor of MRPs. In recent years, more and more vegetable proteins or peptides have been used in the production of flavor enhancers by MR. Soybean peptides have been used to generate a range of flavors, including umami, sweet, salty, and meaty, as a potential flavor precursor (67). MRPs were made utilizing a xylose and soybean peptide method after heating at 100–140°C and pH 7.6 for 2 h. MRPs with cysteine addition presented the minimal bitterness, after heating at 140°C, and the highest umami and saltiness at 100°C (68). Not only soybeans, but other plant-derived proteins are also reported to change the flavor through MR. In umami soup, MRPs of flaxseed protein hydrolysates could enhance the mouthfulness and continuity (68). And hydrolysates or extracts from meat have also been employed to improve the meat-like flavors of food products. However, the main drawback of these studies is that the resulting Maillard reaction products have no clear directivity (chicken, beef, or fish flavor).

To further enhance the flavor, Kang et al. (69) reported that after addition of xylose and L-cysteine to beef hydrolysate, kokumi, meaty, umami, umami-enhancing

and kokumi-enhancing capacity were improved. However, In comparison to meat hydrolysates, meat extracts have poor flavor and aromatic qualities. Enzymatic hydrolysis and MR could turn animal bone extracts into taste components. To solve this problem, ribose was utilized to investigate MRPs generated from beef bone hydrolysates. Enzymatic hydrolysis and heat treatment are reported to promote the production of meat characteristic flavor substance (2-methylpyrazine, dimethyl disulphide, and dimethyl trisulphide) and inhibit the burning taste and formation of bitter substance (2-furanmethanol) (4). Similar results were also observed in swine lard and goat by-product protein hydrolysates, in which aroma compounds were conducive to an increase in the hydrolysis process (70). By markedly increasing the contents of pyrazine and sulfur compounds in the hydrolysate, Flavourzyme could improve the flavor of chicken bone extracts. MR significantly decreased the bitter taste and increased the flavor acceptability of hydrolyzed chicken bone extracts by using Protamex® and Flavourzyme® in a sequential hydrolysis procedure (71). Using chicken as a source of proteins, after thermal treatment with xylose, meat flavor was generated, and the thick, kokumi and freshness of the freshness solution were significantly enhanced (72). Moreover, in the recent study, strong barbecue beef flavor was generated with bone protein hydrolysate (73, 74). To improve the surplus value of fish, heating the low-valued fish hydrolysates with meat hydrolysates, xylose and other additives were optimal for sauce flavor synthesis, in which meaty smell was strengthened and fishy odor was reduced. For example, after xylose reacted with the hydrolysate of shrimp, a product with rich seafood taste and freshness was obtained. After xylose was heated with the polypeptide hydrolysis of shrimp, the resulting MRPs had a rich seafood taste and freshness (75). The hydrolysate of fermented Tilapia fish head could develop a flavor concentrate (31). Overall, a convergence between meat proteins and the flavors of their MRPs was showed, which indicated that we could target the raw materials for MR. However, these studies mainly focused on meat flavor and lacked systematic research on other flavors.

Hydrolysis conditions of raw material

The specific substances with flavor characteristics in MR are affected by specific amino acids, peptides, and proteins. The hydrolyzed products obtained by different peptidases contain different peptide spectral and free amino acids, its MRPs also have different sensory properties. *A. Melleus* contains a large number of peptides below 1,355 Da (probably corresponding to dipeptides or aromatic amino acids). In the meantime, under the hydrolysis of some proteases such as chymotrypsin or pepsin, the proteins were cleaved specifically to produce peptides that had a c-terminal amino acid (76). Grossmann et al. (77) found that the bitter and umami taste of the cricket and mealworm protein samples had an increasing tendency after enzymatic hydrolyses, which coule be clarified by the liberation of amino acids. However, not all proteases play decisive roles in flavor. Five kinds of bovine bone hydrolysates were genarated by single (P-Protamex®, B-bromelain, F-Flavourzyme®) and simultaneous (P+F and B+F) enzymatic hydrolysis, then were heated at 113°C to form MRPs. The proportion of most volatile compounds in P+F-MRPs and B+F-MRPs differed insignificantly as Flavourzyme® reacted with Protamex® or bromelain simultaneously. Volatile components (such as 2-methylpyrazine, dimethyl disulfide and dimethyl trisulfide) were detected in B-MRPs after heating, and did not appear in P/F-MRPs. They contributed to baking, sulfur, and meat flavor, but the difference was not significant. Based on it, comparing the single hydrolysis of F-MRPs with the simultaneous hydrolysis of P+F-MRPs and B+F-MRPs, there was no remarkable difference in the main volatile compounds of the three MRPs. This suggested that only addition of Flavournzyme® was effective in producing major aroma compounds during MR (4). Various studies have fully demonstrated that protease specific cleavage is one of the means to improve the sensory quality of MRPs. However, the mechanism of flavor enhancement by enzymatic hydrolysis was not considered. It would be more meaningful to further study the characteristic precursor peptides that generate flavor substances in MR. Other enzymes besides proteases also contribute to the formation of flavor in MR. For example, meat-like flavors can be created by myrosinase and lipoxygenase in the two-step brom of Brassica proteins (78). Reducing sugars produced by enzymatic hydrolysis of starch play a role in MR, which can alter the production of taste components directly or indirectly (79). The content and reactivity of MR substrate were increased by enzymatic hydrolysis, which provided the prerequisite for the production of flavor. After the selection of raw materials, the type of enzyme can be selected according to the requirements of the reaction and material characteristics. When dealing with substances with high protein content, proteases can be selected for enzymatic digestion to obtain more highly active peptides. As raw materials with high carbohydrate content were utilized, amylase and glycosidase could be used to increase the content of reducing sugar that can participate in MR.

Molecular weight of peptides

Peptides have been considered to be very critical taste active ingredients in foods. Peptides of molecular weight ranging from 1 to 5 kDa have been found to strongly influence the flavor enhancing attributes (umami, continuity, and mouthfulness), and they are called Maillard peptides; which mainly contribute to the kokumi taste (41, 80). The scent of chicken was provided by a peptide fraction of 2–5 kDa in chicken enzymatic hydrolysate. Meanwhile, in MRPs of chicken enzymatic hydrolysate, a peptide fraction < 500 Da contributed to the roasted scent of chicken, a peptide fraction > 1 kDa

formed by cross-linking the peptide fraction 500 Da contributed a kokumi flavor, and a peptide fraction > 3 kDa imparted a bitter taste (81). Low molecular weight (LMW) peptides (<1 kDa) generated in meat during chilled conditioning can act as flavor precursors in the MR with a potential contribution to key volatile organic compound (VOC). The majority of nitrogen-containing volatiles, pyrazines and pyridines, dominated the carnosine mixture, while sulfur-containing VOCs dominated the GSH and Cys Gly peptide mixtures. The peptides with LMW (<1 kDa) are mainly the products of degradation of High molecular weight (HMW) peptides, which are considered as the main contributor of the formation of pyrazines and 2-furfurylpyrrole due to the higher reactivity of the amidogen in these compounds. HMW peptides are the products of cross-linking and polymerization of LMW peptides, which may be formed during the MR. However, peptides with a molecular weight of 128–1,000 Da were found to be primarily responsible for the meat-like flavor, as well as influencing other sensory characteristics (68). Various studies have well demonstrated that peptides with molecular weights < 5 kDa are more suitable, and HMW peptides tend to bring bitter and other odors. Thus, specific enzymatic hydrolysis or ultrafiltration can be used to increase the content of LMW in the reaction system, to increase the consumer preference and acceptability of processed foods.

Reaction conditions of MR

Since the open-chain concentrations of sugars and active forms of amino reactants depend on pH, the parameters significantly influenced the reaction rate and formation of MRPs (15). Firstly, high pH provided favorable conditions for the molecular rearrangement of sugars, and could promote the occurrence of nucleophilic addition reaction (82). Secondly, Amadori compounds are prone to form 1, 2-enolization at pH 8, and tend to react with 2, 3-enolization at pH 9.7. Thirdly, increasing initial reaction pH was beneficial to caramelization, but it had little effect in the range of 6.7–8.0 (83). Therefore, pH might alter the route of MR, causing in variations in the types and contents of flavor compounds in products. During the MR, the consumption of amino groups, the degradation of sugars, free amino acids (FAAs), and peptides facilitated the formation of acidic compounds. For example, after the addition of cysteine to the soybean peptide and D-xylose system, terminal pH was decreased, because cysteine accelerated the formation of formic acid and acetic acid (68). For the first time, Lotfy et al. (16) used enzymatically hydrolyzed quinoa protein as a major precursor for producing thermal process flavorings. By increasing pH from 5 to 9, the odor sensory attributes of the generated process flavor changed from caramel to burnt-coffee. This was due to the fact that low pH favored the production of furans, while high pH preferred the formation of pyrazines. However, pH does not have a significant effect on MRPs in all the cases. Li and Liu (34) discovered that the volatile profiles of heat-treated pork hydrolysate might not unaffected by pH. Volatile compounds such as furfural and furans were formed in similar amounts in heated samples with varying pH values.

MR is composed of a series of complex reactions, in which the sensitivity of each reaction and reactant to temperature are different. Therefore, temperature is also known to directly or indirectly influence the reaction degree and product composition. The MR rate increased significantly with the increase of temperature. For every 10°C increase of temperature, the reaction rate increases 3–5 times. At temperature < 110°C, the system of polypeptide and xylose was given priority to cross-linking reaction. At temperature > 110°C, a series of small molecular compounds of degradation were formed in the peptides system. These small molecular compounds accelerate the transition from pyrazine, sulfur-containing compounds and pyrrole to volatile compounds. Furans are sugar-derived compounds that are commonly generated under high thermal treatment (84). The concentration of furans in the soybean peptides-xylose system rose, as the temperature climbed from 80 to 140°C, demonstrating that furans were formed as a result of severe thermal treatment (68). Similarly, as xylose and chicken hydrolytic peptides were heated at 80–100°C for 60–90 min, the formation of umami-flavor and thick-flavor substances was conducive. While pyrazine, furan and pyridine were heated at high temperature (100–140°C) for 30–60 min, the formation of volatile compounds such as with barbecue and meat flavor was conducive (81). On one hand, after high-temperature treatment, ketones and phenols may be converted into intermediates for heterocyclic compounds or volatilized, and esters could be hydrolyzed into acids and alcohols. On the other hand, Protein hydrolysis may produce more amino acids, peptides, and small molecule compounds to accelerate the MR process. Lower heating temperature (80–100°C) with cysteine added was beneficial to forming umami FAAs, while bitter FAAs were likely formed at temperature ranging from 100 to 120°C which was consistent with the recent study for stewed pork with the high-temperature processing methods (63). However, excessively high temperature would not only generate pungent odor substances such as thiazole, but also destroy the enzyme binding sites of polypeptides and generate some cellulose analogs. The analogs are not easy to be decomposed and absorbed by the human body, thus reducing the nutritional values of food. In addition, at temperature > 110°C, some toxic substances (such as acrylamide and AGEs) are formed, which have certain toxic effects on human body.

MF assistive technology

Recently, new emerging technologies, including pulsed electric field, microwave radiation, high-pressure homogenization and high pressure, have been applied to promote the Maillard reaction with less processing time (35).

MR could be significantly accelerated, since ultrasound provided more energy during proteins grafting (85). Furthermore, ultrasonic treatment has the potential to alter the secondary and tertiary structures of proteins, reducing glycation time and increasing the functional properties of conjugates (86). Under ultrasound treatment, the reactivity between proteins and sugars was extremely low. The protein-dense quaternary and tertiary structures protect the active amino groups, and make the protein graft difficult. In contrast, this process usually requires higher temperature and longer time (usually several days) without ultrasound treatment. As an alternative strategy, ultrasound is an appropriate choice for promoting protein saccharification. MRPs had a higher content of conjugated amino acids after ultrasonic pretreatment, indicating that ultrasonic pretreatment of soybean protein/sugar mixture before heating accelerated the reaction (87). Ultrasound assisting MR has been a promising approach for improving the functional properties of mung bean protein isolates with glucose (88). It could accelerate the MR rate, and improve the content of sulfur containing volatile flavor compounds and antioxidant properties of the products (89). Many studies have found that ultrasonic pretreatment of proteins before enzymolysis hydrolyzed the protein into smaller fragments, resulting in a considerable increase in reaction rate (90, 91). Comparing energy aggregating ultrasound (EGU) and energy dispersing ultrasound (EDU) pretreatments, the taste and overall acceptability of MRPs were improved. Due to the low intensity and uniformity of the ultrasonic waves generated by the EDU, the protein molecule distribution was more uniform, which increased the irregular curvature and surface hydrophobicity of the protein. It also resulted in the increase of the content of peptides and amino acids in the hydrolyzed protein as well as the ratio of small molecule peptides to amino acids, thus promoting the MR between hydrolyzed protein and glucose (11).

Traditional production methods of black garlic could not meet the industrial demand because of long-time, high production cost, high-energy consumption, and uneven product quality. The most important chemical reaction in the production of black garlic is MR, and the major substrates are reducing sugars and amino acids (92). The reducing sugars produced by the degradation of polysaccharides and enzymes are important parts of MR, but the enzymes and substrates are usually isolated at different locations in intact cells. The destruction of cellular structures by high-pressure pretreatment affected the intracellular environment, and especially accelerated the degradation of fructan. MR substrates accumulated rapidly in the early stage of processing, which led to the accelerated arrival of the reducing sugar equilibrium point (RSBP) during the heat treatment. High pressure reduced the production time of black garlic from 24 to 15 d, and the taste was also improved (93).

A new non-thermal food processing method is pulse electric field (PEF). Electric field strength, polarity, pulse time, pulse count, and pulse shape are the basic PEF process parameters. PEF processing has so far been widely employed in the extraction of physiologically active compounds, alteration of biomacromolecules, augmentation of chemical processes, and other aspects (94). PEF processing has the ability to change the microstructure and macromolecular interactions of biomacromolecules while reducing the overall processing time with great efficiency when compared to conventional heating techniques. PEF is particularly vital for improving interactions between proteins and polysaccharides (95). Researchers claim that PEF processing might boost the carbon backbone's internal energy fluctuation, enhance mass transfer, and lower the chemical reaction's activation energy (94). The molecular chains of proteins would be attacked by the free radicals produced by electrolysis or electrochemical reactions when the protein-polysaccharide mixed solution is subjected to the PEF processing, leading to the partial-unfolding of proteins' secondary structure and improved protein-water interactions. Additionally, several previously hidden cationic, surface-free sulfhydryl, and hydrophobic groups on proteins are revealed (95). The delivered electric energy simultaneously induces the depolymerization and breakdown of carbohydrate chains. These modifications facilitate the binding of various reactants and increase the likelihood of collisions between reactive molecules. When the free -NH_2 of proteins links with the -C = O of polysaccharides, covalent interactions take place. By-products of Rainbow Trout (Oncorhynchus mykiss), Dover Sole (Dover Sole) as well as other animal protein (96) and non-dairy plant-based Beverages (97) have been demonstrated to taste better and be more widely accepted when subjected to pulsed electric fields. However, there is presently no large-scale PEF technology available to generate MRPs for the food business. To fully comprehend the interaction between the critical intensity and the thermal consequences of PEF processing, more study is required.

Negative effects

It is widely known that the average human diet contains large amounts of MRPs. A certain degree of browning plays an important role in developing the sensory properties (such as color, aroma, and flavor) which are needed in certain foods. For example, many baked goods, such as cookies and bread, have desired brown color, giving the consumer an impression of high quality. However, excessive MR might also undermine the sensory, flavor and nutritional values of foods, and even produce anti-nutritional or toxic substances such as acrylamide, heterocyclic amine, and advanced glycation final.

MR might affect the color of agricultural products, causing economic losses. The color deterioration of shrimp was noticed due to the multiple effects of lipid oxidation, phenol oxidation, MR, and astaxanthin degradation (98). Pyrazine and

5-hydroxymethyl furfural (5-HMF) were increased in a time-dependent way. Similarly, the internal browning depreciated the economic value of sweet potatoes due to the generation levels of reactive oxygen species, active polyphenols in the browning area were higher than those in the normal area. Intracellular glucose accumulation initiated the MR and led to ROS aggregation (99).

Moreover, MR played a key role in browning during the instant controlled pressure drop-assisted hot air drying of the apple slices which reduced the sensory quality of the slices (100). As one of the carcinogenic MRPs, acrylamide should be prevented from generation in food systems containing reducing sugars and asparagine. To control the acryl amide generation, ultrasound-MR could be used to accelerate MR in the asparagine-glucose model system (100).

The stability of flavor and flavorings is receiving more attention these days. Flavor loss and deterioration are significant restrictions during food processing and storage, particularly at temperatures above room temperature. Because of their instability (such as pyranone and unsaturated diones), MRPs are extremely prone to flavor loss during storage and processing (101). The flavor quality and customer acceptance of food were both lowered as a result of the loss of favorable fragrance components (such as acetaldehyde, butanal, and furfural). The contents of taste components in MRPs were drastically reduced after storage, and the solution's clarity deteriorated. The stability and transparency of Maillard reaction intermediates as a spice precursor also make them a potential substitute for MRPs (102).

In addition to the food system, MR also occurs in the human body, and could pose a health risk. It is known that the superoxides product might oxidize biological macromolecules (such as lipids and proteins) in each stage of MR in the medical field. Diabetes is related to advanced glycation end products (AGEs), as a result of the fact that MR is triggered by an increase in blood sugar level (103). Furthermore, AGEs accumulation in follicles by activating ATF4 in the follicular microenvironment, which triggers inflammation and reduces oocyte competence (104). In a concentration-dependent manner, AGEs significantly accelerated BMSC senescence, induced mitochondrial dysfunction, and blocked mitophagy (43). Therefore, it is necessary to imply intervention measures to control MR under these situations.

Application of MRPs as flavor enhancers

Table 4 showed the latest studies on the role of the Maillard reaction in the production of flavor. By studying the taste characteristics of 1–5 kDa peptides MRPs, the Maillard peptide could enhance the umami and continuity of umami solution and consommé soup (43). Heo et al. (111) investigated on the molecular and sensory properties of y-glutamyl peptides, which are key factors to the Kokumi taste of edible beans (*Phaseolus vulgaris* L.). As added to a savory matrix like sodium chloride and monosodium glutamate solutions or chicken broth, the y-glutamyl peptides greatly improved mouthfullness, complexity, and shelf life. Similarly, the Maillard-peptide and the taste enhancer from long-term ripening of miso (soybean paste) were deemed essential substances, suggesting the characteristic flavor (mouthfulness and continuity) of long-ripened miso. Purified di-, tri-, tetra-, and other short peptides have also been extensively studied in MR systems to provide various flavor and taste characteristics. According to previous study, the cross-linking of peptides in the thermal reaction process played an important role in the aroma and mellow feeling. MR study of rapeseed peptides, cysteine and Xylose showed that high temperature reduced the bitter value of the product, and low temperature promoted the salty and umami-tasting (85). Kang et al. (69) reported that interaction between enzymatic hydrolysis and MR improved the quality of beef flavor by regulating the formation of characteristic aroma precursors. In addition, the possible pathway and mechanism of the characteristic flavor of natural meat were further clarified, forming a new technology for the preparation of high-fidelity MF.

In the recent years, the promising industrial avenues for MFs have a good potential in China due to the rich flavor, however, there is still scope to develop their application. In view of this characteristic, strategies can be applied to obtain MFs directly by chemical synthesis after analyzing the structural characteristics of key flavor compounds. Zhai et al. (112) synthesized 2, 5-dimethylpyrazine, 2,3, 5-trimethylpyrazine and benzyl alcohol by palladium-catalyzed synthesis of 2-enylpyrazine oxides. Kocadagli et al. (32) also prepared 2-acetyl-1-pyrroline, 6-acetyl-1,2,3,4-tetrahydropyridine and 5-acetyl-2,3-dihydro4H-1,4-thiazide to enhance the flavor characteristics of baked foods. However, resulting MRPs were often unstable and highly volatile, especially at higher temperatures (101). In addition, flavor substances with active properties are often derived into other substances through peroxidation, polymerization and condensation, thus changing the overall flavor profile. Among the MRPs, pyrazine is regarded as the most vulnerable key aroma substances. Followed by pyrrole, mercaptans and aldehydes, oxidation and polymerization are the most important factors for the loss. Therefore, during the application and storage of MFs, it is difficult to maintain a stable concentration and flavor enhancing effect, especially in the thermal processing. It has become an important research direction for food scientists to analyze the mechanism of flavor generation and loss, and improve the controllability of flavor substances escape. In addition to high stability, MRIs can also reduce the bitterness of raw materials and increase the umami taste. It also improves the body's perception of salt, which helps reduce salt intake in daily life. But the mechanism of saltiness enhancement of vegetable protein enzymatic hydrolysates warrants future studies (10).

Conclusion

The MRPs not only alter food properties (stability, flavor, color, etc.), but also enhance the functional properties (anti-oxidant, anti-microbial, and anti-browning) of amino acids, peptides and proteins. MRPs have been used as flavor enhancers because of good mouthfeel and umami. Their flavor characteristics could be pleasant floral, nutty, caramel, attractive meat, or even spicy. E-nose, E-tongue, and GC-MS have become the most representative tools to detect flavor components, helping researchers to obtain comprehensive flavor profile. MF depends largely on the proteins, reducing sugars, and conditions (time, temperature, pH, vacuum degree, etc.). After proteins and sugars obtained from different sources react, MRPs of different flavor are obtained. Meanwhile, under different enzymatic hydrolysis conditions, proteins are enzymolyzed into different peptide fragments. In MR, since the open chain concentration of sugars and active form of amino reactants depend on pH, each reaction and reactant has a different sensitivity to temperature and affects the reaction differently.

Except flavor, MR currently has many limitations in terms of the difficulty in controlling the reaction degree, and the instability of the final product. Undesirable substances, which could reduce the flavor and nutrition, might be formed during the reaction. To address these issues, MRI has become a new research focus and has contributed to improving stability and flavor, nevertheless, the generation and mechanism of MRPs still need to be further exploited.

Author contributions

SL, GM, and LW designed the topic. LG and SL prepared the manuscript. HP, XL, and TZ prepared the figures. SL, GM, TZ, and HS reviewed and revised the manuscript. All authors contributed to the article and approved the submitted version.

Funding

This work was funded by Technology Project of Anhui Province 201903a06020024, Technology Project of Anhui Province 202203a06020029, Eight Major Industrial Chain Strengthening and Chain Reinforcing Projects 2021GJ010, Science and Technology Plan Project of Huangshan City 2020KN-04, and Key Research and Development Projects from Anhui Province 202104a06020013.

Conflict of interest

The authors declare that the research was conducted in the absence of any commercial or financial relationships that could be construed as a potential conflict of interest.

Publisher's note

All claims expressed in this article are solely those of the authors and do not necessarily represent those of their affiliated organizations, or those of the publisher, the editors and the reviewers. Any product that may be evaluated in this article, or claim that may be made by its manufacturer, is not guaranteed or endorsed by the publisher.

References

1. Fu Y, Zhang YH, Soladoye OP, Aluko RE. Maillard reaction products derived from food protein-derived peptides: insights into flavor and bioactivity. *Crit Rev Food Sci Nutr.* (2020) 60:3429–42. doi: 10.1080/10408398.2019.1691500

2. Nooshkam M, Varidi M, Verma DK. Functional and biological properties of Maillard conjugates and their potential application in medical and food: a review. *Food Res Int.* (2020) 131:109003. doi: 10.1016/j.foodres.2020.109003

3. Xu Z, Huang G, Xu T, Liu L, Xiao J. Comparative study on the Maillard reaction of chitosan oligosaccharide and glucose with soybean protein isolate. *Int J Biol Macromol.* (2019) 131:601–7. doi: 10.1016/j.ijbiomac.2019.03.101

4. Chiang JH, Eyres GT, Silcock PJ, Hardacre AK, Parker ME. Changes in the physicochemical properties and flavour compounds of beef bone hydrolysates after Maillard reaction. *Food Res Int.* (2019) 123:642–9. doi: 10.1016/j.foodres.2019.05.024

5. Song Y, Du B, Ding Z, Yu Y, Wang Y. Baked red pepper (*Capsicum annuum* L.) powder flavor analysis and evaluation under different exogenous Maillard reaction treatment. *LWT.* (2020) 139:110525. doi: 10.1016/j.lwt.2020.110525

6. Habinshuti I, Chen X, Yu J, Mukeshimana O, Duhoranimana E, Karangwa E, et al. Antimicrobial, antioxidant and sensory properties of Maillard reaction products (MRPs) derived from sunflower, soybean and corn meal hydrolysates. *LWT.* (2019) 101:694–702. doi: 10.1016/j.lwt.2018.11.083

7. Navicha W, Hua Y, Masamba KG, Kong X, Zhang C. Effect of soybean roasting on soymilk sensory properties. *Br Food J.* (2018) 120:2832–42. doi: 10.1108/BFJ-11-2017-0646

8. Chen F, Lin L, Zhao M, Zhu Q. Modification of Cucumaria frondosa hydrolysate through maillard reaction for sea cucumber peptide based-beverage. *LWT.* (2021) 136:110329. doi: 10.1016/j.lwt.2020.110329

9. Wang W, Zhang L, Wang Z, Wang X, Liu Y. Physicochemical and sensory variables of Maillard reaction products obtained from Takifugu obscurus muscle hydrolysates. *Food Chem.* (2019) 290:40–6. doi: 10.1016/j.foodchem.2019.03.065

10. Zhou X, Cui H, Zhang Q, Hayat K, Yu J, Hussain S, et al. Taste improvement of Maillard reaction intermediates derived from enzymatic hydrolysates of pea protein. *Food Res Int.* (2021) 140:109985. doi: 10.1016/j.foodres.2020.109985

11. Habinshuti I, Mu T-H, Zhang M. Structural, antioxidant, aroma, and sensory characteristics of Maillard reaction products from sweet potato protein hydrolysates as influenced by different ultrasound-assisted enzymatic treatments. *Food Chem.* (2021) 361:130090. doi: 10.1016/j.foodchem.2021.130090

12. Sun L-b, Zhang Z-y, Xin G, Sun B-x, Bao X-j, Wei Y-y, et al. Advances in umami taste and aroma of edible mushrooms. *Trends Food Sci Technol.* (2020) 96:176–87. doi: 10.1016/j.tifs.2019.12.018

13. He S, Zhang Z, Sun H, Zhu Y, Zhao J, Tang M, et al. Contributions of temperature and l-cysteine on the physicochemical properties and sensory characteristics of rapeseed flavor enhancer obtained from the rapeseed peptide and d-xylose Maillard reaction system. *Ind Crops Prod.* (2019) 128:455–63. doi: 10.1016/j.indcrop.2018.11.048

14. Liu Z, Zhu Y, Wang W, Zhou X, Chen G, Liu Y. Seven novel umami peptides from Takifugu rubripes and their taste characteristics. *Food Chem.* (2020) 330:127204. doi: 10.1016/j.foodchem.2020.127204

15. Geng J-T, Takahashi K, Kaido T, Kasukawa M, Okazaki E. Relationship among pH, generation of free amino acids, and Maillard browning of dried Japanese common squid *Todarodes pacificus* meat. *Food Chem.* (2019) 283:324–30. doi: 10.1016/j.foodchem.2019.01.056

16. Lotfy SN, Saad R, El-Massrey KF, Fadel HHM. Effects of pH on headspace volatiles and properties of Maillard reaction products derived from enzymatically hydrolyzed quinoa protein-xylose model system. *LWT.* (2021) 145:111328. doi: 10.1016/j.lwt.2021.111328

17. Spotti MJ, Loyeau PA, Marangón A, Noir H, Rubiolo AC, Carrara CR. Influence of Maillard reaction extent on acid induced gels of whey proteins and dextrans. *Food Hydrocoll.* (2019) 91:224–31. doi: 10.1016/j.foodhyd.2019.01.020

18. Singh P, Rao PS, Sharma V, Arora S. Physico-chemical aspects of lactose hydrolysed milk system along with detection and mitigation of maillard reaction products. *Trends Food Sci Technol.* (2021) 107:57–67. doi: 10.1016/j.tifs.2020.11.030

19. Zhou Z, Langrish T. A review of Maillard reactions in spray dryers. *J Food Eng.* (2021) 305:110615. doi: 10.1016/j.jfoodeng.2021.110615

20. Hafsa J, Smach MA, Mrid RB, Sobeh M, Majdoub H, Yasri A. Functional properties of chitosan derivatives obtained through Maillard reaction: A novel promising food preservative. *Food Chem.* (2021) 349:129072. doi: 10.1016/j.foodchem.2021.129072

21. Ahmed T, Wang CK. Black garlic and its bioactive compounds on human health diseases: a review. *Molecules.* (2021) 26:5028. doi: 10.3390/molecules26165028

22. Hou L, Xie J, Zhao J, Zhao M, Fan M, Xiao Q, et al. Roles of different initial Maillard intermediates and pathways in meat flavor formation for cysteine-xylose-glycine model reaction systems. *Food Chem.* (2017) 232:135–44. doi: 10.1016/j.foodchem.2017.03.133

23. Lomelí-Martín A, Martínez LM, Welti-Chanes J, Escobedo-Avellaneda Z. Induced changes in aroma compounds of foods treated with high hydrostatic pressure: a review. *Foods.* (2021) 10:878. doi: 10.3390/foods10040878

24. Deuscher Z, Gourrat K, Repoux M, Boulanger R, Labouré H, Le Quéré JL. Key aroma compounds of dark chocolates differing in organoleptic properties: a GC-O comparative study. *Molecules.* (2020) 25:1809. doi: 10.3390/molecules25081809

25. Bertrand E, Boustany PE, Faulds CB, Berdagué J. The Maillard reaction in food: an introduction. In: *Reference Module in Food Science* (2018).

26. Rufián-Henares JA, Pastoriza S. Browning: non-enzymatic browning. In: *Encyclopedia of Food and Health*, eds B. Caballero, P. M. Finglas, and F. Toldrá. Oxford: Academic Press (2016). p. 515–21.

27. Shen Y, Hu L-T, Xia B, Ni Z-J, Elam E, Thakur K, et al. Effects of different sulfur-containing substances on the structural and flavor properties of defatted sesame seed meal derived Maillard reaction products. *Food Chem.* (2021) 365:130463. doi: 10.1016/j.foodchem.2021.130463

28. Xiao Q, Woo MW, Hu J, Xiong H, Zhao Q. The role of heating time on the characteristics, functional properties and antioxidant activity of enzyme-hydrolyzed rice proteins-glucose Maillard reaction products. *Food Biosci.* (2021) 43:101225. doi: 10.1016/j.fbio.2021.101225

29. Ni Z-J, Liu X, Xia B, Hu L-T, Thakur K, Wei Z-J. Effects of sugars on the flavor and antioxidant properties of the Maillard reaction products of camellia seed meals. *Food Chem.* (2021) 11:100127. doi: 10.1016/j.fochx.2021.100127

30. Du X, Sissons J, Shanks M, Plotto A. Aroma and flavor profile of raw and roasted agaricus bisporus mushrooms using a panel trained with aroma chemicals. *LWT.* (2021) 138:110596. doi: 10.1016/j.lwt.2020.110596

31. Gao P, Xia W, Li X, Liu S. Optimization of the Maillard reaction of xylose with cysteine for modulating aroma compound formation in fermented tilapia fish head hydrolysate using response surface methodology. *Food Chem.* (2020) 331:127353. doi: 10.1016/j.foodchem.2020.127353

32. Kocadagli T, Methven L, Kant A, Parker JK. Targeted precursor addition to increase baked flavour in a low-acrylamide potato-based matrix. *Food Chem.* (2021) 339:128024. doi: 10.1016/j.foodchem.2020.128024

33. Heo J, Adhikari K, Choi KS, Lee J. Analysis of caffeine, chlorogenic acid, trigonelline, and volatile compounds in cold brew coffee using high-performance liquid chromatography and solid-phase microextraction-gas chromatography-mass spectrometry. *Foods.* (2020) 9:1746. doi: 10.3390/foods9121746

34. Li X, Liu S-Q. Effect of pH, xylose content and heating temperature on colour and flavour compound formation of enzymatically hydrolysed pork trimmings. *LWT.* (2021) 150:112017. doi: 10.1016/j.lwt.2021.112017

35. Li Z, Zheng Y, Sun Q, Wang J, Zheng B, Guo Z. Structural characteristics and emulsifying properties of myofibrillar protein-dextran conjugates induced by ultrasound Maillard reaction. *Ultrason Sonochem.* (2021) 72:105458. doi: 10.1016/j.ultsonch.2020.105458

36. Fan M, Xiao Q, Xie J, Cheng J, Sun B, Du W, et al. Aroma compounds in chicken broths of Beijing Youji and commercial broilers. *J Agric Food Chem.* (2018) 66:10242–51. doi: 10.1021/acs.jafc.8b03297

37. Xiong C, Qiang L, Li S, Cheng C, Chen Z, Huang W. *In vitro* antimicrobial activities and mechanism of 1-Octen-3-ol against food-related bacteria and pathogenic fungi. *J Oleo Sci.* (2017) 66:1041–9. doi: 10.5650/jos.ess16196

38. Zannou O, Kelebek H, Selli S. Elucidation of key odorants in Beninese Roselle (*Hibiscus sabdariffa* L.) infusions prepared by hot and cold brewing. *Food Res. Int.* (2020) 133:109133. doi: 10.1016/j.foodres.2020.109133

39. Hidalgo FJ, Lavado-Tena CM, Zamora R. Formation of 3-hydroxypyridines by lipid oxidation products in the presence of ammonia and ammonia-producing compounds. *Food Chem.* (2020) 328:127100. doi: 10.1016/j.foodchem.2020.127100

40. Zhao J, Wang T, Xie J, Xiao Q, Du W, Wang Y, et al. Meat flavor generation from different composition patterns of initial Maillard stage intermediates formed in heated cysteine-xylose-glycine reaction systems. *Food Chem.* (2019) 274:79–88. doi: 10.1016/j.foodchem.2018.08.096

41. Zhan H, Hayat K, Cui H, Hussain S, Ho C-T, Zhang X. Characterization of flavor active non-volatile compounds in chicken broth and correlated contributing constituent compounds in muscle through sensory evaluation and partial least square regression analysis. *LWT.* (2020) 118:108786. doi: 10.1016/j.lwt.2019.108786

42. Zhang N, Yang Y, Wang W, Fan Y, Liu Y. A potential flavor seasoning from aquaculture by-products: an example of takifugu obscurus. *LWT.* (2021) 151:112160. doi: 10.1016/j.lwt.2021.112160

43. Guo Y, Jia X, Cui Y, Song Y, Wang S, Geng Y, et al. Sirt3-mediated mitophagy regulates AGEs-induced BMSCs senescence and senile osteoporosis. *Redox Biol.* (2021) 41:101915. doi: 10.1016/j.redox.2021.101915

44. Yang X, Li Y, Li S, Ren X, Oladejo AO, Lu F, et al. Effects and mechanism of ultrasound pretreatment of protein on the Maillard reaction of protein-hydrolysate from grass carp (Ctenopharyngodon idella). *Ultrason Sonochem.* (2020) 64:104964. doi: 10.1016/j.ultsonch.2020.104964

45. He S, Chen Y, Brennan C, Young DJ, Chang K, Wadewitz P, et al. Antioxidative activity of oyster protein hydrolysates Maillard reaction products. *Food Sci Nutr.* (2020) 8:3274–86. doi: 10.1002/fsn3.1605

46. Andruszkiewicz PJ, D'Souza RN, Corno M, Kuhnert N. Novel Amadori and Heyns compounds derived from short peptides found in dried cocoa beans. *Food Res Int.* (2020) 133:109164. doi: 10.1016/j.foodres.2020.109164

47. Liang S, Zhang T, Fu X, Zhu C, Mou H. Partially degraded chitosan-based flocculation to achieve effective deodorization of oyster (*Crassostrea gigas*) hydrolysates. *Carbohydr Polym.* (2020) 234:115948. doi: 10.1016/j.carbpol.2020.115948

48. Wang Z, Zheng C, Huang F, Liu C, Huang Y, Wang W. Effects of radio frequency pretreatment on quality of tree peony seed oils: process optimization and comparison with microwave and roasting. *Foods.* (2021) 10:3062. doi: 10.3390/foods10123062

49. Zhang Z, Elfalleh W, He S, Tang M, Zhao J, Wu Z, et al. Heating and cysteine effect on physicochemical and flavor properties of soybean peptide Maillard reaction products. *Int J Biol Macromol.* (2018) 120:2137–46. doi: 10.1016/j.ijbiomac.2018.09.082

50. Nakagawa K, Maeda H, Yamaya Y, Tonosaki Y. Maillard reaction intermediates and related phytochemicals in black garlic determined by EPR and HPLC analyses. *Molecules.* (2020). 25:4578. doi: 10.3390/molecules25194578

51. Luo Y, Li S, Ho CT. Key aspects of amadori rearrangement products as future food additives. *Molecules.* (2021) 26:4314. doi: 10.3390/molecules26144314

52. Prud'homme SM, Hani YMI, Cox N, Lippens G, Nuzillard JM, Geffard A. The zebra mussel (*Dreissena polymorpha.*) as a model organism for ecotoxicological studies: a prior 1H NMR spectrum interpretation of a whole body extract for metabolism monitoring. *Metabolites.* (2020) 10:256. doi: 10.3390/metabo10060256

53. Neagu AN, Jayathirtha M, Baxter E, Donnelly M, Petre BA, Darie CC. Applications of tandem mass spectrometry (MS/MS) in protein analysis for biomedical research. *Molecules.* (2022) 27:2411. doi: 10.3390/molecules27082411

54. Saldaña E, Saldarriaga L, Cabrera J, Siche R, Behrens JH, Selani MM, et al. Relationship between volatile compounds and consumer-based sensory characteristics of bacon smoked with different Brazilian woods. *Food Res Int.* (2019) 119:839–49. doi: 10.1016/j.foodres.2018.10.067

55. Petričević S, Marušić Radovčić N, Lukić K, Listeš E, Medić H. Differentiation of dry-cured hams from different processing methods by means of volatile compounds, physico-chemical and sensory analysis. *Meat Sci.* (2018) 137:217–27. doi: 10.1016/j.meatsci.2017.12.001

56. Routray W, Rayaguru K. 2-Acetyl-1-pyrroline: a key aroma component of aromatic rice and other food products. *Food Rev Int.* (2018) 34:539–65. doi: 10.1080/87559129.2017.1347672

57. Cambeiro-Perez N, Gonzalez-Gomez X, Gonzalez-Barreiro C, Perez-Gregorio MR, Fernandes I, Mateus N, et al. Metabolomics insights of the immunomodulatory activities of phlorizin and phloretin on human THP-1 macrophages. *Molecules.* (2021) 26:787. doi: 10.3390/molecules26040787

58. Ahluwalia K, Ebright B, Chow K, Dave P, Mead A, Poblete R, et al. Lipidomics in understanding pathophysiology and pharmacologic effects in inflammatory diseases: considerations for drug development. *Metabolites.* (2022) 12:333. doi: 10.3390/metabo12040333

59. Xing H, Mossine VV, Yaylayan V. Diagnostic MS/MS fragmentation patterns for the discrimination between Schiff bases and their Amadori or Heyns rearrangement products. *Carbohydr Res.* (2020) 491:107985. doi: 10.1016/j.carres.2020.107985

60. Feskens E, Brennan L, Dussort P, Flourakis M, Lindner LME, Mela D, et al. Potential markers of dietary glycemic exposures for sustained dietary interventions in populations without diabetes. *Adv Nutr.* (2020) 11:1221–36. doi: 10.1093/advances/nmaa058

61. Hwang IS, Chon SY, Bang WS, Kim MK. Influence of roasting temperatures on the antioxidant properties, β-glucan content, and volatile flavor profiles of shiitake mushroom. *Foods.* (2020) 10:54. doi: 10.3390/foods10010054

62. Xie Q, Xu B, Xu Y, Yao Z, Zhu B, Li X, et al. Effects of different thermal treatment temperatures on volatile flavour compounds of water-boiled salted duck after packaging. *LWT.* (2022) 154:112625. doi: 10.1016/j.lwt.2021.112625

63. Han D, Zhang C-H, Fauconnier M-L, Jia W, Wang J-F, Hu F-F, et al. Characterization and comparison of flavor compounds in stewed pork with different processing methods. *LWT.* (2021) 144:111229. doi: 10.1016/j.lwt.2021.111229

64. Elhalis H, Cox J, Frank D, Zhao J. Microbiological and chemical characteristics of wet coffee fermentation inoculated with hansinaspora uvarum and *Pichia kudriavzevii* and their impact on coffee sensory quality. *Front Microbiol.* (2021) 12:713969. doi: 10.3389/fmicb.2021.713969

65. Yoo JH, Kim JW, Yong HI, Baek KH, Lee HJ, Jo C. Effects of searing cooking on sensory and physicochemical properties of beef steak. *Food Sci Anim Resources.* (2020) 40:44–54. doi: 10.5851/kosfa.2019.e80

66. Deng S, Xing T, Li C, Xu X, Zhou G. The effect of breed and age on the growth performance, carcass traits and metabolic profile in breast muscle of Chinese indigenous chickens. *Foods.* (2022) 11, 483. doi: 10.3390/foods11030483

67. Tu Y, Xu Y, Ren F, Zhang H. Characteristics and antioxidant activity of Maillard reaction products from α-lactalbumin and 2′-fucosyllactose. *Food Chem.* (2020) 316:126341. doi: 10.1016/j.foodchem.2020.126341

68. Wei CK, Thakur K, Liu DH, Zhang JG, Wei ZJ. Enzymatic hydrolysis of flaxseed (Linum usitatissimum L.) protein and sensory characterization of Maillard reaction products. *Food Chem.* (2018) 263:186–93. doi: 10.1016/j.foodchem.2018.04.120

69. Kang L, Alim A, Song H. Identification and characterization of flavor precursor peptide from beef enzymatic hydrolysate by Maillard reaction. *J Chromatogr B.* (2019) 1104:176–81. doi: 10.1016/j.jchromb.2018.10.025

70. de Araújo Cordeiro ARR, de Medeiros LL, Bezerra TKA, Pacheco MTB, de Sousa Galvão M, Madruga MS. Effects of thermal processing on the flavor molecules of goat by-product hydrolysates. *Food Res Int.* (2020) 138:109758. doi: 10.1016/j.foodres.2020.109758

71. Sun HM, Wang JZ, Zhang CH, Li X, Xu X, Dong XB, et al. Changes of flavor compounds of hydrolyzed chicken bone extracts during Maillard reaction. *Food Sci.* (2015) 79:C2415–26. doi: 10.1111/1750-3841.12689

72. Zhang L, Chen Q, Liu Q, Xia X, Wang Y, Kong B. Effect of different types of smoking materials on the flavor, heterocyclic aromatic amines, and sensory property of smoked chicken drumsticks. *Food Chem.* (2022) 367:130680. doi: 10.1016/j.foodchem.2021.130680

73. Shen DY, Li M-k, Song H-L, Zou T-t, Zhang L, Xiong J. Characterization of aroma in response surface optimized no-salt bovine bone protein extract by switchable GC/GC×GC-olfactometry-mass spectrometry, electronic nose, and sensory evaluation. *LWT.* (2021) 147:111559. doi: 10.1016/j.lwt.2021.111559

74. Xu X, Yu M, Raza J, Song H, Gong L, Pan W. Study of the mechanism of flavor compounds formed via taste-active peptides in bovine bone protein extract. *LWT.* (2021) 137:110371. doi: 10.1016/j.lwt.2020.110371

75. Cai L, Li D, Dong Z, Cao A, Lin H, Li J. Change regularity of the characteristics of Maillard reaction products derived from xylose and Chinese shrimp waste hydrolysates. *LWT Food Sci Technol.* (2016) 65:908–16. doi: 10.1016/j.lwt.2015.09.007

76. Hou X, Yuan Z, Wang X, Cheng R, Zhou X, Qiu J. Peptidome analysis of cerebrospinal fluid in neonates with hypoxic-ischemic brain damage. *Mol Brain.* (2020) 13:133. doi: 10.1186/s13041-020-00671-9

77. Grossmann KK, Merz M, Appel D, De Araujo MM, Fischer L. New insights into the flavoring potential of cricket (Acheta domesticus) and mealworm (*Tenebrio molitor*) protein hydrolysates and their Maillard products. *Food Chem.* (2021) 364:130336. doi: 10.1016/j.foodchem.2021.130336

78. Marcinkowska M, Jeleń HH. Inactivation of thioglucosidase from *Sinapis alba* (white mustard) seed by metal salts. *Molecules.* (2020) 25:4363. doi: 10.3390/molecules25194363

79. Ma R, Jin Z, Wang F, Tian Y. Contribution of starch to the flavor of rice-based instant foods. *Crit Rev Food Sci Nutr.* (2021) 1–12. doi: 10.1080/10408398.2021.1931021

80. Rhyu M-R, Lyall V. Interaction of taste-active nutrients with taste receptors. *Curr Opin Physiol.* (2021) 20:64–9. doi: 10.1016/j.cophys.2020.12.008

81. Liu J, Liu M, He C, Song H, Chen F. Effect of thermal treatment on the flavor generation from Maillard reaction of xylose and chicken peptide. *LWT Food Sci Technol.* (2015) 64:316–25. doi: 10.1016/j.lwt.2015.05.061

82. Hrynets Y, Bhattacherjee A, Betti M. *Nonenzymatic Browning Reactions: Overview*. Amsterdam: Academic Press (2019). p. 233–44.

83. Yu M, He S, Tang M, Zhang Z, Zhu Y, Sun H. Antioxidant activity and sensory characteristics of Maillard reaction products derived from different peptide fractions of soybean meal hydrolysate. *Food Chem.* (2018) 243:249–57. doi: 10.1016/j.foodchem.2017.09.139

84. Zhang H, Chen H, Wang W, Jiao W, Chen W, Zhong Q, et al. Characterization of volatile profiles and marker substances by HS-SPME/GC-MS during the concentration of coconut jam. *Foods.* (2020) 9:347. doi: 10.3390/foods9030347

85. Chen WJ, Ma XB, Wang WJ, Lv RL, Guo MM, Ding T, et al. Preparation of modified whey protein isolate with gum acacia by ultrasound maillard reaction. *Food Hydrocoll.* (2019) 95:298–307. doi: 10.1016/j.foodhyd.2018.10.030

86. Chen L, Chen J, Wu K, Yu L. Improved low pH emulsification properties of glycated peanut protein isolate by ultrasound Maillard reaction. *J Agric Food Chem.* (2016) 64:5531–8. doi: 10.1021/acs.jafc.6b00989

87. Yu H, Zhong Q, Liu Y, Guo Y, Xie Y, Zhou W, et al. Recent advances of ultrasound-assisted Maillard reaction. *Ultrason Sonochem.* (2020) 64:104844. doi: 10.1016/j.ultsonch.2019.104844

88. Abdelhedi O, Mora L, Jemil I, Jridi M, Toldra F, Nasri M, et al. Effect of ultrasound pretreatment and Maillard reaction on structure and antioxidant properties of ultrafiltrated smooth-hound viscera proteins-sucrose conjugates. *Food Chem.* (2017) 230:507–15. doi: 10.1016/j.foodchem.2017.03.053

89. Gouda M, El-Din Bekhit A, Tang Y, Huang Y, Huang L, He Y, et al. Recent innovations of ultrasound green technology in herbal phytochemistry: a review. *Ultrason Sonochem.* (2021) 73:105538. doi: 10.1016/j.ultsonch.2021.105538

90. Jin J, Okagu OD, Yagoub AEA, Udenigwe CC. Effects of sonication on the in vitro digestibility and structural properties of buckwheat protein isolates. *Ultrason Sonochem.* (2021) 70:105348. doi: 10.1016/j.ultsonch.2020.105348

91. Lan M, Li W, Chang C, Liu L, Li P, Pan X, et al. Enhancement on enzymolysis of pigskin with ultrasonic assistance. *Bioengineered.* (2020) 11:397–407. doi: 10.1080/21655979.2020.1736736

92. Ríos-Ríos KL, Montilla A, Olano A, Villamiel M. Physicochemical changes and sensorial properties during black garlic elaboration: a review. *Trends Food Sci Technol.* (2019) 88:459–67. doi: 10.1016/j.tifs.2019.04.016

93. Li F, Cao J, Liu Q, Hu X, Liao X, Zhang Y. Acceleration of the Maillard reaction and achievement of product quality by high

pressure pretreatment during black garlic processing. *Food Chem.* (2020) 318:126517. doi: 10.1016/j.foodchem.2020.126517

94. Niu D, Zeng XA, Ren EF, Xu FY, Li J, Wang MS, et al. Review of the application of pulsed electric fields (PEF) technology for food processing in China. *Food Res Int*. (2020) 137:109715. doi: 10.1016/j.foodres.2020.109715

95. Gieteru SG, Ali MA, Oey I. Optimisation of pulsed electric fields processing parameters for developing biodegradable films using zein, chitosan and poly(vinyl alcohol). *Innov Food Sci Emerg Technol*. (2020) 60:102287. doi: 10.1016/j.ifset.2020.102287

96. Wang M, Zhou J, Collado MC, Barba FJ. Accelerated solvent extraction and pulsed electric fields for valorization of rainbow trout (*Oncorhynchus mykiss*) and sole (*Dover sole*) by-products: protein content, molecular weight distribution and antioxidant potential of the extracts. *Marine Drugs.* (2021) 19:207. doi: 10.3390/md19040207

97. Munekata PES, Domínguez R, Budaraju S, Roselló-Soto E, Barba FJ, Mallikarjunan K, et al. Effect of innovative food processing technologies on the physicochemical and nutritional properties and quality of non-dairy plant-based beverages. *Foods.* (2020) 9:288. doi: 10.3390/foods9030288

98. Li D-Y, Yuan Z, Liu Z-Q, Yu M-M, Guo Y, Liu X-Y, et al. Effect of oxidation and maillard reaction on color deterioration of ready-to-eat shrimps during storage. *LWT.* (2020) 131:109696. doi: 10.1016/j.lwt.2020.109696

99. Fukuoka N, Miyata M, Hamada T, Takeshita E. Histochemical observations and gene expression changes related to internal browning in tuberous roots of sweet potato (*Ipomea batatas*). *Plant Sci.* (2018) 274:476–84. doi: 10.1016/j.plantsci.2018.07.004

100. Gao Z, Zheng J, Chen L. Ultrasonic accelerates asparagine-glucose non-enzymatic browning reaction without acrylamide formation. *Ultrason Sonochem.* (2017) 34:626–30. doi: 10.1016/j.ultsonch.2016.06.041

101. He F, Qian YL, Qian MC. Flavor and chiral stability of lemon-flavored hard tea during storage. *Food Chem.* (2018) 239:622–30. doi: 10.1016/j.foodchem.2017.06.136

102. Cui H, Yu J, Xia S, Duhoranimana E, Huang Q, Zhang X. Improved controlled flavor formation during heat-treatment with a stable Maillard reaction intermediate derived from xylose-phenylalanine. *Food Chem.* (2019) 271:47–53. doi: 10.1016/j.foodchem.2018.07.161

103. Fukuoka N, Hirabayashi H, Hamada T. Oxidative stress via the Maillard reaction is associated with the occurrence of internal browning in roots of sweetpotato (*Ipomoea batatas*). *Plant Physiol Biochem.* (2020) 154:21–9. doi: 10.1016/j.plaphy.2020.05.009

104. Takahashi N, Harada M, Azhary JMK, Kunitomi C, Nose E, Terao H, et al. Accumulation of advanced glycation end products in follicles is associated with poor oocyte developmental competence. *Mol Hum Reprod.* (2019) 25:684–94. doi: 10.1093/molehr/gaz050

105. Hu LT, Elam E, Ni ZJ, Shen Y, Xia B, Thakur K, et al. The structure and flavor of low sodium seasoning salts in combination with different sesame seed meal protein hydrolysate derived Maillard reaction products. *Food Chem.: X*. (2021) 121:100148. doi: 10.1016/j.fochx.2021.100148

106. Sun F, Cui H, Zhan H, Xu M, Hayat K, Tahir MU, et al. Aqueous preparation of maillard reaction intermediate from glutathione and xylose and its volatile formation during thermal treatment. *J Food Sci*. (2019) 84:3584–93. doi: 10.1111/1750-3841.14911

107. Yin M, Shao S, Zhou Z, Chen M, Zhong F, Li Y. Characterization of the key aroma compounds in dog foods by gas chromatography-mass spectrometry, acceptance test, and preference test. *J Agri Food Chem.* (2020) 68:9195–204. doi: 10.1021/acs.jafc.0c03088

108. Wang L, Qiao K, Huang Y, Zhang Y, Xiao J, Duan W. Optimization of beef broth processing technology and isolation and identification of flavor peptides by consecutive chromatography and LC-QTOF-MS/MS. *Food Sci Nutr*. (2020) 8:4463–71. doi: 10.1002/fsn3.1746

109. Li Q, Sun H, Zhang M, and Wu T. (2020). Characterization of the flavor compounds in wheat bran and biochemical conversion for application in food. *J of Food Sci*, 85, 1427–1437.

110. Bak KH, Waehrens SS, Fu Y, Chow CY, Petersen MA, Ruiz-Carrascal J, et al. Flavor characterization of animal hydrolysates and potential of glucosamine in flavor modulation. *Foods*. (2021)10:3008. doi: 10.3390/foods10123008

111. Heo S, Kim JH, Kwak MS, Sung MH, Jeong DW. Functional annotation genome unravels potential probiotic *Bacillus velezensis* strain KMU01 from traditional Korean fermented Kimchi. *Foods.* (2021) 10:563. doi: 10.3390/foods10030563

112. Zhai K, Lai M, Wu Z, Zhao M, Jing Y, Liu P. Synthesis and initial thermal behavior investigation of 2-alkenyl substituted pyrazine N-oxides. *Catal Commun.* (2018) 116:20–6. doi: 10.1016/j.catcom.2018.07.017

frontiers | Frontiers in Nutrition

TYPE Original Research
PUBLISHED 26 September 2022
DOI 10.3389/fnut.2022.998448

OPEN ACCESS

EDITED BY
Gang Fan,
Huazhong Agricultural University, China

REVIEWED BY
Bing Yang,
Agricultural University of Hebei, China
Guang Xin,
Shenyang Agricultural University, China

*CORRESPONDENCE
Yan Zhao
zhaoyan@jxau.edu.cn

SPECIALTY SECTION
This article was submitted to Food Chemistry, a section of the journal Frontiers in Nutrition

RECEIVED 20 July 2022
ACCEPTED 05 September 2022
PUBLISHED 26 September 2022

CITATION
Gao B, Hu X, Xue H, Li R, Liu H, Han T, Tu Y and Zhao Y (2022) The changes of umami substances and influencing factors in preserved egg yolk: pH, endogenous protease, and proteinaceous substance. *Front. Nutr.* 9:998448. doi: 10.3389/fnut.2022.998448

The changes of umami substances and influencing factors in preserved egg yolk: pH, endogenous protease, and proteinaceous substance

Binghong Gao[1,2], Xiaobo Hu[3], Hui Xue[2], Ruiling Li[2], Huilan Liu[2], Tianfeng Han[2], Yonggang Tu[1] and Yan Zhao[1]*

[1]Jiangxi Key Laboratory of Natural Products and Functional Food, Jiangxi Agricultural University, Nanchang, China, [2]Engineering Research Center of Biomass Conversion, Ministry of Education, Nanchang University, Nanchang, China, [3]State Key Laboratory of Food Science and Technology, Nanchang University, Nanchang, China

The study investigated the changes of nucleotides, succinic acid, and free amino acids amounts in yolk and the causes leading to the changes after pickling to uncover the fundamental umami component of preserved egg yolk. The findings demonstrated that while the contents of 5′-adenosine monophosphate (AMP), 5′-cytidine monophosphate (CMP), 5′-guanosine monophosphate (GMP), 5′-uridine monophosphate (UMP), and succinic acid increased after slightly decreasing aspartic acid (Asp) content in preserved egg yolk increased gradually. The contents of 5′-inosine monophosphate (IMP) and other free amino acids were gradually decreased. Comparing the taste activity value (TAV), it was found that the single umami substance, succinic acid, played a key role in inducing the umami taste. In combination with the Spearman correlation analysis, it was shown that the proteinaceous substance, which is the most significant umami component in preserved egg yolk, tended to condense first and subsequently disintegrate in an alkaline environment. The orthogonal partial least squares analysis (OPLS) found that pH was also affected by the changes in proteinaceous substance. These findings offer suggestions for enhancing the pickling procedure and investigating the optimal pickling period for preserved eggs.

KEYWORDS

preserved egg yolk, umami, succinic acid, OPLS, Spearman's correlation

Introduction

The majority of the world's fresh duck egg production and processing occurs in China, where each year, almost 80% of fresh duck eggs are converted into preserved eggs and salted eggs (1). According to a study (2), consumers choose preserved eggs in a range of duck egg products because of their distinct flavor and nutritional worth. Preserved eggs are a fantastic anti-inflammatory and anti-cancer food. Traditional preserved eggs are made by pickling fresh eggs with a mixture of sodium hydroxide, salt, and metal

compounds, and the pickling cycle is usually 4–5 weeks. Recently, to produce a shorter time, better quality preserved eggs. Researchers have created techniques for pickling that are stress free. According to Sun et al. (3), vacuum technology has a three-fold shorter curing time than conventional methods. Strong alkali's effect during pickling causes the proteins in fresh duck eggs to break down into free amino acids and tiny peptides, and the lipids to break down into free fatty acids (4). Therefore, the complex physical and chemical changes in preserved eggs not only improve the nutritional value but also have a significant impact on the formation of their unique flavor. Exploring flavor substances in preserved eggs not only provide a theoretical basis for the processing technology of preserved eggs but also predict the maturity of preserved eggs. Ren et al. (5) found that dimethyl trithioether may be a marker of maturation in preserved eggs. Compared with preserved egg white, preserved egg yolk is rich in dry matter (such as lipids and proteins). Producers are interested in the distinct flavor of preserved egg yolk because it may be utilized to create specialty foods like mooncakes or pasta (2). Therefore, the primary research object for this study was preserved egg yolk.

It is generally believed that alkali induction and Maillard reaction are the main reasons for gel structure formation, color change, and flavor formation in preserved eggs (6). However, in the research on flavor substances, it is found that enzyme activity in food also plays a key role in the formation of flavor substances. One of the most significant biochemical changes during the maturation of fermented meat products is proteolysis, which is crucial for the development of flavor and the softening of texture in the finished product (7). Enzymes produced by microorganisms and endogenous enzymes are the main enzymes in food. According to Rivas-Canedo et al. (8) and Lin et al. (9), variations in the activity of several microbial enzymes and endogenous enzymes are directly related to the synthesis of taste compounds in dry-cured ham and Pixian broad bean paste. It is hypothesized that endogenous protease may be one of the primary causes for the alteration of flavor components in preserved eggs since the strong alkali inhibit the invasion of harmful bacteria and other microorganisms (10).

The research on taste characteristics in preserved egg yolk showed that the umami taste of preserved egg yolk was prominent, and free amino acids, succinic acid, and nucleotides contained in preserved egg yolk had varying degrees of influence on the umami taste of preserved egg yolk (11). Based on previous research, this study focuses on the contents of the umami substance and the factors influencing its change in preserved egg yolk. The primary umami compounds were discovered by examining the changes in nucleotides, succinic acid, and free amino acid concentrations in preserved egg yolk during pickling and combined them with taste activity value (TAV). Furthermore, multivariate statistical analysis was utilized to examine the relationship between pH, endogenous protease, and proteinaceous substance to investigate the factors that affect the umami substance in preserved egg yolk. The investigation of the umami of preserved egg yolk during the pickling process could provide a theoretical basis for the improvement of the pickling process.

Materials and methods

Materials

Methanol, acetonitrile, and acetic acid, chromatographically pure, were purchased from Thermo Fisher Technology China Co., LTD. (Shanghai, China). Sodium hydroxide was provided by the Tianjin Tianshun Lye Co., LTD. (Tianjin, China), edible salt was purchased from the Jiangxi Jiangyan Huakang Industrial Co., LTD. (Jiangxi China), and copper sulfate (food grade) was provided by the Xilong Technology Co., LTD. (Guangdong, China). Casein, trichloroacetic acid, and folinol were purchased from the Beijing Solarbio Technology Co., LTD. (Beijing, China). Sulfosalicylic acid was purchased from the Tianjin Damao Chemical Reagent Factory (Tianjin, China). Standard products: 5′-cytidine monophosphate (CMP), 5′-uridine monophosphate (UMP), succinic acid, 5′-adenosine monophosphate (AMP), 5′-guanosine monophosphate (GMP), 5′-inosine monophosphate (IMP), and 5′-xanthosidic monophosphate (XMP) were purchased from the Beijing Solarbio Technology Co., LTD. (Beijing, China).

Preparation of preserved egg yolk

Fresh duck eggs were obtained from the Tianyun Company in Jiangxi Province, China. Fresh uncracked duck eggs were selected and soaked in a pickling solution containing NaOH (4.5%, m/v), NaCl (3.0%, m/v), and $CuSO_4$ (0.4%, m/v) (10) for 35 days. Samples were taken once a week during the marinading period, with 15 eggs divided into three equal portions. The preserved eggs were shelled and the yolks were removed from the egg whites. All samples of egg yolks were freeze-dried (SCIENTZ-10N, Ningbo ScientzBiotechnology Co., Ltd., Ningbo, China) for subsequent experimental determination.

Determination of nucleotides

Egg yolk samples (0.08 g) were accurately weighed and placed in a 1.5 ml centrifuge tube, and 0.5 ml water and 0.5 ml acetonitrile were added. After that, the samples oscillated for 30 min. The centrifuge tube was placed in a low-temperature centrifuge and centrifuged at 12,000 rpm at 4°C for 5 min. A total of 200 μl of supernatant was taken, and then the frozen centrifugation technology was used for drying. The powder was redissolved in 100 μl ultrapure water.

The Waters ACQUITY UPLC I-Class ULTRA was used for chromatographic separation. Chromatographic conditions: Waters UPLC HSS T3 column (1.8 μm × 2.1 mm × 150 mm); flow rate: 0.26 ml/min; Injection volume was 3 μl; column temperature: 45°C; mobile phase A consisted of 0.1% formic acid and 5 mmol/L ammonium formate, and mobile phase B consisted of methanol. Elution conditions: 0–1 min, 2% B; 1–2.3 min, 2%, 100% B; 2.3–3 min, 100% B; 3–3.1 min, 100%, 2% B; 3.1–5 min, 2% B. The Waters XEVO TQ-S micro-tandem quadrupole mass spectrometry system was used for mass spectrometry analysis. The collection mode was positive ion, and the ion source voltage was 2.0 kV; cone voltage was 10 V; the source temperature was 150°C; the desolvation temperature was 500°C. the auxiliary gas flow rate was 10 L/h and the de-solvent gas flow rate was 1,000 L/h. The peak area of nucleotide data was calculated using the targetLynx quantitative software, and the permissible retention time was 15 s. The quantitative results of nucleotide concentration were obtained by the standard curve method.

Determination of succinic acid

The samples of 0.1 g yolk powder were accurately weighed and fully dissolved with 1.5 ml 80% methanol, extracted with ultrasonic at 45°C for 30 min, and centrifuged at 12,000 rpm for 10 min at 4°C. The supernatant was taken and blow-dried with nitrogen. Mobile phase solution (1 ml) was added for vortex and shock to dissolve.

HPLC conditions: LC-100C18 reversed-phase column (150 mm×4.6 mm, 5 μm; Shanghai Wufeng Scientific Instrument Co., LTD.); mobile phase: 0.1% phosphoric acid aqueous solution, pH: 2.7; the injection volume was 10 μl. The flow rate was 0.7 ml/min. The column temperature was 30°C, and the UV wavelength was 210 nm.

Determination of free amino acids

Egg yolk powder (0.2 g) was accurately weighed and dissolved in 5 ml 10% sulfosalicylic acid, followed by ultrasound for 30 min, and placed overnight at 4°C. After that, the solution (2 ml) was centrifuged at 12,000 rpm for 30 min. The supernatant (20 μl) was transferred through a 0.45 μm microporous membrane and tested by an automatic amino acid analyzer (L-8900, Hitachi, Japan).

Taste activity value

The calculation method of taste activity value (TAV) was the ratio between the concentration of umami substances in food and the umami threshold value (12).

Determination of pH

The determination of pH referred to the analysis method of (13) hygienic standard for eggs and egg products and had been slightly modified. Egg yolk samples (10.0 g) were taken under different pickling periods, diluted to 150 ml with water, and homogenized at 12,000 rpm for 2 min with a homogenizer (T18; IKA, Germany). After the residue was filtered by double-layer gauze, a 50 ml sample was taken and the pH value was measured by PHS-25 (Shanghai Yidian Scientific Instrument Co., Ltd., China).

Determination of TCA soluble peptide

The determination of TCA soluble peptide contents was referenced by Sriket et al. (14). Yolk powder (3.0 g) under different pickling periods was taken, Trichloroacetic acid (27 ml 50 g/L) was added, homogenized at 10,000 rpm for 1 min, and placed in the refrigerator for 1 h and then removed. The supernatant was centrifuged at 8,000 rpm for 5 min. The supernatant (1 ml) was mixed with 1 ml diluted folinol and 5 ml Na_2CO_3 and reacted for 20 min at 40°C. In the multimode reader (PerkinElmer, Massachusetts, USA), the UV wavelength was adjusted to 660 nm to determine the absorbance of the sample and the standard curve. Standard curve drawing: 0, 20, 40, 60, 80, and 100 μg/ml of tyrosine solution (1 ml).

Determination of endogenous protease activity

The determination of endogenous protease activity was slightly modified on the basis of Lu et al. (15). Egg yolk samples (5.0 g) under different curing days were added with 20 ml Tris-HCl at pH 8.0, homogenized and mixed, and soaked at 4°C for 3 h. The supernatant obtained by centrifugation of 8,000 rpm for 10 min was used as crude enzyme extract. The blank sample was set as: 0.8 ml crude enzyme solution + 4 ml Tris-HCl + 1.6 ml 1% casein + 4 ml 10% trichloroacetic acid; The experimental sample was: 0.8 ml crude enzyme solution + 4 ml tris-HCl + 1.6 ml 1% casein + 2.4 ml 10% trichloroacetic acid. The samples were reacted at 35°C for 15 min and centrifuged at 8,000 rpm for 10 min to obtain the supernatant. The absorbance was measured by adjusting the UV absorption wavelength to 275 nm in the multimode reader.

Enzyme activity (U/g) = Δ OD/ [15 min × 0.001 × (0.8 ml ÷ 20 ml) × 5 g].

In the formula, ΔOD is the change of absorption value of the experimental sample and blank sample; 15 min was the reaction time; 0.8 ml was the crude enzyme volume, 20 ml was the total crude enzyme volume, and 5 g was the sample weight.

Statistical analysis

All assays were repeated three times, and the results were expressed as means ± standard deviations. Statistical analyses were performed using a one-way analysis of variance, followed by the Duncan test ($P < 0.05$) using SPSS 26 (SPSS Inc., Chicago, IL). In multivariate statistical analysis, the Spearman correlation analysis was also conducted with SPSS 26. Orthogonal partial least squares (OPLS) analysis of pH, endogenous protease, TCA soluble peptide, and free amino acid were performed using SIMCA-P (Version 14.1, Umetrics, Sweden). The endogenous protease and pH were set as Y, and the TCA soluble peptide and free amino acid were set as X.

Results and discussion

Changes in nucleotide contents during pickling

All the nutrients necessary for the formation and development of duck embryos are present in duck eggs. Ducks manufacture all the genetic compounds in eggs during the initial stages of egg laying through the control of several genes (16). Endocytosis-mediated liver metabolite deposition in the yolk has been discovered to have a significant impact on the generation of duck yolk contents in female ducks (17). Metabolomics analysis of Muscovy duck liver tissue before and after oviposition (18) showed that the nucleotide metabolic pathway was one of the significant pathways. Furthermore, nucleotides are basic components of DNA and RNA, which are the precursor of nucleic acid synthesis in the body. As already stated, endocytosis allows nucleotides to reach the egg yolk and influence embryo development. Nucleotides in duck eggs, however, were rarely mentioned in previous studies. In this study (Table 1), five kinds of nucleotides, namely, AMP, CMP, GMP, IMP, and UMP, were detected in fresh duck egg yolk, suggesting that the nucleotides contained in yolk may be derived from the original accumulation (19). In studies on food flavors, nucleotides have been discovered to have a distinctive umami flavor. The umami nucleotides AMP, GMP, IMP, XMP, HxR (inosine), HX (hypoxanthine), and others were frequently found in food (20). Among them, AMP, GMP, IMP, and XMP are the main umami nucleotides in food, while HxR and HX are bitter substances (21). Excluding IMP, Table 1 demonstrates that changes in other nucleotide contents and total nucleotide contents primarily displayed a tendency in the direction of decline following small increases. During the pickling period, the contents of CMP, UMP, AMP, and GMP varied at different times, among which the peak value of UMP appeared in the third week, the peak value of CMP appeared in the first week, and the peak value of AMP and GMP appeared in the fourth week. The degradation of nucleotides during pickling may be related to the nucleotide change time. An earlier study discovered that temperature and pH at the time are associated with nucleotide breakdown (22). In addition, XMP was only found in fresh duck eggs. It was speculated that some nucleosides were formed due to the XMP transformation reaction in duck eggs (23). Generally speaking, flavor substances with TAV > 1 play a key role in the formation of the overall flavor profile in food, and the higher the TAV value is, the higher the influence of flavor substances on the overall flavor profile is (12). TAV of umami nucleotides in preserved egg yolk was all <1 when compared to each nucleotide (Table 1). The results indicated that individual nucleotide did not promote the umami taste of preserved egg yolk.

Changes in succinic acid contents during pickling

Succinic acid is a crucial umami component in food, as well as a key metabolic intermediate in the body. Istiqamah et al. (24) believed that succinic acid was a key umami substance in *Averrhoa bilimbi L*. Abundant succinic acid was also found in this study. Table 2 shows that after initially falling, the succinic acid content of preserved egg yolks rose. The succinic acid concentration considerably dropped between 0 and 21 days ($P < 0.05$). At this stage, alkaline pickling solution continuously penetrated the egg, and complex chemical changes took place in the egg yolk, which may promote the decarboxylation of succinic acid and lead to a decreasing trend (20). After 21 days, succinic acid content increased gradually ($P < 0.05$). The tendency for the succinic acid level to rise may result from the reactivation of specific metabolic enzymes (25). As can be seen from Table 2, the TAV of succinic acid in preserved egg yolk was far >1, indicating that succinic acid had a positive effect on the umami taste of preserved egg yolk. In addition, the coexistence of succinic acid with glutamic acid, arginine, glycine, and other amino acids could better enrich the umami taste of food (20).

Changes in free amino acid contents during pickling

Free amino acids are crucial flavor components of preserved egg yolks and the primary building blocks of volatile flavor compounds (26). The automatic amino acid analyzer was used to measure the free amino acids in preserved egg yolk during the pickling period (Table 2), and 15 different free amino acids were detected. Other free amino acids and the total amount of free amino acids declined gradually after pickling, with the exception of Asp. The content of Asp was not detected at 0–14 days but increased gradually at 21–35 days. Deng (26) determined free amino acids in preserved egg yolk by high-performance liquid chromatography and found that Asp always

TABLE 1 The changes of nucleotide contents in preserved egg yolk during pickling.

Name	Threshold (mg/100 g)	Content (mg/100 g)						TAV
		0 d	7 d	14 d	21 d	28 d	35 d	MAX
CMP	—	0.0060 ± 0.0005^{c}	0.012 ± 0.000^{a}	0.0086 ± 0.0011^{b}	0.0084 ± 0.0005^{b}	0.0096 ± 0.0023^{b}	0.0089 ± 0.0017^{b}	—
UMP	—	0.173 ± 0.004^{b}	0.343 ± 0.012^{ab}	0.432 ± 0.130^{ab}	0.46 ± 0.30^{ab}	0.35 ± 0.15^{ab}	0.28 ± 0.04^{a}	—
AMP	50	0.012 ± 0.003^{d}	0.020 ± 0.001^{ab}	0.014 ± 0.002^{bc}	0.012 ± 0.000^{bc}	0.023 ± 0.003^{a}	0.016 ± 0.004^{bc}	<0.0005
IMP	25	0.0094 ± 0.0063^{a}	0.002 ± 0.000^{b}	0.0027 ± 0.0006^{b}	0.0024 ± 0.0009^{b}	0.0027 ± 0.0013^{b}	0.0018 ± 0.0003^{b}	<0.0004
GMP	12.5	0.019 ± 0.008^{a}	0.021 ± 0.000^{a}	0.020 ± 0.002^{a}	0.020 ± 0.011^{a}	0.023 ± 0.003^{a}	0.017 ± 0.004^{a}	<0.0020
XMP	—	0.0087 ± 0.0070^{a}	ND	ND	ND	ND	ND	—
Total		0.22 ± 0.03^{a}	0.40 ± 0.01^{a}	0.48 ± 0.13^{a}	0.51 ± 0.31^{a}	0.41 ± 0.15^{a}	0.32 ± 0.05^{a}	

Values in the table are expressed as mean ± standard deviation ($n = 3$); Different superscripts of lowercase letters in the same line indicate significant difference between mean values (abc), $p < 0.05$.

existed in the pickling process. Therefore, it was speculated that the reason why the content of Asp was not detected during 0–14 days in this study might be individual differences in duck eggs. The increase in Asp concentration may be caused by the alkali-induced protein breakdown of egg yolks. Based on the effect of alkali infiltration, it was discovered that during the pickling process of preserved eggs, the high molecular weight protein in the preserved egg yolk was decomposed into small molecular components, such as free amino acids and short peptides (10). From the perspective of the change of the total free amino acids and TCA soluble peptide, the total free amino acid content decreased and the amount of TCA soluble peptide increased, which showed that a higher level of protein breakdown into tiny peptides during the entire pickling process. Moreover, deamination, decarboxylation, and Maillard reaction also occurred in the free amino acids generated during the whole pickling process (27). The contents of free amino acids decreased gradually. Except for Asp, the other 14 kinds of free amino acids had significant changes from 0 to 14 days ($P < 0.05$), while little changes after 14 days. Heavy metal compounds in preserved eggs mainly played a role in the hole blocking in the later stage of preserved eggs, reducing the exchange of internal and external substances (28) and various physical and chemical reactions. Therefore, it was conjectured that it may also be the reason that the decrease of free amino acid contents in the later pickling period (29). By comparing the TAV of free amino acids (Table 2), the TAV values of free amino acids in preserved egg yolk were all <1. The results indicated that individual free amino acid did not promote the umami taste of preserved egg yolk. In conclusion, although the TAV of umami nucleotide and umami amino acid were both <1. As important umami substances, they might work in concert with other ingredients to increase the umami taste of preserved egg yolk.

Change in pH value during pickling

Through pores and corrosion holes on the eggshell, lye slowly seeps inside eggs, changing the pH of the preserved egg yolk during pickling. As shown in Figure 1, the pH of the yolk increased significantly from 0 to 7 days ($P < 0.05$). After 7 days, the increasing trend in pH gradually slowed down and stabilized finally. The substantial pH fluctuations in the yolk during the early stages of pickling may be caused by the lye penetrating the egg more quickly. In addition, Selamassakul et al. (30) believed that the cleavage of hydrophobic amino acids and non-polar amino acids peptide bonds in macromolecular proteins into small peptides and free amino acids would increase the pH value. The protein structure of the yolk's protein was damaged by high pH, which may also have contributed to the yolk's growing pH (10). In the later pickling stage, as the outer yolk gradually hardened and formed a thicker solidified layer (10), the penetration rate of lye molecules gradually decreased and the rising trend of pH value gradually slowed down. Additionally, the acid in the yolk may also be the cause of the gradual pH change (such as acid amino acid). The pH in preserved egg yolk eventually stabilized at around 10.0. The internal and external material exchange gradually slowed down at this point, and the pH change tended to be stable as the solidification of the preserved egg yolk gradually spread to the interior and the heavy metal compounds in the pickling liquid were deposited in the eggshell (10).

Changes in TCA soluble peptide contents and endogenous protease activity during pickling

The term "TCA soluble peptide" refers to all tiny peptides (<10 kDa in molecular weight), free amino acids, and other nitrogen-containing non-protein molecules (31). Preserved egg yolk is rich in protein, mainly including high molecular weight proteins, such as low-density lipoprotein, high-density lipoprotein, active protein, and phosphoprotein (32). In addition to lipids, protein contents are the most important substance in preserved egg yolk (10). Investigating the alterations in proteinaceous substance is therefore necessary. In the process

TABLE 2 The contents of succinic acid and free amino acid in preserved egg yolk during pickling.

Class	Name	Threshold (mg/100 g)	Content (mg/100 g)						TAV
			0 d	7 d	14 d	21 d	28 d	35 d	MAX
Organic acid	Succinic acid	10.6	278.42 ± 2.06^{a}	273.22 ± 1.60^{b}	247.97 ± 3.79^{c}	238.70 ± 1.03^{d}	245.87 ± 0.85^{c}	280.87 ± 1.66^{a}	26.50
Free amino acids	Asp	100	ND	ND	ND	6.16 ± 0.3.9^{a}	5.97 ± 0.29^{a}	6.40 ± 0.28^{a}	0.06
	Thr	260	8.95 ± 0.33^{a}	7.98 ± 0.10^{b}	6.80 ± 0.68^{c}	5.80 ± 0.11^{d}	5.13 ± 0.72^{d}	5.38 ± 0.12^{d}	0.03
	Ser	150	8.06 ± 0.10^{a}	7.05 ± 0.06^{b}	6.13 ± 0.18^{c}	5.69 ± 0.15^{cd}	5.21 ± 0.68^{d}	5.48 ± 0.13^{d}	0.05
	Glu	30	17.45 ± 0.16^{a}	15.60 ± 0.14^{b}	14.81 ± 0.68^{c}	13.41 ± 0.15^{d}	12.85 ± 0.77^{d}	13.14 ± 0.29^{d}	0.58
	Gly	130	2.69 ± 0.02^{a}	2.49 ± 0.02^{b}	2.18 ± 0.14^{c}	2.10 ± 0.02^{cd}	2.01 ± 0.13^{cd}	2.10 ± 0.02^{d}	0.02
	Ala	60	5.87 ± 0.01^{a}	5.05 ± 0.05^{b}	4.63 ± 0.33^{c}	4.31 ± 0.03^{6c}	4.17 ± 0.15^{d}	4.60 ± 0.15^{d}	0.10
	Val	40	7.6 ± 0.07^{a}	7.23 ± 0.05^{a}	6.51 ± 0.43^{b}	5.93 ± 0.14^{c}	5.55 ± 0.46^{c}	5.83 ± 0.14^{c}	0.19
	Met	30	3.96 ± 0.01^{a}	3.58 ± 0.35^{a}	3.11 ± 0.19^{b}	2.81 ± 0.13^{bc}	2.48 ± 0.49^{bc}	2.76 ± 0.17^{c}	0.13
	Ile	90	5.74 ± 0.05^{a}	5.55 ± 0.04^{a}	5.10 ± 0.36^{b}	4.71 ± 0.22^{bc}	4.33 ± 0.41^{c}	4.62 ± 0.12^{c}	0.06
	Leu	50	22.46 ± 0.03^{a}	20.46 ± 0.15^{b}	18.90 ± 1.27^{c}	16.76 ± 0.52^{d}	15.33 ± 1.44^{d}	16.24 ± 0.47^{d}	0.45
	Tyr	–	9.98 ± 0.07^{a}	8.87 ± 0.04^{b}	8.35 ± 0.51^{b}	7.67 ± 0.29^{c}	6.93 ± 0.63^{cd}	7.37 ± 0.28^{d}	–
	Phe	90	20.17 ± 0.24^{a}	11.09 ± 0.22^{b}	12.41 ± 0.47^{b}	12.62 ± 0.10^{b}	12.65 ± 1.27^{b}	12.06 ± 1.98^{b}	0.22
	Lys	50	13.94 ± 0.05^{a}	12.0 ± 0.12^{b}	11.13 ± 0.62^{bc}	10.44 ± 0.30^{bc}	9.34 ± 1.50^{bc}	10.80 ± 1.39^{c}	0.28
	His	20	3.20 ± 0.02^{a}	2.82 ± 0.02^{b}	2.30 ± 2.03^{c}	2.10 ± 0.06^{c}	1.89 ± 0.14^{b}	1.77 ± 0.09^{b}	0.16
	Arg	50	10.56 ± 0.10^{a}	9.55 ± 0.08^{ab}	8.69 ± 0.84^{bc}	8.61 ± 0.44^{bc}	7.39 ± 0.68^{bc}	8.61 ± 1.45^{c}	0.21
	Total		140.72 ± 0.64^{a}	115.31 ± 6.97^{b}	111.06 ± 6.86^{bc}	107.06 ± 1.77^{bc}	100.60 ± 10.60^{bc}	106.92 ± 1.92^{c}	

Values in the table are expressed as mean ± standard deviation ($n = 3$); Different superscripts of lowercase letters in the same line indicate significant difference between mean values (abc), $p < 0.05$.

10.3389/fnut.2022.998448

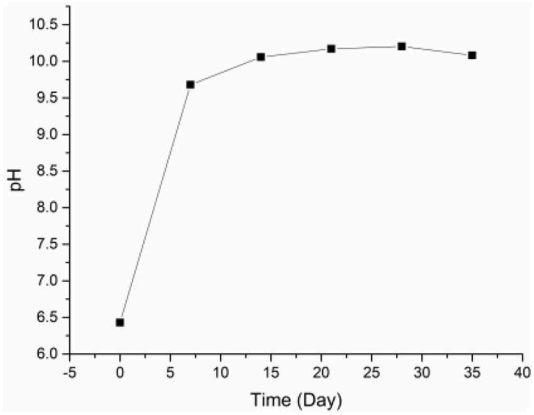

FIGURE 1
The changes of pH value in preserved egg yolks during pickling.

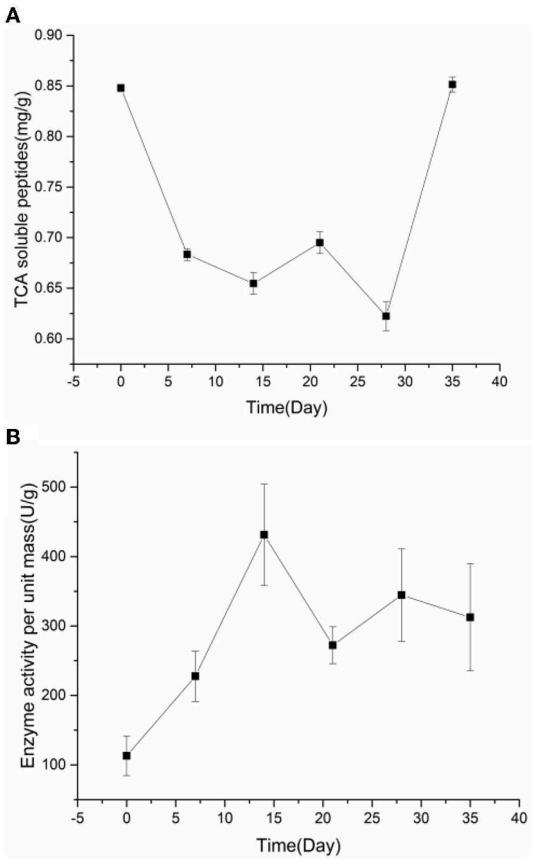

FIGURE 2
The changes of TCA soluble peptide contents **(A)** and the endogenous protease activity **(B)** in preserved egg yolk during pickling.

of pickling, the contents of TCA soluble peptides and free amino acids were changed due to some internal and external environment changes. To a certain extent, variations in the content of TCA soluble peptides could indicate the degree of protein degradation in egg yolk (33). The relationship between pH, endogenous protease, and proteinaceous substance in preserved egg yolk was explored to discover the interrelation of internal and external environmental changes on the protein of preserved egg yolk. Based on the fluctuation change of TCA soluble peptide contents and endogenous protease activity, the whole pickling process was analyzed in stages. Spearman correlation analysis shows the correlation of different influencing factors on the contents of proteinaceous substance in preserved egg yolk. OPLS is performed to further investigate relationships between multiple dependent variables and multiple independent variables. The OPLS-DA score scatter plots demonstrate a trend of intergroup separation about preserved egg yolk at different curing times. The problem of over-fitting is determined by 200 permutation tests. After model verification, principle components are selected the fitting indexes of independent variables (R2X) and the fitting index of the dependent variable (R2Y) demonstrate that principle components explained variations among X and Y variables. Among them, model index rankings are as follows: R2Y (cum) $>$ Q2 (cum) $>$ 0.5, R2Y (cum) - Q2 (cum) $<$ 0.3. The created model has significant predictive power and is stable and dependable. As shown by the results, there is a good agreement between model predictions and observed values.

As shown in Figure 2, TCA soluble peptide contents were significantly decreased from 0 to 14 days ($P < 0.05$), while the activity of endogenous protease was significantly increased ($P < 0.05$). When exploring the gel properties of preserved egg yolk, Yang et al. (10) found that the isoelectric point of amino acids in preserved egg yolk was similar to pH, particles in yolk would accumulate before 14 days. And then some high molecular weight crosslinked proteins would be produced, which reduced the contents of small peptides. The endogenous protease mainly promoted the increase of TCA soluble peptide and free amino acid contents, and pH inhibited the increase of TCA soluble peptide and free amino acid contents in the pickling period when pH changed significantly. As shown in Table 3, spearman correlation analysis showed that the changes of TCA soluble peptide and other free amino acids, apart from Phe, were significantly negatively correlated with the change of pH ($P < 0.001$). The changes in endogenous protease activity were negatively correlated with the changes of proteinaceous substance in preserved egg yolk (Table 4). It was also consistent with the result that, in contrast to the effect of endogenous protease on protein degradation, protein coagulation may play a dominant role in this phase. The OPLS of pH and TCA soluble peptide and free amino acid were as follows (Figure 3A): R2X = 0.996, R2Y = 1, and Q2 = 0.997; the soluble peptide and free amino acid model of endogenous protease and TCA were R2X = 0.928, R2Y = 0.76, and Q2 = 0.691 (Figure 4A). By comparing the data of the two models, R2 and Q2 were both

TABLE 3 Spearman correlation analysis between pH and proteinaceous substance in preserved egg yolk.

Proteinaceous substance	0–14 d	14–28 d	28–35 d
TCA-Soluble peptide	−0.936**	−0.436	−0.706
Asp	–	0.634	−0.667
Thr	−0.910**	−0.923**	−0.132
Ser	−0.910**	−0.889**	−0.261
Glu	−0.936**	−0.881**	−0.29
Gly	−0.910**	−0.427	−0.618
Ala	−0.940**	−0.607	−0.812*
Val	−0.910**	−0.829**	−0.319
Met	−0.910**	−0.769*	−0.191
Ile	−0.914**	−0.803**	−0.522
Leu	−0.910**	−0.889**	−0.319
Tyr	−0.910**	−0.838**	−0.145
Phe	−0.442	0.333	0.029
Lys	−0.910**	−0.829**	−0.058
His	−0.914**	−0.804**	0.058
Arg	−0.910**	−0.65	−0.464

*represents significant correlation ($P < 0.05$); **represents extremely significant correlation ($P < 0.01$).

TABLE 4 Spearman correlation analysis between endogenous protease activity and proteinaceous substance in preserved egg yolk.

Proteinaceous substance	0–14 d	14–28 d	28–35 d
TCA-Soluble peptide	−0.850**	−0.433	−0.29
Asp	–	−0.47	−0.486
Thr	−0.867**	0.433	0.406
Ser	−0.867**	0.383	0.371
Glu	−0.917**	0.533	−0.314
Gly	−0.867**	0.25	0.058
Ala	−0.912**	0.217	0.086
Val	−0.850**	0.467	0.429
Met	−0.833**	0.483	0.464
Ile	−0.828**	0.427	0.486
Leu	−0.833**	0.533	0.429
Tyr	−0.883**	0.25	0.086
Phe	−0.417	−0.217	−0.771
Lys	−0.833**	0.467	0.486
His	−0.845**	0.283	0.543
Arg	−0.833**	0.117	0.6

Values in the table are expressed as mean ± standard deviation ($n = 3$); Different superscripts of lowercase letters in the same line indicate significant difference between mean values, $P < 0.05$; ND: not detected; –: not found; ** represents extremely significant correlation ($P < 0.01$), * represents significant correlation ($P < 0.05$).

<0.5, and R2 was close to 1, indicating that the predicted values and measured values of the two models were consistent. The results showed that the changes in TCA soluble peptide and free amino acid contents also led to changes in pH value and endogenous protease activity. It was worth noting that it had a great impact on the change in pH value.

During the 14–28 days of the pickling period (Figure 2), the contents of TCA soluble peptide were significantly decreased ($P < 0.05$), while the activity of endogenous protease was slightly decreased. The lower endogenous protease activity may have been caused by the increased pH, which was between 10.0 and 10.2 at this stage. Cathepsin and aminopeptidase are the two known egg yolk proteases (34). Cathepsin exists in lysosomes and is mainly activated in acidic environments (35). The alkaline environment inhibits its activity. There are many kinds of aminopeptidase, and its suitable pH range is mainly neutral or alkaline. For example, the suitable pH of leucine aminopeptidase is about 9.5 (8). However, the pH of egg yolk in the later pickling period was stable at about 10–10.2. Therefore, it may be hypothesized that neutral or alkaline endogenous protease contributed in some way to enhancing protein degradation in egg yolk at 0–14 days with the rise in pH. After 14 days, when the pH of egg yolk remained in a relatively steady range, endogenous protease activity was inhibited and protein breakdown was reduced or even stopped. Through Spearman correlation analysis, the changes of proteinaceous substance in preserved egg yolk were significantly negatively correlated with the changes in pH value ($P < 0.001$; Table 3), and positively correlated with the changes in endogenous protease activity (Table 4). This result showed that an alkaline environment still played a leading role in the change of proteinaceous substance in preserved egg yolk. The OPLS of pH and TCA soluble peptide and free amino acid were R2X = 0.883, R2Y = 0.903, and Q2 = 0.704 (Figure 3B). The soluble peptide and free amino acid model of endogenous protease and TCA was R2X = 0.942, R2Y = 0.728, and Q2 = 0.359 (there was a problem of over-fitting in the result) (Figure 4B). At this stage, the changes of internal substances of preserved egg yolk also affected the changes of pH value and endogenous protease activity.

From 28 to 35 days of the pickling period (Figure 2), the contents of TCA soluble peptide showed a significantly increased trend ($P < 0.05$), while the activity of endogenous protease remained in a low range. Through Spearman correlation analysis, it was found that the change of proteinaceous substance in preserved egg yolk had the same trend as 14–28 days. According to the aforementioned findings, the endogenous protease's contribution to this pickling stage was still little when compared to that of the preceding pickling stage. At this stage, the pH was stabled in a different range from the isoelectric point, so that the protein in egg yolk was no longer in a condensed state, and the strong alkaline internal environment

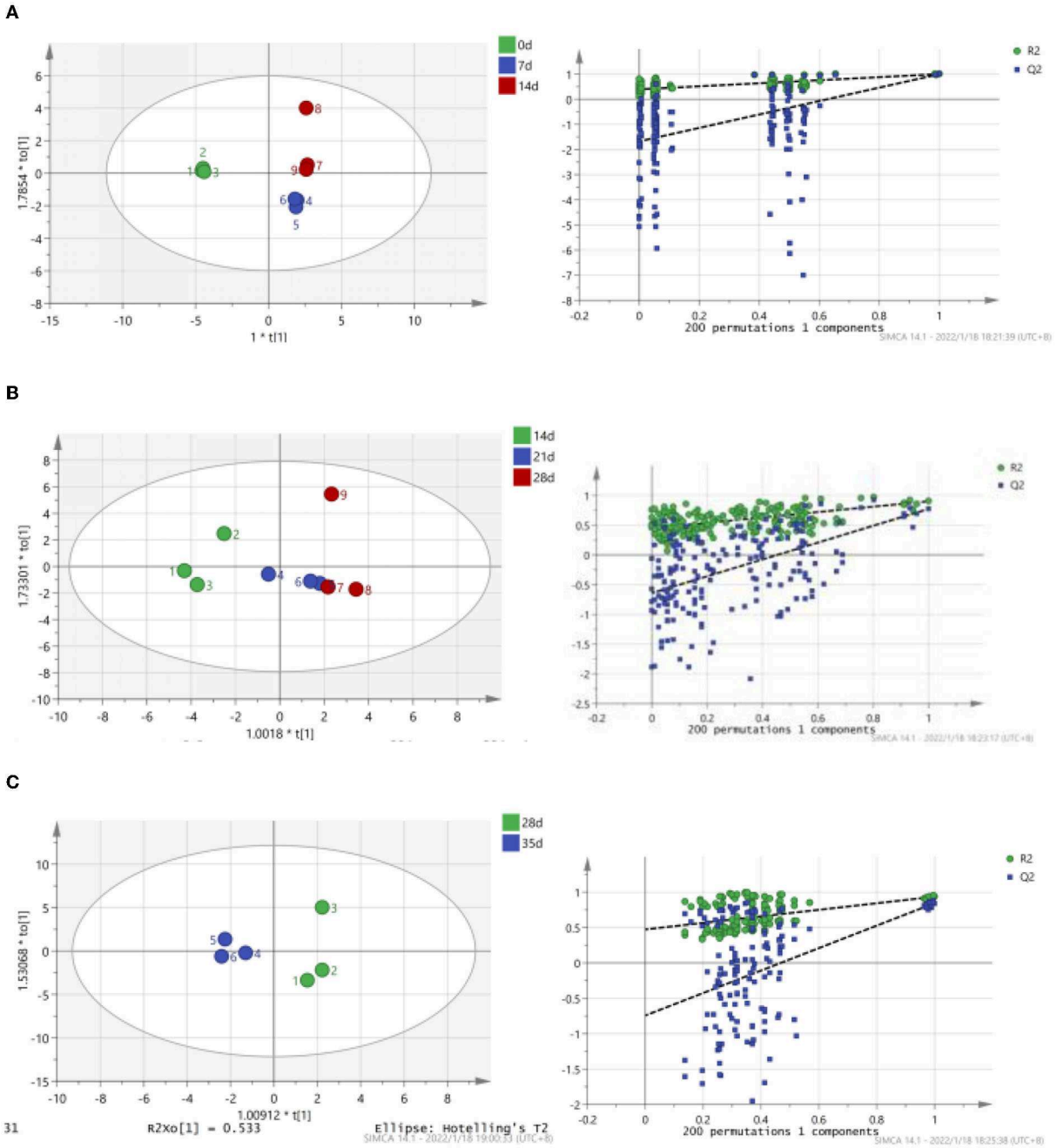

FIGURE 3
Correlation between endogenous pH, TCA soluble peptide and free amino acid contents in preserved egg yolk at different pickling stages (OPLS score chart and replacement test chart of preserved egg yolk at different pickling stages). **(A)**: 0–14 d; **(B)**: 14–28 d; **(C)**: 28–35 d.

caused the degradation of large molecules of protein to form small peptides and free amino acids. Therefore, it could lead that the contents of TCA soluble peptide showed a significant upward trend. Compared to the OPLS, which were established by analyzing the interaction between pH, endogenous protease, and TCA soluble peptides and free amino acid (Figures 3C, 4C), it was found that the models of pH and TCA soluble peptide and free amino acid were R2X = 1, R2Y = 1, Q2 = 1. The model of endogenous protease, TCA soluble peptide, and free amino acid was R2X = 0.88, R2Y = 0.534, and Q2 = −0.141 (there was a problem of over-fitting in the result). The results showed that, at this stage, the changes of proteinaceous

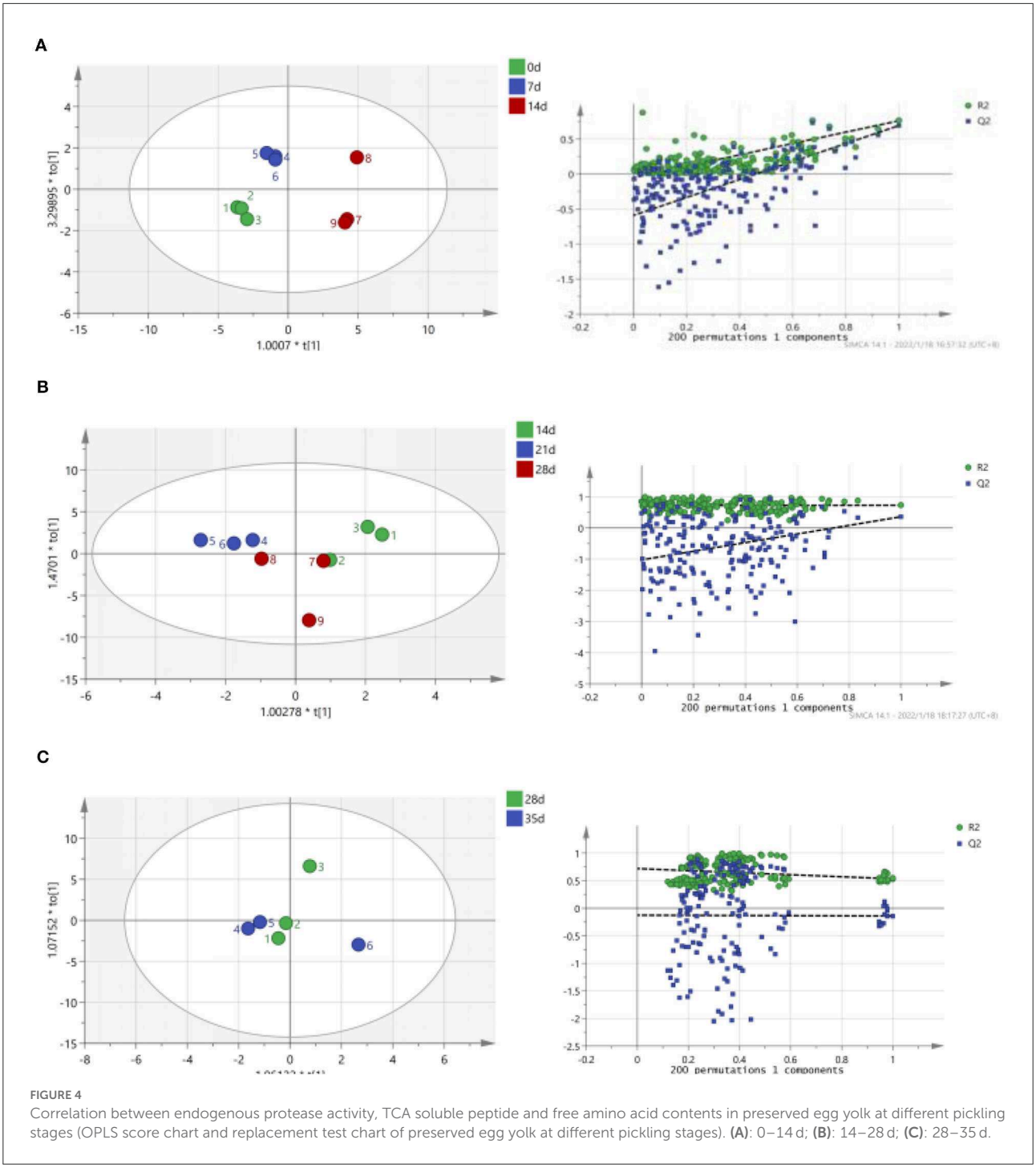

FIGURE 4
Correlation between endogenous protease activity, TCA soluble peptide and free amino acid contents in preserved egg yolk at different pickling stages (OPLS score chart and replacement test chart of preserved egg yolk at different pickling stages). **(A)**: 0–14 d; **(B)**: 14–28 d; **(C)**: 28–35 d.

substance in preserved egg yolk only affected the changes in pH.

According to the study's findings, endogenous protease activity and pH changes were two factors that affected how quickly proteins degraded. In addition, Table 2 shows that the number of free amino acids in preserved egg yolk dropped. This means that preserved egg yolk included a certain amount of tiny peptides, some of which may have umami properties and contribute to the umami flavor of preserved egg yolk.

Conclusion

In this work, the umami substance variations in preserved egg yolk were precisely identified, and the contributing variables

to the content changes were thoroughly investigated. The umami flavor of preserved egg yolks was significantly influenced by succinic acid, according to the TAV data. Correlation analysis showed that, before 14 days, endogenous protease and pH played an important role in the degradation and agglutination of protein molecules in preserved egg yolk respectively. When pH was steady in a higher range after 14 days, its ability to act changed to degradation. The contents of total free amino acids in preserved egg yolk decreased, while the contents of TCA soluble peptide increased significantly. Therefore, in addition to amino acids, nucleotides, and succinic acid, the umami taste of preserved egg yolk may have been created by umami peptides found in TCA soluble peptides. To improve the composition of umami substances in preserved egg yolk, umami peptides in the preserved egg yolk will be further studied.

Data availability statement

The original contributions presented in the study are included in the article/supplementary material, further inquiries can be directed to the corresponding author.

Author contributions

BG: investigation, formal analysis, data curation, and writing—original draft. XH, YT, HX, RL, HL, and TH: writing—review and editing. YZ: conceptualization, funding acquisition, project administration, validation, and writing—review and editing. All authors contributed to the article and approved the submitted version.

Funding

We gratefully acknowledge the financial support provided by the National Natural Science Foundation of China (Grant Nos. 32060551, 31871832, and 31760439).

Conflict of interest

The authors declare that the research was conducted in the absence of any commercial or financial relationships that could be construed as a potential conflict of interest.

Publisher's note

All claims expressed in this article are solely those of the authors and do not necessarily represent those of their affiliated organizations, or those of the publisher, the editors and the reviewers. Any product that may be evaluated in this article, or claim that may be made by its manufacturer, is not guaranteed or endorsed by the publisher.

References

1. Wang Y, Xiong C, Luo W, Li J, Tu Y, Zhao Y. Effects of packaging methods on the quality of heavy metals-free preserved duck eggs during storage. *Poultry Sci.* (2021) 100:101051. doi: 10.1016/j.psj.2021.101051

2. Batool Z, Hu G, Xinyue H, Wu Y, Fu X, Cai Z, et al. A comprehensive review on functional properties of preserved eggs as an excellent food ingredient with anti-inflammatory and anti-cancer aspects. *Food Biosci.* (2021) 44:101347. doi: 10.1016/j.fbio.2021.101347

3. Sun NX, Liu HP, Wen YH, Yuan W, Wu YR, Gao J, et al. Comparative study on Tianjin and Baiyangdian preserved eggs pickled by vacuum technology. *J Food Process Preserv.* (2020). 44:14405. doi: 10.1111/jfpp.14405

4. Zhao Y, Yao Y, Xu M, Wang S, Wang X, Tu Y. Simulated gastrointestinal digest from preserved egg white exerts anti-inflammatory effects on Caco-2 cells and a mouse model of DSS-induced colitis. *J Funct Foods.* (2017) 35:655–65. doi: 10.1016/j.jff.2017.06.028

5. Ren Y, Huang X, Aheto JH, Wang C, Ernest B, Tian X, et al. Application of volatile and spectral profiling together with multimode data fusion strategy for the discrimination of preserved eggs. *Food Chem.* (2021) 343:12851. doi: 10.1016/j.foodchem.2020.128515

6. Luo W, Xue H, Xiong C, Li J, Tu Y, Zhao Y. Effects of temperature on quality of preserved eggs during storage. *Poult Sci.* (2020) 99:3144–57. doi: 10.1016/j.psj.2020.01.020

7. Wang H, Xu J, Liu Q, Chen Q, Sun F, Kong B. Interaction between protease from Staphylococcus epidermidis and pork myofibrillar protein: flavor and molecular simulation. *Food Chem.* (2022) 386:132830. doi: 10.1016/j.foodchem.2022.132830

8. Rivas-Canedo A, Martinez-Onandi N, Gaya P, Nunez M, Picon A. Effect of high-pressure processing and chemical composition on lipid oxidation, aminopeptidase activity and free amino acids of Serrano dry-cured ham. *Meat Sci.* (2021) 172:108349. doi: 10.1016/j.meatsci.2020.108349

9. Lin H, Bi X, Zhou B, Fang J, Liu P, Ding W, et al. Microbial communities succession and flavor substances changes during Pixian broad-bean paste fermentation. *Food Biosci.* (2021) 42:101053. doi: 10.1016/j.fbio.2021.101053

10. Yang Y, Zhao Y, Xu M, Wu N, Yao Y, Du H, et al. Changes in physico-chemical properties, microstructure and intermolecular force of preserved egg yolk gels during pickling. *Food Hydrocoll.* (2019) 89:131–42. doi: 10.1016/j.foodhyd.2018.10.016

11. Gao B, Hu X, Li R, Zhao Y, Tu Y, Zhao Y. Screening of characteristic umami substances in preserved egg yolk based on the electronic tongue and UHPLC-MS/MS. *LWT Food Sci. Technol.* (2021) 152:112396. doi: 10.1016/j.lwt.2021.112396

12. Zhang N, Wang W, Li B, Liu Y. Non-volatile taste active compounds and umami evaluation in two aquacultured pufferfish (*Takifugu obscurus* and *Takifugu rubripes*). *Food Biosci.* (2019) 32:100468. doi: 10.1016/j.fbio.2019.100468

13. GB/T 5009.47-2003. (2021). *Chinese Standard GB/T 5009.47-2003 in Method for Analysis of Hygienic Standard of Egg and Egg Products*. Beijing: The Standard Press of PR China.

14. Sriket C, Benjakul S, Visessanguan W, Hara K, Yoshida A. Retardation of post-mortem changes of freshwater prawn (*Macrobrachium rosenbergii*) stored in ice by legume seed extracts. *Food Chem.* (2012) 135:571–9. doi: 10.1016/j.foodchem.2012.04.121

15. Lu X, Bai Y, Pang Y, Jiang H, Liu X. Effects of storage temperature on texture, endogenous enzymes and water content of Siphonidae and Hymenoptera. *Sci Technol Food Indus.* (2020) 41:281–7 (in Chinese)

16. D'Alessandro A, Righetti PG, Fasoli E, Zolla L. The egg white and yolk interactomes as gleaned from extensive proteomic data. *J Proteomics.* (2010) 73:1028–42. doi: 10.1016/j.jprot.2010.01.002

17. Burley RW, Evans AJ, Pearson JA. Molecular aspects of the synthesis and deposition of hens' egg yolk with special reference to low density lipoprotein. *Poult Sci.* (1993) 72:850–5. doi: 10.3382/ps.0720850

18. Zhu W, Yang W, Wei C, Liu L, Geng Z, Chen X. Comparative analysis of untargeted metabolomics in liver tissues of Muscovy ducks during prelaying and laying. *J China Agric Univ.* (2020) 25:76–85 (in Chinese)

19. Kamel NF, Hady MM, Ragaa NM, Mohamed FF. Effect of nucleotides on growth performance, gut health, and some immunological parameters in broiler chicken exposed to high stocking density. *Livest Sci.* (2021) 253:104703. doi: 10.1016/j.livsci.2021.104703

20. Liu C, Ji W, Jiang H, Shi Y, He L, Gu Z, et al. Comparison of biochemical composition and non-volatile taste active compounds in raw, high hydrostatic pressure-treated and steamed oysters Crassostrea hongkongensis. *Food Chem.* (2021) 344:128632. doi: 10.1016/j.foodchem.2020.128632

21. Guo H, Yang F, Gao B, Yu D, Xu Y, Jiang Q, Xiao W. Analysis on taste difference of Eriocheir sinensis in different cultured waters. *Prog Fish Sci.* (2021) 2021:1–17 (in Chinese)

22. Rotola-Pukkila M, Yang B, Hopia A. The effect of cooking on umami compounds in wild and cultivated mushrooms. *Food Chem.* (2019) 278:56–66. doi: 10.1016/j.foodchem.2018.11.044

23. Dong M, Qin L, Ma L, Zhao Z, Du M, Kunihiko K, et al. Postmortem nucleotide degradation in turbot mince during chill and partial freezing storage. *Food Chem.* (2020) 311:125900. doi: 10.1016/j.foodchem.2019.125900

24. Istiqamah A, Lioe HN, Adawiyah DR. Umami compounds present in low molecular umami fractions of asam sunti—a fermented fruit of *Averrhoa bilimbi* L. *Food Chem.* (2019) 270:338–43. doi: 10.1016/j.foodchem.2018.06.131

25. Hu S, Feng X, Huang W, Ibrahim SA, Liu Y. Effects of drying methods on non-volatile taste components of Stropharia rugoso-annulata mushrooms. *LWT Food Sci Technol.* (2020) 127:109428. doi: 10.1016/j.lwt.2020.109428

26. Deng W. *Changes of Amino Acids and Fatty Acids in Preserved Egg Processing and the Role of Forming Preserved Egg Flavor Master*. Nanchang: NanChang University (2013).

27. Poulsen MW, Hedegaard RV, Andersen JM, de Courten B, Bugel S, Nielsen J, et al. Advanced glycation endproducts in food and their effects on health. *Food Chem Toxicol.* (2013) 60:10–37. doi: 10.1016/j.fct.2013.06.052

28. Renzone G, Novi G, Scaloni A, Arena S. Monitoring aging of hen egg by integrated quantitative peptidomic procedures. *Food Res Int.* (2021) 140:110010. doi: 10.1016/j.foodres.2020.110010

29. Cao D, Feng F, Xiong C, Li J, Xue H, Zhao Y, et al. Changes in lipid properties of duck egg yolks under extreme processing conditions. *Poult Sci.* (2021) 100:101140. doi: 10.1016/j.psj.2021.101140

30. Selamassakul O, Laohakunjit N, Kerdchoechuen O, Ratanakhanokchai K. A novel multi-biofunctional protein from brown rice hydrolysed by endo/endo-exoproteases. *Food Funct.* (2016) 7:2635–44. doi: 10.1039/c5fo01344e

31. Ketnawa S, Rawdkuen S. Application of bromelain extract for muscle foods tenderization. *Food Nutr Sci.* (2011) 02, 393–401. doi: 10.4236/fns.2011.25055

32. Xu L, Gu L, Su Y, Chang C, Wang J, Dong S, et al. Impact of thermal treatment on the rheological, microstructural, protein structures and extrusion 3D printing characteristics of egg yolk. *Food Hydrocoll.* (2019) 100:105399. doi: 10.1016/j.foodhyd.2019.105399

33. Saengsuk N, Laohakunjit N, Sanporkha P, Kaisangsri N, Selamassakul O, Ratanakhanokchai K, et al. Physicochemical characteristics and textural parameters of restructured pork steaks hydrolysed with bromelain. *Food Chem.* (2021) 361:130079. doi: 10.1016/j.foodchem.2021.130079

34. Mann K, Mann M. The chicken egg yolk plasma and granule proteomes. *Proteomics.* (2008) 8:178–91. doi: 10.1002/pmic.200700790

35. Di Spiezio A, Marques ARA, Schmidt L, Thiessen N, Gallwitz L, Fogh J, et al. Analysis of cathepsin B and cathepsin L treatment to clear toxic lysosomal protein aggregates in neuronal ceroid lipofuscinosis. *Biochim Biophys Acta (BBA).* (2021) 1867:166205. doi: 10.1016/j.bbadis.2021.166205

36. Liu H, Ma J, Pan T, Suleman R, Wang Z, Zhang D. Effects of roasting by charcoal, electric, microwave and superheated steam methods on (non)volatile compounds in oyster cuts of roasted lamb. *Meat Sci.* (2021) 172:108324. doi: 10.1016/j.meatsci.2020.108324

frontiers | Frontiers in Nutrition

TYPE Correction
PUBLISHED 24 October 2022
DOI 10.3389/fnut.2022.1064331

OPEN ACCESS

APPROVED BY
Frontiers Editorial Office,
Frontiers Media SA, Switzerland

*CORRESPONDENCE
Yan Zhao
zhaoyan@jxau.edu.cn

SPECIALTY SECTION
This article was submitted to Food Chemistry, a section of the journal Frontiers in Nutrition

RECEIVED 08 October 2022
ACCEPTED 12 October 2022
PUBLISHED 24 October 2022

CITATION
Gao B, Hu X, Xue H, Li R, Liu H, Han T, Tu Y and Zhao Y (2022) Corrigendum: The changes of umami substances and influencing factors in preserved egg yolk: pH, endogenous protease, and proteinaceous substance. *Front. Nutr.* 9:1064331. doi: 10.3389/fnut.2022.1064331

Corrigendum: The changes of umami substances and influencing factors in preserved egg yolk: pH, endogenous protease, and proteinaceous substance

Binghong Gao[1,2], Xiaobo Hu[3], Hui Xue[2], Ruiling Li[2], Huilan Liu[2], Tianfeng Han[2], Yonggang Tu[1] and Yan Zhao[1]*

[1]Jiangxi Key Laboratory of Natural Products and Functional Food, Jiangxi Agricultural University, Nanchang, China, [2]Engineering Research Center of Biomass Conversion, Ministry of Education, Nanchang University, Nanchang, China, [3]State Key Laboratory of Food Science and Technology, Nanchang University, Nanchang, China

KEYWORDS

preserved egg yolk, umami, succinic acid, OPLS, Spearman's correlation

A corrigendum on

The changes of umami substances and influencing factors in preserved egg yolk: pH, endogenous protease, and proteinaceous substance

by Gao, B., Hu, X., Xue, H., Li, R., Liu, H., Han, T., Tu, Y., and Zhao, Y. (2022). *Front. Nutr.* 9:998448. doi: 10.3389/fnut.2022.998448

In the published article, there was an error in affiliation(s).

Instead of "Binghong Gao[1], Xiaobo Hu[2], Hui Xue[1], Ruiling Li[1], Huilan Liu[1], Tianfeng Han[1], Yonggang Tu[3] and Yan Zhao[3]*

[1]Engineering Research Center of Biomass Conversion, Ministry of Education, Nanchang University, Nanchang, China

[2]State Key Laboratory of Food Science and Technology, Nanchang University, Nanchang, China

[3]Jiangxi Key Laboratory of Natural Products and Functional Food, Jiangxi Agricultural University, Nanchang, China," it should be

"Binghong Gao[1,2], Xiaobo Hu[3], Hui Xue[2], Ruiling Li[2], Huilan Liu[2], Tianfeng Han[2], Yonggang Tu[1] and Yan Zhao[1]*

[1]Jiangxi Key Laboratory of Natural Products and Functional Food, Jiangxi Agricultural University, Nanchang, China

[2]Engineering Research Center of Biomass Conversion, Ministry of Education, Nanchang University, Nanchang, China
[3]State Key Laboratory of Food Science and Technology, Nanchang University, Nanchang, China".

The authors apologize for this error and state that this does not change the scientific conclusions of the article in any way. The original article has been updated.

Publisher's note

frontiers | Frontiers in Nutrition

TYPE Original Research
PUBLISHED 28 September 2022
DOI 10.3389/fnut.2022.1015924

OPEN ACCESS

EDITED BY
Gang Fan,
Huazhong Agricultural University, China

REVIEWED BY
Aurea K. Ramírez-Jiménez,
Monterrey Institute of Technology and Higher Education (ITESM), Mexico
Gang Jin,
Ningxia University, China

*CORRESPONDENCE
Xuedan Cao
xuedancao@outlook.com
Xiugui Fang
fangxg640103@163.com

SPECIALTY SECTION
This article was submitted to Food Chemistry, a section of the journal Frontiers in Nutrition

RECEIVED 10 August 2022
ACCEPTED 15 September 2022
PUBLISHED 28 September 2022

CITATION
Cao X, Ru S, Fang X, Li Y, Wang T and Lyu X (2022) Effects of alcoholic fermentation on the non-volatile and volatile compounds in grapefruit (C*itrus paradisi* Mac. cv. Cocktail) juice: A combination of UPLC-MS/MS and gas chromatography ion mobility spectrometry analysis.
Front. Nutr. 9:1015924.
doi: 10.3389/fnut.2022.1015924

Effects of alcoholic fermentation on the non-volatile and volatile compounds in grapefruit (C*itrus paradisi* Mac. cv. Cocktail) juice: A combination of UPLC-MS/MS and gas chromatography ion mobility spectrometry analysis

Xuedan Cao*, Shuijiang Ru, Xiugui Fang*, Yi Li, Tianyu Wang and Xiamin Lyu

Zhejiang Citrus Research Institute, Taizhou, China

Grapefruit has attracted much attention as a functional fruit, of which "Cocktail" is a special variety with low acidity. The present study aimed to investigate the effects of alcoholic fermentation on the non-volatile and volatile compounds of "Cocktail" grapefruit juice. To analyze, a non-targeted metabolomics method based on UPLC-MS/MS and volatiles analysis using GC-IMS were performed. A total of 1015 phytochemicals were identified, including 296 flavonoids and 145 phenolic acids, with noticeably increasing varieties and abundance following the fermentation. Also 57 volatile compounds were detected, and alcoholic fermentation was effective in modulating aromatic profiles of grapefruit juice, with terpenes and ketones decreasing, and alcohols increasing together with esters. Citraconic acid and ethyl butanoate were the most variable non-volatile and volatile substances, respectively. The results provide a wealth of information for the study of "Cocktail" grapefruit and will serve as a valuable reference for the large-scale production of grapefruit fermented juice in the future.

KEYWORDS

GC-IMS, metabolomics, grapefruit juice, alcoholic fermentation, flavonoids

Introduction

In recent years, fermented fruit juice has gained more attention due to its positive effect on human health (1–3). As an alternative to conventional thermal treatments, fermentation allows a low-energy consumption in the process and can affect the phytochemical composition and biological activity of fruit juice owing to the role of microbes (2, 4). As previously reported, lactic acid or alcoholic fermentation had a great impact on the bioactive compounds in citrus juices, such as flavonoids, phenolic acids, limonoids, carotenoids and vitamin A values (5). Additionally, alcoholic fermentation causes a variation in flavor substances, such as essential oils, sugars, lipids, ascorbic acid, and sulfur-containing compounds (6). Although existing studies suggest that alcoholic fermentation can alter the phytochemical composition of citrus juice and affects its function and flavor, however, they often focus on a small number of compounds and the systematic study of all components is needed.

The grapefruit (*Citrus paradisi* Mac.) originated in Barbados in the 18th century via crossing naturally between the pomelo (*Citrus maxima* Burm) and the sweet orange [*Citrus sinensis* (L.) Osbeck], which is now widely distributed in tropical and subtropical regions of the world (7). Grapefruit encompassed various bioactive chemicals like flavonoids, limonoids, carotenoids, organic acids, pectin, fiber, and folic acid (8–11). These bioactive substances endow grapefruit with important biomedical activities such as anti-inflammatory, antibacterial, anticancer, chemopreventive, and blood sugar regulation effects (12–14). Among different grapefruit varieties, "Cocktail" is a special one due to its higher sugar content and lower acidity in comparison with others (15). These properties make "Cocktail" grapefruit a promising raw material for fermented juice production. However, to our knowledge, research on "Cocktail" grapefruit juice and its fermented beverages has not been well studied. In particular, the effect of alcoholic fermentation on the non-volatile and volatile profiles of "Cocktail" grapefruit juice has not been reported.

Metabolomics is a comprehensive analysis, comprising the identification and quantification of as many metabolites as possible in a biological system or a food system (16). The application of this methodology is helpful to understand the relationship between food quality and processing. Wang et al. (17) have employed UPLC-MS/MS and gas chromatography-mass spectrometry (GC-MS) based metabolomics to explore the effects of high-hydrostatic-pressure and high-temperature treatments on the metabolic profiling of tomato juice. Citrus juice, in contrast, has more complex metabolic substances associated with human health that should be of well concern. Goh et al. (18) have applied LC-QTOF/MS to analyze non-volatile compounds in Hongxin and Shatian pomelo juices, and eight dominant compounds were identified and quantified. Likewise, Deng et al. (19) have identified and quantified 14 compounds in grapefruit using UHPLC system. These targeted approaches are more limited as reaching a relatively small number of metabolites, which is unsuitable for the overall metabolites analysis. By contrast, untargeted approach is a more common choice since it covers a wider range of molecules. As for volatile compounds, GC-MS and gas chromatography ion mobility spectrometry (GC-IMS) are extensively analysis tools. Comparatively, GC-IMS is less time-cost due to its ultra-high sensitivity and fast analytical speed (20). Brendel et al. (21) has achieved the differentiation of grapefruit juice and orange juice samples by their volatile profiles using a GC-MS-IMS system, and GC-IMS was found to be more sensitive in the identification of low-abundance volatiles compared with GC-MS. Therefore, GC-IMS technique has recently been applied to detect flavor compounds in fermented products, such as fermented Douchi (22) and alcoholic beverages like cherry wine (23). As a consequence, untargeted methods and GC-IMS are preferred for the overall study of non-volatile and volatile compounds of fruit juices. However, to our knowledge, few studies have adopted the integration of these two techniques to investigate the phytochemical composition and volatile compounds in grapefruit juice and its fermented juice.

In this study, metabolomics techniques based on UPLC-MS/MS and volatiles analysis using GC-IMS were performed to comprehensively analyze the variation of the metabolites and volatile compounds during grapefruit juice fermentation. The aim was to investigate the potential effects of alcoholic fermentation on the non-volatile and volatile substances of "Cocktail" grapefruit juices, which may contribute to the development of "Cocktail" grapefruit products.

Materials and methods

Chemical reagents

Gradient grades of methanol, acetonitrile, and formic acid were purchased from Merck Company (Germany). The internal standard 2-chlorophenylalanine was bought from J&K Chemicals Co., Ltd. (United States). Ultrapure water used was produced by a Millipore Milli-Q system (Millipore, Bedford, MA, United States). Pectinase (10000 U/g) and active dry yeast (*Saccharomyces cerevisiae* BV818) were provided by Jiangsu Ruiyang Biotech Co., Ltd. (Wuxi, China) and Angel Yeast Co., Ltd. (Yichang, China), respectively.

Preparation of grapefruit juice and grapefruit fermented juice

Six-year-old grapefruit trees (*Citrus paradisi* Mac. cv. Cocktail) with similar growth and fruit-bearing capacity were selected, which were grown in the Zhejiang Citrus Research Institute experimental orchard located in Taizhou city, Zhejiang provinces, China (~28°64′N, 121°16′E). Fruits were randomly harvested from these selected trees at commercial maturity

during November to December, and immediately transported to the laboratory. A total of 100 kilograms of fruits with no physical injuries or infections were selected, and then the peels and seeds were removed manually. The grapefruit juice (FJ) sample was obtained by pulp homogenizing with a blender (FPM256, Kenwood, United Kingdom) and filtering through an 80-mesh filter, and stored at −80°C.

For fermentation, the fresh grapefruit juice was treated with 0.05% of pectolytic enzyme and kept at 45° for 1.5 h. After naturally cooled, the juice was inoculated with 200 mg/L of the yeast after the strain was activated in 37° water for 30 mins. The fermentation process lasted for 14 days using 25 L unsealed stainless steel containers, and the temperature was maintained between 18° and 20° (24). The grapefruit fermented juice (FMT) was obtained by discarding the lees and stored at −80°. Fermentation experiments were carried out in triplicate. Then the basic parameters of FJ and FMT were measured according to Castello et al. (1), with sugars and organic acids determined by HPLC methods (25). The quality parameters of FJ and FMT are presented in **Table 1**.

TABLE 1 Quality parameters of grapefruit juice (FJ) and grapefruit fermented juice (FMT).

Parameters	FJ	FMT
pH	3.62 ± 0.01^{b}	3.81 ± 0.01^{a}
Titratable acidity (g citric acid/100 mL)	0.85 ± 0.02^{a}	0.54 ± 0.01^{b}
Total soluble solids (∘Brix)	10.82 ± 0.31^{a}	4.37 ± 0.11^{b}
Alcohol (% v/v)	0.38 ± 0.03^{b}	6.01 ± 0.18^{a}
Sugars (mg/g)		
Glucose	20.99 ± 1.05^{a}	0.29 ± 0.01^{b}
Fructose	27.19 ± 1.08^{a}	1.94 ± 0.21^{b}
Sucrose	59.42 ± 2.00^{a}	nd^{b}
Organic acids (mg/g)		
Oxalic	0.06 ± 0.01^{a}	nd^{b}
Tartaric	0.52 ± 0.03^{a}	0.55 ± 0.03^{a}
Malic	1.63 ± 0.17^{b}	2.01 ± 0.14^{a}
Shikimic	0.07 ± 0.01^{a}	0.02 ± 0.01^{b}
Lactic	nd^{b}	0.23 ± 0.02^{a}
Acetic	nd^{b}	0.10 ± 0.04^{a}
Citric	5.04 ± 0.26^{a}	4.61 ± 0.24^{a}
Quinic	nd	nd
Fumaric	nd	nd

Values are expressed as mean ($n = 3$) ± standard deviation (SD) and "n.d." indicated no detection. Different letters in the same row represent a significant difference at $p < 0.05$.

Metabolites analysis of the grapefruit juice and grapefruit fermented juice by UPLC-MS/MS

Metabolites extraction

After being thawed from the refrigerator at −80°C, the FJ and FMT samples were mixed with vortex for 10 s. As FMT samples contained much lower solid contents than FJ samples, the following extraction processes were slightly different in the two groups. For FJ, 9 mL sample was placed in a 50 mL centrifuge tube and immersed in liquid nitrogen for freezing, after which the sample was completely lyophilized using a SCIENTZ-100F lyophilizer (Xinzhi 100F, Ningbo, China). Then 50 mg of lyophilized FJ sample was taken into a 2 mL EP tube, and 1200 μL of 70% of methanol (containing 2-chlorophenylalanine as internal standard) was added for the extraction. As for FMT samples, 3 mL of thawed sample was taken for lyophilization as above, and then 200 μL extraction solution was added. Afterward, both FJ and FMT samples extraction procedure was performed by vortexing the sample for 15 min and centrifuging (12000 r/min, 4°C) for 3 min. The supernatants were filtered with a 0.22 μm membrane and stored at −80° for analysis. Note that the obtained data of the two groups were corrected according to the corresponding volume before we performed the comparison.

UPLC-MS/MS condition

The sample extracts were analyzed using a UPLC-MS/MS system (UPLC, SHIMADZU Nexera X2; MS, Applied Biosystems 4500 Q TRAP). The analytical conditions were as follows: for UPLC, the Agilent SB-C18 column (1.8 μm, 2.1 mm × 100 mm) was used and the column oven was set to 40°C. The mobile phase consisted of solvent A, pure water with 0.1% formic acid, and solvent B, acetonitrile with 0.1% formic acid. Sample separation was performed with a gradient program that employed the starting conditions of 95% A and 5% B. Within 9 min, a linear gradient to 5% A, 95% B was programmed, and a composition of 5% A, 95% B was kept for 1 min. Subsequently, a composition of 95% A and 5.0% B was adjusted within 1.1 min and kept for 2.9 min. The flow velocity was set as 0.35 mL/min and the injection volume was 4 μL. The effluent was alternatively connected to an ESI-triple quadrupole-linear ion trap (QTRAP)-MS.

ESI-Q TRAP-MS/MS condition: LIT and triple quadrupole (QQQ) scans were acquired on a triple quadrupole-linear ion trap mass spectrometer (Q TRAP), AB4500 Q TRAP UPLC-MS/MS System, equipped with an ESI Turbo Ion-Spray interface, operating in positive and negative ion mode and controlled by Analyst 1.6.3 software (AB Sciex). The ESI source operation parameters were as follows: ion source, turbo spray; source temperature 550°C; ion spray voltage (IS) 5500 V (positive ion mode)/−4500 V (negative ion mode); ion source gas I (GSI), gas II (GSII), curtain gas (CUR) was set at 50, 60, and 25.0 psi, respectively; the collision-activated dissociation (CAD) was high. Instrument tuning and mass calibration were performed with 10 and 100 μmol/L polypropylene glycol solutions in QQQ and LIT modes, respectively. QQQ scans were acquired as multiple reaction monitoring (MRM) experiments with collision gas (nitrogen) set to medium. A specific set of

MRM transitions were monitored for each period according to the metabolites eluted within this period.

Statistical data analysis of metabolites

The metabolomics data of FJ and FMT were processed using the system software analyst (version 1.6.3 Applied Biosystems Company, Framingham, MA, United States). Metware database (MWDB) was adopted for substance characterization which was based on secondary spectrum information. Metabolite quantification was accomplished by MRM analysis of triple quadrupole mass spectrometry. After obtaining the metabolite spectrum analysis data of different samples, the mass spectrum peaks of all substances were integrated by peak area, and the mass spectrum peaks of the same metabolite in different samples were integrated and corrected. Then unsupervised principal component analysis (PCA) was performed by statistics function prcomp within R[1] after the data was unit variance scaled. The heatmap of metabolites was carried out by the R package ComplexHeatmap. VIP (variable importance in projection) values were extracted from the OPLS-DA result, which also contained score plots and permutation plots generated using the R package MetaboAnalystR. Significantly regulated metabolites between groups were determined by VIP $\geq$ 1 and absolute $\log_2$FC (fold change) $\geq$ 1. The data was log-transformed and mean centering before OPLS-DA. To avoid overfitting, a permutation test (200 permutations) was performed. Identified metabolites were annotated using the KEGG Compound database[2], and annotated metabolites were then mapped to the KEGG Pathway database[3].

Volatiles analysis by gas chromatography ion mobility spectrometry

Gas chromatography ion mobility spectrometry condition

Analyses for the identification of characteristic volatile compounds of fruit juice samples were performed on an IMS commercial instrument (Flavorspec®, GAS GmbH, Dortmund, Germany), equipped with an MXT-WAX column (30 m × 0.53 mm id, 0.1 μm film thickness, Restek, United States). For analysis, 2 g of each sample was placed into a 20 mL headspace vial, closed with magnetic caps, and incubated at 40°C for 20 min at 500 rpm/min. Afterward, 500 μL of the headspace gases was automatically injected into the GC-IMS equipment by a heated syringe (65°C). The nitrogen gas (N_2) was used as carrier gas and drift gas, and the column temperature was kept at 60°C under isothermal conditions for timely separation. The programmed flow for carrier gas was set as follows: 2 mL/min for 2 min, then raised to 10 mL/min till 10 min, and ramped up to 100 mL/min in the next 10 min, then maintained at 100 mL/min until 30 min. The drift gas flow rate was held at 150 mL/min. Each analysis was conducted in triplicates.

Gas chromatography ion mobility spectrometry data analysis

The GC-IMS data were collected and processed using LAV software (version 2.2.1, G.A.S., Dortmund, Germany). To avoid significant errors in the multivariate statistical analysis, the spectra were normalized relative to the expected reaction-ion-peak (RIP) position, which was followed by spline interpolation to create a common set of points on the drift-time axis (*X*-axis) of the GC-IMS spectra. Volatile compounds were qualitatively analyzed by comparing the retention indexes and drift times with those in the GC-IMS library. The "Gallery Plot" plug-in of LAV software was used to automatically generate fingerprints, to visually and quantitatively compare the differences in volatiles between FJ and FMT samples. Principal component analysis and differential metabolites analysis were performed by R software.

Results and discussion

Quality parameters

The effect of alcoholic fermentation on the substances and parameters of grapefruit juice were presented in **Table 1**. The titratable acidity decreased by 36.5% after fermentation with an increase in the pH value, which may be owing to the consumption of some organic acids by the yeast as reported by Liu et al. (3). Likewise, the soluble solids content of the fermented juice showed a significant decrease due to the utilization of carbohydrates by the microbial. While a notable increase in alcohol content in fermented grapefruit juice was determined. Moreover, HPLC analysis was carried out to evaluate the changes in sugars and organic acids concentrations. Sucrose, fructose and glucose in the juice were mostly consumed by the yeast, and the consumption of sucrose was the highest among the sugars. Ordoudi et al. (26) reported that almost all the sugars in fruit juice were converted to alcohols at the end of alcoholic fermentation, which was consistent with our results. The concentration of citric acid, the main acid found in the juice, was slightly reduced after the fermentation. Lactic and acetic were detected as the newly formed acidic metabolites within the fermentation.

Organic acids and sugars are known as the most abundant solids present in fruit juice. They are responsible for the sour and sweet taste, and also have a significant effect on the mouthfeel quality. The consumption of sugars by the yeast

1 www.r-project.org
2 http://www.kegg.jp/kegg/compound
3 http://www.kegg.jp/kegg/pathway.html

sharply diminished the sweet taste and resulted in a relatively elevated sour taste of the juice. Since we have selected "Cocktail" grapefruit with lower acidity than other varieties, the fermented juice was more acceptable to consumers in terms of acidity. Besides, as a volatile acid, acetic acid can produce a pleasant acidity at levels below 0.8 g/L in fermented fruit juice (27). Small amounts of lactic acid produced by yeast metabolism can also improve the sensory properties of the juice (28). Taken our results together, the fermented "Cocktail" grapefruit juice is expected to meet the growing demand of consumers for fruit wines with less ethanol and good mouthfeel.

Metabolomics analysis

Data quality assessment

A total of 1015 metabolites were identified in FJ and FMT samples. **Supplementary Figure 1** represented the overlapping display of the mass spectra of mixed QC samples to ensure the reproducibility and reliability of the data. The results showed that the TIC curves of QC samples had a high overlap, indicating the reliability of the results.

Metabolomics analysis of grapefruit juice and grapefruit fermented juice

The metabolite profiles of grapefruit juice samples can be visualized by the heatmap (**Figure 1A**). It showed that the three replicates of each group are clustered together, indicating good homogeneity and high reliability. The metabolites identified in FT and FMT can be classified into 10 major groups, namely flavonoids (296), phenolic acids (145), lipids (95), alkaloids (88), organic acids (80), amino acids (79), lignans and coumarins (69), nucleotides and their derivatives (43), terpenoids (15), and quinines (10). Overall, an obvious difference was found between FMT and FJ, and the abundance of most metabolites increased after alcoholic fermentation, including flavonoids, phenolic acids, amino acids and terpenoids. As shown in **Figure 1B**, the sum of flavonoids and phenolic acids accounted for more than 43% of the total identified compounds. Moreover, our result was in good agreement with previous literature in terms of the variation of flavonoids and phenolic acids after fermentation (29). The elevated content of flavonoids and phenolic acids may be partially owing to the hydrolysis of large original polymers performed by microbial enzymes. Besides, during the fermentation process, the alcohols and the heat generated in the matrix might contribute to the percolation of these bioactive compounds (30).

Multivariate analysis of identified metabolites in grapefruit juice and grapefruit fermented juice

To eliminate the effects of quantity on pattern recognition, we applied a log10 transformation of peak areas for each metabolite and, subsequently, performed PCA and OPLS-DA analysis. We selected the first two principal components, which can explain 85% of the total variation between groups. In the

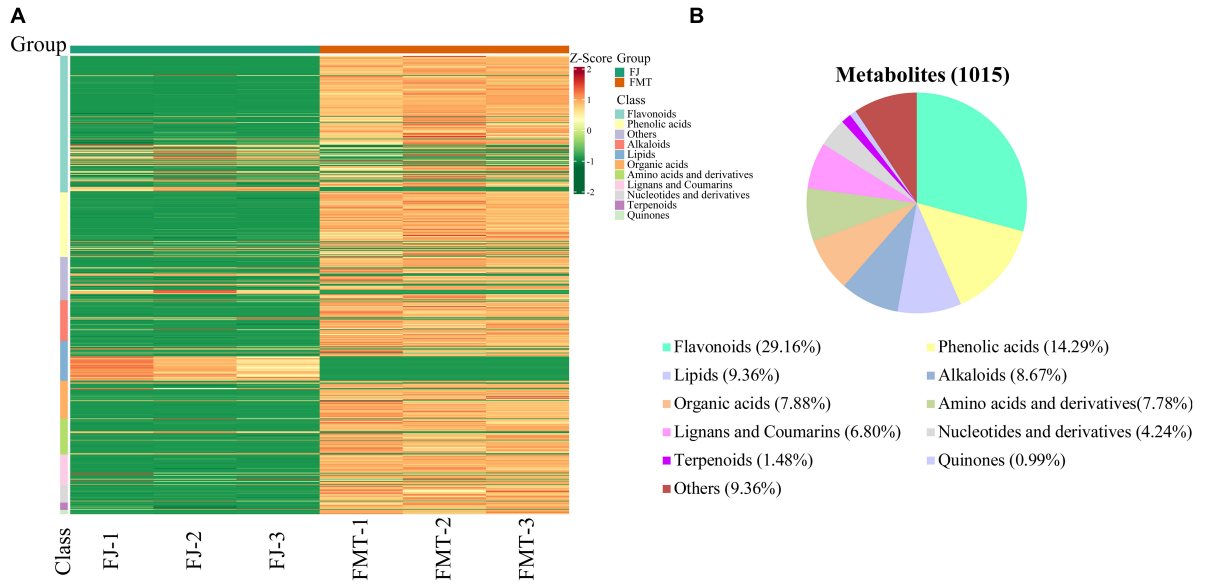

FIGURE 1
Heatmap visualization and proportions of the metabolites identified from grapefruit juice (FJ) and grapefruit fermented juice (FMT). **(A)** Heatmap visualization. The content of each metabolite was normalized to the complete linkage hierarchical clustering. Each example is visualized in a single column, and each metabolite is represented by a single row. Red indicates high abundance, whereas metabolites with low relative abundance are shown in green (the color key scale is right of the heat map). **(B)** Types and proportions of the metabolites identified from FJ and FMT.

PCA scores, each point represents an individual sample, and Figure 2A showed that FJ and FMT were divided into two distinct areas, indicating the difference between FJ and FMT. In comparison to PCA, OPLS-DA is a better approach to processing two classes of datasets to discriminate the metabolites between the samples. As shown in Figure 2B, the horizontal coordinates indicate the scores of the main compounds, reflecting the differences between groups, and the vertical coordinates indicate the scores of the orthogonal components, showing the differences within groups. Accordingly, the OPLS-DA scores plot showed metabolites of the samples presented clear intergroup differences between FJ and FMT. In the model validation permutation test plot of OPLS-DA, the vertical coordinate indicates the accuracy of 200 models in 200 permutation tests, and the arrow indicates the location of the model accuracy (Figure 2C). Here, R2Y, Q2 and R2X values were higher than 0.9 and the *p*-Value is less than 0.05, showing the goodness of the prediction. In addition, the advantages of the S-plot from the supervised OPLS-DA can discriminate the differential constituents in the samples. In the S-plot, each point represents an ion detected using UPLC-MS/MS, where the *X*-axis represents variable contribution, and the *Y*-axis represents variable confidence. In Figure 2D, the variables that changed most significantly were plotted at the top or bottom of

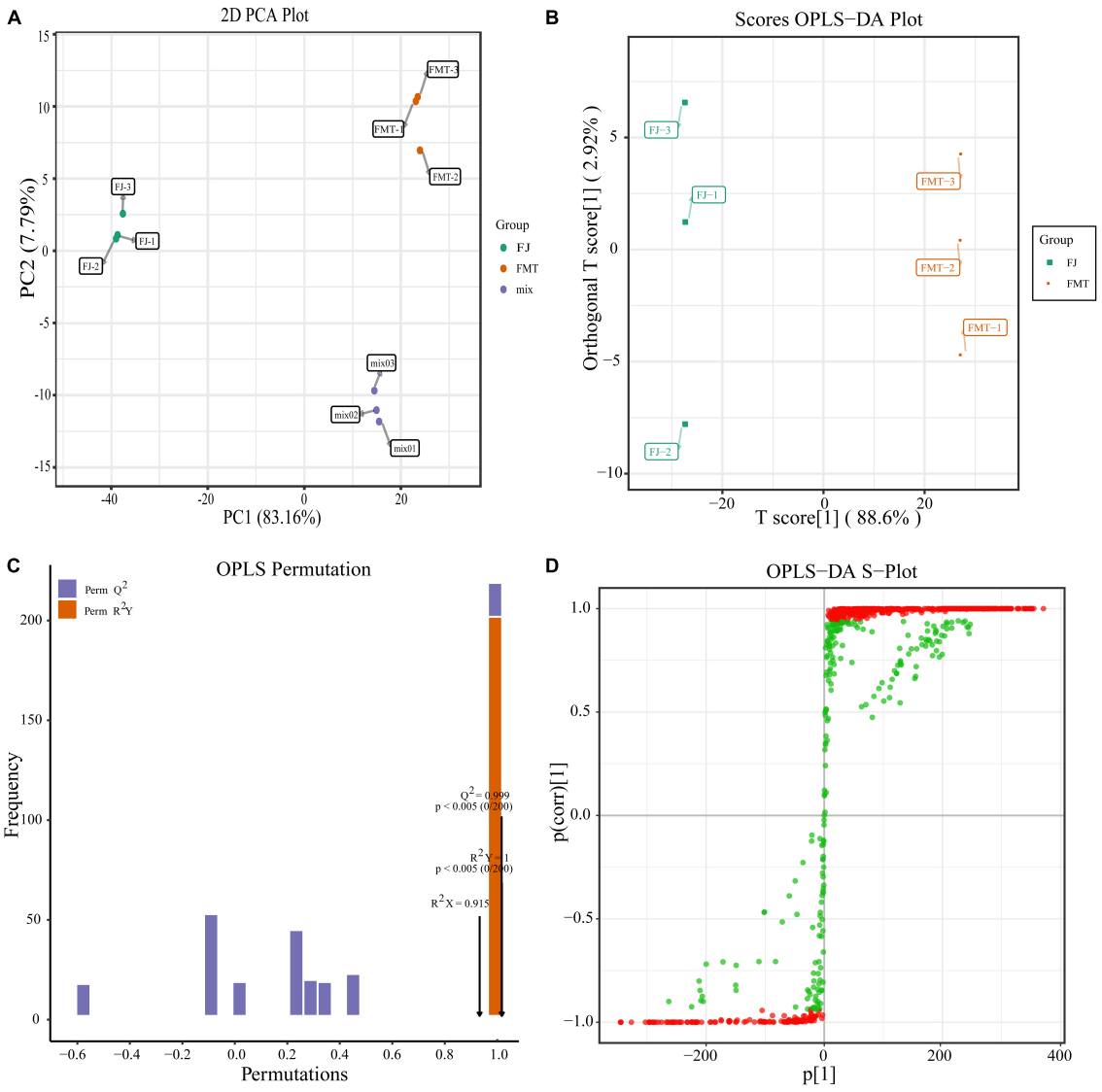

FIGURE 2
Multivariate analysis of identified metabolites. **(A)** PCA analysis of metabolites identified from FJ and FMT. Equal volumes of FJ and FMT samples were mixed as a quality control (QC). **(B)** OPLS-DA model plot of the metabolites identified from FJ and FMT. **(C)** Permutation test for OPLS-DA model validation of FJ and FMT. **(D)** OPLS-DA S-Plot of the samples.

the "S" shape plot, where the red area indicated the VIP value of these metabolites ≥ 1 and the green section meant the VIP < 1. Collectively, both PCA and OPLS-DA analyses suggested that FJ and FMT had different metabolite profiles, indicating that the yeast activities had a great impact on the metabolites of grapefruit juice.

Moreover, further studies based on the VIP value, together with the fold change of the metabolites were carried out by a volcano plot. A total of 752 differential metabolites were identified with the fold change threshold > 2 (or <0.5) and VIP value threshold >1 between FJ and FMT, among which 134 metabolites were decreased and 618 metabolites increased (**Figure 3A**). The significant metabolites could be categorized into more than 10 different classes, including flavonoids, phenolic acids, alkaloids, lipids, organic acids, and amino acids and their derivatives, etc. (**Figure 3B**).

Flavonoids

Flavonoids have been shown to possess a variety of biological activities such as anti-inflammatory properties, cholesterol-lowering and immune system modulation (31). In the present study, 224 flavonoids were detected in the differential metabolites, accounting for approximately one-third of the total differentials, of which 184 increased and 40 decreased (**Supplementary Table 1**). The results indicated that fermentation has changed the flavonoids in grapefruit juice obviously. About 55 flavonoids were newly produced after fermentation, including 24 flavones, 14 dihydroflavones, 9 flavonols, 3 chalcones, 2 isoflavones, 1 dihydroflavonol, 1 flavonoid carbon glycoside, and 1 flavanone. The only 2 flavonoids that disappeared after fermentation were kaempferol-3-O-robinobioside and tricetin-5-O-(6″-malonyl) glucoside. The decline of kaempferol-3-O-robinobioside is likely due to the hydrolysis of glycosides by 3-O-glucosyltransferase produced by the yeast according to Wang et al. (32). Generally, most of the natural flavonoids in citrus exist in the form of glycosides (33). In this study, 137 kinds of flavonoids were identified as glycosides, and the most prominent glycosides in FJ are neohesperidin, hesperidin and naringin. Sicari et al. (34) analyzed the flavonoids in two different grapefruit juice and found naringin, narirutin, poncirin, and naringenin were the major flavonoids with a content ranging from 17.3 to 287.2 mg/L, which was similar to our results.

Previous reports showed that the absorption of flavonoid glycosides by intestinal epithelial cells is lower than flavonoid aglycone (35). And the bioavailability of flavonoid glycosides can be improved after being hydrolyzed into monoglycoside or aglycone forms during the fermentation (36). For instance, *saccharomyces cerevisiae* can degrade neohesperidin and hesperidin and form hesperetin and nobiletin with the action of glycosidases (37). In the present study, there was a significant decrease in flavonoid glycosides in FMT compared with FJ, such as neoeriocitrin, hesperidin, neohesperidin, narirutin, poncirin, didymin, rhoifolin, eriocitrin, isorhoifolin, naringin, while it was found concurrently an increase of their corresponding flavonoid aglycones. Additionally, flavonoids may undergo demethylation during alcoholic fermentation, as proved by the increased level of compounds like 5-demethylnobiletin and 3′-demethylnobiletin in FMT samples (38).

Phenolic acids

Phenolic acids are important bioactive substances in grapefruit juice, which played an important role in the juice function and sensory characteristics (39). The principal phenolic acids found in grapefruit are protocatechuic, neochlorogenic acid, hydroxycinnamic acids and ferulic acid, etc. (40). In this study, 106 kinds of phenolic acids and their derivatives were detected in the differential metabolites, of which 98 increased and 8 decreased after fermentation (**Supplementary Table 1**). Total 53 phenolic acids derivatives such as ferulic acid methyl

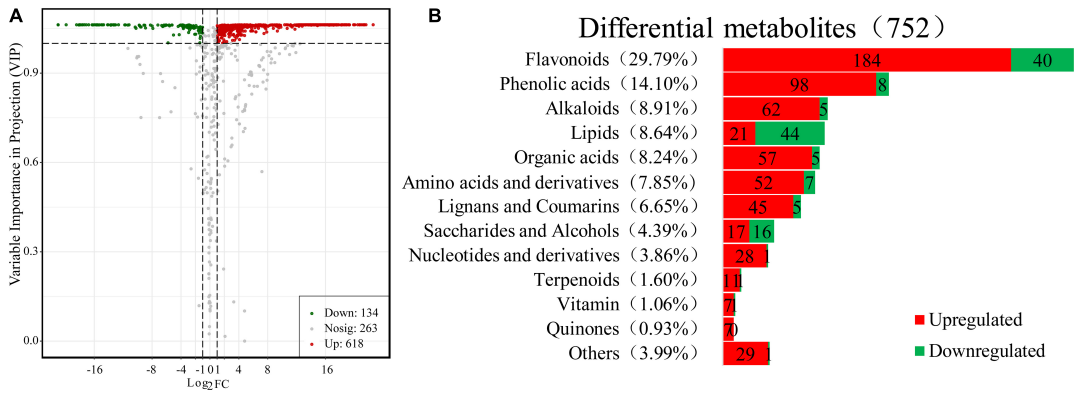

FIGURE 3
Differential metabolites between FJ and FMT. **(A)** Volcano plot of the 752 differential metabolites identified. Differential metabolites were defined as metabolites with VIP ≥ 1 and absolute log_2FC (fold change) ≥ 1 in FMT relative to FJ. **(B)** Column chart depicting the biochemical categories of differential metabolites identified between FJ and FMT.

ester and ethyl ferulate were newly generated, and only 1-O-p-coumaroyl-β-D-glucose and chlorogenic acid disappeared during the fermentation process. As reported by Zuriarrain-Ocio et al. (41), chlorogenic acid can be hydrolyzed by some lactic acid bacteria (LAB) strains to quinic and caffeic acids. Herein, we found the abundance decrease in chlorogenic acid corresponded to a large increase in caffeic acid, this may because *Saccharomyces cerevisiae* and LAB strains have similar conversion functions for chlorogenic acid. Among those ascending phenolic acids, such as salicylic acid, vanillic acid, protocatechuic acid and caffeic acid, have been reported to have antioxidant, antimutagenic, antiproliferative and antimicrobial properties (42). Additionally, newly generated methyl ferulate (FAME) had known function in inhibiting colony formation, inducing morphological change and apoptosis of cancer cells, and FAME also exhibited potential benefits to enhance the sensitivity of colorectal cancer cells to conventional chemotherapeutic drugs (43). Moreover, ethyl ferulate was reported to ameliorate LPS-induced acute lung injury in an AMPK/Nrf2-dependent manner (44). Consequently, the results implied that alcoholic fermentation can enrich bioactive phenolic metabolites in grapefruit juice and potentially improve its health value.

Lipids, organic acids, amino acids, and derivatives

Lipids were the only category in which more compounds were found to decrease, including palmitaldehydes, lauric acid and γ-linolenic acid, etc. Lipids are essential nutrients for yeast alcoholic fermentation, which play an important role in membrane structure, adaptation to stress, or as signaling molecules. Lipid metabolism also generates large intermediate products, for instance, lipid supplementation can greatly stimulate the formation of yeast volatile metabolites (45). As for organic acids, more than 90% of them increased in abundance after fermentation, with citraconic acid being the most abundant followed by aminomalonic acid. Some short-chain fatty acids were newly generated after yeast alcoholic fermentation, such as 2-hydroxybutyric acid, 4-acetamidobutyric acid, 2,3-dihydroxy-3-methylpentanoic acid, 3-methyl-2-oxobutanoic acid, and 2-hydroxyisobutyric acid, etc. Yao et al. (46) has reported short-chain fatty acids, produced by gut microbiome fermentation, played an important role in human immunity and metabolism. Additionally, the significantly increased 3-(4-hydroxyphenyl)-propionic acid in FMT, could inhibit the conversion of macrophages into foam cells by regulating cellular lipid metabolism, and suppressing cellular oxidative stress and inflammation (47). Moreover, fermentation caused an increase in the abundance of most amino acids, with L-cyclopentylglycine being the greatest after fermentation. The increase of free amino acids like L-methionine, L-leucine, L-isoleucine and L-tyrosine were mainly owing to the hydrolyzation of proteins by the proteolytic enzymes produced by the microbial. Also, the abundance of acylated amino acids ascended in the FMT sample, which may arise from the acylation of the respective amino acids activated by CoA or *N*-acylating enzymes (48).

In addition, vitamin C, an important micronutrient in citrus juice, was also significantly increased after fermentation with a fold change of 3.27. Overall, the abundance of most functional (flavonoids, phenolic acids) and nutritional components (amino acids, vitamins, organic acids, etc.) in fermented grapefruit juice increased, indicating that controlled alcoholic fermentation plays an important role in enhancing the nutritional value of grapefruit juice.

KEGG classification and enrichment analysis of differential metabolites

The pathway enrichment analysis of 752 differential metabolites was carried out by the KEGG database. A total of 199 differential metabolites were identified, which were distributed in 84 metabolic pathways (**Supplementary Figure 2**). Subsequently, we conducted the KEGG pathway enrichment analysis to identify differences in metabolic pathways between FJ and FMT (**Supplementary Figure 3**). The specialized metabolic pathways included flavonoid biosynthesis, pyrimidine metabolism, tropane, piperidine and pyridine alkaloid biosynthesis, valine, leucine and isoleucine biosynthesis, and phenylalanine metabolism, etc.

In particular, we focused on the changes of metabolites in the flavonoid synthesis pathway. According to **Supplementary Figure 2**, a total of 23 metabolites were annotated to the flavonoid biosynthesis pathway, accounting for 11.56% of the total metabolites annotated, which was the highest except for the metabolic pathway and biosynthesis of secondary metabolites pathway. **Supplementary Figure 4** detailed the biotransformation involved in flavonoid biosynthesis, and the abundance changes of relevant compounds were notated. Many of the metabolites were monitored after fermentation with an upregulation (red). This is probably due to the biocatalytic action of newly generated enzymes by the yeast, such as flavonoid 3′,5′-hydroxylase, flavonoid 3′-monooxygenase, and flavonoid 4′-O-methyltransferase (32).

Volatile profiles analysis

Visual topographic plot comparison of volatile compounds in grapefruit juice and grapefruit fermented juice

The results of the qualitative analysis of volatile compounds in the samples are listed in **Table 2**. Except for 8 unidentified compounds, a total of 57 components were tentatively identified from the GC-IMS library, containing 20 esters, 13 aldehydes, 8 terpenes, 7 ketones, 7 alcohols, 1 acid, and 1 ether. We detected more volatile compounds with GC-IMS in this study than in previous studies (49, 50), which helped to better understand the

TABLE 2 Qualitative analysis of volatile compounds in the grapefruit juice.

Class	Compound	CAS	Formula	MW	RI	Rt [sec]	Dt [RIP rel]
Aldehydes	Non-anal	C124-19-6	$C_9H_{18}O$	142.2	1401.7	1026.948	1.47202
	Octanal-M	C124-13-0	$C_8H_{16}O$	128.2	1299.3	822.172	1.40575
	Octanal-D	C124-13-0	$C_8H_{16}O$	128.2	1299.3	822.17	1.82885
	(E)-2-Hexenal	C6728-26-3	$C_6H_{10}O$	98.1	1232.2	715.257	1.18357
	Heptanal	C117-71-7	$C_7H_{14}O$	114.2	1197.3	665.432	1.33426
	2-Methyl-2-pentenal	C623-36-9	$C_6H_{10}O$	98.1	1165.7	603.152	1.50041
	Hexanal	C66-25-1	$C_6H_{12}O$	100.2	1102.5	488.97	1.56224
	Diethyl acetal	C105-57-7	$C_6H_{14}O_2$	118.2	913.3	295.415	1.03213
	3-Methylbutanal	C590-86-3	$C_5H_{10}O$	86.1	933	308.829	1.41831
	Propanal-M	C123-38-6	C_3H_6O	58.1	820.2	239.525	1.04633
	Propanal-D	C123-38-6	C_3H_6O	58.1	820.2	239.525	1.14997
	2-Methylpropanal	C78-84-2	C_4H_8O	72.1	832.5	246.232	1.28485
	Butanal	C123-72-8	C_4H_8O	72.1	918.3	298.769	1.29337
	Furfural	C98-01-1	$C_5H_4O_2$	96.1	1494	1254.592	1.09324
	Methacrolein	C78-85-3	C_4H_6O	70.1	896.2	284.265	1.04773
Esters	Ethyl nonanoate	C123-29-5	$C_{11}H_{22}O_2$	186.3	1533.8	1367.68	1.53253
	Butyl hexanoate	C626-82-4	$C_{10}H_{20}O_2$	172.3	1434.1	1101.743	1.4534
	Ethyl Acetate	C141-78-6	$C_4H_8O_2$	88.1	903.1	288.708	1.33455
	Ethyl formate	C109-94-4	$C_3H_6O_2$	74.1	881.1	274.736	1.21102
	Methyl acetate	C79-20-9	$C_3H_6O_2$	74.1	851.2	256.851	1.19541
	Ethyl propanoate	C105-37-3	$C_5H_{10}O_2$	102.1	975.1	339.569	1.45807
	Ethyl lactate	C97-64-3	$C_5H_{10}O_3$	118.1	1359.8	937.574	1.13555
	Ethyl isobutyrate	C97-62-1	$C_6H_{12}O_2$	116.2	984.5	346.834	1.56313
	Propyl acetate	C109-60-4	$C_5H_{10}O_2$	102.1	994.4	354.659	1.47794
	Isobutyl acetate	C110-19-0	$C_6H_{12}O_2$	116.2	1030.6	394.341	1.61424
	Methyl 3-methylbutanoate	C556-24-1	$C_6H_{12}O_2$	116.2	1022.4	384.84	1.53899
	Ethyl butanoate	C105-54-4	$C_6H_{12}O_2$	116.2	1051.9	420.051	1.56455
	Ethyl 3-methylbutanoate	C108-64-5	$C_7H_{14}O_2$	130.2	1066	437.935	1.65116
	Ethyl 2-methylbutanoate	C7452-79-1	$C_7H_{14}O_2$	130.2	1081.5	458.615	1.65179
	Isoamyl acetate	C123-92-2	$C_7H_{14}O_2$	130.2	1139	551.952	1.74908
	3-methylbutyl propanoate	C105-68-0	$C_8H_{16}O_2$	144.2	1187.5	648.433	1.83892
	Ethyl hexanoate-M	C123-66-0	$C_8H_{16}O_2$	144.2	1246.2	736.379	1.33906
	Ethyl hexanoate-D	C123-66-0	$C_8H_{16}O_2$	144.2	1244.7	733.969	1.80492
	Ethyl octanoate-M	C106-32-1	$C_{10}H_{20}O_2$	172.3	1450.2	1140.763	1.48179
	Ethyl octanoate-D	C106-32-1	$C_{10}H_{20}O_2$	172.3	1451.9	1145.019	2.03799
	Ethyl crotonate	C623-70-1	$C_6H_{10}O_2$	114.1	1147	566.823	1.19847
	Isobutyl butyrate	C539-90-2	$C_8H_{16}O_2$	144.2	1145.9	564.829	1.33362
Acids	Acetic acid-M	C64-19-7	$C_2H_4O_2$	60.1	1500.7	1272.94	1.06007
	Acetic acid-D	C64-19-7	$C_2H_4O_2$	60.1	1501.3	1274.602	1.15549
Ketones	2-Heptanone	C110-43-0	$C_7H_{14}O$	114.2	1187.7	648.824	1.6202
	Cyclopentanone	C120-92-3	C_5H_8O	84.1	1151.4	575.125	1.11402
	1-Penten-3-one-D	C1629-58-9	C_5H_8O	84.1	1041.4	407.196	1.31183
	1-Penten-3-one-M	C1629-58-9	C_5H_8O	84.1	1042.3	408.314	1.07757
	4-Methyl-2-pentanone-M	C108-10-1	$C_6H_{12}O$	100.2	1028.2	391.547	1.18121
	4-Methyl-2-pentanone-D	C108-10-1	$C_6H_{12}O$	100.2	1026.7	389.87	1.47794
	2-Pentanone	C107-87-9	$C_5H_{10}O$	86.1	1000.6	360.807	1.36862
	2-Butanone	C78-93-3	C_4H_8O	72.1	917.5	298.21	1.24368
	Acetone	C67-64-1	C_3H_6O	58.1	841.4	251.262	1.11874
Ethers	Dimethyl sulfide	C75-18-3	C_2H_6S	62.1	795.7	226.67	0.95972

(Continued)

TABLE 2 (Continued)

Class	Compound	CAS	Formula	MW	RI	Rt [sec]	Dt [RIP rel]
Alcohols	1-Hexanol	C111-27-3	$C_6H_{14}O$	102.2	1372.5	963.788	1.33005
	2-Methyl-1-propanol-M	C78-83-1	$C_4H_{10}O$	74.1	1108.2	498.313	1.17198
	2-Methyl-1-propanol-D	C78-83-1	$C_4H_{10}O$	74.1	1108.5	498.856	1.35563
	1-Propanol-M	C71-23-8	C_3H_8O	60.1	1054.6	423.404	1.11164
	1-Propanol-D	C71-23-8	C_3H_8O	60.1	1056.8	426.198	1.25405
	Ethanol	C64-17-5	C_2H_6O	46.1	946.5	318.33	1.12584
	2-Propanol	C67-63-0	C_3H_8O	60.1	934.6	309.947	1.09034
	1-Butanol	C71-36-3	$C_4H_{10}O$	74.1	1161.8	595.425	1.37816
	3-Methyl-1-butanol	C123-51-3	$C_5H_{12}O$	88.1	1223.6	702.646	1.48018
Terpenes	γ-Terpinene	C99-85-4	$C_{10}H_{16}$	136.2	1261.4	759.891	1.22027
	Limonene-M	C5989-27-5	$C_{10}H_{16}$	136.2	1205.5	676.851	1.22414
	Limonene-D	C5989-27-5	$C_{10}H_{16}$	136.2	1204.8	675.81	1.29176
	Limonene-T	C5989-27-5	$C_{10}H_{16}$	136.2	1205.5	676.85	1.66077
	α-Phellandrene	C99-83-2	$C_{10}H_{16}$	136.2	1187.2	647.786	1.21834
	Myrcene-M	C123-35-3	$C_{10}H_{16}$	136.2	1175.9	623.912	1.22027
	Myrcene-D	C123-35-3	$C_{10}H_{16}$	136.2	1175.9	623.91	1.28789
	Myrcene-T	C123-35-3	$C_{10}H_{16}$	136.2	1175.9	623.91	1.711
	β-Pinene-M	C127-91-3	$C_{10}H_{16}$	136.2	1132.9	540.871	1.21834
	β-Pinene-D	C127-91-3	$C_{10}H_{16}$	136.2	1132.9	540.87	1.63758
	(-)-β-Pinene	C18172-67-3	$C_{10}H_{16}$	136.2	1118.1	514.921	1.21834
	α-Pinene-M	C80-56-8	$C_{10}H_{16}$	136.2	1035.3	399.93	1.22096
	α-Pinene-D	C80-56-8	$C_{10}H_{16}$	136.2	1034.4	398.81	1.66677
	Terpinolene	C586-62-9	$C_{10}H_{16}$	136.2	1299.5	822.682	1.20762

RI and Rt mean retention index and retention time, respectively. Dt indicates migration time, where [RIP rel] refers to normalization treatment.

variation of volatiles before and after fermentation. In addition, several single compounds were found to produce multiple signals or spots (dimers, trimers, and even polymers). It has been reported that the formation of dimers or trimers is related to the high proton affinity or high concentration of the compounds in the analytes, and the compounds with high concentration could accelerate the combination of neutral molecules and proton molecules to form dimmers Lantsuzskaya (Krisilova) et al. (51).

Figure 4A shows GC-IMS topographical plots of volatile compounds in grapefruit juice before and after fermentation. The ordinate represents the retention time of volatile compounds during GC separation, and the abscissa represents the ion migration time (after normalization). The red vertical line on the left is the reactive ion peak (RIP), each point on the right of the RIP represents a volatile compound extracted from the samples. The color and area of the signals represent the signal intensity of the compounds. Darker colors and larger area spots indicate that the content of the volatile substances was higher. As shown, most of the signals appear in the retention time of 200 to 800 s and the drift time of 1.0 to 1.8 ms. It was observed the volatile compounds changed dramatically after fermentation.

The contribution of volatile aroma compounds to the overall composition and sensory perception of fruit wines is well recognized. To further analyze the specific effects of fermentation on the volatile flavor substances of grapefruit juice, fingerprint profiles of volatiles in FJ and FMT were generated according to the Gallery Plot plug-in (Figure 4B), enabling an intuitive comparison of the differences in volatile compounds between the two groups of samples. Each row of the graph represents the signal peak of a volatile compound contained in one sample, and each column indicates the comparison between different samples for the same volatile compound. The shade of the color represents the content of the volatile compound, the brighter the color, the higher the content and vice versa (the numbered peaks are those not identified). As seen in Figure 4B, FT samples showed high contents of ethyl nonanoate, butyl hexanoate, ethyl formate, nonanal, octanal, heptanal, hexanal, 2-methylpropanal, propanal, acetal, E-2-hexenal, 2-methyl-2-pentenal, methacrolein, γ-pinene, limonene, α-phellandrene, myrcene, β-pinene, α-pinene, (-)-β-pinene, 2-propanol, 2-heptanone, 1-penten-3-one, 2-butanone, 4-methyl-2-pentanone, and acetone, which could form the flavor profile of fresh grapefruit juice. Compared with FT, FMT samples showed less content in aldehydes like 2-methyl-2-pentenal, hexanal, heptanal as

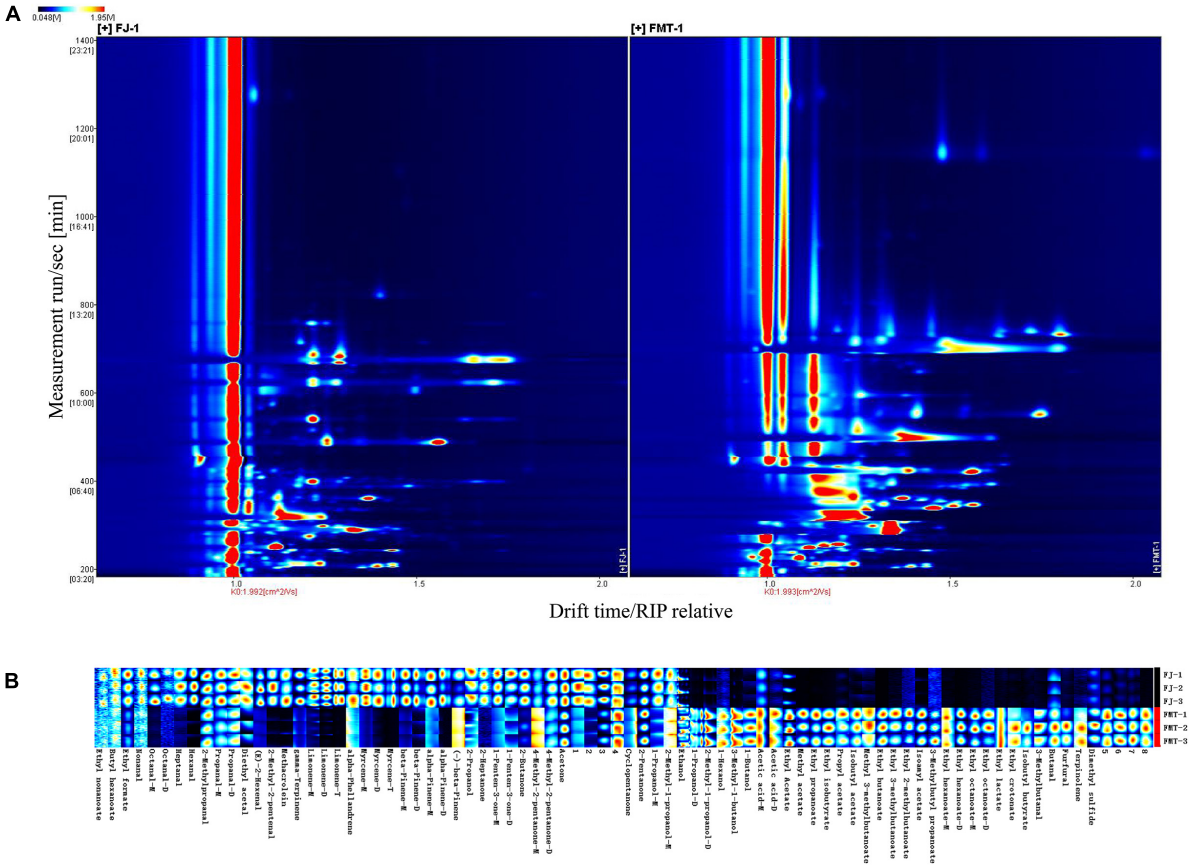

FIGURE 4
Gas chromatography-mass spectrometry spectrum of the FJ and FMT samples (**A**, a top view) and Gallery plot fingerprint of volatile substances **(B)**.

well as terpenes like limonene, myrcene and β-pinene, while showed higher content in esters such as ethyl butanoate, ethyl propanoate, ethyl isobutyrate, methyl acetate and alcohols like ethanol, 3-methyl-1-butanol and 1-butanol.

Principal component analysis and OPLS-DA analysis

Principal component analysis of volatiles was used to analyze the difference between FJ and FMT samples (**Figure 5A**). Based on the first principal component (PC1 = 88.11%) and the second principal component (PC2 = 5.44%), two groups were separated clearly, indicating that fermentation can alter the volatile composition of grapefruit juice. A comparison of the volatile characteristics of FJ and FMT using the OPLS-DA model is shown in **Figure 5B**. As calculated, R2Y of the model was 1, Q2 and R2X were both greater than 0.9, and the p-Value is less than 0.05, indicating that the model is of goodness. As a result, both PCA and OPLS-DA results indicated the flavor profiles of grapefruit juice changed dramatically before and after fermentation.

Effect of fermentation on the volatiles in grapefruit juice

The effect of fermentation on grapefruit juice is reflected in the total amount and composition of volatile substances. According to volatile profiles abundance, the total amount of volatiles after fermentation was higher than unfermented juice, increasing about 80% compared to FJ samples. In addition, the composition of the volatiles has changed obviously *via* fermentation (**Figure 5C**). Terpenes accounted for the highest percentage in FJ, followed by alcohols. In contrast, the highest volatiles in FMT were alcohols, followed by esters, and terpenes accounting for only 2.2% (**Figure 5D**). Fan et al. (52) also observed significant changes in volatile compounds in orange juice after fermentation, with most terpenes disappearing after fermentation and esters being the most abundant aromatically compounds. For these phenomena, it was suggested the terpenes decrease may be owing to the transformations by yeast. For example, limonene could be transformed to carveol, trans-2,8-methadien-1-ol, and cis-2,8-methadien-1-ol by yeast via hydroxylation, and the simple adsorption by yeast cells may also result in the massive loss of aroma compounds during

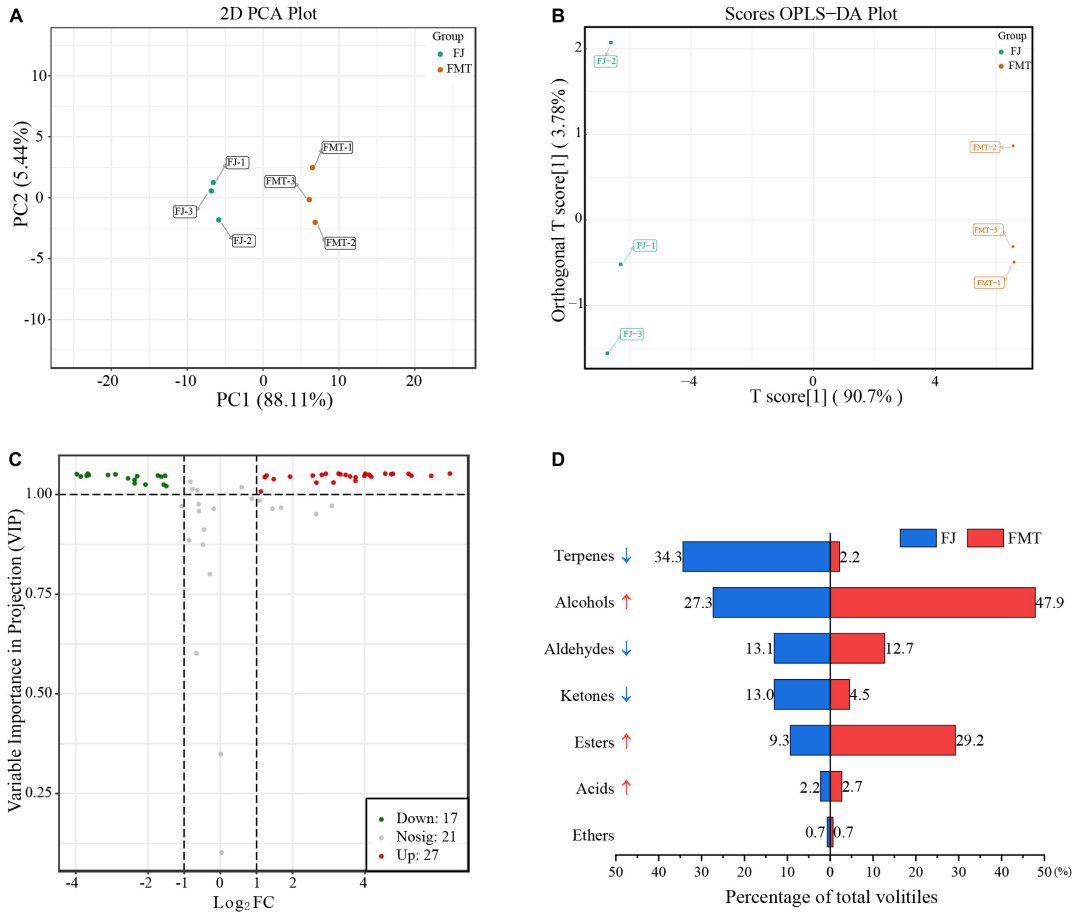

FIGURE 5
Multivariate analysis of volatile compounds. **(A)** PCA analysis of volatile compounds from FJ and FMT. **(B)** OPLS-DA model plot of the volatile compounds from FJ and FMT. **(C)** Volcano plot of differential metabolites. **(D)** Volatile substances changes of different categories between FJ and FMT.

the fermentation process (53). In addition, monoterpene and sesquiterpene hydrocarbons were primarily distributed in the pulp (74.0 and 87.2%) and cloud (7.3 and 14.9%) of citrus juice (54), while the insoluble cloud and pulp turned into a precipitate after alcoholic fermentation. Herein, the FMT was obtained by collecting the supernatants of fermented juice without the precipitation, in which some terpenes may also be lost together. The only exception is the increase in terpinolene content after fermentation. Terpinolene has been reported not to be degraded or transformed by the yeast (53), and previous studies showed it can be also derived from the decomposition of limonene (55), which may account for its raised level. Given that the flavor of grapefruit juice depends on the combined effects of multiple aroma compounds, the analysis of these volatiles compounds is summarized by category as follows.

Terpenes

Terpene was one of the most abundant volatiles in grapefruit juice, and limonene exhibited the highest concentration in both FJ and FMT, which agreed with the results of the previous study (56). As reported, most of the detected terpenes imparted citrusy, fruity, piney and woody notes. For example, limonene and α-pinene both contribute citrus-like, pungent aromas (57). β-pinene was described as woody and piney, while myrcene contributed most of the green, fruity notes. Fermentation caused a dramatic decrease in terpenes and may result in a reduction of citrusy flavor in juice. Nevertheless, terpenes may contribute to the overall flavor to a smaller extent than other ingredients such as esters and alcohols, due to the relatively higher sensory threshold (57). Thus, the reduction of terpenes content may have a limited effect on the aroma. In contrast, compounds such as esters, organic acids and alcohols with low sensory thresholds may have a greater impact on juice flavor.

Esters

A total of 20 esters were detected in grapefruit juice, which were known to contribute to the "top note" of fruit and citrus flavors (58). Controlled alcoholic fermentation can

increase the content of juice esters, owing to the generated by-products that were produced in the yeast decomposition of sugars. After fermentation, the proportion of esters in the volatiles of grapefruit juice increased from 9.3% (FJ) to 29.2% (FMT). Among these esters, ethyl acetate was the most abundant compound both before and after fermentation. Ethyl butyrate, ethyl hexanoate, methyl acetate, ethyl propanoate, ethyl isobutyrate, propyl acetate, isobutyl acetate and isoamyl acetate all showed a content increase in FMT samples. As reported, isoamyl acetate confers a banana aroma characteristic and has a high aggregate value for the food industry (59). Ethyl butyrate and ethyl hexanoate are responsible for the fruity odor and act as important contributors to the desired flavor in orange products (58). Selli et al. (60) identified 63 compounds in Turkish Kozan wine and found that alcohols, followed by esters, were the most abundant aromatic compounds in orange wine. Uniquely, the content of methyl acetate was high in fresh juice with only less than ethyl acetate, yet showed a decline after fermentation, implying that yeast could also consume or degrade some esters during the growth. Ethyl formate has been reported to have antimicrobial activity (61), while yeast may achieve suitable growth conditions via the degradation of ethyl formate. Although there is no direct evidence to confirm this speculation, the reports that ethyl formate could be hydrolyzed into formic acid and ethanol by *Aeromonas salmonicida* and the formed formic acid would participate in the cyclic metabolism of carboxylic acid (62), which may provide some information.

Alcohols

The concentration of alcohols in FMT was much higher than that in FJ, indicating that the fermentation resulted in a huge change in the alcoholic aroma. Ethanol was the highest alcohol both in FJ and FMT, imparting the sweet and wine notes for the juices. Likewise, 1-Propanol contributed to the sweet and wine notes, while 3-methyl-1-butanol (isoamylol), 1-butanol and 1-hexanol enhanced the fruity note. Interestingly, alcohols could contribute to the absorption of phenolic compounds in the human intestine, in addition to enhancing the flavor of the juice (1). Combined with the former result that alcoholic fermentation can increase the abundance of flavonoids and phenolic acids in the juice, it was suggested that fermented grapefruit juice can be served as a wellness drink to promote human health.

Acids, aldehydes, and ketones

Concerning other volatile constituents, including acids, aldehydes and ketones, it was found that only one volatile acid, i.e., acetic acid was detected from the current samples. Acetic acid content was higher in FMT than that in FJ samples, which was similar to a previous report (63). A total of 14 aldehydes were detected in the juice, and the concentrations of 8 aldehydes showed a dramatic decrease after fermentation, including octanal, heptanal, 2-methyl-2-pentenal, (E)-2-hexenal, hexanal, diethyl acetal, propanal and methacrolein. The reduction was likely due to oxidation and/or enzymatic degradation occurring during yeast fermentation (30). For example, propanal can be oxidized to produce propionic acid and utilized by the yeast, and aldehydes and ketones would be transformed into corresponding biogenic amines by the microbial enzymes (63). On the other hand, 4 aldehydes increased after fermentation, namely 3-methylbutanal, butanal, 2-methyl-1-propanol and furfural, which may be the oxidation products of alcohols with the raising level. Seven ketones were detected, five of which decreased significantly, including 2-heptanone (fruity, spicy and woody), 4-methyl-2-pentanone (green, herbal, fruity), 1-penten-3-one (fresh and pungent), 2-butanone (fruity) and acetone (apple and pungent). Among them, 1-penten-3-one has been characterized as an impact aroma compound in grapefruit, orange juice, olive oil, or tomatoes due to a very low odor threshold of 0.94 μg/L (64). However, 1-penten-3-oneis prone to degradation due to its instability in the heat treatment or storage progress (64).

Collectively, fermented grapefruit juice had a reduction in the abundance of most terpenes and ketones contributing to "fruity," "citrus-like" notes, and the increase of the esters with "green," "fruity" notes. In addition, the newly generated esters and alcohols could endow the fermented juice with fruitiness and wine flavor. It indicated that alcoholic fermentation induced changes in the aroma profile and enriched the flavor of grapefruit juice. The study is a comprehensive analysis of the functional and volatile compounds in fermented grapefruit juice, yet still requires refinement in the next work. Besides, more efforts should be made to perform the functional evaluation of fermented grapefruit juice *in vitro* and *in vivo* models, aiming to obtain more information on its efficacy.

Conclusion

In this study, an abundant number of metabolites were generated from "Cocktail" grapefruit juice fermented by *Saccharomyces cerevisiae*. Metabolites in grapefruit juice after alcoholic fermentation can be effectively evaluated by wide-target metabolomics, and GC-IMS allows a well-visualized differentiation between fermented and unfermented grapefruit juice. The integration of these two techniques achieves a comprehensive analysis of non-volatile and volatile metabolites in grapefruit juice, which provides a wide perspective to further understand or evaluate the effect of alcoholic fermentation on the biochemical composition of citrus juices. Grapefruit juice was identified to be rich in flavonoids and phenolic acids, and fermentation can lead to a notable increase in the variety and abundance of these bioactive components. Meanwhile, Lipids, organic acids, amino acids and other classes of compounds also underwent significant changes. Additionally, alcoholic fermentation was effective in modulating grapefruit aromatic profiles, especially in the enrichment of juice aroma compounds with the "fruity" notes (ethyl butyrate, ethyl

hexanoate, isoamyl acetate, 1-butanol, etc.) and "winey" notes (ethanol, 1-propanol, 1-hexanol, etc.). It is expected that the obtained results will serve as a valuable reference for the large-scale production of grapefruit fermented juice and its functional enhancements in the future, as well as inspiring research on the formation mechanism of key flavor substances in the juice and the transformation process of major functional compounds during fermentation.

Data availability statement

The original contributions presented in this study are included in the article/**Supplementary material**, further inquiries can be directed to the corresponding authors.

Author contributions

XC, XF, and SR designed the study. XC, YL, and TW collected the data and participated in the design of the experimental. XL participated in manuscript preparation and revision. All authors contributed to the article and approved the submitted version.

Funding

This research was funded by the Key Research and Development Program of Zhejiang Province, China, grant numbers: 2022C02078 and 2022C02012.

Acknowledgments

The authors thank Huang Xiu and Ke Fuzhi for providing fruit materials and cultivar identification.

Conflict of interest

The authors declare that the research was conducted in the absence of any commercial or financial relationships that could be construed as a potential conflict of interest.

Publisher's note

All claims expressed in this article are solely those of the authors and do not necessarily represent those of their affiliated organizations, or those of the publisher, the editors and the reviewers. Any product that may be evaluated in this article, or claim that may be made by its manufacturer, is not guaranteed or endorsed by the publisher.

Supplementary material

The Supplementary Material for this article can be found online at: https://www.frontiersin.org/articles/10.3389/fnut.2022.1015924/full#supplementary-material

References

1. Castello F, Fernández-Pachón M-S, Cerrillo I, Escudero-López B, Ortega Á, Rosi A, et al. Absorption, metabolism, and excretion of orange juice (poly) phenols in humans: The effect of a controlled alcoholic fermentation. *Arch Biochem Biophys.* (2020) 695:108627. doi: 10.1016/j.abb.2020.108627

2. Hashemi SMB, Jafarpour D. Fermentation of bergamot juice with *Lactobacillus plantarum* strains in pure and mixed fermentations: Chemical composition, antioxidant activity and sensorial properties. *LWT.* (2020) 131:109803. doi: 10.1016/j.lwt.2020.109803

3. Liu B, Yuan D, Li Q, Zhou X, Wu H, Bao Y, et al. Changes in organic acids, phenolic compounds, and antioxidant activities of lemon juice fermented by *Issatchenkia terricola*. *Molecules.* (2021) 26:6712. doi: 10.3390/molecules26216712

4. Filannino P, Di Cagno R, Gobbetti M. Metabolic and functional paths of lactic acid bacteria in plant foods: Get out of the labyrinth. *Curr Opin Biotechnol.* (2018) 49:64–72. doi: 10.1016/j.copbio.2017.07.016

5. Cerrillo I, Escudero-López B, Hornero-Méndez D, Martín F, Fernández-Pachón M-S. Effect of alcoholic fermentation on the carotenoid composition and provitamin A content of orange juice. *J Agric Food Chem.* (2014) 62:842–9. doi: 10.1021/jf404589b

6. Mapelli-Brahm P, Barba FJ, Remize F, Garcia C, Fessard A, Mousavi Khaneghah A, et al. The impact of fermentation processes on the production, retention and bioavailability of carotenoids: An overview. *Trends Food Sci Technol.* (2020) 99:389–401. doi: 10.1016/j.tifs.2020.03.013

7. Xi W, Zhang G, Jiang D, Zhou Z. Phenolic compositions and antioxidant activities of grapefruit (*Citrus paradisi* Macfadyen) varieties cultivated in China. *Int J Food Sci Nutr.* (2015) 66:858–66. doi: 10.3109/09637486.2015.1095864

8. Patil BS, Jayaprakasha GK, Chidambara Murthy KN, Vikram A. Bioactive compounds: Historical perspectives, opportunities, and challenges. *J Agric Food Chem.* (2009) 57:8142–60. doi: 10.1021/jf9000132

9. Uckoo RM, Jayaprakasha GK, Balasubramaniam VM, Patil BS. Grapefruit (*Citrus paradisi* Macfad) phytochemicals composition is modulated by household processing techniques. *J Food Sci.* (2012) 77:C921–6. doi: 10.1111/j.1750-3841.2012.02865.x

10. Xi W, Fang B, Zhao Q, Jiao B, Zhou Z. Flavonoid composition and antioxidant activities of Chinese local pummelo (*Citrus grandis* Osbeck.) varieties. *Food Chem.* (2014) 161:230–8. doi: 10.1016/j.foodchem.2014.04.001

11. Zhang Y, Liu Y, Liu F, Zheng X, Xie Z, Ye J, et al. Investigation of chromoplast ultrastructure and tissue-specific accumulation of carotenoids in citrus flesh. *Sci Hortic.* (2019) 256:108547. doi: 10.1016/j.scienta.2019.108547

12. Mallick N, Khan RA. Effect of *Citrus paradisi* and *Citrus sinensis* on glycemic control in rats. *Afr J Pharmacy and Pharmacol.* (2015) 9:60–4. doi: 10.5897/AJPP2014

13. Memariani Z, Abbas SQ, Ul Hassan SS, Ahmadi A, Chabra A. Naringin and naringenin as anticancer agents and adjuvants in cancer combination therapy: Efficacy and molecular mechanisms of action, a comprehensive narrative review. *Pharmacol Res.* (2021) 171:105264. doi: 10.1016/j.phrs.2020.105264

14. Zhao Z, Liao N. Bergamottin induces DNA damage and inhibits malignant progression in melanoma by modulating miR-145/Cyclin D1 axis. *Onco Targets Ther.* (2021) 14:3769–81. doi: 10.2147/OTT.S275322

15. Zheng H, Zhang Q, Quan J, Zheng Q, Xi W. Determination of sugars, organic acids, aroma components, and carotenoids in grapefruit pulps. *Food Chem.* (2016) 205:112–21. doi: 10.1016/j.foodchem.2016.03.007

16. Utpott M, Rodrigues E, Rios A, de O, Mercali GD, Flôres SH. Metabolomics: An analytical technique for food processing evaluation. *Food Chem.* (2022) 366:130685. doi: 10.1016/j.foodchem.2021.130685

17. Wang X, Chen F, Ma L, Liao X, Hu X. Non-volatile and volatile metabolic profiling of tomato juice processed by high-hydrostatic-pressure and high-temperature short-time. *Food Chem.* (2022) 371:131161. doi: 10.1016/j.foodchem.2021.131161

18. Goh RMV, Pua A, Liu SQ, Lassabliere B, Leong K-C, Sun J, et al. Characterisation of volatile and non-volatile compounds in pomelo by gas chromatography-olfactometry, gas chromatography and liquid chromatography-quadrupole time-of-flight mass spectrometry. *J Essent Oil Res.* (2020) 32:132–43. doi: 10.1080/10412905.2019.1677272

19. Deng M, Dong L, Jia X, Huang F, Chi J, Muhammad Z, et al. The flavonoid profiles in the pulp of different pomelo (*Citrus grandis* L. Osbeck) and grapefruit (*Citrus paradisi* Mcfad) cultivars and their in vitro bioactivity. *Food Chem.* (2022) 15:100368. doi: 10.1016/j.fochx.2022.100368

20. Yu H, Guo W, Xie T, Ai L, Tian H, Chen C. Aroma characteristics of traditional Huangjiu produced around Winter Solstice revealed by sensory evaluation, gas chromatography–mass spectrometry and gas chromatography–ion mobility spectrometry. *Food Res Int.* (2021) 145:110421. doi: 10.1016/j.foodres.2021.110421

21. Brendel R, Schwolow S, Rohn S, Weller P. Volatilomic profiling of citrus juices by dual-detection HS-GC-MS-IMS and machine learning—an alternative authentication approach. *J Agric Food Chem.* (2021) 69:1727–38. doi: 10.1021/acs.jafc.0c07447

22. Chen Y, Li P, Liao L, Qin Y, Jiang L, Liu Y. Characteristic fingerprints and volatile flavor compound variations in Liuyang Douchi during fermentation via HS-GC-IMS and HS-SPME-GC-MS. *Food Chem.* (2021) 361:130055. doi: 10.1016/j.foodchem.2021.130055

23. Su Z, Liu B, Ma C. Analyses of the volatile compounds in cherry wine during fermentation and aging in bottle using HS-GC-IMS. *Food Sci Technol Res.* (2021) 27:599–607. doi: 10.3136/fstr.27.599

24. Bi J, Li H, Wang H. Delayed bitterness of citrus wine is removed through the selection of fining agents and fining optimization. *Front Chem.* (2019) 7:185. doi: 10.3389/fchem.2019.00185

25. Yu H, Zhang Y, Zhao J, Tian H. Taste characteristics of Chinese bayberry juice characterized by sensory evaluation, chromatography analysis, and an electronic tongue. *J Food Sci Technol.* (2018) 55:1624–31. doi: 10.1007/s13197-018-3059-4

26. Ordoudi SA, Mantzouridou F, Daftsiou E, Malo C, Hatzidimitriou E, Nenadis N, et al. Pomegranate juice functional constituents after alcoholic and acetic acid fermentation. *J Funct Foods.* (2014) 8:161–8. doi: 10.1016/j.jff.2014.03.015

27. Vilela A. Use of nonconventional yeasts for modulating wine acidity. *Fermentation.* (2019) 5:27. doi: 10.3390/fermentation5010027

28. Benito Á, Calderón F, Benito S. Mixed alcoholic fermentation of *Schizosaccharomyces pombe* and *Lachancea thermotolerans* and its influence on mannose-containing polysaccharides wine Composition. *AMB Exp.* (2019) 9:1–8. doi: 10.1186/s13568-019-0738-0

29. Cuadros-Inostroza Á, Verdugo-Alegría C, Willmitzer L, Moreno-Simunovic Y, Vallarino JG. Non-targeted metabolite profiles and sensory properties elucidate commonalities and differences of wines made with the same variety but different cultivar clones. *Metabolites.* (2020) 10:220. doi: 10.3390/metabo10060220

30. Multari S, Guzzon R, Caruso M, Licciardello C, Martens S. Alcoholic fermentation of citrus flavedo and albedo with pure and mixed yeast strains: Physicochemical characteristics and phytochemical profiles. *LWT.* (2021) 144:111133. doi: 10.1016/j.lwt.2021.111133

31. Samtiya M, Aluko RE, Dhewa T, Moreno-Rojas JM. Potential health benefits of plant food-derived bioactive components: an overview. *Foods.* (2021) 10:839. doi: 10.3390/foods10040839

32. Wang Y, Li H, Li X, Wang C, Li Q, Xu M, et al. Widely targeted metabolomics analysis of enriched secondary metabolites and determination of their corresponding antioxidant activities in *Elaeagnus angustifolia* var. *Orientalis* (L.) Kuntze fruit juice enhanced by *Bifidobacterium animalis* subsp. Lactis HN-3 fermentation. *Food Chem.* (2022) 374:131568. doi: 10.1016/j.foodchem.2021.131568

33. Yang M, Jiang Z, Wen M, Wu Z, Zha M, Xu W, et al. Chemical variation of Chenpi (citrus peels) and corresponding correlated bioactive compounds by LC-MS metabolomics and multibioassay analysis. *Front Nutr.* (2022) 9:825381. doi: 10.3389/fnut.2022.825381

34. Sicari V, Pellicanò TM, Giuffrè AM, Zappia C, Capocasale M, Poiana M. Physical chemical properties and antioxidant capacities of grapefruit juice (*Citrus paradisi*) extracted from two different varieties. *Int Food Res J.* (2018) 25:1978–84.

35. Actis-Goretta L, Dew TP, Lévèques A, Pereira-Caro G, Rein M, Teml A, et al. Gastrointestinal absorption and metabolism of hesperetin-7-O-rutinoside and hesperetin-7-O-glucoside in healthy humans. *Mol Nutr Food Res.* (2015) 59:1651–62. doi: 10.1002/mnfr.201500202

36. Shakour ZTA, Fayek NM, Farag MA. How do biocatalysis and biotransformation affect citrus dietary flavonoids chemistry and bioactivity? A review. *Crit Rev Biotechnol.* (2020) 40:689–714. doi: 10.1080/07388551.2020.1753648

37. Xu A, Xiao Y, He Z, Liu J, Wang Y, Gao B, et al. Use of non-saccharomyces yeast co-fermentation with saccharomyces cerevisiae to improve the polyphenol and volatile aroma compound contents in nanfeng tangerine wines. *J Fungi.* (2022) 8:128. doi: 10.3390/jof8020128

38. Queiroz Santos VA, Nascimento CG, Schmidt CAP, Mantovani D, Dekker RFH, da Cunha MAA. Solid-state fermentation of soybean okara: Isoflavones biotransformation, antioxidant activity and enhancement of nutritional quality. *LWT.* (2018) 92:509–15. doi: 10.1016/j.lwt.2018.02.067

39. Tran AM, Nguyen TB, Nguyen VD, Bujna E, Dam MS, Nguyen QD. Changes in bitterness, antioxidant activity and total phenolic content of grapefruit juice fermented by *Lactobacillus* and *Bifidobacterium* strains. *Acta Aliment.* (2020) 49:103–10. doi: 10.1556/066.2020.49.1.13

40. Ahmed W, Azmat R, Mehmood A, Ahmed R, Liaquat M, Khan SU, et al. Comparison of storability and seasonal changes on new flavonoids, polyphenolic acids and terepene compounds of *Citrus paradisi* (grapefruit) cv. Shamber through advance methods. *J Food Meas Charact.* (2021) 15:2915–21. doi: 10.1007/s11694-021-00815-y

41. Zuriarrain-Ocio A, Zuriarrain J, Etxebeste O, Dueñas MT, Berregi I. Evolution of main polyphenolics during cidermaking. *LWT.* (2022) 167:113798. doi: 10.1016/j.lwt.2022.113798

42. Gruz J, Novák O, Strnad M. Rapid analysis of phenolic acids in beverages by UPLC–MS/MS. *Food Chem.* (2008) 111:789–94. doi: 10.1016/j.foodchem.2008.05.014

43. Abaza, M, Afzal M, Al-Attiyah R, Guleri R. Ferulic acid methylester from *Tamarix aucheriana*, shows anticancer activity against human colorectal cancer cells: underlying molecular mechanisms. *FASEB J.* (2015) 29:936.10. doi: 10.1096/fasebj.29.1_supplement.936.10

44. Wu Y, Wang Y, Gao Z, Chen D, Liu G, Wan B, et al. Ethyl ferulate protects against lipopolysaccharide-induced acute lung injury by activating AMPK/Nrf2 signaling pathway. *Acta Pharmacol Sin.* (2021) 42:2069–81. doi: 10.1038/s41401-021-00742-0

45. Tesnière C. Importance and role of lipids in wine yeast fermentation. *Appl Microbiol Biotechnol.* (2019) 103:8293–300. doi: 10.1007/s00253-019-10029-4

46. Yao Y, Cai X, Fei W, Ye Y, Zhao M, Zheng C. The role of short-chain fatty acids in immunity, inflammation and metabolism. *Crit Rev Food Sci Nutr.* (2022) 62:1–12. doi: 10.1080/10408398.2020.1854675

47. Zhang Y-Y, Li X-L, Li T-Y, Li M-Y, Huang R-M, Li W, et al. 3-(4-Hydroxyphenyl) propionic acid, a major microbial metabolite of procyanidin A2, shows similar suppression of macrophage foam cell formation as its parent molecule. *RSC Adv.* (2018) 8:6242–50. doi: 10.1039/C7RA13729J

48. Mindt M, Walter T, Kugler P, Wendisch VF. Microbial engineering for production of N-functionalized amino acids and amines. *Biotechnol J.* (2020) 15:1900451. doi: 10.1002/biot.201900451

49. Shaw PE, Moshonas MG, Hearn CJ, Goodner KL. Volatile constituents in fresh and processed juices from grapefruit and new grapefruit hybrids. *J Agric Food Chem.* (2000) 48:2425–9. doi: 10.1021/jf0001076

50. Ahmed S, Rattanpal HS, Gul K, Dar RA, Sharma A. Chemical composition, antioxidant activity and GC-MS analysis of juice and peel oil of grapefruit varieties cultivated in India. *J Integr Agric.* (2019) 18:1634–42. doi: 10.1016/S2095-3119(19)62602-X

51. Lantsuzskaya (Krisilova) EV, Krisilov AV, Levina AM. Structure of the cluster ions of ketones in the gas phase according to ion mobility spectrometry and ab initio calculations. *Russ J Phys Chem A.* (2015) 89:1838–42. doi: 10.1134/S0036024415100179

52. Fan G, Xu X, Qiao Y, Xu Y, Zhang Y, Li L, et al. Volatiles of orange juice and orange wines using spontaneous and inoculated fermentations. *Eur Food Res Technol.* (2009) 228:849. doi: 10.1007/s00217-008-0992-x

53. Slaghenaufi D, Indorato C, Troiano E, Luzzini G, Felis GE, Ugliano M. Fate of grape-derived terpenoids in model systems containing active yeast cells. *J Agric Food Chem.* (2020) 68:13294–301. doi: 10.1021/acs.jafc.9b08162

54. Brat P, Rega B, Alter P, Reynes M, Brillouet J-M. Distribution of volatile compounds in the pulp, cloud, and serum of freshly squeezed orange juice. *J Agric Food Chem.* (2003) 51:3442–7. doi: 10.1021/jf026226y

55. Sun R, Xing R, Zhang J, Wei L, Ge Y, Deng T, et al. Authentication and quality evaluation of not from concentrate and from concentrate orange juice by HS-SPME-GC-MS coupled with chemometrics. *LWT.* (2022) 162:113504. doi: 10.1016/j.lwt.2022.113504

56. Lee H, Choi S, Kim E, Kim Y-N, Lee J, Lee D-U. Effects of pulsed electric field and thermal treatments on microbial reduction, volatile composition, and sensory properties of orange juice, and their characterization by a principal component analysis. *Appl Sci.* (2021) 11:186. doi: 10.3390/app11010186

57. Feng S, Suh JH, Gmitter FG, Wang Y. Differentiation between flavors of sweet orange (*Citrus sinensis*) and mandarin (*Citrus reticulata*). *J Agric Food Chem.* (2018) 66:203–11. doi: 10.1021/acs.jafc.7b04968

58. Ren J-N, Tai Y-N, Dong M, Shao J-H, Yang S-Z, Pan S-Y, et al. Characterisation of free and bound volatile compounds from six different varieties of citrus fruits. *Food Chem.* (2015) 185:25–32. doi: 10.1016/j.foodchem.2015.03.142

59. Rossi SC, Vandenberghe LPS, Pereira BMP, Gago FD, Rizzolo JA, Pandey A, et al. Improving fruity aroma production by fungi in SSF using citric pulp. *Food Res Int.* (2009) 42:484–6. doi: 10.1016/j.foodres.2009.01.016

60. Selli S, Canbas A, Varlet V, Kelebek H, Prost C, Serot T. Characterization of the most odor-active volatiles of orange wine made from a Turkish cv. Kozan (*Citrus sinensis* L. Osbeck). *J Agric Food Chem.* (2008) 56:227–34. doi: 10.1021/jf072231w

61. Zaitoon A, Lim L-T, Scott-Dupree C. Activated release of ethyl formate vapor from its precursor encapsulated in ethyl Cellulose/Poly (Ethylene oxide) electrospun nonwovens intended for active packaging of fresh produce. *Food Hydrocoll.* (2021) 112:106313. doi: 10.1016/j.foodhyd.2020.106313

62. Yao X, Wang K, Zhang S, Liang S, Li K, Wang C, et al. Degradation of the mixture of ethyl formate, propionic aldehyde, and acetone by *Aeromonas salmonicida*: A novel microorganism screened from biomass generated in the citric acid fermentation industry. *Chemosphere.* (2020) 258:127320. doi: 10.1016/j.chemosphere.2020.127320

63. Li H, Jiang D, Liu W, Yang Y, Zhang Y, Jin C, et al. Comparison of fermentation behaviors and properties of raspberry wines by spontaneous and controlled alcoholic fermentations. *Food Res Int.* (2020) 128:108801. doi: 10.1016/j.foodres.2019.108801

64. Mall V, Sellami I, Schieberle P. New degradation pathways of the key aroma compound 1-penten-3-one during storage of not-from-concentrate orange juice. *J Agric Food Chem.* (2018) 66:11083–91. doi: 10.1021/acs.jafc.8b04334

frontiers | Frontiers in Nutrition

TYPE Original Research
PUBLISHED 03 October 2022
DOI 10.3389/fnut.2022.1022600

OPEN ACCESS

EDITED BY
Mingquan Huang,
Beijing Technology and Business University, China

REVIEWED BY
Guangsen Fan,
Beijing Technology and Business University, China
Liang Yang,
Moutai Institute, China

*CORRESPONDENCE
Shuang Chen
shuangchen@jiangnan.edu.cn

SPECIALTY SECTION
This article was submitted to Food Chemistry, a section of the journal Frontiers in Nutrition

RECEIVED 18 August 2022
ACCEPTED 08 September 2022
PUBLISHED 03 October 2022

CITATION
Yan Y, Lu J, Nie Y, Li C, Chen S and Xu Y (2022) Characterization of volatile thiols in Chinese liquor (Baijiu) by ultraperformance liquid chromatography–mass spectrometry and ultraperformance liquid chromatography–quadrupole-time-of-flight mass spectrometry. *Front. Nutr.* 9:1022600. doi: 10.3389/fnut.2022.1022600

Characterization of volatile thiols in Chinese liquor (Baijiu) by ultraperformance liquid chromatography–mass spectrometry and ultraperformance liquid chromatography–quadrupole-time-of-flight mass spectrometry

Yan Yan[1,2], Jun Lu[3], Yao Nie[2], Changwen Li[3], Shuang Chen[2]* and Yan Xu[2]

[1]School of Liquor and Food Engineering, Guizhou University, Guiyang, China, [2]Laboratory of Brewing Microbiology and Applied Enzymology, Key Laboratory of Industrial Biotechnology of Ministry of Education, School of Biotechnology, Jiangnan University, Wuxi, China, [3]Guizhou Guotai Liquor Group Co., Ltd., Renhuai, China

Volatile thiols give a unique flavor to foods and they have been extensively studied due to their effects on sensory properties. The analytical assay of volatile thiols in food is hindered by the complexity of the matrix, and by both their high reactivity and their typically low concentrations. A new ultraperformance liquid chromatography (UPLC) strategy has been developed for the identification and quantification of volatile thiols in Chinese liquor (Baijiu). 4,4′-Dithiodipyridine reacted rapidly with eight known thiols to form derivatives, which provided a diagnostic fragment ion (*m/z* 143.5) for tandem mass spectrometry (MS/MS). To screen for new thiols, Baijiu samples were analyzed by means of UPLC–MS/MS screening for compounds exhibiting the diagnostic fragment ion (*m/z* X→143.5). New peaks with precursor ions of *m/z* 244, 200 and 214 were detected. Using UPLC with quadrupole-time-of-flight mass spectrometry (UPLC–Q-TOF–MS) and authentic standards, ethyl 2-mercaptoacetate, 1-butanethiol, and 1-pentanethiol were identified in Baijiu for the first time. Commercial Baijiu samples were analyzed with the new method and the distribution of 11 thiols was revealed in different Baijiu aroma-types. The aroma contribution of these thiols was evaluated by their odoractivity values (OAVs), with the result that 7 of 11 volatile thiols

had OAVs > 1. In particular, methanethiol, 2-furfurylthiol, and 2-methyl-3-furanthiol had relatively high OAVs, indicating that they contribute significantly to the aroma profile of Baijiu.

KEYWORDS

thiols, Baijiu, UPLC-MS/MS, quantification, odor activity value

Introduction

Baijiu (Chinese liquor) is a locally-produced, distilled alcoholic beverage that has been very popular for thousands of years and is produced using a unique traditional solid-state fermentation process (1, 2). It is typically made from sorghum or a mixture of wheat, barley, corn, rice, and sorghum. Baijiu is produced using traditional spontaneous fermentation processes with an assortment of microbial communities involved (3). The characteristic aroma of Baijiu can vary considerably, resulting from differences in raw materials, production processes, and flavor components. Baijiu is generally classified into 12 aroma types (4). At present, soy sauce aroma-type Baijiu (SSAB) (5, 6), strong aroma-type Baijiu (SAB) (7, 8), light aroma-type Baijiu (LAB) (9, 10), and roasted sesame-like aroma-type Baijiu (RSAB) (11, 12) are the four common Baijiu aroma-types in China.

The popularity of Baijiu arises mainly from its pleasant taste and the odor active compounds in its volatile fraction. More than 1,870 volatile compounds have been identified in Baijiu, including esters, alcohols, ketones, acids, aldehydes, nitrogenous compounds, and sulfur compounds (4). Despite this great complexity, only a small number of compounds are responsible for the majority of the olfactory sensation Baijiu provides. Some sulfur containing compounds are among the most important for Baijiu flavor (13, 14). In particular, volatile thiols, known historically as mercaptans, have the general structure, R-SH, and exhibit important sensory effects to Baijiu, because their concentrations are much higher than their low odor thresholds (12, 15, 16). Therefore, their determination and insights into their concentrations could help to improve the sensory quality of Baijiu and modulate its sensory attributes.

Several methods for analyzing volatile thiols in Baijiu have been developed, all using gas chromatography (GC) (12, 17). However, profiling volatile thiols in Baijiu remains a bottleneck with GC-based methods. The complexity of the Baijiu sample matrix, the typically low concentrations of volatile thiols and their low detection-sensitivity in electron-impact mass spectrometry (EIMS), means that few of them can be identified using GC–MS. Only one volatile thiol was detected in Baijiu by HS-SPME–GC–MS (18). Although pulsed flame photometric detection (PFPD) and sulfur chemiluminescence detection (SCD) are highly selective and sensitive for the quantification of volatile thiols, they provide little identification information, except for their chromatographic retention time. As a result, additional and cumbersome identification procedures are required. Only three volatile thiols were identified by HS-SPME–GC–PFPD, and four volatile thiols were identified by GC × GC–SCD in Baijiu (13, 16). In addition, current GC-based methods for Baijiu volatiles are in general, laborious and time consuming, and some of them involve multiple sample manipulation steps, during which volatile thiols can be lost, or degraded. These limitations have led to the need for a simple, rapid method that enables the identification and quantification of Baijiu volatile thiols.

To improve the sensitivity and selectivity of the measurement method, and stabilize the sulfanyl, thiols from wine and coffee are usually derivatized prior to separation and analysis using liquid chromatography-electrospray ionization mass spectrometry (LC–ESI-MS) (19, 20). 4,4'-Dithiodipyridine (DTDP) is one of the available derivatization reagents. Thiols derivatized with DTDP show increased hydrophobicity, decreased polarity volatility, and stronger affinity for protonation, resulting in an enhanced LC signal for separation and positive-mode ESI-MS detection, which enables the quantification of thiols at ng/L levels in wine (21, 22).

As a result of the low odor thresholds of most volatile thiols, in combination with their low concentrations, it is likely that some potent volatile thiols remain to be discovered in Baijiu. Therefore, we developed a method to identify the volatile thiols by UPLC–MS/MS and UPLC–Q-TOF–MS, rather than adopting a conventional GC approach. The UPLC–MS/MS method was applied to a range of Baijiu samples to investigate the volatile thiol profile.

Materials and methods

Samples

Four aroma-types Baijiu samples were under investigation: 8 SSAB samples, 6 SAB samples, 6 RSAB samples, and 7 LAB samples. The detailed information is given in **Supplementary Table 1**. The samples were stored at room temperature and without light before analysis.

TABLE 1 Optimized multiple-reaction-monitoring (MRM) parameters for the derivatizeds thiol in Baijiu.

No.	Compounds	Retention time	Precursor ion	Product ion	Cone voltage	Collision energy	Type
1	Methanethiol	1.45	158.0	110.7	23	19	Quantifier
			158.0	143.1	23	20	Qualifier
2	Ethanethiol	2.46	172.0	143.0	23	19	Quantifier
			172.0	110.2	24	21	Qualifier
3	Ethyl 2-mercaptoacetate	2.66	230.0	143.4	25	27	Quantifier
			230.0	201.1	27	29	Qualifier
4	2-Furfurylthiol	4.06	223.7	143.8	21	19	Quantifier
			223.7	81.3	24	21	Qualifier
5	2-Sulfanylethanol	6.95	187.6	173.0	21	15	Quantifier
			187.6	143.6	22	17	Qualifier
6	2-Methyl-3-furanthiol	8.94	224.0	110.6	23	25	Quantifier
			224.0	143.8	23	23	Qualifier
7	Benzenemethanethiol	9.03	234.0	143.9	23	17	Quantifier
			234.0	110.5	25	23	Qualifier
8	3-Mercaptohexyl acetate	15.59	286.2	143.3	23	23	Quantifier
			286.2	81.3	24	25	Qualifier
9	Ethyl 2-mercaptopropionate	4.97	244.0	143.2	25	27	Quantifier
			244.0	110.2	27	29	Qualifier
10	1-Butanethiol	10.78	199.7	143.4	25	19	Quantifier
			199.7	110.7	25	28	Qualifier
11	1-Pentanethiol	16.39	214.0	143.2	27	17	Quantifier
			214.0	110.5	27	19	Qualifier

Chemicals and materials

The thiols studied were methanethiol, ethanethiol, ethyl 2-mercaptoacetate, 2-furfurylthiol, 2-sulfanylethanol, 2-methyl-3-furanthiol, benzenemethanethiol, 3-mercaptohexyl acetate, ethyl 2-mercaptopropionate, 1-butanethiol, 1-pentanethiol. The internal standard was 2-phenylethanethiol. All analytes were provided commercially at high-purity grade (>°96%) by Sigma-Aldrich (Shanghai, China). Ethylenediaminetetraacetic acid disodium salt (EDTA-Na_2), 4,4'-Dithiodipyridine (DTDP, 97%), acetaldehyde (99%), and formic acid (99%) were bought from J&K Chemical Corp., (Beijing, China). C18 solid-phase extraction cartridges (6 mL, 500 mg) were purchased from ANPEL (Shanghai, China). LC–MS grade acetonitrile were purchased from Merck (Sigma-Aldrich, Shanghai, China).

Sample preparation and derivatization

A modified derivatization method for the analysis of thiols in Baijiu was used according to a previously described procedure (21). A solution of the Baijiu sample (20 mL) was spiked with 10 μL of 2-phenylethanethiol (6 mg/L) and used as an internal standard solution. The sample was diluted with water (20 mL, Millipore, USA) to a final concentration of about 25% ethanol by volume. EDTA-Na_2 (40 mg), 50% acetaldehyde (160 μL), and freshly thawed DTDP (10 mM, 400 μL) was then added to the resulting solution. The mixture was vortex-assisted stirred for 5 min and rested for 25 min at room temperature. The sample was loaded onto a SPE cartridge, which was previously pretreated with 6 mL of methanol, followed by 6 mL of water. The column was washed with 50% methanol (12 mL). The analytes retained by SPE were eluted with methanol (3 mL) and concentrated to a final volume of 400 μL under nitrogen. The solution was filtered (0.22 μm) and stored at 4°C.

Mass spectrometry method development

A triple-quadrupole mass spectrometer (Xevo TQ-S, Waters, Milford, USA) was performed with positive ionization mode. The multiple-reaction-monitoring (MRM) conditions were optimized with infusion of derivatized thiols at 10 μL/min. Based on the mass spectra (**Supplementary Figure 1**) with the MassLynx software using the sample tune and develop method, two ion transitions were chosen for the quantification (quantifier) and the confirmation (qualifier) (23). **Table 1** lists the best MRM parameters for each derived thiol with the following instrument settings: capillary voltage, 3 kV; desolvation temperature, 500°C; gas, 800 L/h.

Ultraperformance liquid chromatography–mass spectrometry instrumentation and conditions

The thiols were separated by using an UPLC system (Waters, Milford, USA) equipped with a vacuum degasser, a binary solvent manager, and an autosampler. As stationary phase an analytical column (waters BEH C18, 100 × 2.1 mm, 1.7 μm) was used. Flow-rate was 0.3 mL/min and the composition of eluents was: solvent A (0.1% formic acid in water) and solvent B (0.1% formic acid in acetonitrile). The linear gradient for solvent B was as follows: 0 min, 15%; 13 min, 22%; 14 min, 30%; 18 min, 35%; 18.5 min, 100%; 21.5 min, 100%; and 22 min, 15%. The injection volume was set at 10 μ L.

The derivatization Baijiu sample was analyzed by means of UPLC–MS/MS using precursor ion scan screening for compounds releasing the diagnostic ion (m/z X→143.5) (24). In the source, cone voltage of 23 V and collision energy of 20 eV was applied. The eleven derivatives were quantified in MRM mode by monitoring their corresponding precursor ion, product ion, cone voltage, and collision energy, respectively (**Table 1**). Each Baijiu sample was tested in three different sessions to obtain an average value.

Thiols identification by ultraperformance liquid chromatography–quadrupole-time-of-flight mass spectrometry

The derivatized Baijiu sample was carried out by UPLC system (Waters, Milford, USA), coupled to a SYNAPT Q–TOF mass spectrometer (Waters, Milford, USA), using the following operation parameters: capillary voltage: 3,500 V; cone voltage: 20 V; collision energy: 20 eV; source temperature: 100°C; desolvation temperature: 400°C; desolvation gas flow: 700 L/h; cone gas flow: 50 L/h. The analytical column, mobile phase, and linear gradient were the same as those in the UPLC–MS/MS. The precursor ions were selected from UPLC–MS/MS spectra, which were produced by precursor ion scan mode. Then, the target ions were fragmented by collision-induced dissociation.

Method validation

Thiols standard solutions at different concentrations were obtained by diluting their corresponding stock solutions using a 50% ethanol-water solution and derivatized *via* the workflow developed in this study. The linearity of the derivatized thiol was evaluated according to the relative peak area versus the concentration and expressed using the correlation coefficient (R^2). Relative to the calibration curve, thiol standards were added to the Baijiu samples at low, medium and high concentration levels. The recovery was calculated based on the concentrations of thiols measured in the spiked and non-spiked Baijiu samples. The intra-day precision was evaluated using the repeated analysis of 11 thiols found in the same Baijiu sample five times on the same day and the inter-day precision was determined on five consecutive days. The limits of detection (LOD) and limits of quantitation (LOQ) of the thiols were determined at their concentrations when the signal/noise (S/N) ratio was 3 and 10, respectively (25).

Determination of odor thresholds

Using a previously proposed method (26), the thiol odor thresholds were detected in a 46% ethanol-water solution using three-alternative forced choice tests. A sensory panel consisting of 20 panelists, 10 males, and 10 females, with an average age of 25 years. The odor activity value (OAV) was defined by dividing the concentration of the thiol to its odor threshold (27, 28).

Statistical analyses

The Masslynx software (waters) was used to process the data of UPLC–MS/MS and UPLC–Q-TOF–MS. Statistical analyses were carried out by using the Microsoft Excel 2010. Principal component analysis (PCA) of the concentrations of thiols in four different aroma-types Baijiu by XLSTAT 2018 software. Variable importance for projection (VIP) values were carried out using the SIMCA software.

Results and discussion

Identification of new thiols in Baijiu by ultraperformance liquid chromatography–mass spectrometry and ultraperformance liquid chromatography–quadrupole-time-of-flight mass spectrometry

Ultraperformance liquid chromatography–mass spectrometry analysis of derivatized thiols using multiple-reaction-monitoring

For the development of the MRM method, each commercial thiol standard derivative (1–8) was directly

infused into the MS ion source in positive mode. The cone voltage (1–50 V) and collision energy (1–35 eV) were optimized to obtain the precursor ion and product ion with maximum fragment ion abundance. Table 1 lists the optimal MRM parameters for each thiol derivative based on their response and ion fragmentation (Supplementary Figure 1). All the derivatized thiols have a diagnostic ion observed between *m/z* 143 and 144 corresponding to a disulfanylpyridine group arising from the derivatized portion of the precursor ion. The fragmentation pathways and ions were similar to those previously reported (21); the fragment ion observed at *m/z* 143.5 in this study was used as the diagnostic ion for identification of the derivatized thiols (Figure 1A). To obtain a good separation of the derivatized thiols, several parameters in the chromatography method were systematically varied, allowing the derivatized thiols to be separated within 17 min, using the optimized gradient elution procedure (Figure 1B).

Precursor ion scan of *m/z* 143.5 in Baijiu by ultraperformance liquid chromatography–mass spectrometry

Based on the fragmentation behavior mentioned above, the *m/z* 143.5 peak was chosen as the diagnostic ion for the derivatized thiols. To improve the detection sensitivity of the constituent of interest, the volume of the SSAB sample was increased to 120 mL, to obtained a higher concentration of derivatized thiols. Based on the cone voltage and collision energy of the derivatized thiols (1–8), a cone voltage of 23 V and collision energy of 20 eV, were found to maximize the fragment ion abundance of the peak between *m/z* 143 and 144, for most of the derivatized thiols. Under these conditions, precursor ion scanning of *m/z* 143.5 was applied, to produce a single-ion chromatogram (Figure 2A). Following the diagnostic ion screening (*m/z* X→143.5), the peaks corresponding to the derivatized thiol candidates were exposed from the total ion chromatogram. Eight peaks (1–8) were identified as known thiols in Baijiu, by comparing the chromatographic retention

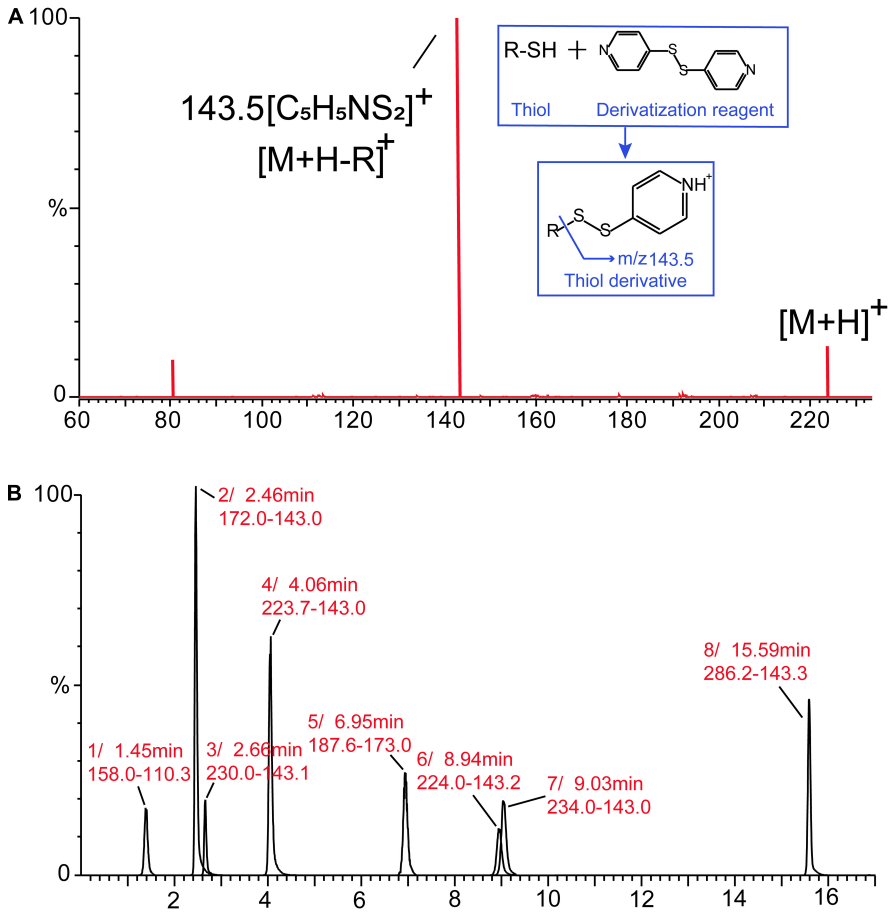

FIGURE 1
Mass spectrometry (MS/MS) spectrum of the derivatized thiols **(A)**. Multiple-reaction-monitoring (MRM) analysis of the derivatized thiol standards (1–8) in positive mode by ultraperformance liquid chromatography (UPLC)–mass spectrometry (MS/MS) **(B)**.

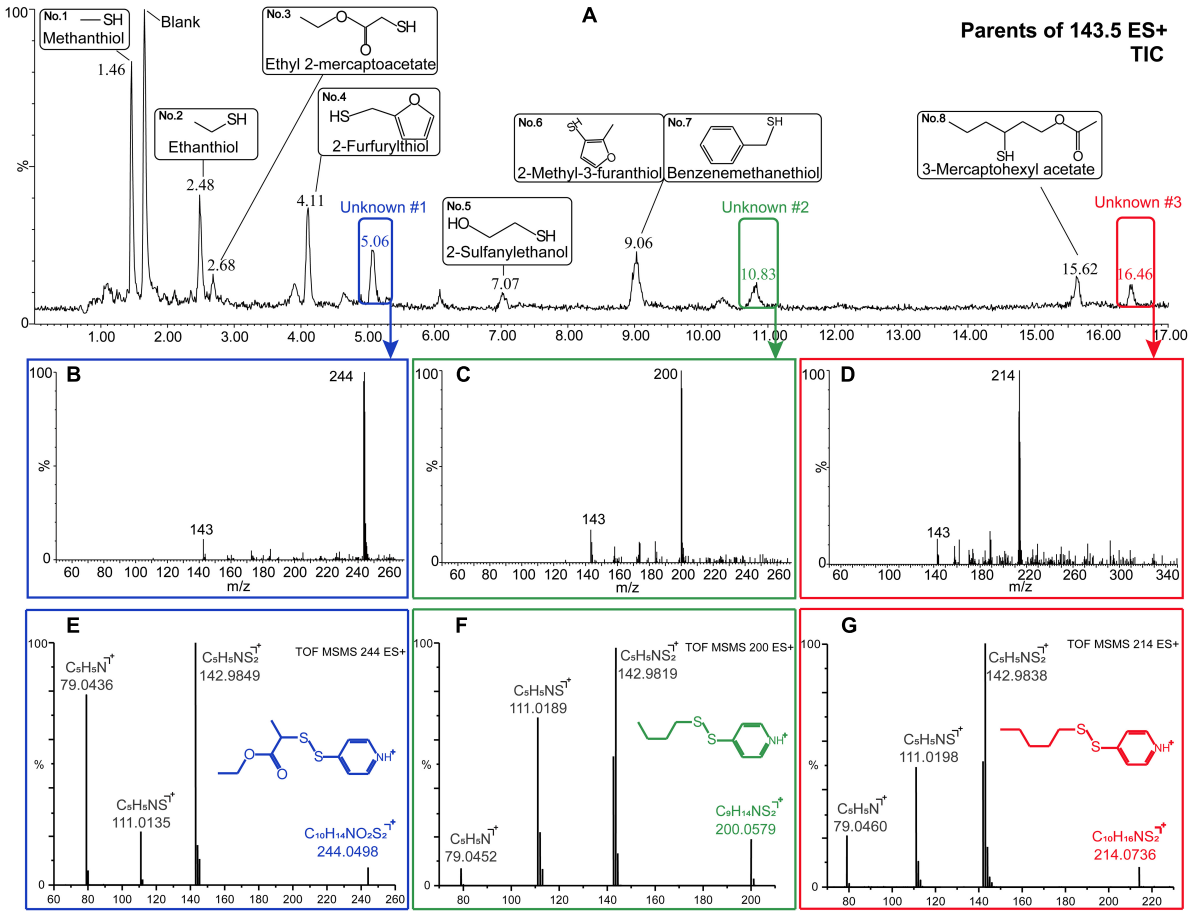

FIGURE 2
Analysis of the derivatized Baijiu sample using precursor mode and ultraperformance liquid chromatography (UPLC)–mass spectrometry (MS/MS) screening for compounds releasing a disulfanylpyridin ion (*m/z* X→143.5) **(A)**. MS spectra of the three unknown peaks by UPLC–MS/MS **(B–D)**. MS peaks observed at 5.06 (unknown #1), 10.83 (unknown #2), and 16.46 min (unknown #3) using ultraperformance liquid chromatography quadrupole-time-of-flight mass spectrometry (UPLC–Q-TOF–MS) and their corresponding elemental composition **(E–G)**.

time (Figure 1B) and MS fragmentation, with the authentic standards. Other than the eight known peaks, Figure 2A also shows three new peaks, unknown #1 (5.06 min), unknown #2 (10.83 min), and unknown #3 (16.46 min) in the chromatogram; three precursor ions at *m/z* 244, 200 and 214 were extracted from the three peaks, respectively (Figures 2B–D). The three peaks appeared to be potential new thiols, so their structures were identified using the following UPLC–Q-TOF–MS method.

New thiols in Baijiu

Quadrupole-time-of-flight mass spectrometry (Q-TOF–MS) was chosen because it can measure accurate masses with high resolution and provides the best information on the molecular composition of the compound of interest, so that its molecular formula can be confirmed, or a preliminary determination made (29, 30). UPLC–Q-TOF–MS analysis revealed the mass of unknown #1 to be *m/z* 244.0498 $[M + H]^+$, corresponding to a molecular formula of $C_{10}H_{13}NO_2S_2$ (Figure 2E). Its main MS/MS fragments were m/z 142.9849 $[M + H]^+$ ($C_5H_5NS_2^+$), 111.0135 $[M + H]^+$ ($C_5H_5NS^+$), and 79.0436 $[M + H]^+$ ($C_5H_5N^+$). The corresponding neutral losses of 101.0649, 31.9714, and 31.9699 appear to be losses of $C_5H_9O_2$, S, and S, respectively, which appear to be fragments of the thiol after derivatization.

The derivatization reagent accounts for $C_5H_5N_S$, so the molecular formula of unknown #1 was $C_5H_{10}O_2S$. The candidate thiols were screened and identified using the database of flavor molecules ([1],[2]accessed in May 2022), then verified by comparison with authentic standard. Unknown #1 was identified as ethyl 2-mercaptopropionate. UPLC–Q-TOF–MS analysis revealed the accurate mass of unknown #2 to be *m/z* 200.0579 $[M + H]^+$, corresponding to a molecular formula of $C_9H_{14}NS_2$ (Figure 2F). The retention time of

1 https://cosylab.iiitd.edu.in/flavordb/
2 https://www.vcf-online.nl/VcfHome.cfm

unknown #3 was 16.46 min and its molecular ion mass was 214.0736 $[M + H]^+$, corresponding to a molecular formula of $C_{10}H_{16}NS_2$ (Figure 2G). Subtracting the formula of the derivatizing reagent gave the molecular formula of unknown #2 and #3 as $C_4H_{10}S$ and $C_5H_{12}S$, respectively. The database of flavor molecules and comparison with authentic standards unambiguously identified these compounds as 1-butanethiol and 1-pentanethiol, respectively. To our knowledge, this is the first time ethyl 2-mercaptopropionate, 1-butanethiol, and 1-pentanethiol have been detected in Baijiu. Ethyl 2-mercaptopropionate has been reported to be an important odorant, which correlates with age in wine (31). 1-Butanethiol and 1-pentanethiol have burned and sulfuryl odor qualities, which are the odorants of fruit brandy and coffee (32, 33).

Analytical characteristics of the ultraperformance liquid chromatography–mass spectrometry method

To check the performance and reliability of the newly developed method, quality parameters such as linear range, limit of detection (LOD), limit of quantification (LOQ), precision, and accuracy were determined.

Linear range, limits of detection, and limits of quantitation

Linearity was evaluated for each thiol over at least seven different concentrations. The experimentally-determined linear ranges covered a wide concentration range (up to 819 μg/L). The correlation coefficients (R^2) for the thiol derivatives were in the range 0.9911–0.9978. The LOD and LOQ obtained for the thiol derivatives were in the ranges 0.001–0.012 μg/L and 0.003–0.037 μg/L, respectively (Table 2). All LOQs of the thiol derivatives were below their respective odor thresholds (Table 3), making this method suitable for combined chemical analysis and sensory experiments. The UPLC–MS/MS method also performed better than GC for quantification of the volatile thiols (Table 4). For example, the LOQ of 2-furfurylthiol was 0.003 μg/L by UPLC–MS/MS, 200 times lower than by HS-SPME–GC–PFPD (0.60 μg/L) (13). In addition, the UPLC–MS/MS yielded an LOD of 0.001 μg/L for 2-methyl-3-furanthiol, 170 times lower than the 0.17 μg/L achieved by HS-SPME–GC–PFPD (34). Many methods have been proposed for the analysis of thiols in Baijiu, with common techniques involving GC. Several methods such as HS-SPME, SBSE, HS-SPME arrow, and direct injection (DI) coupled with GC are widely used for extraction of thiols in Baijiu. The PFPD, SCD, and TOFMS are highly selective and sensitive for sulfur determination. Compared with previous GC analytical methods for the number of thiols analyzed in Baijiu (Supplementary Figure 2), 11 thiols were studied in the present study [11 vs. 4 with GC × GC–SCD (16), 3 with GC–PFPD (13), 1 with HS-SPME Arrow–GC–MS (18), 0 with LLE–GC × GC–TOFMS (35), 0 with HS-SPME–GC–MS (36), 0 with SBSE–GC–MS (37), and 0 with DI–GC–MS (38)].

Precision and accuracy

The method for precision measurement was based on stable instrument status, and the results were recorded as the intra- and inter-day precision with a number of replicates (n = 5) (Table 5). The RSDs of the intra-day measurements varied between 0.31% (1-pentanthiol) and 3.58% (ethyl 2-mercaptoacetate), and the inter-day RSDs varied between 5.24% (ethyl 2-mercaptoacetate) and 11.79% (methanethiol). The accuracy of the method was determined based on the recoveries. The recoveries of the thiol derivatives were all between 81.2% (methanethiol) and 106.7% (1-pentanthiol) at the three different concentration levels studied (low, medium, and high concentrations in the calibration graphs).

TABLE 2 Linear range, correlation coefficient (R^2), limits of detection (LOD), and limits of quantitation (LOQ) of the established method for derivatized thiols.

No.	Compounds	Linear equation	Linear range (μg/L)	R^2	LOD (μg/L)	LOQ (μg/L)
1	Methanethiol	$y = 0.1028x + 0.0183$	0.8–819.2	0.9978	0.012	0.037
2	Ethanethiol	$y = 0.8996x + 0.4628$	0.8–819.2	0.9936	0.008	0.024
3	Ethyl 2-mercaptoacetate	$y = 4.6146x + 0.1797$	0.03–30.72	0.9967	0.002	0.007
4	2-Furfurylthiol	$y = 0.5528x + 0.1985$	0.05–102.4	0.9933	0.001	0.003
5	2-Sulfanylethanol	$y = 3.5746x + 0.8394$	0.01–10.24	0.9950	0.002	0.005
6	2-Methyl-3-furanthiol	$y = 0.9625x - 0.0310$	0.02–10.24	0.9935	0.001	0.003
7	Benzenemethanethiol	$y = 4.1164x - 0.0676$	0.01–10.24	0.9959	0.002	0.007
8	3-Mercaptohexyl acetate	$y = 4.9971x - 0.0122$	0.01–10.24	0.9926	0.002	0.007
9	Ethyl 2-mercaptopropionate	$y = 9.7719x + 0.2881$	0.01–10.24	0.9911	0.002	0.005
10	1-Butanethiol	$y = 1.3153x - 0.0227$	0.01–20.48	0.9929	0.004	0.012
11	1-Pentanthiol	$y = 1.4120x - 0.6857$	0.05–51.2	0.9962	0.007	0.023

TABLE 3 The thiol concentrations in different aroma types Baijiu and their corresponding odor activity values (OAVs) range.

No.	Compound	Odor description[a]	Threshold (μg/L)	Concentration (μg/L)				OAV			
				SSAB	RSAB	SAB	LAB	SSAB	RSAB	SAB	LAB
1	Methanethiol	Burnt rubber, gasoline	2.2	229–513	78–245	33–104	2–10	104–233	35–111	15–47	0.9–4.5
2	Ethanethiol	Onion, rubber	0.8	6.7–32.1	5.3–28.4	1.7–7.3	Nd[c]	8.4–40.1	6.6–35.5	2.1–9.1	-
3	Ethyl 2-mercaptoacetate	Cooked vegetable	120	1.3–9.3	0.9–3.3	0.1–0.4	Nd	<0.1	<0.1	<0.1	-
4	2-Furfurylthiol	Coffee, roasted sesame seeds	0.1	11.2–37.8	6.1–21.3	1.7–6.1	0.5–1.9	112–378	61–213	17–61	5–19
5	2-Sulfanylethanol	Garbage, grilled	130	0.03–0.08	0.03–0.07	0.03–0.05	Nd–0.03	<0.1	<0.1	<0.1	<0.1
6	2-Methyl-3-furanthiol	Roasted meat, fried	0.0048	1.0–2.5	0.9–2.8	0.07–0.13	0.08–0.31	208–521	188–583	14.6–27.1	16.7–64.6
7	Benzenemethanethiol	Smoke, roasted	0.01	0.76–3.68	0.09–0.30	0.02–0.05	Nd	76–368	9–30	2–5	-
8	3-Mercaptohexyl acetate	Grapefruit, passion fruit	0.09[b]	0.05–0.13	Nd–0.08	Nd–0.05	Nd	<0.1	<0.1	<0.1	-
9	Ethyl 2-mercaptopropionate	Animal, burnt	13.23[b]	0.64–1.41	0.11–0.34	0.02–0.08	Nd	<0.1	<0.1	<0.1	-
10	1-Butanethiol	Burned, roasted	0.5[b]	1.8–7.6	1.6–8.3	0.07–0.22	Nd	3.6–15.2	3.2–16.6	0.1–0.4	-
11	1-Pentanthiol	Burned, roasted	0.3[b]	1.9–6.2	0.5–3.8	Nd	Nd	6.3–20.7	1.7–12.7	-	-

[a]Odor description are taken from online databases (Flavornet: http://www.flavornet.org; The Good Scents Company: http://www.thegoodscentscompany.com; FlavorDB: https://cosylab.iiitd.edu.in/flavordb/). [b]Odor threshold detected in this study. [c]Nd, not detected.

TABLE 4 Comparison of analytical methods for thiols in Baijiu.

Compounds	HS-SPME–GC–PFPD[12]		LLE–GC × GC–SCD[16]		HS-SPME Arrow–GC–MS[18]		This study	
	LOD	LOQ	LOD	LOQ	LOD	LOQ	LOD	LOQ
Methanethiol	26	86	-	-	-	-	0.012	0.037
Ethanethiol	3.3	11	-	-	-	-	0.008	0.024
2-Furfurylthiol	0.18	0.60	0.12	0.20	0.016	0.053	0.001	0.003
2-Methyl-3-furanthiol	0.17	0.58	0.10	0.21	-	-	0.001	0.003
Benzenemethanethiol	-	-	0.07	0.11	-	-	0.002	0.007

Analysis of practical samples

Quantitation of thiols in Baijiu samples and odor activity value analysis

To determine the practical utility of the new method, it was applied to a variety of typical aroma-type Baijiu samples obtained from diverse regions. The determined concentrations of 11 thiols are shown in **Supplementary Table 2**. The OAV can be used to evaluate the sensory contribution of an aroma compound, because it is obtained by dividing the concentration of the thiol by its odor threshold. An OAV much greater than 1 means that the compound may contribute to the odor of the Baijiu (39, 40).

The thiol concentrations in different Baijiu aroma types and their corresponding OAV ranges were determined (**Table 3**). When compared with the other samples, SSAB was characterized by a higher total thiol concentration. The concentrations of seven thiols in SSAB were higher than their corresponding odor thresholds. Methanethiol (229–513 μg/kg, OAVs 104–233), 2-furfurylthiol (11.2–37.8 μg/kg, OAVs 112–378), and 2-methyl-3-furanthiol (1.0–2.5 μg/kg, OAVs 208–521), which have been identified as important aroma compounds for SSAB in previous reports, were also confirmed in this study (34, 41). Two notable thiols, 1-butanethiol (1.8–7.6 μg/L, OAVs 4–15), and 1-pentanethiol (1.9–6.2 μg/L, OAVs 6–21), were quantified in Baijiu for the first time, in trace amounts, but their low odor thresholds still result in significant OAVs.

A total of 7 thiols with OAVs > 1 was found in RSAB. The highest OAV was found for 2-methyl-3-furanthiol (0.9–2.8 μg/kg, OAVs 188–583), which has a roasted meat odor and was identified in RSAB for the first time in this study.

10.3389/fnut.2022.1022600

TABLE 5 Recovery and precision of the established method for derivatized thiols.

No.	Compounds	Spiked level (μg/L)	Recovery (%)	Precision (RSD,%)	
				Intra-day	Inter-day
1	Methanethiol	1	81.2	1.21	7.09
		400	96.8	0.89	8.25
		800	92.5	3.55	11.79
2	Ethanethiol	1	82.5	2.41	6.55
		400	84.6	1.70	8.54
		800	88.5	2.55	11.20
3	Ethyl 2-mercaptoacetate	0.1	88.6	0.63	7.62
		5	92.6	3.21	5.24
		50	97.1	3.58	5.67
4	2-Furfurylthiol	0.1	84.7	1.48	7.89
		10	96.0	1.39	9.31
		100	104.1	1.62	6.79
5	2-Sulfanylethanol	0.02	83.9	2.30	10.28
		0.2	96.5	1.87	6.55
		2	98.3	0.43	7.51
6	2-Methyl-3-furanthiol	0.05	82.5	2.51	9.27
		0.5	104.5	0.97	8.41
		5	96.3	1.88	6.08
7	Benzenemethanethiol	0.05	83.6	3.27	9.50
		0.5	99.4	3.09	7.06
		5	86.7	1.07	7.98
8	3-Mercaptohexyl acetate	0.05	82.2	3.58	5.29
		0.5	83.6	2.96	9.88
		5	96.4	3.06	7.65
9	Ethyl 2-mercaptopropionate	0.02	90.3	0.72	7.35
		0.2	105.4	1.20	8.41
		2	88.4	1.15	8.93
10	1-Butanethiol	0.05	83.0	2.46	6.57
		0.5	81.5	1.86	9.22
		5	96.3	3.20	9.08
11	1-Pentanthiol	0.2	83.9	0.31	7.80
		2	106.7	2.31	6.91
		10	103.6	0.82	9.35

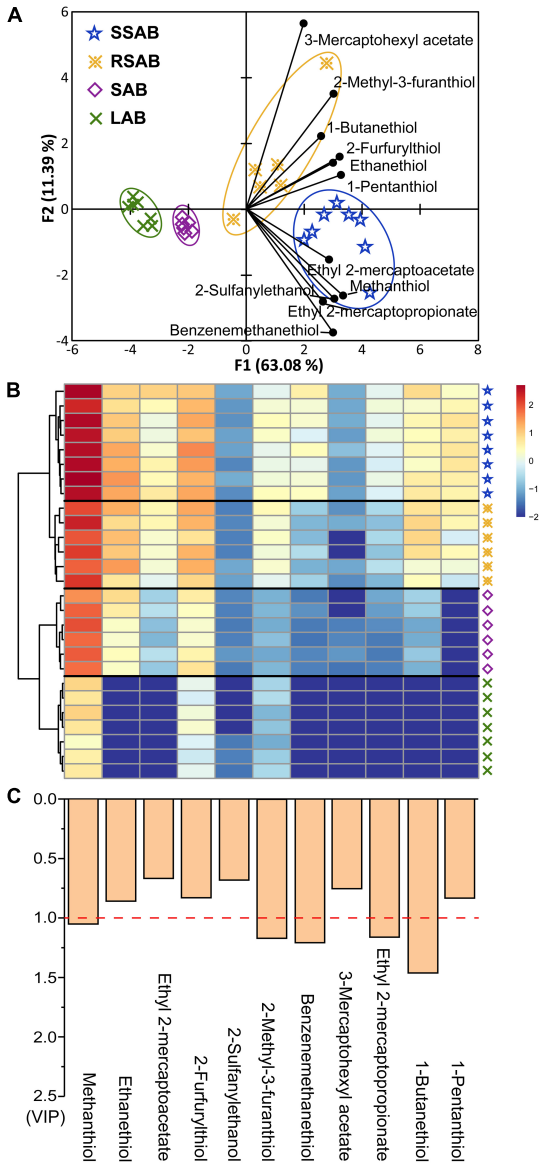

FIGURE 3
Principal component analysis (PCA) of the thiols in four aroma-types Baijiu samples **(A)**. Heat map of thiols **(B)**. The histogram shows the value of variable importance for projection (VIP) **(C)**.

2-Furfurylthiol (6.1–21.3 μg/kg, OAVs 61–213) was found at a concentration much higher than its odor threshold, and determined to be a typical potent odorant of RSAB (12). In the process of RSAB fermentation, *Saccharomyces cerevisiae* generates 2-furfurylthiol using furfural and L-cysteine as precursors (42). The OAVs of ethanethiol (6.6–35.5), benzenemethanethiol (9–30), 1-butanethiol (3.2–16.6), and 1-pentanethiol (1.7–12.7) exceeded their odor thresholds, indicating that they may contribute significantly to the overall aroma profile.

Five thiols were found at concentrations higher than their odor thresholds in SAB. Of these thiols, methanethiol was present at the highest concentration (33–104 μg/kg, OAVs 15–47), followed by ethanethiol (1.7–7.3 μg/kg, OAVs 2–9) and 2-furfurylthiol (1.7–6.1 μg/kg, OAVs 17–61). Lower concentrations were observed for 2-methyl-3-furanthiol (0.07–0.13 μg/kg, OAVs 15–27) and benzenemethanethiol

(0.02–0.05 μg/kg, OAVs 2–5), which was present at concentrations below 1 μg/L in all samples. Only four thiols were found in LAB. Among them, methanethiol (2–10 μg/L, OAVs 1–5), 2-furfurylthiol (0.5–1.9 μg/L, OAVs 5–19) and 2-methyl-3-furanthiol (0.08–0.31 μg/L, OAVs 17–65) had OAVs > 1. These findings will facilitate further study of the contribution of thiols to the aroma of Baijiu.

Statistical analysis of thiols

Principal components analysis (PCA) is an unsupervised method for expressing the similarities and differences of groups of samples (43, 44). PCA analysis was performed on the thiol concentrations (detailed data in **Supplementary Table 2**) to visualize graphically, the thiol concentrations found in the different Baijiu aroma-types. The PCA scores plot (**Figure 3A**) clearly distinguished the four different Baijiu aroma-types. The first two principal components PCA (PC1 and PC2) accounted for 74.47% of the variation, indicating that the thiols significantly affect the flavor characteristics of Baijiu (45). Moreover, heat map and hierarchical cluster analysis were also visualized differences within the different Baijiu aroma-types (**Figure 3B**). The SSAB samples were characterized by the highest thiol concentrations and were all grouped on the far right of the PCA bi-plot. In contrast, the LAB samples with lowest thiol concentrations were on the far left.

To identify the most discriminative thiols contributing to different Baijiu aroma-types, important compounds were calculated (46). Generally, variable importance for projection (VIP) values are considered a significant contributor to different samples. Thiols with VIP > 1.0 are the most relevant for explaining the different Baijiu aroma-types (47). Five thiols (methanethiol, 2-methyl-3-furanthiol, benzenemethanethiol, ethyl 2-mercaptopropionate, and 1-butanethiol) could be considered as being responsible for the differences in the aroma characteristics between Baijiu aroma-types (**Figure 3C**).

Conclusion

In this study, a novel strategy using UPLC–MS/MS and UPLC–Q-TOF–MS, was developed to identify thiols in Baijiu. The unique and consistent MS/MS fragmentation pathway of the DTDP-thiol derivatives provides a powerful way to expand the number of quantifiable thiols, and identify unknown thiols by targeting a diagnostic ion (*m/z* 143.5). In addition to the eight known thiols detected in the Baijiu samples, three new thiols were detected and identified (ethyl 2-mercaptopropionate, 1-butanethiol, and 1-pentanethiol) using the strategy developed in this study. In addition, a method using UPLC–MS/MS has been developed and validated to quantify thiols in Baijiu. Seven thiols were suggested as important aroma contributors for Baijiu based on OAVs. Five thiols could be used as markers for different Baijiu aroma-types.

Data availability statement

The original contributions presented in this study are included in the article/**Supplementary material**, further inquiries can be directed to the corresponding author.

Author contributions

YY: conceptualization, methodology, investigation, and writing—original draft. JL, YN, and CL: methodology and resources. SC: conceptualization, writing—review and editing, project administration, and funding acquisition. YX: resources, funding acquisition, and writing—review and editing. All authors have read and approved the final manuscript.

Funding

This work was supported by the National Natural Science Foundation of China (32172331) and Guizhou Science and Technology Program [(2021) General project 137].

Conflict of interest

Author JL and CL were employed by Guizhou Guotai Liquor Group Co., Ltd.

The remaining authors declare that the research was conducted in the absence of any commercial or financial relationships that could be construed as a potential conflict of interest.

Publisher's note

Supplementary material

The Supplementary Material for this article can be found online at: https://www.frontiersin.org/articles/10.3389/fnut.2022.1022600/full#supplementary-material

References

1. Jin GY, Zhu Y, Xu Y. Mystery behind Chinese liquor fermentation. *Trends Food Sci Technol*. (2017) 63:18–28. doi: 10.1016/j.tifs.2017.02.016

2. Ye H, Wang J, Shi J, Du J, Zhou Y, Huang M, et al. Automatic and intelligent technologies of solid-state fermentation process of Baijiu production: applications, challenges, and prospects. *Foods*. (2021) 10:680. doi: 10.3390/foods10030680

3. Wu Q, Zhu Y, Fang C, Wijffels RH, Xu Y. Can we control microbiota in spontaneous food fermentation?-Chinese liquor as a case example. *Trends Food Sci Technol*. (2021) 110:321–31. doi: 10.1016/j.tifs.2021.02.011

4. Liu H, Sun B. Effect of fermentation processing on the flavor of baijiu. *J Agric Food Chem*. (2018) 66:5425–32. doi: 10.1021/acs.jafc.8b00692

5. Yang L, Fan W, Xu YGC. × GC-TOF/MS and UPLC-Q-TOF/MS based untargeted metabolomics coupled with physicochemical properties to reveal the characteristics of different type daqus for making soy sauce aroma and flavor type baijiu. *LWT-Food Sci Technol*. (2021) 146:111416. doi: 10.1016/j.lwt.2021.111416

6. Yan Y, Chen S, Nie Y, Xu Y. Quantitative analysis of pyrazines and their perceptual interactions in soy sauce aroma type Baijiu. *Foods*. (2021) 10:441. doi: 10.3390/foods10020441

7. Qian Y, Zhang L, Sun Y, Tang Y, Li D, Zhang H, et al. Differentiation and classification of Chinese Luzhou-flavor liquors with different geographical origins based on fingerprint and chemometric analysis. *J Food Sci*. (2021) 86:1861–77. doi: 10.1111/1750-3841.15692

8. Gao J, Liu G, Li A, Liang C, Ren C, Xu Y. Domination of pit mud microbes in the formation of diverse flavour compounds during Chinese strong aroma-type Baijiu fermentation. *LWT-Food Sci Technol*. (2021) 137:110442. doi: 10.1016/j.lwt.2020.110442

9. Niu Y, Yao Z, Xiao Z, Zhu G, Zhu J, Chen J. Sensory evaluation of the synergism among ester odorants in light aroma type liquor by odor threshold, aroma intensity and flash GC electronic nose. *Food Res Int*. (2018) 113:102–14. doi: 10.1016/j.foodres.2018.01.018

10. Wang Z, Wang Y, Zhu T, Wang J, Huang M, Wei J, et al. Characterization of the key odorants and their content variation in Niulanshan Baijiu with different storage years using flavor sensory omics analysis. *Food Chem*. (2022) 376:131851. doi: 10.1016/j.foodchem.2021.131851

11. Shen T, Liu J, Wu Q, Xu Y. Increasing 2-furfurylthiol content in Chinese sesame-flavored Baijiu via inoculating the producer of precursor l-cysteine in Baijiu fermentation. *Food Res Int*. (2020) 138:109757. doi: 10.1016/j.foodres.2020.109757

12. Sha S, Chen S, Qian M, Wang C, Xu Y. Characterization of the typical potent odorants in Chinese roasted sesame-like flavor type liquor by headspace solid phase microextraction-aroma extract dilution analysis, with special emphasis on sulfur-containing odorants. *J Agric Food Chem*. (2017) 65:123–31. doi: 10.1021/acs.jafc.6b04242

13. Chen S, Sha S, Qian M, Xu Y. Characterization of volatile sulfur compounds in Moutai liquors by headspace solid-phase microextraction gas chromatography-pulsed flame photometric detection and odor activity value. *J Food Sci*. (2017) 82:2816–22. doi: 10.1111/1750-3841.13969

14. Sun J, Wang Z, Sun B. Low quantity but critical contribution to flavor: review of the current understanding of volatile sulfur-containing compounds in Baijiu. *J Food Compos Anal*. (2021) 103:104079. doi: 10.1016/j.jfca.2021.104079

15. Chen L, Capone DL, Jeffery DW. Analysis of potent odour-active volatile thiols in foods and beverages with a focus on wine. *Molecules*. (2019) 24:2472. doi: 10.3390/molecules24132472

16. Song X, Zhu L, Wang X, Zheng F, Zhao M, Liu Y, et al. Characterization of key aroma-active sulfur-containing compounds in Chinese Laobaigan Baijiu by gas chromatography-olfactometry and comprehensive two-dimensional gas chromatography coupled with sulfur chemiluminescence detection. *Food Chem*. (2019) 297:124959. doi: 10.1016/j.foodchem.2019.124959

17. Niu Y, Yao Z, Xiao Q, Xiao Z, Ma N, Zhu J. Characterization of the key aroma compounds in different light aroma type Chinese liquors by GC-olfactometry, GC-FPD, quantitative measurements, and aroma recombination. *Food Chem*. (2017) 233:204–15. doi: 10.1016/j.foodchem.2017.04.103

18. Zhang X, Wang C, Wang L, Chen S, Xu Y. Optimization and validation of a head space solid-phase microextraction-arrow gas chromatography-mass spectrometry method using central composite design for determination of aroma compounds in Chinese liquor (Baijiu). *J Chromatogr A*. (2019) 1610:460584. doi: 10.1016/j.chroma.2019.460584

19. Chen L, Capone DL, Jeffery DW. Identification and quantitative analysis of 2-methyl-4-propyl-1,3-oxathiane in wine. *J Agric Food Chem*. (2018) 66:10808–15. doi: 10.1021/acs.jafc.8b04027

20. Quintanilla-Casas B, Dulsat-Serra N, Cortes-Francisco N, Caixach J, Vichi S. Thiols in brewed coffee: assessment by fast derivatization and liquid chromatography-high resolution mass spectrometry. *LWT-Food SciTechnol*. (2015) 64:1085–90. doi: 10.1016/j.lwt.2015.07.010

21. Capone DL, Ristic R, Pardon KH, Jeffery DW. Simple quantitative determination of potent thiols at ultratrace levels in wine by derivatization and high-performance liquid chromatography-tandem mass spectrometry (HPLC-MS/MS) analysis. *Anal Chem*. (2015) 87:1226–31. doi: 10.1021/ac503883s

22. Mafata M, Stander MA, Thomachot B, Buica A. Measuring thiols in single cultivar south african red wines using 4,4-dithiodipyridine (DTDP) derivatization and ultraperformance convergence chromatography-tandem mass spectrometry. *Foods*. (2018) 7:138. doi: 10.3390/foods7090138

23. Danek M, Fang XY, Tang J, Plonka J, Barchanska H. Simultaneous determination of pesticides and their degradation products in potatoes by MSPD-LC-MS/MS. *J Food Compos Anal*. (2021) 104:104129. doi: 10.1016/j.jfca.2021.104129

24. Meyer S, Dunkel A, Hofmann T. Sensomics-assisted elucidation of the tastant code of cooked crustaceans and taste reconstruction experiments. *J Agric Food Chem*. (2016) 64:1164–75. doi: 10.1021/acs.jafc.5b06069

25. Venisse N, Cambien G, Robin J, Rouillon S, Nadeau C, Charles T, et al. Development and validation of an LC-MS/MS method for the simultaneous determination of bisphenol A and its chlorinated derivatives in adipose tissue. *Talanta*. (2019) 204:145–52. doi: 10.1016/j.talanta.2019.05.103

26. Dong W, Shi K, Liu M, Shen C, Li A, Sun X, et al. Characterization of 3-methylindole as a source of a "mud"-like off-odor in strong-aroma types of base Baijiu. *J Agric Food Chem*. (2018) 66:12765–72. doi: 10.1021/acs.jafc.8b04734

27. Wang J, Ming Y, Li Y, Huang M, Luo S, Li H, et al. Characterization and comparative study of the key odorants in Caoyuanwang mild-flavor style Baijiu using gas chromatography-olfactometry and sensory approaches. *Food Chem*. (2021) 347:129028. doi: 10.1016/j.foodchem.2021.129028

28. Bi S, Wang A, Lao F, Shen Q, Liao X, Zhang P, et al. Effects of frying, roasting and boiling on aroma profiles of adzuki beans (*Vigna angularis*) and potential of adzuki bean and millet flours to improve flavor and sensory characteristics of biscuits. *Food Chem*. (2021) 339:127878. doi: 10.1016/j.foodchem.2020.127878

29. Muehlwald S, Buchner N, Kroh LW. Investigating the causes of low detectability of pesticides in fruits and vegetables analysed by high-performance liquid chromatography-Time-of-flight. *J Chromatogr A*. (2018) 1542:37–49. doi: 10.1016/j.chroma.2018.02.011

30. Feng T, Wu Y, Zhang Z, Song S, Zhuang H, Xu Z, et al. Purification, identification, and sensory evaluation of kokumi peptides from agaricus bisporus mushroom. *Foods*. (2019) 8:43. doi: 10.3390/foods8020043

31. Picard M, Thibon C, Redon P, Darriet P, de Revel G, Marchand S. Involvement of dimethyl sulfide and several polyfunctional thiols in the aromatic expression of the aging bouquet of red bordeaux wines. *J Agric Food Chem*. (2015) 63:8879–89. doi: 10.1021/acs.jafc.5b03977

32. Dziekonska-Kubczak U, Pielech-Przybylska K, Patelski P, Balcerek M. Development of the method for determination of volatile sulfur compounds (VSCs) in fruit brandy with the use of HS-SPME/GC-MS. *Molecules*. (2020) 25:1232. doi: 10.3390/molecules25051232

33. Charles-Bernard M, Roberts DD, Kraehenbuehl K. Interactions between volatile and nonvolatile coffee components. 2. Mechanistic study focused on volatile thiols. *J Agric Food Chem*. (2005) 53:4426–33. doi: 10.1021/jf048020y

34. Wang L, Fan S, Yan Y, Yang L, Chen S, Xu Y. Characterization of potent odorants causing a pickle-like off-odor in Moutai-aroma type Baijiu by comparative aroma extract dilution analysis, quantitative measurements, aroma addition, and omission studies. *J Agric Food Chem*. (2020) 68:1666–77. doi: 10.1021/acs.jafc.9b07238

35. Zhu S, Lu X, Ji K, Guo K, Li Y, Wu C, et al. Characterization of flavor compounds in Chinese liquor Moutai by comprehensive two-dimensional gas chromatography/time-of-flight mass spectrometry. *Anal Chim Acta*. (2007) 597:340–8. doi: 10.1016/j.aca.2007.07.007

36. Ding X, Wu C, Huang J, Zhou R. Characterization of interphase volatile compounds in Chinese Luzhou-flavor liquor fermentation cellar analyzed by head space-solid phase micro extraction coupled with gas chromatography mass spectrometry (HS-SPME/GC/MS). *LWT-Food Sci Technol*. (2016) 66:124–33. doi: 10.1016/j.lwt.2015.10.024

37. Fan W, Shen H, Xu Y. Quantification of volatile compounds in Chinese soy sauce aroma type liquor by stir bar sorptive extraction and gas chromatography-mass spectrometry. *J Sci Food Agric*. (2011) 91:1187–98. doi: 10.1002/jsfa.4294

38. Sun J, Zhao D, Zhang F, Sun B, Zheng F, Huang M, et al. Joint direct injection and GC–MS chemometric approach for chemical profile and sulfur compounds of sesame-flavor Chinese Baijiu (Chinese liquor). *Eur Food Res Technol*. (2017) 244:145–60. doi: 10.1007/s00217-017-2938-7

39. Dunkel A, Steinhaus M, Kotthoff M, Nowak B, Krautwurst D, Schieberle P, et al. Nature's chemical signatures in human olfaction: a foodborne perspective for future biotechnology. *Angew Chem Int Ed Engl*. (2014) 53:7124–43. doi: 10.1002/anie.201309508

40. Zhu W, Cadwallader KR. Streamlined approach for careful and exhaustive aroma characterization of aged distilled liquors. *Food Chem X*. (2019) 3:100038. doi: 10.1016/j.fochx.2019.100038

41. Yan Y, Chen S, Nie Y, Xu Y. Characterization of volatile sulfur compounds in soy sauce aroma type Baijiu and changes during fermentation by GC × GC-TOFMS, organoleptic impact evaluation, and multivariate data analysis. *Food Res Int*. (2020) 131:109043. doi: 10.1016/j.foodres.2020.109043

42. Zha M, Yin S, Sun B, Wang X, Wang C. STR3 and CYS3 contribute to 2-furfurylthiol biosynthesis in Chinese sesame-flavored Baijiu yeast. *J Agric Food Chem*. (2017) 65:5503–11. doi: 10.1021/acs.jafc.7b01359

43. Cserhati T. Data evaluation in chromatography by principal component analysis. *Biomed Chromatogr*. (2010) 24:20–8. doi: 10.1002/bmc.1294

44. Lieb VM, Esquivel P, Cubero Castillo E, Carle R, Steingass CB. GC-MS profiling, descriptive sensory analysis, and consumer acceptance of Costa Rican papaya (*Carica papaya* L.) fruit purees. *Food Chem*. (2018) 248:238–46. doi: 10.1016/j.foodchem.2017.12.027

45. He F, Duan J, Zhao J, Li H, Sun J, Huang M, et al. Different distillation stages Baijiu classification by temperature-programmed headspace-gas chromatography-ion mobility spectrometry and gas chromatography-olfactometry-mass spectrometry combined with chemometric strategies. *Food Chem*. (2021) 365:130430. doi: 10.1016/j.foodchem.2021.130430

46. He Y, Liu Z, Qian M, Yu X, Xu Y, Chen S. Unraveling the chemosensory characteristics of strong-aroma type Baijiu from different regions using comprehensive two-dimensional gas chromatography-time-of-flight mass spectrometry and descriptive sensory analysis. *Food Chem*. (2020) 331:127335. doi: 10.1016/j.foodchem.2020.127335

47. Zhang H, Du H, Xu Y. Volatile organic compound-mediated antifungal activity of *Pichia* spp. and its effect on the metabolic profiles of fermentation communities. *Appl Environ Microbiol*. (2021) 87:e02992-20. doi: 10.1128/aem.02992-20.

frontiers | Frontiers in Nutrition

TYPE Original Research
PUBLISHED 05 October 2022
DOI 10.3389/fnut.2022.1018534

OPEN ACCESS

EDITED BY
Yanyan Zhang,
University of Hohenheim, Germany

REVIEWED BY
Yanqun Xu,
Zhejiang University, China
Zhengke Zhang,
Hainan University, China

*CORRESPONDENCE
Jian Li
lijian@th.btbu.edu.cn

SPECIALTY SECTION
This article was submitted to Food Chemistry, a section of the journal Frontiers in Nutrition

RECEIVED 13 August 2022
ACCEPTED 08 September 2022
PUBLISHED 05 October 2022

CITATION
Zeng X, Wang L, Fu Y, Zuo J, Li Y, Zhao J, Cao R and Li J (2022) Effects of methyl salicylate pre-treatment on the volatile profiles and key gene expressions in tomatoes stored at low temperature.
Front. Nutr. 9:1018534.
doi: 10.3389/fnut.2022.1018534

Effects of methyl salicylate pre-treatment on the volatile profiles and key gene expressions in tomatoes stored at low temperature

Xiangquan Zeng[1], Libin Wang[2], Yingli Fu[1], Jinhua Zuo[3], Yan Li[1], Jingling Zhao[1], Rui Cao[1] and Jian Li[1]*

[1]Department of Food Quality and Safety, School of Food and Health, Beijing Engineering and Technology Research Center of Food Additives, Beijing Technology and Business University, Beijing, China, [2]School of Light Industry and Food Science, Nanjing Forestry University, Nanjing, Jiangsu, China, [3]Beijing Vegetable Research Center, Beijing Academy of Agriculture and Forestry Science, Beijing, China

Tomato is one of the most widely cultivated horticultural plants in the world, while the key volatile compounds of tomato fruits generally derive from fatty acid, carotenoid, phenylalanine, and branched-chain amino acid pathways. As an important endogenous signal molecule, methyl salicylate (MeSA) plays a crucial role in the fruit ripening process of plant. Recently, it has been demonstrated that MeSA can maintain the flavor quality of full ripe tomatoes after cold-storage preservation. However, few research teams attempted to investigate the effects of MeSA plus low temperature treatment on the different volatile biosynthetic pathways of tomatoes previously. Therefore, in this study, the effects of methyl salicylate pre-treatment (0.05 mM MeSA, 24 h) on the volatile profile and flavor-related key gene expressions of tomato fruits stored at 10°C were evaluated for the first time. Our results showed that the loss of volatile compounds in low temperature-treated tomato fruits could be effectively alleviated by MeSA pre-treatment. Although MeSA had no remarkable effect on the formation of carotenoid pathway- and branched-chain amino acid pathway-related volatiles in tomatoes subjected to low temperature, the content of fatty acid pathway-related volatiles (including *cis*-3-hexenal, hexanal, and *trans*-2-hexenal) in full red fruits of 10°C MeSA group was remarkably higher than that of 10°C control group. Furthermore, MeSA pre-treatment significantly up-regulated the expression of *LOXC* or *LOXD* gene in low temperature-treated fruits at breaker or full red stage, respectively. In conclusion, pre-treatment with MeSA might avoid the loss of aromatic compounds in tomato fruits stored at low temperature by activating the fatty acid pathway.

KEYWORDS

methyl salicylate, low temperature, tomato, volatile biosynthetic pathways, flavor compounds

Introduction

Tomato is one of the most widely cultivated horticultural plants in the world, which accounts for 23% of total output in the whole fruit and vegetable market (1, 2). It has been demonstrated that tomato fruits are rich in vitamins, flavonoids, carotenoids, and other bioactive compounds (3). As an important sensory quality parameter for tomato fruit, the aroma is closely associated with the consumers' acceptance of tomatoes. Nowadays, over 400 volatile compounds have been identified in tomatoes, including primary aromatic compounds and a series of secondary aromatic compounds (4). Among them, aldehydes, alcohols, ketones, esters, phenols, and sulfurs play important roles in the flavor of tomatoes.

The key volatile compounds of tomato fruits usually derive from fatty acid, carotenoid, phenylalanine, and branched-chain amino acid pathways (5). It is reported that C6-aroma compounds can be synthesized from fatty acid pathway in tomato fruits, which are a large group of flavor substances with grassy and green odors, including hexanal, *cis*-3-hexenal, and *trans*-2-hexenal (6–8). Specifically, linolenic acid or linoleic acid is catalyzed by lipoxygenases (*LOX*s) and hydroperoxide lyase (*HPL*) to form hexanal or *cis*-3-hexenal, respectively. Under the action of aldehyde dehydrogenase 2 (*ADH2*), these compounds can be reduced to the corresponding alcohols (4). Furthermore, the aromatic compounds with fruity flavors such as neral, geranial, geranylacetone, 6-methyl-5-hepten-2-one, β-ionone, are derived from β-carotene precursors via carotenoid pathway in tomatoes. Carotenoids are able to be degraded by the carotenoid cleavage dioxygenase (*LeCCD*s) to form primary oxidation products, which further transform into volatile compounds under the actions of enzyme catalysis and acid hydrolysis (9).

Also, the volatiles synthesized from phenylalanine pathway have significant effects on the overall flavor of tomato fruits, containing 2-phenylacetaldehyde, 2-phenylethanol, methyl salicylate, guaiacol, eugenol, catechol, 1-nitro-2-ethylbenzene, and 2-phenylacetonitrile (10). On the one hand, phenylalanine can be catalyzed by phenylalanine ammonia lyase (*PAL*) to form *trans*-cinnamic acid, which further passes through different metabolic branches to form salicylic acid. One the other hand, amino acid decarboxylase (*LeAADC*) is able to promote the transformation of phenylalanine into phenylethylamine (11). Alternatively, the formation of aromatic compounds with floral smell (e.g., 2-phenylacetaldehyde and 2-phenylethanol) are related with the effects of *LeAADC* and phenethylamine reductase (*PAR*) (12). Regarding the branched-chain amino acid pathway, isoleucine and leucine are the representative precursors of aromatic components with caramel flavor (e.g., 2-methylbutyraldehyde, 3-methylbutyraldehyde, 2-methylbutanol, and 3-methylbutanol), fruity and spicy flavor (e.g., isovaleronitrile and isobutyl acetate) as well as green and fruity flavor (e.g., 2-isobutylthiazole). Notably, branched-chain amino acid aminotransferases (*SlBCAT*s) are essential for the synthesis of these components (13).

Based on previous studies, the flavor of tomato fruits can be significantly influenced by their varieties and maturity stages as well as different postharvest treatments (including ethylene, low temperature, and hormone treatments) (14). Cold storage is shown to be one of the most effective postharvest treatment methods to prolong the shelf life of horticultural products (15). However, it may inhibit the flavor formation of tomato fruits. For instance, Wang et al. (6) investigated the changes of volatile compounds in tomatoes at the green ripening stage under low temperature (5°C) (6). The results showed that the level of twelve important compounds (including aldehydes and alcohols) in tomato fruits significantly decreased after treating under low temperature. In addition, the ripening process, ethylene release, and the respiratory rate of tomatoes were also inhibited by low temperature treatment although no obvious mechanical injury was observed. It was worth mentioning that the volatile content of fruits stored at 5°C was at a very low level before the color-breaking stage. In the research of Ponce-Valadez et al. (16), they observed that storing at 12.5°C over 9 days could lead to a decrease of total aroma volatiles in tomatoes, especially for hexanal, hexanol and *cis*-3-hexenol (16). Nevertheless, there was no significant difference in consumer's flavor perception between the fruits treated at 12.5 and 20°C.

Methyl salicylate (MeSA), a plant volatile organic compound, is synthesized from salicylate acid (SA) and essential for the growth, development as well as functions of plants (17). As an important endogenous signal molecule, MeSA plays a crucial role in defense mechanism activation, responses against several abiotic and biotic stresses as well as the fruit ripening process (18). In recent years, postharvest treatment with MeSA has drawn increasing interest due to its effects on extending the shelf-life of fresh agricultural products and reducing their low-temperature susceptibility (19). For instance, the chilling injury symptoms of tomatoes exposed to 0.01 mM of MeSA for hours at room temperature were significantly less severe than those of control (20). Interestingly, in a previous investigation, it was found that MeSA pre-treatment could effectively improve the flavor quality of full ripe "FL 47" tomatoes after cold storage as well (6). To be specific, MeSA remarkably suppressed the loss of some key aroma volatiles (including geranylacetone, geranial, and MeSA) in tomato fruits subjected to chilling temperature. However, little information about the effects of MeSA plus low temperature treatment on the volatile biosynthetic pathways (fatty acid, carotenoid, phenylalanine, and branched-chain amino acid pathways) of tomato fruits was provided. Consequently, we aimed to explore the roles of MeSA pre-treatment in the flavor components and flavor-related key gene expressions of tomatoes stored at low temperature in the present study.

Materials and methods

Plant materials

Mature green (G) "FL 47" tomatoes were harvested from a commercial field in Fort Pierce, FL. In the current research, fruits with moderate size and no obvious mechanical damage were selected and used in the following experiment.

Methyl salicylate plus low temperature treatment

One hundred and forty-four uniform and defect-free fruits with an average weight of 270 g were divided into two groups. Half of them were treated with MeSA at 20°C for 24 h, while the left fruits were stored in air. In terms of the MeSA treated group, the fruits were placed in a 45 L airtight glass container, from the top of which a 7 cm diameter filter paper disc soaked in 222.9 μL of MeSA was suspended. The final chemical vapor concentration in the container was 0.05 mM. After fumigating for 24 h at 20°C, the container was opened, and ventilated for 12 h. Subsequently, all fruits were further classified into four groups (36 fruits each group), respectively. To be specific, 72 fruits with and without MeSA pre-treatment were stored at 20°C for ripening, while another half were transferred to 10°C for 10 days before ripening at 20°C. The samples at G stage (0 day) and other three maturity stages [full red (R), pink (P), and breaker (BR) stages] were collected in this study. For 20°C control group, tomato fruits reached to BR, P or R stage on the 4th, 10th, or 14th day after MeSA pre-treatment, respectively. By contrast, it took 5, 11, or 14 days for fruits in the 20°C MeSA group to reach to BR, P or R stage after MeSA pre-treatment, respectively. The ripening of fruits in 10°C control and 10°C MeSA groups was significantly delayed by low temperature treatment. Particularly, tomatoes in 10°C control group reached to BR, P, or R stage on the 13th, 22nd, or 28th day after MeSA pre-treatment, respectively, whilst it took 13, 21, or 27 days for the fruits of 10°C MeSA group to reach the corresponding stage after treating with MeSA.

Volatile compound analysis

Volatile compound analysis was performed using gas chromatography-olfactometry-mass spectrometry (GC-O-MS) according to the method of Li et al. (21), with some modifications (21). Briefly, a sharp stainless steel knife was used to remove the peels from three tomato fruits at the same maturation stage per replicate, then the pulp tissues was squeezed into juice (Baijie, S-308, China). Subsequently, 10.0 g of juice was mixed with 1.0 g of NaCl solution and immediately transferred to a 40 mL headspace bottle, which was incubated in a 60°C thermostatic water bath for 10 min to activate volatile compounds. Volatiles compounds were separated by a DB-WAX capillary column (30 m × 0.25 mm × 0.25 μm) and further identified by 7890B Agilent GC coupled to 5977A mass spectrometer detector (Agilent Technologies, USA). The temperature programming was as follows: The initial temperature (35°C) was held for 0 min before increasing to 180°C at a rate of 3°C/min, then it ramped to 230°C at a rate of 15°C/min and maintained for 2 min. High purity helium was utilized as the carrier gas at a flow rate of 1.3 mL/min, while electron impact ionization at electron energy of 70 eV and a mass range of m/z 50–500 amu were used for MS.

Three assessors trained over 2 weeks were employed to conduct GC-O-MS analysis. The panel members determined aroma intensities using a ten-point intensity scale, wherein 1, 5, and 10 corresponded to weak intensity, moderate intensity, and extreme intensity, respectively. Each sample was sniffed by assessor panelists twice, and the parameters such as aroma descriptions, retention time and intensity value were recorded. The peak was considered the active aroma only if at least two experimenters found similar odor at the same retention time.

RNA isolation and cDNA preparation for expression analysis

The total RNA was isolated from the pulp of tomatoes based on the method described by Singh et al. (22). Subsequently, the reversed transcription of RNA to cDNA was performed using the Revert Aid First-Strand cDNA Synthesis Kit (Fermentas, Madison, WI, USA) in accordance with the manufacturer's instructions. To verify the expression patterns revealed by the RNA-seq technology, quantitative real-time PCR (qRT-PCR) analysis was conducted in our research. Genes tested included *LOX*s, *ADH2*, *HPL*, *LeCCD*s, and *SlBCAT*s. Gene specific primers for selected genes were designed by online software,[1] while the melt curve was used to analyze the amplification curve specificity. Besides, qRT-PCR analysis was performed using Fast SYBR Mixture on a Bio-Rad CFX connected with real-time PCR detection system, and the incubation conditions of test was based on a two-step method: 95°C for first 10 min, followed by 40 cycles of 95°C for 15 s and 60°C for 60 s. Relative expression level was calculated based on the $2^{-\Delta\ \Delta\ Ct}$ method using actin as an internal reference gene. Three biological replicates were used for all qRT-PCR experiments and average data from three was plotted.

Statistical analysis

The volatile compounds were identified by comparing their retention indexes (RI) and mass—fragmented patterns with

1 https://mafft.cbrc.jp/alignment/server/

standards, mass spectra in the NIST Database, and/or previously published studies (23). All the experiments were performed by triplicate assays, and the results were expressed as the means ± standard deviation (SD) using SPSS 19.0 (USA) for windows. The statistical significances of data were determined using one-way analysis of variance (ANOVA) followed by the comparison of Duncan's Multiple Range Test (DMRT), p-values < 0.05 were regarded as significant.

Results and discussion

The volatile profiles and key gene expressions of tomato fruits stored at 20°C

As shown in Table 1, a total of 37 volatile compounds in "FL 47" tomato fruits were identified by GC-O-MS analysis, containing 16 aldehydes, five alcohols, five ketones, two esters, four hydrocarbons, three oxygen-containing heterocyclic compounds, as well as two sulfur and nitrogen-containing heterocyclic compounds. The findings were similar to those of Wang et al. (6), they identified 42 volatile compounds in full ripe "FL 47" tomatoes by headspace-solid-phase micro-extraction-GC-MS (HS-SPME-GC-MS) analysis (6). It was shown in Figure 1 that the content of aldehydes was the highest in volatile compounds of most groups and their flavors were described as green. As the tomato fruits ripened, the aldehyde content significantly increased. In line with Xi et al. (24), *cis*-3-hexenal was the most predominant compound among 16 aldehydes (24), while its percentage in total volatiles of tomatoes at P or R stage without any treatment was 38.48 or 69.89%, respectively (Table 2).

Furthermore, the alcohols or ketones were the second most abundant volatile compounds, the odor of which was described as malt or flora, respectively. However, the variation trend of alcohol and ketone contents with maturity was different from that of aldehyde content. The alcohol level in flavor components of fruits without any treatment continuously increased prior to the P stage, while decreased at R stage. By contrast, the concentration of ketones at BR, or P stage was relatively lower than those at G and R stage. It might be attributed to the difference in the biosynthetic pathways of these aromatic compounds (22). It was worthwhile to note that 3-methylbutanol or acetone was the major alcohol or ketone compound in volatiles of the control, respectively. When the fruit was at R stage, the level of 3-methylbutanol or acetone could reach to 16.85 or 8.14%. On the basis of the data of volatile composition, green and malt might be the main flavors in the whole odor description of tomato fruits (Table 1).

To investigate the effects of postharvest treatments on the volatile biosynthetic pathways of tomatoes, the volatile compounds were divided into four groups in the current research as well, including fatty acid pathway- (*cis*-3-hexenal, hexanal, trans-2-hexenal, 1-pentanol, and 1-penten-3-one), carotenoid pathway- (6-methyl-5-hepten-2-one and geranyl

TABLE 1 The retention index and odor descriptions of the volatile compounds identified by the GC-MS analysis.

Volatile compounds	Retention index	Odor description
Aldehydes		
Butanal	590	Pungent, green
Isovaleraldehyde	890	Malt
2-Methylbutanal	647	Malt
Tiglic aldehyde	1,101	Green, fruit
trans-2-Pentenal	828	Strawberry, fruit, tomato
cis-3-Hexenal	771	Leafy, green
Hexanal	773	Grass, tallow, fat
trans-2-Hexenal	828	Green, leafy
Heptanal	875	Fat, citrus
trans, trans-2, 4-Hexadienal	886	Green
Benzaldehyde	948	Almond, burnt sugar
Octanal	970	Fat, soap, green
Benzeneacetaldehyde	1,062	Honey, sweet
2-Octenal	987	Green leafy, walnut
Non-anal	1,059	Fat, citrus, green
Hydrocarbons		
α-Pinene	910	Pine, turpentine
p-Cymene	994	Solvent, gasoline, citrus
$_D$-Limonene	998	Lemon, orange
Terpinolene	1,049	Pine, plastic
Alcohols		
2-Methylpropanol	614	Wine, solvent, bitter
3-Methylbutanol	707	Whiskey, malt, burnt
2-Methylbutanol	711	Malt, wine, onion
1-Pentanol	1,107	Balsamic
3-Methylpentanol	817	Pungent
Ketones		
Acetone	534	Pungent, irritating, floral
2-Butanone	592	Sweet
1-Penten-3-one	661	Fruity, floral, green
6-Methyl-5-hepten-2-one	951	Fruity, floral
Geranyl acetone	1,368	Sweet, floral, estery
Oxygen-containing heterocyclic compounds		
2-Methylfuran	595	Chocolate
2-Ethyl furan	675	Rum, coffee and chocolate
2-pentyl-furan	996	Green bean, butter
Esters		
Butyl acetate	759	Pear
2-Methylbutyl acetate	866	Fruit
Sulfur- and nitrogen-containing heterocyclic compounds		
2-Isobutylthiazole	1,002	Tomato leafy, green
Dimethyl-disulfide	1,071	Onion, cabbage, putrid

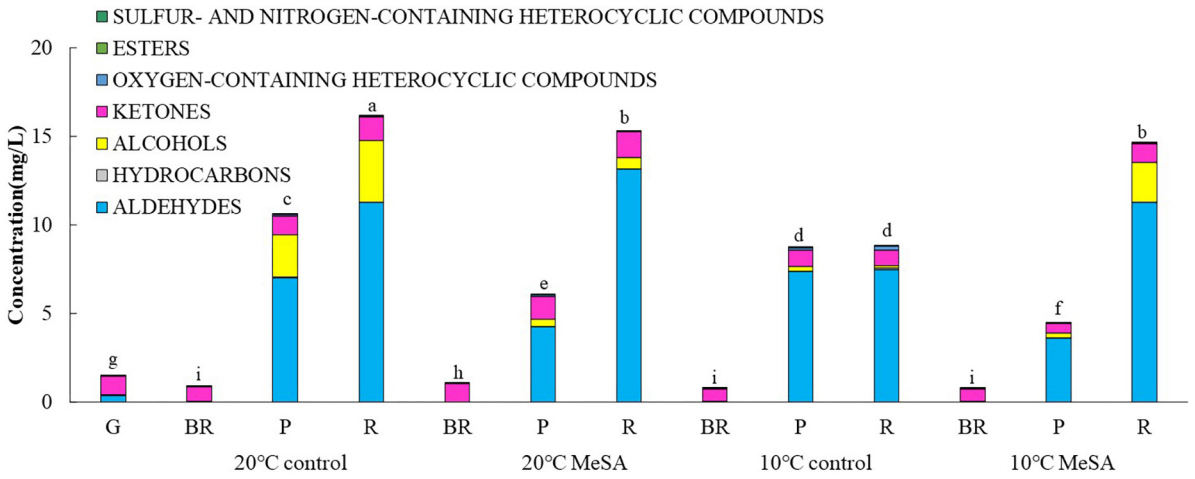

FIGURE 1
Effects of methyl salicylate (MeSA) on the contents of different types of volatile compounds in low temperature-treated tomato fruits. Data are expressed as mean ± SD (n = 3), repeated measures one-way ANOVA followed by Duncan's multiple range test (DMRT). Data marked with the same letter were no significant difference at $p < 0.05$.

acetone), phenylalanine pathway- (MeSA) and branched-chain amino acid pathway-related volatiles (2-methylbutanal, 3-methylbutanal, 2-methylbutanol, and 2-isobutylthiazole) (25). It could be found in **Figure 2** that no MeSA was detected in the volatiles of tomato fruits, possibly due to the difference in the analytic method utilized in the present study. In addition, fatty acid pathway- and branched-chain amino acid pathway-related volatiles played more important roles in the aromatic compounds of tomato fruits in 20°C control group than carotenoid-related volatiles, while their levels gradually increased with the ripening of fruits. The contents of fatty acid pathway-related volatiles in fruits at P and R stages were significantly higher than those of other volatiles, while branched-chain amino acid pathway-related volatiles were the main components of aromatic compounds in tomatoes at BR stage. Additionally, the concentration of fatty acid pathway-related volatiles in fruits of 20°C control group at R stage was approximately 2.78-fold that of branched-chain amino acid pathway-related volatiles. Hence, it seemed that the fatty acid and branched-chain amino acid pathways could be greatly activated to promote the formation of relevant flavor components when the tomatoes ripened.

A series of key genes were selected to further verified the data obtained in volatile analysis, such as *LOX*s, *ADH2*, *HPL*, *LeCCD*s, and *SlBCAT*s. *LOX*s (*LOXA*, *LOXB*, *LOXC*, *LOXD*, and *LOXE*), *ADH2* and *HPL* are one of the key enzymes involving the synthesis fatty acid pathway-related volatiles in tomato fruits (26). As shown in **Figure 3**, there was no significant difference in the relative expression of *LOXA*, *LOXB* and *LOXE* genes among the fruits at different maturity stages stored at 20°C, while the relative expressions of *LOXC* and LOXD genes in tomatoes at P and R stages were remarkably higher compared with those at G and BR stages. When the fruits were at R stage, the relative expression of *LOXC* and *LOXD* genes was 882.4 or 241.4% higher than that of fruits at G stage. According to Chen et al. (27), *LOXC* was chloroplast-targeted and generated volatile C6 flavor compounds from both linoleic and linolenic acid, whilst *LOXD* could participate in the biosynthesis of jasmonic acid (27). Although no significant difference was observed in the *ADH2* gene expression of tomato fruits at four maturity stages without any treatments, the relative expression of *HPL* gene gradually reduced with the ripening of tomatoes (**Figure 4**). The expression level of *HPL* gene in fruits at R stage was on 41.2% that in those at G stage. Our data was similar to those obtained by Chen et al. (28) and Zhang et al. (29), they believed that the production of C6 aldehydes led to the changes in *HPL* gene expression (28, 29).

Carotenoid cleavage can occur at any conjugated double bonds by *LeCCD*s to form an aldehyde or ketone (30). Two genes (*LeCCD1A-N* and *LeCCD1B*) were chosen in the present study, it was observed that the relative expression of *LeCCD* genes in tomato fruits decreased before the BK stage and then slowly increased (**Figure 5**). There was no significant difference in the *LeCCD* gene expression levels among the fruits at different maturity stages stored at 20°C, which was in accordance with the findings of Jing et al. (31). In terms of branched-chain amino acid pathway, *slBCAT*s are able to catalyze the initial step of degradation of leucine, isoleucine and valine to synthesize various flavor components (32). **Figure 6** showed that the relative expressions of *slBCAT1* and *slBCAT2* genes in tomatoes of 20°C control group remarkably decreased with the ripening of fruits, which was probably brought about by the volatile production at different maturity stages (33). The *slBCAT1* or *slBCAT2* gene expression level in fruits at R stage stored at 20°C

TABLE 2 Effects of methyl salicylate (MeSA) pre-treament on the volatile profiles of tomato fruits stored at low temperature.

Concentration (mg/L) compounds	20°C control				20°C MeSA			10°C control			10°C MeSA		
	G	BR	P	R	BR	P	R	BR	P	R	BR	P	R
Aldehydes													
Butanal	-	-	0.00379^{bc}	0.01009^{a}	-	0.00514^{b}	0.00797^{a}	-	0.00060^{d}	0.00163^{cd}	-	-	0.00375^{bc}
Isovaleraldehyde	0.001172^{e}	-	0.68416^{c}	0.85113^{ab}	-	0.78050^{ac}	0.85590^{a}	-	0.22263^{d}	0.86813^{a}	-	0.06435^{e}	0.74258^{bc}
2-Methylbutanal	-	-	-	-	-	-	-	-	-	-	-	-	-
Tiglic aldehyde	-	-	0.65628^{b}	0.91665^{a}	-	0.69762^{b}	0.80697^{ab}	-	-	0.72970^{b}	-	-	0.72407^{b}
trans-Pentenal	-	-	-	0.00927^{b}	-	-	0.02077^{a}	0.00318^{c}	-	-	-	-	0.01319^{b}
cis-3-Hexenal	-	-	4.08108^{bd}	7.29117^{ab}	-	1.93157^{de}	8.87602^{a}	-	5.69925^{ac}	4.45166^{bd}	-	2.70142^{ce}	7.41624^{ab}
Hexanal	0.367712^{de}	-	1.25997^{ac}	1.55635^{ac}	-	0.73528^{ce}	1.71419^{a}	-	1.17889^{ad}	1.12850^{ad}	-	0.82166^{be}	1.63075^{ab}
trans-2-Hexenal	-	-	0.37929^{cd}	0.63588^{ac}	-	0.09721^{d}	0.81403^{a}	-	0.27169^{cd}	0.29695^{cd}	-	0.00274^{d}	0.72669^{ab}
Heptanal	-	-	0.00467^{c}	0.01183^{a}	-	0.00573^{c}	0.01260^{a}	-	0.00195^{de}	0.00422^{cd}	-	-	0.00824^{b}
trans, trans-2, 4-Hexadienal	--	-	-	-	-	-	-	0.00624	-	-	-	-	-
Benzaldehyde	-	-	0.00052^{c}	0.00106^{b}	-	0.00058^{c}	0.00117^{b}	-	-	0.00031^{d}	-	-	0.00139^{a}
Octanal	-	0.00060^{a}	-	-	-	-	-	0.00054^{a}	-	-	-	-	-
Benzeneacetaldehyde	-	-	-	-	-	-	0.05162	-	-	-	-	-	-
2-Octenal	-	-	-	-	-	-	0.00523	-	-	-	-	-	-
Non-anal	0.000119^{c}	0.00032^{a}	-	0.00011^{cd}	0.00018^{b}	-	0.00010^{d}	-	-	-	-	-	-
Hydrocarbons													
α-Pinene	0.000112^{de}	0.00024^{ae}	0.00016^{ce}	0.00011^{de}	0.00026^{a-d}	0.00010^{de}	0.00008^{de}	0.00036^{ab}	0.00006^{e}	0.00042^{a}	0.00021^{b-e}	0.00012^{de}	0.00031^{a-c}
p-Cymene	-	0.00015^{bc}	-	0.00142^{a}	0.00021^{b}	-	-	0.00002^{cd}	-	-	0.00013^{b-d}	0.00003^{cd}	-
D-Limonene	0.50085^{b}	-	0.02252^{de}	0.01393^{ef}	-	0.01398^{ef}	0.01192^{f}	0.03462^{c}	0.01967^{df}	0.06383^{a}	0.01259^{ef}	0.02425^{d}	0.02895^{cd}
Terpinolene	-	-	-	0.00062^{a}	-	-	0.00002^{bc}	-	-	0.00008^{b}	-	-	0.00005^{bc}
Alcohols													
2-Methylpropanol	-	-	0.01730^{c}	0.03770^{b}	0.00108^{g}	0.01204^{d}	0.04019^{a}	-	0.00348^{e}	0.00357^{e}	-	-	0.00318^{f}
3-Methylbutanol	-	-	1.85744^{c}	2.72023^{a}	-	1.91057^{c}	2.40270^{b}	-	0.93333^{d}	1.72721^{c}	-	0.06917^{e}	1.84948^{c}
2-Methylbutanol	-	0.01592^{g}	0.47700^{c}	0.64783^{a}	-	0.42209^{d}	0.57772^{b}	-	0.20312^{f}	0.36492^{e}	-	0.18759^{f}	0.34749^{e}
1-Pentanol	-	-	-	-	-	-	-	-	-	-	-	-	-
3-Methylpentanol	-	-	0.03911^{b}	0.06448^{a}	-	-	0.03954^{b}	-	0.03455^{b}	0.03783^{b}	-	-	0.02846^{b}
Ketones													
Acetone	1.040855^{cd}	0.81874^{def}	1.07578^{bcd}	1.31415^{ab}	1.02152^{cd}	1.22290^{abc}	1.47779^{a}	0.68821^{ef}	0.95501^{cde}	0.88831^{de}	0.72412^{ef}	0.56623^{f}	1.04710^{cd}
2-Butanone	-	-	0.00284^{d}	0.00757^{a}	-	0.00386^{c}	0.00598^{b}	-	0.00045^{ef}	0.00122^{e}	-	-	0.00281^{d}
1-Penten-3-one	-	-	-	-	-	-	-	-	-	-	-	-	-

(Continued)

10.3389/fnut.2022.1018534

TABLE 2 (Continued)

Concentration (mg/L) compounds	20°C control				20°C MeSA				10°C control				10°C MeSA			
	G	BR	P	R	BR	P	R		BR	P	R		BR	P	R	
6-Methyl-5-hepten-2-one	-	-	0.01048^{b}	0.02199^{a}	-	0.01978^{a}	-		-	0.00017^{b}	0.02246^{a}		-	-	0.00890^{b}	
Geranyl acetone	-	-	-	-	-	-	-		-	-	-		-	-	-	
Oxygen-containing heterocyclic compounds																
2-Methylfuran	0.000673^{c}	0.00026^{d}	0.00073^{c}	0.00103^{b}	0.00068^{c}	0.00103^{b}	0.00199^{a}		-	0.00016^{de}	0.00013^{de}		-	0.00007^{de}	-	
2-Ethyl furan	-	0.00749^{ab}	0.00771^{ab}	0.00974^{a}	0.00968^{a}	0.00607^{ab}	0.00783^{ab}		0.01028^{a}	0.00866^{ab}	0.00528^{ab}		0.00819^{ab}	0.00793^{ab}	0.00820^{ab}	
2-pentyl-furan	-	0.00163^{g}	0.07296^{d}	0.01794^{f}	-	0.11360^{b}	-		0.00245^{g}	0.09487^{c}	0.21697^{a}		0.00205^{g}	0.00255^{g}	0.03856^{e}	
Esters																
Butyl acetate	-	-	0.00205^{c}	0.00259^{b}	-	0.00360^{a}	0.00262^{b}		-	0.00066^{d}	0.00257^{b}		-	-	0.00072^{d}	
2-Methylbutyl acetate	-	0.00008^{h}	0.00006^{i}	-	0.00124^{a}	0.00041^{f}	0.00061^{e}		0.00068^{d}	0.00074^{c}	0.00097^{b}		0.00028^{g}	-	-	
Sulfur- and nitrogen-containing heterocyclic compounds																
2-Isobutylthiazole	-	-	-	-	-	-	-		0.00131^{a}	-	-		-	0.00083^{b}	-	
Dimethyl-disulfide	0.00128^{c}	-	-	-	-	-	-		-	0.00661^{a}	-		-	0.00203^{b}	-	
Total volatiles	1.462008	0.84543	10.6059	16.14487	1.03845	6.06163	15.29267		0.74789	8.69958	8.813554		0.74757	4.4509	14.63111	

Data are expressed as mean ± SD ($n = 3$), repeatedmeasures one-way ANOVA followed by Duncan's test formultiple comparisons. Datamarked with the same letter were no significant difference at $P < 0.05$.

was 26.5 or 80.7% lower in comparison to that in those at G stage, respectively. In short, it seemed that the production of volatile compounds in tomato fruits was mainly influenced by their maturity through regulating fatty acid and branched-chain amino acid pathways.

Effects of low temperature on the volatile profiles and key gene expressions of tomato fruits

It was shown in Table 2 that the total volatile contents in tomato fruits of 10°C control group were much lower compared to those of 20°C control group. When the fruits were at R stage, the total volatile content in fruits of 10°C control group was only 54.6% that a of 20°C control group. In line with previous studies (24), the formation of all types of aromatic compounds in tomatoes were considerably inhibited by low temperature treatment as well (Figure 1). The aldehyde, alcohol or ketone level in fruits at R stage stored at 20°C was 1. 51-, 25. 99-, or 1.47-fold that at 10°C, respectively.

Although there was no significant difference in the level of carotenoid pathway-related volatiles in fruits between 10°C control and 20°C control groups, the formation fatty acid pathway- and branched-chain amino acid pathway-related volatiles in tomatoes were suppressed by low temperature treatment (Figure 2). In fatty acid, carotenoid or branched-chain amino acid pathway, no significant difference was observed in the relative expressions of *LOXA*, *LOXE*, *ADH2*, *HPL, LeCCD1A-N*, *LeCCD1B, SlBCAT1,* and *SlBCAT2* genes in fruits at R stage between 20°C control group and 10°C control group (Figures 3–6). Whereas, low temperature treatment remarkably enhanced the expression levels of *LOXB* and *LOXC* genes as well as inhibited the *LOXD* gene expression level. At R stage, the relative expression of *LOXB*, *LOXC*, or *LOXD* gene in fruits of 10°C control group was 149.6, 209.5, or 6.2% that of 20°C control group, respectively. It seemed that low temperature treatment could greatly reduce the formation of fatty acid pathway-related volatiles through inhibiting the *LOXD* activity in tomatoes.

Effects of methyl salicylate and methyl salicylate plus low temperature treatment on the volatile profiles and key gene expressions of tomato fruits

Methyl salicylate pre-treatment is a common postharvest technique to reduce the chilling injury of tomato fruits (34). Table 2 showed that the total volatile content of tomatoes in 20°C MeSA group was a little lower as compared to that in 20°C control group, which was consistent with the results of Wang et al. (6). At P stage, the aldehyde or alcohol level in

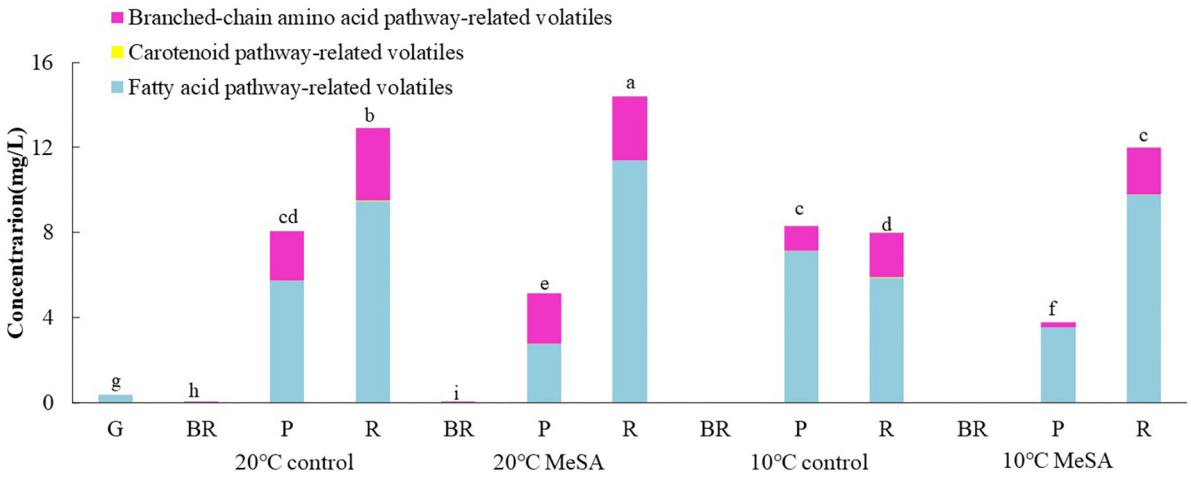

FIGURE 2
Effects of methyl salicylate (MeSA) pre-treatment on the levels of fatty acid pathway-, carotenoid pathway-, and branched-chain amino acid pathway-related volatiles in tomato fruits stored at low temperature. Data are expressed as mean ± SD (n = 3), repeated measures one-way ANOVA followed by Duncan's multiple range test (DMRT). Data marked with the same letter were no significant difference at $p < 0.05$.

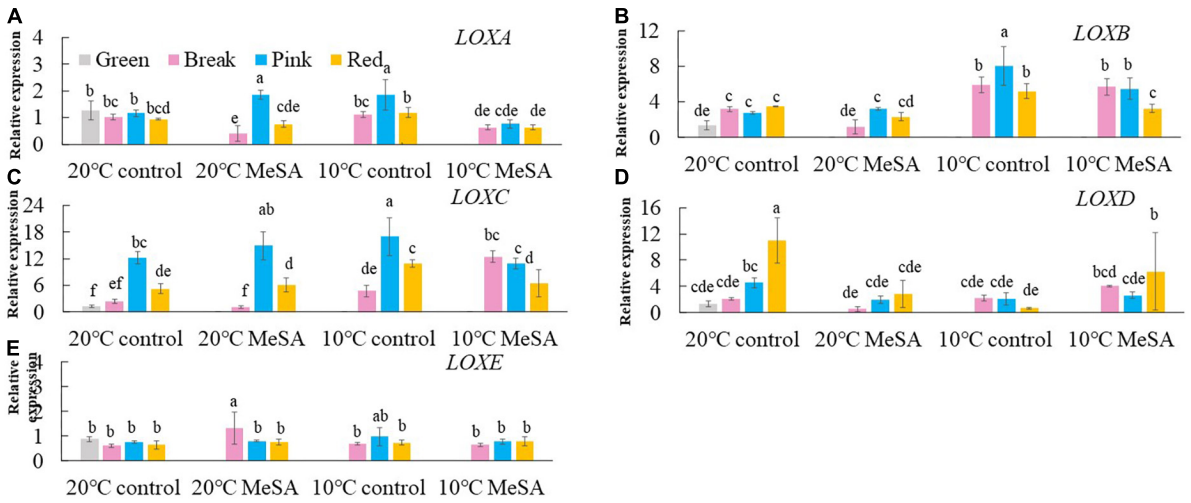

FIGURE 3
Effects of methyl salicylate (MeSA) pre-treatment on the relative expressions of *LOXA* **(A)**, *LOXB* **(B)**, *LOXC* **(C)**, *LOXD* **(D)**, and *LOXE* **(E)** genes in tomato fruits stored at low temperature. Data are expressed as mean ± SD (n = 3), repeated measures one-way ANOVA followed by DMRT. Data marked with the same letter were no significant difference at $p < 0.05$.

fruits of 20°C MeSA group was 60.6 or 17.7% that of 20°C control group, respectively (Figure 1). In addition, the decrease of volatile compounds in low-temperature treated tomato fruits was effectively alleviated by MeSA pre-treatment. The total volatile content of fruits at R stage in 10°C MeSA group was 66.0% higher in comparison with that in 10°C control group, while the level of aldehydes, alcohols, or ketones in tomatoes at R stage in 10°C MeSA group was 1. 51-, 16. 69-, or 1.16-fold that in 10°C control group, respectively. Notably, MeSA pre-treatment significantly increased the *cis*-3-hexenal, hexanal and *trans*-2-hexenal levels in fruits subjected to low temperature. The enhancement of these aroma compounds was possibly associated with the direct action to *LOX* and β-oxidation pathways by regulating activities and expressions of *LOX*, *ADH*, *HPL*, and a series of other enzymes (35). Thereby, the effects of MeSA on the volatiles derived from different pathways and key gene expressions in low temperature-treated tomato fruits were further estimated in our research.

As shown in Figure 2, on the one hand, no significant difference was found in the levels of carotenoid pathway- and branched-chain amino acid pathway-related aroma compounds in fruits at R stage between 10°C MeSA group and 10°C

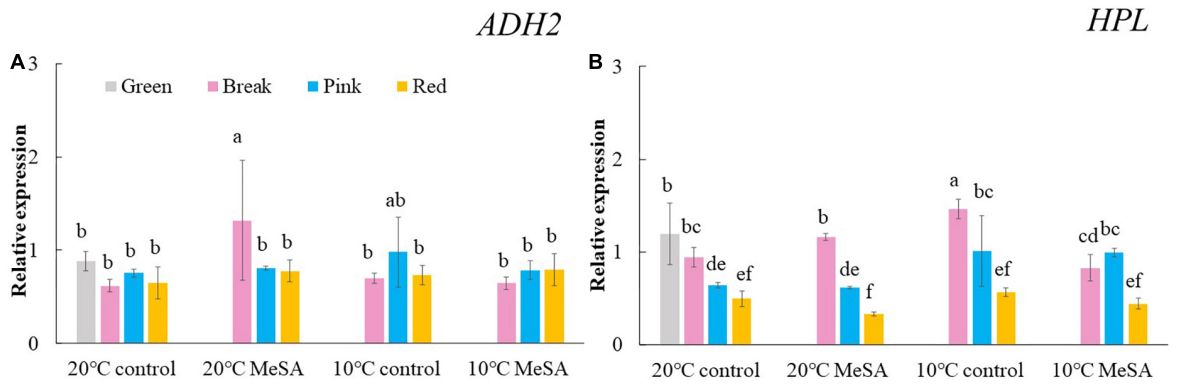

FIGURE 4
Effects of methyl salicylate (MeSA) pre-treatment on the relative expressions of *ADH2* **(A)** and *HPL* **(B)** genes in tomato fruits stored at low temperature. Data are expressed as mean ± SD (n = 3), repeated measures one-way ANOVA followed by DMRT. Data marked with the same letter were no significant difference at $p < 0.05$.

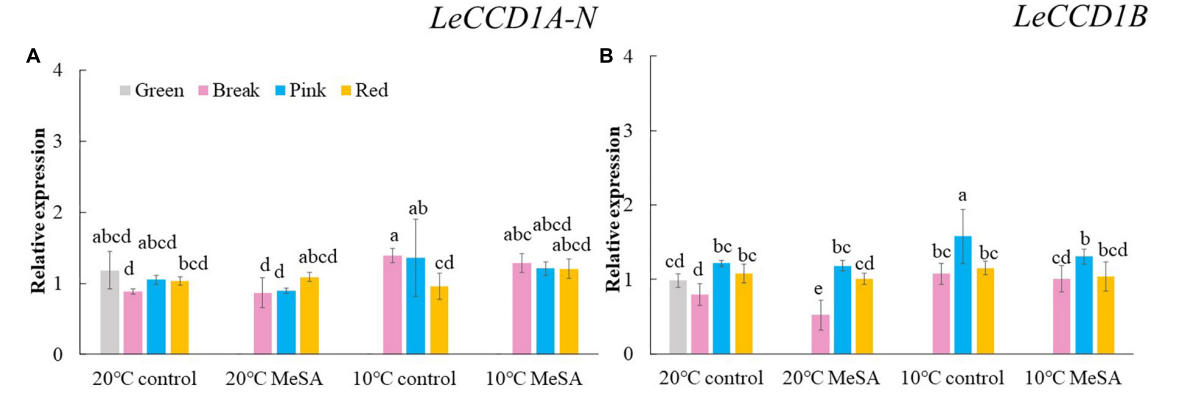

FIGURE 5
Effects of methyl salicylate (MeSA) pre-treatment on the relative expressions of *LeCCD1A-N* **(A)** and *LeCCD*1B **(B)** genes in tomato fruits stored at low temperature. Data are expressed as mean ± SD (n = 3), repeated measures one-way ANOVA followed by DMRT. Data marked with the same letter were no significant difference at $p < 0.05$.

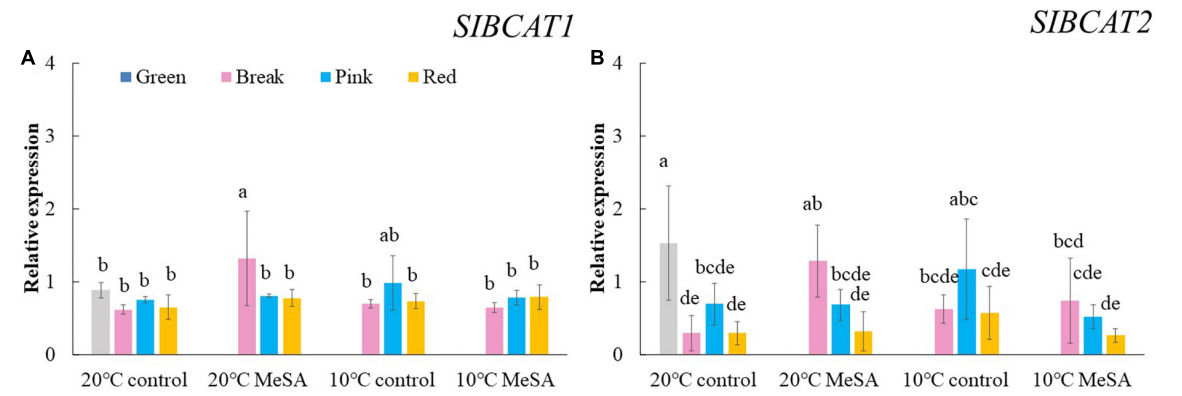

FIGURE 6
Effects of methyl salicylate (MeSA) pre-treatment on the relative expressions of *slBCAT1* **(A)** and *slBCAT2* **(B)** genes in tomato fruits stored at low temperature. Data are expressed as mean ± SD (n = 3), repeated measures one-way ANOVA followed by DMRT. Data marked with the same letter were no significant difference at $p < 0.05$.

control group. On the other hand, the biosynthesis of fatty acid pathway-related aroma compounds in tomatoes at P stage under 20°C was suppressed by MeSA pre-treatment. Whereas, the content of these components in tomatoes treated by MeSA greatly increased when the fruits turned red. The phenomenon was observed by Liu et al. (36) as well, they put forward that a high concentration of exogenous MeSA would increase endogenous salicylic acid concentration and induce cell damage in plants, which could subsequently result in the increased emission of fatty acid-derived compounds. Naturally, it was easily understood that the administration of MeSA in tomatoes stored at 10°C considerably inhibited the decrease of fatty acid pathway-related volatiles.

LOX pathway contributes to the formation of fruity note flavors in various fruits, including pears, kiwifruits and peaches (35, 37, 38). It was shown in **Figure 3** that there was no significant difference in the expression levels of *LOXA*, *LOXB*, *LOXC*, and *LOXE* genes in fruits at R stage between 20°C MeSA group and 20°C control group. However, MeSA pre-treatment remarkably down-regulated the expression of *LOXD* gene in full red tomatoes stored under 20°C, which might be brought about by the protective effects of MeSA against the reduced membrane integrity in fruits (39). Regarding low temperature-treated tomato fruits at different maturity stages, MeSA pre-treatment had no significant effect on the expression of *LOXE* gene. In response to chilling injury, the relative expressions of *LOXA* and *LOXB* genes in low temperature-treated fruits at R stage were down-regulated by MeSA pre-treatment. Nevertheless, treating fruits with MeSA and low temperature greatly up-regulated the *LOXC* gene expression at BK stage as well as *LOXD* gene expression at R stage (**Figures 3C,D**). Specifically, the *LOX* gene expression level in fruits (BK stage) or *LOXD* gene expression level in fruits (R stage) of 10°C MeSA group was 160.9% or 80.8% higher compared to that of 10°C control group, respectively. A higher expression of *LOX* genes could promote the formation of straight-chain alcohols, esters and lactones (34). Thus, the results obtained in volatile analysis were confirmed by those of qRT-PCR experiment.

ADH2 plays crucial roles in the reaction of aldehydes into alcohols (40), while *HPL* is essential for the green note flavors on account of its effects on the biosynthesis of aldehydes and oxoacids (41). As shown in **Figure 4**, MeSA pre-treatment had no remarkable impact on the *ADH2* and *HPL* expression levels in low temperature-treated tomatoes at P and R stages. We hypothesized that the increase of alcohols and esters in volatile compounds of tomatoes at R stage in 10°C MeSA group was probably caused by the up-regulation effects of MeSA on the relative expression of alcohol o-acyltransferase rather than *ADH2* (42). *LeCCDs* and *slBCAT*s are involved in the metabolism carotenoid pathway- and branched-chain amino acid pathway-related volatiles. **Figures 5**, **6** showed that there was no significant difference in the relative expressions of LeCCD1A-N, LeCCD1B, slBCAT1 and slBCAT2 genes between 20°C MeSA group and 20°C control group, which was matched with the data of volatile analysis. Overall, MeSA pre-treatment might avoid the loss of volatiles compounds in tomato fruits stored at low temperature through activating the fatty acid pathway.

Conclusion

In the present investigation, the effects of MeSA pre-treatment on the volatile profile and volatile biosynthesis pathways of low temperature-treated tomatoes were studied. Our results indicated that low temperature treatment could inhibit the biosynthesis of aromatic components in tomato fruits at P and R stages. Whereas, MeSA pre-treatment was able to effectively alleviate the loss of volatile compounds in tomato fruits stored at 10°C, especially aldehydes, alcohols and ketones. Notably, the level of fatty acid pathway-related volatiles (including *cis*-3-hexenal, hexanal and *trans*-2-hexenal) in full red fruits of 10°C MeSA group was significantly higher as compared to that of 10°C control group, although MeSA pre-treatment had no remarkable effect on the formation of carotenoid pathway- and branched-chain amino acid pathway-related flavor components in tomatoes treated by low temperature. Based on the data of qRT-PCR analysis, MeSA plus low temperature treatment remarkably up-regulated the *LOXC* or *LOXD* gene expression in fruits at BK or R stage compared to low temperature treatment, while there was no significant difference in the relative expressions of *ADH2*, *HPL*, *LeCCD*, and *slBCAT* genes between 20°C MeSA group and 20°C control group. In a nutshell, the loss of aromatic compounds in low temperature-treated tomato fruits could be suppressed by MeSA pre-treatment through activating the fatty acid pathway.

Data availability statement

The original contributions presented in this study are included in the article/supplementary material, further inquiries can be directed to the corresponding author.

Author contributions

XZ: resources (lead), writing—original draft (lead), and funding acquisition (lead). LW and JHZ: supervision (supporting). YF, YL, JLZ, and RC: writing—review and editing (supporting). JL: conceptualization (lead), funding acquisition (lead), supervision (lead), and writing—review and editing (lead). All authors contributed to the article and approved the submitted version.

Funding

This work was supported by the National Natural Science Foundation of China (No: 31772038) and the Research Foundation for Youth Scholars of Beijing Technology and Business University (Project No: QNJJ2022-10).

Conflict of interest

The authors declare that the research was conducted in the absence of any commercial or financial relationships that could be construed as a potential conflict of interest.

Publisher's note

All claims expressed in this article are solely those of the authors and do not necessarily represent those of their affiliated organizations, or those of the publisher, the editors and the reviewers. Any product that may be evaluated in this article, or claim that may be made by its manufacturer, is not guaranteed or endorsed by the publisher.

References

1. Zou J, Chen J, Tang N, Gao Y, Hong M, Wei W. Transcriptome analysis of aroma volatile metabolism change in tomato (*Solanum lycopersicum*) fruit under different storage temperatures and 1-MCP treatment. *Postharvest Biol Technol.* (2018) 135:57–67. doi: 10.1016/j.postharvbio.2017.08.017

2. Fritz EL, Rosenberg BR, Lay K, Mihailovi A, Papavasiliou FN. A comprehensive analysis of aid's effects on the transcriptome and methylome of activated b cells. *Nat Immunol.* (2013) 14:749–55. doi: 10.1038/ni.2616

3. Garbowicz K, Liu Z, Alseekh S, Tieman D, Taylor M, Kuhalskaya A, et al. Quantitative trait loci analysis identifies a prominent gene involved in the production of fatty acid-derived flavor volatiles in tomato. *Mol Plant.* (2018) 11:1147–65. doi: 10.1016/j.molp.2018.06.003

4. Wang L, Baldwin EA, Bai J. Recent advance in aromatic volatile research in tomato fruit: the metabolisms and regulations. *Food Bioprocess Tech.* (2016) 9:203–16. doi: 10.1007/s11947-015-1638-1

5. Mathieu S, Cin VD, Fei Z, Li H, Bliss P, Taylor MG. Flavour compounds in tomato fruits: identification of loci and potential pathways affecting volatile composition. *J Exp Bot.* (2009) 60:325–37. doi: 10.1093/jxb/ern294

6. Wang L, Baldwin EA, Plotto A, Luo W, Raithore S, Yu Z, et al. Effect of methyl salicylate and methyl jasmonate pre-treatment on the volatile profile in tomato fruit subjected to chilling temperature. *Postharvest Biol Technol.* (2015) 108:28–38. doi: 10.1016/j.postharvbio.2015.05.005

7. Zeng X, Jiang W, Du Z, Kokini JL. Encapsulation of tannins and tannin-rich plant extracts by complex coacervation to improve their physicochemical properties and biological activities: a review. *Crit Rev Food Sci.* (2022). [Epub ahead of print]. doi: 10.1080/10408398.2022.2075313

8. Zeng X, Li H, Jiang W, Li Q, Xi Y, Wang X, et al. Phytochemical compositions, health-promoting properties and food applications of crabapples: a review. *Food Chem.* (2022) 386:132789. doi: 10.1016/j.foodchem.2022.132789

9. da Silva Souza MA, Peres LE, Freschi JR, Purgatto E, Lajolo FM, Hassimotto NM. Changes in flavonoid and carotenoid profiles alter volatile organic compounds in purple and orange cherry tomatoes obtained by allele introgression. *J Sci Food Agric.* (2020) 100:1662–70. doi: 10.1002/jsfa.10180

10. Gonda I, Davidovich-Rikanati R, Bar E, Lev S, Jhirad P, Meshulam Y, et al. Differential metabolism of L-phenylalanine in the formation of aromatic volatiles in melon (*Cucumis melo* L.) fruit. *Phytochemistry.* (2018) 148:122–31. doi: 10.1016/j.phytochem.2017.12.018

11. Espino-Díaz M, Sepúlveda DR, González-Aguilar G, Olivas GI. Biochemistry of apple aroma: a review. *Food Technol Biotech.* (2016) 54:375–94. doi: 10.17113/ftb.54.04.16.4248

12. Tieman D, Taylor M, Schauer N, Fernie AR, Hanson AD, Klee HJ. Tomato aromatic amino acid decarboxylases participate in synthesis of the flavor volatiles 2-phenylethanol and 2-phenylacetaldehyde. *Proc Natl Acad Sci USA.* (2006) 103:8287–92. doi: 10.1073/pnas.0602469103

13. Matysik S, Herbarth O, Mueller A. Determination of microbial volatile organic compounds (MVOCs) by passive sampling onto charcoal sorbents. *Chemosphere.* (2009) 76:114–9. doi: 10.1016/j.chemosphere.2009.02.010

14. Li J, Di T, Bai J. Distribution of volatile compounds in different fruit structures in four tomato cultivars. *Molecules.* (2019) 24:2594. doi: 10.3390/molecules24142594

15. Gomes BL, Fabi JP, Purgatto E. Cold storage affects the volatile profile and expression of a putative linalool synthase of papaya fruit. *Food Res Int.* (2016) 89:654–60. doi: 10.1016/j.foodres.2016.09.025

16. Ponce-Valadez M, Escalona-Buendía HB, Villa-Hernández JM, de León-Sánchez FD, Rivera-Cabrera F, Alia-Tejacal I, et al. Effect of refrigerated storage (12.5 ℃) on tomato (Solanum lycopersicum) fruit flavor: a biochemical and sensory analysis. *Postharvest Biol Technol.* (2016) 111:6–14. doi: 10.1016/j.postharvbio.2015.07.010

17. Li H, Suo J, Han Y, Liang C, Jin M, Zhang Z, et al. The effect of 1-methylcyclopropene, methyl jasmonate and methyl salicylate on lignin accumulation and gene expression in postharvest 'Xuxiang'kiwifruit during cold storage. *Postharvest Biol Technol.* (2017) 124:107–18. doi: 10.1016/j.postharvbio.2016.10.003

18. Min D, Li F, Zhang X, Shu P, Cui X, Dong L, et al. Effect of methyl salicylate in combination with 1−methylcyclopropene on postharvest quality and decay caused by Botrytis cinerea in tomato fruit. *J Sci Food Agric.* (2018) 98:3815–22. doi: 10.1002/jsfa.8895

19. Giménez MJ, Valverde JM, Valero D, Zapata PJ, Castillo S, Serrano M. Postharvest methyl salicylate treatments delay ripening and maintain quality attributes and antioxidant compounds of 'early lory' sweet cherry. *Postharvest Biol Technol.* (2016) 117:102–9. doi: 10.1016/j.postharvbio.2016.02.006

20. Ding CK, Wang CY, Gross KC, Smith DL. Reduction of chilling injury and transcript accumulation of heat shock proteins in tomato fruit by methyl jasmonate and methyl salicylate. *Plant Sci.* (2001) 161:1153–9. doi: 10.1016/S0168-9452(01)00521-0

21. Li J, Fu Y, Bao X, Li H, Zuo J, Zhang M, et al. Comparison and analysis of tomato flavor compounds using different extraction methods. *J Food Meas Charact.* (2020) 14:465–75. doi: 10.1007/s11694-019-00102-x

22. Singh RK, Srivastava S, Chidley HG, Nath P, Sane VA. Overexpression of mango alcohol dehydrogenase (MiADH1) mimics hypoxia in transgenic tomato and alters fruit flavor components. *Agri Gene.* (2018) 7:23–33. doi: 10.1016/j.aggene.2017.10.003

23. Li J, Fu Y, Bao X, Li H, Zuo J. Optimization of solid phase microextraction combined with gas chromatography−mass spectrometry (GC−MS) to analyze aromatic compounds in fresh tomatoes. *J Food Biochem.* (2019) 43:e12858. doi: 10.1111/jfbc.12858

24. Xi Y, Li Q, Yan J, Baldwin E, Plotto A, Rosskopf E, et al. Effects of harvest maturity, refrigeration and blanching treatments on the volatile profiles of ripe "Tasti-Lee" Tomatoes. *Foods.* (2021) 10:1727. doi: 10.3390/foods10081727

25. Tieman D, Zhu G, Resende MF Jr., Lin T, Nguyen C, Bies D. A chemical genetic roadmap to improved tomato flavor. *Science.* (2017) 355:391–4. doi: 10.1126/science.aal1556

26. Upadhyay RK, Mattoo AK. Genome-wide identification of tomato (*Solanum lycopersicum* L.) lipoxygenases coupled with expression profiles during plant development and in response to methyl-jasmonate and wounding. *J Plant Physiol.* (2018) 231:318–28. doi: 10.1016/j.jplph.2018.10.001

27. Chen Z, Chen X, Yan H, Li W, Li Y, Cai R, et al. The lipoxygenase gene family in poplar: identification, classification, and expression in response to MeJA treatment. *PLoS One.* (2015) 10:e0125526. doi: 10.1371/journal.pone.0125526

28. Chen G, Hackett R, Walker D, Taylor A, Lin Z, Grierson D. Identification of a specific isoform of tomato lipoxygenase (TomloxC) involved in the generation of fatty acid-derived flavor compounds. *Plant Physiol.* (2004) 136:2641–51. doi: 10.1104/pp.104.041608

29. Zhang B, Shen JY, Wei WW, Xi WP, Xu CJ, Ferguson I, et al. Expression of genes associated with aroma formation derived from the fatty acid pathway during peach fruit ripening. *J Agric Food Chem.* (2010) 58:6157–65. doi: 10.1021/jf100172e

30. Vogel JT, Tan BC, McCarty DR, Klee HJ. The carotenoid cleavage dioxygenase 1 enzyme has broad substrate specificity, cleaving multiple carotenoids at two different bond positions. *J Biol Chem.* (2008) 283:11364–73. doi: 10.1074/jbc.M710106200

31. Jing G, Li T, Qu H, Yun Z, Jia Y, Zheng X, et al. Carotenoids and volatile profiles of yellow-and red-fleshed papaya fruit in relation to the expression of carotenoid cleavage dioxygenase genes. *Postharvest Biol Technol.* (2015) 109:114–9. doi: 10.1016/j.postharvbio.2015.06.006

32. Kochevenko A, Araújo WL, Maloney GS, Tieman DM, Do PT, Taylor MG, et al. Catabolism of branched chain amino acids supports respiration but not volatile synthesis in tomato fruits. *Mol Plant.* (2012) 5:366–75. doi: 10.1093/mp/ssr108

33. Yang X, Song J, Fillmore S, Pang X, Zhang Z. Effect of high temperature on color, chlorophyll fluorescence and volatile biosynthesis in green-ripe banana fruit. *Postharvest Biol Technol.* (2011) 62:246–57. doi: 10.1016/j.postharvbio.2011.06.011

34. Zhang X, Shen L, Li F, Meng D, Sheng J. Methyl salicylate-induced arginine catabolism is associated with up-regulation of polyamine and nitric oxide levels and improves chilling tolerance in cherry tomato fruit. *J Agr Food Chem.* (2011) 59:9351–7. doi: 10.1021/jf201812r

35. Zhou D, Sun Y, Li M, Zhu T, Tu K. Postharvest hot air and UV-C treatments enhance aroma-related volatiles by simulating the lipoxygenase pathway in peaches during cold storage. *Food Chem.* (2019) 292:294–303. doi: 10.1016/j.foodchem.2019.04.049

36. Liu B, Kaurilind E, Jiang Y, Niinemets Ü. Methyl salicylate differently affects benzenoid and terpenoid volatile emissions in *Betula pendula*. *Tree Physiol.* (2018) 38:1513–25. doi: 10.1093/treephys/tpy050

37. Li G, Jia H, Li J, Li H, Teng Y. Effects of 1-MCP on volatile production and transcription of ester biosynthesis related genes under cold storage in 'Ruanerli'pear fruit (*Pyrus ussuriensis* Maxim.). *Postharvest Biol Technol.* (2016) 111:168–74. doi: 10.1016/j.postharvbio.2015.08.011

38. Yin XR, Zhang Y, Zhang B, Yang SL, Shi YN, Ferguson IB, et al. Effects of acetylsalicylic acid on kiwifruit ethylene biosynthesis and signaling components. *Postharvest Biol Technol.* (2013) 83:27–33. doi: 10.1016/j.postharvbio.2013.03.012

39. Glowacz M, Bill M, Tinyane PP, Sivakumar D. Maintaining postharvest quality of cold stored 'Hass' avocados by altering the fatty acids content and composition with the use of natural volatile compounds–methyl jasmonate and methyl salicylate. *J Sci Food Agric.* (2017) 97:5186–93. doi: 10.1002/jsfa.8400

40. Vancanneyt G, Sanz C, Farmaki T, Paneque M, Ortego F, Castañera P. Hydroperoxide lyase depletion in transgenic potato plants leads to an increase in aphid performance. *Proc Natl Acad Sci USA.* (2001) 98:8139–44. doi: 10.1073/pnas.141079498

41. Cano-Salazar J, López ML, Crisosto CH, Echeverría G. Volatile compound emissions and sensory attributes of 'Big Top'nectarine and 'Early Rich'peach fruit in response to a pre-storage treatment before cold storage and subsequent shelf-life. *Postharvest Biol Technol.* (2013) 76:152–62. doi: 10.1016/j.postharvbio.2012.10.001

42. Ortiz A, Graell J, López ML, Echeverría G, Lara I. Volatile ester-synthesising capacity in 'Tardibelle'peach fruit in response to controlled atmosphere and 1-MCP treatment. *Food Chem.* (2010) 123:698–704. doi: 10.1016/j.foodchem.2010.05.037

frontiers | Frontiers in Nutrition

TYPE Original Research
PUBLISHED 12 October 2022
DOI 10.3389/fnut.2022.1022156

OPEN ACCESS

EDITED BY
Yanyan Zhang,
University of Hohenheim, Germany

REVIEWED BY
Mingyu Yin,
Shanghai Ocean University, China
Shengjun Chen,
South China Sea Fisheries Research Institute (CAFS), China

*CORRESPONDENCE
Yaxin Sang
sangyaxin@sina.com
Jie Gao
gaojiehbu@163.com

†These authors have contributed equally to this work

SPECIALTY SECTION
This article was submitted to Food Chemistry, a section of the journal Frontiers in Nutrition

RECEIVED 18 August 2022
ACCEPTED 21 September 2022
PUBLISHED 12 October 2022

CITATION
Wang Y, Tian G, Mao K, Chitrakar B, Wang Z, Liu J, Bai X, Sang Y and Gao J (2022) Effects of four cooking methods on flavor and sensory characteristics of scallop muscle. *Front. Nutr.* 9:1022156. doi: 10.3389/fnut.2022.1022156

Effects of four cooking methods on flavor and sensory characteristics of scallop muscle

Yueyao Wang[1], Guifang Tian[1], Kemin Mao[1], Bimal Chitrakar[1], Zhongxuan Wang[1], Jie Liu[2], Xinzhong Bai[2], Yaxin Sang[1*†] and Jie Gao[1*†]

[1]College of Food Science and Technology, Hebei Agricultural University, Baoding, China, [2]Shandong Longsheng Food Co., Ltd., Laoling, China

This work aimed to explore the influence of four different cooking methods (Boiling, roasting, frying, and microwaving) on the sensory characteristics of scallop muscles. Headspace-gas chromatography-ion mobility spectrometry (HS-GC-IMS) and electronic nose (e-nose) were combined to analyze the aroma of scallops. Combined with the results of free amino acids and electronic tongue (e-tongue), the taste changes of different samples were analyzed. Furthermore, texture profile and microstructure analysis jointly showed the influence of cooking methods on texture. The results showed that frying was the most suitable cooking method for scallop muscle because it resulted the best tasted products, boiled scallops retain the highest similarity to fresh scallops. Besides, a higher level of lipid oxidation and Maillard reaction resulted in significant increase in aldehydes, ketones, furans, umami, and sweet amino acid. For the boiled sample, the loss of water-soluble compounds and less fat oxidation resulted in fewer flavor substances and free amino acids, along with looser organizational structure and poorer sensory quality. The research showed that besides the texture of scallop muscle, volatile organic compounds and free amino acids as well as their mutual roles in taste and smell were also important to sensory receptivity.

KEYWORDS

scallop, volatile flavor compounds, free amino acid, HS-GC-IMS, electronic nose, electronic tongue

Introduction

Scallop is a major cultivated shellfish in China and its the annual production output ranks top in the world. More than 90% was produced in China (1). Scallop varieties, namely *Argopecten irradians*, *Patinopecten yessoensis*, and *Chlamys farreri* are the three major scallops produced in the coastal areas of China (2). Among them, *Argopecten irradians* are mainly cultivated in northern coastal areas belonging to Shandong and Liaoning province. As a common kind of shellfish, *Argopecten irradians* are widely produced and consumed because of their short growth cycle and fast growth speed (3). However, fresh scallops easily deteriorate in a short time and generate an off-flavor,

which limits their long-distance transport and storage life. Cooking can make the scallop safe to consume by killing pathogens; at the same time, its flavor is improved to a various degree. In recent years, there have been many studies on the effects of different cooking methods on the flavor, taste and sensory properties of aquatic products. Chen et al. (4) compared tilapia muscles heated through microwaving, roasting, steaming, and boiling and found that the four heating methods had significantly different influence on the flavor. Besides, due to varying heating principles, heating temperatures and other factors, different heating methods affect food organization and structure, which ultimately affect the food taste by changing muscle fiber structure and water contents. Lee et al. (5) found that palatability of white-striping chicken breasts changed after heating and the meat roasted in an oven tasted harder and chewier than that cooked by sous-vide. At present, the research on scallop mainly focuses on the influence of drying method on its flavor and taste substances (6, 7); however, there is little research on its cooking method. Therefore, the changes in flavor and sensory characteristics due to different cooking methods may be an interesting area in the sensory study of scallops.

However, the way to assess the flavor of heated products is as important as heating methods. HS-GC-IMS is an emerging flavor analytical instrument. Being highly sensitive, it can not only qualitatively and quantitatively analyze volatile organic compounds but also compare different samples of flavor substances more intuitively. E-nose and e-tongue are the bionic systems that simulate human senses of smell and taste; however, they have weaknesses as well. For example, they can't identify concrete substances; so, they can't fully replace the analytical instruments or sensory analysis (8). In recent years, the combined use of multiple instruments has become a popular trend, as it can provide more comprehensive and diversified information for the research on food flavor and taste characteristics (9). Established literature combined HS-GC-IMS, e-nose, e-tongue and amino acid detection to represent the flavor and taste changes of salmonid. The results showed that multiple instruments can complement each other in validating analysis results, thereby differentiating samples in a more comprehensive and effective manner (10). However, no report about the application of the combined use of these instruments to scallops have been available so far.

This work combined HS-GC-IMS and e-nose to analyze the aroma of scallop muscle after various cooking methods, including boiled in water, roasted, fried and heated by microwave. Combining the free amino acids in scallops and e-tongue results, we analyzed the taste changes of scallop muscle heated in different ways. Through sensory assessment, microstructure observation and texture profile analysis, we analyzed the sensory characteristics of heated scallop muscle. Finally, we analyzed how sensory assessment was correlated to taste and aroma. The research results can provide a basis for choosing the heating method suitable for scallop muscle for better sensory properties.

Materials and methods

Materials

Fresh scallops (*Argopectens irradias*) and corn oil were purchased from a local supermarket in Baoding, Hebei, China. Chemicals, such as sulfosalicylic acid, sodium citrate and ninhydrin were obtained from Sinopharm Chemical Reagent Co., Ltd. (Shanghai, China). The mixed amino acid standard solution (HPLC grade, amino acids in this standard were 2.5 μmol per mL in 0.1 N HCl, except L-cystine at 1.25 μmol per mL) was purchased from Sigma-Aldrich Chemical Co. (St. Louis, MO, USA).

Treatment of samples

Fresh scallops were cleaned and shell-removed to get muscle parts; they were divided into five groups. The scallop without cooking was the control sample (CK). For boiling cooking, the sample was heated in boiling water for 10 min (BS). The roasted scallops (RS) were prepared by dry roasting inside a preheated oven (200°C) for 10 min; the samples were turned over at the fifth min. Scallops were fried in a pan containing preheated corn oil (150°C) for 6 min (FS). Microwaved scallops (MS) were obtained by heating them in a microwave oven at 400 W for 2 min. After cooling, all the samples were packed in zip-lock aluminum bags and kept in a fridge until further analysis.

Volatile compounds analysis by headspace-gas chromatography-ion mobility spectrometry

Headspace-gas chromatography-ion mobility spectrometry (HS-GC-IMS) (FlavourSpec®, G.A.S., Dortmund, Germany) was used to analyze the volatile compounds of scallop muscle following the method of Li et al. (11) with slight modification. Before analysis, 2 g of the sample was taken into a 20 mL glass bottle and then incubated with swirling at 500 r/min for 10 min at 80°C. Then, a syringe heated to 85°C was used to inject 1.0 mL of headspace gas. The chromatographic column used was MXT-5 (15 m × 0.53 mm i.d., 1°μm film thickness; Restek Corporation, Bellefonte, PA, USA). Nitrogen (99.99% purity) was used as the carrier gas.

The elution program was as follows: 2 mL/min for 2 min; 10 mL/min within 8 min; 100 mL/min within 10 min; and 150 mL/min within 20 min. At 45°C, the substance was ionized and further separated in the IMS ionization chamber. During

analysis, C4-C9 n-ketones (Sinopharm Chemical Reagent Co., Ltd., Beijing, China) was used as reference to identify the retention index (RI) of the substance. Then, RI and drift time (DT) were compared with GC × IMS Library.

Free amino acids analysis by automatic amino acid analyzer

The method of Zhang et al. (12) was used to analyze free amino acids by using an amino acid analyzer (Biochrom 30+, UK) with slight modification. An accurately weighed (2 g) ground sample was dissolved in 10 mL of water and kept for 24 h. The supernatant was mixed with sulfosalicylic acid (5%, v/v). The mixture was centrifuged at 6,000 × g for 10 min and the supernatant was dried in a rotary evaporator; the residue was dissolved in 1 mL sodium citrate buffer and then filtered through 0.45 μm filter for the detection free amino acids at 570 nm (440 nm was used for proline detection). Standard curves were prepared by using external standards. Altogether, 17 free amino acids considered were: glycine (Gly), alanine (Ala), arginine (Arg), glutamic acid (Glu), cysteine (Cys), tyrosine (Tyr), methionine (Met), lysine (Lys), aspartic acid (Asp), proline (Pro), threonine (Thr), isoleucine (Ile), leucine (Leu), histidine (His), phenylalanine (Phe), valine (Val), and serine (Ser).

Electronic nose analysis

The PEN-3 electronic nose (Airsense Technology Co., Ltd., Germany) was used to differentiate the flavor of raw scallop muscle from that of the scallop muscles cooked in four different ways. The e-nose had 10 metal receptors in total. Each receptor was sensitive to a specific type of substances. Sample (2.0 g) was cut into 2 mm × 2 mm pieces and put into a 20 mL glass bottle; after incubation at 60°C for 10 min, testing was done for 120 s. The e-nose was cleaned before each testing.

Electronic tongue analysis

The SA-4028 electronic tongue (Ensoul, Beijing, China) was used to differentiate the taste of raw scallop muscle from cooked samples. Accurately weighed (10 g) cut sample was mixed with deionized water at 1:8 ratio and homogenized (Supor, Hangzhou, China) for 2 min at 32,000 r/min until well mixed. Supernatant was collected after centrifugation at 10,000 × g for 10 min, which was used for e-tongue analysis. The electronic tongue used sensors to detect soluble substances in the liquid sample to generate a signal response value of each sensor for analysis (13).

Sensory evaluation analysis

Ten trained tasters (1:1 male: female ratio; aged between 20 and 25) were selected to assess sensory characteristics. Each taster had an independent space and was not disturbed by another taster. The scallop muscle sample was presented in a clean and transparent cup with a random 3-digit code. After each tasting, the panelist was normalized their mouth by a bite of biscuit and then cleaned with water. Scores were given for odor, taste, texture, and appearance; the average score from all the panelists was considered for the data analysis.

Texture profile and microstructure analysis

Using TMS-Pro texture profile analyzer (FTC, USA) with a cylindrical probe (50 mm dia.), texture parameters were analyzed (14). The measurement speed was 1 mm/s with a deformation of 30%; two consecutive compressions were made within a 5 s interval time. For microstructure analysis, samples were cut into cubes (5 mm × 5 mm × 1 mm) and fixed on the sample support using a double-sided adhesive tape. The sample was viewed through scanning electron microscope (SU8010, Hitachi, Japan) at 500× magnification after coating with gold under vacuum (15).

Statistical analysis

Correlation analysis of the differences among the samples was conducted using the SPSS 23.0 software (IBM, Armonk, NY, USA). The significance of the differences was conducted with Duncan multiple comparison method, considering $P < 0.05$ as the significant difference. Origin 2021 was used to conduct radar map-based visual analysis of the samples. Advanced Heatmap Plots was performed using the OmicStudio tools from https://www.omicstudio.cn. Main component analysis was performed using https://www.chiplot.online/. Correlation analysis and graphic presentations were generated using the R "corrplot" package (16). For correlation network diagram, cytoscape (Version 3.9.1) was used.

Results and discussion

Analysis of volatile flavor compounds in scallop samples

Headspace-gas chromatography-ion mobility spectrometry was used to identify the volatile organic compounds in scallop muscle and analyze the change in flavor components among different samples. **Figure 1A** was the HS-GC-IMS topographic

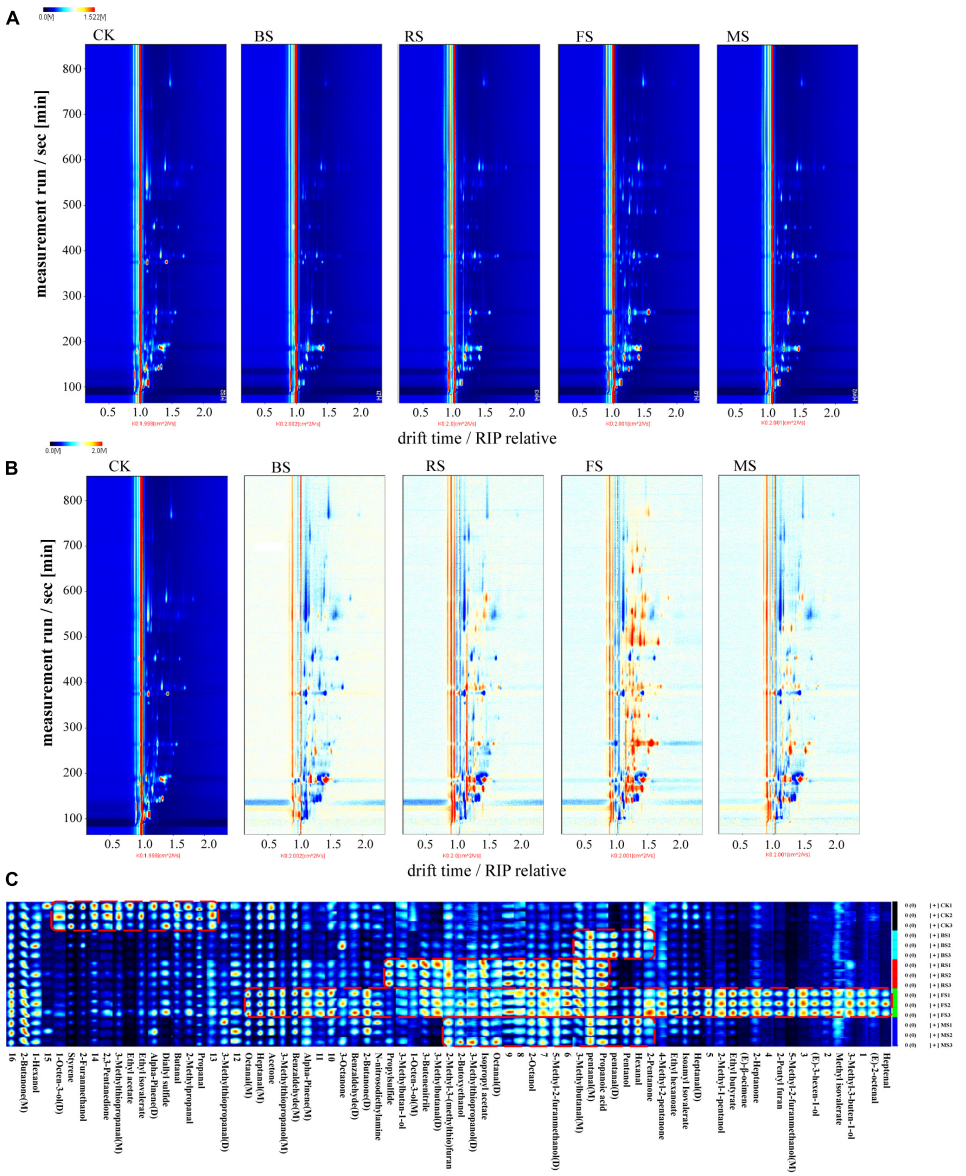

FIGURE 1
Headspace-gas chromatography-ion mobility spectrometry (HS-GC-IMS) topographic plots and gallery plot of five treatment groups. **(A)** Topographic plot of HS-GC-IMS spectra; **(B)** Comparison of spectrogram results. **(C)** Gallery plot of five treatment groups. (M) and (D) denote monomer and dimer, respectively (CK, the control group; BS, boiled sample; RS, oven heated sample; FS, fried sample; MS, microwaved sample).

plot of the five samples. Each point on the left and right sides of RIP peak (reactive ion peak) represented a volatile flavor substance. The darker the red was, the higher the content was. It can be seen that the flavor components in the sample are well separated. Some substances disappeared and others appeared in different cooking steps. Figure 1B showed the comparison of the topographic plots of the five samples of scallops, through which we can observe the changes caused by the four heating methods to the flavor substances of scallops more clearly. The flavor substance topographic plot of raw scallop muscle was used as the reference. The red spots indicated an increased concentration of flavor substances, while the blue spots indicated their decreased concentration. These four cooking methods showed the changes in flavor substances in various degrees; the highest increase was observed in the fried scallop, while the lowest increase was found in the boiled ones.

By testing and analyzing through HS-GC-IMS (Table 1), the volatile organic compounds in raw scallop muscle and the scallop muscle cooked in different ways were 48 in number; the varieties included 12 aldehydes, 11 alcohols, 7 ketones, 7 esters, 1 acid, and 10 others; aldehydes and alcohols were the major compounds. Most aldehydes and ketones showed

TABLE 1 Contents of volatile compounds in scallops identified by HS-GC-IMS.

S.No	Volatile compounds	CAS#	Formula	Retention index	Retention time (sec)	Drift time (a.u.)	Peak volume (a.u)				
							Raw	Boiled	Roasted	Fried	Microwaved
	Aldehydes										
1	Octanal (M)	C124130	C8H16O	998.6	585.19	1.40355	1560.84 ± 189.75^{bc}	1,149.96 ± 89.48^{c}	1,591.63 ± 220.91^{bc}	2,338.03 ± 158.42^{a}	1,658.26 ± 471.04^{b}
2	Octanal (D)	C124130	C8H16O	980.3	551.031	1.41421	232.85 ± 28.60^{b}	324.16 ± 42.80^{ab}	457.44 ± 34.30^{a}	460.66 ± 49.02^{a}	405.18 ± 158.58^{a}
3	Butanal	C123728	C4H8O	606.4	148.651	1.1028	1,684.24 ± 337.55^{a}	835.52 ± 243.06^{b}	608.64 ± 159.10^{b}	696.62 ± 132.22^{b}	483.23 ± 97.56^{b}
4	Heptanal (M)	C111717	C7H14O	893.4	390.536	1.32983	1,810.60 ± 204.96^{b}	1,090.96 ± 98.65^{c}	1,637.35 ± 79.79^{b}	2,236.26 ± 141.40^{a}	1,565.95 ± 427.46^{b}
5	Heptanal (D)	C111717	C7H14O	891.2	387.193	1.69606	580.77 ± 136.37^{b}	212.80 ± 43.22^{c}	392.64 ± 61.97^{bc}	987.33 ± 165.29^{a}	443.71 ± 234.14^{bc}
6	Hexanal	C66251	C6H12O	765.5	247.461	1.25116	969.34 ± 79.94^{b}	1,719.31 ± 202.63^{a}	583.14 ± 176.96^{b}	1,895.02 ± 113.63^{a}	2,131.80 ± 482.75^{a}
7	Pentanal (M)	C110623	C5H10O	685.1	182.891	1.18647	338.24 ± 15.51^{c}	1,220.24 ± 129.07^{a}	915.73 ± 126.91^{b}	915.02 ± 94.67^{b}	1,225.22 ± 67.69^{a}
8	Pentanal (D)	C110623	C5H10O	688.8	184.604	1.42917	534.70 ± 76.20^{d}	4,202.00 ± 638.70^{a}	1,380.45 ± 414.08^{c}	2,412.52 ± 188.12^{b}	2,787.59 ± 618.32^{b}
9	2-Methylpropanal	C78842	C4H8O	591.1	142	1.2895	1,292.00 ± 200.15^{a}	380.77 ± 43.57^{c}	499.28 ± 159.83^{b}	878.90 ± 292.51^{b}	387.50 ± 126.03^{c}
10	Propanal	C123386	C3H6O	501	102.771	1.05695	4,461.92 ± 605.51^{a}	2,752.13 ± 237.34^{b}	2,617.10 ± 83.29^{b}	2,920.20 ± 407.09^{b}	2,330.30 ± 123.09^{b}
11	3-Methylthiopropanal (D)	C3268493	C4H8OS	897.3	397.733	1.08839	272.26 ± 156.74	269.34 ± 140.22	262.81 ± 81.65	433.24 ± 179.28	539.24 ± 158.28
12	3-Methylthiopropanal (M)	C3268493	C4H8OS	909.9	421.061	1.0907	646.15 ± 67.5^{b}	245.65 ± 48.67^{c}	402.43 ± 66.15^{c}	1,051.41 ± 183.06^{a}	673.04 ± 198.11^{b}
13	3-Methylbutanal (D)	C590863	C5H10O	647.9	166.712	1.40053	171.15 ± 48.04^{b}	343.78 ± 147.69^{b}	1,042.69 ± 340.18^{a}	1,246.63 ± 121.38^{a}	148.23 ± 63.22^{b}
14	3-Methylbutanal (M)	C590863	C5H10O	643.3	164.716	1.17038	1,293.70 ± 155.10^{c}	1,697.49 ± 281.11^{b}	2,581.91 ± 232.83^{a}	2,598.72 ± 56.93^{a}	1,197.87 ± 139.95^{c}
15	Benzaldehyde (D)	C100527	C7H6O	962.3	517.846	1.46872	194.27 ± 23.70^{a}	108.77 ± 70.00^{b}	115.89 ± 21.79^{b}	221.67 ± 61.04^{a}	170.39 ± 59.60^{ab}
16	Benzaldehyde (M)	C100527	C7H6O	961.1	515.695	1.14858	1,241.38 ± 131.71^{a}	656.23 ± 132.56^{b}	1,050.69 ± 125.63^{a}	1,379.00 ± 191.09^{a}	1,101.30 ± 321.41^{a}
17	(E)-2-octenal	C2548870	C8H14O	1, 054.1	693.07	1.33622	61.48 ± 15.73^{b}	58.99 ± 14.06^{b}	54.80 ± 21.18^{b}	177.81 ± 28.53^{a}	70.34 ± 23.48^{b}
18	Heptenal	C18829555	C7H12O	946.5	488.68	1.66426	79.79 ± 8.77^{b}	85.94 ± 28.43^{b}	86.67 ± 14.32^{b}	321.66 ± 73.04^{a}	74.11 ± 5.01^{b}
	Ketones										
19	2,3-Pentanedione	C600146	C5H8O2	694.7	189.449	1.30753	1732.37 ± 498.37^{a}	494.01 ± 55.05^{b}	432.95 ± 71.98^{b}	789.69 ± 262.76^{b}	466.76 ± 53.94^{b}
20	2-Butanone (M)	C78933	C4H8O	582.7	138.338	1.06914	1,499.15 ± 187.65^{b}	1,242.16 ± 144.04^{b}	1,432.49 ± 244.06^{b}	1,905.86 ± 42.34^{a}	1,962.82 ± 240.26^{a}
21	2-Butanone (D)	C78933	C4H8O	586	139.77	1.24463	947.80 ± 141.81^{c}	434.01 ± 148.43^{c}	907.54 ± 325.54^{c}	2,385.43 ± 267.10^{a}	1,735.36 ± 594.31^{b}
22	Acetone	C67641	C3H6O	509.5	106.491	1.12538	4,966.29 ± 728.31^{ab}	1,825.95 ± 692.47^{d}	3,339.89 ± 658.00^{c}	5,492.55 ± 788.33^{a}	3,790.89 ± 996.56^{bc}
23	2-Pentanone	C107879	C5H10O	691.8	187.072	1.3674	427.62 ± 32.96^{b}	475.25 ± 97.95^{ab}	348.00 ± 41.85^{b}	624.80 ± 147.93^{a}	418.66 ± 66.63^{b}
24	4-Methyl-2-pentanone	C108101	C6H12O	718.5	208.908	1.17828	127.92 ± 28.52^{c}	212.12 ± 20.45^{b}	222.42 ± 44.79^{b}	453.20 ± 35.22^{a}	201.42 ± 8.58^{b}
25	2-Heptanone	C110430	C7H14O	883.4	378.117	1.25837	193.63 ± 33.67^{b}	160.24 ± 31.00^{b}	204.95 ± 29.57^{b}	473.34 ± 11.90^{a}	178.63 ± 27.94^{b}
26	3-Octanone	C106683	C8H16O	979	548.637	1.29835	230.43 ± 87.28	383.83 ± 221.98	247.59 ± 33.49	353.25 ± 200.17	326.75 ± 138.64
	Alcohols										
27	1-Octen-3-ol (M)	C3391864	C8H16O	1, 005.1	597.833	1.16261	268.00 ± 82.05^{bc}	116.62 ± 36.97^{c}	422.15 ± 146.50^{a}	308.75 ± 23.25^{ab}	148.50 ± 45.34^{c}
28	1-Octen-3-ol (D)	C3391864	C8H16O	981.2	552.815	1.5881	376.05 ± 67.13^{a}	134.96 ± 26.77^{b}	140.26 ± 9.65^{b}	189.29 ± 20.11^{b}	142.10 ± 24.14^{b}

(Continued)

10.3389/fnut.2022.1022156

TABLE 1 (Continued)

S.No	Volatile compounds	CAS#	Formula	Retention index	Retention time (sec)	Drift time (a.u.)	Peak volume (a.u)				
							Raw	Boiled	Roasted	Fried	Microwaved
29	2-Furanmethanol	C98000	C5H6O2	879.6	373.738	1.11127	2,126.07 ± 508.77^{a}	940.06 ± 477.91^{b}	559.21 ± 59.22^{b}	612.04 ± 72.76^{b}	428.35 ± 128.47^{b}
30	Pentanol	C71410	C5H12O	762.5	245.031	1.5084	272.27 ± 53.88^{bc}	561.85 ± 86.42^{ab}	104.90 ± 21.23^{c}	635.18 ± 95.36^{a}	797.66 ± 362.90^{a}
31	1-Hexanol	C111273	C6H14O	868.5	360.73	1.31603	215.32 ± 52.28	251.55 ± 26.40	186.63 ± 60.89	233.42 ± 28.26	218.71 ± 10.15
32	5-Methyl-2-furanmethanol (D)	C3857258	C6H8O2	962.2	517.639	1.27804	125.71 ± 8.02^{b}	117.75 ± 25.06^{b}	281.24 ± 73.18^{a}	307.69 ± 20.07^{a}	247.10 ± 24.81^{a}
33	5-Methyl-2-furanmethanol (M)	C3857258	C6H8O2	947.6	490.757	1.25894	141.27 ± 32.12^{b}	96.65 ± 5.06^{b}	101.41 ± 5.06^{b}	1,273.85 ± 163.04^{a}	128.85 ± 9.19^{b}
34	2-Methyl-1-pentanol	C105306	C6H14O	838.4	325.853	1.29886	65.51 ± 3.96^{c}	60.15 ± 2.30^{c}	61.27 ± 3.56^{c}	204.06 ± 4.68^{a}	75.80 ± 6.04^{b}
35	3-Methylthiopropanol (D)	C505102	C4H10OS	979.6	549.783	1.45532	101.01 ± 6.51	113.81 ± 41.62	172.54 ± 26.15	139.22 ± 44.61	147.65 ± 69.63
36	3-Methylthiopropanol (M)	C505102	C4H10OS	977.9	546.755	1.10208	3,943.78 ± 830.80^{a}	753.65 ± 62.89^{b}	1,009.20 ± 190.33^{b}	1,409.18 ± 585.99^{b}	1,008.06 ± 267.41^{b}
37	(E)-3-Hexen-1-ol	C928972	C6H12O	840.3	327.949	1.51447	46.73 ± 4.22^{b}	46.89 ± 5.42^{b}	46.43 ± 11.29^{b}	139.90 ± 9.70^{a}	41.03 ± 2.47^{b}
38	3-Methyl-3-buten-1-ol	C763326	C5H10O	718.9	209.301	1.29057	53.01 ± 4.34^{c}	63.28 ± 6.17^{c}	81.48 ± 14.34^{b}	183.96 ± 8.32^{a}	54.35 ± 7.62^{c}
39	3-Methylbutan-1-ol	C123513	C5H12O	728.2	216.879	1.23522	245.47 ± 49.00^{b}	166.00 ± 17.49^{b}	332.23 ± 57.31^{a}	226.05 ± 20.41^{b}	193.90 ± 64.42^{b}
40	2-Octanol	C123966	C8H18O	998.1	584.168	1.45925	279.90 ± 49.86^{d}	353.53 ± 14.36^{c}	727.53 ± 7.01^{a}	772.08 ± 53.17^{a}	603.05 ± 33.20^{b}
	Esters										
41	Isoamyl isovalerate	C659701	C10H20O2	1, 092	766.687	1.47268	959.87 ± 191.18^{b}	496.31 ± 35.18^{d}	674.76 ± 123.03^{cd}	1,457.78 ± 130.53^{a}	818.84 ± 193.30^{bc}
42	Ethyl hexanoate	C123660	C8H16O2	996.6	581.156	1.81994	256.86 ± 61.17^{b}	158.51 ± 17.83^{b}	244.71 ± 64.05^{b}	520.51 ± 93.99^{a}	274.56 ± 110.95^{b}
43	Ethyl isovalerate	C108645	C7H14O2	935	467.501	1.26531	432.74 ± 161.90^{a}	177.01 ± 31.59^{b}	208.06 ± 37.82^{b}	262.17 ± 63.22^{b}	192.50 ± 31.34^{b}
44	Ethyl butyrate	C105544	C6H12O2	786.9	265.993	1.56437	681.82 ± 213.13^{b}	572.15 ± 63.23^{b}	696.44 ± 169.79^{b}	4,443.93 ± 275.36^{a}	870.54 ± 339.52^{b}
45	Ethyl acetate	C141786	C4H8O2	601.7	146.601	1.33466	1,175.58 ± 580.67^{a}	220.51 ± 83.34^{b}	205.97 ± 114.91^{b}	247.50 ± 125.96^{b}	100.61 ± 25.34^{b}
46	Isopropyl acetate	C108214	C5H10O2	591.3	142.074	1.15412	529.36 ± 34.19^{c}	632.95 ± 125.79^{c}	1,534.86 ± 353.64^{a}	1,159.58 ± 40.41^{b}	1,073.59 ± 16.61^{b}
47	Methyl isovalerate	C556241	C6H12O2	777.8	257.532	1.19206	127.50 ± 25.58^{b}	144.16 ± 9.51^{b}	130.68 ± 11.36^{b}	198.83 ± 5.29^{a}	136.10 ± 6.00^{b}
	Acids										
48	Propanoic acid	C79094	C3H6O2	691.9	187.137	1.26579	617.76 ± 72.72^{c}	1,349.68 ± 161.62^{b}	1,563.14 ± 64.98^{a}	1,461.05 ± 51.72^{ab}	1,383.61 ± 89.50^{ab}
	Others										
49	Alpha-pinene (D)	C80568	C10H16	927	452.716	1.22059	736.52 ± 415.78	354.36 ± 53.59	439.73 ± 98.28	476.24 ± 254.62	578.43 ± 307.72
50	Alpha-pinene (M)	C80568	C10H16	909.2	419.79	1.21006	185.08 ± 40.16^{cd}	119.70 ± 25.63^{d}	258.78 ± 70.75^{bc}	405.78 ± 60.52^{a}	313.68 ± 33.08^{b}
51	(E)-β-ocimene	C13877913	C10H16	1, 029.1	644.414	1.2656	83.19 ± 13.15^{b}	72.30 ± 11.98^{b}	74.79 ± 6.67^{b}	420.05 ± 20.73^{a}	73.04 ± 6.28^{b}
52	Styrene	C100425	C8H8	881	375.364	1.41468	1,723.65 ± 232.59^{a}	435.69 ± 130.12^{b}	425.91 ± 64.50^{b}	605.36 ± 41.94^{b}	354.22 ± 141.50^{b}
53	Diallyl sulfide	C592881	C6H10S	862.7	354.041	1.11647	375.31 ± 65.71^{a}	75.68 ± 9.36^{c}	214.94 ± 34.93^{b}	266.66 ± 106.20^{b}	56.41 ± 0.76^{c}
54	Propylsulfide	C111477	C6H14S	891.1	387.109	1.14974	349.82 ± 30.77^{c}	565.59 ± 5.73^{b}	1,266.11 ± 26.28^{a}	434.59 ± 43.40^{bc}	570.64 ± 176.16^{b}
55	2-Butoxyethanol	C111762	C6H14O2	896.4	396.148	1.21184	217.05 ± 44.65^{c}	226.11 ± 58.50^{c}	317.04 ± 45.64^{bc}	375.60 ± 55.29^{ab}	429.36 ± 63.73^{a}
56	3-Butenenitrile	C109751	C4H5N	643.3	164.697	1.25904	307.53 ± 46.13^{b}	492.47 ± 116.01^{b}	1,340.36 ± 274.60^{a}	1,240.22 ± 15.03^{a}	407.97 ± 62.35^{b}
57	*N*-nitrosodiethylamine	C55185	C4H10N2O	894	391.749	1.53126	179.82 ± 48.54^{ab}	99.23 ± 11.83^{b}	124.26 ± 20.65^{b}	266.18 ± 61.57^{a}	187.48 ± 67.70^{ab}
58	2-Pentyl furan	C3777693	C9H14O	983.8	557.568	1.2612	137.25 ± 10.24^{b}	138.10 ± 11.86^{b}	151.58 ± 6.42^{b}	557.24 ± 61.12^{a}	160.59 ± 20.89^{b}
59	2-Methyl-3-(methylthio) furan	C63012975	C6H8OS	946	487.809	1.15364	125.04 ± 14.21^{c}	110.25 ± 20.14^{c}	215.20 ± 27.37^{a}	117.54 ± 3.15^{c}	177.24 ± 26.79^{b}

(M) and (D) denote monomer and dimer, respectively. Superscript a, b, c, and d in the same row denotes significantly different at $P < 0.05$.

10.3389/fnut.2022.1022156

stronger response signals in the fried samples. The HS-GC-IMS gallery plot of the volatile flavor compounds in different samples were shown in **Figure 1C**, in which, each row represented the response signals of the volatile flavor compounds in one sample, and each column represented the response signals of each volatile flavor compound in different samples. The gallery plot enabled more intuitive comparison between the volatile flavor compounds in scallop samples. The categories of flavor substances in all samples were similar but the contents were different. Different cooking methods resulted different characteristic flavors, among which, the FS was loaded with a greater variety of volatile compounds with higher contents, while the result was opposite for the BS. The increase of such compounds in RS and MS samples was similar in terms of flavor areas. Except the BS samples, the contents of aldehydes and ketones increased after heating, particularly in case of fried samples, which was indicated by more red spots in the HS-GC-IMS topographic plots, ultimately contributing to rich flavors. The change might be resulted from the fact that the fried scallops absorbed unsaturated fatty acid from the oil during frying, which caused more lipid oxidation in the FS samples; the process was accelerated by the higher frying temperature (17). The lower contents of ketones and aldehydes in the BS samples was probably related to the lower heating temperature boiling water. During boiling, some oil and hydrolysis of scallops fat might get hydrolyzed into fatty acids and dissolved in water, causing the loss of flavor substances (18).

Aldehydes were mainly generated from lipid oxidation and protein degradation, with the lower odor thresholds and having bigger influence on scallop flavor (19). Aldehydes changed most significantly in the fried scallops: compared with the control samples, the fried samples showed higher contents of heptenal, (E)-2-octenal, heptanal, hexanal, octanal, pentanal, 3-methylbutanal, and 3-methylthiopropanal (M). Besides, the boiled scallops contained much more contents of hexanal, pentanal and 3-methylbutanal (M) than the control samples. The roasted scallops contained more contents of pentanal, octanal (D) and 3-methylbutanal, while the microwaved scallops contained increased contents of pentanal, octanal (D), and hexanal. The identified aldehydes were mainly fatty aldehydes, generated from lipid oxidation and degradation. For example, hexanal (Fruit and leaf fragrances), heptanal (Nuts fragrance and green fragrance of fruit), octanal (Fruit and fatty odors) were also found in aquatic products like silver carps, tunas, and sturgeons (11, 20). Butanal gives green aroma and fruit fragrance and pentanal gives almond flavor (21, 22). In addition, (E)-2-octenal and heptenal derived from linoleic acid provide the fatty flavor (23). Branched aldehyde is generated from amino acid through Strecker degradation. For example, benzaldehyde commonly seen in meat products produces an almond-like sweet flavor, showing the smallest content in the boiled samples (21). 3-Methylthiopropanal conferred onion-like and meat aroma (22).

Ketones are mainly from lipid oxidation (19). The contents of most ketones in the fried samples were significantly higher than those in other samples. 2-Heptanone was thought to contribute to the meat aroma (24). 2-Pentanone, whose content was equally higher in the fried scallops than other samples, give food creamy and cheesy flavors (21). 2-Butanone increased significantly in the fried and microwaved scallops.

The main flavor substances in scallop muscles at the cooking stage were aldehydes and alcohols (6). However, unlike aldehydes, alcohols have higher odor thresholds, contributing smaller influence on flavor. 3-Methylthiopropanol, whose content was higher in raw and heated scallops, contributing a sweet onion flavor. 1-Octen-3-ol decreased after heating. It is a commonly seen flavor substance in aquatic products, known to contribute a peculiar smell of mushroom and mud, which decreases upon heating (25). 5-Methyl-2-furanmethanol, which increased significantly in the roasted, microwaved and fried scallops, provided a roast smell. 3-Methylbutan-1-ol gives an almond smell, with the content higher in the roasted scallops (22).

Esters provide sweet and fruit flavors; for example, ethyl hexanoate, ethyl acetate, and ethyl butyrate (26). Esters are esterified with the alcohols and free fatty acid generated from lipid oxidation (20). The content of isopropyl acetate increased after heating. Ethyl butyrate in the fried scallops was much more than that in other samples. Ethyl isovalerate and ethyl acetate decreased sharply after heating, probably because the content of volatile esters decreased as the heating temperature rises (17). There was only one kind of acid in scallops: propanoic acid, which increased after heating. Furans are important flavor substances in meat; they are generally generated from sugar degradation products, formed through Maillard reaction and usually have the meat and sweet flavor (19). The contents of 2-pentyl furan and 2-Methyl-3-(methylthio) furan were significantly higher in the fried and roasted scallops. Among them, 2-pentyl furan is commonly seen in meat as an important flavor substance and has fruit fragrance (27).

Free amino acids contents in scallop samples

Figure 2 was the heat map (the data were normalized with z-score) for free amino acids contents in scallops cooked by tested methods. The results showed that the roasted and fried scallops shared a higher level of similarity and can be clustered together. Except Pro, the roasted and fried scallops contained more sweet amino acids (Gly, Thr, Ser, Ala, and Arg), umami amino acids (Asp and Glu) and odorless amino acid (Cys) than other samples. In the microwaved scallops, sweet amino acids (Thr, Ser, and Arg) and umami amino acids (Asp and Glu) increased significantly than the control samples. Among them, Gly and Ala were the main sources of

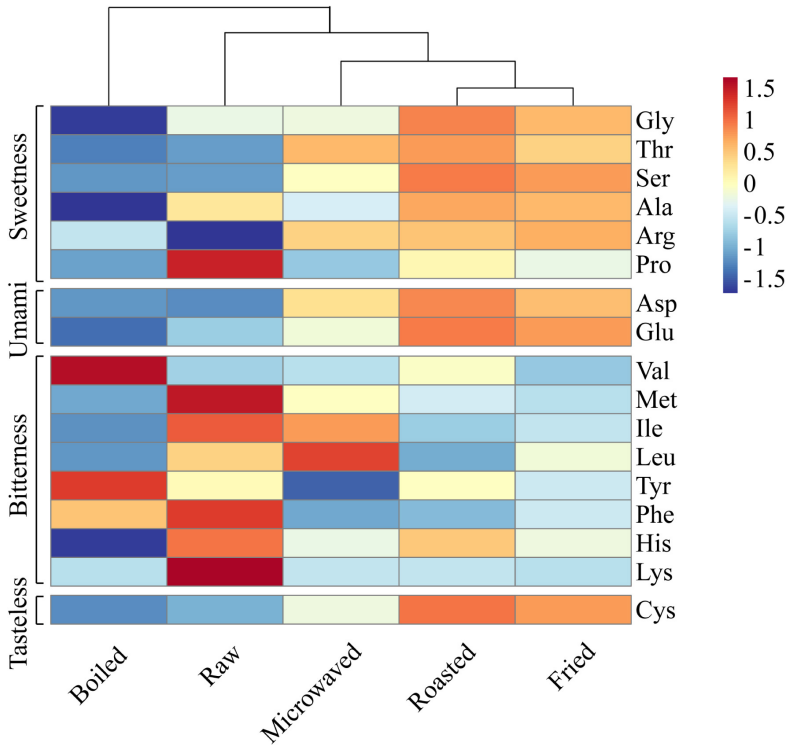

FIGURE 2
Heat map clustering of free amino acids in raw and cooked scallops.

sweetness of shellfish (28). In terms of bitter amino acids, the red region representing high content was mainly concentrated in the control samples, while the blue region representing low content was mainly concentrated in the fried samples. Compared with other samples, the boiled scallops contained lower contents of most free amino acids, which was probably because the flavor compounds were dissolved in water during the boiling process (29). Heating duration and temperature differences also affected the protein degradation and caused further changes in amino acid contents (7). The heating medium in boiling was water; temperature of which was lower, while microwave heating lasted for a shorter time. Both heating methods feature less water loss, limiting the increase of amino acids (30). As the taste substances, free amino acids are crucial to food taste (31), with content changes contributing to the umami and sweet taste of scallop muscle.

E-nose analysis of scallop samples

The principal component analysis method was used to develop the spatial distribution map, as shown in **Figure 3A** for different samples. PC1 and PC2 were 98.48 and 1.4%, respectively; the combined contribution rate was 99.88%, indicating that e-nose was able to differentiate well among the samples. The control and the boiled samples were distributed in the right half of the map, while the roasted, microwaved and fried samples were distributed in the left half. The control sample was far away from the samples cooked in the four different ways, indicating that all the four cooking methods caused changes to the smell of samples. The boiled sample was the closest to the control samples, followed by the roasted sample and then microwaved and fried samples. That means that the boiled sample had the smell closest to the control samples, while the fried and microwaved samples had the smell, which was the most different from the control samples. The radar map (**Figure 3B**) further supported the PCA results. Besides, their differences were mainly reflected in two metal receptors, including W1W (Sensitive to many terpenes and organic sulfur compounds) and W2W (Sensitive to aromatic compounds and organic sulfide); the fried and microwaved sample were the most responsive and the control sample was the least one. This was consistent with the HS-GC-MS results, where 3-methylthiopropanal (an organic sulfide) contributed most to the signal changes of W1W and W2W metal receptors (**Figure 3B**).

E-tongue analysis of scallop samples

The principal component analysis method was used to develop the spatial distribution map (**Figure 3C**) of different

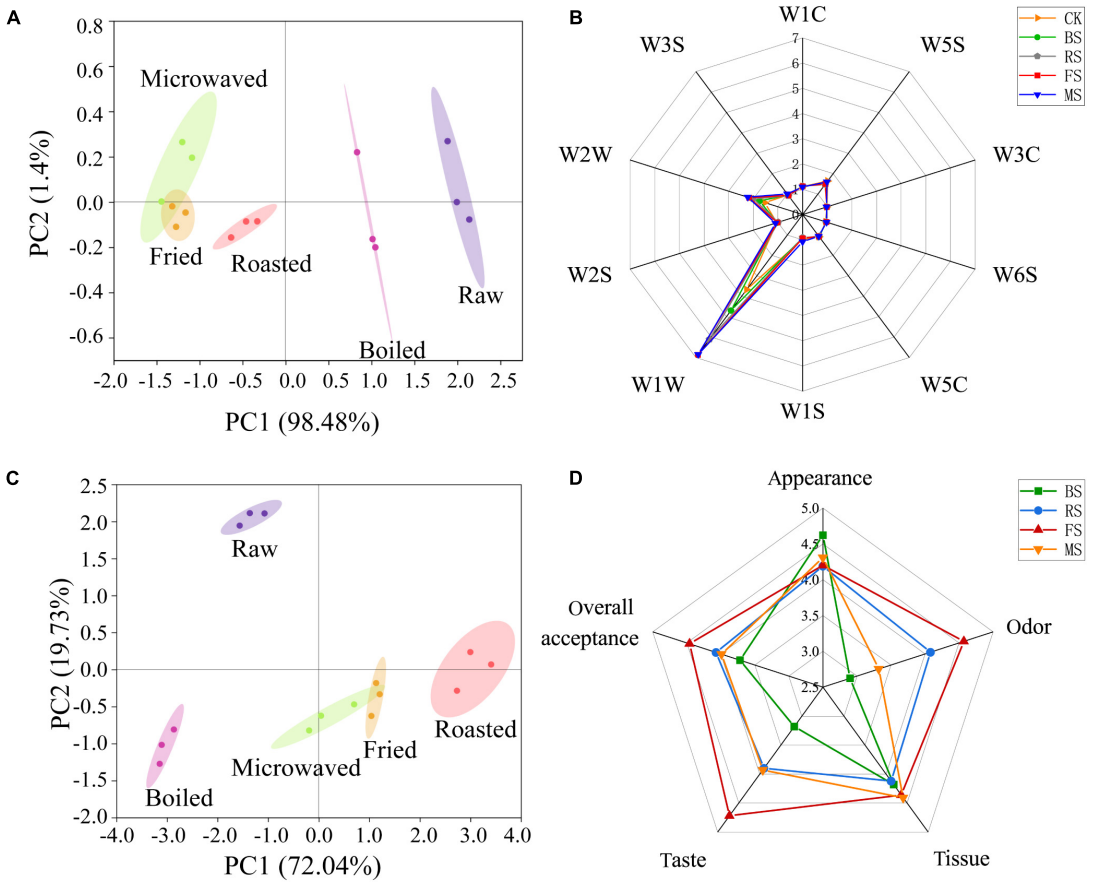

FIGURE 3
Electronic nose, electronic tongue, and sensory evaluation analysis of raw and cooked scallops. **(A)** Principal component analysis of electronic nose results. **(B)** Radar graph of electronic nose results. **(C)** Principal component analysis of electronic tongue results. **(D)** Radar graph of sensory evaluation results (CK, the control group; BS, boiled sample; RS, oven heated sample; FS, fried sample; MS, microwaved sample).

samples. PC1 and PC2 were 72.04 and 19.73%, respectively, and the combined contribution rate was 91.77%, indicating that e-tongue was able to differentiate well among the samples. The control sample was located in the second quadrant, far away from the samples cooked in four different ways, indicating all the four cooking methods caused changes to the taste of the scallop muscle. Only the fried and microwaved samples overlapped, indicating that the two samples had similar taste, while other samples differed greatly in taste.

Sensory evaluation of scallop samples

The radar map for the sensory assessment of scallop muscle cooked by different ways is shown in Figure 3D. The samples differed little in appearance among samples but differed greatly in smell and taste. In terms of smell, the fried and roasted samples had higher sensory scores. In terms of taste, the fried, roasted and microwaved samples had higher scores. Overall, the fried sample was more receptive than other samples, while the boiled sample was least receptive. The sensory scores for smell and taste varied greatly among samples, affecting the overall receptivity to a greater degree. Interestingly, associated with the results of the e-nose- and e-tongue-principal component analysis, boiled samples were highly similar to raw samples in taste and volatile odor substances. On the one hand, this high degree of similarity seems to better achieve the goal of maintaining the original sensory qualities of fresh scallops. However, it should not be ignored that the boiled samples obtained the lowest sensory score among the cooked samples. Therefore, this way of cooking is not the best way to meet the needs of consumers.

The analysis of microstructures and texture profiles in scallop samples

The TPA method was used to simulate the secondary chewing process in human oral cavity and analyze the influence

10.3389/fnut.2022.1022156

TABLE 2 Changes in the texture of heating scallops.

Groups	Hardness (N)	Springiness (mJ)	Chewiness (mJ)
Boiled	2.77 ± 0.31^{b}	1.71 ± 0.09^{b}	2.25 ± 0.13^{b}
Roasted	4.03 ± 0.67^{a}	2.34 ± 0.10^{a}	4.01 ± 1.08^{a}
Fried	3.00 ± 0.60^{b}	2.02 ± 0.23^{ab}	2.46 ± 0.48^{b}
Microwaved	2.93 ± 0.15^{b}	1.91 ± 0.45^{ab}	2.35 ± 0.14^{b}

Superscript a, b, and c in the same column denotes significantly different at $P < 0.05$.

of different cooking methods on the taste of scallop muscle. The roasted sample was much harder and chewier than the other three samples; also, it was much more elastic than the boiled sample (Table 2).

We used the scanning electron microscopy to observe the microstructure of the section of scallop muscle cooked in different ways. The muscle fibers in the control sample were arranged most loosely, while the seams among muscle bundles notably shrank after heating during cooking by different methods, probably caused by the loss of water during heating (Figure 4). The muscle fibers in the boiled and microwaved samples were arranged relatively loose, while the muscle fibers in the fried and roasted samples were tightly arranged with smaller seams. Such difference in muscle fiber arrangement might be the reason behind the difference in hardness, elasticity and chewiness values (32). Besides, the muscle fibers of microwaved sample were arranged in the most disorder manner, probably related to the principle of microwave heating, ultimately improving the tenderness of scallop muscle (15). Unlike frying, boiling or roasting, where the transmission of heat takes place through conduction from outside to inside of the material being heated, microwave system heats food through water molecular friction (30), which involves fast high-frequency vibrations and molecular polarization (33).

Correlation analysis of the data

Taste, volatile, and texture are important factors affecting the sensory assessment of foods. One physicochemical indicator cannot reflect the cross-effect of these factors on sensory (34). So, we used correlation analysis to further explore the effect.

The results of the e-nose and the correlation heat map for volatile organic compounds identified through HS-GC-IMS (Figure 5A; $P < 0.05$) showed the correlation between the e-nose metal receptor signals and the concentration of flavor substances. Significant correlation appeared in W1W and W2W metal receptors; W1W metal receptor (Sensitive to many terpene and organic sulfur compounds) showed a significant positive correlation with octanal, 3-methylthiopropanal, 2-butanone, 4-methyl-2-pentanone, 5-methyl-2-furanmethanol, 2-methyl-1-pentanol, 3-methyl-3-buten-1-ol, 2-octanol, ethyl hexanoate, ethyl butyrate, isopropyl acetate, propanoic acid, 2-butoxyethanol, 3-butenenitrile, and 2-pentyl furan, while W2W metal receptor (Sensitive to aromatic compounds and organic sulfide) was significant positively correlated with octanal, 3-methylthiopropanal, 2-butanone, 4-methyl-2-pentanone, 5-methyl-2-furanmethanol, 2-octanol, isopropyl acetate, propanoic acid, and 2-butoxyethanol. Such compounds affected the e-nose results to a larger degree.

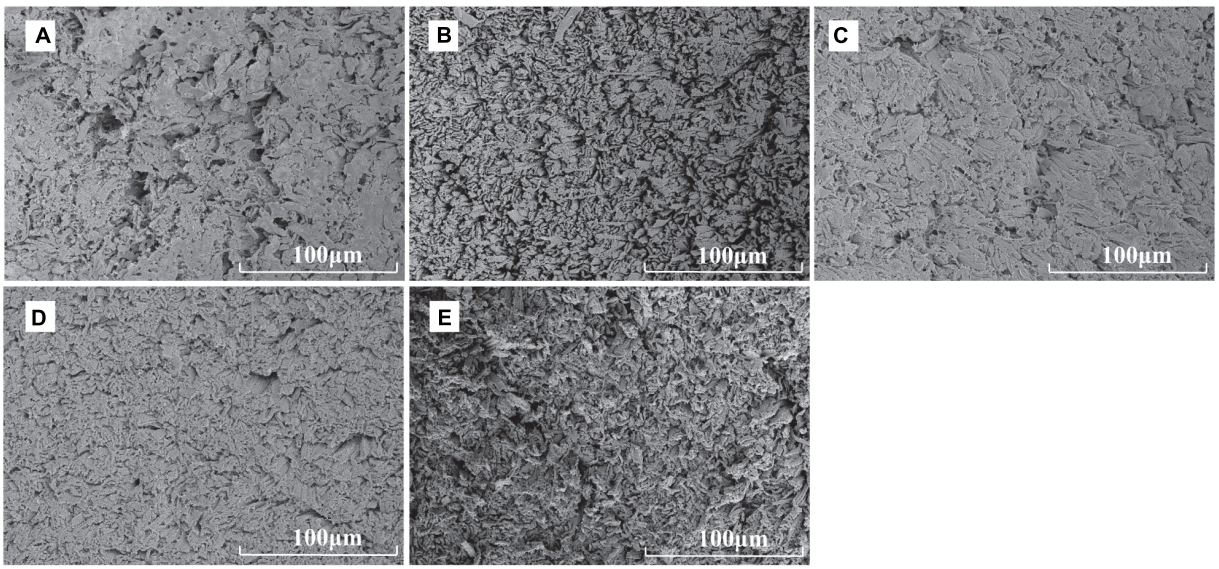

FIGURE 4
Scanning electron micrographs of raw and cooked scallops (500× magnification, **(A)** CK, the control group; **(B)** BS, boiled sample; **(C)**: RS, oven-heated sample; **(D)** FS, fried sample; **(E)** MS, microwaved sample).

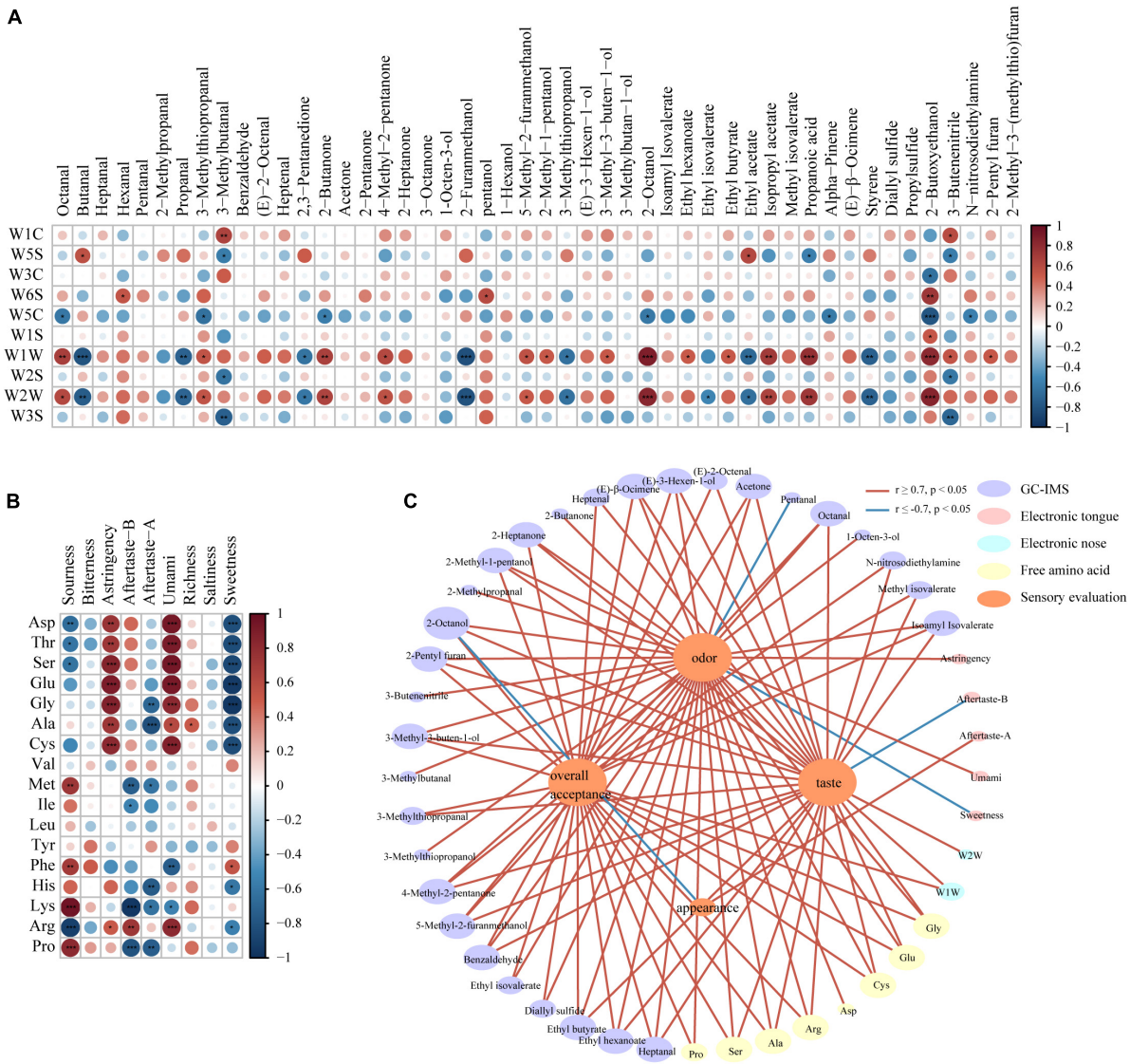

FIGURE 5
Correlation analysis: **(A)** Between volatile compounds with e-nose results and **(B)** between free amino acids with e-tongue results (*0.01 < P < 0.05, **0.001 < P < 0.01; ***P < 0.001). **(C)** Correlation networks between volatile compounds, e-nose results, free amino acids, e-tongue results with sensory scores, based on Pearson correlation coefficients ($|r| > 0.7$, $P < 0.05$) (Red represents positive correlations, and blue represents negative correlations).

Many researches showed that free amino acids (FAAs) were positively correlated to taste (35). According to the e-tongue results and the heat map for the contents of free amino acids (**Figure 5B**; $P < 0.05$), the contents of Asp, Thr, Ser, Glu, Gly, Ala, Cys, and Arg had significant positive correlation with the umami signal and convergence signal of e-tongue, and was negatively correlated to the sweet signal of e-tongue. The acid signal of e-tongue was negatively correlated with Asp, Thr, Ser, and Arg, while positively correlated with Met, Phe, Lys, and Pro. The aftertaste signal of e-tongue was negatively correlated with Gly, Ala, Met, Ile, His, Lys, and Pro, while positively correlated with Arg. Besides, Phe and Lys were negatively correlated with the umami signal; Arg was positively correlated with the umami signal; His and Arg were negatively correlated with the sweet signal; Phe was positively correlated with the sweet signal; all the 17 free amino acids had no significant correlation with the bitter and salty signals of e-tongue.

Glu and Asp were umami amino acids; both of them showed a significant positive correlation ($P < 0.001$) with the umami signal of e-tongue. Glu was positively correlated with the sensory score of taste and overall sensory score ($|r| \geq 0.7$, $P < 0.05$). Besides, as shown in **Figure 5B**, Arg was positively correlated with the umami signal, while Phe was positively correlated

with the acid signal, which was consistent with previous results ($0.001 < P < 0.01$) (28, 31).

Figure 5C is the network diagram showing how sensory scores are correlated to volatile organic compounds, free amino acids contents, e-nose results and e-tongue results ($|r| \geq 0.7$, $P < 0.05$). Among the 48 volatile flavor compounds separated through HS-GC-IMS, 30 compounds were correlated with sensory scores. Among them, 23 flavor compounds, including benzaldehyde, heptanal, and 2-pentyl furan, were positively correlated with the sensory score of odor; pentanal was negatively correlated with the sensory score of odor; 23 flavor compounds, including octanal, and heptanal were positively correlated with the sensory score of taste; 23 flavor compounds, including octanal, and benzaldehyde were positively correlated with overall sensory scores. Eight of the 17 free amino acids were significantly correlated with the sensory scores. The contents of Ala, Glu, Arg, Ser, Gly, and Cys were positively correlated with taste, odor and overall sensory scores. Besides, the content of Pro and Asp were positively correlated with the sensory score of odor, while the content of Pro was positively correlated with the overall sensory score. E-nose sensor W1W was positively correlated with the overall sensory score. Only the aftertaste-B signal of e-tongue was negatively correlated with the sensory score of taste. As the sensory score of structure had no significant correlation with other indicators, it was not indicated in the figure.

Among the free amino acids that were positively correlated with the sensory score of taste and the overall sensory score, all the free amino acids had sweet or umami taste except Cys (which is tasteless free amino acid) ($|r| \geq 0.7$, $P < 0.05$). However, sweet free amino acids, including Gly, Thr, Ser, and Ala were negatively correlated with the sweet results of e-tongue ($P < 0.001$), probably related to the limitations of e-tongue. Shen et al. (36) pointed out that the electric potential sensor of e-tongue might absorb compounds, leading to differences between the response value of the sensor and sensory scores. Like all the analytical systems, e-tongue can't fully replace human senses, because human eating involves chewing and is a process featuring dynamic sensing of taste. However, e-tongue can only measure liquid samples under static condition, which cannot simulate a complete eating process (13).

Interestingly, some researches showed 3-methylthiopropanal was able to positively activate human T1R1/T1R3, the taste receptor of umami (37). In this research, the content of 3-methylthiopropanal increased in the fried and microwaved samples, which was positively correlated with the taste sensory score. Besides, many volatile organic compounds separated through HS-GC-IMS had important positive role in the taste, smell and overall sensory scores. That indicated that rich flavor compounds not only offered the tasters a better smell experience, but also affected taste feelings. FAAs can make the precursor of flavor substances, changing food flavors together with volatile organic compounds (38). The interactions between senses of smell and taste were also seen in the results of Merlo et al. (39).

Conclusion

This research provided a comprehensive method that uses HS-GC-IMS, e-nose, e-tongue, sensory analysis, and free amino acid tests to identify the sensory characteristics of scallop muscle cooked in different ways. It also explained the differences of taste among samples through texture profile and microstructure analysis. Overall results showed that fried scallop had the best sensory score, probably because of the significant increase in aldehydes and ketones, caused by a higher degree of lipid oxidation and Maillard reaction as well as the increase in furans, umami, and sweet free amino acids. Boiled scallop had the lowest sensory score, probably related to the decrease in sweet and umami amino acids, caused by the loss of water-soluble compounds and fewer contents of volatile organic compounds. The interactions between senses of smell and taste resulted from volatile organic compounds and free amino acids were crucial to the formation of the sensory quality of scallop.

Data availability statement

The original contributions presented in this study are included in the article/Supplementary material, further inquiries can be directed to the corresponding authors.

Author contributions

YW and JG conceived and designed the study. YW performed the experiments, analyzed the data, and wrote the manuscript. ZW and KM performed the statistical analysis. GT, JG, BC, and XB contributed to revisions of the manuscript. YS, JG, XB, and JL projected administration. All authors have read and approved the manuscript.

Funding

This work was supported by the National Key R&D Program of China (2019YFD0902003) and the Study on Key Technology of Preparation of Compound Flavoring by Biocatalysis.

Conflict of interest

JL and XB were employed by Shandong Longsheng Food Co., Ltd.

The remaining authors declare that the research was conducted in the absence of any commercial or financial relationships that could be construed as a potential conflict of interest.

Publisher's note

All claims expressed in this article are solely those of the authors and do not necessarily represent those of their affiliated organizations, or those of the publisher, the editors and the reviewers. Any product that may be evaluated in this article, or claim that may be made by its manufacturer, is not guaranteed or endorsed by the publisher.

Supplementary material

The Supplementary Material for this article can be found online at: https://www.frontiersin.org/articles/10.3389/fnut.2022.1022156/full#supplementary-material

References

1. Anonymous. *Scallops - Various Species: Sources, Quantities and Cultivation Methods*. (2022). Available online at: https://www.seafish.org/responsible-sourcing/aquaculture-farming-seafood/species-farmed-in-aquaculture/aquaculture-profiles/scallops/sources-quantities-and-cultivation-methods/#:~:text=Scallops%20are%20farmed%20across%20the%20globe%2C%20and%20was,together%20produced%20almost%20204%2C000%20tonnes%20in%202016%202.2022 (accessed July 27, 2022).

2. Zhang X, Cheng J, Han D, Zhao X, Chen X, Liu Y. Geographical origin traceability and species identification of three scallops (*Patinopecten yessoensis, Chlamys farreri*, and *Argopecten irradians*) using stable isotope analysis. *Food Chem.* (2019) 299:125107. doi: 10.1016/j.foodchem.2019.125107

3. Yang B, Gao X, Zhao J, Liu Y, Lui H-K, Huang T-H, et al. Massive shellfish farming might accelerate coastal acidification: a case study on carbonate system dynamics in a bay scallop (*Argopecten irradians*) farming area, North Yellow Sea. *Sci Total Environ.* (2021) 798:149214. doi: 10.1016/j.scitotenv.2021.149214

4. Chen J, Tao L, Zhang T, Zhang J, Wu T, Luan D, et al. Effect of four types of thermal processing methods on the aroma profiles of acidity regulator-treated tilapia muscles using E-nose, HS-SPME-GC-MS, and HS-GC-IMS. *LWT.* (2021) 147:111585. doi: 10.1016/j.lwt.2021.111585

5. Lee B, Park CH, Kong C, Kim YS, Choi YM. Muscle fiber and fresh meat characteristics of white-striping chicken breasts, and its effects on palatability of sous-vide cooked meat. *Poult Sci.* (2021) 100:101177. doi: 10.1016/j.psj.2021.101177

6. Chen Z, Zhu Y, Cao W, Zhou L, Zhang C, Qin X, et al. Novel insight into the role of processing stages in nutritional components changes and characteristic flavors formation of noble scallop *Chlamys nobilis* adductors. *Food Chem.* (2022) 378:132049. doi: 10.1016/j.foodchem.2022.132049

7. Yin M, Matsuoka R, Yanagisawa T, Xi Y, Zhang L, Wang X. Effect of different drying methods on free amino acid and flavor nucleotides of scallop (*patinopecten yessoensis*) adductor muscle. *Food Chem.* (2022) 396:133620. doi: 10.1016/j.foodchem.2022.133620

8. Grassi S, Benedetti S, Magnani L, Pianezzola A, Buratti S. Seafood freshness: e-nose data for classification purposes. *Food Control.* (2022) 138:108994. doi: 10.1016/j.foodcont.2022.108994

9. Yang Y, Qian MC, Deng Y, Yuan H, Jiang Y. Insight into aroma dynamic changes during the whole manufacturing process of chestnut-like aroma green tea by combining GC-E-Nose, GC-IMS, and GC × GC-TOFMS. *Food Chem.* (2022) 387:132813. doi: 10.1016/j.foodchem.2022.132813

10. Duan Z, Dong S, Dong Y, Gao Q. Geographical origin identification of two salmonid species via flavor compound analysis using headspace-gas chromatography-ion mobility spectrometry combined with electronic nose and tongue. *Food Res Int.* (2021) 145:110385. doi: 10.1016/j.foodres.2021.110385

11. Li X, Xie W, Bai F, Wang J, Zhou X, Gao R, et al. Influence of thermal processing on flavor and sensory profile of sturgeon meat. *Food Chem.* (2022) 374:131689. doi: 10.1016/j.foodchem.2021.131689

12. Zhang X, Zheng Y, Feng J, Zhou R, Ma M. Integrated metabolomics and high-throughput sequencing to explore the dynamic correlations between flavor related metabolites and bacterial succession in the process of Mongolian cheese production. *Food Res Int.* (2022) 160:111672. doi: 10.1016/j.foodchem.2022.132740

13. Ross CF. Considerations of the use of the electronic tongue in sensory science. *Curr Opin Food Sci.* (2021) 40:87–93. doi: 10.1016/j.cofs.2021.01.011

14. Yi J, Xu Q, Hu X, Dong P, Liao X, Zhang Y. Shucking of bay scallop (*Argopecten irradians*) using high hydrostatic pressure and its effect on microbiological and physical quality of adductor muscle. *Innov Food Sci Emerg Technol.* (2013) 18:57–64. doi: 10.1016/j.ifset.2013.02.010

15. Zhou Y, Hu M, Wang L. Effects of different curing methods on edible quality and myofibrillar protein characteristics of pork. *Food Chem.* (2022) 387:132872. doi: 10.1016/j.foodchem.2022.132872

16. Wei T, Simko V, Levy M, Xie Y, Jin Y, Zemla J. Package 'corrplot'. *Statistician.* (2017) 56:e24.

17. Luo X, Xiao S, Ruan Q, Gao Q, An Y, Hu Y, et al. Differences in flavor characteristics of frozen surimi products reheated by microwave, water boiling, steaming, and frying. *Food Chem.* (2022) 372:131260. doi: 10.1016/j.foodchem.2021.131260

18. Yu Y, Wang G, Yin X, Ge C, Liao G. Effects of different cooking methods on free fatty acid profile, water-soluble compounds and flavor compounds in Chinese Piao chicken meat. *Food Res Int.* (2021) 149:110696. doi: 10.1016/j.foodres.2021.110696

19. Li W, Chen YP, Blank I, Li F, Li C, Liu Y. GC × GC-ToF-MS and GC-IMS based volatile profile characterization of the Chinese dry-cured hams from different regions. *Food Res Int.* (2021) 142:110222. doi: 10.1016/j.foodres.2021.110222

20. Wang F, Gao Y, Wang H, Xi B, He X, Yang X, et al. Analysis of volatile compounds and flavor fingerprint in Jingyuan lamb of different ages using gas chromatography–ion mobility spectrometry (GC–IMS). *Meat Sci.* (2021) 175:108449. doi: 10.1016/j.meatsci.2021.108449

21. Xie Q, Xu B, Xu Y, Yao Z, Zhu B, Li X, et al. Effects of different thermal treatment temperatures on volatile flavour compounds of water-boiled salted duck after packaging. *LWT.* (2022) 154:112625. doi: 10.1016/j.lwt.2021.112625

22. Yu J, Lu K, Zi J, Yang X, Xie W. Characterization of aroma profiles and aroma-active compounds in high-salt and low-salt shrimp paste by molecular sensory science. *Food Biosci.* (2022) 45:101470. doi: 10.1016/j.fbio.2021.101470

23. Li H, Geng W, Haruna SA, Zhou C, Wang Y, Ouyang Q, et al. Identification of characteristic volatiles and metabolomic pathway during pork storage using HS-SPME-GC/MS coupled with multivariate analysis. *Food Chem.* (2022) 373:131431. doi: 10.1016/j.foodchem.2021.131431

24. Bassam SM, Noleto-Dias C, Farag MA. Dissecting grilled red and white meat flavor: its characteristics, production mechanisms, influencing factors and chemical hazards. *Food Chem.* (2022) 371:131139. doi: 10.1016/j.foodchem.2021.131139

25. Chen X, Luo J, Lou A, Wang Y, Yang D, Shen QW. Duck breast muscle proteins, free fatty acids and volatile compounds as affected by curing methods. *Food Chem.* (2021) 338:128138. doi: 10.1016/j.foodchem.2020.128138

26. Deng S, Liu Y, Huang F, Liu J, Han D, Zhang C, et al. Evaluation of volatile flavor compounds in bacon made by different pig breeds during storage time. *Food Chem.* (2021) 357:129765. doi: 10.1016/j.foodchem.2021.129765

27. Li C, Al-Dalali S, Wang Z, Xu B, Zhou H. Investigation of volatile flavor compounds and characterization of aroma-active compounds of water-boiled salted duck using GC–MS–O, GC–IMS, and E-nose. *Food Chem.* (2022) 386:132728. doi: 10.1016/j.foodchem.2022.132728

28. Liu T-T, Xia N, Wang Q-Z, Chen D-W. Identification of the non-volatile taste-active components in crab sauce. *Foods.* (2019) 8:324. doi: 10.3390/foods8080324

29. Li R, Sun Z, Zhao Y, Li L, Yang X, Chen S, et al. Effect of different thermal processing methods on water-soluble taste substances of tilapia fillets. *J Food Composit Anal.* (2022) 106:104298. doi: 10.1016/j.jfca.2021.104298

30. Tang D, Wang R, He X, Chen X, Huo X, Lü X, et al. Comparison of the edible quality of liquid egg with different cooking methods and their antioxidant activity after in vitro digestion. *Food Res Int.* (2021) 140:110013. doi: 10.1016/j.foodres.2020.110013

31. Liu YX, Zhang YY, Zheng J, Chen JN, Huang XH, Dong XP, et al. Seasonal variations in free amino acid, 5 '-nucleotide, and lipid profiles of scallop (*Patinopecten yessoensis*) revealed by targeted and untargeted metabolomic approaches. *LWT Food Sci Technol.* (2022) 154:112881. doi: 10.1016/j.lwt.2021.112881

32. Liu R, Yang L, Yang T, Qin M, Li K, Bao W, et al. Effect of nitric oxide treatment on pork meat quality, microstructure, and total bacterial count during postmortem aging. *Meat Sci.* (2022) 190:108806. doi: 10.1016/j.meatsci.2022.108806

33. Rodríguez R, Alvarez-Sabatel S, Ríos Y, Rioja P, Talens C. Effect of microwave technology and upcycled orange fibre on the quality of gluten-free muffins. *LWT.* (2022) 158:113148. doi: 10.1016/j.lwt.2022.113148

34. Zhu Y, Zhou X, Chen YP, Liu Z, Jiang S, Chen G, et al. Exploring the relationships between perceived umami intensity, umami components and electronic tongue responses in food matrices. *Food Chem.* (2022) 368:130849. doi: 10.1016/j.foodchem.2021.130849

35. Zhang S, Zhang C, Qiao Y, Xing L, Kang D, Khan IA, et al. Effect of flavourzyme on proteolysis, antioxidant activity and sensory qualities of Cantonese bacon. *Food Chem.* (2017) 237:779–85. doi: 10.1016/j.foodchem.2017.06.026

36. Shen X, Wang Y, Ran L, Liu R, Sun X, Hu L, et al. Flavor deterioration of liquid endosperm in postharvest tender coconut revealed by LC-MS-based metabolomics. GC-IMS and E-tongue. *Postharvest Biol Technol.* (2022) 187:111866. doi: 10.1016/j.postharvbio.2022.111866

37. Toda Y, Nakagita T, Hirokawa T, Yamashita Y, Nakajima A, Narukawa M, et al. Positive/negative allosteric modulation switching in an umami taste receptor (T1R1/T1R3) by a natural flavor compound, methional. *Sci Rep.* (2018) 8:11796. doi: 10.1038/s41598-018-30315-x

38. Hu Y, Tian Y, Zhu J, Wen R, Chen Q, Kong B. Technological characterization and flavor-producing potential of lactic acid bacteria isolated from traditional dry fermented sausages in northeast China. *Food Microbiol.* (2022) 106:104059. doi: 10.1016/j.fm.2022.104059

39. Merlo TC, Manuel Lorenzo J, Saldana E, Patinho I, Oliveira AC, Menegali BS, et al. Relationship between volatile organic compounds, free amino acids, and sensory profile of smoked bacon. *Meat Sci.* (2021) 181:108596. doi: 10.1016/j.meatsci.2021.108596

frontiers | Frontiers in Nutrition

TYPE Original Research
PUBLISHED 18 October 2022
DOI 10.3389/fnut.2022.1003126

OPEN ACCESS

EDITED BY
Gang Fan,
Huazhong Agricultural University, China

REVIEWED BY
Madhuresh Dwivedi,
National Institute of Technology Rourkela, India
Baoguo Sun,
Beijing Technology and Business University, China
Yong-Quan Xu,
Tea Research Institute (CAAS), China

*CORRESPONDENCE
Rui-Ming Luo
wyr2013tymk@163.com

SPECIALTY SECTION
This article was submitted to Food Chemistry, a section of the journal Frontiers in Nutrition

RECEIVED 25 July 2022
ACCEPTED 20 September 2022
PUBLISHED 18 October 2022

CITATION
Wang YR, Wang SL and Luo RM (2022) Evaluation of key aroma compounds and protein secondary structure in the roasted Tan mutton during the traditional charcoal process. *Front. Nutr.* 9:1003126. doi: 10.3389/fnut.2022.1003126

Evaluation of key aroma compounds and protein secondary structure in the roasted Tan mutton during the traditional charcoal process

Yong-Rui Wang[1], Song-Lei Wang[2] and Rui-Ming Luo[2]*

[1]College of Agriculture, Ningxia University, Yinchuan, China, [2]College of Food and Wine, Ningxia University, Yinchuan, China

The traditional charcoal technique was used to determine the changes in the key aroma compounds of Tan mutton during the roasting process. The results showed that the samples at the different roasting time were distinguished using GC-MS in combination with PLS-DA. A total of 26 volatile compounds were identified, among which 14 compounds, including (*E*)-2-octenal, 1-heptanol, hexanal, 1-hexanol, heptanal, 1-octen-3-ol, 1-pentanol, (*E*)-2-nonenal, octanal, 2-undecenal, nonanal, pentanal, 2-pentylfuran and 2-methypyrazine, were confirmed as key aroma compounds through the odor activity values (OAV) and aroma recombination experiments. The OAV and contribution rate of the 14 key aroma compounds were maintained at high levels, and nonanal had the highest OAV (322.34) and contribution rate (27.74%) in the samples after roasting for 10 min. The content of α-helix significantly decreased ($P < 0.05$), while the β-sheet content significantly increased ($P < 0.05$) during the roasting process. The content of random coils significantly increased in the samples roasted for 0–8 min ($P < 0.05$), and then no obvious change was observed. At the same time, β-turn content had no obvious change. Correlation analysis showed that the 14 key aroma compounds were all positively correlated with the content of α-helix and negatively correlated with the contents of β-sheet and random coil, and also positively correlated with the content of β-turn, except hexanal and 2-methypyrazine. The results are helpful to promoting the industrialization of roasted Tan mutton.

KEYWORDS

roasted Tan mutton, key aroma compounds, OAVS, aroma recombination experiment, protein secondary structure, correlation analysis

Introduction

Regardless of religious restrictions, mutton is extensively consumed owing to its great nutritional value, including iron, zinc, high-quality protein, fat and vitamins (1). The consumption of mutton in China, the world's largest mutton production and consumption country, has steadily increased (2).

Tan sheep, one of the most well-known and popular sheep in Ningxia Hui Autonomous Region of China, have frequently boarded the official dinner to entertain international guests (3). The unique geographical environment, forage grass and water quality of the Ningxia region result in a low "off-flavor" of Tan mutton.

Roasted mutton, including roasted sheep leg and mutton shashlik, is a classic and handy meal that is popular across the world (4). During the roasting process of mutton, the reactions, like Maillard reaction, lipid oxidation and the interactions between the components of the meat produce a large number of aroma compounds (5). The aroma compounds, including aliphatic aldehydes, ketones, alcohols, acids and esters, were usually generated by lipid degradation, and these compounds were responsible for the animal species-specific meat aroma (6, 7). The heterocyclic compounds, like nitrogen-containing and oxygen-containing, as well as sulfur-containing chemicals, are regularly produced by the Maillard process and contribute to the fundamental aroma of meat (8). Furthermore, the interaction between the Maillard reaction and the lipid degradation also plays a significant role in the generation of the cooked meat aroma (9). However, the overall aroma of Tan mutton can be altered by modifying the manufacturing conditions, and temperature is an important factor in this process (10).

In the recent 40 years, the key aroma compounds in many types of meat were evaluated by GC-MS combined with GC-O and odor active values (OAV) (8). Based on OAV, a series of compounds, such as hexanal, 1-octen-3-ol, nonanal and octanal, were confirmed as the primary aroma compounds in roasted mutton using a typical charcoal roasting method (11). Different roasting methods, including microwave, electricity and superheated steam, also produced similar aroma compounds in roasted mutton (12–14). However, to our knowledge, little has been known about the changes in aroma compounds or odor expression and its alterations during the roasting process. It is thus necessary to understand the relationship between the changes and key control factors of aroma compounds in roasted mutton, thereby helping producers control the aroma of products (15).

Protein can combine with aroma compounds (16). When the protein's capacity to attach to the aromatic compounds changes, it impacts the retention of the aroma compounds in the product, which has a substantial impact on the product's aroma perception (17). Polypeptides' original conformation was broken during the roasting process, resulting in increased thermal motion, loss of secondary and tertiary structure, and rupture of intermolecular forces, such as electrostatic or non-polar interactions and disulfide bonds (18–20). As a result, the meat's sensory quality after cooking, like tenderness and aroma, was affected by the denaturation of proteins and changes in fiber structure resulting from heat treatment (21, 22). The appropriateness of meat for cooking is determined mostly by macroscopical factors. However, microstructure changes in meat after cooking are the basis and causes of these macroscopical alterations, which have received little attention so far (23).

Thus, the study aimed to (i) select the key aroma compounds by GC-O and study the changes of these compounds in the composition and concentration using GC-MS in roasted Tan mutton during the traditional charcoal process; (ii) identify the key aroma compounds in roasted Tan mutton using OAV and aroma recombination tests; (iii) study the changes in the protein secondary structure of roasted Tan mutton during the roasting process; (iv) determine correlation between the protein secondary structure and key aroma compounds in roasted Tan mutton.

Materials and methods

Materials

The Tan mutton used in this experiment was randomly obtained from the hind legs of Yanchi Tan sheep (30 ± 1 kg, 9 months age) from Ningxia Xinhai Food Co., Ltd. (Yanchi, China). The following chemicals were purchased from Sigma-Aldrich (Shanghai, China): 1,2-dichlorobenzene (internal standard, 99.7%) and n-alkanes (C_5-C_{32}, 98%), hexanal (95%), heptanal (97%), 1-heptanol (97%), benzaldehyde (99.5%), 2-methypyrazine (99%), (*E*)-2-undecenal (96%), pentanal (99%), octanal (99%), 1-hexanol (99%), 1-pentanol (99%), (*E*)-2-octenal (97%), nonanal (99.5%), (*E*)-2-nonenal (97%), 2-pentylfuran and 1-octen-3-ol (98%). Methanol (analytical grade) was purchased from Thermo Fisher Scientific Co., Ltd. (Shanghai, China).

Sample preparation

The bones were removed from the leg of the Tan sheep, and then the mutton washed with tap water to clean the blood and other impurities on the surface (24). After washing, the mutton was cut into small pieces (1.5 × 1.5 × 1.0 cm). Then eight pieces of Tan mutton were put into iron sticks, and then placed on the fire for grilling. The Tan mutton was roasted on a barbeque grill 5 cm from the charcoal fire at 250–270°C, flipping over the clusters every 20 s. The water content of tan mutton decreased from (raw meat) 69.34–72.02 to 48.33–53.25% (roasting for 14 min). The sensory assessment findings revealed that 10 min was the optimal roasting period for the mutton, and the mutton roasted for 10 min had the best flavor and overall acceptability with the unanimous agreement of panelists. The core and surface temperatures of the roasted Tan mutton at 10 min were 79.5–81.2 and 85.6–95.7°C, respectively. The samples were roasted for 0, 2, 4, 6, 8, 10, 12, and 14 min. Three replicate samples (eight iron sticks each) were prepared and subjected to the following analyses.

Aroma analysis

GC-MS analysis

Aroma analysis of roasted Tan mutton was performed by a GC-MS system (GC-MS 2010 plus, SHIMADZU, Japan) jointed with solid-phase microextraction (SPME) fiber. Briefly, 2 ± 0.01 g of the sample after crushed were placed into a 15 mL headspace bottle with 4 μL of internal standard (1,2-dichlorobenzene, 6.42 μg/mL in methanol). After mixing with a vortex, the headspace bottle was sealed with a PTFE diaphragm, and placed in a water bath at 55°C for 20 min. The aged SPME fiber (50/30 μm DVB / CAR / PDMS) was inserted into a sealed extraction bottle and kept on the top of the mutton sample for adsorption for 30 min, and then transferred to the GC inlet for desorption at 250°C for 5 min. The chromatographic capillary column was DB-WAX (30 m×0.25 mm×0.25 μm, Agilent Technologies, Santa Clara, CA). The GC and MS were carried out in accordance with our previous study (25).

GC-O analysis

A GC system equipped with an olfactory detection port (GC 2014, SHIMADZU, Japan) and a DB-WAX column (60 m × 0.25 mm × 0.25 μm; Agilent Technologies, Inc.) was used for GC-O analysis The GC conditions were the same as for the GC-MS. The effluent was divided in a 1:1 ratio between the MS and the sniffer port. This sniffing experiment was conducted by three professional appraisers. They were required to keep track of the retention time according to the time of the stopwatch and describe the aroma characteristics as soon as they appear in the sniffing port.

Identification and quantitation of aroma compounds

The aroma compounds of roasted Tan mutton were identified using a mass spectrometry library (MS), linear retention indices (LRI) and odor characteristics (O) in comparison to authentic flavor standards (S) (Table 1). The retention of a homologous sequence of n-alkanes (C_5-C_{32}) was used to compute the LRI. The odorants were validated by comparing the retention time and ion fragments of samples with authentic flavor standards in GC-MS analysis under similar chromatographic conditions. As an internal standard, 1,2-dichlorobenzene was used to semiquantify the aroma compounds. In particular, a 5-point calibration curve was used to measure the quantities of odorants (OAV >1) in an odorless mutton model. The odorless mutton model, in a nutshell, consisted of an odorless mutton matrix, realistic flavor criteria and ultrapure water. The odorless mutton matrix was made according to previous studies (4, 26), with some modifications. Briefly, diethyl ether and n-pentane were added to the mutton (diethyl ether–n-pentane–mutton puree ratio of 2:1:1, m/m/m). After shaking for 12 h, the organic solvent was extracted 5 times. The samples were then frozen in an FD-1A-50 freeze-dryer using liquid nitrogen (Shanghai Zheng-Qiao Science Instrument Plant, Ltd., Beijing, China) at −50°C for 24 h. Sensory panelists assessed the aroma characteristics of roasted mutton and the recombination model.

Protein secondary structure analysis

The protein's secondary structure of roasted Tan mutton was determined using attenuated total reflection (ATR) by Fourier transform infrared spectroscopy (FTIR; Bruker, Germany). Roasted mutton was vacuum-frozen (freezing temperature −25°C, cold trap temperature −30°C, vacuum degree 20 Pa), dried for 48 h and then crushed into 200 mesh powder. Then 2 mg sample of roasted mutton were added with 100 mg KBr, placed in a mortar to grind and crush until evenness, and then pressed into thin slices for analysis by mid-infrared spectroscopy. The instrument's parameters included absorbance spectra ranging from 500 to 4000 cm^{-1}, a resolution of 4 cm^{-1}, and a scan rate of 100 times. The protein secondary structure information was contained in the amide I spectrum in the mid-IR spectral range of 1700–1600 cm^{-1}, which was caused by the expansion vibration of C = O (27). The superposition of different protein secondary structure peak components resulted in the formation of the amide I band. The second-order derivation and deconvolution technique were used to further deconstruct the peaks in the amide I band of the original protein infrared spectra that were not discernable into multiple sub-peaks. Peakfit 4.12 software was used to perform deconvolution and curve-fitting on the amide I band distribution.

Sensory evaluation

The sensory evaluation was carried out in accordance with previous reports (28, 29). The panelists consisted of 10 graduate students (five males and five females, aged from 22 to 25) who did not suffer rhinitis and were non-smokers (30, 31). Before the experiments, ISO 4121:2003 and GB/T 29604-2013 guidelines were used to train all panelists for 30 days. Firstly, the aroma characteristics of a 54-aroma kit (Le Nez du Vin®, France) were distinguished and described for 20 days (once 5 days, each training lasting for 1 h). Secondly, five olfactory qualities, including meaty, fatty, roasty, grassy, and sweet, were chosen for the panelists to assess the aroma quality of roasted Tan mutton. This assessment lasted for 30 min and was performed 15 times within 30 days. Finally, these panelists were qualified to do the sensory evaluation. The sensory evaluation panel evaluated the sensory properties of roasted Tan mutton on a five-point

TABLE 1 Identification of aroma compounds in roasted Tan mutton for 0–14 min.

No.	Volatile compounds[a]	Threshold (μg/kg)[b]	RI		Odor description	ID[e]
			Literature[c]	Calculated[d]		
1	1-Heptanol	5.4	1462	1473	floral	MS,O,RI,S
2	1-Hexanol	5.6	1359	1351	green, fruity, oily	MS,O,RI,S
3	1-Nonanol	46	1673	1770	rose, citrus	MS,O,RI
4	1-Octanol	120	1573	1558	fatty, waxy	MS,O,RI
5	1-Octen-3-ol	1	1456	1462	mushroom	MS,O,RI,S
6	1-Pentanol	150	1274	1275	sweet, balsamic	MS,O,RI,S
7	2,3-Butanediol	/	1583	1584	green	MS,O,RI
8	(*E*)-2-Heptenal	40	1291	1286	herbaceous, green, oily	MS,O,RI
9	(*E*)-2-Nonenal	0.19	1517	1514	green, fatty, tallowy	MS,O,RI,S
10	(*E*)-2-Octenal	3	1396	1392	sweet, fatty, mild	MS,O,RI,S
11	(*E*)-2-Undecenal	0.78	1755	1754	green, fruity, fatty	MS,O,RI,S
12	Hexanal	4.5	1064	1068	floral, fruity, fatty	MS,O,RI,S
13	Octanal	0.59	1273	1277	fruity, nutty, oily	MS,O,RI,S
14	Heptanal	2.8	1163	1160	herbaceous, green, oily	MS,O,RI,S
15	Benzaldehyde	750	1534	1528	bitter almond, aromatic, popcorn	MS,O,RI
16	Nonanal	1.1	1369	1367	sweet melon	MS,O,RI,S
17	Pentanal	12	964	967	woody, fatty	MS,O,RI,S
18	Acetic acid	99	1401	1398	sour, pungent, strong	MS,O,RI
19	Hexanoic acid	890	1854	1857	lamby, oily	MS,O,RI
20	Decanoic acid	10	2281	2269	rancid, oily	MS,O,RI
21	Nonanoic acid	6.8	2174	2173	rancid, oily, fatty	MS,O,RI
22	Octanoic acid	3	2067	2075	cheesy, waxy	MS,O,RI
23	Hexanoic acid methyl ester	77	1189	1192	fruity	MS,O,RI
24	6-Methyl-5-hepten-2-one	68	1342	1361	roasted peanuts, tallowy	MS,O,RI
25	2-Pentylfuran	6	1215	1228	vegetable, earthy	MS,O,RI,S
26	2-Methypyrazine	30	1238	1243	roasted, meaty	MS,O,RI,S

[a]The aroma compounds in roasted mutton. [b]Aroma thresholds obtained from reference Sohail et al. (8). [c]Data in literature. [d]Data determined according to the retention time of n-alkanes (C_5-C_{32}). [e]Identification analysis. MS, mass spectrometry; LRI, linear retention indices; O, odor qualities; S, authentic flavor standards.

scale (4∼5: very strong, 3∼4: strong, 2∼3: medium, 1∼2: weak, 0∼1: very weak). To avoid odor interaction between samples, panelists were required to take a 30 s break during the experiment.

Statistical analysis

Excel was used to analyze the average value and standard deviation of the data, and the data were expressed as means ± standard deviation. Duncan's multiple range test ($P < 0.05$) was used to analyze differences between individual means using SPSS 19.0 software (IBM Corporation, USA). The PCA chart of the electronic nose data was made by SIMCA14.0 software. The Pearson correlation analysis was performed by R software. The other graphs were made by Origin 18C software.

Results

Discrimination of roasted Tan mutton

To discriminate the samples of roasted Tan mutton, GC-MS was coupled with PLS-DA. As shown in Figure 1A, the PLS-DA score plot showed a distinct separation of the eight sample groups. R^2X, R^2Y and Q^2 values of 0.982, 0.983, and 0.951 were obtained, indicating that the built model was stable and predictive. The raw meat and sample roasted for 2 min located in the first quadrant of the PLS-DA score plot (Figure 1B), among which hexanoic acid methyl ester was the major chemical family forming the odors of raw meat. The mutton samples roasted for 4, 6, and 8 min located in the second quadrant. This distribution was heavily influenced by alcohols and aldehydes, including 1-octene-3-ol, 1-nonanol, 1-octanol, pentanal, heptanal, (*E*)-2-nonenal, (*E*)-2-octenal,

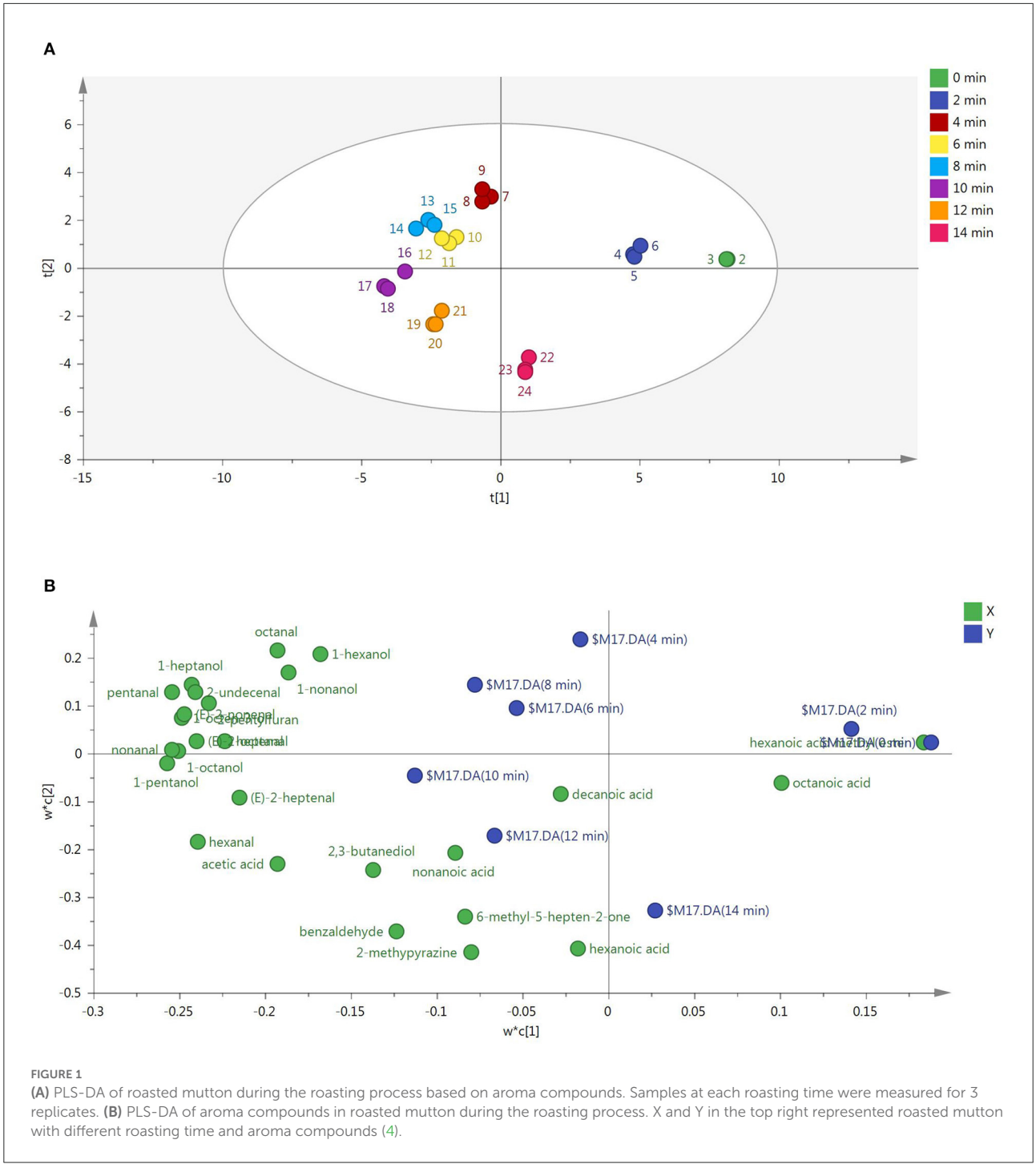

FIGURE 1
(A) PLS-DA of roasted mutton during the roasting process based on aroma compounds. Samples at each roasting time were measured for 3 replicates. **(B)** PLS-DA of aroma compounds in roasted mutton during the roasting process. X and Y in the top right represented roasted mutton with different roasting time and aroma compounds (4).

otanal, 1-hexanol, 1-heptanol, nonanal, (*E*)-2-undecenal, and 2-pentylfuran. The mutton samples roasted for 10 and 12 min appeared in the third quadrant related to 1-pentanol, hexanal, (*E*)-2-heptenal, decanoic acid, nonanoic acid, hexanoic acid, acetic acid, 2,3-butanediol, 6-methyl-5-hepten-2-one, 2-methylpyrazine, and benzaldehyde. The mutton sample with roasting for 14 min appeared in the fourth quadrant related to octanoic acid.

The changes in composition and concentrations of aroma compounds in roasted Tan mutton

As shown in Tables 1, 2, a total of 26 aroma compounds were identified using DB-WAX columns in all samples, including seven alcohols, 10 aldehydes, five acids, two heterocyclics, one ester and one ketone. In comparison, no significant changes

TABLE 2 Quantitation analysis of aroma compounds in roasted Tan mutton during the roasting process.

No.	Volatile compounds	Calibration equations	R^2	Volatile flavor compounds retention (μg/kg)							
				0 min	2 min	4 min	6 min	8 min	10 min	12 min	14 min
1	1-Heptanol	y = 0.2391x + 0.0178	0.9855	2.19 ± 0.19f	3.12 ± 0.04f	12.68 ± 1.39b	12.15 ± 0.24bc	14.18 ± 0.69a	11.17 ± 0.22cd	10.07 ± 0.42d	7.50 ± 0.12e
2	1-Hexanol	y = 0.0517x + 0.0232	0.9928	11.52 ± 0.05e	11.89 ± 0.30e	16.38 ± 0.70c	24.09 ± 1.48a	16.89 ± 0.88bc	18.42 ± 1.09b	13.95 ± 0.68d	11.00 ± 0.46e
3	1-Nonanol	—	—	0.77 ± 0.18c	0.85 ± 0.09c	2.17 ± 0.12b	2.26 ± 0.24b	2.21 ± 0.17b	2.20 ± 0.17b	3.04 ± 0.15a	ND
4	1-Octanol	—	—	4.38 ± 0.02e	14.21 ± 0.46d	24.30 ± 1.31b	19.79 ± 1.74c	27.16 ± 2.71b	32.91 ± 2.41a	26.54 ± 1.08b	18.62 ± 2.09c
5	1-Octen-3-ol	y = 0.0296x + 0.0156	0.9904	102.26 ± 0.92f	130.07 ± 5.86e	236.43 ± 9.34c	328.55 ± 24.08a	304.24 ± 4.07b	320.31 ± 3.77ab	228.43 ± 5.55cd	209.03 ± 5.64d
6	1-Pentanol	y = 0.4106x + 0.0144	0.9915	11.75 ± 0.17e	22.42 ± 1.12d	139.81 ± 3.39b	138.68 ± 7.65b	136.51 ± 5.06b	153.06 ± 4.08a	132.53 ± 2.76b	122.45 ± 2.02c
7	2,3-Butanediol	—	—	10.44 ± 0.81d	10.86 ± 0.78d	6.61 ± 0.14e	36.92 ± 2.08a	11.36 ± 1.00d	33.88 ± 1.62b	26.75 ± 1.70c	28.97 ± 1.84c
8	(*E*)-2-Heptenal	—	—	1.36 ± 0.04f	1.12 ± 0.011f	3.88 ± 0.43e	11.36 ± 0.20d	22.24 ± 1.77a	17.39 ± 0.38b	12.86 ± 0.69c	12.65 ± 0.24cd
9	(*E*)-2-Nonenal	y = 0.5312x + 0.0312	0.9832	0.30 ± 0.03c	0.21 ± 0.06c	4.16 ± 0.30a	3.90 ± 0.04a	3.92 ± 0.70a	4.03 ± 0.19a	3.11 ± 0.10b	2.59 ± 0.31b
10	(*E*)-2-Octenal	y = 0.6473x + 0.0023	0.9649	0.53 ± 0.02d	2.19 ± 0.09cd	5.29 ± 0.65b	13.65 ± 2.15a	15.14 ± 1.45a	15.21 ± 0.77a	13.86 ± 0.52a	3.97 ± 0.16bc
11	2-Undecenal	y = 0.5374x + 0.0457	0.9826	0.20 ± 0.02g	0.43 ± 0.10f	1.72 ± 0.13c	1.26 ± 0.10d	2.19 ± 0.03a	1.89 ± 0.04b	1.31 ± 0.07d	0.96 ± 0.08e
12	Hexanal	y = 0.0182x + 0.0010	0.9915	23.62 ± 0.49g	94.90 ± 2.14f	234.41 ± 6.56e	378.74 ± 8.10d	430.31 ± 3.70c	658.11 ± 13.18a	565.49 ± 5.17b	423.28 ± 11.34c
13	Octanal	y = 0.2946x + 0.0373	0.9842	13.16 ± 0.24e	138.49 ± 2.98c	150.21 ± 2.96b	155.72 ± 8.35ab	161.79 ± 2.83a	159.96 ± 3.20a	131.08 ± 2.25c	66.98 ± 1.39d
14	Heptanal	y = 0.2338x + 0.0164	0.9699	10.02 ± 0.02d	115.33 ± 7.37c	120.75 ± 6.71c	137.88 ± 3.06ab	143.28 ± 3.94a	137.45 ± 5.47a	131.79 ± 3.14b	112.10 ± 2.14c
15	Benzaldehyde	—	—	ND	11.69 ± 1.06d	19.07 ± 2.09c	16.95 ± 1.72cd	19.90 ± 3.08c	115.32 ± 4.95b	120.18 ± 3.28ab	121.23 ± 1.75a
16	Nonanal	y = 0.3696x + 0.1004	0.9825	13.21 ± 0.45g	113.76 ± 4.96f	226.13 ± 7.67d	222.06 ± 10.86d	242.08 ± 4.90c	354.57 ± 5.84a	297.53 ± 5.75b	139.83 ± 2.35e
17	Pentanal	y = 0.0627x + 0.0241	0.9864	ND	23.69 ± 1.92d	125.04 ± 4.66a	122.51 ± 1.69a	120.53 ± 3.58a	121.23 ± 7.27a	109.66 ± 1.96b	55.08 ± 1.88c
18	Acetic acid	—	—	3.05 ± 0.08e	8.06 ± 0.89d	15.17 ± 1.36c	18.39 ± 0.66b	19.00 ± 0.53b	16.54 ± 3.10bc	23.59 ± 0.99a	25.17 ± 1.43a
19	Hexanoic acid	—	—	4.81 ± 0.12d	5.79 ± 0.32c	3.20 ± 0.20e	6.16 ± 0.43c	5.73 ± 0.28c	5.62 ± 0.49c	7.58 ± 0.21b	9.90 ± 0.42a
20	Decanoic acid	—	—	0.56 ± 0.05bc	0.58 ± 0.13bc	0.37 ± 0.09d	0.94 ± 0.07a	0.35 ± 0.02d	0.64 ± 0.14bc	0.69 ± 0.01b	0.51 ± 0.03cd
21	Nonanoic acid	—	—	0.92 ± 0.06c	0.81 ± 0.16c	0.60 ± 0.08d	0.84 ± 0.04c	0.81 ± 0.02c	1.34 ± 0.12a	1.11 ± 0.10b	0.86 ± 0.04c
22	Octanoic acid	—	—	1.28 ± 0.13a	0.71 ± 0.02c	ND	1.01 ± 0.10b	0.76 ± 0.76c	0.78 ± 0.78c	ND	0.94 ± 0.09b
23	Hexanoic acid methyl ester	—	—	14.32 ± 0.67a	ND	ND	ND	ND	ND	ND	ND
24	6-Methyl-5-hepten-2-one	—	—	10.52 ± 0.06c	11.20 ± 0.88bc	11.74 ± 0.01^{bc}	11.58 ± 0.82bc	11.65 ± 0.34bc	11.97 ± 0.53b	14.41 ± 1.24a	14.61 ± 0.61a
25	2-Pentylfuran	y = 0.5325x + 0.0186	0.9749	1.55 ± 0.09e	1.60 ± 0.31e	31.89 ± 2.80^{b}	22.25 ± 1.05c	36.33 ± 1.95a	34.58 ± 0.96ab	17.44 ± 1.66d	19.86 ± 1.77cd
26	2-Methypyrazine	y = 0.9420x + 0.0125	0.9683	ND	ND	ND	ND	11.33 ± 1.06d	53.28 ± 1.13c	77.54 ± 2.23b	101.70 ± 3.09a

The results were presented as means and standard errors. ND, not detected.

10.3389/fnut.2022.1003126

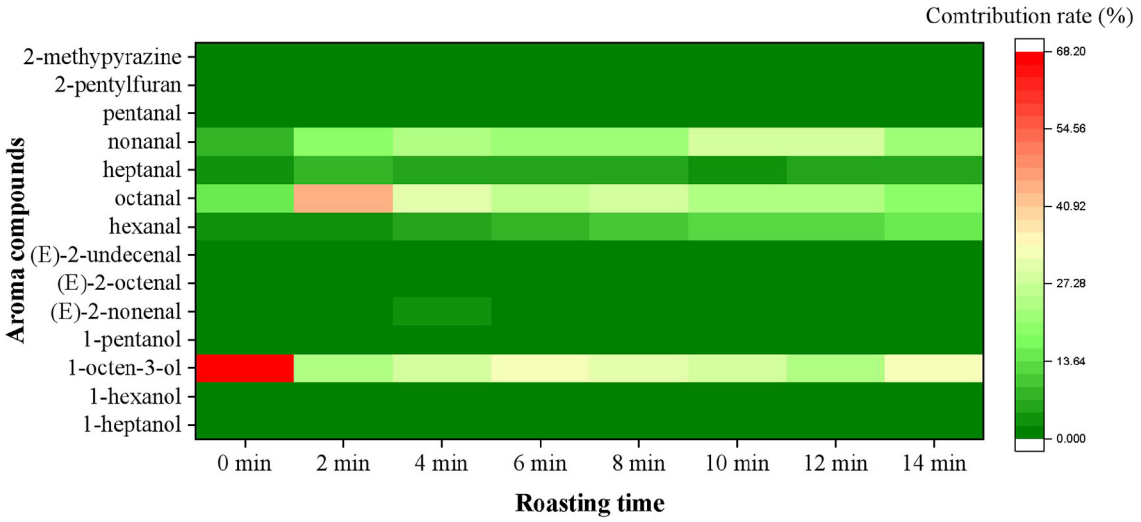

FIGURE 2
Changes of contribution rates of aroma compounds (OAV > 1) in roasted Tan mutton during the roasting process.

in any of the odorants were found across the eight samples ($P > 0.05$). Aldehydes and alcohols accounted for more than 65% of all odorants. Methyl ester hexanoic acid was identified in the raw meat and disappeared after roasting for 2 min. Compared with the mutton samples roasted for 2–14 min, the concentration of octanoic acid was significantly higher ($P < 0.05$) in the raw meat. In contrast, benzaldehyde and pentanal appeared in the mutton roasted for 2 min, with a high concentration in the mutton roasted for 14 min. 1-octanol, hexanal, 1-pentanol, 2-pentylfuran, heptanal, 2,3-butanediol, (*E*)-2-heptenal, octanal, (*E*)-2-octenal, nonanal and nonanoic acid were found to have the highest concentrations in the mutton roasted for 8 and 10 min. The mutton roasted for 14 min had the highest concentrations of 6-methyl-5-hepten-2-one, acetic acid, and hexanoic acid. Interestingly, 2-methypyrazine had the highest concentration in the sample roasted for 14 min.

In all stages, hexanal, heptanal, (*E*)-2-octenal, (*E*)-2-heptenal, nonanal, and octanal were the most important aldehydes, and hexanal had the highest concentration. 1-octen-3-ol was the most important alcohol in roasted Tan mutton. The concentrations of most aldehydes and alcohols rose dramatically in roasted Tan mutton after 2–10 min of roasting ($P < 0.05$), but reduced after 12–14 min of roasting. In particular, hexanal (658.11 μg/kg), nonanal (354.57 μg/kg), heptanal (137.45 μg/kg), pentanal (121.23 μg/kg), octanal (159.96 μg/kg) and 1-octen-3-ol (320.31 μg/kg) may significantly contribute to the aroma of roasted Tan mutton after 10 min.

Key aroma compounds in roasted Tan mutton

The OAV and contribution rate were calculated to better understand the significance of each aroma compound. As shown in Figure 2, a total of 14 aroma compounds, including (*E*)-2-octenal, 1-heptanol, hexanal, 1-hexanol, heptanal, 1-octen-3-ol, 1-pentanol, (*E*)-2-nonenal, octanal, (*E*)-2-undecenal, nonanal, pentanal, 2-pentylfuran and 2-methypyrazine were initially found as the key aroma compounds in roasted Tan mutton because their OAVs surpassed 1. Among them, there were eight aldehydes, four alcohols, one pyrazine and one furan. The concentrations and OAV of 14 key aroma compounds rose considerably ($P < 0.05$) from 0 to 10 min, but significantly decreased ($P < 0.05$) from 10 to 14 min. Only 7 of the 14 key aroma compounds with OAV greater than 1 may play critical roles in aroma expression in raw meat, including 1-hexanol, 1-octen-3-ol, (*E*)-2-nonenal, hexanal, octanal, heptanal, and nonanal. In comparison with raw meat, 14 key odorants were all observed and remained at high levels in the samples for 10 min, among which hexanal (146.24), nonanal (322.33), octanal (271.11), and 1-octen-3-ol (320.31) had the highest OAV. Particularly, the concentration and OAV of nonanal exhibited the highest level in the mutton roasted for 10 min. The contribution rate was further used to demonstrate the importance of each aroma compound. The nonanal (27.74%), 1-octen-3-ol (27.57%), octanal (23.34%), and hexanal (12.59%) primarily contributed to the aroma of roasted mutton for 10 min. Furthermore, the sensory panelists unanimously agreed

that the recombination model of 14 key aroma compounds generated the usual meaty, grassy, roasty, fatty, and sweet aromas associated with the roasted mutton (Figure 3). The recombination model's similarity was rated 4.8 out of 5, indicating that the 14 aroma compounds were the key aroma compounds of roasted Tan mutton.

Change of protein secondary structure in roasted Tan mutton

FT-IR spectroscopy is a commonly used and reliable method in the analysis of protein secondary structure. Our second-derivative band placements were consistent with previous studies showing that mid-IR spectra in the range of 1645–1662 cm^{-1} accounted for the α-helix band, the β-sheet band located at 1612–1640 cm^{-1} and 1682–1697 cm^{-1}, the β-turn band located at 1662–1682 cm^{-1}, and the random coil located at 1637–1645 cm^{-1} (32, 33). Fourier self-deconvolution, second derivative, and Gaussian curve-fitting were used in this investigation to quantitatively examine the spectra's second derivative (34). As shown in Table 3 and Figure 4, there was a reduction in the α-helix content ($P < 0.05$), and an increase in the β-sheet ($P < 0.05$) across all of the samples. The content of random coils significantly increased in the samples roasted for 0–8 min ($P < 0.05$), but afterward, no discernible change was found. At the same time, there were no significant changes in the content of β-turn. The contents of α-helix and β-sheet of protein from roasted Tan mutton decreased, and the contents of β-turn and random coil increased. Higher levels of α-helix and β-sheet indicated a more stable secondary structure, whereas higher contents of β-turn and random coil indicated a more flexible protein structure (35).

Discussion

Aldehydes and alcohols are the pivotal aroma compounds in roasted Tan mutton

The pivotal aroma compounds in meat were aldehydes and alcohols, such as hexanal, nonanal, octanal, and 1-octen-3-ol (36). In this study, 12 aldehydes and alcohols were identified out of 14 key aroma compounds, with a percentage contribution of 98.91–99.95% in the aroma of roasted Tan mutton. Nonanal had the highest OAV (322.34) and contribution rate (27.74%) especially, followed by 1-octen-3-ol, octanal and hexanal in the mutton roasted for 10 min. According to the investigation, lipid

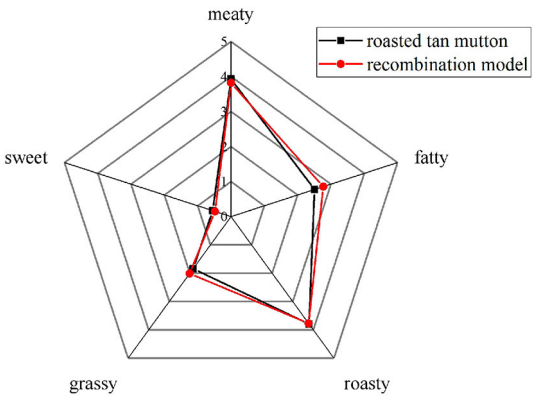

FIGURE 3
Aroma profiles in roasted Tan mutton and recombination model.

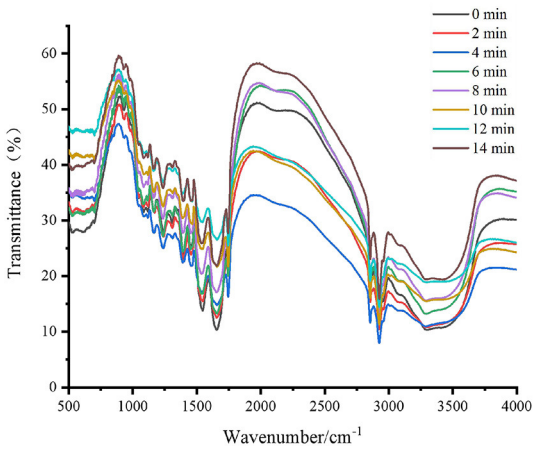

FIGURE 4
Fourier transform infrared spectroscopy (500–4000 cm^{-1}) from roasted Tan mutton at different roasting time.

TABLE 3 Relative percentage of protein secondary structure of roasted Tan mutton.

	0 min	2 min	4 min	6 min	8 min	10 min	12 min	14 min
α-helix (%)	37.66 ± 0.27a	35.23 ± 0.25b	33.05 ± 0.12c	28.20 ± 0.41d	26.81 ± 0.39e	26.55 ± 0.14e	24.85 ± 0.07f	24.43 ± 0.16f
β-sheet (%)	17.13 ± 0.10f	19.70 ± 0.40e	20.67 ± 0.50d	22.69 ± 0.45c	23.16 ± 0.20c	25.67 ± 0.35b	26.11 ± 0.16ab	26.46 ± 0.21a
β-turn (%)	13.69 ± 0.31a	12.48 ± 0.20d	12.22 ± 0.36d	12.65 ± 0.24cd	13.08 ± 0.14bc	13.49 ± 0.20ab	13.20 ± 0.17ab	13.56 ± 0.33ab
random coil (%)	31.52 ± 0.27e	32.59 ± 0.52d	34.06 ± 0.33c	36.48 ± 0.30a	36.95 ± 0.08a	34.29 ± 0.22c	35.84 ± 0.06b	35.55 ± 0.32b

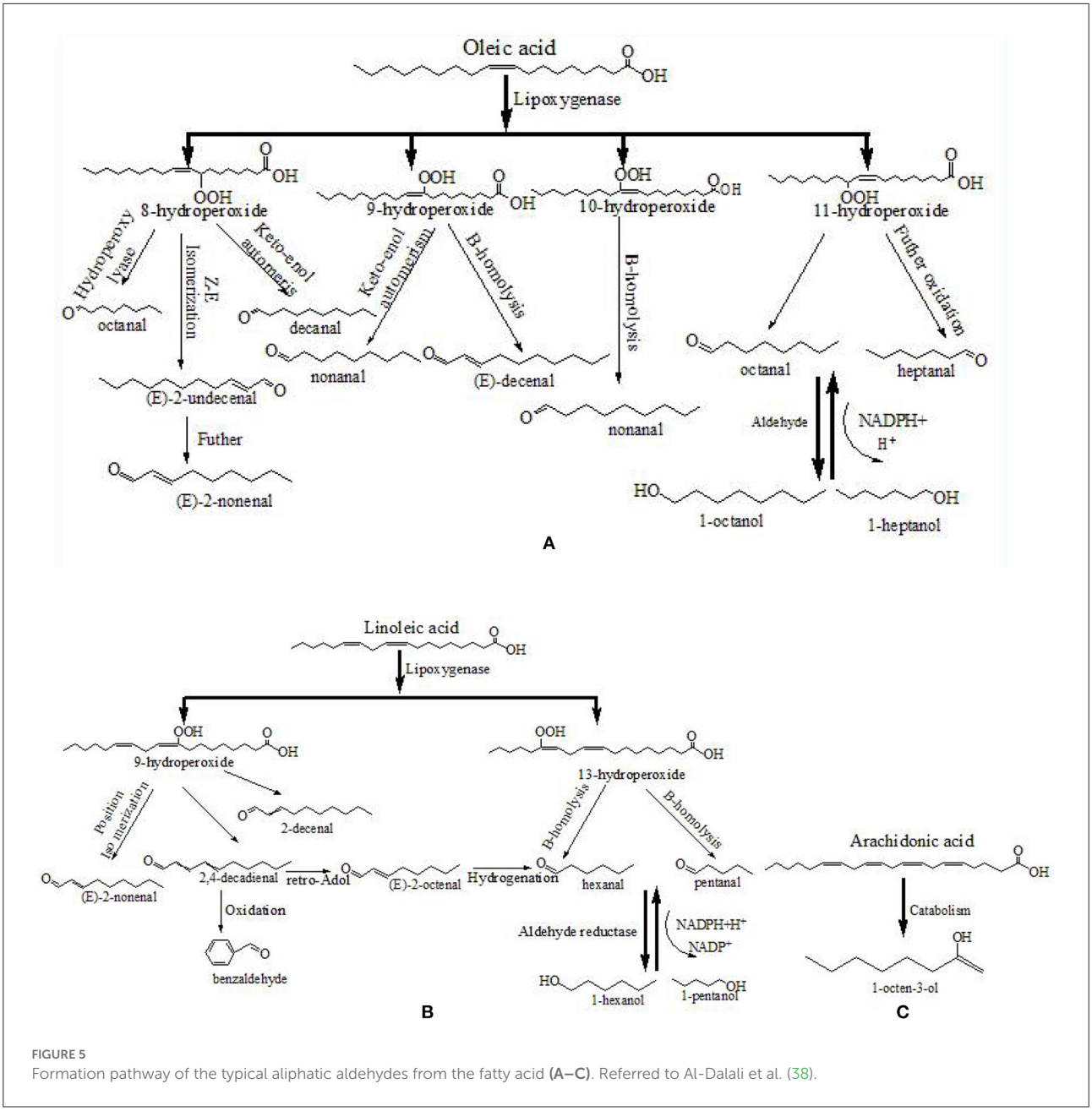

FIGURE 5
Formation pathway of the typical aliphatic aldehydes from the fatty acid **(A–C)**. Referred to Al-Dalali et al. (38).

oxidation products, such as 1-octen-3-ol, heptanal, hexanal and octanal, had the highest concentrations and OAV in the roasted mutton (4, 13, 37). Although the concentrations of aldehydes and alcohols varied depending on the roasting procedure, these compounds remained the most prominent aroma compounds in the roasted mutton (11).

Unsaturated fatty acids were the primary contributors to the formation of fatty aldehydes and alcohols. In various livestock and poultry meat, oleic acid is the common monounsaturated fatty acid, while linoleic acid, linolenic acid, and arachidonic acid are the common polyunsaturated fatty acids (8). Figure 5 depicts the formation pathway of some aliphatic aldehydes and alcohols from fatty acid degradation. First, hydroperoxides of fatty acids are formed by removing the hydrogen-free radical from the alkyl radical, adding O_2, and absorbing the hydrogen-free radical (39). The hydroperoxides are then fractured, which results in the generation of volatile chemicals. As shown in Figure 5, the decomposition of oleic acid 8- and 11-hydroperoxides may result in the formation of octanal and decanal, respectively (40). The decomposition of linoleic acid 9- and 13-hydroperoxides may result in the formation of (*E*, *E*)-2,4-decadienal and hexanal, respectively (38, 41). Furthermore,

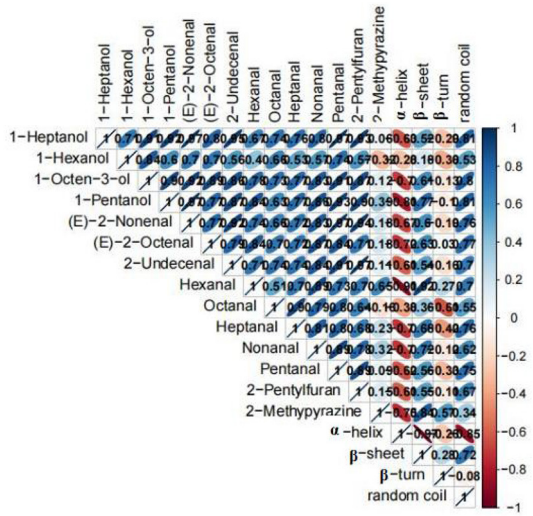

FIGURE 6
Correlation matrix between parameters of proteins structures (α-helix, β-sheet, β-turn, and random coil) and key aroma compounds.

the generated aldehydes can undergo further reactions, such as alcohol or acid transformation or retro-aldol condensation (9, 42). The decomposition of 9- and 13-hydroperoxides of linoleic acid can produce (*E*, *E*)-2,4-decadienal, and the retro-aldolization of (*E*, *E*)-2,4-decadienal can result in the formation of (*E*)-2-octenal.

As for the 14 key aroma compounds in roasted Tan mutton, the major source of 1-octen-3-ol, which has a mushroom odor, is arachidonic acid (38, 43). Hexanal, pentanal, heptanal, (*E*)-2-nonenal, (*E*)-2-octenal, 1-pentanol and 2-pentylfuran are derived from the oxidized linoleic acid, while octanal, 1-hexanol, 1-heptanol nonanal and 2-undecenal are mainly oxidized from oleic acid. Furthermore, 2-methypyrazine may also be generated from lipid-Maillard interaction and a higher pH value contributed to its generation (44, 45).

Protein secondary structure in roasted Tan mutton

Protein is a key quality indicator in the roasted meat, influencing the color, texture and flavor of the meat (46–48). Particularly, some physiologically active enzymes in meat have a direct impact on meat tenderness (49). The amide I band is the most useful band to analyze secondary structural information of proteins. The alterations in the FTIR band in the current investigation were in accordance with previous studies showing that the level of β-sheet gradually increased and the α-helix content decreased during roasting process (50, 51). The decrease of α-helix content suggested that myofibrillar proteins were uncoiling and nonpolar amino acids were exposed to the surface of proteins in roasted Tan mutton (51, 52). The exposure to nonpolar amino acids led to the improvement of surface hydrophobicity, and this improvement was sensitive to the change in roasting temperature (53). The interaction between nonpolar amino acids was greatly strengthened, leading to protein aggregation when roasted at high temperatures (54). Protein aggregation significantly altered the structure of proteins, and β-sheet was shown to be intimately associated with protein aggregation (55). The increase of β-sheet content in roasted Tan mutton during the roasting process may be due to the effects of heating on the reconstruction of unfolded myofibrillar proteins and the aggregation of myofibrillar proteins *via* hydrophobic interaction between nonpolar amino acids (56, 57). Interestingly, an increased content of random coils was observed in the samples roasted for 0–8 min, suggesting that random coils were formed as a result of extreme denaturation of myofibrillar proteins (58).

Relationship between protein secondary structure and key aroma compounds

Many flavor compounds, including ketones, aldehydes and esters, bind to proteins *via* hydrophobic interactions (59–61). During the roasting process, a high energy input may cause a significant degree of denaturation and destruction of the secondary structure (62, 63). Changes in the microstructure of macromolecules, such as changes in protein conformation (α-helix, β-sheet, and β-turn), can alter the interaction between volatile chemicals and proteins (64). Finally, the phase equilibrium of the flavor compound system may be broken.

To understand the relationship between the structure of proteins and the key aroma compounds during the roasting process, the Pearson correlation analysis was performed (Figure 6). The 14 key aroma compounds were all positively correlated with α-helix and were all negatively correlated with β-sheet and random coil in the amide I band and were also positively correlated with β-turn except hexanal and 2-methypyrazine. Among them, hexanal both had the highest correlation coefficient with α-helix and β-sheet.

Conclusion

Thermal processing methods have a significant influence on the aroma of mutton. In this study, 14 aroma compounds, including 1-heptanol, 1-hexanol, 1-octen-3-ol, 1-pentanol, (*E*)-2-nonenal (*E*)-2-octenal, (*E*)-2-undecenal, hexanal, octanal, heptanal, nonanal, pentanal, 2-pentylfuran, and 2-methypyrazine, were identified as key aroma compounds

in roasted Tan mutton under charcoal grilling conditions. Among them, the key aroma compounds were aldehydes and alcohols. A reduction in the α-helix content ($p < 0.05$) and an increase in the β-sheet level ($p < 0.05$) were observed during the whole roasting process. Furthermore, random coil content significantly increased in the samples roasted for 0–8 min and β-turn content did not change. Correlation analysis showed that 14 key aroma compounds were all positively correlated with α-helix and negatively correlated with β-sheet and random coil in the amide I band, and were also positively correlated with β-turn except hexanal and 2-methypyrazine. In the next step, we will study the key volatile compounds of common condiments to lay the foundation for revealing the interaction between the aroma of roasted Tan mutton and condiments, which is helpful to promoting the industrialization of roasted Tan mutton.

Data availability statement

The original contributions presented in the study are included in the article/supplementary material, further inquiries can be directed to the corresponding author.

Author contributions

Y-RW: conceptualization, methodology, software, data curation, and writing—original draft preparation. S-LW: visualization and investigation. R-ML: software, validation, and writing—reviewing and editing. All authors contributed to the article and approved the submitted version.

Funding

The State Key Research and Development Plan (2018YFD0400101), the Natural Science Foundation of China (31660484), and the Key Research and Development Plan of Ningxia Hui Autonomous Region (2019BEH03002) provided financial assistance for this work.

Conflict of interest

The authors declare that the research was conducted in the absence of any commercial or financial relationships that could be construed as a potential conflict of interest.

Publisher's note

All claims expressed in this article are solely those of the authors and do not necessarily represent those of their affiliated organizations, or those of the publisher, the editors and the reviewers. Any product that may be evaluated in this article, or claim that may be made by its manufacturer, is not guaranteed or endorsed by the publisher.

References

1. Qi SS, Wang P, Zhan P, Tian HL. Characterization of key aroma compounds in stewed mutton (goat meat) added with thyme (*Thymus vulgaris* L.) based on the combination of instrumental analysis and sensory verification. *Food Chem.* (2022) 371:131111. doi: 10.1016/j.foodchem.2021.131111

2. Fan H, Fu W. Analysis of supply and demand changes in China's mutton market based on partial equilibrium model. *Acta Agri Zhejiangensis.* (2020) 32:1123–32.

3. Cheng L, Liu G, He J, Wan G, Ma C, Ban J, et al. Non-destructive assessment of the myoglobin content of Tan sheep using hyperspectral imaging. *Meat Sci.* (2019) 167:107988. doi: 10.1016/j.meatsci.2019.107988

4. Liu H, Hui T, Fang F, Li SB, Wang ZY, Zhang DQ, et al. The formation of key aroma compounds in roasted mutton during the traditional charcoal process. *Meat Sci.* (2022) 184:108689. doi: 10.1016/j.meatsci.2021.108689

5. Fan MD, Xiao QF, Xie JC, Cheng J, Sun BG, Du WB, et al. Aroma compounds in chicken broths of Beijing Youji and commercial broilers. *J Agri Food Chem.* (2018) 66:10242–51. doi: 10.1021/acs.jafc.8b03297

6. Bassam SM, Noleto-Dias C, Farag MA. Dissecting grilled red and white meat flavor: its characteristics, production mechanisms, influencing factors and chemical hazards. *Food Chem.* (2022) 371:131139. doi: 10.1016/j.foodchem.2021.131139

7. Zhao J, Wang M, Xie J, Zhao M, Hou L, Liang J, et al. Volatile flavor constituents in the pork broth of black-pig. *Food Chem.* (2017) 226:51–60. doi: 10.1016/j.foodchem.2017.01.011

8. Sohail A, Al-Dalali S, Wang JN, Xie JC, Shakoor A, Asimi S, et al. Aroma compounds identified in cooked meat: a review. *Food Res Int.* (2022) 157:111385. doi: 10.1016/j.foodres.2022.111385

9. Wang TZ, Zhen DW, Tan J, Xie JC, Cheng J, Zhao J, et al. Characterization of initial reaction intermediates in heated model systems of glucose, glutathione, and aliphatic aldehydes. *Food Chem.* (2020) 305:125482. doi: 10.1016/j.foodchem.2019.125482

10. Ortner E, Granvogl M. Thermally induced generation of desirable aroma-active compounds from the glucosinolate sinigrin. *J Agri Food Chem.* (2018) 66:2485–90. doi: 10.1021/acs.jafc.7b01039

11. Liu H, Ma J, Pan T, Suleman R, Wang Z, Zhang D, et al. Effects of roasting by charcoal, electric, microwave and superheated steam methods on (non)volatile compounds in oyster cuts of roasted lamb. *Meat Sci.* (2021) 172:108324. doi: 10.1016/j.meatsci.2020.108324

12. Adelina NM, Wang H, Zhang LG, Zhao YH. Comparative analysis of volatile profiles in two grafted pine nuts by headspace-SPME/GC-MS and electronic nose as responses to different roasting conditions. *Food Res Int.* (2021) 140:110026. doi: 10.1016/j.foodres.2020.110026

13. Franciscoa VC, Almeida LC, Junior SB, Neto JO, Nassu RT. Química. *Nova.* (2020) 43:435–41. doi: 10.21577/0100-4042.20170505

14. Xiao X, Hou C, Zhang D, Li X, Ren C, Ijaz M, et al. Effect of pre- and post-rigor on texture, flavor, heterocyclic aromatic amines and sensory evaluation of roasted lamb. *Meat Sci.* (2020) 169:108220. doi: 10.1016/j.meatsci.2020.108220

15. Liu H, Huang J, Hu Q, Chen Y, Lai K, Xu J, et al. Dual-fiber solid-phase microextraction coupled with gas chromatography-mass spectrometry for the analysis of volatile compounds in traditional Chinese dry-cured ham. *J Chromato B.* (2020) 1140:121994. doi: 10.1016/j.jchromb.2020.121994

16. Wang K, Li C, Wang B, Yang W, Luo S, Zhao Y, et al. formation of macromolecules in wheat gluten/starch mixtures during twin-screw extrusion: Effect of different additives. *J Sci Food Agri.* (2017) 97:5131–8. doi: 10.1002/jsfa.8392

17. Guichard E. Flavour retention and release from protein solutions. *Biotechnol Adv.* (2006) 24:226–9. doi: 10.1016/j.biotechadv.2005.11.003

18. Hu L, Ren S, Shen Q, Chen J, Ye X, Ling J, et al. Proteomic study of the effect of different cooking methods on protein oxidation in fish fillets. *RSC Adv.* (2017) 7:27496–505. doi: 10.1039/C7RA03408C

19. Yu T, Morton J, Clerens S, Dyer J. Cooking-induced protein modifications in meat. *Comp Rev Food Sci Food Safety.* (2017) 16:141–59. doi: 10.1111/1541-4337.12243

20. Nawaz A, Li E, Khalifa I, Walayat N, Liu J, Irshad S, et al. Effect of Different Processingn methods on quality, structure, oxidative properties and water distribution properties of fish meat-based snacks. *Foods.* (2021) 10:2467. doi: 10.3390/foods10102467

21. Kong F, Tang J, Lin M, Rasco B. Thermal effects on chicken and salmon muscles: Tenderness, cook loss, area shrinkage, collagen solubility and microstructure. *LWT - Food Sci Technol.* (2007) 41:1210–22. doi: 10.1016/j.lwt.2007.07.020

22. Pérez-Juan M, Kondjoyan A, Picouet P, Realini CE. Effect of marination and microwave heating on the quality of semimembranosus and semitendinosus muscles from Friesian mature cows. *Meat Sci.* (2012) 92:107–14. doi: 10.1016/j.meatsci.2012.04.020

23. Liu H, Wang Z, Suleman R, Shen Q, Zhang D. Effect of protein thermal stability and protein secondary structure on the roasted mutton texture and colour from different cuts. *Meat Sci.* (2019) 156:52–8. doi: 10.1016/j.meatsci.2019.05.014

24. Zhan P, Tian HL, Zhang XM, Wang LP. Contribution to aroma characteristics of mutton process flavor from the enzymatic hydrolysate of sheep bone protein assessed by descriptive sensory analysis and gas chromatography olfactometry. *J Chromato B.* (2013) 922:1–8. doi: 10.1016/j.jchromb.2012.12.026

25. Wang YR, Luo RM, Wang SL. Water distribution and key aroma compounds in the process of beef roasting. *Front Nutr.* (2022) 9:978622. doi: 10.3389/fnut.2022.978622

26. Bressanello D, Liberto E, Cordero C, Sgorbini B, Rubiolo P, Pellegrino G, et al. Chemometric modeling of coffee sensory notes through their chemical signatures: Potential and limits in defining an analytical tool for quality control. *J Agri Food Chem.* (2018) 66:7096–109. doi: 10.1021/acs.jafc.8b01340

27. Sun S, Guo B, Wei Y, Fan M. Multi-element analysis for determining the geographical origin of mutton from different regions of China. *Food Chem.* (2011) 124:1151–6. doi: 10.1016/j.foodchem.2010.07.027

28. Biffin TE, Smith MA, Bush RD, Collins D, Hopkins DL. The effect of electrical stimulation and tenderstretching on colour and oxidation traits of alpaca (*Vicunga pacos*) meat. *Meat Sci.* (2019) 156:125–30. doi: 10.1016/j.meatsci.2019.05.026

29. Schmidberger PC, Schieberle P. Changes in the key aroma compounds of raw shiitake mushrooms (Lentinula edodes) induced by pan-frying as well as by rehydration of dry mushrooms. *J Agri Food Chem.* (2020) 68:4493–506. doi: 10.1021/acs.jafc.0c01101

30. Pu DD, Duan W, Huang Y, Zhang YY, Sun BG, Ren FZ, et al. Characterization of the key odorants contributing to retronasal olfaction during bread consumption. *Food Chem.* (2020) 318:126520. doi: 10.1016/j.foodchem.2020.126520

31. Pu DD, Zhang YY, Zhang HY, Sun BG, Ren FZ, Chen HT, et al. Characterization of the key aroma compounds in traditional Hunan Smoke-Cured Pork Leg (Larou, THSL) by aroma extract dilution analysis (AEDA), odor activity value (OAV), and sensory evaluation experiments. *Foods.* (2020) 9:413. doi: 10.3390/foods9040413

32. Singh A, Lahlali R, Vanga SK, Karunakaran C, Orsat V, Raghavan V, et al. Effect of high electric field on secondary structure of wheat gluten. *Int J Food Prop.* (2016) 19:1217–26. doi: 10.1080/10942912.2015.1076458

33. Vanga SK, Wang J, Orsat V, Raghavan V. Effect of pulsed ultrasound, a green food processing technique, on the secondary structure and in-vitro digestibility of almond milk protein. *Food Res Int.* (2020) 137:109523. doi: 10.1016/j.foodres.2020.109523

34. Zhou LY, Zhang Y, Zhao CB, Lin HJ, Wang ZJ, Wu F, et al. Structural and functional properties of rice bran protein oxidized by peroxyl radicals. *Int J Food Prop.* (2017) 20:1456–67. doi: 10.1080/10942912.2017.1352596

35. Zhang ZY, Yang YL, Zhou P, Zhang X, Wang JY. Effects of high pressure modification on conformation and gelation properties of myofibrillar protein. *Food Chem.* (2017) 217:678–86. doi: 10.1016/j.foodchem.2016.09.040

36. Zhang J, Pan D, Zhou G, Wang Y, Dang Y, He J, et al. The changes of the volatile compounds derived from lipid oxidation of boneless dry-cured hams during processing. *Eur J Lipid Sci Technol.* (2019) 121:1900135. doi: 10.1002/ejlt.201900135

37. Liu H, Hui T, Fang F, Ma QL, Li SB, Zhang DQ, et al. Characterization and discrimination of key aroma compounds in pre- and postrigor roasted mutton by GC-O-MS, GC E-Nose and aroma recombination experiments. *Foods.* (2021) 10:2387. doi: 10.3390/foods10102387

38. Al-Dalali S, Li C, Xu B. Insight into the effect of frozen storage on the changes in volatile aldehydes and alcohols of marinated roasted beef meat: Potential mechanisms of their formation. *Food Chem.* (2022) 385:132629. doi: 10.1016/j.foodchem.2022.132629

39. Domínguez R, Pateiro M, Gagaoua M, Barba FJ, Zhang W, Lorenzo JMA, et al. Comprehensive review on lipid oxidation in meat and meat products. *Antioxidants.* (2019) 8:429. doi: 10.3390/antiox8100429

40. Merlo TC, Lorenzo JM, Saldāna E, Patinho I, Oliveira AC, Menegali BS, et al. Relationship between volatile organic compounds, free amino acids, and sensory profile of smoked bacon. *Meat Sci.* (2021) 181:108596. doi: 10.1016/j.meatsci.2021.108596

41. Du WB, Zhao MY, Zhen DW, Tan J, Wang TZ, Xie JC, et al. Key aroma compounds in Chinese fried food of youtiao. *Flavour Frag J.* (2019) 35:88–98. doi: 10.1002/ffj.3539

42. Al-Dalali S, Li C, Xu B. Effect of frozen storage on the lipid oxidation, protein oxidation, and flavor profile of marinated raw beef meat. *Food Chem.* (2022) 376:131881. doi: 10.1016/j.foodchem.2021.131881

43. Zang MW, Wang L, Zhang ZQ, Zhang KH, Li D, Li XM, et al. Changes in flavour compound profiles of precooked pork after reheating (warmed-over flavour) using gas chromatography–olfactometry–mass spectrometry with chromatographic feature extraction. *Int J Food Sci Technol.* (2019) 55:978–87. doi: 10.1111/ijfs.14306

44. Resconi VC, Bueno M, Escudero A, Magalhaes D, Ferreira V, Campo MM, et al. Ageing and retail display time in raw beef odour according to the degree of lipid oxidation. *Food Chem.* (2018) 242:288–300. doi: 10.1016/j.foodchem.2017.09.036

45. Li ZZ, Ha M, Frank D, McGilchrist P, Warner RD. Volatile profile of dry and wet aged beef loin and its relationship with consumer flavour liking. *Foods.* (2021) 10:3113. doi: 10.3390/foods10123113

46. Berhe DT, Engelsen SB, Hviid M, Lametsch R. Raman spectroscopic study of effect of the cooking temperature and time on meat proteins. *Food Res Int.* (2014) 66:123–31. doi: 10.1016/j.foodres.2014.09.010

47. Han Z. Meng-jie Cai MJ, Cheng JH, Sun DW. Effects of constant power microwave on the adsorption behaviour of myofibril protein to aldehyde flavour compounds. *Food Chem.* (2021) 336:127728. doi: 10.1016/j.foodchem.2020.127728

48. Guo X, Wang YQ, Lu SL, Wang JY, Fu HH, Gu BY, et al. Changes in proteolysis, protein oxidation, flavor, color and texture of dry-cured mutton ham during storage. *LWT Food Sci Technol.* (2021) 149:111860. doi: 10.1016/j.lwt.2021.111860

49. Becker A, Boulaaba A, Pingen S, Krischek C, Klein G. Low temperaturecooking of pork meat-physicochemical and sensory aspects. *Meat Sci.* (2016) 118:82–8. doi: 10.1016/j.meatsci.2016.03.026

50. Xu XL, Han MY, Fei Y, Zhou GH. Raman spectroscopic study of heat-induced gelation of pork myofibrillar proteins and its relationship with textural characteristic. *Meat Sci.* (2010) 87:159–64. doi: 10.1016/j.meatsci.2010.10.001

51. Zhou CY, Cao JX, Zhuang XB, Bai Y, Li CB, Xu XL, et al. Evaluation of the secondary structure and digestibility of myofibrillar proteins in cooked ham. *CyTA J Food.* (2019) 17:78–86. doi: 10.1080/19476337.2018.1554704

52. Chelh I, Gatellier P, Sante-Lhoutellier V. Technical note: a simplified procedure for myofibril hydrophobicity determination. *Meat Sci.* (2006) 74:681–3. doi: 10.1016/j.meatsci.2006.05.019

53. Zhou CY, Pan DD, Sun YY, Li CB, Xu XL, Cao JX, et al. The effect of cooking temperature on the aggregation and digestion rate of myofibrillar proteins in Jinhua ham. *J Sci Food Agri.* (2018) 98:3563–70. doi: 10.1002/jsfa.8872

54. Xie J, Qin M, Cao Y, Wang W. Mechanistic insight of photo-induced aggregation of chicken egg white lysozyme: The interplay between hydrophobic interactions and formation of inter-molecular disulfide bonds. *Proteins Struct Funct Bioinform.* (2011) 79:2505–16. doi: 10.1002/prot.23074

55. Nault L, Vendrely C, Brechet Y, Bruckert F, Weidenhaupt M. Peptides that form beta-sheets on hydrophobic surfaces accelerate surface-induced insulin amyloidal aggregation. *FEBS Lett.* (2013) 587:1281–6. doi: 10.1016/j.febslet.2012.11.036

56. Bouraoui M, Nakai S, Li-Chan E. *In situ* investigation of protein structure in pacific whiting surimi and gels using Raman spectroscopy. *Food Res Int.* (1997) 30:65–72. doi: 10.1016/S0963-9969(97)00020-3

57. Okuno A, Kato M, Taniguchi Y. Pressure effects on the heat-induced aggregation of equine serum albumin by FT-RT spectroscopic study: Secondary structure, kinetic and thermodynamic properties. *Biochem Biophysica Acta.* (2007) 1774:652–60. doi: 10.1016/j.bbapap.2007.03.003

58. Yoshidome T, Kinoshita M. Physical origin of hydrophobicity studied in terms of cold denaturation of proteins: comparison between water and simple fluids. *Phys Chem Chem Phys.* (2012) 14:14554–66. doi: 10.1039/c2cp41738c

59. Viry O, Boom R, Avisona S, Pascu M, Bodnár I. A predictive model for flavor partitioning and protein-flavor interactions in fat-free dairy protein solutions. *Food Res Int.* (2018) 109:52–8. doi: 10.1016/j.foodres.2018.04.013

60. Pelletier E, Kai S, Guichard E. Measurement of interactions between β-lactoglobulin and flavor compounds (esters, acids, and pyrazines) by affinity and exclusion size chromatography. *J Agri Food Chem.* (1998) 46:1506–9. doi: 10.1021/jf970725v

61. Guichard E, Langourieux S. Interactions between β-lactoglobulin and flavour compounds. *Food Chem.* (2000) 71:301–8. doi: 10.1016/S0308-8146(00)00181-3

62. Ying D, Hlaing MM, Lerisson J, Pitts K, Cheng L, Sanguansri L, et al. Physical properties and FTIR analysis of rice-oat flour and maize-oat flour based extruded food products containing olive pomace. *Food Res Int.* (2017) 100:665–73. doi: 10.1016/j.foodres.2017.07.062

63. Lou XW, Yang QL, Sun YY, Pan DD, Cao JX. The effect of microwave on the interaction of flavour compounds with G-actin from grass carp (Catenopharyngodon idella). *J Sci Food Agri.* (2017) 97:3917–22. doi: 10.1002/jsfa.8325

64. Yang QL, Lou XW, Wang Y, Pan DD, Sun YY, Cao JX, et al. Effect of pH on the interaction of volatile compounds with the myofibrillar proteins of duck meat. *Poultry Sci.* (2017) 96:1963–9. doi: 10.3382/ps/pew413

frontiers | Frontiers in Nutrition

TYPE Original Research
PUBLISHED 28 October 2022
DOI 10.3389/fnut.2022.1007164

OPEN ACCESS

EDITED BY
Mingquan Huang,
Beijing Technology and Business University, China

REVIEWED BY
Nattakorn Kuncharoen,
Kasetsart University, Thailand
Bowen Wang,
Beijing Technology and Business University, China

*CORRESPONDENCE
Lin Zhang
t20131501@csuft.edu.cn
Liangzhong Zhao
sys169@163.com

SPECIALTY SECTION
This article was submitted to Food Chemistry, a section of the journal Frontiers in Nutrition

RECEIVED 30 July 2022
ACCEPTED 20 September 2022
PUBLISHED 28 October 2022

CITATION
Zhou X, Zhou W, He X, Deng Y, Li L, Li M, Feng X, Zhang L and Zhao L (2022) Effects of post-fermentation on the flavor compounds formation in red sour soup.
Front. Nutr. 9:1007164.
doi: 10.3389/fnut.2022.1007164

Effects of post-fermentation on the flavor compounds formation in red sour soup

Xiaojie Zhou[1,2,3,4], Wenhua Zhou[1,3], Xiaojie He[2,4], Yaxin Deng[2,4], Liangyi Li[1,3], Ming Li[2,4], Xuzhong Feng[4,5], Lin Zhang[1,3]* and Liangzhong Zhao[2,4]*

[1]College of Food Science and Engineering, Central South University of Forestry and Technology, Changsha, China, [2]College of Food and Chemical Engineering, Shaoyang University, Shaoyang, China, [3]Hunan Key Laboratory of Processed Food for Special Medical Purpose, Changsha, China, [4]Hunan Provincial Key Laboratory of Soybean Products Processing and Safety Control, Shaoyang, China, [5]Shenzhen Shanggutang Food Development Co., Ltd., Shenzhen, China

Red Sour Soup (RSS) is a traditional fermented food in China. After two rounds of fermentation, sour soup has a mellow flavor. However, the microbial composition and flavor formation processes in post-fermentation in RSS are unclear. This study investigates the bacteria composition of RSS during the post-fermentation stage (0–180 days) using high-throughput sequencing. The results show that lactic acid bacteria (LAB) are dominant during the post-fermentation process, and their abundance gradually increases with fermentation time. Additionally, gas chromatography-mass spectrometry was used to detect volatile flavor compounds in the post-fermentation process. Seventy-seven volatile flavor compounds were identified, including 24 esters, 14 terpenes, 9 aromatic hydrocarbons, 9 alkanes, 6 heterocyclic compounds, 3 alcohols, 3 acids, 3 ketones, 2 phenols, 2 aldehydes, 1 amine, and 1 other. Esters and aromatic hydrocarbons are the main volatile compounds in RSS during the post-fermentation process. Orthogonal partial least squares screening and correlation analysis derived several significant correlations, including 48 pairs of positive correlations and 19 pairs of negative correlations. Among them, *Acetobacter* spp., *Clostridium* spp. and *Sporolactobacillus* spp. have 15, 14, 20 significant correlation pairs, respectively, and are considered the most important bacterial genera post-fermentation. Volatile substances become abundant with increasing fermentation time. LAB are excessive after more than 120 days but cause a drastic reduction in volatile ester levels. Thus, the post-fermentation time should be restricted to 120 days, which retains the highest concentrations of volatile esters in RSS. Overall, these findings provide a theoretical basis to determine an optimal post-fermentation time duration, and identify essential bacteria for manufacturing high-quality starter material to shorten the RSS post-fermentation processing time.

KEYWORDS

bacterial diversity, effect mechanism, post-fermentation, red sour soup (RSS), volatile compounds

Introduction

In China, fermentation has more than 3,000 years of history, and there are representative traditional fermented foods with unique characteristics for different regions or ethnic groups (1–3). Sour soup is a well-known traditional fermented food with a thousand years of history originating from a minority group in Guizhou of Kaili, China (4). It has been used as a condiment due to its unique flavor and high nutritional value. It can promote digestion, regulate intestinal flora, improve free radical scavenging and enhance immunity (5). Sour soup is categorized as Red Sour Soup (RSS) and white sour soup due to the differences in raw materials and fermentation process (6). RSS is mainly made of fresh red pepper and tomato, fermented for a few months by spontaneous fermentation without starter material (7). RSS's widely used production technology includes two anaerobic fermentation stages: pre-fermentation and post-fermentation (8). Pre-fermentation is the separate fermentation process of tomato and pepper in a jar for 3 to 12 months. Post-fermentation is a mixture of pre-fermented tomatoes and peppers in proportion, with an appropriate number of auxiliary materials added, such as rice milk, and then put into a jar for fermentation for 1 to 6 months.

Like other fermented vegetables, the fermentation process of RSS involves complex microbial communities. Many studies demonstrated that the fermented food flavor is mainly attributed to the contribution of microbial communities in succession (2, 3, 9). When investigating the flavor components of commercial sour soup, it was found that predominantly volatile flavor compounds are esters and terpenoids (10–12). Esters are mainly derived from raw materials and the metabolites of microorganisms, while terpenoids mainly come from the raw material itself. Lactobacillus, Weissella and yeast were previously detected in RSS, with lactic acid bacteria (LAB) playing a leading role (13). LAB secretes large amounts of lactic acid, which not only participate in the reaction to produce abundant esters to enrich the volatile flavor but also generates extreme environmental pressure to inhibit the growth of miscellaneous bacteria and improve product quality. Additionally, some studies have found that fungi and bacteria played a role in the fermentation of sour soups. But, the presence of fungi seemed to incur the risk of some toxins that could produce an unpleasant flavor (9). However, the microbiota succession of RSS during post-fermentation and its relationship with the specific flavor of RSS remains unclear.

Various methods were undertaken to study bacterial diversity, including microbial isolation and cultivation, polymerase chain reaction-denaturing gradient gel electrophoresis (PCR-DGGE), and DNA cloning libraries (14–16). However, the conventional methods of microorganism investigation take time and have low sensitivity. In contrast, the high-throughput sequencing method has the advantages of short sequencing time and high sequencing flux, allowing it to determine the full diversity of microbial flora (17, 18). Headspace solid-phase microextraction coupled with gas chromatography-mass spectrometry (HS-SPME-GC-MS) with high sensitivity has been widely chosen to determine volatile compounds in samples (19, 20). Recently, these techniques have been used to detect microbial and flavor compounds in traditionally brewed foods (21, 22). Orthogonal partial least squares discriminant analysis (OPLS-DA) and Pearson correlation analysis have been widely applied to investigate the relationship between microorganisms and flavor substances in fermented foods (23, 24).

Currently, some studies explored the dynamic changes of microbial communities and flavor substances and the correlation between bacterial communities and flavor substances in RSS (8, 11, 12). However, most researchers focus on the kinds of bacteria and flavor compounds in RSS during the pre-fermentation process (7–9, 12). The correlation between bacterial successions and the production of volatile aromatic substances during the post-fermentation is unclear. This study performs HS-SPME-GC-MS to evaluate the correlation between bacterial communities and volatile aromatic substances in four different post-fermentation stages (0–180 days) of RSS. The results will enable the characterization of condiment fermentation mechanisms, while providing a theoretical framework for directional regulation of RSS.

Materials and methods

Sample collection and analysis

The RSS samples were provided by Kaili Lianghuan Biotechnology Co., Ltd (Guizhou, China). The RSS was manufactured according to Li et al. (8). The sample production process was: (1) mix pepper and distilled water with a ratio of 1:2 (wt/wt). Once smashed, add 30 g/kg of salt, followed by storage in fermenting jars for 30 days. (2) Fresh tomato was directly chopped and ground into a colloid sauce, 30 g/kg salt was added, and fermented in jars for 30 days. (3) Mix the finished fermentation products of (1) and (2) in a ratio of 1:3, then add 1% (wt/wt) rice milk, and transfer into the jar. The fermentation tank was then loaded, and the product was fermented for 180 days. Four groups of samples were collected at the appropriate fermentation time points (0 days, 60 days, 120 days, and 180 days) with six replicates per group. The test samples were from batches with different post-fermentation times and labeled sequentially as F-A (0 days), F-B (60 days), F-C (120 days) and F-D (180 days). Samples were prepared by mixing equal amounts of the mixture from five points, consisting of the four corners and the midpoint of the fermentation tank: upper (1 sample), middle (2 samples), left (1 sample), right (1 sample) and bottom (1 sample). The mixed

samples were collected in sterilized sampling bottles. Twenty-four samples were collected in sterilized vials, transported on dry ice to the laboratory, and stored at –80°C for analysis.

Illumina MiSeq sequencing

The total DNA from each 5 mL sample of sour soup was extracted using the E.Z.N.A.® Soil DNA Kit (Omega Bio-Tek, Norcross, GA, United States) following instructions provided by the manufacturer. Agarose gel electrophoresis was performed to check DNA quality, and a NanoDrop 2000 UV-vis spectrophotometer (Thermo Scientific, Wilmington, USA) was used to measure the final DNA concentration and purity. Using a thermocycler PCR system (GeneAmp 9700, ABI, USA), primers 338F (5′-ACTCCTACGGGAGGCAGCAG-3′) and 806R (5′-GGACTACHVGGGTWTCTAAT-3′) were used to amplify the V3-V4 hypervariable regions of the bacterial 16S rDNA gene [Lin et al. (10)]. For the PCR reaction, the following program was used: 3 min of denaturation at 95°C, 27 cycles of 30 s each at 95°C, 30 s for annealing at 55°C, and 45 s for elongation at 72°C, followed by a final extension at 75°C for 5 min. This reaction was performed in triplicate in a 20 μL mixture containing 4 μL of 5 × FastPfu Buffer, 2 μL of 2.5 mmol/L dNTPs, 0.8 μL of each primer (5 μmol/L), 0.4 μL of FastPfu Polymerase and 10 ng of template DNA. The AxyPrep DNA Gel Extraction Kit (Axygen Biosciences, Union City, CA, USA) was used to extract PCR products from a 2% agarose gel and purify them further. The QuantiFluor™-ST system (Promega, USA) was used to quantify the DNA according to the manufacturer's protocol. Purified amplicons were sequenced on an Illumina MiSeq platform (Illumina, San Diego, USA) using equimolar pooling and paired-end sequencing (2 × 300 bp). Quantitative library concentrations were measured using a Qubit v.3.0 Fluorometer (Invitrogen, Carlsbad, CA, USA). The library was quantified to 10 nmol/L. Illumina MiSeq (Illumina, San Diego, CA, USA) was used for the PE250/FE300 paired-end sequencing, and data were read using MiSeq Control Software (Illumina, San Diego, CA, USA).

Volatile flavor component analysis

Volatile organic compounds (VOCs) of RSS samples were analyzed using HS-SPME-GC/MS according to previously reported methods (8) with some modifications. Samples (1 g) of RSS were immediately transferred to Agilent headspace vials (Agilent, Palo Alto, CA, USA) with a NaCl-saturated solution to inhibit enzyme reactions. Crimp-top caps with TFE-silicone septa (Agilent) were used to seal the vials. Each vial was incubated at 60°C for 10 min. Following this, a 65 μm carboxen-polydimethylsiloxane fiber (Supelco, Bellefonte, PA, USA) was inserted in the sample's headspace for 20 min at 60°C. To extract the VOCs from the fiber coating, the injection port of a high-performance gas chromatography instrument (Model 7890B, Agilent) was heated to 250°C for 5 min in splitless mode after sampling. The identification and quantification of VOCs were undertaken using an Agilent Model 7890B GC and a 7000D mass spectrometer (Agilent), equipped with a 30 m × 0.25 mm × 1.0 μm DB-5MS (5% phenyl-polymethylsiloxane) capillary column. Helium (99.999% purity) was used as the carrier gas at a linear velocity of 1.0 mL/min. The injector temperature was maintained at 250°C and the detector at 280°C. The oven temperature was programmed from 40°C (maintained for 5 min) to 280°C (maintained for 5 min) with a rate of 6°C/min. Spectra were recorded at 70 eV using electron impact ionization mode (EI) and scanned in an m/z range of 30–350 amu at 1 s intervals. The temperatures of the quadrupole mass detector, ion source and transfer line were set at 150, 230, and 280°C, respectively. The volatile compounds were identified by comparing the mass spectra with the MetWare data system library.[1]

Statistical analysis

Sequence clustering was performed using VSEARCH (v. 1.9.6) (the similarity level was set to 97%). Silva 132 was used as the 16S rRNA reference database. Species classification analysis of the operational taxonomic units (OTUs) was carried out using the RDP Classifier (Ribosomal Database Program) Bayesian algorithm. The alpha diversity indices were calculated based on the OTU analysis results. Principal component analysis (PCA) and Pearson's correlation were performed with selected signals obtained through chromatogram processing in SPSS 22.0 (SPSS 22.0 for Windows, SPSS, Chicago, Illinois, USA).

Results

Overview of illumina MiSeq sequencing data for red sour soup samples

Based on the 97% similarity of OTUs, **Figure 1** shows the rarefaction curve of the bacterial community. Approximately 8,000 sequences provided sufficient coverage of all taxa in the four groups, and the number of observed OTUs stabilized beyond this point.

Under the 97% similarity threshold of OTUs, the alpha diversity indices of four sample groups were used to assess differences in the abundance and diversity of bacteria. The observed species, Shannon, Simpson, ACE, Chao1 and Good's coverage indices are shown in **Table 1**. The results indicate

1 http://www.metware.cn/

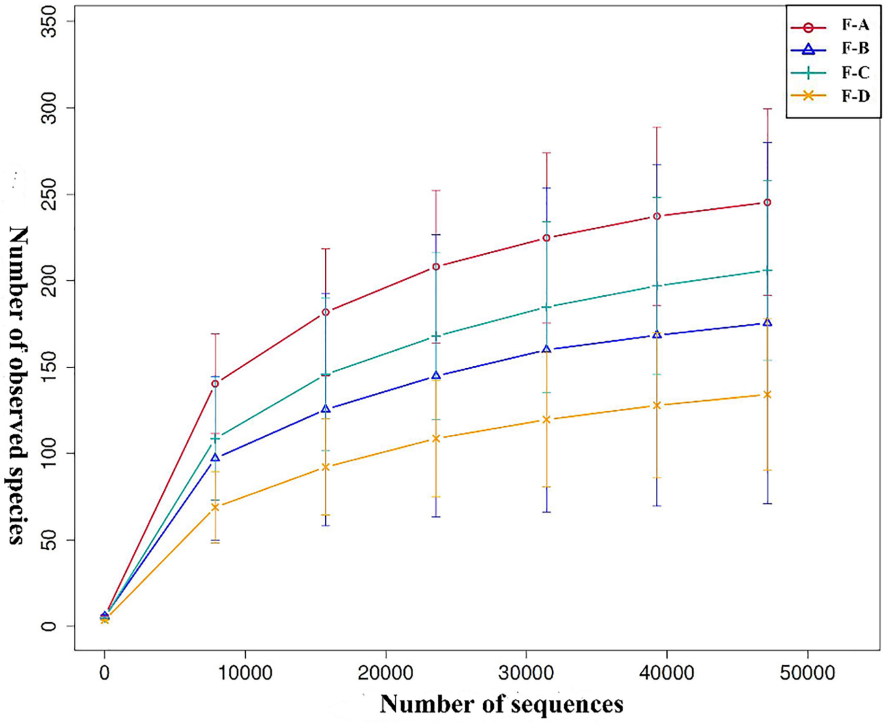

FIGURE 1
Rarefaction curve analysis of different sour soup samples at different post-fermentation stages. Each line of a different color represents data from each sample group. F-A, F-B, F-C and F-D refer to the sour soup samples fermented for 0 days, 60 days, 120 days, and 180 days, respectively. The abscissa denotes the number of sequences, and the ordinate denotes the number of observed OTUs.

TABLE 1 Sequencing data and alpha diversity analysis.

Groups	Observed species	Shannon	Simpson	Chao1	ACE	Good's coverage
F-A	230.4 ± 25.29^{a}	3.61 ± 0.41^{a}	0.84 ± 0.03^{a}	242.3 ± 27.23^{a}	248.0 ± 26.54^{a}	1 ± 0^{a}
F-B	97.2 ± 14.03^{b}	2.92 ± 0.58^{ab}	0.76 ± 0.13^{a}	103.2 ± 15.34^{b}	106.3 ± 10.78^{b}	1 ± 0^{a}
F-C	231.7 ± 39.46^{a}	2.85 ± 0.49^{ab}	0.79 ± 0.03^{a}	265.8 ± 32.21^{a}	281.4 ± 30.26^{a}	1 ± 0^{a}
F-D	122.3 ± 16.27^{b}	1.97 ± 0.09^{b}	0.58 ± 0.01^{b}	136.6 ± 13.46^{b}	143.6 ± 18.03^{b}	1 ± 0^{a}

[1]F-A, F-B, F-C and F-D refer to the sour soup samples fermented for 0 days, 60 days, 120 days and 180 days, respectively. a, b, c, d, e, Statistical analysis was performed by one-way ANOVA (Tukey's test, $P < 0.05$).

that the Good's coverage index of each group is equal to 1, indicating that the sequencing depth of all samples was sufficient to provide a reliable overall representation of the bacteria. The highest value of observed species is found in group F-C (120 days), followed by groups F-A (0 days) and F-D (180 days), and finally, F-B (60 days). Similar trends are found in the Chao1 and ACE indices. These results indicate that at 120 days of fermentation, the RSS has the highest bacterial richness. The Shannon and Simpson indices decrease gradually with increasing fermentation time, illustrating that the diversity of bacteria in RSS decreases with fermentation time.

From Figure 2, the values of OTUs in RSS are significantly different at the four post-fermentation stages. The standard and unique OTUs drawn are represented using Venn diagrams, which more intuitively show the uniqueness and overlap of sample OTUs composition. The total OTUs in the F-A, F-B, F-C and F-D groups are 766, 645, 685 and 371, respectively. Figure 2 showed that their shared OTUs were 342, 315, 200, 238, 176, and 212 in the intersection of F-A and F-B, F-A and F-C, F-A and F-D, F-B and F-C, F-B and F-D, F-C and F-D, respectively. At the initial stage of post-fermentation (0–60 days), the number of intersectional OTUs was 342 (Figure 2A). Surprisingly, that gradually decreases to 315 and 200 when the fermentation time increases to 120 and 180 days (Figures 2B,C). According to Figures 2D–F, the uniqueness of OTUs mainly occurs between the 120 days and 180 days samples. At the other fermentation times, there are minimal changes in the uniqueness of OUTs.

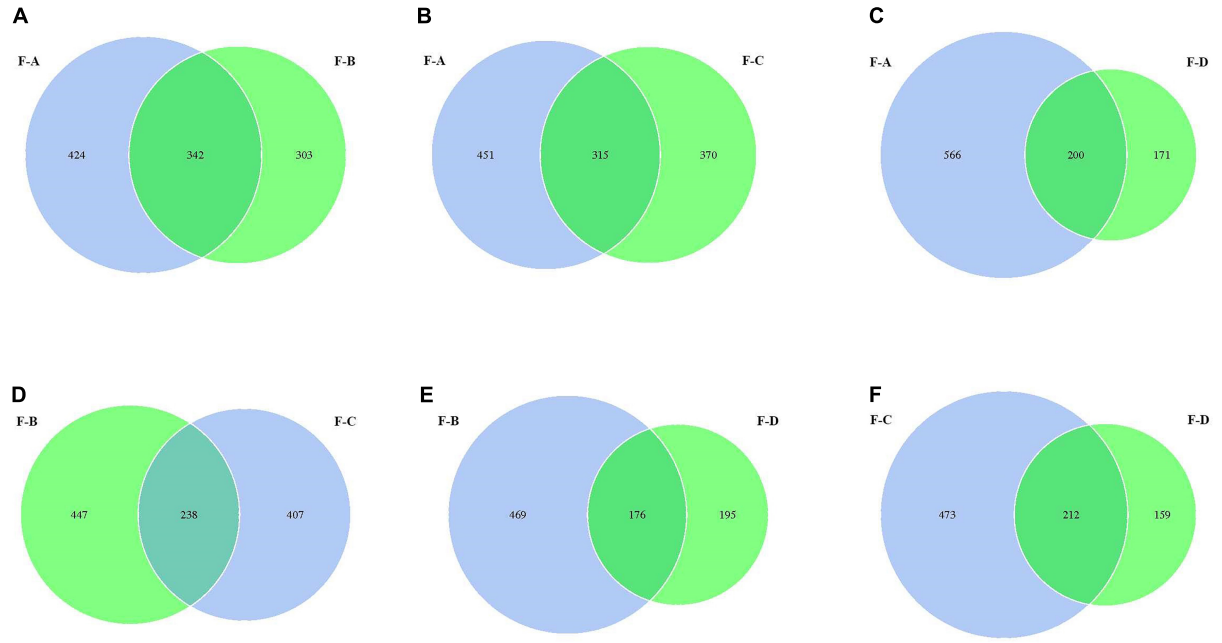

FIGURE 2
The Venn analysis of the bacterial composition in red sour soup based on OUT levels. Each circle represents a sample, the numbers of circles and overlapping parts represent the number of OTUs shared between samples, and the numbers without overlapping parts represent the number of unique OTUs of samples.

Microbiota community in red sour soup at different fermentation stages

The phylum and genus of the bacteria were distinguished based on the OTUs level to investigate the bacterial compositions in detail. More than 30 phyla and 364 genera are detected in RSS samples during post-fermentation, and the top 10 most abundant groups are shown in (Figure 3). Firmicutes (72.94–99.18%), Proteobacteria (0.16–23.16%) and Actinobacteriota (0.11–7.39%) are the dominant phyla in the fermentation process of sour soup, accounting for more than 90% (Figure 3A). Interestingly, Firmicutes decrease at 120 days and then increase with increasing fermentation time. Proteobacteria and Actinobacteriota exhibited a gradually decreasing trend during the post-fermentation process. Miscellaneous bacteria gradually decrease during fermentation, indicating that increasing the fermentation time can reduce the miscellaneous bacteria content.

At the genus level (Figure 3B), the main genera were detected at a high abundance ($\geq$ 1% in at least one sample), including *Lactobacillus* spp., *Ralstonia* spp., *Clostridium* spp., *Acetobacter* spp., *Stenotrophomonas* spp., *Pseudomonas* spp., *Propionibacterium* spp., *Pediococcus* spp., *Halomonas* spp., and *Aliidiomarina* spp. Among them, LAB are the dominant bacteria (60–98%), consisting of *Lentilactobacillus* spp., *Lactiplantibacillus* spp., *Schleiferilactobacillus* spp., *Lactobacillus* spp., *Sporolactobacillus* spp., *Pediococcus* spp., *Limosilactobacillus* spp., *Loigolactobacillus* spp., *Levilactobacillus* spp., *Lacticaseibacillus* spp., *Companilactobacillus* spp., *Liquorilactobacillus* spp., *Ligilactobacillus* spp. and others, especially *Lentilactobacillus* spp. (39.02–86.23%). The levels of these bacteria decrease at 60 days (60.35%) and then increase with increasing post-fermentation time (120–180 days). The second-most abundant is *Ralstonia* spp., accounting for 0.17–10.41%. The content of *Ralstonia* spp. was high at the beginning of post-fermentation, especially at 60 days of fermentation (10.41%), and sharply decreased to 0.12–0.02% during the later stages. The levels of *Acetobacter* spp. and *Clostridium* spp. significantly increased after 60 days of fermentation time, accounting for 9.23% and 10.73%, respectively, but were lower at other fermentation points. The content of *Stenotrophomonas* spp. was high during the initial post-fermentation stage (0 days, 6.44%) but gradually decreased with fermentation and disappeared entirely at 180 days.

Analysis of enrichment of metabolic pathways

The Kyoto Encyclopedia of Genes and Genomes (KEGG) is an integrated database resource for associating genomic sequences with biological functions. Figure 4 shows the dynamic change of microbial function predicted for RSS

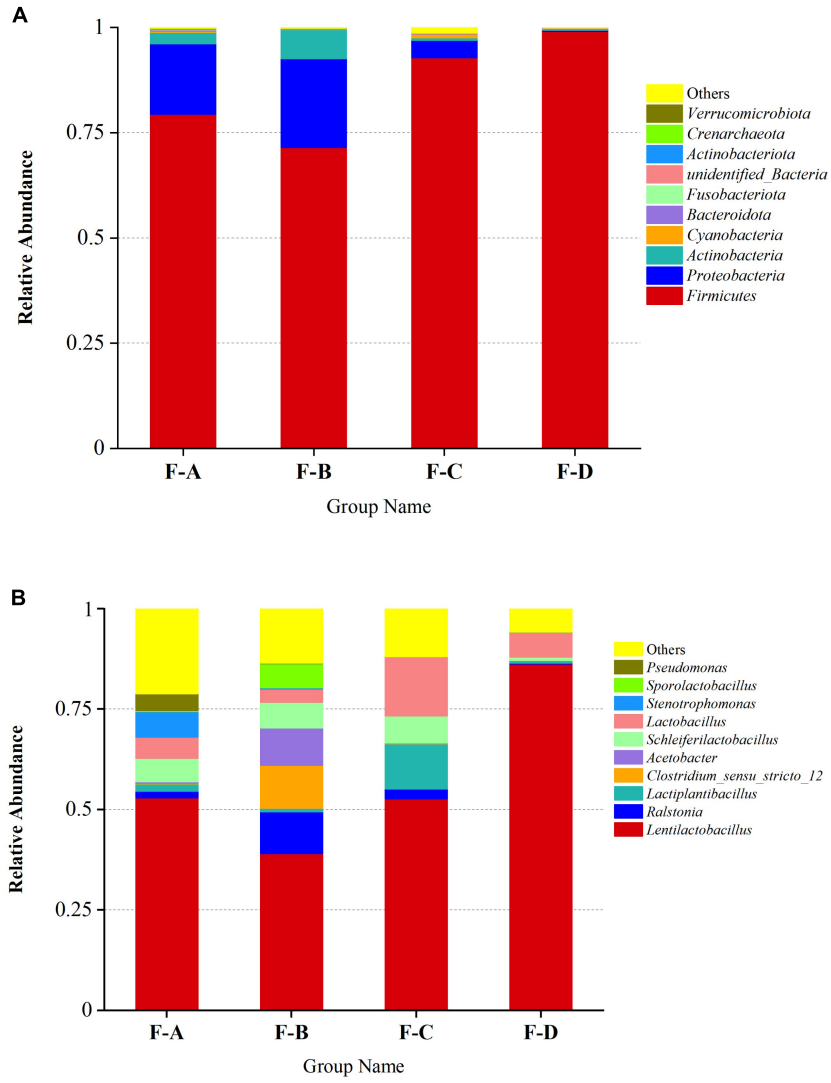

FIGURE 3
Relative abundance of bacteria in RSS samples at the phylum **(A)** and genus **(B)** levels at different post-fermentation stages. F-A, F-B, F-C and F-D refer to the sour soup samples fermented for 0 days, 60 days, 120 days, and 180 days, respectively. Each column represents a sample group containing a variety of bacteria.

during post-fermentation. Figure 4A shows the composition of level 1 KEGG pathways in bacteria from samples during different post-fermentation stages. The functionality of the bacteria in RSS is mainly for metabolic activity, including carbohydrates, amino acids, energy, nucleotide, cofactor, vitamin, terpenoid substances and poly ketone metabolism. The most important metabolic pathways are carbohydrates and amino acid metabolism. Second, glycan and other secondary metabolites that are involved in synthesis and metabolism (Supplementary Figure 1). These metabolic activities provide the unique flavor of RSS.

As shown in Figure 4D, the intensity of carbohydrate metabolism increases gradually with the post-fermentation time. It reaches the maximum at 180 days, which may be related to the abundance of LAB (25). Much evidence shows that the function of carbohydrate metabolism is mainly assigned to LAB in the vegetable fermentation process, and carbohydrate metabolism contributes to the survival of LAB in various environments (26–28). The metabolism of carbohydrates through glycolytic and citrate cycle pathways can produce acids and substrates for amino acid metabolism, as well as some by-products (29). The intermediate pyruvate is also a core compound in producing organic acids, ethanol and esters (30). Finally, the intensity of amino acid metabolism reaches a peak value at 60 days. The metabolic activity of terpenes decreased with fermentation time. Secondly, the abundance of gene annotations related to genetic information and environment process was high, and both reached the highest value at

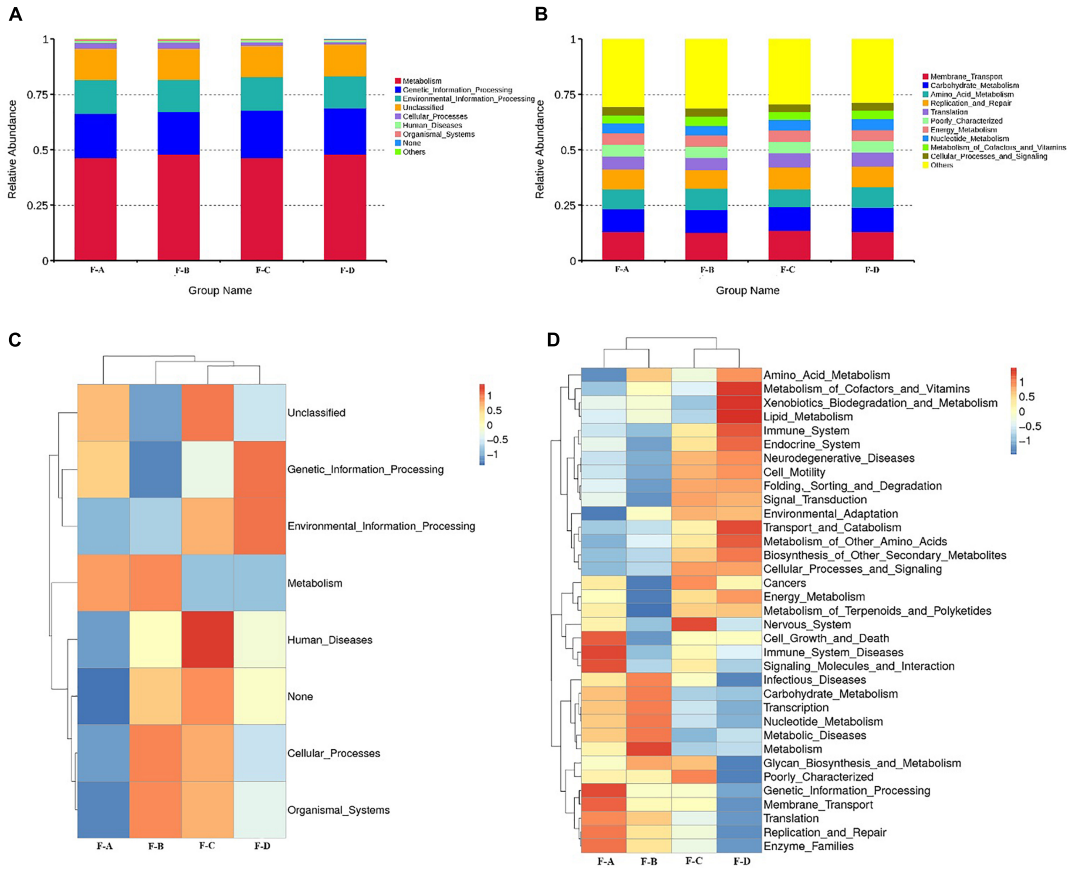

FIGURE 4
Abundance of Primary Function of bacteria at level 1 **(A)**, level 2 **(B)**, and cluster heatmap of Primary Function of bacteria at the level 1 **(C)**, and level 2 **(D)** by Picrust in RSS samples.

120 days. Genetic annotations related to human disease have also been detected. However, with increasing fermentation times, the abundance of genetic annotations related to human disease gradually decreased and reached the lowest level at 180 days, consistent with decreasing miscellaneous bacteria content (Table 1).

The composition of volatile compounds in red sour soup

Flavor substances are one of the critical indices to evaluate the quality of fermented foods. In the fermentation process, various substrates can be converted into distinctive metabolites through biocatalytic reactions of microorganisms, causing unique flavors in RSS. Thus, the RSS samples at four stages of the fermentation process between 0 and 180 days were investigated using HSPE-GC-MS. Table 2 shows a total of 77 kinds of volatile flavor compounds were detected in RSS samples, including 24 esters, 14 terpenes, 9 aromatic hydrocarbons, 9 alkanes, 6 heterocyclic compounds, 3 alcohols, 3 acids, 3 ketones, 2 phenols, 2 aldehydes, 1 amine, and 1 classified as other.

Figure 5 shows that esters are the dominant volatile substances in RSS during the post-fermentation process. The percentage of esters between 0 and 120 days of post-fermentation was insignificant, but it dramatically decreased to 25.36% from approximately 39.80% at 180 days. Furthermore, aromatic hydrocarbons (18.19–25.79%), terpenoids (6.99–15.01%), and heterocyclic compounds (4.21–5.92%) increased gradually during post-fermentation. Alcohols (2.57–6.08%) and alkanes (4.03–5.74%) suddenly decreased at 120 days of fermentation, while aldehydes (2.79–7.76%) suddenly decreased at 60 days and recovered to higher levels at 180 days (6.99%). Phenolic substances (4.20–8.44%) peaked at 60 days (8.44%), initially increased with fermentation time (0–60 days) and then decreased significantly (60–180 days).

Esters are abundant in the RSS fermentation process and usually have floral and fruity smells (12, 31). The high esters content includes propanoic acid propyl ester (propyl propionate), 1-butanol 3-methyl-acetate (isoamyl acetate), methyl salicylate, hexadecanoic acid ethyl ester (ethyl cetylate),

TABLE 2 Aroma compounds detected by GC-MS in different samples.

Classification	Compounds	RT	F-A	F-B	F-C	F-D
amines	m-Aminophenylacetylene	1.21E + 01	0.04 ± 0.000^{a}	0.04 ± 0.005^{a}	0.03 ± 0.000^{a}	0.03 ± 0.005^{a}
alcohols	3-methyl-1-butanol	3.09E + 00	6.26 ± 0.212^{a}	5.83 ± 0.094^{a}	2.29 ± 0.105^{b}	4.99 ± 1.115^{a}
	Benzyl alcohol	1.02E + 01	0.12 ± 0.005a	0.06 ± 0.046a	0.09 ± 0.006a	0.12 ± 0.005a
	6-methyl-5-hepten-2-ol	9.06E + 00	0.24 ± 0.000a	0.19 ± 0.015a	0.19 ± 0.027a	0.21 ± 0.065a
aromatic hydrocarbons	2-methoxyphenol	1.17E + 01	10.22 ± 0.404^{c}	5.98 ± 0.151^{d}	12.28 ± 0.173^{b}	14.49 ± 0.424^{a}
	Naphthalene	1.46E + 01	1.34 ± 0.207^{a}	1.28 ± 0.076^{a}	1.40 ± 0.058^{a}	1.17 ± 0.175^{a}
	4-ethyl-2-methoxyphenol	1.71E + 01	1.42 ± 0.062^{c}	4.41 ± 0.064^{a}	3.77 ± 0.112^{b}	3.90 ± 0.185^{b}
	Mesitylene	8.34E + 00	0.08 ± 0.026^{a}	0.11 ± 0.005^{a}	0.08 ± 0.006^{a}	0.06 ± 0.005^{a}
	1-methyl-3-(1-methylethyl)-benzene	9.96E + 00	1.33 ± 0.139^{b}	1.16 ± 0.067^{b}	1.74 ± 0.085^{b}	2.66 ± 0.504^{a}
	1-ethenyl-3,5-dimethylbenzene	1.19E + 01	0.62 ± 0.065^{b}	0.56 ± 0.065^{b}	0.69 ± 0.027^{b}	0.97 ± 0.115^{a}
	pentamethylbenzene	1.53E + 01	0.45 ± 0.225^{a}	0.19 ± 0.087^{ab}	0.29 ± 0.086^{ab}	0.09 ± 0.005^{b}
	1,2,3,4-tetrahydro-1,4,6-trimethylnaphthalene	1.54E + 01	0.29 ± 0.046^{b}	0.41 ± 0.087^{b}	1.17 ± 0.025^{a}	0.33 ± 0.017^{b}
	2-ethylbenzene-1,4-diol	1.47E + 01	3.68 ± 0.158^{a}	4.11 ± 0.446^{a}	1.66 ± 0.027^{b}	2.11 ± 0.055^{b}
phenols	Eugenol	1.92E + 01	5.58 ± 0.153^{c}	8.13 ± 0.354^{a}	6.68 ± 0.261^{b}	4.12 ± 0.139^{d}
	5-pentyl-1,3-benzenediol	2.34E + 01	0.26 ± 0.005^{b}	0.31 ± 0.036^{a}	0.12 ± 0.006^{c}	0.08 ± 0.005^{c}
other	4-chlorobutanoic anhydride	1.91E + 01	0.12 ± 0.005^{b}	0.18 ± 0.026^{a}	0.11 ± 0.015^{b}	0.15 ± 0.006^{ab}
aldehydes	Benzaldehyde	8.11E + 00	0.76 ± 0.026^{c}	0.56 ± 0.025^{d}	0.88 ± 0.026^{b}	1.57 ± 0.085^{a}
	2,4-dimethylbenzaldehyde	1.55E + 01	7.00 ± 0.667^{a}	2.23 ± 0.101^{c}	4.99 ± 0.172^{b}	5.42 ± 0.655^{b}
acids	Non-anoic acid	1.72E + 01	2.39 ± 0.304^{a}	2.75 ± 0.456^{a}	2.02 ± 0.147^{a}	3.00 ± 0.565^{a}
	Octanoic acid	1.45E + 01	0.68 ± 0.031^{c}	1.25 ± 0.048^{b}	1.29 ± 0.046^{b}	2.19 ± 0.037^{a}
	Butanoic acid	3.98E + 00	0.06 ± 0.046^{a}	0.16 ± 0.041^{a}	0.12 ± 0.005^{a}	0.02 ± 0.037^{a}
terpenes	3-Carene	1.06E + 01	0.28 ± 0.025^{c}	0.22 ± 0.017^{d}	0.40 ± 0.028^{b}	0.60 ± 0.035^{a}
	gamma-Terpinene	1.10E + 01	0.07 ± 0.005^{c}	0.07 ± 0.005^{c}	0.10 ± 0.009^{b}	0.18 ± 0.006^{a}
	(E)-1-(2,6,6-trimethyl-1,3-cyclohexadien-1-yl)-2-buten-1-on	1.99E + 01	1.68 ± 0.005^{c}	2.16 ± 0.167^{b}	1.83 ± 0.066^{c}	2.51 ± 0.109^{a}
	D-limonene	1.01E + 01	0.69 ± 0.058^{b}	0.65 ± 0.019^{b}	0.80 ± 0.005^{b}	1.18 ± 0.155^{a}
	trans-beta-ionone	1.81E + 01	0.33 ± 0.016^{b}	0.05 ± 0.005^{b}	0.03 ± 0.005^{b}	6.75 ± 0.587^{a}
	(S)-(+)-alpha-phellandrene	9.42E + 00	0.28 ± 0.006^{b}	0.23 ± 0.017^{c}	0.25 ± 0.006^{c}	0.36 ± 0.015^{a}
	(+)-alpha-pinene	1.03E + 01	0.07 ± 0.000^{c}	0.06 ± 0.016^{c}	0.27 ± 0.025^{b}	0.36 ± 0.025^{a}
	(1S)-6,6-dimethyl-2-methylene-bicyclo[3.1.1]heptane	8.95E + 00	0.46 ± 0.026^{c}	0.40 ± 0.035^{c}	1.05 ± 0.068^{b}	1.36 ± 0.202^{a}
	2,6,10,10-tetramethyl-1-oxaspiro[4.5]dec-6-ene	1.78E + 01	1.62 ± 0.101^{b}	2.54 ± 0.104^{a}	2.42 ± 0.163^{a}	0.09 ± 0.005^{c}
	4-isopropyl-6-methyl-1-methylene-1,2,3,4-tetrahydronaphthalene	2.67E + 01	0.03 ± 0.000^{ab}	0.03 ± 0.006^{ab}	0.02 ± 0.000^{b}	0.04 ± 0.005^{a}
	2,6-dimethyl-2,4,6-octatriene	1.18E + 01	0.22 ± 0.005^{c}	0.20 ± 0.005^{c}	0.27 ± 0.007^{b}	0.38 ± 0.036^{a}
	alpha-dehydro-ar-himachalene	2.36E + 01	0.01 ± 0.000^{c}	0.01 ± 0.000^{b}	0.01 ± 0.000^{a}	0.01 ± 0.000^{c}
	Ionone	2.30E + 01	0.91 ± 0.005^{b}	3.07 ± 0.217^{a}	0.75 ± 0.036^{b}	0.07 ± 0.001^{c}
	1, 1, 5-trimethyl-1, 2-dihydronaphthalene	2.06E + 01	0.35 ± 0.026^{b}	0.46 ± 0.035^{b}	1.21 ± 0.058^{a}	1.15 ± 0.136^{a}
ketones	Isophorone	1.10E + 01	0.13 ± 0.002^{b}	0.12 ± 0.006^{b}	0.13 ± 0.015^{b}	0.17 ± 0.016^{a}
	Tropinone	1.06E + 01	0.08 ± 0.005^{a}	0.08 ± 0.005^{ab}	0.07 ± 0.001^{b}	0.07 ± 0.001^{ab}
	1-(4-hydroxy-3-thienyl)-ethanone	8.38E + 00	0.69 ± 0.105^{a}	0.71 ± 0.076^{a}	0.62 ± 0.037^{a}	0.63 ± 0.105^{a}
alkanes	Tetradecane	2.06E + 01	0.07 ± 0.004^{a}	0.07 ± 0.005^{a}	0.06 ± 0.005^{a}	0.06 ± 0.006^{a}
	Pentadecane	2.31E + 01	4.41 ± 0.121^{a}	4.89 ± 0.405^{a}	3.38 ± 0.073^{b}	4.45 ± 0.527^{a}
	Hexadecane	2.54E + 01	0.09 ± 0.005^{b}	0.11 ± 0.005^{a}	0.07 ± 0.001^{b}	0.08 ± 0.006^{b}
	Heptadecane	2.76E + 01	0.29 ± 0.026^{ab}	0.32 ± 0.007^{a}	0.23 ± 0.006^{c}	0.25 ± 0.027^{bc}
	Octadecane	2.98E + 01	0.08 ± 0.005^{a}	0.08 ± 0.006^{a}	0.08 ± 0.004^{a}	0.08 ± 0.005^{a}
	Heneicosane	2.75E + 01	0.03 ± 0.005^{a}	0.04 ± 0.005^{a}	0.03 ± 0.005^{a}	0.03 ± 0.001^{a}
	2,6,10-trimethyl-tetradecane	2.27E + 01	0.05 ± 0.003^{b}	0.08 ± 0.005^{a}	0.05 ± 0.001^{b}	0.06 ± 0.005^{b}
	2-methyl-pentadecane	2.46E + 01	0.01 ± 0.001^{b}	0.02 ± 0.001^{a}	0.01 ± 0.002^{b}	0.02 ± 0.001^{b}
	2,6,11,15-tetramethyl-hexadecane	2.38E + 01	0.14 ± 0.026^{a}	0.14 ± 0.007^{a}	0.12 ± 0.005^{a}	0.12 ± 0.006^{a}

(Continued)

TABLE 2 (Continued)

Classification	Compounds	RT	F-A	F-B	F-C	F-D
heterocyclic compounds	2-isobutylthiazole	1.02E + 01	2.01 ± 0.036^{a}	2.84 ± 0.315^{b}	3.39 ± 0.058^{a}	2.83 ± 0.206^{b}
	7,9-di-tert-butyl-1-oxaspiro(4,5)deca-6,9-diene-2,8-dione	3.18E + 01	0.18 ± 0.055^{a}	0.19 ± 0.055^{a}	0.21 ± 0.027^{a}	0.13 ± 0.055^{a}
	4H-pyran-4-one	8.91E + 00	1.45 ± 0.076^{a}	1.23 ± 0.048^{a}	1.18 ± 0.079^{a}	1.28 ± 0.215^{a}
	1-(2-furanyl)-1-propanone	1.03E + 01	0.36 ± 0.025^{a}	0.33 ± 0.027^{ab}	0.28 ± 0.026^{b}	0.33 ± 0.029^{ab}
	4-isobutylpyrimidine	9.36E + 00	0.14 ± 0.015^{a}	0.12 ± 0.005^{a}	0.11 ± 0.003^{a}	0.14 ± 0.026^{a}
	2,4a-epidioxy-5,6,7,8-tetrahydro-2,5,5,8a-tetramethyl-2H-1-benzopyran	1.67E + 01	0.07 ± 0.002^{b}	0.02 ± 0.005^{b}	0.00 ± 0.003^{b}	1.22 ± 0.101^{a}
esters	Isobutyl acetate	3.39E + 00	0.23 ± 0.015^{a}	0.17 ± 0.006^{b}	0.24 ± 0.017^{a}	0.03 ± 0.004^{c}
	Propanoic acid, propyl ester (Propyl propionate)	4.32E + 00	6.00 ± 0.143^{a}	3.64 ± 0.139^{c}	4.65 ± 0.272^{b}	1.16 ± 0.136^{d}
	1-Butanol, 3- methyl-, acetate (Isoamyl acetate)	5.85E + 00	1.03 ± 0.062^{c}	1.82 ± 0.127^{b}	1.79 ± 0.108^{b}	2.77 ± 0.404^{a}
	Hexanoic acid, ethyl ester (Ethyl hexanoate)	9.22E + 00	0.03 ± 0.002^{a}	0.04 ± 0.001^{a}	0.04 ± 0.003^{a}	0.03 ± 0.001^{a}
	Propanoic acid, 2- hydroxy-, ethyl ester (Ethyl lactate)	6.66E + 00	0.58 ± 0.023^{a}	0.19 ± 0.064^{b}	0.33 ± 0.035^{ab}	0.45 ± 0.148^{ab}
	Butanedioic acid, diethyl ester (Diethyl succinate)	1.45E + 01	0.23 ± 0.006^{d}	1.09 ± 0.085^{b}	0.81 ± 0.016^{c}	1.44 ± 0.202^{a}
	Benzoic acid, ethyl ester (Ethyl benzoate)	1.42E + 01	0.12 ± 0.005^{b}	0.15 ± 0.037^{b}	0.14 ± 0.005^{b}	0.83 ± 0.007^{a}
	Methyl salicylate	1.48E + 01	16.26 ± 0.282^{b}	10.38 ± 0.115^{c}	17.62 ± 0.184^{a}	9.32 ± 0.767^{d}
	Linalyl acetate	1.22E + 01	0.45 ± 0.036^{b}	0.41 ± 0.095^{b}	0.53 ± 0.037^{b}	1.06 ± 0.118^{a}
	alpha-Terpinyl acetate	1.50E + 01	0.37 ± 0.045^{a}	0.30 ± 0.057^{a}	0.25 ± 0.076^{a}	0.32 ± 0.027^{a}
	Benzoic acid, 2- hydroxy-, ethyl ester (Ethyl salicylate)	1.70E + 01	0.81 ± 0.045^{c}	0.28 ± 0.016^{d}	1.07 ± 0.035^{b}	1.44 ± 0.038^{a}
	Dodecanoic acid, ethyl ester (Ethyl laurinate)	2.52E + 01	0.05 ± 0.001^{b}	0.39 ± 0.045^{a}	0.03 ± 0.001^{b}	0.03 ± 0.005^{b}
	Methyl tetradecanoate	2.81E + 01	0.01 ± 0.002^{b}	0.02 ± 0.001^{a}	0.01 ± 0.004^{b}	0.01 ± 0.003^{b}
	Tetradecanoic acid, ethyl ester (Ethyl myristate)	2.96E + 01	0.09 ± 0.015^{b}	0.50 ± 0.046^{a}	0.04 ± 0.003^{b}	0.07 ± 0.003^{b}
	Hexadecanoic acid, ethyl ester (Ethyl cetylate)	3.36E + 01	4.30 ± 0.765^{b}	10.49 ± 0.758^{a}	2.01 ± 0.186^{c}	1.49 ± 0.285^{c}
	Isopropyl palmitate	3.54E + 01	0.36 ± 0.057^{b}	0.50 ± 0.116^{a}	0.16 ± 0.015^{c}	0.04 ± 0.006^{c}
	Hexadecanoic acid, methyl ester (Methyl palmitate)	3.23E + 01	0.34 ± 0.045^{b}	0.82 ± 0.066^{a}	0.34 ± 0.009^{b}	0.46 ± 0.075^{b}
	Isopropyl myristate	3.16E + 01	0.02 ± 0.004^{b}	0.06 ± 0.003^{a}	0.01 ± 0.004^{c}	0.01 ± 0.001^{d}
	Ethyl 9-hexadecenoate	3.32E + 01	0.01 ± 0.002^{b}	0.05 ± 0.005^{a}	0.01 ± 0.003^{c}	0.01 ± 0.002^{c}
	n-propyl acetate	2.78E + 00	6.24 ± 0.48^{b}	6.11 ± 0.456^{b}	7.73 ± 0.535^{a}	3.52 ± 0.386^{c}
	Phthalic acid, butyl hex-3-yl ester	3.28E + 01	1.73 ± 0.092^{a}	0.62 ± 0.165^{b}	0.39 ± 0.025^{c}	0.43 ± 0.027^{c}
	(Z, Z)-9.12-octadecadienoic acid, methyl ester (methyl linoleate)	3.83E + 01	0.02 ± 0.001^{b}	0.03 ± 0.002^{a}	0.00 ± 0.000^{c}	0.00 ± 0.000^{c}
	Linoleic acid ethyl ester (Ethyl Linoleate)	3.66E + 01	0.04 ± 0.006^{b}	0.10 ± 0.005^{a}	0.01 ± 0.002^{c}	0.01 ± 0.001^{c}
	Ethyl 13-methyl-tetradecanoate	3.09E + 01	0.48 ± 0.021^{a}	0.47 ± 0.055^{a}	0.44 ± 0.037^{a}	0.43 ± 0.026^{a}

[2] RT refers to the retention time. F-A, F-B, F-C and F-D refer to the sour soup samples fermented for 0 days, 60 days, 120 days and 180 days, respectively. Statistical analysis was performed using one-way ANOVA (Tukey's test, $P < 0.05$).

n-propyl acetate, methyl salicylate and butyl hex-3-yl ester phthalic acid. Propyl propionate and butyl hex-3-yl ester phthalic acid levels decrease over time, while isoamyl acetate and benzoic acid, 2- hydroxy-, ethyl ester (Ethyl salicylate) increase with post-fermentation time. Ethyl cetylate and n-propyl acetate initially showed an increasing trend but then decreased, peaking at 60 and 120 days of fermentation, respectively. Finally, methyl salicylate had a decreasing trend before 60 days and then increased up to the 120-day point.

The aromatic hydrocarbon compounds also account for many of the total volatile compounds. Among them, 2-methoxyphenol, naphthalene, 4-ethyl-2-methoxyphenol, 1-methyl-3-(1-methylethyl)-benzene and 2-ethylbenzene-1,4-diol occurred at high percentages. 2-methoxyphenol exhibited a decreasing trend before 60 days and then increased, while it was inverse to 4-ethyl-2-methoxyphenol. The concentration of 1-methyl-3-(1-methylethyl)-benzene increased during the post-fermentation time, while that of 2-ethylbenzene-1,4-diol was the opposite. Terpenes are often derived from plants, and the most abundant terpenes included (E)-1-(2,6,6-trimethyl-1,3-cyclohexadien-1-yl)-2-buten-1-one, D-limonene, trans-beta-ionone, (1S)-6,6-dimethyl-2-methylene-bicyclo[3.1.1]heptane, 2,6,10,10-tetramethyl-1-oxaspiro[4.5]dec-6-ene, and ionone. (E)-1-(2,6,6-trimethyl-1,3-cyclohexadien-1-yl)-2-buten-1-one fluctuated with post-fermentation and reached a peak at 180 days. Meanwhile, D-limonene, trans-beta-ionone and (1S)-6,6-dimethyl-2-methylene-bicyclo[3.1.1]heptane increased with

10.3389/fnut.2022.1007164

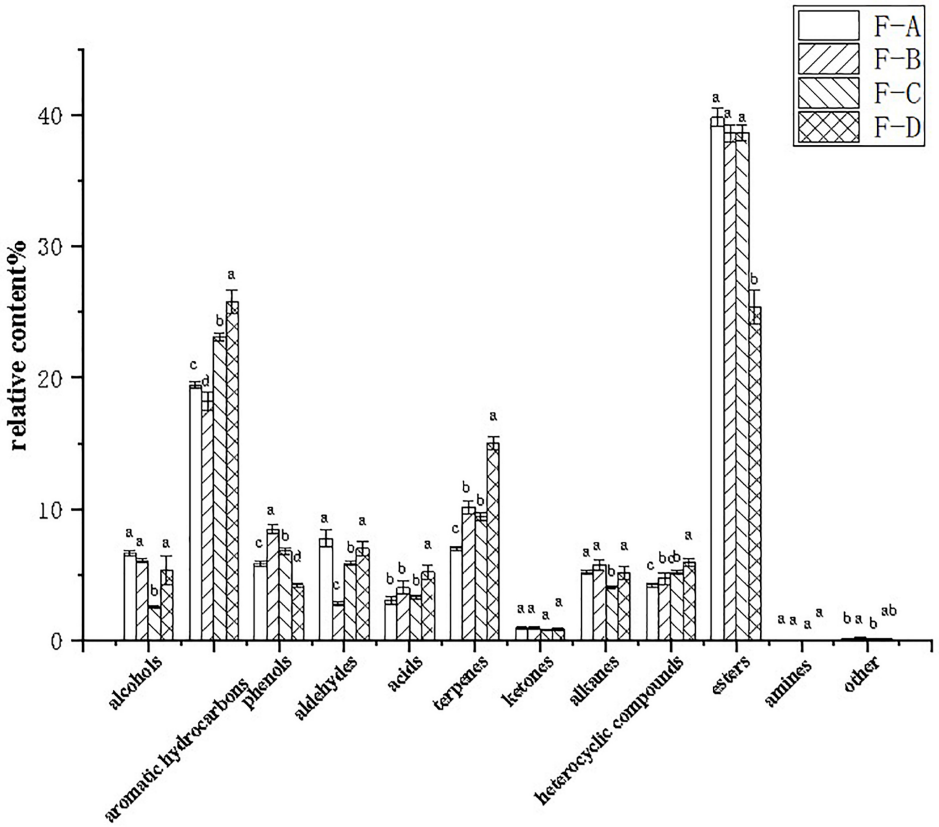

FIGURE 5
Relative percentages of volatile compounds in RSS samples at different post-fermentation stages. F-A, F-B, F-C, and F-D refer to the sour soup samples fermented for 0 days, 60 days, 120 days and 180 days, respectively. Each column represents a variety of substances in each sample. Statistical analysis was performed by one-way ANOVA (Tukey's test, $P < 0.05$).

fermentation time. 2,6,10,10-tetramethyl-1-oxaspiro[4.5]dec-6-ene first increased and then decreased. Other substances present at high contents included 2-isobutylthiazol, 4H-pyran-4-one, 3-methyl-1-butanol and pentadecane.

Principal component analysis analysis of volatile compounds

Principal component analysis (PCA) analysis was undertaken to compare the differences of volatile substances in RSS with different fermentation days. As shown in **Figure 6**, different samples were distinguished, and parallel samples were pooled. According to the first principal component, F-A and F-B were close together, indicating they were similar and clustered into one category. Taking the second principal component into account, all samples were relatively close. Therefore, the differences between these samples can primarily be explained using the first principal component. As can be seen from the overall distance, the changes in volatile substances were relatively small in the early stage of post-fermentation (0–60 days) and became more extensive in the later stage of post-fermentation (120–180 days).

Correlation between microbiota and volatile components of red sour soup

Pearson correlation analysis was employed to evaluate the relationship between the dominant bacteria and the predominant volatile components in RSS. OPLS was applied to screen the critical volatile components with variable importance in projection (VIP) values greater than 1. Pearson correlation analysis was undertaken for RSS's top 10 most abundant bacteria and the main volatile compounds. Cytoscope software was used to portray the results through a visualization network. As shown in **Figure 7**, 67 significant correlations are identified. *Acetobacter* spp., *Clostridium* spp. and *Sporolactobacillus* spp. have over ten significant correlations, especially *Sporolactobacillus* spp., and all three bacteria are primarily correlated with esters. *Acetobacter* mainly correlated with benzoic acid, 2- hydroxy-, ethyl ester (ethyl salicylate), (Z, Z)-9.12-octadecadienoic acid,

10.3389/fnut.2022.1007164

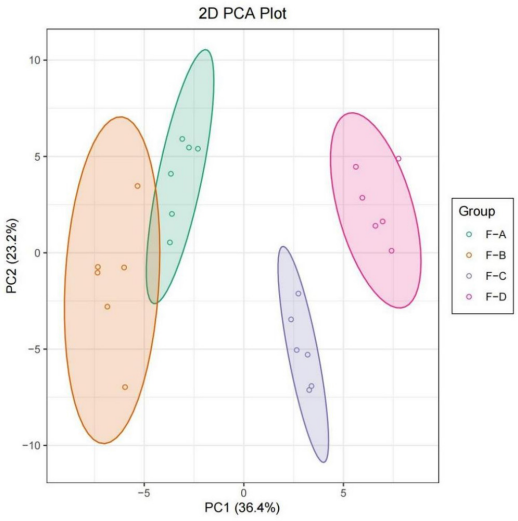

FIGURE 6
PCA plot based on HS-SPME-GC/MS results for RSS from different post-fermentation stages. F-A, F-B, F-C and F-D refer to the sour soup samples fermented for 0 days, 60 days, 120 days, and 180 days, respectively.

methyl ester (methyl linoleate), hexadecanoic acid, methyl ester (methyl palmitate), methyl tetradecanoate, dodecanoic acid, ethyl ester (ethyl laurinate), hexadecanoic acid, ethyl ester (ethyl cetylate), tetradecanoic acid, ethyl ester (ethyl myristate), isopropyl myristate, linoleic acid ethyl ester (ethyl linoleate) and ethyl 9-hexadecenoate. *Clostridium* spp. mainly correlate with benzoic acid, 2- hydroxy-, ethyl ester (ethyl salicylate), (Z, Z)-9.12-octadecadienoic acid, methyl ester (methyl linoleate), hexadecanoic acid, methyl ester (methyl palmitate), methyl tetradecanoate, hexadecanoic acid, ethyl ester (ethyl cetylate), dodecanoic acid, ethyl ester (ethyl laurinate), tetradecanoic acid, ethyl ester (ethyl myristate), isopropyl myristate, linoleic acid ethyl ester (ethyl linoleate), and ethyl 9-hexadecenoate. *Sporolactobacillus* spp. mainly correlate with benzoic acid, 2- hydroxy-, ethyl ester (ethyl salicylate), (Z, Z)-9.12-octadecadienoic acid, methyl ester (methyl linoleate), hexadecanoic acid, methyl ester (ethyl cetylate), methyl tetradecanoate, hexadecanoic acid, ethyl ester (ethyl cetylate), dodecanoic acid, ethyl ester (ethyl laurinate), tetradecanoic acid, ethyl ester (ethyl myristate), isopropyl myristate, linoleic acid ethyl ester (ethyl linoleate) and ethyl 9-hexadecenoate. *Acetobacter*, *Clostridium* spp. and *Sporolactobacillus* spp. also correlate with 2-methoxyphenol, 2,4-dimethyl-benzaldehyde, and hexadecane.

Discussion

Red sour soup (RSS) is a traditional Chinese fermented food with a history of several thousand years (32). Its fermentation process relies mainly on LAB, acetic acid bacteria and *Clostridium* spp., which produce a refreshingly sour taste. As reported in previous studies, naturally fermented sour soup has more flavor after a longer fermentation time (more than 87 days) (33). However, for practical purposes, commercial production generally shortens the production period to 1–2 months by adding dominant strains (34, 35). This study aims to investigate the effect of fermentation time on the quality of RSS, the microbial composition and volatile flavor substances in RSS during the post-fermentation process.

Lactic acid bacteria (LAB) is commonly chosen as a starter material in various vegetable fermentation processes, such as Sichuan paocai, Korean kimchi, German sauerkraut and North-eastern Chinese pickles (36–39). LAB could convert fermentable sugars into lactic acid and other organic acids (40), which could help to produce flavor compounds in foods through fermentation (41). The gradual accumulation of acids will inhibit the growth of other microorganisms so that LAB gradually become the dominant bacteria (42, 43). Meanwhile, the diversity of LAB may also contribute to the production of volatile flavored compounds (13). As shown in **Figure 3**, LAB is the main bacteria in RSS in the post-fermentation process, consistent with sour soup's widely reported microbial composition (4, 12, 13, 31, 32, 44). Notably, the central populations of LAB are *Sporolactobacillus* spp., *Lentilactobacillus* spp., *Lactiplantibacillus* spp., and *Lactobacillus* spp. *Sporolactobacillus* spp. predominantly correlate with 2- hydroxy-, ethyl ester, methyl ester, methyl ester, ethyl ester, ethyl ester, ethyl ester, linoleic acid ethyl ester, benzoic acid, hexadecanoic acid, and other volatile flavor compounds. *Lentilactobacillus* spp. is mainly related to benzoic acid ethyl ester, linalyl acetate, and propanoic acid propyl ester. *Lactiplantibacillus* spp. mainly correlate with α-deshydro-ar-himachalene, naphthalene, and octadecane, while *Lactobacillus* spp. mainly correlate with hexanoic acid ethyl ester and methyl salicylate. However, as Lin et al. reported, excessive LAB may inhibit the production of flavor substances, especially esters (12). The current study report that the lactic acid bacteria reached the highest content at 180 days, while the ester content decreased. A hypothesis was suggested that the underlying reason could relate to excess LAB inhibiting the growth of yeast and microorganisms related to ester production. The growth of yeast can produce many alcohols as precursors of esters (45). LAB inhibits yeast growth by producing bacteriostatic substances or robbing trace nutrients for fungal growth (46, 47).

Acetobacter spp. can produce acetic acid and are ubiquitous in the fermentation of various kinds of vinegar (48). Acetic acid production significantly contributes to the generation of esters from alcohols and can make the fermented product more aromatic (49). In addition, there is evidence that acetic acid bacteria can increase the total fatty acid content of the fermentation by breaking down amino acids (50). Pearson correlation analysis results

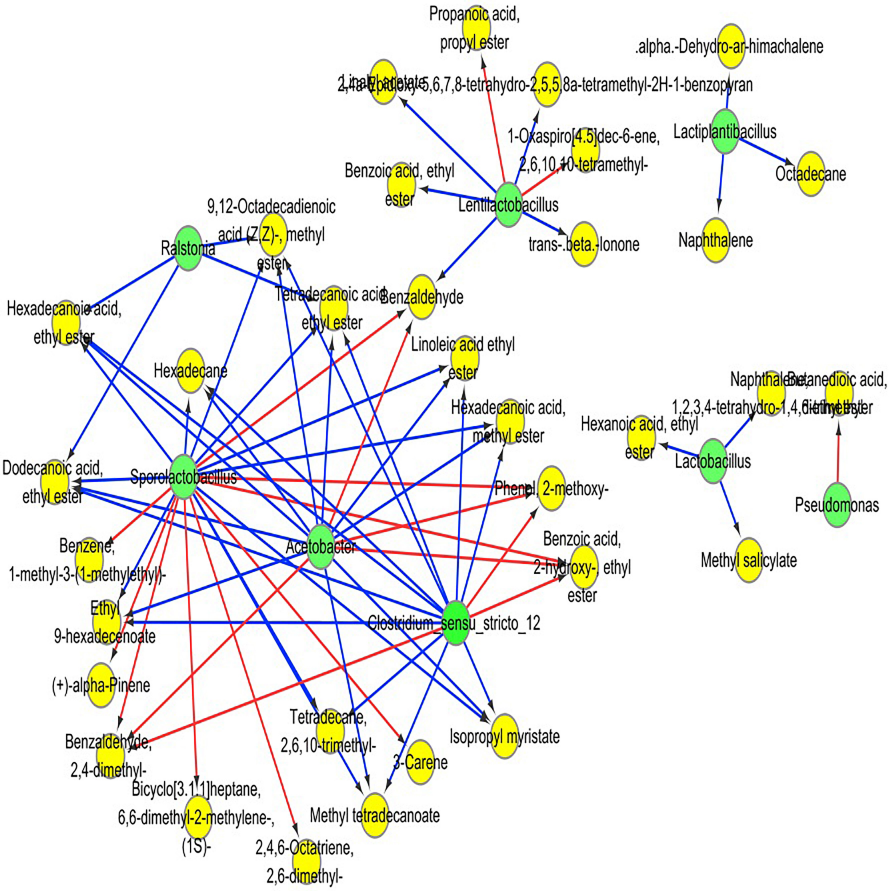

FIGURE 7
Heatmap of correlation analysis between dominant bacteria and some highly differential volatile components, based on Pearson's correlation coefficients. The red line shows a positive correlation, and the blue line shows a negative correlation. Green circles indicate microorganisms, and yellow circles indicate volatile substances.

indicate that in the post-fermentation process of RSS, *Acetobacter* spp. is positively correlated with a variety of esters, including (Z,Z)-9.12-octadecadienoic acid-methyl ester, 2-hydroxy-benzoic acid ethyl ester, dodecanoic acid ethyl ester, ethyl 9-hexadecenoate, hexadecanoic acid ethyl ester, hexadecanoic acid methyl ester, isopropyl myristate, linoleic acid ethyl ester, methyl tetradecanoate, and tetradecanoic acid ethyl ester.

Clostridium spp. are usually found in wine fermentation (51, 52). Acetyl coenzyme A can be synthesized via the reverse β-oxidation pathway by *Clostridium* spp. and then converted to butyric acid. Octanoic acid can be synthesized through a similar metabolic pathway by *Clostridium* spp. (53). Low concentrations of butyric acid are essential flavor compounds in many foods. However, the high concentration of butyric acid would create an unpleasant smell. Therefore, butyric acid is best kept at a low concentration during fermentation (54). The current study also detected butyric and caprylic acids as volatile flavor compounds.

Small amounts of *Ralstonia* spp. were also detected. *Ralstonia* spp. are usually found in soil and presumably were introduced by raw materials during production (55). In some cases, *Ralstonia* spp. are pathogenic and causes bacterial infections, and levels were inhibited later during fermentation (180 days) (56). Meanwhile, esters positively related with *Ralstonia* spp., such as (Z,Z)-9.12-octadecadienoic acid, methyl ester, dodecanoic acid ethyl ester, hexadecanoic acid ethyl ester, and tetradecanoic acid ethyl ester also decreased significantly at 180 days. However, its role in fermentation is unclear.

Hydrocarbons, including alkanes and aromatic hydrocarbons, were also detected during fermentation. Aromatic hydrocarbons have a unique aroma, but aromatic hydrocarbon compounds have a higher flavor threshold and may not significantly affect flavor. Nevertheless, at a specific

concentration, they give fermented products a fuller flavor (57). Terpenoids are mainly produced by plants and have floral and woody scents. During fermentation, terpenoids are released due to the transformation of microorganisms, increasing terpenoid levels. LAB has been shown to release potential volatile terpenes through enzymatic hydrolysis (58–68). There may be a positive correlation between terpenoids' content and consumers' affection (60). High concentrations of aldehydes are often thought to be the unpleasant taste of vegetable fermentation, and lactic fermentation usually reduces the levels of related aldehydes (61). The current study found that aldehydes are negatively correlated with bacterial levels. Benzaldehyde and 2-4 dimethylbenzaldehyde are detected in our study, and give the fermentation desirable sensory properties, such as almond, bitter almond, cherry and sweet tastes (62, 63).

After a long post-fermentation process, the contents of volatile compounds, especially esters, acids, terpenes and aromatic compounds, were more abundant, indicating that a longer fermentation time was beneficial to expanding the volatile flavor. However, the data illustrate that when fermentation time is prolonged and between 120 and 180 days, the contents of the esters decrease. This may be due to the excessive LAB, which could inhibit the production of flavor substances (11). Due to the low flavor threshold of esters, even small changes in the concentrations of esters can directly impact the sour soup's sensory quality (49). Thus, these results indicate that the optimal post-fermentation time is around 120 days in the RSS preparation process.

Conclusion

This study investigated the relationship between microbial composition and volatile flavor substances in RSS during the post-fermentation process. *Acetobacter* spp., *Clostridium* spp. and *Sporolactobacillus* spp. influenced volatile flavor compound levels significantly. In addition, with the passage of fermentation time (0–120 days), the amounts of LAB and volatile flavor substances accumulate. Unfortunately, although LAB are overabundant in the lengthy post-fermentation time (180 days), esters production in RSS are inhibited. Thus, the fermentation time of RSS should be controlled at around 120 days. Notably, *Acetobacter* spp., *Clostridium* spp. and *Sporolactobacillus* spp. can be considered starter material for RSS fermentation and warrants further research.

Data availability statement

The data presented in this study are deposited in the NCBI repository, accession number: PRJNA857173.

Author contributions

XZ: writing—original draft and conceptualization. WZ: conceptualization. LZ and LZZ: writing—review and editing. ML and XF: visualization. XH, YD, and LL: software and formal analysis. All authors contributed to the article and approved the submitted version.

Funding

This work was supported by the Natural Science Foundation of Hunan Province (Nos. 2022JJ50241 and 2022JJ31009), The project of the Hunan Education Department (No. 21C0623), The Science and Technology Innovation Program of Hunan Province (Nos. 2017TP1021, 2019TP1028, 2019SK2122, 2019TP2011, 2019NK4229, 2021GK4024, and 2021GK4022), The Science and Technology Support Project of Guizhou Province (No. [2020]1Y150) and the Open Project of Hunan Provincial Key Laboratory of Soybean Products Processing and Safety Control (DZPJG202005), and Innovation and Entrepreneurship Training for College Students of Shaoyang University plan project (No. 86).

Conflict of interest

Author XF was employed by Shenzhen Shanggutang Food Development Co., Ltd.

The remaining authors declare that the research was conducted in the absence of any commercial or financial relationships that could be construed as a potential conflict of interest.

Publisher's note

Supplementary material

The Supplementary Material for this article can be found online at: https://www.frontiersin.org/articles/10.3389/fnut.2022.1007164/full#supplementary-material

References

1. Xiao X, Li J, Xiong H, Tui W, Zhu Y, Zhang J. Effect of extrusion or fermentation on physicochemical and digestive properties of barley powder. *Front Nutr.* (2022) 8:794355. doi: 10.3389/fnut.2021.794355

2. Chen W, Lv X, Tran VT, Maruyama JI, Han KH, Yu JH. From traditional to modern: progress of molds and yeasts in Fermented-Food production. *Front Microbiol.* (2022) 13:876872. doi: 10.3389/fmicb.2022.876872

3. Zhang Y, Liu Y, Yang W, Huang J, Liu Y, Huang M, et al. Characterization of the potent aroma compounds in preserved egg yolk by gas chromatography-olfactometry, quantitative measurements, and odor activity value. *J Agric Food Chem.* (2018) 66:6132–41. doi: 10.1021/acs.jafc.8b01378

4. Xiong K, Han F, Wang Z, Du M, Chen Y, Tang Y, et al. Screening of dominant strains in red sour soup from Miao nationality and the optimization of inoculating fermentation conditions. *Food Sci Nutr.* (2021) 9:261–71. doi: 10.1002/fsn3.1992

5. Cong S, Li Z, Yu L, Liu Y, Cheng M. Integrative proteomic and lipidomic analysis of Kaili Sour Soup-mediated attenuation of high-fat diet-induced nonalcoholic fatty liver disease in a rat model. *Nutr Metab.* (2021) 18:26. doi: 10.1186/s12986-021-00553-4

6. Zhou W. Hmong's delicious food-Vinegar soup. *Jiangsu Condiment Subsid Food.* (2004) 4:27–8. doi: 10.16782/j.cnki.32-1235/ts.2004.04.011

7. Zhou D. Analysis and research on nutrients in Kaili red sour soup. *China Condiment.* (2015) 40:5. doi: 10.3969/j.issn.1000-9973.2015.05.033

8. Li D, Duan F, Tian Q, Zhong D, Wang X, Jia L. Physiochemical, microbiological and flavor characteristics of traditional Chinese fermented food Kaili Red Sour Soup. *LWT Food Sci Technol.* (2021) 142:110933. doi: 10.1016/j.lwt.2021.110933

9. Lin L, Du F, Zeng J, Liang Z, Zhang X, Gao X. Deep insights into fungal diversity in traditional Chinese sour soup by Illumina MiSeq sequencing. *Food Res Int.* (2020) 137:109439. doi: 10.1016/j.foodres.2020.109439

10. Lin L, Wu J, Chen X, Huang L, Zhang X, Gao X. The role of the bacterial community in producing a peculiar smell in Chinese fermented sour soup. *Microorganisms.* (2020) 8:1270. doi: 10.3390/microorganisms8091270

11. Wang C, Zhang Q, He L, Li C. Determination of the microbial communities of Guizhou Suantang, a traditional Chinese fermented sour soup, and correlation between the identified microorganisms and volatile compounds. *Food Res Int.* (2020) 138:109820. doi: 10.1016/j.foodres.2020.109820

12. Lin LJ, Zeng J, Tian QM, Ding XQ, Zhang XY, Gao XY. Effect of the bacterial community on the volatile flavor profile of a Chinese fermented condiment – Red sour soup – During fermentation. *Food Res Int.* (2022) 155:111059. doi: 10.1016/j.foodres.2022.111059

13. Liu N, Pan J, Miao S, Qing L. Microbial community in Chinese traditional fermented acid rice soup (rice-acid) and its correlations with key organic acids and volatile compounds. *Food Res Int.* (2020) 137:109672. doi: 10.1016/j.foodres.2020.109672

14. Wu, Y, Yang K, Shi M, Lyu P, Wang D, Li L, et al. High-throughput sequencing combined with traditional microbial culturable method to study microbial diversity and community changes in soy sauce moromi. *Food Ferment Ind.* (2022) 1–11. doi: 10.13995/j.cnki.11-1802/ts.031469

15. Wei Q, Wang H, Chen Z, Lv Z, Xie Y, Lu F. Profiling of dynamic changes in the microbial community during the soy sauce fermentation process. *Appl Microbiol Biotechnol.* (2013) 97:9111–9. doi: 10.1007/s00253-013-5146-9

16. Liu N, Lu Z, Wang L, Yu Y, Li G, Shi J, et al. Clone library analysis of enzyme genes in metabolic pathway for acetoin production in the fermentation of Zhenjiang aromatic vinegar. *Chin J Appl Environ Biol.* (2017) 23:134–9.

17. De Filippis F, Parente E, Ercolini D. Metagenomics insights into food fermentations. *Microb Biotechnol.* (2017) 10:91–102. doi: 10.1111/1751-7915.12421

18. Li Q, Kang J, MaXiao Z, Li P, Liu L, Hu X. Microbial succession and metabolite changes during traditional serofluid dish fermentation. *LWT Food Sci Technol.* (2017) 84:771–9. doi: 10.1016/j.lwt.2017.06.051

19. Seo HS, Lee S, Singh D, Park MK, Kim YS, Shin HW, et al. Evaluating the headspace volatolome, primary metabolites, and aroma characteristics of Koji fermented with *Bacillus amyloliquefaciens* and *Aspergillus oryzae*. *J Microbiol Biotechnol.* (2018) 28:1260–9. doi: 10.4014/jmb.1804.04017

20. Svečnjak L, Jović O, Prđun S, Rogina J, Marijanoviæ Z, Car J, et al. Influence of beeswax adulteration with paraffin on the composition and quality of honey determined by physico-chemical analyses, 1 H NMR, FTIR-ATR and HS-SPME/GC–MS. *Food Chem.* (2019) 291:187–98. doi: 10.1016/j.foodchem.2019.03.151

21. Lin Y, Lin Y, Cai T, Lan W. High-throughput sequencing of microbial community diversity and dynamics during douchi fermentation. *PLoS One.* (2016) 11:e0168166. doi: 10.1371/journal.pone.0168166

22. Fei Y, Li L, Chen L, Zheng Y, Yu B. High-throughput sequencing and culture-based approaches to analyze microbial diversity associated with chemical changes in naturally fermented tofu whey, a traditional Chinese tofu-coagulant. *Food Microbiol.* (2018) 76:69–77. doi: 10.1016/j.fm.2018.04.004

23. Liu Z, Wang Z, Sun J, Ni L. The dynamics of volatile compounds and their correlation with the microbial succession during the traditional solid-state fermentation of Gutian Hong Qu glutinous rice wine. *Food Microbiol.* (2020) 86:103347. doi: 10.1016/j.fm.2019.103347

24. Hu S, He C, Li Y, Yu Z, Chen Y, Wang Y, et al. The formation of aroma quality of dark tea during pile-fermentation based on multi-omics. *LWT Food Sci Technol.* (2021) 147:111491. doi: 10.1016/j.lwt.2021.111491

25. Du F, Zhang X, Gu H, Song J, Gao X. Dynamic changes in the bacterial community during the fermentation of traditional Chinese fish sauce (TCFS) and their correlation with TCFS quality. *Microorganisms.* (2019) 7:371. doi: 10.3390/microorganisms7090371

26. Liu D, Zhang C, Zhang J, Xin X, Liao X. Metagenomics reveals the formation mechanism of flavor metabolites during the spontaneous fermentation of potherb mustard (*Brassica juncea var. Multiceps*). *Food Res Int.* (2021) 148:110622. doi: 10.1016/j.foodres.2021.110622

27. Xiao M, Huang T, Xu Y, Peng Z, Liu Z, Guan Q, et al. Metatranscriptomics reveals the gene functions and metabolic properties of the major microbial community during Chinese Sichuan Paocai fermentation. *Food Microbiol.* (2021) 98:103573. doi: 10.1016/j.fm.2020.103573

28. Jun Z, Shuaishuai W, Lihua Z, Qilong M, Xi L, Mengyang N, et al. Culture-dependent and -independent analysis of bacterial community structure in Jiangshui, a traditional Chinese fermented vegetable food. *LWT Food Sci Technol.* (2018) 96:244–50. doi: 10.1016/j.lwt.2018.05.038

29. Liu S, Chen Q, Zou H, Yu Y, Zhou Z, Mao J, et al. A metagenomic analysis of the relationship between microorganisms and flavor development in Shaoxing mechanized huangjiu fermentation mashes. *Int J Food Microbiol.* (2019) 303:9–18. doi: 10.1016/j.ijfoodmicro.2019.05.001

30. Xiao M, Peng Z, Hardie WJ, Huang T, Liu Z, Zhang Y, et al. Exploring the typical flavors formation by combined with metatranscriptomics and metabolomics during Chinese Sichuan paocai fermentation. *LWT Food Sci Technol.* (2022) 153:112474. doi: 10.1016/j.lwt.2021.112474

31. Cui Y, Qu X. Genetic mechanisms of prebiotic carbohydrate metabolism in lactic acid bacteria: emphasis on *Lacticaseibacillus casei* and *Lacticaseibacillus paracasei* as flexible, diverse and outstanding prebiotic carbohydrate starters. *Trends Food Sci Technol.* (2021) 115:486–99. doi: 10.1016/j.tifs.2021.06.058

32. Zhou X, Liu Z, Xie L, Li L, Zhou W, Zhao L. The correlation mechanism between dominant bacteria and primary metabolites during fermentation of red sour soup. *Foods.* (2022) 11:341. doi: 10.3390/foods11030341

33. He Y, Li G, Li Y, Luo X, Luo Q, Shi B, et al. Analysis of trend of microflora and flavor components in red sour soup during fermentation. *Sci Technol Food Ind.* (2022) 28:301.doi: 10.13386/j.issn1002-0306.2021120301

34. Zheng S, Hu P. Study on quality change of red sour soup fermented by lactic acid bacteria. *China Condiment.* (2019) 44:65–70. doi: 10.3969/j.issn.1000-9973.2019.08.012

35. Wu S, Li J, Long L, Yang T, Wang Y, Li G. Quality change of red sour soup during natural fermentation and lactic acid bacteria intensified fermentation. *China Brew.* (2020) 39:75–8. doi: 10.11882/j.issn.0254-5071.2020.10.015

36. Xiao Y, Xiong T, Peng Z, Liu C, Huang T, Yu H, et al. Correlation between microbiota and flavors in fermentation of Chinese Sichuan Paocai. *Food Res Int.* (2018) 114:123–32. doi: 10.1016/j.foodres.2018.06.051

37. Park KY, Jeong JK, Lee YE, Daily JW. Health benefits of kimchi (Korean fermented vegetables) as a probiotic food. *J Med Food.* (2014) 17:6–20. doi: 10.1089/jmf.2013.3083

38. Cho SK, Shin SY, Lee SJ, Li L, Moon JS, Kim DJ, et al. Simple synthesis of isomaltooligosaccharides during Sauerkraut fermentation by addition of *Leuconostoc* starter and sugars. *Food Sci Biotechnol.* (2015) 24:1443–6. doi: 10.1007/s10068-015-0185-x

39. An F, Sun H, Wu J, Zhao C, Li T, Huang H, et al. Investigating the core microbiota and its influencing factors in traditional Chinese pickles. *Food Res Int.* (2021) 147:110543. doi: 10.1016/j.foodres.2021.110543

40. Ashaolu TJ, Reale A. A holistic review on Euro-Asian lactic acid bacteria fermented cereals and vegetables. *Microorganisms.* (2020) 8:1–24. doi: 10.3390/microorganisms8081176

41. Qin H, Sun Q, Pan X, Qiao Z, Yang H. Microbial diversity and biochemical analysis of Suanzhou: a traditional Chinese fermented cereal gruel. *Front Microbiol.* (2016) 7:1311. doi: 10.3389/fmicb.2016.01311

42. Adams MR, Hall CJ. Growth inhibition of food-borne pathogens by lactic and acetic acids and their mixtures. *Int J Food Sci Technol.* (1988) 23:287–92. doi: 10.1111/j.1365-2621.1988.tb00581.x

43. Gao Z, Daliri EBM, Wang JUN, Liu D, Chen S, Ye X, et al. Inhibitory effect of lactic acid bacteria on foodborne pathogens: a review. *J Food Prot.* (2019) 82:441–53. doi: 10.4315/0362-028X.JFP-18-303

44. Li J, Wang X, Wu W, Jiang J, Feng D, Shi Y, et al. Comparison of fermentation behaviors and characteristics of tomato sour soup between natural fermentation and dominant bacteria-enhanced fermentation. *Microorganisms.* (2022) 10:640. doi: 10.3390/microorganisms10030640

45. De Roos J, De Vuyst L. Microbial acidification, alcoholization, and aroma production during spontaneous lambic beer production. *J Sci Food Agric.* (2019) 99:25–38. doi: 10.1002/jsfa.9291

46. SLU Library,. *Fungal Inhibitory Lactic Acid Bacteria*. Sweden: Open access publications in the SLU publication database (2022).

47. Bayrock DP, Ingledew WM. Inhibition of yeast by lactic acid bacteria in continuous culture: nutrient depletion and/or acid toxicity? *J Ind Microbiol Biotechnol.* (2004) 31:362–8. doi: 10.1007/s10295-004-0156-3

48. Sokollek SJ, Hertel C, Hammes WP. Description of *Acetobacter oboediens* sp. nov. and *Acetobacter pomorum* sp. nov., two new species isolated from industrial vinegar fermentations. *Int J Syst Bacteriol.* (1998) 48:935–40. doi: 10.1099/00207713-48-3-935

49. Settanni L, Corsetti A. The use of multiplex PCR to detect and differentiate food- and beverage-associated microorganisms: a review. *J Microbiol Methods.* (2007) 69:1–22. doi: 10.1016/j.mimet.2006.12.008

50. Kruis AJ, Bohnenkamp AC, Patinios C, van Nuland YM, Levisson M, Mars AE, et al. Microbial production of short and medium chain esters: enzymes, pathways, and applications. *Biotechnol Adv.* (2019) 37:107407. doi: 10.1016/j.biotechadv.2019.06.006

51. Fang G-Y, Chai L-J, Zhong X-Z, Lu Z-M, Zhang X-J, Wu L-H, et al. Comparative genomics unveils the habitat adaptation and metabolic profiles of clostridium in an artificial ecosystem for liquor production. *Msystems.* (2022):e297–322. doi: 10.1128/msystems.00297-22

52. Lawson Anani Soh A, Ralambotiana H, Ollivier B, Prensier G, Tine E, Garcia JL. *Clostridium thermopalmarium* sp. nov., a moderately thermophilic butyrate-producing bacterium isolated from palm wine in senegal. *Syst Appl Microbiol.* (1991) 14:135–9. doi: 10.1016/S0723-2020(11)80291-2

53. Xu Y, Zhao J, Liu X, Zhang C, Zhao Z, Li X, et al. Flavor mystery of Chinese traditional fermented baijiu: the great contribution of ester compounds. *Food Chem.* (2022) 369:130920. doi: 10.1016/j.foodchem.2021.130920

54. Hawthorne DB, Shaw RD, Davine DF, Kavanagh TE, Clarke BJ. Butyric acid off-flavors in beer: origins and control. *J Am Soc Brew Chem.* (1991) 49:4. doi: 10.1094/asbj-49-0004

55. Denny T. Plant pathogenic *Ralstonia* species. *Plant Assoc Bact.* (2006) 2006:573–644. doi: 10.1007/978-1-4020-4538-7_16

56. Ryan MP, Adley CC. *Ralstonia* spp.: emerging global opportunistic pathogens. *Eur J Clin Microbiol Infect Dis.* (2014) 33:291–304. doi: 10.1007/s10096-013-1975-9

57. Dan T, Chen H, Li T, Tian J, Ren W, Zhang H, et al. Influence of *Lactobacillus* plantarum P-8 on fermented milk flavor and storage stability. *Front Microbiol.* (2019) 9:3133. doi: 10.3389/fmicb.2018.03133

58. Sarry JE, Günata Z. Plant and microbial glycoside hydrolases: volatile release from glycosidic aroma precursors. *Food Chem.* (2004) 87:509–21. doi: 10.1016/j.foodchem.2004.01.003

59. Klerk D. *Co-Expression of Aroma Liberating Enzymes in a Wine Yeast Strain.* Ph.D. thesis. Matieland: Institute for Wine Biotechnology (2009). p. 86–7.

60. Melgarejo P, Calín-Sánchez Á, Vázquez-Araújo L, Hernández F, Martínez JJ, Legua P, et al. Volatile composition of pomegranates from 9 Spanish cultivars using headspace solid phase microextraction. *J Food Sci.* (2011) 76:S114–20. doi: 10.1111/j.1750-3841.2010.01945.x

61. Liu Y, Chen H, Chen W, Zhong Q, Zhang G, Chen W. Beneficial effects of tomato juice fermented by *lactobacillus plantarum* and *Lactobacillus Casei*: antioxidation, antimicrobial effect, and volatile profiles. *Molecules.* (2018) 23:2366. doi: 10.3390/molecules23092366

62. Genovese A, Gambuti A, Piombino P, Moio L. Sensory properties and aroma compounds of sweet Fiano wine. *Food Chem.* (2007) 103:1228–36. doi: 10.1016/j.foodchem.2006.10.027

63. Hong M, Li J, Chen Y, Qi B, Huang Y, Wu J, et al. Impact of mixed non-Saccharomyces yeast during fermentation on volatile aroma compounds of Vidal blanc icewine. *Lwt Food Sci Technol.* (2021) 145:111342. doi: 10.1016/j.lwt.2021.111342

64. Hu Y, Zhang L, Wen R, Chen Q, Kong B. Role of lactic acid bacteria in flavor development in traditional Chinese fermented foods: A review. *Crit Rev Food Sci.* (2022) 62:2741–55. doi: 10.1080/10408398.2020.1858269

65. Jung M, Kim J, Lee SH, Whon TW, Sung H, Bae J, et al. Role of combinated lactic acid bacteria in bacterial, viral, and metabolite dynamics during fermentation of vegetable food, kimchi. *Food Res Int.* (2022) 157:111261. doi: 10.1016/j.foodres.2022.111261

66. Sevindik O, Guclu G, Agirman B, Selli S, Kadiroglu P, Bordiga M, et al. Impacts of selected lactic acid bacteria strains on the aroma and bioactive compositions of fermented gilaburu (*Viburnum opulus*) juices. *Food Chem.* (2022) 378:132079. doi: 10.1016/j.foodchem.2022.132079

67. Pang X, Chen C, Huang X, Yan Y, Chen J, Han B. Influence of indigenous lactic acid bacteria on the volatile flavor profile of light-flavor Baijiu. *LWT* (2021) 147:111540. doi: 10.1016/j.lwt.2021.111540

68. Xu X, Wu B, Zhao W, Lao F, Chen F, Liao X, et al. Shifts in autochthonous microbial diversity and volatile metabolites during the fermentation of chili pepper (*Capsicum frutescens* L.). *Food Chem.* (2021) 335:127512. doi: 10.1016/j.foodchem.2020.127512

frontiers | Frontiers in Nutrition

TYPE Original Research
PUBLISHED 10 November 2022
DOI 10.3389/fnut.2022.1000271

OPEN ACCESS

EDITED BY
Yanyan Zhang,
University of Hohenheim, Germany

REVIEWED BY
Yucheng Zheng,
Fujian Agriculture and Forestry University, China
Yi Yu,
Wuhan University, China
Manjunatha Gowda,
Indian Institute of Horticultural Research (ICAR), India

*CORRESPONDENCE
Ning Liu
liuning@nercv.org
Zhanhui Wu
wuzhanhui@nercv.org

SPECIALTY SECTION
This article was submitted to Food Chemistry, a section of the journal Frontiers in Nutrition

RECEIVED 22 July 2022
ACCEPTED 24 October 2022
PUBLISHED 10 November 2022

CITATION
Liu N, Hu M, Liang H, Tong J, Xie L, Wang B, Ji Y, Han B, He H, Liu M and Wu Z (2022) Physiological, transcriptomic, and metabolic analyses reveal that mild salinity improves the growth, nutrition, and flavor properties of hydroponic Chinese chive (*Allium tuberosum* Rottler ex Spr). *Front. Nutr.* 9:1000271. doi: 10.3389/fnut.2022.1000271

Physiological, transcriptomic, and metabolic analyses reveal that mild salinity improves the growth, nutrition, and flavor properties of hydroponic Chinese chive (*Allium tuberosum* Rottler ex Spr)

Ning Liu[1,2]*, Manman Hu[1,2], Hao Liang[1,2], Jing Tong[1,2], Long Xie[1,2], Baoju Wang[1,2], Yanhai Ji[1,2], Beibei Han[1,2], Hongju He[1,3], Mingchi Liu[1,2] and Zhanhui Wu[1,2]*

[1]National Engineering Research Center for Vegetables (Institute of Vegetable Sciences), Beijing Academy of Agriculture and Forestry Sciences, Beijing, China, [2]Key Laboratory of Urban Agriculture (North China), Ministry of Agriculture and Rural Affairs, Beijing, China, [3]Institute of Agri-Food Processing Science, Beijing Academy of Agriculture and Forestry Sciences, Beijing, China

Environmental stressors such as salinity have pronounced impacts on the growth, productivity, nutrition, and flavor of horticultural crops, though yield loss sometimes is inevitable. In this study, the salinity influences were evaluated using hydroponic Chinese chive (*Allium tuberosum*) treated with different concentrations of sodium chloride. The results demonstrated that lower salinity could stimulate plant growth and yield. Accordingly, the contents of soluble sugar, ascorbic acid, and soluble protein in leaf tissues increased, following the decrease of the nitrate content, under mild salinity (6.25 or 12.5 mM NaCl). However, a higher level of salinity (25 or 50 mM NaCl) resulted in growth inhibition, yield reduction, and leaf quality deterioration of hydroponic chive plants. Intriguingly, the chive flavor was boosted by the salinity, as evidenced by pungency analysis of salinity-treated leaf tissues. UPLC-MS/MS analysis reveals that mild salinity promoted the accumulation of glutamic acid, serine, glycine, and proline in leaf tissues, and thereby enhanced the umami and sweet flavors of Chinese chive upon salinity stress. Considering the balance between yield and flavor, mild salinity could conduce to hydroponic Chinese chive cultivation. Transcriptome analysis revealed that enhanced pungency could be ascribed to a salt stress-inducible gene, *AtuFMO1*, associated with the biosynthesis of S-alk(en)yl cysteine sulphoxides (CSOs). Furthermore, correlation analysis suggested that

two transcription factors, AtubHLH and AtuB3, were potential regulators of *AtuFMO1* expressions under salinity. Thus, these results revealed the molecular mechanism underlying mild salinity-induced CSO biosynthesis, as well as a practical possibility for producing high-quality Chinese chive hydroponically.

KEYWORDS

***Allium tuberosum*, cysteine sulphoxides, hydroponics, flavor, crop growth, mild salinity**

Introduction

Chinese chive (*Allium tuberosum* Rottler ex Spr), a leafy vegetable belonging to the *Allium* genus, has been widely cultivated in China, Japan, India, and many other Asian countries. The leaves, flowers, and tender inflorescences of Chinese chive were, and are, consumed primarily owing to its pungent and sweet flavor, and the ability to enhance the flavor of other foods (1). The unique flavor of Chinese chive is largely attributed to its ability to biosynthesize a series of sulfur-containing metabolites, namely S-alk(en)yl cysteine sulphoxides (CSOs), stored in the cytoplasm (1, 2). CSOs are non-volatile, odorless, and chemically stable molecules and are the flavor precursors of *Allium* crops (1, 3). Upon the damage of plant tissues through cooking, chewing, or chopping, alliinase compartmentalized in the vacuoles hydrolyzes CSOs, thereby producing sulfenic acid, pyruvic acid, and ammonia. Subsequently, the spontaneous degradation of sulfenic acids generates an array of odorous, volatile, sulfur-containing compounds, which make essential contributions to the final taste and smell (4, 5). Furthermore, many of these breakdown products are known for their chemopreventive properties (6, 7), and therefore Chinese chive as a promisingly functional vegetable becomes more and more popular in the current food inventory.

Inspired by the urgent demand for safer and more sustainable food production, a hydroponic system has been employed in Chinese chive cultivation. The synthetic "underground" environment nearly eradicates the occurrence of chive gnat (*Bradysia odoriphaga*), which is cryptic in the rooting soil and inflicts more than half yield loss annually in North China (8). As a result, the application of high toxic insecticides could be dramatically reduced under the new production style. Unexpectedly, the leafy tissues of hydroponic chive often taste less pungent presumably due to the reduced secondary metabolism and enhanced primary metabolism in hydroponic Chinese chive (9). Indeed, the sufficient nutrient supply and excellent growth conditions favor the primary metabolism, resulting in lower accumulation of nutrition-related, secondary metabolites in hydroponic vegetables. Several definitive studies also reported that the nutrient and flavor deterioration of hydroponic vegetables is a major cause of consumer complaints (10), suggesting it is a common issue frustrating hydroponic farmer. With respect to the hydroponic chive, the decline of flavor intensity is primarily associated with the reduction of total CSO accumulations in its leafy tissues (9). Considering that people usually favor soil-grown products with a much stronger pungency, it becomes necessary to increase the flavor intensity of hydroponic Chinese chive to ensure the sustainable development of the hydroponic sector.

The CSO biosynthesis pathways have been investigated in *Allium* species (11–13). Initially, plants uptake and assimilate sulfate into cysteine, methionine, and thereafter glutathione, and in *Allium* species, further convert to CSOs that are essential for flavor production and the repertoire of nitrogen and sulfur (1). The CSO metabolic process is very complicated involving many enzymes and regulatory proteins. Sulfate uptake and distribution are managed by a family of sulfate transporters (SULTRs) in different plant organs or tissues (14). The sulfur assimilation pathway has been investigated intensively, and analysis of Arabidopsis mutant has identified several genes encoding key enzymes, such as ATP-sulfurylase (ATPS), adenosine-5'-phosphosulfate reductase (APR), sulfite reductase (SiR), O-acetylserine sulfhydrylase (OASTL), in transition from inorganic sulfur to cysteine (14). The production of GSH is catalyzed by two enzymes, cysteine ligase (GCL) and glutathione synthetase (GS), and glutathione serves as the direct substrate for CSO biosynthesis (15). Only two groups of enzymes, γ-glutamyl transpeptidase (GGT) which catalyzes the removal of the γ-glutamyl group from the biosynthetic intermediates, and flavin-containing monooxygenase (FMO) which catalyzes the sulfide into sulfoxide, were characterized to date (16, 17). Although the CSO metabolic pathways have been explored in several *Allium* species (11, 18), limited information is available on the effects of environmental stimuli on the CSO biosynthesis, and the corresponding regulation mechanisms at the molecular level remains intangible.

Environmental stressors such as salinity, drought, high/low temperature, and UV-irradiation have pronounced impacts on the nutrients, flavor, and taste in horticultural products, though yield loss sometimes is unavoidable under such stressed conditions. Under sub-optimal or adverse growth conditions,

plants enhance the production of secondary metabolites that play major roles in the adaptation of plants to the stress conditions (19). On the other hand, the accumulation of such metabolites contributes to the specific odors, tastes, and smells in horticultural plants. For example, 100 mM NaCl treatment could promote the accumulation of methyl cysteine sulfoxide, thus increasing the pungency of the onion bulb (20). In tomato cultivations, saline irrigation has been successfully employed in improving the vegetable quality in terms of carbohydrates, carotenoids, organic acids, and amino acids in fruits (21). However, the salinity effects on vegetable growth and quality are still controversial. Most studies on salt stress and tolerance have revealed that severe salinity impedes vegetable growth and performance. A recent study on onion seedlings argued that sulfur metabolism remained unaffected by salinity stresses (22). According to these findings, it seems that the plant responsive behaviors are determined to a large extent by the salinity levels, and an appropriate level of salinity has potential to promote the quality of horticultural plants.

Considering that salinity levels could be easily and accurately manipulated in the hydroponic system, it is plausible that salinity stress might be an efficient approach to stimulate the biosynthesis of CSOs in chive plants subjected to sub-optimal growth conditions. Nevertheless, in the current literature, there are few studies on the adaptations to various salinity concentrations, especially on the effects on growth and nutritional profiles, in Chinese chive. Therefore, our study aims to identify the threshold concentration of salinity in hydroponic Chinese chive cultivations that could improve the flavor without a loss in crop productivity. Furthermore, the regulatory mechanisms of salinity-induced CSO biosynthesis were also investigated *via* integrated transcriptome and targeted metabolome analysis. These findings attempt to develop a practical technique for improving the flavor of Chinese chive cultivated hydroponically and to explore the underlying molecular mechanism of CSO biosynthesis in response to salinity.

Materials and methods

Plant material, growth conditions, and salinity treatments

Seeds of *A. tuberosum* cultivar "791" were sown in a 32-cell tray with granulated rockwool irrigated with 1/4 strength of Hoagland's medium once a day. On May 4, 2018, 2-month-old seedlings were transplanted to a hydroponic system using the deep flow technique (DFT) under LED lamps and 10/14 h light/dark photoperiod. The temperature and relatively humidity conditions in the greenhouse were 22 ± 3°C/18 ± 3°C (day/night) and 60–70%, respectively. The chive plants were supplied with the nutrient solution as previously described (23). The pH and the electrical conductivity (EC) of the nutrient solution were adjusted to 6.5 and 1.4 dS m^{-1}, respectively. The nutrient solutions used in the hydroponic cultivation system were renewed twice a month. In the first year, Chinese chive plants were kept growing without any harvesting in order to promote rhizome growth. Chinese chive plant is perennial vegetable, and the major edible parts are its aboveground organs including leaf and pseudostem. According to the agricultural practice for hydroponic Chinese chive, the aboveground tissues (leaves) were harvested its once a month since 2021. On May 1, 2022, the 3-year-old plants were subjected to different salt stress treatments. For hardening to salinity stress, 3-yearold chive plants were exposed to 6.25 mM NaCl (EC 2.0 dS m^{-1}), 12.5 mM NaCl (EC 2.7 dS m^{-1}), 25 mM NaCl (EC 3.4 dS m^{-1}), and 50 mM NaCl (EC 4.8 dS m^{-1}) by adding NaCl to nutrient solutions. After 30-day-growth, leaf tissues were sampled from chive plants grown in the nutrient solution supplemented with 6.25 mM (S1), 12.5 mM (S2), 25 mM (S3), or 50 mM (S4) NaCl. The leaf tissues collected from untreated Chinese chive plants (Con) was used as controls. For RNA extraction experiments, these samples collected from at least 10 individual chive plants were immediately frozen in liquid nitrogen, and then stored in -80°C until use. Sample collections were performed on separate days for three biological replicates.

Leaf quality assessment

The indicators of leaf quality include soluble sugar content (SS), total soluble protein content (TSP), ascorbic acid content (AsA), nitrate content (Nit), chlorophyll a content (Chl a), chlorophyll b content (Chl a), and carotenoids content (Car). Analysis of leaf quality was conducted using the third and fourth mature leaves of 30-day harvesting plants, which reflected the common practice in the commercial production of hydroponic Chinese chive. All indicators were determined by referring to previous methods (24).

Identification and quantitative analysis of free amino acids and their metabolites

Amino acids and their metabolites were analyzed by MetWare Biotechnology Co., Ltd. (Wuhan, China) based on the AB Sciex QTRAP 6500 LC-MS/MS platform. The leaf samples were vacuum freeze-dried and then grounded into powder using a homogenizer (MM400, Retsch, Germany). 50 mg of powder were dissolved in 500 μL 70% methanol (v/v) and vortexed for 3 min. After centrifugation at 12,000 r/min for 10 min at 4°C, 300 μL of supernatant was transferred into a new centrifuge tube and was stored the supernatant in a -20°C freezer for 30 min. Then the supernatant was centrifuged again at 12,000

r/min for 10 min at 4°C. After centrifugation, transfer 200 μL of supernatant through Protein Precipitation Plate for further LC-MS analysis.

Ultra-performance liquid chromatography (UPLC) was performed using the Shimadzu Nexera X2 instrument (Shimadzu, Japan) equipped with an ACQUITY BEH Amide column (1.7 μm, 2.1 × 100 mm). The mobile phase was composed of ultrapure water with 2 mM ammonium acetate and 0.04% formic acid (solvent A) and acetonitrile with 2 mM ammonium acetate and 0.04% formic acid (solvent B). The gradient was started at 90% B (0–1.2 min); decreased to 60% B (9 min); 40% B (10–11 min); finally ramped back to 90% B (11.01–15 min). The column temperature was set to 40°C, and the injection volume was 2 μ L.

AB 6500^{+} QTRAP® LC-MS/MS System, equipped with an ESI Turbo Ion-Spray interface, operating in both positive and negative ion modes. The ESI source operation was carried out as follows: turbo spray in the ion source, 550°C for source temperature; ionic spray (IS) voltage, 5,500 V (positive ion mode)/-4,500 (negative ion mode); Curtain gas (CUR) was set at 35.0 psi; DP and CE for individual MRM transitions were done with further DP and CE optimization. A specific set of MRM transitions were monitored for each period according to the amino acid eluted within this period. All experiments were conducted on three replicates.

Pungency measurement

The pungency of Chinese chive was analyzed using the onion procedure with a few modifications (11). Leaf samples were homogenized and centrifuged to obtain the clean juice of the Chinese chive, and the 20-fold diluted juice was split in half. One-half juice was mixed with an equal volume of 2.5% trichloroacetic acid immediately to deactivate the juice alliinase for the background pyruvate acid; the other half was incubated at room temperature for 3 min. After that, both were reacted with an equal volume of 0.0125% 2, 4-dinitrophenyl hydrazine at 37°C for 5 min. Then 5 volume of 0.6 M NaOH was added to terminate the reaction, and the absorbance was measured by spectrophotometer at the wavelength of 520 nm. Pyruvate determinations were made against a sodium pyruvate standard curve.

Transcriptome analysis

Total RNA was extracted with Trizol according to the manufacturer's instructions. RNA quantity and quality were examined using a NanoDrop 2000 spectrophotometer (Thermo Fisher Scientific, USA) to ensure structural integrity for further experiments. RNA-Seq libraries were prepared were sequenced at the Illumina NovaSeq 6000 platform to an average depth of 50 million reads per sample.

Sequence reads were filtered using SeqPrep[1] and Sickle[2] to remove the low-quality and adaptor sequences. Clean reads were assembled *via* the Trinity de novo assembly program[3] and TransRate.[4] Sequences were handled with CD-HIT[5] program to reduce the transcript redundancy, and finally, the assembly quality was evaluated using BUSCO (Benchmarking Universal Single-Copy Orthologs)[6] program with default configurations. Finally, several databases including Non-redundant (Nr) database,[7] Pfam,[8] Swiss-Prot,[9] COG (Clusters of Orthologous Groups of proteins),[10] Gene Ontology (GO) database,[11] were used to perform functional annotation on the unigenes, and the E-value was set to 1×10^{-3}.

Bowtie program (version 0.12.7) was applied to map clean reads to all the assembled transcripts by the "single-end" method with parameter "-v 3 -a –phred64-quals." The number of mapped clean reads for each unigene was then counted and normalized into reads per kb per million reads (RPKM) to calculate the expression level of the unigene. Three data sets from the same organ or tissues were treated as a group, and differential expression analysis of two groups was performed using the DESeq R package (version 1.10.1). In this analysis, the false discovery rate (FDR) was used to calculate the threshold *P*-value in significance tests, and then the results of *P*-values were adjusted by Benjamin and Hochberg's method. FDR < 0.001 and $p < 0.05$ as the threshold to determine significant differences in comparisons between two samples.

Quantitative reverse-transcription PCR

Total RNA isolation, reverse transcription with oligo $(dT)_{18}$ (Invitrogen, USA), and quantitative reverse-transcription PCR were performed as described previously (25). The gene expression analysis was performed using TB Green premix (Takara Biotech., Dalian, China) on a CFX96 Real-Time PCR system (BioRad, Hercules, USA). The reaction protocol followed the manufacturer's instructions: 1 cycle at 98°C for 30 s; 45 cycles at 95°C for 5 s, 58°C for 30 s, and 72°C for 30 s; and 4°C until removal. A housekeeping gene DN253_c0_g1 was used as internal control for expression analyses (26). The sequences of specific primers are listed in **Supplementary Table 1**.

1 https://github.com/jstjohn/SeqPrep
2 https://github.com/najoshi/sickle
3 https://github.com/trinityrnaseq/trinityrnaseq
4 http://hibberdlab.com/transrate/
5 https://www.bioinformatics.org/cd-hit/
6 http://busco.ezlab.org
7 http://www.ncbi.nlm.nih.gov
8 http://pfam.xfam.org/
9 http://web.expasy.org/docs/swiss-prot_guideline.html
10 http://www.ncbi.nlm.nih.gov/COG/
11 http://geneontology.org

Statistical analysis

IBM SPSS Statistics for Windows version 25.0 (IBM Corp., USA) and GraphPad Prism version 8.0 (GraphPad Software, USA) were used for statistical analyses. Turkey's multiple range test and one-way ANOVA were used to compare differences between treatment and control groups.

Results

Effects of salinity stress on the plant growth and yield in hydroponic Chinese chive

The growth and yield of hydroponic Chinese chive were remarkably influenced by different concentrations of sodium chloride in the nutrient solutions (**Figure 1A**). S1 (6.25 mM) and S2 (12.5 mM) could stimulate plant growth, and the plant height, leaf length, leaf width, leaf number, and biomass were higher than that of controls (**Figures 1A,B**). The treatments with S3 (25.0 mM) and S4 (50 mM) inhibited plant growth, and these plants exhibited stress symptoms of wilting, leaf senescence, reduced height, and biomass (**Figures 1A,B**), and S4 plants finally failed to produce aboveground tissues after the second harvest. Accordingly, the theoretical yield of Chinese chive was slightly increased under S1 or S2 treatments, while it decreased dramatically under S3 and S4 treatments (**Figure 1C**). Thus, the results suggested that a low concentration of NaCl (S1 or S2) could promote the growth of Chinese chive, whereas higher concentrations (S3 or S4) disrupted the normal growth, and even resulted in the plant death.

To investigate the salinity effects on the rhizome zone/organs in Chinese chive, root activity was also analyzed using triphenyltetrazolium chloride (TTC) method. The results suggested that three was no significant difference in root activities under S1 and S2 treatments, whereas root activities were significantly reduced under S3 and S4 treatments (**Figure 1C**). The expression of two marker genes that correlated with environmental stresses was analyzed, and the qRT-PCR data suggested that either lower concentrations (S1 and S2) or higher concentrations (S3 and S4) of NaCl did induce the expression of two abiotic stress marker genes, AtuLTI 6B and AtuLTP (**Figure 1D**), suggesting that the exposure to NaCl did stimulate plant responses to salinity stress at the molecular levels. Thus, S3 and S4 might represent the moderate (or high) salinity whereas S1 and S2 might be defined as the mild salinity according to the severity of adverse effects on the plants.

Effects of salinity stress on the leaf quality

As the leaf is the common edible part of the Chinese chive, the representative quality traits of leaf tissues were analyzed in this study. The content of photosynthetic pigments was significantly influenced by the different concentrations of NaCl treatments. The results showed that the contents of chlorophyll a and b, total chlorophyll were significantly higher under S1 and S2 treatments; On the contrary, the contents of chlorophyll were decreased dramatically under S3 and S4 treatments (**Table 1**). In particular, the content of total chlorophyll reached the peak at S1 or S2, and increased by 1.28, 1.27 times compared to the controls. Additionally, the content of carotenoids was significantly reduced in four salinity-treated samples.

When plants were treated by salinity, the contents of soluble sugar, ascorbic acid, and soluble protein were higher than that of control in the presence of 6.25 mM NaCl, albeit they significantly increased under 12.5 mM NaCl treatment (**Figure 2A**), However, the nutritional quality of Chinese chive was markedly declined with the continuing increase of salinity levels such as S3 and S4 (**Figure 2A**). Besides, the nitrate content in the leaves decreased significantly, however, no significant difference between salinity treatments was observed (**Figure 2A**), suggesting that the reductions were independent of salt concentrations.

To investigate the salinity effects on the flavor, a pungency test was conducted by measuring the enzymatically produced pyruvate (EPY) of leaf tissues under various salinity treatments. Strikingly, the pungency level exhibited about a twofold increase in S1 treatment and probably reached its peak at S2 treatment (**Figure 2B**). Unexpectedly, the pungency of chive plants decreased with the elevation of salt stress whereas it was still significantly higher than that of controls (**Figure 2B**). Together, the results suggested that mild salinity could contribute to the improvements in leaf quality and flavor intensity, whereas exposure of chive plants to moderate or high salinity could cause the deterioration in leaf quality.

Leaf amino acid and derivatives profiles of NaCl-treated Chinese chive

The contents of free amino acids (FAA) and derivatives were investigated with leaves of salinity-treated hydroponic chive plants. A total of 20 amino acids, including 9 essential amino acids, were identified in all leaf samples. **Table 2** shows the list of all amino acids and their content in mg·100 g^{-1} among different samples. To a large extent, the composition of FAAs was similar between the stressed and control samples. In leaf tissues, glutamic acid was the most abundant amino acid,

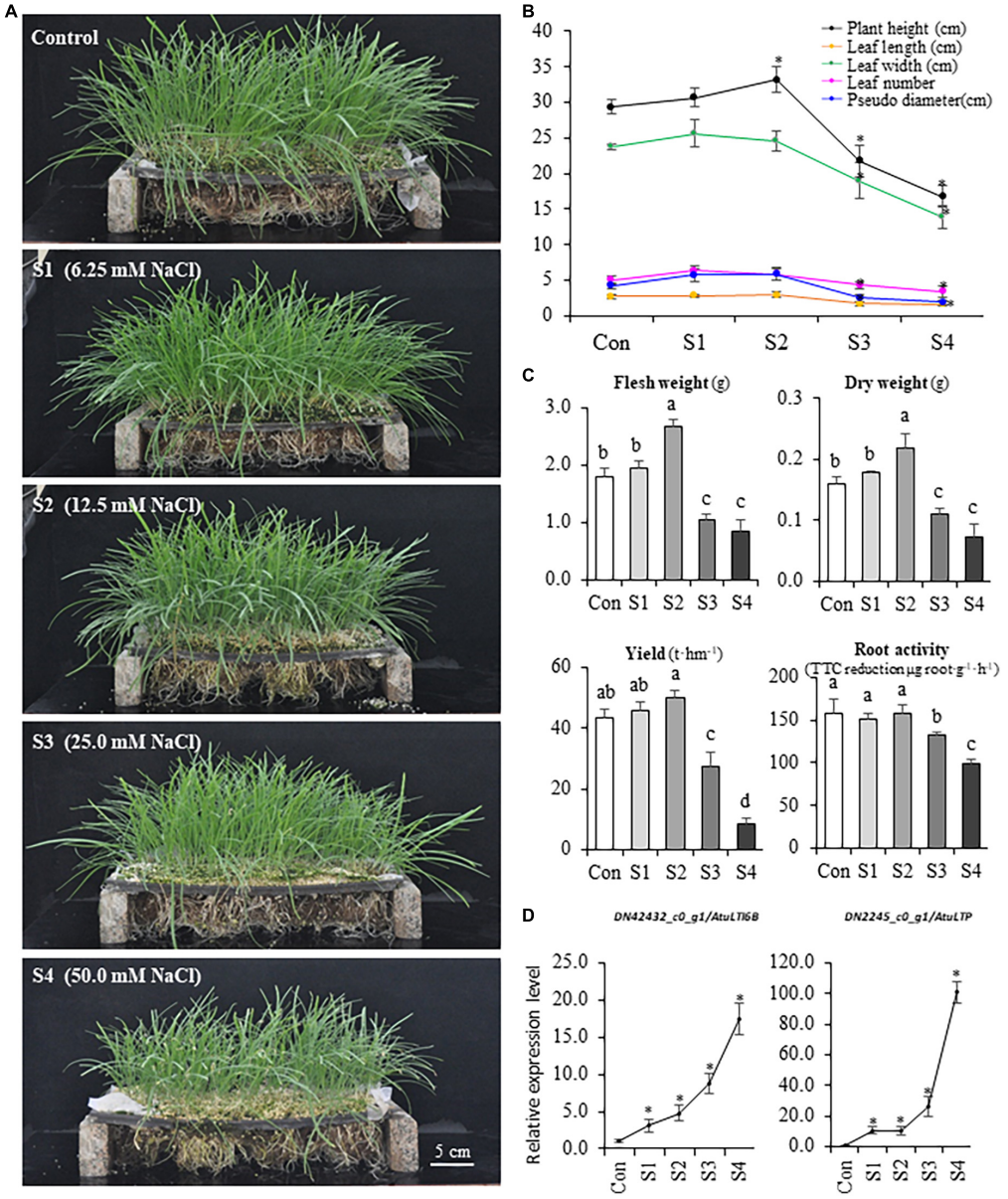

FIGURE 1
The variations of phenotype and physiology of Chinese chive under different levels of salinity. **(A)** Phenotypes of hydroponic Chinese chive plants grown under different NaCl concentrations for 30 days. **(B)** Changes of plant height, leaf width, leaf length, leaf number, and pseudo-stem diameter under salinity treatments. **(C)** Changes of fresh weight, dry weight, yield, and root activity of salinity- treated Chinese chive plants. Results represent the means ± *SD* of 10 replicates. **(D)** Expression patterns of stress marker genes. Data are means ± *SD* of three biological replicates. Different letters indicate significant differences at $p < 0.05$ determined by one-way ANOVA, while stars represent significant differences between treatments and controls according to the Student's *t*-test analysis ($p < 0.05$).

followed by glutamine, aspartic acid, asparagine, and serine, which account for 88.2–90.0% of total FAAs; nevertheless, other FAAs occurred in trace amounts in our analysis.

According to the flavor and taste of amino acids, they could be divided into four groups: umami, sweetness, bitterness, and tasteless (Table 2). The umami group includes glutamic and aspartic acids, whose content varied from 46.4 to 57.0% of total FAAs among different samples. The sweetness group was represented by glutamine, asparagine, serine, glycine, alanine, threonine, protein, etc., and these amino acids account for 41.6–52.1% of total FAAs in Chinese chive. Thus, our findings suggested that umami and sweet FAAs are major amino acids, which reflected the characteristic flavor of Chinese chive.

Generally speaking, the content of total FAAs gradually decreased in the leaf tissues with the increases in salinity levels, albeit different amino acids showed their specific responses

TABLE 1 Photosynthetic pigments of hydroponic Chinese chive under different saline cultures.

	Chl a ($mg \cdot g^{-1}$)	Chl b ($mg \cdot g^{-1}$)	Total Chl ($mg \cdot g^{-1}$)	Car ($mg \cdot g^{-1}$)
Con	0.57 ± 0.09b	0.27 ± 0.09b	0.85 ± 0.03b	0.18 ± 0.03a
S1	0.75 ± 0.07a	0.33 ± 0.03a	1.09 ± 0.05a	0.12 ± 0.02b
S2	0.73 ± 0.06a	0.35 ± 0.02a	1.08 ± 0.05a	0.10 ± 0.02b
S3	0.49 ± 0.03c	0.22 ± 0.01c	0.73 ± 0.05c	0.09 ± 0.01b
S4	0.46 ± 0.07c	0.22 ± 0.03c	0.71 ± 0.04c	0.09 ± 0.01b

All data are expressed as mean ± standard deviation ($n = 6$). Means within each column and main effect followed by different letters are significantly different ($p < 0.05$) according to Turkey's multiple-range test.

upon the salinity treatments. A heatmap is provided to illustrate the metabolic variations of FAAs in salinity-treated samples (Figure 2C). According to their responsive profiles under different levels of salinity, the FAAs could be simply divided into two groups (Figure 2C). Group I include proline, serine, tryptophan, glutamic acid, cysteine, isoleucine, and leucine, concentrations of which increased in response to salt stresses. For example, salinity treatments affected proline most remarkably, as its concentrations in S3 samples doubled compared to the controls in leaf samples. Notably, several CSO biosynthesis-related amino acids, like serine, cysteine, and glutamic acid, exhibited relatively maximum accumulation in S1 or S2 samples. The second group consisted of aspartic acid, asparagine, glycine, arginine, etc., and their contents decreased or keep unchanged under different salinity stresses (Figure 2C).

Other than FAAs, a total of 51 amino acid derivatives were identified in our metabolic analysis. Among them, glutathione represented the most abundant organosulfur metabolite (Supplementary Table 3), suggesting that Chinese chive might use glutathione as a sulfur reservoir; however, others occurred at trace level (< 0.01 mg g^{-1}). A heatmap was made to compare the accumulation profiles of eight non-proteinogenic, s-containing amino acids (Figure 2D). The results indicated that the accumulation patterns of glutathione, S-sulfo-L-cysteine, and D-homocysteine are similar to cysteine, glutamic acid, and serine. Besides, Succinic-Acid, γ-Aminobutyric acid and L-Citrulline were abundant derivatives in Chinese chive (Supplementary Table 3). Of these derivatives, the relatively high abundance of γ-Aminobutyric acid is noteworthy as it has been widely used as a dietary supplement.

Transcriptomic analysis of Chinese chive under salinity stresses

Leaf samples from salinity-treated (S1, S2, and S3) and control plants were used for transcriptome sequencing. 50 mM NaCl-treated samples (S4) were excluded from the transcriptome analysis due to the severe loss of crop yield and economic values. In the experiments, a total of 93.96 Gb of clean reads were obtained from 12 RNA-Sequencing libraries, and the average Q30 value is 94.96%, suggesting a high sequencing accuracy in the RNA-Seq experiments (Supplementary Table 4). The mapping ratio varied from 79.39 to 81.73%, which indicated that the transcriptome assembly had good sequencing read coverage. Principle Component Analysis (PCA) analysis suggested that samples from S1 and S2 groups were clustered closely (Supplementary Figure 1A), implying that the distance between them was relatively close. Samples from other groups were clustered separately. Therefore, the result exhibited a scattered distribution of S1/2, S3, and control, which indicated that the transcriptomic data were suitable for further analysis. After de novo assembly and redundancy reduction, 197,470 unigenes with an E90N50 size of 2,278 bp and GC content of 35.97%, were generated for further analysis (Supplementary Table 5). The average BUSCO score was 72.9%, suggesting that the assembly has the most near-universal single-copy genes. All unigenes were further functionally annotated against public databases, namely, Nr, GO, KEGG, COG, SwissProt, and Pfam, and the results suggested that more than one-quarter of unigenes could match a sequence in the aforementioned database (Supplementary Table 6).

To identify differentially expressed genes (DEGs), the FPKM (fragments per kilobase of transcript per million mapped reads) value was calculated to analyze gene expression patterns, and DEGs were filtered by setting a threshold of $|\log2(\text{Fold Change})| \geq 1$ and FDR ≤ 0.05. A total of 2,840 DEGs were identified in our transcriptomic analysis. 154 (67 upregulated, 87 downregulated), 251 (78 upregulated, 173 downregulated), 1,723 (1,243 upregulated, 480 downregulated), 129 (69 upregulated, 60 downregulated), and 1,324 (1,056 upregulated, 268 downregulated), and 1,806 (1,315 upregulated, 491 downregulated) DEGs were obtained among Con vs. S1, Con vs. S2, Con vs. S3, S1 vs. S2, S2 vs. S3, and S1 vs. S3, respectively (Figure 3A and Supplementary Figure 1B). Consistent with the growth phenotypes, a larger number of DEGs in S3 vs. control and S3 vs. S1 comparisons were observed, whereas there were fewer DEGs identified from Con vs. S1 and S1 vs. S2 comparisons (Figure 3B). The results provide additional supporting evidence that S1 or S2 represented mild stresses because they only mobilized a small number of genes, while moderate stress (S3) could induce the expression of more genes under a harsher environment.

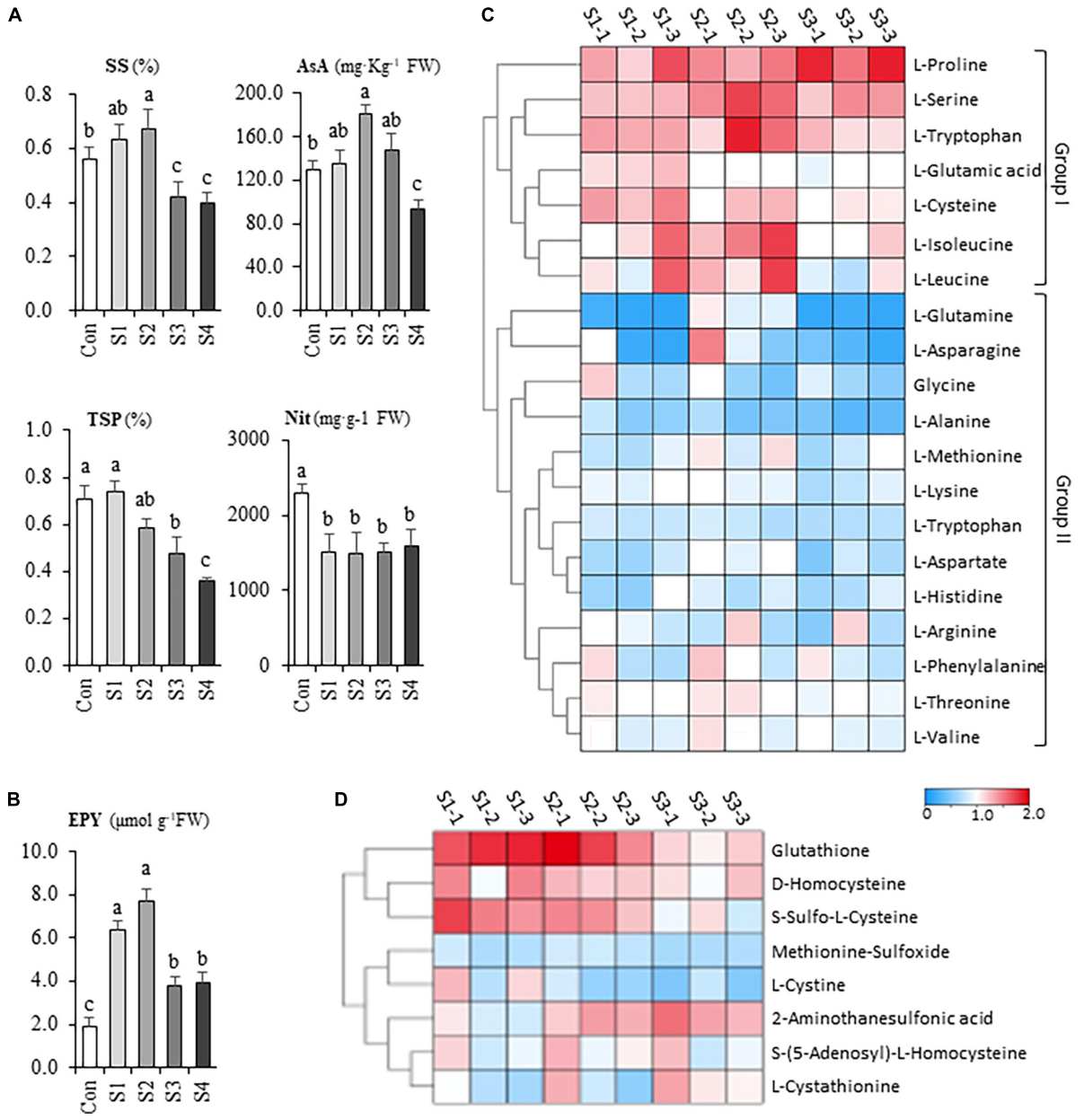

FIGURE 2
The salinity effects on the nutritional and flavor property of hydroponic Chinese chive. **(A)** The contents of soluble sugar (SS), ascorbic acid (AsA), total soluble protein (TSP), nitrate (Nit) of Chinese chive under various salinity treatments. **(B)** The gross flavor intensity assay of leaf tissues in salt stress-treated Chinese chive. Flavor intensity was estimated by the yield of the enzymatically produced pyruvate (EPY) derived from the hydrolysis reaction of cysteine sulfoxides. Results represent the means ± *SD* of 10 replicates. Different letters indicate significant differences at $p < 0.05$ determined by one-way ANOVA. Cluster heatmaps indicate the fold changes of the contents in free amino acid **(C)** and S-containing derivatives **(D)** between salinity-treated samples and controls.

To obtain an overview of the functions of these DEGs between salinity treatments and controls, KEGG enrichment analysis was conducted with the DEGs identified from S1 vs. Con, S2 vs. Con, and S3 vs. Con comparisons. Interestingly, in addition to the pathways involved in MAPK signaling, plant hormone signal transduction, and other salt stress-responsive process, some sulfur-related, flavonoid biosynthesis, and glutathione metabolism pathways were also significantly enriched in all three comparison groups (Figure 3C). These results showed that the sulfur-metabolic pathways were implicated in plant responses to salinity stress.

A total of 2,840 DEGs were classified into 8 clusters by performing K-means analysis and hierarchical clustering (Figure 3D). Interestingly, DEGs in cluster_3 (91 unigenes)

TABLE 2 Changes of free amino acid content in hydroponic Chinese chive under different salinity stresses.

Free amino acids (μg·100 g^{-1})		Con	S1	S2	S3
Umami	Glu	716.65 ± 11.217 ^{c}	837.16 ± 119.46^{a}	761.89 ± 16.145^{ab}	702.22 ± 54.266^{c}
	Asp	428.65 ± 50.196	330.19 ± 24.254	322.25 ± 27.37	296.28 ± 40.393
Sweetness	Ser	144.74 ± 2.496^{c}	180.55 ± 4.922^{b}	230.14 ± 17.373^{a}	196.25 ± 16.013^{b}
	Ala	73.22 ± 16.109	57.78 ± 6.593	46.12 ± 11.246	45.91 ± 3.432
	Thr	71.62 ± 12.519	57.48 ± 8.307	68.07 ± 4.658	61.27 ± 2.204
	Gly	55.53 ± 24.118^{a}	37.13 ± 9.619^{b}	44.68 ± 7.373^{b}	14.66 ± 2.423^{c}
	Pro	16.49 ± 2.459^{b}	22.98 ± 3.347^{a}	23.50 ± 2.044^{a}	28.72 ± 1.358^{a}
	Gln	5.47 ± 0.548	5.58 ± 0.640	5.71 ± 0.143	5.27 ± 0.515
	Asn	1.80 ± 0.250^{a}	0.30 ± 0.029^{b}	1.66 ± 0.056^{a}	0.31 ± 0.078^{b}
Bitterness	His	14.18 ± 1.54	9.47 ± 1.704	13.09 ± 0.978	9.21 ± 3.338
	Arg	9.84 ± 2.454	6.53 ± 1.024	7.57 ± 0.889	6.89 ± 1.479
	Val	7.90 ± 0.962	7.18 ± 0.175	7.59 ± 0.248	7.15 ± 0.492
	Ile	2.11 ± 0.359^{b}	2.57 ± 0.135^{ab}	3.11 ± 0.201^{a}	2.25 ± 0.196^{b}
	Leu	2.14 ± 0.622^{ab}	2.4 ± 0.055^{ab}	2.83 ± 0.196^{a}	1.82 ± 0.115^{b}
	Met	0.65 ± 0.123^{a}	0.38 ± 0.009^{b}	0.33 ± 0.014^{b}	0.23 ± 0.004^{b}
	Trp	0.03 ± 0.001^{b}	0.04 ± 0.002^{ab}	0.04 ± 0.009^{a}	0.03 ± 0.004^{ab}
	Phe	0.50 ± 0.100	0.44 ± 0.028	0.42 ± 0.149	0.39 ± 0.188
Tasteless	Lys	11.43 ± 2.59	8.64 ± 1.213	11.27 ± 0.429	9.04 ± 2.678
	Tyr	4.36 ± 0.229^{a}	3.94 ± 0.150^{ab}	4.05 ± 0.127^{ab}	3.30 ± 0.579^{b}
	Cys	0.33 ± 0.006^{b}	0.45 ± 0.046^{a}	0.40 ± 0.051^{ab}	0.35 ± 0.030^{b}
Total		2306.6 ± 198.740^{a}	2137.5 ± 196.215^{ab}	2278.1 ± 85.339^{a}	1953.4 ± 180.126^{b}

Values are expressed as average ± standard deviation ($n = 3$). These lowercase superscript letters within the same line denote significant differences between means at $p < 0.05$.

and cluster_6 (102 unigenes) whose expression reached their peaks at either S1 or S2, were worthy of particular interest (**Figure 3E**), because these expression behaviors might be associated with their potential roles in metabolic responses to mild salinity. Although no significant pathways were enriched among cluster_3 DEGs, cluster_6 DEGs enriched several sulfur-metabolic processes, such as glutathione metabolism, cysteine and methionine metabolism, and sulfur metabolism, among the top 20 enrichment pathways (**Supplementary Figure 1C**). Given that pathway enrichment results, DEGs in cluster_6 might play crucial and active roles in plant salt tolerance, as well as leaf nutritional and flavor attributes.

Expression analysis of the differentially expressed genes associated with cysteine sulphoxide biosynthesis

Since the sulfate assimilation and CSO biosynthesis pathways in Chinese chive have been explored in our previous study (11), emphasis was put on the expression changes of genes related to the sulfur and CSO metabolism. In this analysis, seven DEGs were annotated as sulfate metabolism-related enzymes such as sulfate transporters (SULTRs), sulfite reductase (SiR), glutathione synthetase (GS), and flavin-containing monooxygenase (FMO), which are involved in sulfur transportation, assimilation, or CSO biosynthesis pathways (**Figure 4A**). According to the presence of an expression peak at S1/2 or S3, these DEGs could be simply classified into two groups. DEGs in the first group were upregulated with the elevation of salinity levels and were represented by *AtuSULTR1.1*/DN140030_c0_g1, *AtuGS1*/DN22568_c0_g1, and *AtuGS2*/DN22568_c0_g2 genes. In contrast, expression of the second group gene, such as *AtuFMO1*/DN32881_c0_g1, *AtuSiR*/DN7313_c0_g2, *AtuGS2*/DN26059_c0_g1, and *AtuSULTR1.3*/DN17834_c2_g1 genes, peaked at S1 or S2, and then dramatically decreased at S3 (**Figure 4A**), suggesting an association with mild salinity. Among them, DN32881_c0_g1 deserved more attention because FMO was regarded as the key enzyme in the CSO biosynthesis pathway. A phylogenetic analysis was generated by the neighbor-joining method by using the amino acid sequences of Arabidopsis FMOs and DN32881_c0_g1. The phylogenetic tree indicated that *AtuFMO1* and *AtFMO1*/At1g19250 were clustered in the same clade (**Figure 4B**), suggesting that DN32881_c0_g1 might also encode a putative flavin-containing monooxygenase. In our experiments, the transcript abundance of AtuFMO1 was at relatively low levels under unstressed conditions, while mild salinity stress elevated the expression of *AtuFMO1* by 37.7 and 44.1 times at S1 and S2, respectively, in leaf tissues; nevertheless, *AtuFMO1* expression, compared to the controls, decreased upon moderate stress. Likewise, similar expression

patterns were also observed for *AtuSiR*/DN7313_c0_g2 and *AtuGS2*/DN26059_c0_g1, indicating the second group of DEGs plays important role in increasing the flavor intensity of hydroponic Chinese chives.

In addition to these CSO-biosynthetic enzyme-coding genes, 103 DEGs were annotated as putative transcriptional factors (TFs) in the transcriptome analysis. Among those TFs, MYB, AP2/ERF, and bHLH were the most abundant TF families that were differentially expressed during the plant adaption process to the salinity perturbations, followed by the NAC, WRKY, Zinc finger, bZIP, and LBD families (**Supplementary Table 7**). Assuming that FMO were possible targets of some transcription factors (TFs), all these genes should share similar expression profiles. Thus, clustering analysis was conducted to identify the candidate TFs which had correlative variations in gene expressions under the elevated levels of salinity, and all differentially expressed TFs were grouped into 4 clusters (**Figure 4C**). To a large extent, expression levels of cluster I and II TFs increased significantly accompanied by the increase in salinity levels, reflecting their positive associations with the salt challenge. Conversely, most TF genes in clusters III and IV displayed the highest expression at either S1 or S2, and lowest expression at S3, implying that they might be involved in the plant responses to high salinity. Interestingly, AtuFMO1 and 12 TFs were classified in the subclade α of clade IV, indicating that these TFs shared similar expression behavior with *AtuFMO1* (**Figure 4C**). Furthermore, concerning the candidate TFs in cluster IV_α TFs, Pearson's correlation analyses were performed based on the RNA-Seq and leaf pungency data (**Figure 5**). A strong positive Pearson's correlation ($r^2 = 0.719$, $p < 0.01$) was found between AtubHLH/DN6046_c0_g2 and enhanced pungency, and expression of AtuB3/DN11964_c0_g1 also showed moderate positive correlations with leaf pungency ($r^2 = 0.578$, $p < 0.05$). Thus, these results indicated that the two TFs (AtubHLH and AtuB3) might be the positive regulators of *AtuFMO1* expressions in salt stress-inducible CSO biosynthesis.

Verification of differentially expressed genes by qRT-PCR

Although Illumina RNA-seq data provides preliminary information on the expression behavior of genes, in some instances, there are some discrepancies between *in silico* analysis and experimental data. Thus, qRT-PCR analysis was conducted to determine the transcript accumulation of CSO-biosynthetic genes (*AtuSULTR1.1*, *AtuSULTR1.2*, *AtuSiR*, *AtuGS1*, *AtuGS2*, *AtuGS3*, and *AtuFMO1*) in different salinity-treated samples. In our analysis, we noticed that expression patterns of *AtuSULTR1.2* were slightly different from what was detected from RNA-Seq analysis (**Figure 6**), probably due to the expression fluctuation between different sets of samples. However, *AtuSULTR1.1*, *AtuGS1*, and *AtuGS3* exhibited maximum expression at S3, whereas expression of *AtuSiR*, AtuGS2, and AtuFMO1 peaked at S1 or S2 (**Figure 6**), which were consistent with that of the RNA-Seq dataset. Similarly, we found that the expression trends of candidate TF genes (*AtubHLH*, *AtuERF*, and *AtuB3*) were consistent with those detected in the RNA-Seq dataset (**Figure 6**). Therefore, the transcriptome data and the qRT-PCR data show a similar trend, indicating that the transcriptome sequencing data was reliable.

Discussion

Mild salinity improved the growth and yield of hydroponic chive

High concentrations of salt, mostly just Na^+ and Cl^-, have negative effects on plant growth and development. However, it has been reported that many plants respond positively to the lower level of Na^+ (27). Indeed, mild salinity can be beneficial in some conditions, though moderate or high salt stresses are detrimental to the majority of plants. Na^+ is a potential substitute for K^+ in executing some metabolic functions particularly when potassium is deficient, as they are chemically and structurally similar (28, 29). Accordingly, depending on the ambient Na^+ concentrations, Na^+ can be either beneficial or detrimental in the agricultural system, and the appropriate level of salinity stress could contribute to the plant growth and final yield.

Application of NaCl has been studied earlier in some horticultural plants such as cabbage (*Brassica rapa* L.), tomato (*Solanum Lycopersicum*), and maize sprouts (*Zea mays* L.), indicating that salinity could be used for improving crop performance (30–32). Studies in cabbage seedlings indicated that low salinity (50 mM NaCl) did not show repressive effects on the total biomass, whereas high salinity (100 mM NaCl) caused a reduction in total biomass of nearly 50% in cabbage (31). Similarly, low levels of salinity (40 and 80 mM NaCl) could stimulate plant growth by the production of broader leaves and the enhanced accumulation of assimilates in sugar beet (33). In this study, different salinity levels were used to investigate their influences on the plant growth, yield, and flavor of the chive plants. Our results demonstrate that mild salinity (6.25 and 12.5 mM NaCl) promoted plant growth and biomass accumulation, while exposure to higher salinity (25 and 50 mM NaCl) hampered plant growth and development. One possible general explanation for these responsive behaviors could be ascribed to the species-specific threshold of salt concentrations at which plants show sensitivity to excessive salinity. The presence of small amounts of NaCl in the rooting medium might only impose relatively weak stress that stimulated the plant growth in the Chinese chive, or these minimum Na+ could be utilized as a "nutrient" instead of K^+ by chive plants. Thus, below a threshold concentration

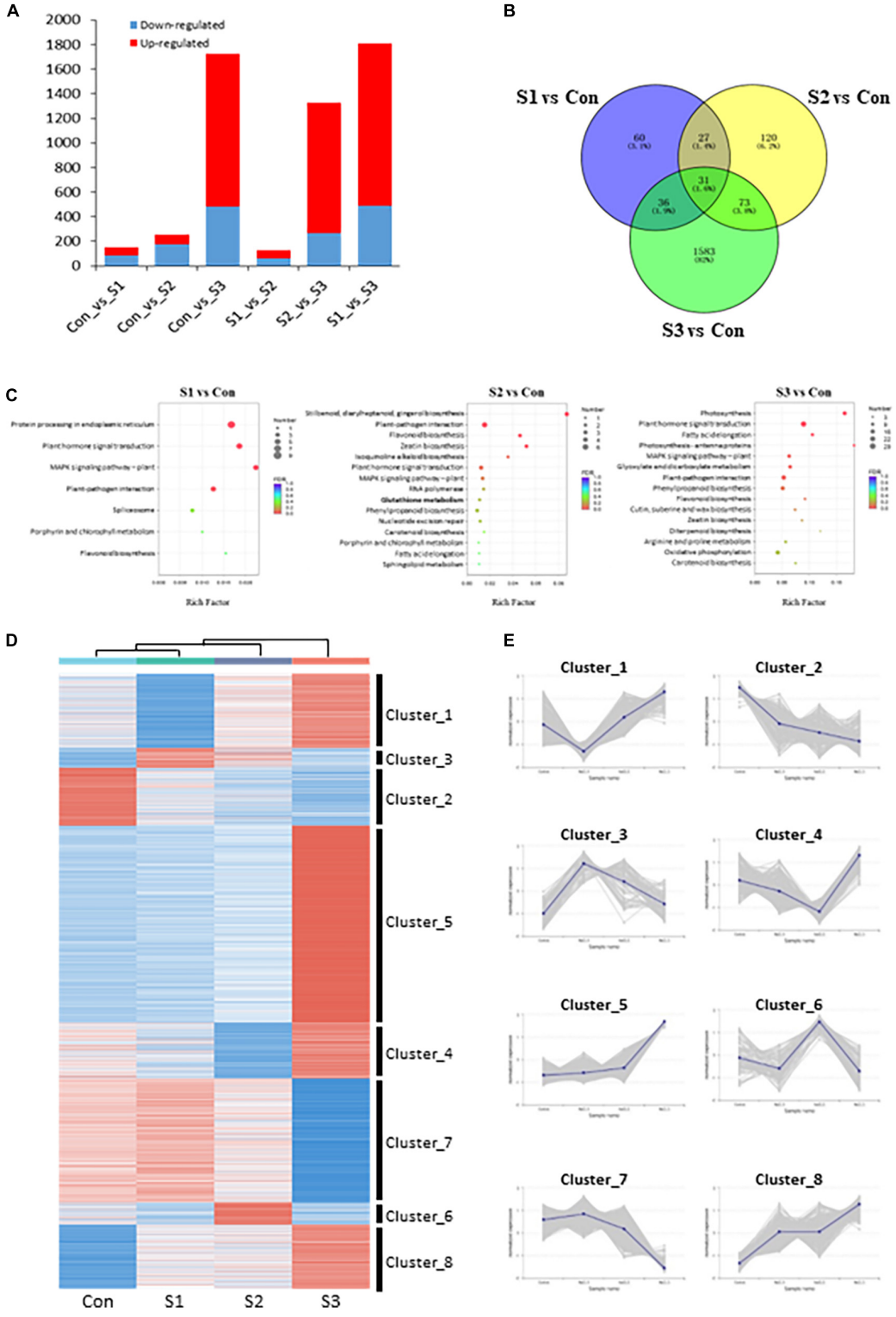

FIGURE 3
Transcriptome overview of Chinese chive under salinity treatments. **(A)** Number of DEGs in each comparison. **(B)** Venn diagram of DEGs between salinity-treated and control samples. **(C)** KEGG pathway enrichments of DEGs in various salinity treatments. **(D)** K-means analysis and hierarchical clustering of DEGs under different salt stress treatments. Heatmap shows gene expression profiles of each cluster under salinity-treated and control samples. **(E)** Expression changes of DEGs with consistent expression patterns. The shadow area was composed of multiple lines of gene expression lines chart.

10.3389/fnut.2022.1000271

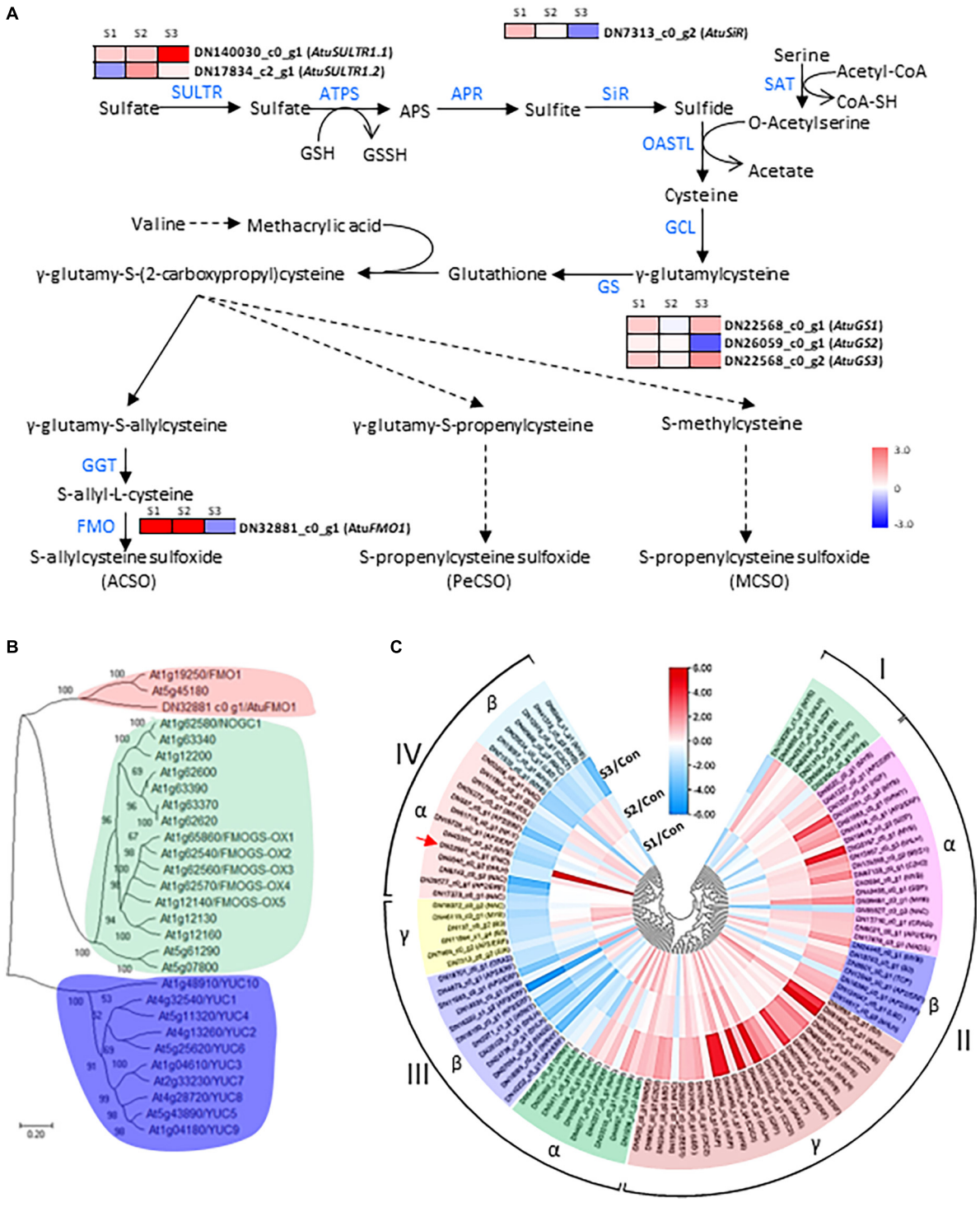

FIGURE 4
Analysis of CSO-biosynthetic genes and their corresponding transcription factors under salinity treatments. **(A)** Schematic presentation of CSO biosynthesis in Chinese chive. The scale bar indicates expression changes under salinity treatments, and colors from blue to red indicate the fold change for each gene between salinity treatment and control. **(B)** A neighbor-joining tree was constructed based on the alignment of AtuFMO1 and 28 FMO protein sequences from Arabidopsis thaliana. The percent bootstrap support for 500 replicates is shown on each branch with > 50% support. **(C)** Clustering analysis of AtuFMO1 and the differentially expressed TF genes under salinity treatments. The color scale represents rescaled log2 fold change values. The color scale above the heatmap shows the expression level, and red indicates high transcript abundance while green indicates low abundance.

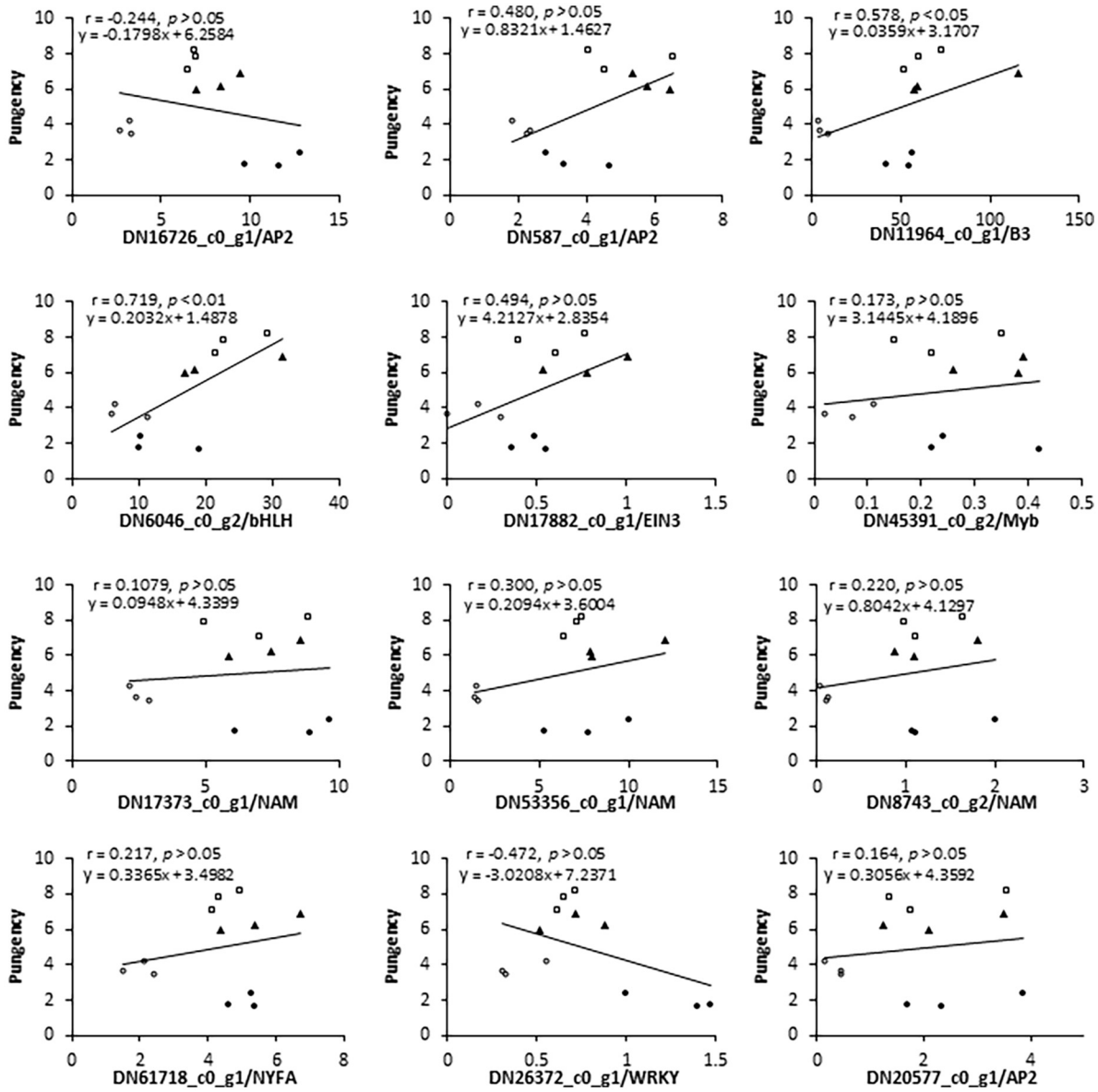

FIGURE 5
Pearson's correlation coefficient and linear regression analyses of the relationship between flavor indicator (leaf pungency) and expression (RNA-Seq data) of selected genes. Above the figure, γ represents the coefficient of determination and y represents an equation by the linear regression model.

of salt, the plant growth seemed unaffected despite the delicately metabolic perturbations, which were manifested in the plant salt tolerance to mild salinity. Nevertheless, with the continuing increase of salinity levels, excessive Na^+ caused morphological alterations (reduction in leaf number, leaf size, plant height, etc.) and physiological disorders (root activity, photosynthetic activity, etc.), and metabolic changes (proline biosynthesis, antioxidant accumulations, etc.) of chive plants. When salinity levels went beyond the plant's adaptability, significant reductions in crop growth resulted in severe yield loss. For instance, the biomass was reduced by roughly 40 and 60% at 100 and 200 mM NaCl treatments, respectively, in hydroponic onions (22). Apparently, the salinity levels were much higher compared to our experiments, which far surpassed plant tolerance and impeded the normal growth of onion seedlings. Although we found that 12.5 mM NaCl is the optimal concentration for hydroponic chive in our experiments, it might be unsuitable for other crops. Therefore, when NaCl was used as a stressor in hydroponic cultivation, identification of the threshold level of salinity, in our opinion, should be considered since the sensitivity to NaCl stress is variable among different crop species.

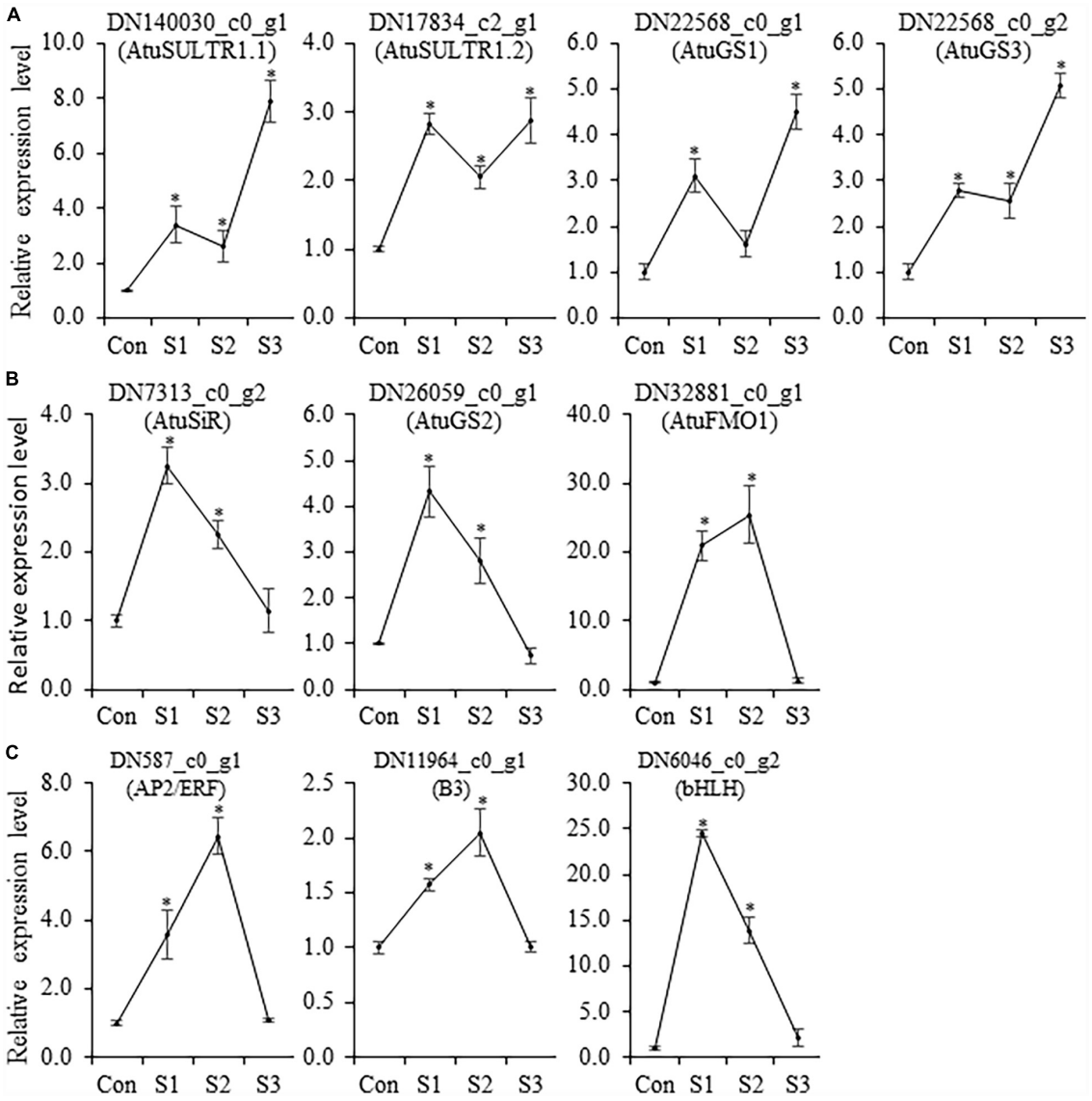

FIGURE 6
Transcriptome analysis of salinity-treated Chinese chive. **(A)** Principal component analysis (PCA) of RNA-Seq data of salt stress-treated and control samples. **(B)** Venn diagram of all DEGs among salinity treatments and control. **(C)** KEGG analysis of cluster_6 DEGs reveals the enrichment of some sulfur metabolism-related pathways.

The composition of free amino acids in Chinese chive

Despite carbohydrates and dietary fiber, FAAs are of importance in the nutritional, medicinal, and sensory values of *Allium* crops. The FAA analysis of the onion bulb suggested that Arg and Gln are the most abundant amino acids, which account for 50% of total FAAs (34). Likewise, a recent study on triploid onion (*A. cornutum*) reached nearly identical conclusions, which correlates with the hypothesis that onions use Arg as a nitrogen reservoir (35). In garlic (*A. sativum*) cloves, Arg, Asp, Glu, and Thr were the top four amino acids, which account for 80% of total FAAs (36). It was proposed that the high content of Arg is the characteristic of the *Allium* species (36). However, UPLC-MS/MS analysis with leaf tissues revealed that the dominant FAAs were Glu, Gln, Asp, and Asn, which accounted for 88.2–90.6% of total FAAs in the salinity-treated and control plants. Our results corroborate a previous investigation with the Chinese chive cultivar "Sanbuchu," which showed that Glu, Asp, His, and Ala were the prominent amino acids in leaf samples (37). Contrary to earlier reports on onion or garlic (34, 35), it was somewhat surprising that lower content of Arg was present in the leaf of Chinese chive. One possible explanation for the discrepancy is due to the species-specific accumulation of amino

acids in Chinese chive. However, another study revealed that Glu, Arg, Gly, Asp, and Ser were the major amino acids in the seed tissues of Chinese chive, which is similar to observations in onion bulbs and garlic cloves (38). Arguably, the accumulation of amino acids might vary among different organs, resulting in the discrepancy of FAA compositions among different findings. Hence, a further in-depth study is required to explore the variations in the composition of FAAs in different organs and species of *Allium* vegetables.

It is well established that FAAs evoke specific taste and flavor sensations, which contributes to the characteristic flavor of food. Previous studies also demonstrated that humans are capable of detecting the taste of amino acids at concentrations in the range from μM to mM levels. A comparison of the detection threshold values for of amino acids confirmed that Glu has the lowest threshold whereas Gly has the highest threshold. For example, the thresholds of L-Glutamic acid, L-Asparagine, and L-serine are 0.063, 0.182, and 2.09 mM, respectively (39). As the percentage water content of Chinese chive was 92% around, the Glu concentrations in leaf tissues should be ranged from 5.1 to 5.84 mM, and accordingly, the Asp concentrations were ranged from 2.38 to 3.44 mM. Thus, the rough calculations indicate that umami amino acids (Glu and Asp) could have distinctive umami taste, because the *in planta* concentrations of Glu and Asp is far above the thresholds as perceived by humans. Interestingly, Ser concentrations ranged from 1.47 to 2.33 mM, which is close to the threshold. Conversely, concentrations of other amino acids except His and Lys are far below their thresholds, and to a large extent, their contributions to flavor and taste might be unneglectable (**Supplementary Table 2**). Together, the majority of abundant FAAs belongs to the umami and sweetness groups, which is consistent with the fact that Chinese chive elicits savoriness and sweet taste. Human taste receptors are far more sensitive to glutamate than any other amino acids, and thus Glu is regarded as the most umami taste substance in food (40). Interestingly, it is notable that S1 treatment significantly stimulated the accumulation of Glu, whereas Asp content decreased slightly. Therefore, the results indicated that the umami taste and flavor could be improved in mild salinity-treated Chinese chives.

Enhanced flavor and cysteine sulphoxide metabolic pathway under salinity

A broad spectrum of the primary and secondary metabolites that plant produced against salinity are also fundamental sources for the odors, tastes, and smells of vegetable products. On one hand, some of those metabolites are directly or indirectly associated with the scavenging of reactive oxygen species (ROS) under salinity stress in plant cells. The majority of sulfur-containing compounds, such as amino acids (cysteine and methionine), vitamins (biotin and thiamine), peptides (glutathione, thioredoxin, and phytochelatins), and other S-containing intermediates of S-metabolism (lipoic acid, allyl-cysteine sulfoxides, and glucosinolates), are involved in the ROS detoxification (41). It has been generally accepted that plants accumulate glutathione (GSH) to maintain cellular redox hemostasis under stressed conditions (42). In *Arabidopsis thaliana* and *Brassica oleracea*, salinity stress-triggered GSH accumulation by activating the expression of two cysteine biosynthesis-related genes encoding adenosine-5'-phosphosulfate reductase (APR) and sulfate adenylyl-transferase (SAT) was upregulated (43). In this study, S-metabolic pathways such as glutathione metabolism, cysteine, methionine metabolism, and sulfur metabolism, were significantly enriched in the KEGG analysis of DEGs specific to mild salinity, indicating a low level of salinity was sufficient to activate the accumulation of sulfur-related metabolites.

On the other hand, these secondary metabolites are also useful in improving the medicinal, nutritive, and flavor attributes of vegetables. Practically, the application of NaCl in hydroponic solutions has been implemented to improve the taste, smell, or color of several vegetables including asparagus, broccoli, and beet (44). For example, an increase in glucosinolates contents under elevated salinity has been reported in some Brassicaceae species such as broccoli (45). Anthocyanins are implicated as functional ingredients beneficial to human health in many vegetables (46). Under salinity stress, upregulation of anthocyanins that mitigated the adverse effects of ROS could improve the nutrient and flavor of vegetables (46). Nevertheless, as mentioned earlier, high salinity could decrease anthocyanin biosynthesis, especially in these salt-sensitive plants (47). In these experiments, we noticed that plant exposure to mild salinity promoted the production of CSO biosynthesis-related FAAs (Glu, Ser, and Cys) as well as the S-containing intermediate (GSH), and their accumulation could contribute to the increases in plant tolerance as well as flavor intensity in Chinese chive. As a consequence, the pungency level of salinity-treated chives was enhanced significantly and even reached the comparable level of soil-grown counterparts.

Regulation mechanism underlying the increased cysteine sulphoxide biosynthesis under mild salinity

The CSO biosynthetic framework was proposed earlier, and the functions of several key genes in the pathway have been explored recently (11, 48). Among these identified DEGs, AtuFMO1 deserved more attention because its strikingly responsive expression behavior was closely associated with pungency changes under salt treatments. Considering that the roles of AsFMO1 (*Allium sativum* FMO1) were highlighted in the S-allyl cysteine sulphoxide (ACSO) biosynthesis in garlic

(16), it is tempting to conclude that the AtuFMO1 might directly participate in the salinity-induced biosynthesis of CSO in Chinese chive.

Except for the structural genes, MYB TFs are essential to the sulfur metabolism and abiotic stress signaling pathway. For example, MYB28, MYB34, and MYB51, members of the R2R3 MYB subfamily, are induced by sulfur deficiency and abiotic stresses (49). Despite MYBs, some bHLH TFs such as MYC2/bHLH06, MYC3/bHLH05, and MYC4/bHLH04 were also involved in the biosynthesis of glucosinolates, the dominant S-containing metabolites in Brassicales, *via* the formation of MYB-bHLH complex (50). Moreover, AP2/ERF TFs were also among the potential regulators of the MYB-bHLH complex (51). Consistent with the findings in Arabidopsis, our results found that a number of TF genes including bHLH, MYB, and AP2/ERF, were co-expressed with *AtuFMO1*. In particular, the expression of two TFs (*AtubHLH*/DN6046_c0_g2 and *AtuB3*/DN11964_c0_g1) had strong positive correlations with the total CSO biosynthesis-related metabolites, implying that they might be potential regulators of the CSO biosynthesis pathways in Chinese chive. Intriguingly, the expression *AtubHLH* and *AtuB3* could be induced by salinity stress. Taken together, our results suggest that mild salinity treatment can promote the expression of bHLH and B3 TFs, which further stimulated the transcription of *AtuFMO1* and consequently CSO biosynthesis.

Conclusion

An appropriate level of salt stress could balance the production and quality of horticultural plants. Our study revealed that mild salinity could stimulate plant growth and improve the nutrition and flavor values of hydroponic Chinese chive, which presents a trade-off between yield, nutrition, and flavor. Notably, the enhanced flavor is strongly correlated with the expression of *AtuFMO1*/DN32881_c0_g1 and two corresponding regulators, *AtubHLH* and *AtuB3*. These genes might play crucial roles in regulating CSO biosynthesis in Chinese chive under salinity stresses. To the best of our knowledge, this is the first report which investigated the effects of mild salinity on the flavor formation, as well as the underlying mechanism, in Chinese chive, which provides novel insights into the interactions between environment and flavor production in *Allium* crops.

Data availability statement

The original contributions presented in this study are included in the article/**Supplementary material**, further inquiries can be directed to the corresponding authors.

Author contributions

MH, HL, YJ, JT, BW, and LX contributed to the data collection and analysis. NL conceived the experiment, designed the study, wrote, and revised the manuscript. HH, ML, and ZW were the supervisor of the project. All authors reviewed and accepted the content of the final manuscript.

Funding

This project was financially supported by the "Special Financial Funds (CZZJ202209)" and "Young Talent Supporting Program (YCXTD00002-10)" of the Beijing Academy of Agriculture and Forestry Sciences, the China Agriculture Research System Grant (CARS-24-B-02), the "Science Innovation Program (KYCX202001-09)" of National Engineering Research Center for Vegetables, and Beijing Agriculture Innovation Consortium (BAIC01-2022).

Acknowledgments

We thank Changlong Wen (National Engineering Research Center for Vegetables) for kindly providing the technical assistance for the qRT-PCR experiments and also thank to Wei Liu (National Engineering Research Center for Vegetables) for fruitful discussions on this manuscript.

Conflict of interest

The authors declare that the research was conducted in the absence of any commercial or financial relationships that could be construed as a potential conflict of interest.

Publisher's note

Supplementary material

The Supplementary Material for this article can be found online at: https://www.frontiersin.org/articles/10.3389/fnut.2022.1000271/full#supplementary-material

References

1. Rabinowitch HD, Currah L. *Allium Crop Science: Recent Advances*. Wallingford: CABI Publishing (2002). doi: 10.1079/9780851995106.0000

2. Rose P, Whiteman M, Moore PK, Zhu YZ. Bioactive S-alk (en) yl cysteine sulfoxide metabolites in the genus Allium: the chemistry of potential therapeutic agents. *Nat Prod Rep.* (2005) 22:351–68. doi: 10.1039/b417639c

3. Stoll A, Seebeck E. Chemical investigations on alliin, the specific principle of garlic. *Adv Enzymol Relat Areas Mol Biol.* (1951) 11:377–400. doi: 10.1002/9780470122563.ch8

4. Ellmore GS, Feldberg RS. Allin lyase localization in bundle sheaths of the garlic clove (*Allium sativum*). *Am J Bot.* (1994) 81:89–94. doi: 10.1002/j.1537-2197.1994.tb15413.x

5. Manabe T, Hasumi A, Sugiyama M, Yamazaki M, Saito K. Alliinase [S-alk(en)yl- L-cysteine sulfoxide lyase] from *Allium tuberosum* (Chinese chive). *Eur J Biochem.* (1998) 257:21–30. doi: 10.1046/j.1432-1327.1998.2570021.x

6. Gross M. All about *Allium*. *Curr Biol.* (2021) 31:R1449–52. doi: 10.1016/j.cub.2021.11.006

7. Nicastro HL, Ross SA, Milner JA. Garlic and onions: their cancer prevention properties. *Cancer Prev Res.* (2015) 8:181–9. doi: 10.1158/1940-6207.CAPR-14-0172

8. Chen C, Shi X, Desneux N, Han P, Gao X. Detection of insecticide resistance in *Bradysia odoriphaga* Yang et Zhang (Diptera: Sciaridae) in China. *Ecotoxicology.* (2017) 26:868–75. doi: 10.1007/s10646-017-1817-0

9. Han BB, Wang BJ, Tong J, Liu MC, Wu ZH, Meng YL, et al. Effects of amino acid treatments on growth,quality,and yield of hydroponic Chinese chive. *Chin Veg.* (2022) 05:74–80.

10. Marles RJ. Mineral nutrient composition of vegetables, fruits and grains: the context of reports of apparent historical declines. *J Food Compos Anal.* (2017) 56:93–103. doi: 10.1016/j.jfca.2016.11.012

11. Liu N, Tong J, Hu M, Ji Y, Wang B, Liang H, et al. Transcriptome landscapes of multiple tissues highlight the genes involved in the flavor metabolic pathway in Chinese chive (*Allium tuberosum*). *Genomics.* (2021) 113:2145–57. doi: 10.1016/j.ygeno.2021.05.005

12. Yamaguchi Y, Kumagai H. Characteristics, biosynthesis, decomposition, metabolism and functions of the garlic odour precursor, S-allyl(l)cysteine sulfoxide. *Exp Ther Med.* (2020) 19:1528–35. doi: 10.3892/etm.2019.8385

13. Yoshimoto N, Saito K. S-alk(en)ylcysteine sulfoxides in the genus *Allium*: proposed biosynthesis, chemical conversion, and bioactivities. *J Exp Bot.* (2019) 70:4123–37. doi: 10.1093/jxb/erz243

14. Takahashi H. Regulation of sulfate transport and assimilation in plants. *Int Rev Cell Mol Biol.* (2010) 281:129–59. doi: 10.1016/S1937-6448(10)81004-4

15. Mitrová K, Svoboda P, Milella L, Ovesná J. Alliinase and cysteine synthase transcription in developing garlic (*Allium sativum* L.) over time. *Food Chem.* (2018) 251:103–9. doi: 10.1016/j.foodchem.2017.12.090

16. Yoshimoto N, Onuma M, Mizuno S, Sugino Y, Nakabayashi R, Imai S, et al. Identification of a flavin-containing S-oxygenating monooxygenase involved in alliin biosynthesis in garlic. *Plant J.* (2015) 83:941–51. doi: 10.1111/tpj.12954

17. Yoshimoto N, Yabe A, Sugino Y, Murakami S, Sai-Ngam N, Sumi S, et al. Garlic gamma-glutamyl transpeptidases that catalyze deglutamylation of biosynthetic intermediate of alliin. *Front Plant Sci.* (2014) 5:758. doi: 10.3389/fpls.2014.00758

18. Rajkumar H, Ramagoni RK, Anchoju VC, Vankudavath RN, Syed AUZ. De novo transcriptome analysis of *Allium cepa* L. (onion) bulb to identify allergens and epitopes. *PLoS One.* (2015) 10:e0135387. doi: 10.1371/journal.pone.0135387

19. Akula R, Ravishankar GA. Influence of abiotic stress signals on secondary metabolites in plants. *Plant Signal Behav.* (2011) 6:1720–31. doi: 10.4161/psb.6.11.17613

20. Chang P-T, Randle WM. Sodium chloride in nutrient solutions can affect onion growth and flavor development. *HortScience.* (2004) 39:1416. doi: 10.21273/HORTSCI.39.6.1416

21. Saito T, Matsukura C, Ban Y, Shoji K, Sugiyama M, Fukuda N, et al. Salinity stress affects assimilate metabolism at the gene-expression level during fruit development and improves fruit quality in tomato (*Solanum lycopersicum* L.). *J Jpn Soc Hort Sci.* (2008) 77:61–8. doi: 10.2503/jjshs1.77.61

22. Aghajanzadeh TA, Reich M, Hawkesford MJ, Burow M. Sulfur metabolism in *Allium cepa* is hardly affected by chloride and sulfate salinity. *Arch Agron Soil Sci.* (2019) 65:945–56. doi: 10.1080/03650340.2018.1540037

23. Wu ZH, Maruo T, Shinohara Y. Effect of total nitrogen concentration of nutrient solution in DFT system on the initial growth and nutrient uptake of Chinese chive (*Allium tuberosum* Rottler ex Spreng.). *J Jpn Soc Hort Sci.* (2008) 77:173–9. doi: 10.2503/jjshs1.77.173

24. He R, Zhang Y, Song S, Su W, Hao Y, Liu H. UV-A and FR irradiation improves growth and nutritional properties of lettuce grown in an artificial light plant factory. *Food Chem.* (2021) 345:128727. doi: 10.1016/j.foodchem.2020.128727

25. Liu N, Staswick PE, Avramova Z. Memory responses of jasmonic acid-associated *Arabidopsis* genes to a repeated dehydration stress. *Plant Cell Environ.* (2016) 39:2515–29. doi: 10.1111/pce.12806

26. Tong J, Hu M, Han B, Ji Y, Wang B, Liang H, et al. Determination of reliable reference genes for gene expression studies in Chinese chive (*Allium tuberosum*) based on the transcriptome profiling. *Sci Rep.* (2021) 11:16558. doi: 10.1038/s41598-021-95849-z

27. Furumoto T, Yamaguchi T, Ohshima-Ichie Y, Nakamura M, Tsuchida-Iwata Y, Shimamura M, et al. A plastidial sodium-dependent pyruvate transporter. *Nature.* (2011) 476:472–5. doi: 10.1038/nature10250

28. Amtmann A, Sanders D. Mechanisms of Na+ uptake by plant cells. In: Callow JA editor. *Advances in Botanical Research.* (Vol. 29), London: Academic Press (1998). p. 75–112. doi: 10.1016/S0065-2296(08)60310-9

29. Barreto RF, Prado RdM, Bodelão NC, Teixeira GCM. Na improves the growth of K-deficient but not K-sufficient kale. *Food Chem.* (2022) 370:131017. doi: 10.1016/j.foodchem.2021.131017

30. He W, Luo H, Xu H, Zhou Z, Li D, Bao Y, et al. Effect of exogenous methyl jasmonate on physiological and carotenoid composition of yellow maize sprouts under NaCl stress. *Food Chem.* (2021) 361:130177. doi: 10.1016/j.foodchem.2021.130177

31. Reich M, Aghajanzadeh T, Helm J, Parmar S, Hawkesford MJ, De Kok LJ. Chloride and sulfate salinity differently affect biomass, mineral nutrient composition and expression of sulfate transport and assimilation genes in *Brassica rapa*. *Plant Soil.* (2017) 411:319–32. doi: 10.1007/s11104-016-3026-7

32. Yin YG, Kobayashi Y, Sanuki A, Kondo S, Fukuda N, Ezura H, et al. Salinity induces carbohydrate accumulation and sugar-regulated starch biosynthetic genes in tomato (*Solanum lycopersicum* L. cv. 'Micro-Tom') fruits in an ABA- and osmotic stress-independent manner. *J Exp Bot.* (2010) 61:563–74. doi: 10.1093/jxb/erp333

33. Hajiboland R, Joudmand A, Fotouhi K. Mild salinity improves sugar beet (*Beta vulgaris* L.) quality. *Acta Agric Scand B Soil Plant Sci.* (2009) 59:295–305. doi: 10.1080/09064710802154714

34. Hansen SL. Content of free amino acids in onion (*Allium cepa* L.) as influenced by the stage of development at harvest and long-term storage. *Acta Agric Scand B Soil Plant Sci.* (2001) 51:77–83. doi: 10.1080/090647101753483796

35. Fredotović Ž, Soldo B, Šprung M, Marijanović Z, Jerković I, Puizina J. Comparison of organosulfur and amino acid composition between triploid onion *Allium cornutum* clementi ex visiani, 1842, and common onion *Allium cepa* L., and evidences for antiproliferative activity of their extracts. *Plants.* (2020) 9:98. doi: 10.3390/plants9010098

36. Ueda Y, Kawajiri H, Miyamura N, Miyajima R. Content of some sulfur-containing components and free amino acids in various strains of garlic. *Nippon Shokuhin Kogyo Gakkaishi.* (1991) 38:429–34. doi: 10.3136/nskkk1962.38.429

37. Jang SJ, Kuk YI. Effects of biostimulants on primary and secondary substance contents in lettuce plants. *Sustain.* (2021) 13:2441. doi: 10.3390/su13052441

38. Hu G, Lu Y, Wei D. Chemical characterization of Chinese chive seed (*Allium tuberosum* Rottl.). *Food Chem.* (2006) 99:693–7. doi: 10.1016/j.foodchem.2005.08.045

39. Schiffman SS, Sennewald K, Gagnon J. Comparison of taste qualities and thresholds of D- and L-amino acids. *Physiol Behav.* (1981) 27:51–9. doi: 10.1016/0031-9384(81)90298-5

40. Vandenbeuch A, Kinnamon SC. Glutamate: tastant and neuromodulator in taste buds. *Adv Nutr.* (2016) 7:823S–7S. doi: 10.3945/an.115.011304

41. Khan NA, Khan MIR, Asgher M, Fatma M, Masood A, Syeed S. Salinity tolerance in plants: revisiting the role of sulfur metabolites. *J Plant Biochem Physiol.* (2014) 2:2. doi: 10.4172/2329-9029.1000120

42. Gong B, Sun S, Yan Y, Jing X, Shi Q. Glutathione metabolism and its function in higher plants adapting to stress. In: Gupta DK, Palma JM, Corpas FJ editors. *Antioxidants and Antioxidant Enzymes in Higher Plants*. Cham: Springer International Publishing (2018). p. 181–205. doi: 10.1007/978-3-319-75088-0_9

43. Queval G, Thominet D, Vanacker H, Miginiac-Maslow M, Gakière B, Noctor G. H2O2-activated up-regulation of glutathione in *Arabidopsis* involves induction

of genes encoding enzymes involved in cysteine synthesis in the chloroplast. *Mol Plant.* (2009) 2:344–56. doi: 10.1093/mp/ssp002

44. Maathuis FJM. Sodium in plants: perception, signalling, and regulation of sodium fluxes. *J Exp Bot.* (2013) 65:849–58. doi: 10.1093/jxb/ert326

45. López-Berenguer C, Martínez-Ballesta MDC, Moreno DA, Carvajal M, García-Viguera C. Growing hardier crops for better health: salinity tolerance and the nutritional value of broccoli. *J Agric Food Chem.* (2009) 57:572–8. doi: 10.1021/jf802994p

46. Khoo HE, Azlan A, Tang ST, Lim SM. Anthocyanidins and anthocyanins: colored pigments as food, pharmaceutical ingredients, and the potential health benefits. *Food Nutr Res.* (2017) 61:1361779. doi: 10.1080/16546628.2017.1361779

47. Daneshmand F, Arvin MJ, Kalantari KM. Physiological responses to NaCl stress in three wild species of potato in vitro. *Acta Physiol Plant.* (2009) 32:91. doi: 10.1007/s11738-009-0384-2

48. Yoshimoto, N., and Saito, K. (2019). S-alk(en)ylcysteine sulfoxides in the genus *Allium*: proposed biosynthesis, chemical conversion, and bioactivities. *J. Exp. Bot.* 70, 4123–4137. doi: 10.1093/jxb/erz243

49. Naing AH, Kim CK. Roles of R2R3-MYB transcription factors in transcriptional regulation of anthocyanin biosynthesis in horticultural plants. *Plant Mol Biol.* (2018) 98:1–18. doi: 10.1007/s11103-018-0771-4

50. Pireyre M, Burow M. Regulation of MYB and bHLH transcription factors: a glance at the protein level. *Mol Plant.* (2015) 8:378–88. doi: 10.1016/j.molp.2014.11.022

51. Li F, Chen B, Xu K, Wu J, Song W, Bancroft I, et al. Genome-wide association study dissects the genetic architecture of seed weight and seed quality in rapeseed (*Brassica napus* L.). *DNA Res.* (2014) 21:355–67. doi: 10.1093/dnares/dsu002

frontiers | Frontiers in Nutrition

TYPE Original Research
PUBLISHED 01 December 2022
DOI 10.3389/fnut.2022.1022590

OPEN ACCESS

EDITED BY
Mingquan Huang,
Beijing Technology and Business University, China

REVIEWED BY
Honglei Tian,
Shaanxi Normal University, China
Ruichang Gao,
Jiangsu University, China

*CORRESPONDENCE
Yu Qiao
qiaoyu412@sina.com
Guangquan Xiong
xiongguangquan@163.com

SPECIALTY SECTION
This article was submitted to Food Chemistry, a section of the journal Frontiers in Nutrition

RECEIVED 18 August 2022
ACCEPTED 10 November 2022
PUBLISHED 01 December 2022

CITATION
Zhou M, Shi G, Deng Y, Wang C, Qiao Y, Xiong G, Wang L, Wu W, Shi L and Ding A (2022) Study on the physicochemical and flavor characteristics of air frying and deep frying shrimp (crayfish) meat. *Front. Nutr.* 9:1022590. doi: 10.3389/fnut.2022.1022590

Study on the physicochemical and flavor characteristics of air frying and deep frying shrimp (crayfish) meat

Mingzhu Zhou[1,2], Gangpeng Shi[1,2], Yi Deng[1,2], Chao Wang[2], Yu Qiao[1]*, Guangquan Xiong[1]*, Lan Wang[1], Wenjin Wu[1], Liu Shi[1] and Anzi Ding[1]

[1]Key Laboratory of Cold Chain Logistics Technology for Agro-Product, Ministry of Agriculture and Rural Affairs, Institute of Agro-Product Processing and Nuclear Agricultural Technology, Hubei Academy of Agricultural Sciences, Wuhan, China, [2]Key Laboratory of Fermentation Engineering (Ministry of Education), Hubei Key Laboratory of Industrial Microbiology, Hubei Provincial Cooperative Innovation Center of Industrial Fermentation, Hubei University of Technology, Wuhan, China

This study aimed to compare the changes in the quality characteristics of air-fried (AF) shrimp meat and deep-fried (DF) shrimp meat at different frying temperatures (160, 170, 180, 190°C). Results showed that compared with DF, the moisture and fat content of air-fried shrimp meat (AFSM) was lower, while the protein content was higher. At the same frying temperature, the fat content of the AFSM was 4.26–6.58 g/100 g lower than that of the deep-fried shrimp meat (DFSM). The smell of the AFSM and DFSM was significantly different from that of the control group. The results of the electronic tongue showed that each of the two frying methods had its flavor profile. Gas chromatography-ion mobility spectrometry (GC-IMS) identified 48 compounds, and the content of volatile compounds detected in AFSM was lower than that in DFSM. Among them, the highest level of volatile compound content was found in the DF-190. E-2-pentenal, 2-heptenal (E), and methyl 2-methyl butanoate were identified only in DFSM. In addition, a total of 16 free amino acids (FAAs) were detected in shrimp meat. As judged by sensory evaluation, the AFSM at 170°C was the most popular among consumers.

KEYWORDS

shrimps, air frying, deep frying, physicochemical properties, flavor characteristics

Introduction

Deep-fried (DF) is a traditional method of cooking with a century-old history (1). The frying process concerns the transfer of heat between the food and the hot oils. Frying could produce some unique flavor characteristics, owing to chemical reactions like browning reaction, Millard reaction, caramelization, and lipid oxidation, which are attractive to consumers (2). In addition, some free amino acids (FAAs) produced by proteolysis and Strecker degradation may be liable for the

distinctive flavor of deep-fried shrimp meat (DFSM). But unacceptable characteristics to consumers also originated during DF. The high oil of fried food was getting more and more attention from consumers. Research has determined that excessive intake of fats enhances the hazard of hypertension and obesity (3). Also, the traditional frying method needs high energy. Therefore, it is necessary to develop a technology to reduce the oil content of fried products without compromising product quality. So far, modified methods of alternative frying technology have been developed, including vacuum frying, AF, microwave frying, microwave-assisted vacuum frying, and ultrasound-treated frying (4).

Air-fried (AF) is a rapid cooking technology. This is achieved by spraying hot air around the ingredients to promote uniform contact between the food and the hot air. This process is carried out in an air fryer apparatus that simulates the movement of heat flow in boiling oil, dehydrating the sample and making it crispy. Compared to traditional DF, AF can lessen the oil content of fried foods. Also, it can form the characteristic shell of fried food due to dehydration (5). Moreover, AF has the advantage of inhibiting the formation of acrylamide (6). Compared with DF foods, the oil content of AF food exhibits 70–80% lower and the acrylamide content can be reduced by about 90% (7). The main component of French fries is starch, but crawfish shrimp meat contains a lot of protein as well as a small amount of fat, which results in a significantly different frying mechanism between the two kinds of food. Cao et al. (8) found that the oil content of AF chicken nuggets was 25% lower than that of DF chicken nuggets. AF was a healthier frying method that can reduce oxidative deterioration of lipids.

Procambarus clarkii is a crustacean. It contains vitamins, polyunsaturated fatty acids (PUFA), and protein (9). Diverse cooking techniques are acting on shrimp meat, comprising frying, baking, steaming, etc. (10). Among them, frying is popular with people due to its appearance, texture, taste, and flavor. However, the health of fried foods with high oil content has attracted increasing attention recently, and researchers have revealed that excessive intake of fat will increase the risk of obesity, high blood pressure, and cardiovascular disease (3). In recent years, AF has been applied to the processing technology of fish and shrimp. Joshy et al. (11) have used the AF technique to prepare a fish cutlet-a popular fish snack with low-fat content and better protein content. Yu et al. (12) found that AF can be regarded as a healthier technique than deep-fat-fried surimi. Heat treatment has been shown to induce lipid oxidation due to the disruption of cell membranes and hemoglobin denaturation, as well as the release of free iron, which promotes lipid oxidation of the product (13). This in turn causes losses to the fried product, and the extent of losses depends on cooking conditions, etc. (14). Therefore, conditions such as cooking temperature have an important effect on the lipid oxidation reaction of crayfish meat (14). And the result of air-frying on the lipid oxidation in prawns with different temperatures was evaluated by Song et al. (9). The results show that temperature plays an important role in influencing the lipid profile of air-fried shrimp and low-temperature turn frying (140–160°C) is less detrimental to the quality of shrimp meat. To date, there has been no comparative study on the physicochemical and flavor characteristics of air-fried shrimp meat (AFSM) and DFSM.

This study would compare the effect of AF and DF on the physicochemical and flavor characteristics of shrimp meat, and discuss the different operating temperatures of frying on the quality characteristics of shrimp meat, namely, the nutrients (moisture, oil, and protein content), physicochemical (color, texture, sensory), and flavor. Meanwhile, it can also identify the optimal AF and DF temperature for producing shrimp meat. These studies provide a basis for the development of healthy fried food.

Materials and methods

Raw materials

Fresh crayfish was obtained from a local market in Wuhan (Longitude: 114.29, Latitude: 30.48), Hubei province of China, and immediately transported to the laboratory at 0–4°C to maintain vigorous vitality. Crayfish with similar body weights (30.00 ± 2.00 g) were selected as experimental samples. The shrimp meat of the crayfish was taken out and washed with pure water, then the surface moisture was blot-dried using absorbent papers.

Frying process

The shrimp meat was divided into three groups, each weighing 100.00 ± 2.00 g. The non-fried shrimp meat was used as the control group. The other two groups were DF and air fried, respectively. For DF, a household deep fryer (model: XJ-15301, Shenzhen, China) with a rated power of 1400 W was used. The shrimp meat was fried in 2 L soybean oil at 160, 170, 180, and 190°C, respectively. Considering that the DF time should not be too long (15), the frying time was set to 2 min. Because AF is an oil-free food processing technology, no oil was applied during the frying of the shrimp meat process. For AF, an air fryer (model: S-2021TS, Shenzhen, China) with a rated power of 1300 W was used, which was preheated at the set temperature for 3 min before the experiment. The shrimp meat was fried in an AF pan at 160, 170, 180, and 190°C for 10 min, and flipped every 5 min. Subsequently, shrimp meat was removed from fryers and cooled down to room temperature before further analysis.

Nutritional composition analysis

Proximate analysis of DF, AF, and control samples was carried out as per AOAC (16). Moisture, protein,

fat, and ash contents of shrimp meat at varying process conditions were measured.

Color and texture analysis

The color meter (model: CR-400, Konica Minolta Holdings, Inc. (Tokyo, Japan) was used to measure the surface color of shrimp meat. The color of the shrimp meat surface was expressed as L* (lightness), a* (redness-greenness), and b* (yellowness-blueness).

Texture profile analysis was performed according to Fan et al. (17). The shrimp meat as described in Section "Frying process" were placed on the loading platform of a TA-XT 2i/50 texture analyzer (Stable Micro Systems, Ltd., Surrey, UK). A P/2 cylindrical probe was used to measure the surface hardness and springiness of the shrimp meat.

Electronic nose analysis

The smell analysis was performed using a Pen III (Airsense, Germany) E-nose system. The PEN III system contained 10 different MOS (metal oxide semiconductor) and the sensors are described in Table 1. Approximately 2.00 g of the shrimp meat and 2 mL 0.18 g/mL NaCl were placed into a 40 ml headspace vial and incubated at 60°C for 30 min. The headspace gas was extracted into the MOS sensors at a constant rate of 300 mL min^{-1}. The flush time and measurement time were 100 and 120 s, respectively.

Electronic tongue analysis

According to Miao et al. (18), shrimp meat was detected by using ASTREE II (Alpha M.O.S France). Approximately 2.00 g of shrimp meat was mixed with 100 ml of distilled water to extract taste substances. The mixture was kept for 30 min and centrifuged, then the water phase was obtained as a measurement sample. Sensors were calibrated and diagnosed before the shrimp meat test. Subsequently, Sensors were dipped in the extract solution.

Gas chromatography-ion mobility spectrometry

According to Xing et al. (19), an analysis of shrimp meat was performed using a GC-IMS instrument (FlavourSpec® in the G.A.S. Department of Shandong HaiNeng Science Instrument Co., Ltd., Shandong, China). Shrimp meat (1.00 g) was homogenized with 10 ml distilled water and 1.00 g NaCl and incubated in a 20 ml headspace bottle for 15 min at 80°C. Gas chromatography (GC) was performed with a column (FS-SE-54-CB-1, 15 m × 0.53 mm × 1.0 μm) to separate the volatile components. The chromatographic was programmed as follows: 2 ml/min for 2 min, 10 ml/min for 8 min, 100 ml/min for 10 min, and 150 ml/min for 10 min. Nitrogen at a flow rate of 150 ml/min was used as the drift gas for IMS, and the temperature was set at 45°C. The GC-IMS data analysis used the functional software Laboratory Analytical Viewer and two plug-ins Reporter and Gallery Plot to construct a 2D topography and fingerprint of the volatile compounds of the samples, and the GC-IMS from the instrument software National Institute of Standards and Technology (NIST) and G.A.S. The volatile compounds were identified by the drift time (DT) of the standard compounds in the database. The relative amounts of the identified volatiles were expressed as the average of the peak areas. Peak intensities of volatile compounds detected by GC-IMS were used for principal component analysis (PCA) to distinguish the differences between different frying temperatures.

TABLE 1 Effect of frying method and temperature on basic nutritional components, color, and texture of shrimp meat.

Group	Moisture content (g/100 g)	Fat (g/100 g)	Protein (g/100 g)	L*	a*	b*	Surface hardness (N)	Springiness
CK	81.04 ± 0.47^{a}	0.50 ± 0.16^{h}	16.44 ± 0.12^{f}	51.74 ± 0.09^{c}	1.72 ± 0.15^{de}	11.56 ± 0.11^{d}	24.63 ± 5.58^{f}	22.92 ± 8.34^{d}
DF-160	72.72 ± 0.08^{b}	5.57 ± 0.06^{d}	19.65 ± 1.36^{e}	73.93 ± 0.25^{b}	1.07 ± 0.16^{e}	11.89 ± 0.81^{d}	83.22 ± 9.22^{e}	52.63 ± 1.83^{ab}
DF-170	69.91 ± 0.42^{c}	6.19 ± 0.14^{c}	21.12 ± 0.11^{d}	74.49 ± 1.36^{b}	2.76 ± 0.35^{cd}	16.41 ± 1.80^{c}	95.77 ± 3.37^{de}	53.09 ± 0.79^{a}
DF-180	67.16 ± 0.10^{de}	7.70 ± 0.28^{b}	22.97 ± 0.16^{c}	74.90 ± 2.23^{b}	3.43 ± 0.25^{abc}	17.84 ± 1.06^{bc}	111.55 ± 11.13^{de}	51.39 ± 2.47^{ab}
DF-190	64.70 ± 0.11^{f}	9.24 ± 0.09^{a}	24.01 ± 0.03^{c}	72.50 ± 2.82^{b}	3.90 ± 0.74^{ab}	18.49 ± 0.29^{bc}	134.76 ± 15.70^{d}	49.35 ± 1.44^{abc}
AF-160	68.06 ± 0.16^{d}	1.31 ± 0.09^{g}	28.37 ± 0.21^{b}	77.36 ± 0.51^{a}	1.68 ± 0.38^{de}	18.13 ± 3.02^{bc}	188.18 ± 19.56^{c}	48.18 ± 1.38^{bc}
AF-170	66.78 ± 0.44^{e}	1.48 ± 0.15^{fg}	29.13 ± 0.13^{b}	74.76 ± 0.55^{b}	2.73 ± 0.40^{cd}	18.47 ± 1.65^{bc}	198.33 ± 20.18^{c}	51.07 ± 0.70^{ab}
AF-180	63.40 ± 1.03^{g}	1.75 ± 0.06^{f}	31.81 ± 0.09^{a}	74.68 ± 0.43^{b}	3.14 ± 0.69^{bc}	19.39 ± 1.20^{b}	242.00 ± 57.45^{b}	48.83 ± 1.00^{abc}
AF-190	62.35 ± 0.16^{h}	2.66 ± 0.31^{e}	32.50 ± 0.23^{a}	72.59 ± 0.66^{b}	4.34 ± 1.27^{a}	22.82 ± 0.71^{a}	353.41 ± 65.65^{a}	46.31 ± 1.20^{c}

Values carrying different letters at the same time indicate statistically significant differences according to Duncan's multiple range test ($p < 0.05$). DF, shrimp meat was treated with deep frying; AF, shrimp meat was treated with air frying; 160, 170, 180, 190: The fried temperature of shrimp meat is expressed as 160, 170, 180, and 190°C.

Free amino acid determination

Free amino acids were measured according to Yu et al. (20). Amino Acid Automatic Analyzer L-8900 (Hitachi, Tokyo) was employed to analyze shrimp meat. Shrimp meat (2.00 g) was homogenized with 15 ml of 5% trichloroacetic acid for 1 min. Then it was placed in a refrigerator at 4°C for 2 h and centrifuged at 9,000 r/min for 15 min with 10 ml supernatant. The 5 ml supernatant was taken out, and the pH was adjusted to 2.0 with 6 mol/L NaOH, then the volume was expanded with distilled water to 10 ml. One milliliter of the extract was filtered using a 0.22 μm membrane filter and applied to an automatic amino acid analyzer.

Sensory evaluation

The sensory evaluation group consisted of 5 boys and 5 girls with an age range of 23–28 years. These panelists received 8 weeks of training, twice a week for 30 min each time. Samples were then randomly assigned to 10 trained panelists. Each panelist scored the samples for each treatment. The basis of sensory scoring was developed by Cao et al. (8) which describes each classification in a 1–5 score. Each indicator is described in a graded manner and divided into three levels: ideal (5 points), more ideal (4 points), moderate (3 points), poor (2 points), and unsatisfactory (1 point). The sensory characteristics of DFSM and AFSM were evaluated by four sensory indicators including color, odor, taste, and texture.

Statistical analysis

Statistical analysis was performed using Origin 2017 (Microcal Software, Inc., Northampton, MA, USA) and DPS software (Zhejiang University, Hangzhou, China). All the data were obtained from at least three repeats. Differences among samples were evaluated using analysis of variance (ANOVA) and Duncan's multiple-range test ($P < 0.05$).

Results and discussion

Changes in basic nutritional components, color, and texture

The nutritional ingredients, chromaticity, and texture properties of fried shrimp meat were shown in **Table 1**. It can be observed that the DFSM and AFSM both decreased in moisture content compared to the control group. The moisture content of the AFSM was slightly lower than that of the DFSM. The reason might be that the AFSM was prepared in a closed system, which would transfer water molecules through a rapid air-flowing mechanism. Meanwhile, the moisture content of AFSM and DFSM reduced with the increase in frying temperature. It may be that the transfer rate of water molecules was accelerated with the increase of AF temperature; while with the increase of DF temperature, the exogenous oils were transferred to the shrimp meat tissues, then the water was accelerated to evaporate. On the other hand, the fat content of raw shrimp meat was 0.50 g/100 g, while that of cooked shrimp meat varied between 5.57 g/100 g and 9.24 g/100 g in DF and between 1.31 and 2.66 g/100 g in AF. On average, the fat content of the AFSM was 74% lower than that of the DFSM. More specifically, the fat content of AF-160, AF-190, DF-160, and DF-190 was 1.31, 2.66, 5.57, and 9.24 g/100 g, respectively. The AFSM was reduced in fat content in contrast to the DFSM because of the absence of oil. This result was following studies conducted on AF fish (12). According to the study of Moreira and Barrufet (21), the high-fat content of DFSM may be stemmed from the equilibrium reaction between the adhesion and drainage of the shrimp surface when the shrimp meat is removed from the oil. Furthermore, when the frying temperature increased, the fat content of samples was also found to be increasing. Since no oil was used for frying, the enhancement of fat content in AFSM may be due to the expulsion of fat from shrimp meat as no other liquid would replace the water removed from the pores of the shrimp meat; With the increase in temperature, the moisture of fried shrimp meat was accelerated to evaporate, and the content of exogenous oil into the shrimp meat tissue increased, which made the oil content increased. In addition, the protein content of raw shrimp meat was 16.44 g/100g, and the AFSM was increased in protein content compared to the DFSM. The protein content increased significantly at increasing frying temperature. This is mainly due to the variation in moisture content. In summary, it shows that AFSM possesses the characteristics of low fat and high protein.

Color parameter is one of the most important quality attributes of fried foods, and also plays an important role in appearance evaluation, which directly impacts consumers' liking for fried foods. The color change of fried food is mainly related to non-enzymatic browning reactions such as chemical oxidation, caramelization, and Maillard reaction (22). The variation of L* (lightness), a* (redness-greenness), and b* (yellowness-blueness) in AFSM and DFSM was shown in **Table 1**. The L* value is a key parameter for the brightness of fried products (23). The L* values of AF and fried shrimp were significantly higher compared to the control group (51.74), which indicated that the lightness of AF and fried shrimp was higher than that of raw shrimp meat. As the AF temperature increased, the lightness of shrimp meat gradually decreased from 77.36 to 72.59, which was attributed to the water loss and reduced light reflection, thus leading to the browning and darkening of the surface of AFSM (14); However, the redness and yellowness value of shrimp meat gradually increased with the increase of the frying temperature. The a* and b* value of

the control group was 1.72 and 11.56, and they rose to 3.90 and 18.49 after DF under 190°C. Conclusively, the values of redness and yellowness were the highest in AFSM. It was believed that a high redness value was directly associated with the generation of acrylamide (24). In general, a high yellowness value suggested more golden shrimp meat, which was acceptable and desirable for fried products.

The texture changes of fried products might depend on the joint action of heat and mass transfer and chemical reactions occurred in the frying process (25). The textural changes are mainly due to protein denaturalization, water evaporation, and tissue browning (26). These changes would greatly affect the likability of the consumers on the products. As presented in Table 2, the surface hardness and springiness of the control group were 24.63 N and 22.92 N. The surface hardness of frying shrimp meat increased as the frying temperature rose, which reached the maximum value of 353.41 N and 134.76 N at 190°C for AFSM and DFSM, respectively. The surface hardness of AFSM was significantly higher than DFSM ($p < 0.05$), and the reason might be that the surface layer of the shrimp meat gradually forms a hard shell during the air-frying process (8). There was no significant difference in springiness between AFSM and DFSM, but a sudden drop of springiness occurred when the temperature climbed up to 190°C; Such variation in springiness may be caused by the uniform and uneven thermal denaturation of myosin and actin (27).

TABLE 2 The performance description of the sensor.

Array serial number	Sensor name	Representative material species	Performance description
1	W1C	Aromatic	Aromatic constituents, benzene
2	W5S	Broad range	High sensitivity and sensitive to nitrogen oxides
3	W3C	Aromatic	Sensitive aroma, ammonia
4	W6S	Hydrogen	Mainly selective for hydrides
5	W5C	Arom-aliph	Short-chain alkane aromatic component
6	W1S	Broad-methane	Sensitive to methyl
7	W1W	Sulfur-organic	Sensitive to sulfides
8	W2S	Broad-alcohol	Sensitive to alcohols, aldehydes, and ketones
9	W2W	Sulph-chlor	Aromatic ingredients, sensitive to organic sulfides
10	W3S	Methane-aliph	Sensitive to long-chain alkanes

Electronic nose response

Electronic noses can be used to determine the odor of a sample, and slight variations in volatile compounds in the sample may lead to differences in sensor response. Data were collected through sample testing and the results of 118–120 s were selected for principal component analysis, which was used to reflect the differences between samples. As shown in Figure 1A, it indicates that the first and second principal components were 80.90 and 17.99%, respectively. This principal component accounted for 98.89% of the total variance. In the scatter plot, shrimp meat from different treatments was well-separated. The AF group and DF group were respectively located on the left and right sides of the PCA, indicating that the smell of the AFSM and DFSM was significantly different from that of the CK group. In AF, the smell of shrimp meat fried at 160°C was significantly different from that fried at 170, 180, and 190°C. In DF, the smell attributes of shrimp meat fried at 160 and 170°C were similar, and there was no difference between shrimp meat fried at 180 and 190°C. E-nose showed a good ability to differentiate fried shrimp through 10 sensors. Response values from 10 sensors were shown in Figure 1B. The sensors W2W, W2S, W1W, and W1S contributed most to the fried shrimp meat, suggesting that sulph-chlor, broad-alcohol, sulfur-organic, and broad-methane had the greatest influence on the odor of fried shrimp (Table 2). Meanwhile, Figure 1B also indicated that W2W, W2S, W1W, and W1S sensors could be effective to distinguish CK, DF, and AF samples. The flavor detected by W2W, W2S, and W1S likely made the greatest contribution to the odor contour of the DFSM, which was probably owing to the high degree of lipid oxidation during deep-frying (28). The lipid oxidation in the frying oil could directly affect the flavor of DF food (29).

Electronic tongue

The electronic tongue is a simulation of the human tongue to analyze, identify and judge the sample measured, and the data obtained is processed by multivariate statistical methods to quickly reflect the quality information of the sample as a whole and achieve the identification and classification of the sample. Figure 2 exhibited the principal component analysis (PCA) and discriminant factor analysis (DFA) diagram which summarized the overall connections between the AFSM and the DFSM. For shrimp meat, the PC1 and PC2 explained 98.81% of the total variation, and the PC1 and PC2 were,

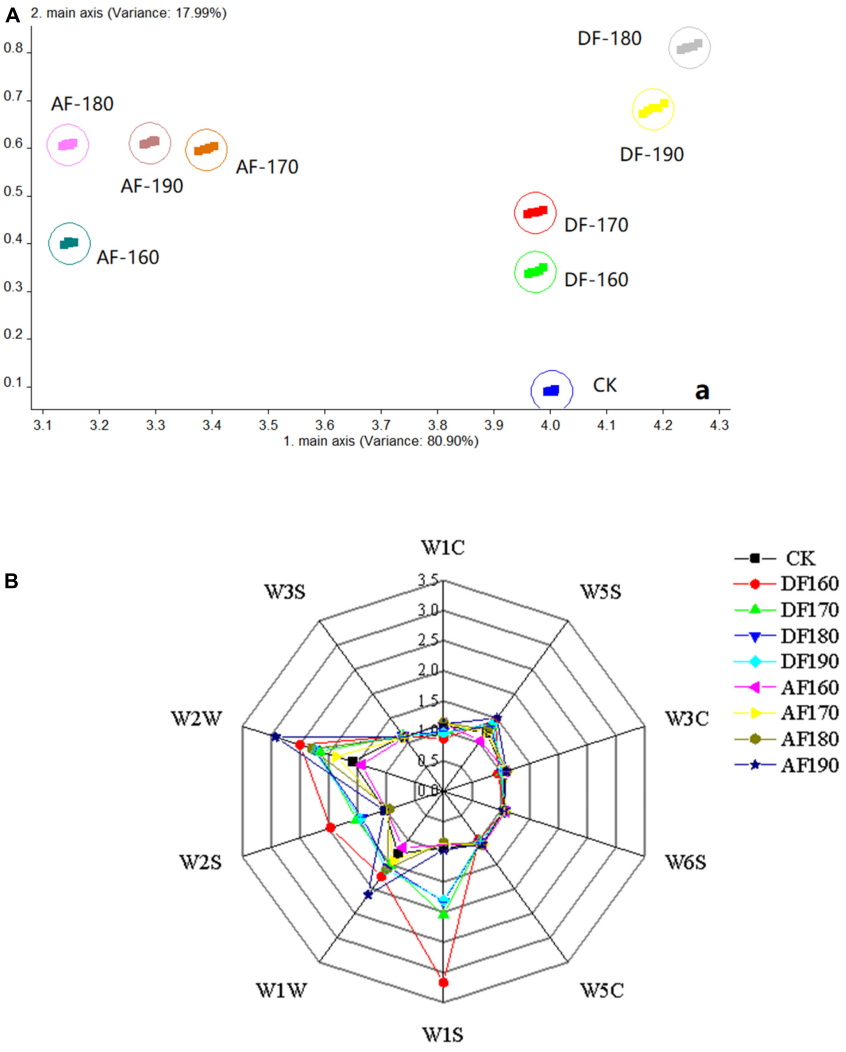

FIGURE 1
Effect of frying method and temperature on the principal component analysis (PCA) of shrimp meat smell **(A)** and sensor signal value **(B)**. DF, shrimp meat was treated with deep frying; AF, shrimp meat was treated with air frying; 160, 170, 180, 190: The fried temperature of shrimp meat is expressed as 160, 170, 180, and 190°C.

respectively, 89.81 and 9.00% (Figure 2A), indicating that the PC1 and PC2 cover the vast majority of taste information of the shrimp meat (30). Meanwhile, the discrimination index reached 90, which certificated that there was a dramatic difference between the tastes of shrimp meat of different frying methods. Compared with the control group, significant changes from the DF and AF groups proved that the taste of shrimp meat depended on the frying method. This difference might be due to the lipid oxidation and Maillard reactions (28). PCA was performed to identify the shrimp meat with different treatments. To better investigate the differences in shrimp meat under different temperatures, DFA was used (Figure 2B). DF1 and DF2 explained 73.95 and 18.37% of the sample variances, respectively. The total contribution (92.32%) indicated that DFA could better distinguish these samples. The data collected by the two frying methods were distributed in different areas of the DFA diagram, indicating that the shrimp meat showed different flavor characteristics after different frying treatments. In addition, there was no overlap in the distribution of data collected at different temperatures for the same frying method, which indicated that the flavor of shrimp was affected by the frying temperature. The result agreed with that obtained by E-nose.

Gas chromatography-ion mobility spectrometry

The differences in volatile compounds in shrimp meat with different frying methods were analyzed by GC–IMS. In Figure 3,

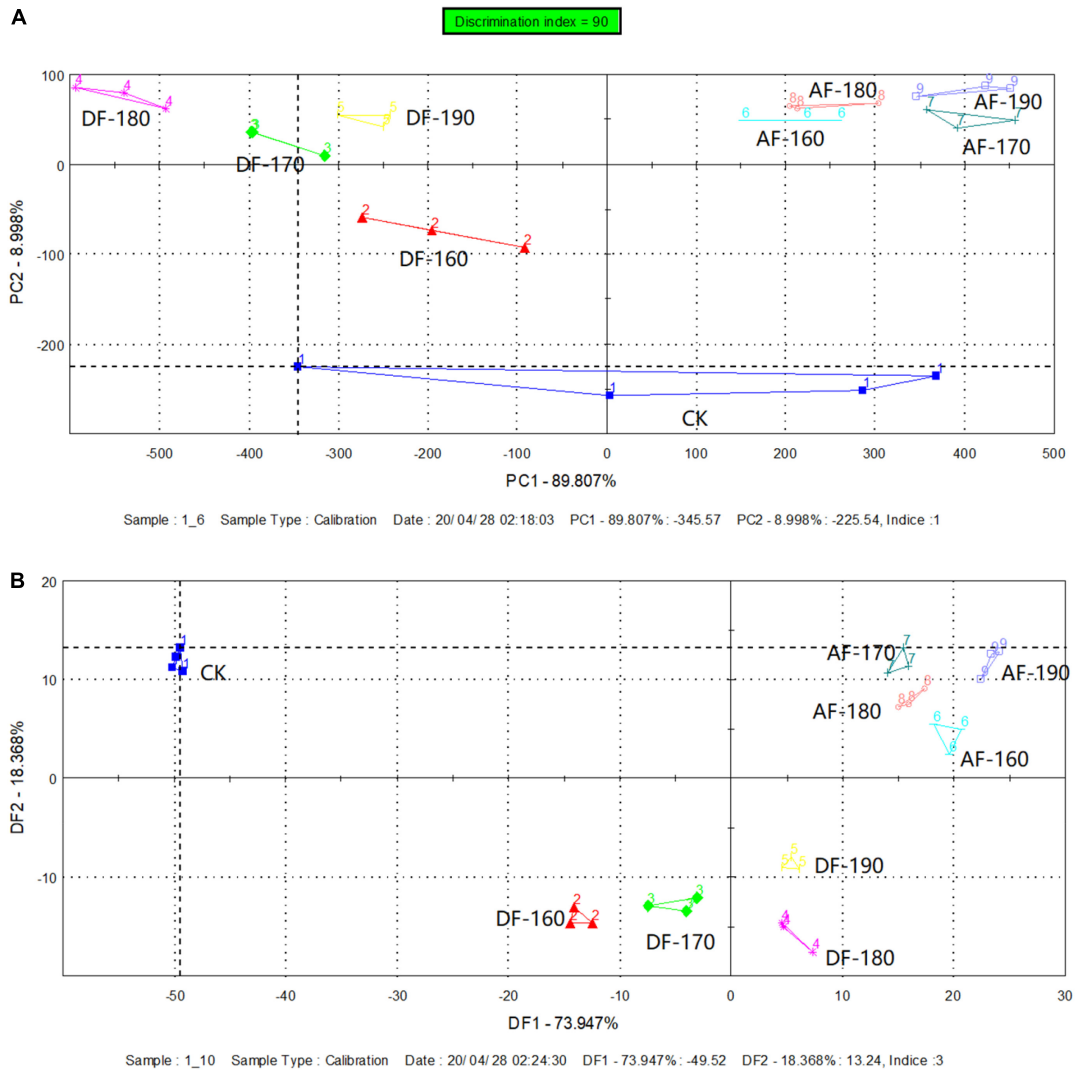

FIGURE 2
Effect of frying method and temperature on principal component analysis (PCA) **(A)** and discriminant factor analysis (DFA) **(B)** of shrimp meat taste. DF, shrimp meat was treated with deep frying; AF, shrimp meat was treated with air frying; 160, 170, 180, 190: The fried temperature of shrimp meat is expressed as 160, 170, 180, and 190°C.

the ordinate and the abscissa denote the retention time and drift time, respectively. The red vertical line in the figure represents the reactive ion peak (RIP). Each point on the right of RIP represents a volatile compound. The darker the color, the higher the concentration. To comprehensively compare the differences between volatile compounds, the peak signal graph was listed by the gallery plot plug-in of the LAV software for intuitive comparison. In **Figure 4**, each row represents all detected signal peaks, and each column represents the signal peak of the same volatile compound under different frying methods and temperatures. The brighter the signal peak, the higher the content of the compound. Due to their different concentrations, it was observed that certain single compounds might produce dimers (31). The formation of dimers was also associated with its high proton affinity, consistent with the research (32). As shown in **Figure 4**, fingerprinting was used to analyze the differences in the volatile compound content of shrimp meat under different frying methods and temperatures. A total of 48 typical target compounds were identified by the GC × IMS Library (**Figure 4** and **Tables 3**, **4**). The signal intensities of 3-methylbutanol, and n-hexanol in fresh shrimp meat were much higher than that in AFSM, while fresh shrimp meat was much lower than DFSM. In addition, E-2-pentenal, 2-heptenal (E), and methyl 2-methylbutanoate were identified only in DFSM.

As shown in **Tables 3**, **4**, these compounds represent six classes, including aldehydes, ketones, alcohols, esters, pyrazines, and other compounds. The generation of these volatile compounds was closely associated with the degradation of

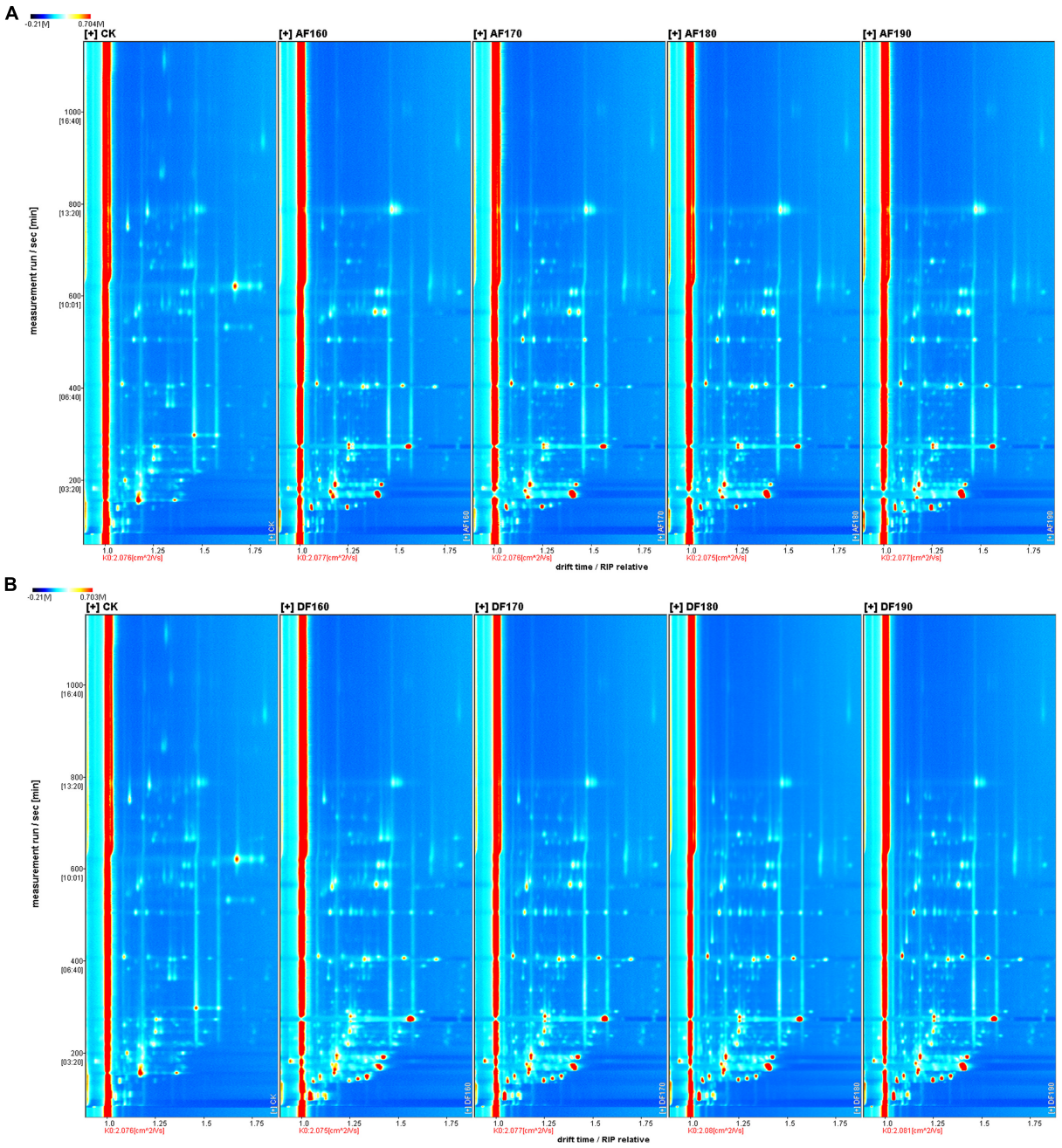

FIGURE 3
Effect of frying temperature on the gas-phase ion mobility spectrum (GC-IMS) of AFSM **(A)** and the GC-IMS of DFSM **(B)**. DF, shrimp meat was treated with deep frying; AF, shrimp meat was treated with air frying; 160, 170, 180, 190: The fried temperature of shrimp meat is expressed as 160, 170, 180, and 190°C.

lipids and proteins through both enzymatic and non-enzymatic reactions (19). The volatile compound's peak area of the DFSM was significantly higher than that of the AFSM, which might be because oil was added to the DFSM. Generally, oil could have a great influence on lipid oxidation, which is crucial to the generation of the typical aroma (33). Among them, the highest level of volatile compounds peak area appeared in the DF-190 (36714.12). The peak area of aldehydes in fried shrimp meat increased. The aldehydes peak area was found to increase remarkably as the frying temperature rose. It can be speculated that high temperatures could promote the generation of some aldehydes. DF-190 had the highest peak area for aldehydes

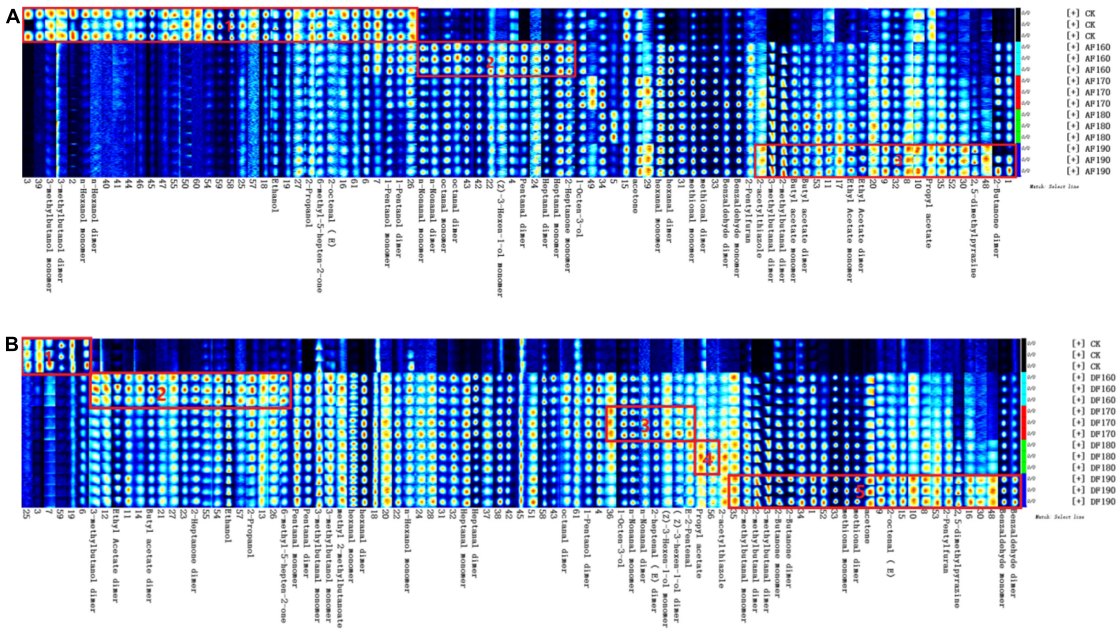

FIGURE 4
Effect of frying temperature on the volatile flavor compounds of AFSM **(A)** and the volatile flavors of DFSM **(B)**. DF, shrimp meat was treated with deep frying; AF, shrimp meat was treated with air frying; 160, 170, 180, 190: The fried temperature of shrimp meat is expressed as 160, 170, 180, and 190°C.

TABLE 3 Types and peak areas of volatile flavor compounds in fried crayfish shrimp meat.

Group	Volatile flavor compounds (Peak volume)						
	Aldehydes	Ketones	Alcohols	Ester	Pyrazines	Others	Total
CK	5496.75 ± 821.66^{e}	1546.49 ± 58.14^{c}	3466.02 ± 394.49^{e}	629.29 ± 44.68^{g}	100.71 ± 21.34^{f}	52.07 ± 15.79^{d}	11291.32 ± 1273.54^{d}
DF-160	18048.29 ± 286.80^{cd}	3322.79 ± 406.39^{ab}	8821.25 ± 20.43^{a}	3465.77 ± 227.21^{a}	138.86 ± 19.76^{e}	109.57 ± 10.68^{c}	33906.52 ± 765.19^{b}
DF-170	20269.01 ± 809.49^{bc}	3809.61 ± 210.49^{ab}	8021.44 ± 210.53^{b}	2512.76 ± 159.17^{c}	189.65 ± 25.14^{d}	140.54 ± 4.75^{b}	34943.00 ± 1245.11^{ab}
DF-180	20417.28 ± 799.82^{b}	3778.44 ± 358.69^{ab}	7456.99 ± 233.03^{c}	2309.09 ± 49.43^{d}	410.73 ± 22.77^{b}	145.45 ± 12.86^{b}	34517.98 ± 869.06^{b}
DF-190	22201.41 ± 376.47^{a}	4277.52 ± 256.85^{a}	6676.62 ± 130.39^{d}	2791.46 ± 46.86^{b}	596.59 ± 14.92^{a}	170.52 ± 3.73^{a}	36714.12 ± 444.52^{a}
AF-160	19123.21 ± 790.03^{cd}	3502.92 ± 185.13^{ab}	2506.86 ± 28.23^{fg}	954.12 ± 22.54^{f}	148.12 ± 2.44^{e}	114.82 ± 11.59^{c}	26350.05 ± 932.18^{c}
AF-170	19866.67 ± 437.90^{bc}	3956.14 ± 331.90^{ab}	2539.78 ± 165.08^{f}	1030.52 ± 30.99^{ef}	196.38 ± 13.33^{d}	119.61 ± 20.72^{c}	27709.11 ± 326.03^{c}
AF-180	20012.88 ± 554.68^{bc}	3074.23 ± 500.60^{b}	2175.09 ± 81.31^{g}	1102.97 ± 25.63^{ef}	244.71 ± 15.56^{c}	106.08 ± 5.70^{c}	26715.95 ± 992.71^{c}
AF-190	20709.24 ± 765.51^{b}	3464.52 ± 1217.99^{ab}	2269.30 ± 68.82^{fg}	1162.58 ± 77.66^{e}	410.42 ± 11.61^{b}	117.10 ± 12.01^{c}	28133.16 ± 1928.08^{c}

Values carrying different letters at the same time indicate statistically significant differences according to Duncan's multiple range test ($p < 0.05$). DF, shrimp meat was treated with deep frying; AF, shrimp meat was treated with air frying; 160, 170, 180, 190: The fried temperature of shrimp meat is expressed as 160, 170, 180, and 190°C.

(22201.41), which contains 2-methylbutanal, 3-methylbutanal, methylal, 2-octanal (E), benzaldhyde, and other substances. Esters were significantly lower in AFSM than in DFSM, and there was no significant effect of frying temperature on the peak area of esters. Alcohols was produced by the reaction of alkoxy radicals, generated during the process of lipid oxidation, with another fatty molecule (34). The alcohol peak area of the DFSM was the highest, followed by that of the CK group peak area ($p < 0.05$), and the AFSM was the lowest. In addition, the content of 2,5-dimethylpyrazine and 2-pentylfuran increased with the increase in temperature. These heterocyclic compounds might be produced by Strecker degradation and aldehyde condensation in the Maillard reaction during heating.

The result of the PCA was shown in Figure 5, the volatile compounds show a difference among the frying shrimp meat. As shown in the figure, the volatile compounds of the AF and DFSM were quite significantly different from that of the CK group. In AF, the volatile compounds of shrimp meat fried at 160°C were significantly different from that fried at 170, 180, and 190°C. In DF, the volatile components of fried shrimp at 160 and 170°C were similar, and there was no significant difference between 180 and 190°C.

10.3389/fnut.2022.1022590

TABLE 4 Qualitative results of GC-IMS of fried crayfish shrimp meat.

Count	Compound	CAS	Formula	MW	RI	RI reference value (44, 45)	Rt [s]	Dt [RIPrel]	Comment
1	2-Butanone	C78933	C_4H_8O	72.1	586.0	587.4	141.297	1.06217	Dimer
2	2-Butanone	C78933	C_4H_8O	72.1	587.6	604.1	142.116	1.24556	
3	Pentanal	C110623	$C_5H_{10}O$	86.1	689.9	699.2	192.075	1.18273	
4	Pentanal	C110623	$C_5H_{10}O$	86.1	689.9	699.2	192.075	1.42469	Monomer
5	Ethyl acetate	C141786	$C_4H_8O_2$	88.1	601.2	618.1	148.668	1.09698	Dimer
6	Ethyl acetate	C141786	$C_4H_8O_2$	88.1	603.4	619.6	149.76	1.33725	Monomer
7	2-Methylbutanal	C96173	$C_5H_{10}O$	86.1	662.1	668.8	178.152	1.15896	Dimer
8	2-Methylbutanal	C96173	$C_5H_{10}O$	86.1	655.9	667.4	175.149	1.40092	Monomer
9	3-Methylbutanal	C590863	$C_5H_{10}O$	86.1	636.1	633.8	165.594	1.17254	Dimer
10	3-Methylbutanal	C590863	$C_5H_{10}O$	86.1	638.4	645.3	166.686	1.40602	Monomer
11	Hexanal	C66251	$C_6H_{12}O$	100.2	789.7	802.2	275.74	1.25445	Dimer
12	Hexanal	C66251	$C_6H_{12}O$	100.2	788.3	801.1	274.122	1.56593	Monomer
13	Butyl acetate	C123864	$C_6H_{12}O_2$	116.2	803.6	813.4	291.91	1.23439	Dimer
14	Butyl acetate	C123864	$C_6H_{12}O_2$	116.2	801.9	815.4	289.889	1.62138	Monomer
15	1-Pentanol	C71410	$C_5H_{12}O$	88.1	756.5	770.9	246.632	1.24973	Dimer
16	1-Pentanol	C71410	$C_5H_{12}O$	88.1	757.0	773.9	247.036	1.50811	Monomer
17	3-Methylbutanol	C123513	$C_5H_{12}O$	88.1	724.4	730.7	220.355	1.23911	Dimer
18	3-Methylbutanol	C123513	$C_5H_{12}O$	88.1	724.9	730.7	220.759	1.49042	Monomer
19	Methional	C3268493	C_4H_8OS	104.2	901.1	907.3	412.445	1.08947	Dimer
20	Methional	C3268493	C_4H_8OS	104.2	899.9	909.9	410.052	1.39814	
21	2-Heptanone	C110430	$C_7H_{14}O$	114.2	887.6	891	389.943	1.26068	
22	2-Heptanone	C110430	$C_7H_{14}O$	114.2	887.4	896	389.609	1.63488	Monomer
23	Heptanal	C111717	$C_7H_{14}O$	114.2	897.2	887.8	404.946	1.3282	Dimer
24	Heptanal	C111717	$C_7H_{14}O$	114.2	896.5	889.3	403.612	1.69897	Monomer
25	n-Non-anal	C124196	$C_9H_{18}O$	142.2	1104.6	1109.5	789.187	1.47463	Dimer
26	n-Non-anal	C124196	$C_9H_{18}O$	142.2	1103.6	1104	787.405	1.9464	Monomer
27	Octanal	C124130	$C_8H_{16}O$	128.2	1003.8	1007.2	609.194	1.39423	Dimer
28	Octanal	C124130	$C_8H_{16}O$	128.2	1004.1	1007.0	609.788	1.82353	
29	6-Methyl-5-hepten-2-one	C110930	$C_8H_{14}O$	126.2	986.3	—	576.522	1.17579	
30	Benzaldehyde	C100527	C_7H_6O	106.1	949.9	963.7	506.426	1.15303	
31	Benzaldehyde	C100527	C_7H_6O	106.1	949.6	962.8	505.832	1.46704	
32	Ethanol	C64175	C_2H_6O	46.1	514.8	512.3	106.862	1.04563	
33	Acetone	C67641	C_3H_6O	58.1	520.9	519.7	109.795	1.11586	
34	2-Propanol	C67630	C_3H_8O	60.1	520.1	514.0	109.429	1.08309	
35	Propyl acetate	C109604	$C_5H_{10}O_2$	102.1	718.7	711.7	215.672	1.15993	
36	E-2-Pentenal	C1576870	C_5H_8O	84.1	740.8	740.6	233.767	1.10517	
37	Methyl 2-methylbutanoate	C868575	$C_6H_{12}O_2$	116.2	777.8	—	264.029	1.18837	
38	(Z)-3-Hexen-1-ol	C928961	$C_6H_{12}O$	100.2	842.0	—	336.689	1.23522	
39	(Z)-3-Hexen-1-ol	C928961	$C_6H_{12}O$	100.2	841.7	—	336.398	1.51614	
40	n-Hexanol	C111273	$C_6H_{14}O$	102.2	866.0	878.5	364.678	1.32262	
41	n-Hexanol	C111273	$C_6H_{14}O$	102.2	864.2	878.8	362.637	1.63724	
42	2,5-Dimethylpyrazine	C123320	$C_6H_8N_2$	108.1	918.0	—	445.015	1.11588	
43	2-Heptenal (E)	C18829555	$C_7H_{12}O$	112.2	950.0	967	506.519	1.25442	
44	2-Heptenal (E)	C18829555	$C_7H_{12}O$	112.2	949.5	966	505.592	1.66892	
45	1-Octen-3-ol	C3391864	$C_8H_{16}O$	128.2	978.7	990	561.802	1.15748	
46	2-Pentylfuran	C3777693	$C_9H_{14}O$	138.2	988.7	—	581.012	1.25414	
47	2-Acetylthiazole	C24295032	C_5H_5NOS	127.2	1018.0	—	634.528	1.12647	
48	2-Octenal (E)	C2548870	$C_8H_{14}O$	126.2	1060.6	1061	710.704	1.33063	

"RI" represents the retention index calculated on FS-SE-54-CB column using n-ketones C4–C9 as external standard. "—" indicates that no reference value was found.

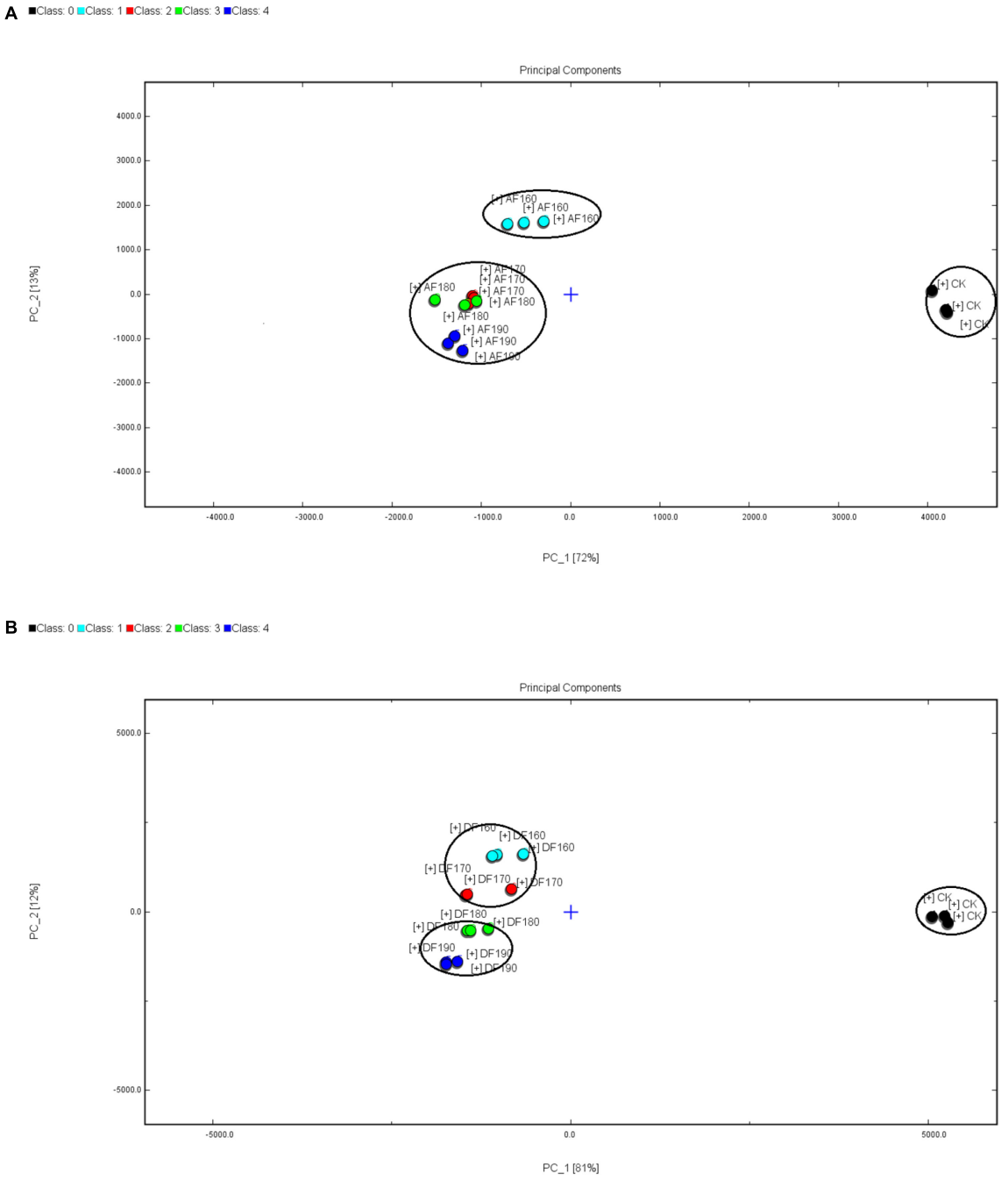

FIGURE 5
Effect of frying temperature on the principal component analysis (PCA) of AFSM **(A)** and the principal component analysis (PCA) of DFSM **(B)**. DF, shrimp meat was treated with deep frying; AF, shrimp meat was treated with air frying; 160, 170, 180, 190: The fried temperature of shrimp meat is expressed as 160, 170, 180, and 190°C.

Free amino acids analysis

Free amino acids are commonly used as quality indicators for various fish and crustacean species. The content of FAAs is essential for the evaluation of protein-rich products. The content of free amino acids in shrimp meat is shown in Table 5, and 16 FAAs were identified. The main FAAs in raw shrimp meat were arginine (1617.31 ± 3.47 mg/g) and histidine (80.00 ± 0.38 mg/g), which are associated with bitter taste (35). Six essential amino acids (EAAs) were included in the 16 FAAs, and the EAA content is the main factor affecting the nutritional value of the protein. In raw shrimp meat, the EAA content

TABLE 5 Effect of frying method and temperature on the FAAs of shrimp meat.

Types	FAAs (mg/g)								
	CK	DF-160	DF-170	DF-180	DF-190	AF-160	AF-170	AF-180	AF-190
Aspartic Asp	1.87 ± 0.03^{c}	0.60 ± 0.05^{f}	3.13 ± 0.25^{a}	1.18 ± 0.08^{e}	0.55 ± 0.20^{f}	1.57 ± 0.01^{d}	2.62 ± 0.06^{b}	1.67 ± 0.01^{d}	1.62 ± 0.06^{d}
Serine Ser	34.92 ± 0.42^{a}	11.27 ± 0.18^{g}	23.54 ± 1.47^{d}	19.88 ± 0.49^{e}	10.49 ± 2.57^{g}	16.90 ± 0.12^{f}	24.18 ± 0.18^{d}	29.53 ± 0.11^{b}	27.45 ± 0.24^{c}
Glutamic Glu	18.69 ± 0.27^{b}	10.50 ± 0.04^{e}	22.72 ± 4.91^{a}	11.05 ± 0.06^{de}	6.32 ± 3.99^{f}	18.23 ± 0.06^{bc}	17.95 ± 0.12^{bc}	14.64 ± 0.14^{cd}	15.51 ± 0.09^{bc}
Alanine Ala	69.60 ± 0.11^{b}	10.64 ± 0.20^{g}	130.09 ± 4.61^{a}	31.38 ± 0.55^{e}	16.24 ± 2.81^{f}	38.87 ± 0.45^{d}	48.39 ± 0.53^{c}	36.80 ± 0.34^{d}	47.00 ± 0.43^{c}
Glycine Gly	72.26 ± 0.12^{a}	14.06 ± 0.17^{g}	64.43 ± 2.14^{b}	26.09 ± 0.50^{e}	18.62 ± 3.32^{f}	39.26 ± 0.38^{c}	39.59 ± 0.36^{c}	34.49 ± 0.36^{d}	38.59 ± 0.32^{c}
Cysteine Cys	–	–	1.01 ± 0.08^{a}	–	–	–	–	–	–
Valine Val	23.48 ± 0.02^{a}	7.84 ± 1.60^{e}	16.33 ± 0.36^{c}	16.26 ± 0.11^{c}	11.23 ± 1.07^{d}	15.91 ± 1.50^{c}	19.01 ± 1.37^{b}	16.72 ± 1.35^{c}	20.06 ± 1.37^{b}
Methionine Met	45.47 ± 0.43^{a}	9.82 ± 0.38^{f}	22.68 ± 0.75^{b}	13.08 ± 0.54^{e}	13.20 ± 2.20^{e}	20.58 ± 0.88^{c}	16.28 ± 0.34^{d}	22.44 ± 0.58^{b}	20.13 ± 0.10^{c}
Isoleucine Ile	15.77 ± 0.05^{a}	1.84 ± 0.09^{h}	8.37 ± 0.29^{d}	7.26 ± 0.16^{e}	4.81 ± 0.89^{g}	6.59 ± 0.06^{f}	11.49 ± 0.08^{b}	7.04 ± 0.05^{ef}	10.27 ± 0.09^{c}
Leucine Leu	28.25 ± 0.08^{a}	4.91 ± 0.08^{g}	17.42 ± 0.53^{c}	14.26 ± 0.38^{d}	9.33 ± 1.54^{f}	11.73 ± 0.06^{e}	19.57 ± 0.23^{b}	13.60 ± 0.11^{d}	20.08 ± 0.17^{b}
Tyrosine Tyr	50.14 ± 3.51^{a}	17.35 ± 0.24^{de}	26.96 ± 0.30^{b}	10.42 ± 0.16^{e}	18.73 ± 1.34^{cd}	27.89 ± 0.07^{b}	25.02 ± 11.02^{bc}	11.37 ± 0.08^{e}	12.49 ± 0.05^{de}
Phenylalanine Phe	24.82 ± 0.68^{a}	7.52 ± 0.34^{i}	13.34 ± 0.34^{e}	12.53 ± 0.35^{f}	9.48 ± 1.04^{h}	11.52 ± 0.11^{g}	17.13 ± 0.14^{c}	14.86 ± 0.02^{d}	18.59 ± 0.16^{b}
Lysine Lys	60.80 ± 0.02^{a}	16.85 ± 0.30^{g}	34.64 ± 1.18^{b}	25.88 ± 0.46^{e}	19.02 ± 3.50^{f}	26.84 ± 0.25^{e}	29.53 ± 0.27^{d}	31.94 ± 0.29^{c}	36.66 ± 0.30^{b}
Histidine His	80.00 ± 0.38^{a}	21.00 ± 0.43^{h}	57.24 ± 1.56^{b}	25.73 ± 0.64^{g}	18.46 ± 3.16^{i}	28.73 ± 0.23^{f}	31.78 ± 0.24^{e}	54.22 ± 0.48^{c}	43.87 ± 0.33^{d}
Arginine Arg	1617.31 ± 3.47^{a}	410.08 ± 5.96^{f}	1069.45 ± 35.45^{b}	704.46 ± 12.80^{e}	643.01 ± 121.40^{e}	821.27 ± 8.19^{d}	694.63 ± 6.83^{e}	962.14 ± 9.29^{c}	1048.39 ± 7.76^{b}
Proline Pro	27.42 ± 0.16^{b}	14.01 ± 0.19^{e}	17.37 ± 0.35^{d}	20.77 ± 0.68^{c}	11.29 ± 5.07^{e}	19.87 ± 0.19^{cd}	25.48 ± 0.29^{b}	30.94 ± 0.48^{a}	30.71 ± 0.35^{a}
TFAA	2170.8	558.29	1528.72	940.23	810.78	1195.76	1022.65	1282.4	1381.42
FAA	224.76	61.08	261.28	110.35	63.51	134.7	152.6	148.07	160.88
EAA	198.59	48.78	112.78	89.27	67.07	93.17	113.01	106.6	125.79

Values carrying different letters at the same time indicate statistically significant differences according to Duncan's multiple range test ($p < 0.05$). DF, shrimp meat was treated with deep frying; AF, shrimp meat was treated with air frying; 160, 170, 180, 190: The fried temperature of shrimp meat is expressed as 160, 170, 180, and 190°C.

was 198.59 mg/g. During food processing, the composition and content of FAAs can change significantly depending on the processing conditions. The total content of FAAs in fried shrimp meat was obviously decreased compared to the control group ($P < 0.05$). These changes can be attributed to heating-induced protein denaturation, decomposition of FAAs, and different interactions between FAAs and the filling oil (36). Aubourg (37) reported that the filling medium and/or interaction with oxidized lipids may lead to the loss of FAAs. The total free amino acid (TFAA) content in AFSM was significantly higher than that in DFSM ($P < 0.05$), indicating that AF reduced the loss of TFAA compared with DF, which may be due to the interaction between FAAs and frying medium caused by DF treatment.

TABLE 6 Effect of frying method and temperature on sensory scores of shrimp meat.

Group	Sensory evaluation
CK	–
DF-160	3.31 ± 0.17^{d}
DF-170	4.18 ± 0.00^{a}
DF-180	4.01 ± 0.06^{ab}
DF-190	3.95 ± 0.09^{b}
AF-160	3.60 ± 0.00^{c}
AF-170	4.20 ± 0.10^{a}
AF-180	4.10 ± 0.17^{ab}
AF-190	3.90 ± 0.20^{b}

Values carrying different letters at the same time indicate statistically significant differences according to Duncan's multiple range test ($p < 0.05$). DF, shrimp meat was treated with deep frying; AF, shrimp meat was treated with air frying; 160, 170, 180, 190: The fried temperature of shrimp meat is expressed as 160, 170, 180, and 190°C.

In fried shrimp meat, Ala, Gly, and Arg were the most abundant FAAs. Ala can be converted to acetaldehyde with a sweet taste by Strecker degradation (38). The acetaldehyde produced can further promote the formation of alkyl pyrazines with a strong aroma (39). DF-170 had the highest Ala content of 130.09 mg/g. Gly, together with hydroxyproline, is an indicator of the presence of connective tissue, principally collagen, and plays a key role in its stability (40). Gly is associated with a sweet taste (35). DF-170 had the highest Gly content of 64.43 mg/g. The amount of Arg in fried shrimp meat was significantly lower compared to the control group ($P < 0.05$). Shahidi found that Arg can be found in many types of seafood (41). Despite the bitter character, the presence of large amounts of Arg gives the food a palatable taste. When the concentration of some bitter amino acids is below their threshold, it can enhance the sweetness and taste of other amino acids, thus improving the overall taste (42). DF-170 and AF-190 had the highest Arg content of 1069.45 and 1048.39 mg/g, respectively.

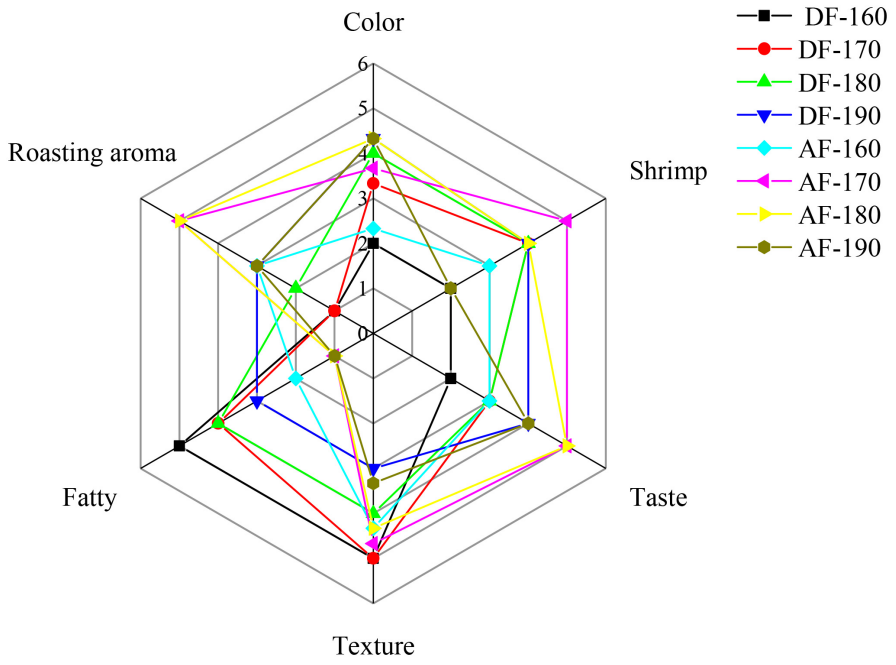

FIGURE 6
Effect of frying method and temperature on the sensory description of shrimp meat taste. DF, shrimp meat was treated with deep frying; AF, shrimp meat was treated with air frying; 160, 170, 180, 190: The fried temperature of shrimp meat is expressed as 160, 170, 180, and 190°C.

It is noteworthy that Glu has a significant impact on flavor due to its low threshold (0.3) and synergistic effect with IMP. The loss of Glu is of great interest because although Glu is a non-essential amino acid, it is an important source of nitrogen that is associated with and even contributes to taste perception (43). Except for DF-170, AFSM had the lowest Glu loss. Cys can react with reducing sugars to produce furan, which can improve the overall flavor of fried shrimp meat. However, Cys was only detected in DF-170.

Changes in sensory scores

As shown in Table 6, it can be seen of overall acceptance that the sensory score for DFSM was close to AFSM, and the sensory scores reached the maximum when the frying temperature was 170°C, which were 4.18 and 4.20. In terms of color, both DF and AF frying methods scored between 3 and 4, with AF-180 and AF-190 scoring the highest, which is consistent with the results of b* values in color determination, indicating that yellowness value is one of the most important indicators for consumers when choosing fried products. The AFSM and DFSM were provided with a special roasting aroma and fatty aroma. The roasting aroma score of the AFSM was higher than that of the DFSM, the scores of AF-170 and AF-180 were the highest. But the fatty aroma score of the AFSM was lower than that of the DFSM, probably because volatile flavor contributed more in the DFSM, as analyzed by "GC-IMS." However, at the lower frying temperature, DFSM was given a greasy feeling, which made the shrimp meat less sensual. The texture score of AFSM is significantly lower than that of DFSM. This is consistent with the results for surface hardness and elasticity, mainly due to the higher moisture loss in the AF treatment compared to the DF treatment, resulting in the formation of a hard outer shell with increased hardness and decreased elasticity of the samples. As can be seen from Figure 6, the texture property score decreases with increasing frying temperature under the same frying method, which is also due to higher moisture loss due to increasing temperature, thus making the hardness increase and elasticity decrease.

Conclusion

The results showed that the evolution of the physicochemical and flavor characteristics of shrimp meat was significantly different in the temperatures of frying. Compared with DF, the AF gave shrimp meat the characteristics of low fat and high protein, and it could reduce the fat content by approximately 4.26–6.58 g/100g. The 16 FAAs were detected in fried shrimp meat. Except for DF-170, the total FAAs content of AFSM was significantly higher than that of DFSM shrimps ($p < 0.05$). The degree of lipid degradation in AF was lower in comparison with that in DF. But the texture characteristics

of DFSM were better than AFSM. The 48 volatile components were detected in fried shrimp, and aldehydes, ketones, alcohols, and esters were the main contributors to the flavor of fried shrimp meat. The total amount of volatile compounds detected in DFSM was higher than that in AFSM. E-2-pentenal, 2-heptenal (E), and methyl 2-methylbutanoate were identified only in DFSM. The fat, protein content, and surface hardness of frying shrimp meat all increased with the increase in frying temperature. As judged by sensory evaluation, the shrimp meat AF at 170°C was the most popular among consumers. Overall, AF is a healthier frying method for fried foods and is a worthwhile alternative.

Data availability statement

The original contributions presented in this study are included in the article/supplementary material, further inquiries can be directed to the corresponding authors.

Author contributions

MZ: experiments, statistical analysis of data, and writing – original draft. GS: experiments, statistical analysis of data, and writing – original draft. YD: statistical analysis of data and writing – original draft. CW: experimental design and review and editing. YQ: experimental design, conceptualization, and visualization. GX: project proposal and research methodology. LW, WW, LS, and AD: review and editing. All authors contributed to the article and approved the submitted version.

Funding

This work was funded by the Major Program of Technical Innovation of Hubei Province (2019ABA087).

Conflict of interest

The authors declare that the research was conducted in the absence of any commercial or financial relationships that could be construed as a potential conflict of interest.

Publisher's note

All claims expressed in this article are solely those of the authors and do not necessarily represent those of their affiliated organizations, or those of the publisher, the editors and the reviewers. Any product that may be evaluated in this article, or claim that may be made by its manufacturer, is not guaranteed or endorsed by the publisher.

References

1. Choe E, Min DB. Chemistry of deep-fat frying oils. *J Food Sci.* (2007) 72:77–86. doi: 10.1111/j.1750-3841.2007.00352.x

2. Bou R, Navas JA, Tres A, Codony R, Guardiola F. Quality assessment of frying fats and fried snacks during continuous deep-fat frying at different large-scale producers. *Food Control.* (2012) 27:254–67. doi: 10.1016/j.foodcont.2012.03.026

3. Saguy IS, Dana D. Integrated approach to deep fat frying: engineering, nutrition, health, and consumer aspects. *J Food Eng.* (2003) 56:143–52. doi: 10.1016/S0260-8774(02)00243-1

4. Devi S, Zhang M, Ju R, Bhandari B. Recent development of innovative methods for efficient frying technology. *Crit Rev Food Sci Nutr.* (2020) 61:3709–24. doi: 10.1080/10408398.2020.1804319

5. Abd Rahman NA, Abdul Razak SZ, Lokmanalhakim LA, Taip FS, Mustapa Kamal SM. Response surface optimization for hot air-frying technique and its effects on the quality of sweet potato snack. *J Food Process Eng.* (2017) 40:e12507. doi: 10.1111/jfpe.12507

6. Teruel MR, Gordon M, Linares MB, Garrido MD, Ahromrit A, Niranjan K. A comparative study of the characteristics of French fries produced by deep fat frying and air frying. *J Food Sci.* (2015) 80:E349–58. doi: 10.1111/1750-3841.12753

7. Sansano M, Juan-Borrás M, Escriche I, Andrés A, Heredia A. Effect of pretreatments and air-frying, a novel technology, on acrylamide generation in fried potatoes. *J Food Sci.* (2015) 80:T1120–8. doi: 10.1111/1750-3841.12843

8. Cao Y, Wu GC, Zhang F, Xu L, Jin Q, Huang J, et al. A comparative study of physicochemical and flavor characteristics of chicken nuggets during air frying and deep frying. *J Am Oil Chem Soc.* (2020) 97:901–13. doi: 10.1002/aocs.12376

9. Song G, Li L, Wang H, Zhang M, Yu X, Wang J, et al. Real-time assessing the lipid oxidation of prawn (*Litopenaeus vannamei*) during air-frying by iKnife coupling rapid evaporative ionization mass spectrometry. *Food Control.* (2020) 111:107066. doi: 10.1016/j.foodcont.2019.107066

10. Brookmire L, Mallikarjunan P, Jahncke M, Grisso R. Optimum cooking conditions for shrimp and Atlantic salmon. *J Food Sci.* (2013) 78:S303–13. doi: 10.1111/1750-3841.12011

11. Joshy CG, Ratheesh G, Ninan G, Ashok KK, Ravishankar CN. Optimizing air-frying process conditions for the development of healthy fish snack using response surface methodology under correlated observations. *J Food Sci Technol.* (2020) 57:2651–8. doi: 10.1007/s13197-020-04301-z

12. Yu X, Li L, Xue J, Wang J, Song G, Zhang Y, et al. Effect of air-frying conditions on the quality attributes and lipidomic characteristics of surimi during processing. *Innov Food Sci Emerg Technol.* (2020) 60:102305. doi: 10.1016/j.ifset.2020.102305

13. Kristinova V, Mozuraityte R, Aaneby J, Storrø I, Rustad T. Iron-mediated peroxidation in marine emulsions and liposomes studied by dissolved oxygen consumption. *Eur J Lipid Sci Technol.* (2014) 116:207–25. doi: 10.1002/ejlt.201300301

14. Cropotova J, Mozuraityte R, Standal IB, Rustad T. Assessment of lipid oxidation in Atlantic mackerel (*Scomber scombrus*) subjected to different antioxidant and sous-vide cooking treatments by conventional and fluorescence microscopy methods. *Food Control.* (2019) 104:1–8. doi: 10.1016/j.foodcont.2019.04.016

15. Andrés A, Arguelles Á, Castelló ML, Heredia A. Mass transfer and volume changes in French fries during air frying. *Food Bioproc Tech.* (2013) 6:1917–24. doi: 10.1007/s11947-012-0861-2

16. AOAC. *Official Methods of Analysis*. 19th ed. Rockville, MD: Association of official analytical chemists (2012).

17. Fan H, Fan D, Huang J, Zhao J, Yan B, Ma S, et al. Cooking evaluation of crayfish (*Procambarus clarkia*) subjected to microwave and conduction heating: a visualized strategy to understand the heat-induced quality changes of food. *Innov Food Sci Emerg Technol.* (2022) 62:102368. doi: 10.1016/j.ifset.2020.102368

18. Miao H, Qin L, Bao H, Wang X, Miao S. Effects of different freshness on the quality of cooked tuna steak. *Innov Food Sci Emerg Technol.* (2017) 44:67–73. doi: 10.1016/j.ifset.2017.07.017

19. Xing T, Zong J, Yu Z, Zhong Q, Ming X, Shu T. Evaluation by electronic tongue and headspace-GC-IMS analyses of the flavor compounds in fry-cured pork with different salt content. *Food Res Int.* (2020) 137:109456. doi: 10.1016/j.foodres.2020.109456

20. Yu D, Xu Y, Regenstein JM, Xia W, Yang F, Jiang Q, et al. The effects of edible chitosan-based coatings on flavor quality of raw grass carp (*Ctenopharyngodon idellus*) fillets during refrigerated storage. *Food Chem.* (2018) 242:412. doi: 10.1016/j.foodchem.2017.09.037

21. Moreira RG, Barrufet MA. A new approach to describe oil absorption in fried foods: a simulation study. *J Food Eng.* (1998) 35:1–22. doi: 10.1016/S0260-8774(98)00020-X

22. Fan LP, Zhang M, Mujumdar A. Vacuum frying of carrot chips. *Dry Technol.* (2005) 23:645–56. doi: 10.1081/DRT-200054159

23. Zeng H, Chen J, Zhai J, Wang H, Xia W, Xiong YL. Reduction of the fat content of battered and breaded fish balls during deep-fat frying using fermented bamboo shoot dietary fiber. *LWT Food Sci Technol.* (2016) 73:425–31. doi: 10.1016/j.lwt.2016.06.052

24. Mogol BA, GõKmen V. Computer vision-based analysis of foods: a nondestructive colour measurement tool to monitor quality and safety. *J Sci Food Agric.* (2014) 94:1259–63. doi: 10.1002/jsfa.6500

25. Troncoso E, Pedreschi F, Zúñiga RN. Comparative study of physical and sensory properties of pre-treated potato slices during vacuum and atmospheric frying. *LWT Food Sci Technol.* (2008) 42:187–95. doi: 10.1016/j.lwt.2008.05.013

26. Asokapandian S, Swamy GJ, Hajjul H. Deep fat frying of foods: a critical review on process and product parameters. *Crit Rev Food Sci Nutr.* (2020) 60:3400–13. doi: 10.1080/10408398.2019.1688761

27. Ishiwatari N, Fukuoka M, Sakai N. Effect of protein denaturation degree on texture and water state of cooked meat. *J Food Eng.* (2013) 117:361–9. doi: 10.1016/j.jfoodeng.2013.03.013

28. Santos CSP, Cunha SC, Casal S. Deep or air frying? A comparative study with different vegetable oils. *Eur J Lipid Sci Technol.* (2017) 119:1600375. doi: 10.1002/ejlt.201600375

29. Chang C, Wu G, Zhang H, Jin Q, Wang X. Deep-fried flavor: characteristics, formation mechanisms, and influencing factors. *Crit Rev Food Sci Nutr.* (2020) 60:1496–514. doi: 10.1080/10408398.2019.1575792

30. Salum P, Guclu G, Selli S. Comparative evaluation of key aroma-active compounds in raw and cooked red mullet (*Mullus barbatus*) by aroma extract dilution analysis. *J Agric Food Chem.* (2017) 65:8402–8. doi: 10.1021/acs.jafc.7b02756

31. Arce L, Gallegos J, Garrido-Delgado R, Medina LM, Sielemann S, Wortelmann T. Ion mobility spectrometry a versatile analytical tool for metabolomics applications in food science. *Curr Metabolomics.* (2015) 2:264–71. doi: 10.2174/2213235X0399915021210294

32. Lantsuzskaya EV, Krisilov AV, Levina AM. Structure of aldehyde cluster ions in the gas phase, according to data from ion mobility spectrometry and AB initio calculations. *Russ J Phys Chem A.* (2015) 89:1590–4. doi: 10.1134/S0036024415090204

33. Jin G, He L, Zhang J, Yu X, Wang J, Huang F. Effects of temperature and NaCl percentage on lipid oxidation in pork muscle and exploration of the controlling method using response surface methodology (RSM). *Food Chem.* (2011) 131:817–25. doi: 10.1016/j.foodchem.2011.09.050

34. Armenteros M, Toldrá F, Aristoy MC, Ventanas J, Estévez M. Effect of the partial replacement of sodium chloride by other salts on the formation of volatile compounds during ripening of dry-cured ham. *J Agric Food Chem.* (2012) 60:7607–15. doi: 10.1021/jf3013772

35. Duan W, Huang Y, Xiao J, Zhang Y, Tang Y. Determination of free amino acids, organic acids, and nucleotides in 29 elegant spices. *Int J Food Sci Nutr.* (2020) 8:3777–92. doi: 10.1002/fsn3.1667

36. Özyurt G, Kafkas E, Etyemez M. Effect of the type of frying oil on volatile compounds of goatfish (*Upeneus pori*) during cold storage. *Int J Food Sci Technol.* (2011) 46:2598–602. doi: 10.1111/j.1365-2621.2011.02789.x

37. Aubourg SP. Loss of quality during the manufacture of canned fish products. *Food Sci Technol Int.* (2001) 7:199–215. doi: 10.1177/108201301772660169

38. Feng Y, Cai Y, Fu X, Zheng L, Xiao Z, Zhao M. Comparison of aromaactive compounds in broiler broth and native chicken broth by aroma extract dilution analysis (AEDA), odor activity value (OAV) and omission experiment. *Food Chem.* (2018) 265:274–80. doi: 10.1016/j.foodchem.2018.05.043

39. Müller R, Rappert S. Pyrazines: occurrence, formation and biodegradation. *Appl Microbiol Biotechnol.* (2010) 85:1315–20. doi: 10.1007/s00253-009-2362-4

40. Chen Y, Ye R, Wang Y. Acid-soluble and pepsin-solublecollagens from grass carp (*Ctenopharyngodon idella*) skin: a com-parative study on physicochemical properties. *Int J Food Sci Technol.* (2015) 50:186–93. doi: 10.1111/ijfs.12675

41. Shahidi F, Aishima T, Abou-Gharbia HA, Youssef M, Adel A, Shehata Y. Effect of processing on flavor precursor amino acids and volatiles of sesame paste (tehina). *J Am Oil Chem Soc.* (1997) 74:667–78. doi: 10.1007/s11746-997-0199-5

42. Lioe HN, Apriyantono A, Takara K, Wada K, Yasuda M. Umami taste enhancement of MSG/NaCl mixtures by subthreshold L-α-aromatic amino acids. *J Food Sci.* (2005) 70:S401–5. doi: 10.1111/j.1365-2621.2005.tb11483.x

43. Sarower MG, Hasanuzzaman AFM, Biswas B, Abe H. Taste producing components in fish and fisheries products: a review. *Int J Food Ferment Technol.* (2013) 2:113–21.

44. Guo XY, Schwab W, Ho CT, Song CK, Wan XC. Characterization of the aroma profiles of oolong tea made from three tea cultivars by both GC-MS and GC-IMS. *Food Chem.* (2022) 376:131933. doi: 10.1016/j.foodchem.2021.131933

45. Cui ZK, Yan H, Manoli T, Mo HZ, Li HB, Zhang H. Changes in the volatile components of squid (*Illex argentinus*) for different cooking methods via headspace-gas chromatography-ion mobility spectrometry. *Food Sci Nutr.* (2020) 8:5748–62. doi: 10.1002/fsn3.1877

frontiers | Frontiers in Nutrition

TYPE Original Research
PUBLISHED 06 December 2022
DOI 10.3389/fnut.2022.1031594

OPEN ACCESS

EDITED BY
Yanyan Zhang,
University of Hohenheim, Germany

REVIEWED BY
Fuping Zheng,
Beijing Technology and Business University, China
Ivan Salmerón,
Autonomous University of Chihuahua, Mexico

*CORRESPONDENCE
Guangli Xia
glxia@sina.com
Yilin You
yilinyou@cau.edu.cn

†These authors have contributed equally to this work

SPECIALTY SECTION
This article was submitted to Food Chemistry, a section of the journal Frontiers in Nutrition

RECEIVED 30 August 2022
ACCEPTED 14 November 2022
PUBLISHED 06 December 2022

CITATION
Wang Y, Wang M, Li W, Wang X, Kong W, Huang W, Zhan J, Xia G and You Y (2022) Indigenous yeast can increase the phenolic acid and volatile ester compounds in Petit Manseng wine.
Front. Nutr. 9:1031594.
doi: 10.3389/fnut.2022.1031594

Indigenous yeast can increase the phenolic acid and volatile ester compounds in Petit Manseng wine

Yanyu Wang[1,2,3†], Miao Wang[1,2,3†], Wenjuan Li[1,3], Xinyuan Wang[1], Weifu Kong[1,2], Weidong Huang[1], Jicheng Zhan[1], Guangli Xia[3,4*] and Yilin You[1*]

[1]Beijing Key Laboratory of Viticulture and Enology, College of Food Science and Nutritional Engineering, China Agricultural University, Beijing, China, [2]Yantai Research Institute, China Agricultural University, Yantai, Shandong, China, [3]Yantai Pula Valley Winery Management Co., Ltd., Yantai, Shandong, China, [4]College of Pharmacy, Binzhou Medical University, Yantai, Shandong, China

Introduction: Indigenous yeasts are generally found in grapes, vineyards, and natural environments. Sequential inoculation and fermentation with non-*Saccharomyces cerevisiae* yeast (H30) and *Saccharomyces cerevisiae* (YT13) also improve the flavor of wine.

Methods: This study sequentially inoculated fermented Petit Manseng and natural grape juice with native H30 and YT13 selected from vineyards in Yantai, China.

Results and discussion: The sensory characteristics of Petit Manseng wine were evaluated by detecting the primary organic acids, phenolic acid compounds, and volatile ester compounds. The results showed that the lactic acid content of the natural wine fermented sequentially with H30 and YT13 increased by 490 μg/L compared with the control group, while the ferulic acid content was 1.4 times that of the single-yeast fermentation group. Furthermore, butyrolactone and anthocyanidin propionate were present in the mixed fermentation group, increasing the aroma complexity of Petit Manseng wine and providing high-quality yeast resources that increase the regional characteristics when producing dry white wine.

KEYWORDS

indigenous yeasts, Petit Manseng wine, phenolic acid compounds, volatile ester compounds, sensory characteristics

Introduction

Of all the yeasts studied, the most attention has been given to *Saccharomyces cerevisiae*, as it is best adapted to survive in these harsh conditions of a wine ferment. In fact, for the majority of untreated wine ferments, *S. cerevisiae* will be the single dominant yeast present at the end of fermentation (1). *Saccharomyces cerevisiae* is the main microorganism responsible for alcohol fermentation, contributing significantly to the alcohol content, taste, and aroma of wine. The major difference between how

wine yeasts produce aroma compounds during fermentation stems from the production of enzymes. Yeasts contain genes that encode enzymes that perform important roles in their survival (2). And modern gene sequencing techniques have shown that some non-*Saccharomyces* yeasts encode for a greater amount of extracellular enzymes than *S. cerevisiae* (3). However, Non-*Saccharomyces cerevisiae* produces a large amount of volatile acid and sulfide during fermentation, giving wine a bad smell and adversely impacting its quality. It is considered the cause of pollution and deterioration during wine production (4). In a study of indigenous *Saccharomyces cerevisiae*, it was found that due to the diversity of indigenous *Saccharomyces* yeasts, there is a much wider range of extracellular enzymes produced during a wild fermentation than when inoculating with a monoculture of *S. cerevisiae*, which played a key role in improving wine flavor (5). Therefore, Indigenous Saccharomyces yeasts isolated from grapes can emphasize the specificity of the terroir, and can contribute to an increased market visibility of wine, due to their production of aromatic compounds which are formed during the fermentation, including higher alcohols, esters, terpenes, and volatile thiols (6).

Indigenous *Saccharomyces cerevisiae* is mainly derived from the microbial population on the surfaces of mature grapes. Due to differences in grape varieties, cultivation methods, and geographic locations, indigenous strains diversely affect the grapes from different regions (7). In Europe, winemakers are more inclined to use indigenous yeast strains when producing wine to increase its typicality (8). In Slovenia, indigenous yeast strains selected from Moscato and Welsh Riesling grapes have been shown to increase the content of 3-mercaptoacetate, linalool, geraniol, and 2-phenylethanol in wine and reduce the 3-mercapto-1-hexanol level. Changes in the concentration of these substances provide Sauvignon Blanc wine with a more intense aroma (6). However, although the NI6 indigenous yeast from the Parr region of South Africa contains high-yield 3-mercapto-1-hexanol, it provides Syrah wines with pleasant "jam", "smoky", and "spicy" aromas (9).

The essential role of *Saccharomyces cerevisiae* and non-*Saccharomyces cerevisiae* is also reflected in the color and taste of the wine. The study found that *Schizosaccharomyces pombe* and *Meyerozyma guilliermondii* showed a higher ability than the control group to produce hydroxycinnamate decarboxylase significantly increasing the vitisin A and B derivative yield, enhancing the color stability of the wine (10, 11). In addition, certain types of yeast that degrade or produce organic acids during the fermentation process can also play a role in color protection. Previous studies indicated that the anthocyanin concentration in the sequential fermentation group using *Lachancea percherrima* was 8–10% higher than that of the control group (12). The indigenous *Saccharomyces cerevisiae* from France and Northern Italy produced higher concentrations of glycerin, malic acid, and succinic acid during the fermentation process and lower concentrations of ethanol, acetic acid, and acetaldehyde, enhancing the acidity and softness of the wine (13–16). Various regions in China contain abundant yeast resources that require further exploration. Our research group collected 85 non-*Saccharomyces cerevisiae* samples from different regions in China, including Yantai, Huailai, Fangshan, and Shangri-La, for early-stage testing. This study uses *p*-nitrophenyl-β-D-glucoside (pNPG) and the Bradford method to determine the β-glucosidase activity and protein content of the primary strains. The indigenous wild non-*Saccharomyces cerevisiae,* H30, from the Yantai region displays high β-glucosidase activity and is selected based on its specific enzyme activity (17).

Materials and methods

Petit Manseng sample

Five-year-old Petit Mensang collected from Beigezhuang Village, Yantai, China. The harvested and selected samples were pressed by bladder press and the extracted grape juice was used for subsequent experiments.

Yeast strain

Yeast strains were selected from indigenous *Saccharomyces cerevisiae* YT13 and non-*Saccharomyces cerevisiae* H30 that had been isolated from grapes in Penglai, Yantai, China. The EC1118 commercial yeast (French Raman) was used for the control group. Commercial *Saccharomyces cerevisiae* was cultured in a yeast extract peptone dextrose (YPD) medium (yeast extract 10 g/L, peptone 20 g/L, glucose 20 g/L) to obtain the single strain liquid, while the indigenous yeast, which had been frozen at −80°C, was thawed and rewarmed, then inoculated in YPD liquid medium, and amplified to obtain the single bacterial solution. This single bacterial solution was added into sterile grape juice at the inoculation ratio of 10% (v/v), until the strain grew to more than 10^7 CFU/mL.

Chemicals

Anhydrous sodium carbonate, Folin phenol, sodium chloride, acetic acid, methanol, 2-octanol, tartaric acid, malic acid, lactic acid, citric acid and succinate were purchased from Shanghai Macklin Biomedical Co., Ltd. (Shanghai, China). Gallic acid, *p*-coumaric acid, protocatechuic acid, gentian acid, chlorogenic acid, ferulic acid, caffeic acid and vanillic acid were purchased from Shanghai Aladdin Biochemical Technology Co., Ltd. (Shanghai, China). Glucose, agar, and glycerol purchased from China Sinopharm Chemical Reagent Factory (Shanghai, China). Peptone and yeast extract were purchased

from Beijing Shuangxuan Microbial Culture Product Medium Factory (Beijing, China). WLN medium was purchased from Shanghai Junrui Biotechnology Co., Ltd. (Shanghai, China). Cross-linked polyvinylpyrrolidone (PVPP) was purchased from Beijing Solarbio Science and Technology Co., Ltd. (Beijing, China). Ethyl acetate was purchased from Tianjin Fuyu Fine Chemical Co., Ltd. (Tianjin, China). Anhydrous ethanol was purchased from Shanghai Forneeds Biotechnology Factory (Shanghai, China). Potassium sulfite was purchased from Enartis (Italy). Pure water was obtained from an Elix ultrapure water purification system.

Fermentation process

The clarified grape juice was filtered through 1 and 0.45 μm filter membranes to obtain the sterilized grape juice, of which 2 L was transferred into a 2.5 L glass fermentation tank. The control group of this experiment was commercial Saccharomyces cerevisiae EC1118 single strain inoculation and fermentation, and indigenous *Saccharomyces cerevisiae* YT13 was used as another single strain fermentation group. In the mixed strain group, non-*Saccharomyces cerevisiae* H30 was inoculated first, and EC1118 and YT13 were inoculated on the fourth day of fermentation. All inoculate proportion was 1%. After inoculation, all samples were fermented at 16°C. The inoculation grouping and fermentation of the natural grape juice were consistent with the abovementioned steps for the sterilization of grape juice, and the specific grouping is shown in **Table 1**. The fermentation of the samples was monitored by measuring Brix values daily. At the end of fermentation, residual sugar content in the different treatment groups was detected using a wine analyzer (F17-WineScan FT120, Foss Co., Ltd., Hillerød, Denmark). When sugar content reached below 4 g/L, the fermentation was stopped by the addition of potassium sulfite. The wine was then poured into glass bottles and stored at 4°C for subsequent detection.

Determination of organic acids

The organic acids produced by fermentation were detected by high performance liquid chromatography (HPLC), according to a method previously described in the literature. The wine samples were filtered by 0.22 μm aqueous microporous membrane and then analyzed by HPLC. Chromatographic conditions were as follows: Waters XBridge C18 chromatographic column (4.6 mm × 250 mm, 5 μm), column temperature of 35°C, detection wavelength of photodiode array detector (PDA) of 210 nm, isocratic elution, mobile phase ratio of 0.1% phosphoric acid solution:methanol = 97.5:2.5, flow rate of 0.8 mL/min, and injection volume of 10 μL. The establishment of the standard working curve was performed as follows: Five mixed standard samples of different concentrations were accurately prepared, stored at 4°C, and subsequently detected under the above chromatographic conditions. Five standard curves were obtained, with peak area as the ordinate and mass concentration of substance as the abscissa. The peak sequence of each standard sample was found to be as follows: tartaric acid, 3.5 min; malic acid, 4.2 min; lactic acid, 5.18 min; citric acid, 6.55 min; and succinic acid, 7.7 min.

Determination of phenolic acids

A wine sample of 10 mL was centrifuged after vortex oscillation with ethyl acetate of equal volume. The supernatant was centrifuged three times (10 min each time) in a 100 mL round-bottom flask and then dried by vacuum distillation at 35°C. The residue was dissolved with 2 mL 50% chromatographic methanol and stored at −20°C for subsequent chromatographic analysis (18). The chromatographic conditions were as follows, according to a method slightly modified by Chen (19). For gradient elution, mobile phase A was methanol-acetic acid-water (volume ratio 10:2:88), mobile phase B was methanol, the flow rate was 0.8 mL/min, and in the elution program: 0–25 min, B was 0–15%; 25–45 min, B was 15–50%; and 45–53 min, B was 50–0%. The column temperature was 30°C, injection 20 μL. Standard working solution: 2 mg/mL standard solution was diluted with methanol to 0.05, 5, 15, 30, 40, and 60 mg/L standard solution, then stored at −20°C. Mixed standard working solution: 80 μL of vanillic acid (2 mg/mL) and 100 μL of other phenolic compounds were dissolved together in chromatographic methanol and diluted to 10 mL, which was then used as the mother solution for further use. The solution was diluted into five standard solutions at different concentrations and stored at −20°C until needed.

TABLE 1 Fermentation test groups.

Grape juice nature	Yeast inoculation method	Types of yeast inoculation
Sterilization	Single yeast inoculation	EC1118 (control)
		YT13
	Sequential inoculation	H30 + EC1118
		H30 + YT13
Nature	Single yeast inoculation	EC1118 (control)
		YT13
	Sequential inoculation	H30 + EC1118
		H30 + YT13

This test was performed on two fermentation systems: sterilization and natural fermentation. Each system comprised four groups. Except for the control group (EC1118), the test groups were as follows: YT13 *Saccharomyces cerevisiae* fermentation (YT13); H30 fermentation for 3 days, followed by inoculation with EC1118 for sequential fermentation (H30 + EC1118); H30 fermentation for 3 days, followed by inoculation with YT13 for sequential fermentation (H30 + YT13).

The peak sequences of each standard sample were as follows: gallic acid, 4.3 min; protocatechuic acid, 7.2 min; gentiopic acid, 11.1 min; chlorogenic acid, 12.9 min; caffeic acid, 15.2 min; vanillic acid, 20.1 min; p-coumaric acid, 25.7 min; ferulic acid, 28.65 min. In the qualitative analysis, cholic acid was detected at 320 nm and the other substances were detected at 280 nm. The identification was carried out by comparing the retention time and spectrum with the pure standard. An external method was used for quantitative analysis.

Determination of volatile esters

Headspace solid phase microextraction gas chromatography-mass spectrometry (HS-*SPME-GC-MS)* was used to detect the aroma compounds in samples, as described by Li et al. (20). A 3 mL wine sample was placed in a 10 mL headspace bottle, to which 0.5 g NaCl powder, 0.3 g PVPP, 3 μL concentration of 0.822 g/L 2-octanol internal standard and a magnetic rotor were added, after which it was sealed with a bottle cap with a rubber gasket. The extraction head of the SPME fiber assembly was aged for 1 h at the inlet of the gas chromatography, at an aging temperature of 250°C. The aged extraction head [divinylbenzene/carboxen/*polydimethylsiloxane* (DVB/CAR/PDMS)] was inserted into the headspace part of the sample bottle, 1 cm away from the liquid surface. The sample was heated and stirred at 50°C and 350 rpm for 50 min, whereafter the extraction head was taken out and inserted into the GC inlet (Thermo Scientific) at 250°C for 5 min. Each sample was measured three times in parallel.

The GC conditions were as follows: The column was a TG-5SILMS (30 m × 0.25 mm × 0.25 μm) capillary column. The carrier gas was high purity helium, and the flow rate was 1.2 mL/min. Solid-phase microextraction was manually injected using the non-split mode. The inlet temperature was 250°C. The column temperature heating program was initialized at 40°C, maintained for 2 min, heated to 230°C at the rate of 5°C/min, then maintained for 5 min. The MS conditions were as follows: interface temperature was 250°C, ion source temperature was 230°C, ionization mode was EI, electron ionization energy was 70 eV, full scan mode acquisition signal, and the scanning range (m/z) was 30–450 amu. For the qualitative analysis, different flavor components were separated by GC to form their respective chromatographic peaks, which were analyzed and identified by GC-MS-computer. The mass spectra of each component were retrieved and analyzed via the online National Institute of Standards and Technology (NIST) mass spectral library. Combined with the relevant literature, artificial analysis was carried out to confirm the chemical components of the flavor substances. Only substances with similarity (SI) greater than 600 and triplicate detection were retained. For the semi-quantitative analysis, the following internal standard method was applied: Using an MS full ion scanning (Scan) map, combined with the comparative results of NIST2011 and the related literature reference, the aroma substances were qualitatively screened. Using the semi-quantitative method, the average value of three replicates was taken as the relative content of the aroma substances.

Sensory evaluation

A tasting group comprised of seven members conducted sensory evaluation and analysis on the dry white wines fermented by different yeasts in this study. A five-point intensity method was used to evaluate the aromas of the fermented products. Seven aroma characteristics, namely alcoholic odor, floral aroma, citrus fruit, tropical fruit, temperate fruit, fermented aroma, and adverse aroma, were selected according to the international Wine and Spirit Education Trust (WSET) wine tasting guidelines. In addition, the appearance (color and clarity), aroma (intensity, coordination, freshness, and complexity) and taste (mellowness, balance, and aftertaste) of each sample were scored, for a total score of 100 points.

Statistical analysis method

IBM SPSS Statistics 26 software was used for significance difference analysis. Analysis of variance (ANOVA) was used; $n = 3$; and $p < 0.05$ indicated significant difference. The results were expressed as mean ± standard deviation. GraphPad Prism 8.0 software was used to draw the broken line diagrams, scatter plots and column diagrams of chemical components in the samples at different fermentation times. The principal component analysis (PCA) chart was created using OriginPro2021 software, while the flavor radar chart was drawn using Excel software.

Results

The effect of indigenous yeast fermentation on the basic physicochemical indexes of Petit Manseng dry white wine

In order to explore the fermentation performance of the two indigenous yeasts (YT13 and H30) in sterilized grape juice and natural grape juice, YT13, H30 + YT13, and H30 + EC1118 were used to ferment Petit Manseng grape juice, while commercial *Saccharomyces cerevisiae* EC1118 was used as the control. The pH value, sugar content, total acid content, alcohol content, and total phenol content of the samples were determined at the beginning and end of fermentation. The results are shown in **Table 2**.

10.3389/fnut.2022.1031594

TABLE 2 Basic physical and chemical indicators of Petit Manseng grape juice and wine.

Detection indicator	Grape juice	Sterilization group				Natural group			
		Control	YT13	H30 + EC1118	H30 + YT13	Control	YT13	H30 + EC1118	H30 + YT13
Fermentation days (days)	0	19	22	23	23	13	17	15	15
pH	3.1 ± 0.02	3.1 ± 0.05^{a}	3.2 ± 0.02^{a}	3.1 ± 0.05^{a}	3.2 ± 0.04^{a}	3.1 ± 0.04^{a}	3.2 ± 0.01^{a}	3.1 ± 0.03^{a}	3.1 ± 0.03^{a}
Sugar content (g/L)	230 ± 0.10	1.9 ± 0.02^{a}	2.3 ± 0.01^{a}	1.9 ± 0.07^{a}	2.0 ± 0.13^{a}	1.4 ± 0.01^{d}	1.7 ± 0.09^{c}	1.9 ± 0.12^{b}	2.3 ± 0.05^{a}
Total acid (g/L)	8.8 ± 0.04	9.4 ± 0.05^{ab}	9.6 ± 0.04^{a}	9.3 ± 0.05^{b}	9.3 ± 0.04^{b}	9.3 ± 0.03^{a}	9.3 ± 0.11^{a}	9.3 ± 0.10^{a}	9.3 ± 0.08^{a}
Alcohol (%Vol)	N.D.	13.2 ± 0.06^{a}	13 ± 0.10^{a}	13.2 ± 0.06^{a}	13.1 ± 0.09^{a}	13.1 ± 0.07^{a}	13 ± 0.10^{a}	13.3 ± 0.12^{a}	13.2 ± 0.01^{a}
Total phenol (mg/L)	N.D.	375.47 ± 10.67^{b}	372.17 ± 8.00^{b}	394.81 ± 1.33^{a}	387.74 ± 2.00a^{b}	340.33 ± 7.67^{b}	362.97 ± 11.01^{a}	354.24 ± 7.34a^{b}	295.99 ± 1.00^{c}

The control group was inoculated with commercial *Saccharomyces cerevisiae* EC1118 (EC1118), while the test groups are treated as follows: YT13 *Saccharomyces cerevisiae* fermentation (YT13); H30 fermentation for 3 days, followed by inoculation with EC1118 for sequential fermentation (H30 + EC1118); H30 fermentation for 3 days, followed by inoculation with YT13 for sequential fermentation (H30 + YT13). In the table, N.D. means not detected. Different letters indicate significant differences at $p < 0.05$.

The Petit Manseng grape juice displayed an initial pH value of 3.1, an initial sugar content of 230 g/L, and a total acid content of 8.8 g/L. In the sterile group, the sugar content of the wine fermented with commercial *Saccharomyces cerevisiae* EC1118 decreased rapidly, while the fermentation process was completed after 19 days. The indigenous *Saccharomyces cerevisiae* YT13 obtained from Penglai was used in the single-yeast fermentation and sequential inoculation fermentation groups, while the fermentation process was completed 23 days after yeast inoculation. The fermentation speed of the Petit Manseng natural grape juice was faster than the fermentation process of the sterilized grape juice, which could be attributed to the loss of macromolecular nutrients during filtration and sterilization. The viability and sugar consumption rate of the commercial *Saccharomyces cerevisiae* EC1118 (control group) was higher in both groups, reducing the fermentation process. After fermentation, the pH of the Petit Manseng wine displayed minimal changes, while the total acid content was significantly higher than that of the grape juice. This could be ascribed to the effect of the yeast, which increased the organic acid content, such as lactic acid and succinic acid. Previous studies showed that different yeast strains affected the polyphenol content in wine. In this study, the result regarding the total phenol content in the Petit Manseng wine fermented with different yeasts showed no significant differences between the sterilization groups. The total phenol content in the natural grape juice group fermented with *Saccharomyces cerevisiae* YT13 was 362.97 ± 11.01 mg/L, which was significantly higher than in the control group. However, the total phenol content of the mixed fermentation group using H30 + YT13 was significantly lower than in all treatment groups.

Indigenous yeast increases the organic acid content of Petit Manseng dry white wine

As shown in Table 3, the type, concentration, and ratio of organic acids play a vital role in wine and can adjust the acid-base balance, maintain the pH value at a relatively low level, affect the taste, and even improve the aroma by affecting the esterification reaction. Organic acids are not only essential for the taste of wine but also determine its acidity. Studies have shown that the content and ratio of organic acids produced by different yeast strains vary. Therefore, this study used liquid chromatography to examine the wine fermented using grape juice and natural grape juice. Five organic acids were detected, including tartaric acid, malic acid, succinic acid, lactic acid, and lemon acid.

During the fermentation test of the Petit Manseng sterilized grape juice, no significant differences were evident in the malic acid, citric acid, and succinic acid content. However, the lactic acid and tartaric acid levels vary significantly. The lactic acid content (1.87 ± 0.10 g/L) in the H30 + YT13

TABLE 3 The content of organic acids in wine fermented from Petit Manseng grape juice.

Organic acid content (g/L)	Sterilization group				Natural group			
	Control	YT13	H30 + EC1118	H30 + YT13	Control	YT13	H30 + EC1118	H30 + YT13
Tartaric acid	4.05 ± 0.34^{ab}	3.79 ± 0.03^{b}	3.92 ± 0.01^{ab}	4.39 ± 0.03^{a}	4.11 ± 0.09^{ab}	3.97 ± 0.03^{bc}	3.84 ± 0.01^{c}	4.20 ± 0.01^{a}
Malic acid	6.25 ± 0.30^{a}	4.10 ± 3.34^{a}	6.66 ± 0.40^{a}	6.96 ± 0.43^{a}	6.71 ± 0.08^{b}	6.77 ± 0.03^{a}	7.31 ± 0.65^{a}	6.96 ± 0.10^{a}
Lactic acid	1.24 ± 0.001^{c}	1.64 ± 0.01^{ab}	1.37 ± 0.25^{bc}	1.87 ± 0.10^{a}	1.38 ± 0.09^{a}	1.61 ± 0.01^{a}	1.56 ± 0.01^{a}	1.87 ± 0.07^{a}
Citric acid	0.67 ± 0.03^{a}	0.86 ± 0.27^{a}	0.51 ± 0.54^{a}	0.69 ± 0.01^{a}	0.75 ± 0.04^{b}	0.79 ± 0.05^{b}	1.02 ± 0.01^{a}	0.85 ± 0.03^{b}
Succinic acid	2.04 ± 0.05^{a}	1.99 ± 0.16^{a}	1.33 ± 0.78^{a}	1.14 ± 0.07^{a}	0.87 ± 0.03^{b}	1.82 ± 0.02^{a}	1.66 ± 0.01^{a}	0.70 ± 0.19^{b}
Total content	14.16 ± 0.40	12.4 ± 2.69	13.80 ± 1.41	15.06 ± 0.41	13.83 ± 0.25	14.96 ± 0.02	15.40 ± 0.48	14.52 ± 0.27

The control group was inoculated with commercial *Saccharomyces cerevisiae* EC1118 (EC1118), while the test groups are treated as follows: YT13 *Saccharomyces cerevisiae* fermentation (YT13); H30 fermentation for 3 days, followed by inoculation with EC1118 for sequential fermentation (H30 + EC1118); H30 fermentation for 3 days, followed by inoculation with YT13 for sequential fermentation (H30 + YT13). Different letters indicate significant differences at $p < 0.05$.

TABLE 4 The content of phenolic acids in wine fermented from Petit Manseng grape juice.

Phenolic acid content (mg/L)	Sterilization group				Natural group			
	Control	YT13	H30 + EC1118	H30 + YT13	Control	YT13	H30 + EC1118	H30 + YT13
Gallic acid	3.79 ± 0.14^{a}	4.32 ± 0.12^{a}	4.37 ± 0.16^{a}	4.17 ± 0.24^{a}	3.85 ± 0.13^{a}	4.33 ± 0.42^{a}	4.26 ± 0.49^{a}	4.29 ± 0.50^{a}
Protocatechuic acid	4.42 ± 0.32^{b}	5.62 ± 0.21^{a}	4.24 ± 0.405^{c}	5.15 ± 0.08^{a}	4.08 ± 0.08^{c}	4.42 ± 0.315^{b}	4.49 ± 0.23^{b}	4.63 ± 0.63^{a}
Gentisic acid	0.46 ± 0.01^{ab}	0.59 ± 0.10^{a}	0.40 ± 0.04^{b}	0.57 ± 0.05^{a}	0.53 ± 0.06^{b}	0.62 ± 0.16^{a}	0.68 ± 0.05^{a}	0.55 ± 0.06^{b}
Chlorogenic acid	2.29 ± 0.91^{ab}	3.50 ± 0.45^{a}	1.86 ± 0.47^{b}	2.63 ± 0.01^{ab}	2.71 ± 0.33^{ab}	3.43 ± 0.14^{a}	2.59 ± 0.22^{b}	3.26 ± 0.38^{ab}
Caffeic acid	2.43 ± 0.02^{a}	2.43 ± 0.71^{a}	2.76 ± 0.04^{a}	2.64 ± 0.30^{a}	2.01 ± 0.13^{a}	2.30 ± 0.19^{a}	2.425 ± 0.40^{a}	2.45 ± 0.25^{a}
Vanillic acid	0.11 ± 0.002^{a}	0.14 ± 0.01^{a}	0.11 ± 0.01^{a}	0.14 ± 0.01^{a}	0.11 ± 0.001^{b}	0.15 ± 0.004^{a}	0.12 ± 0.01^{b}	0.12 ± 0.01^{b}
P-coumaric acid	0.35 ± 0.14^{a}	0.12 ± 0.03^{ab}	0.07 ± 0.09^{b}	0.12 ± 0.04^{ab}	0.34 ± 0.09^{a}	0.11 ± 0.12^{c}	0.39 ± 0.05^{a}	0.29 ± 0.01^{b}
Ferulic acid	0.43 ± 0.03^{a}	0.55 ± 0.09^{a}	0.45 ± 0.02^{a}	0.54 ± 0.01^{a}	0.41 ± 0.02^{d}	0.51 ± 0.06^{c}	0.61 ± 0.09^{b}	0.78 ± 0.05^{a}
Total content	14.27 ± 1.76	17.27 ± 3.63	14.25 ± 3.39	15.95 ± 1.00	14.03 ± 0.84	15.88 ± 2.42	15.58 ± 1.54	16.36 ± 1.9

The control group was inoculated with commercial *Saccharomyces cerevisiae* EC1118 (EC1118), while the test groups are treated as follows: YT13 *Saccharomyces cerevisiae* fermentation (YT13); H30 fermentation for 3 days, followed by inoculation with EC1118 for sequential fermentation (H30 + EC1118); H30 fermentation for 3 days, followed by inoculation with YT13 for sequential fermentation (H30 + YT13). Different letters indicate significant differences at $p < 0.05$.

group was the highest, significantly exceeding the control group level (1.24 ± 0.001 g/L). Although the tartaric acid content difference was not as significant as that of lactic acid, its level in the H30 + YT13 group (4.39 ± 0.03 g/L) was still significantly higher than the control group (4.05 ± 0.34 g/L). Except for the lactic acid content, significant differences were evident in the Petit Manseng wine fermented with natural grape juice. The tartaric acid content (4.20 ± 0.01 g/L) was highest in the wine of the H30 + YT13 group, which was consistent with the results of the sterilization system. However, these results were inconsistent with previous studies in which the malic acid content of cider fermented with the mixed strain containing *Schizosaccharomyces pombe* and *Saccharomyces cerevisiae* was lower than that of the wine subjected to single yeast fermentation. Although the lactic acid content of the three groups, ranging from 1.56 to 1.61 g/L, showed no significant differences, these values were all higher than in the control group (1.38 ± 0.09 g/L). The citric acid content (1.02 ± 0.01 g/L) of the H30 + EC1118 group was significantly higher than in the other groups. The succinic acid test results differed from that of the sterilization system, and its content in the YT13 and H30 + EC1118 groups was significantly higher than in the other two groups. In general, whether it was the sterile or natural group, the organic acid content in wine fermented with indigenous yeast was significantly higher than that in the control group.

Indigenous yeast increases the phenolic acid content of Petit Manseng dry white wine

Phenolic acids represent important polyphenolic compounds in wine, displaying antioxidant properties and playing a role in human nutrition and health. This study detected a total of eight phenolic acids (namely gallic acid, protocatechuic acid, gentisic acid, chlorogenic acid, caffeic acid, vanillic acid, *p*-Coumaric acid, and ferulic acid) in the wines fermented with filtered and sterilized grape juice.

As shown in Table 4, no significant differences were evident in gallic acid, caffeic acid, vanillic acid, and ferulic acid in the sterilized Petit Manseng grape juice fermented

wine. Except for coumaric acid, the phenolic acid content of the single-bacteria and mixed-bacteria fermentations using YT13 was higher than in the control group, confirming the high quality of indigenous strains. However, the results for the H30 + EC1118 mixed fermentation exhibited an opposite trend. The protocatechuic acid (4.24 ± 0.405 g/L), gentisic acid (0.40 ± 0.04 g/L), chlorogenic acid (1.86 ± 0.47 g/L), and soybean acid (0.07 ± 0.09 g/L) levels were all significantly lower than the control group. In the H30 + YT13 mixed fermentation group, the levels of these four phenolic acids were 5.15 ± 0.08, 0.57 ± 0.05, 2.63 ± 0.01, and 0.12 ± 0.04 g/L, significantly higher than the H30 + EC1118 group. It is speculated that this is due to a decrease in the phenolic acid content caused by the interaction between H30 and EC1118. However, whether the significant difference between the phenolic acid production by YT13 and EC1118 is related to the characteristics of the individual yeasts remains unclear and requires further exploration. Furthermore, the indigenous microorganism variety in the Yantai natural grape juice caused changes in the phenolic acid levels. As shown in Table 4, the highest total phenolic acid content in the Petit Manseng wine fermented with natural grape juice reached 16.36 ± 1.9 mg/L, while the levels in the three test groups were higher than in the control group (14.03 ± 0.84 mg/L). Except for gallic acid and caffeic acid, significant differences were apparent in the content of the other phenolic acids. The protocatechuic acid levels in the three groups were 4.42 ± 0.315, 4.49 ± 0.23, and 4.63 ± 0.63 mg/L, which were significantly higher than in the control group (4.08 ± 0.08 mg/L), while the vanillic acid content (0.15 ± 0.004 mg/L) was highest in the YT13 test group. The H30 + EC1118 group displayed the highest gentisic acid level, reaching 0.68 mg/L. The chlorogenic acid detection results were consistent with the sterilization system, exhibiting the highest level (3.43 ± 0.14 mg/L) in the YT13 test group. The *p*-coumaric acid content (0.39 ± 0.05 mg/L) of the H30 + EC1118 group was the highest of the four groups.

These results indicated that the levels of other phenolic acid compounds in the YT13-fermented wine were higher than in the control group except for coumaric acid. The total phenolic acid content also verified this conclusion.

Indigenous yeast increases the relative content of the volatile ester compounds in Petit Manseng dry white wine

Volatile compounds are affected by many factors. Studies have found that gallic acid and *p*-coumaric acid can spontaneously bind to linalool and its glycosides via hydrogen bonding and dispersion, effectively controlling the release and regulating the overall aroma of wine features. Therefore, this study used gas chromatography and mass spectrometry for volatile compound detection. The sterilized Petit Manseng wine exhibited 55 different volatile compounds, including 18 alcohols, 16 acids, 12 esters, six aldehydes and ketones, and three other compounds. A total of 52 different volatile aroma components were detected in the natural Petit Manseng wine, including 16 alcohols, 16 acids, 12 esters, five aldehydes and ketones, and three other compounds. To more intuitively compare the differences between the natural wines and the sterile wines fermented with different yeasts, the OriginPro 2021 software was used to perform principal component analysis on the data via dimensionality reduction processing. Figure 1 shows the principal component analysis results regarding the volatile compounds in the sterilized Petit Manseng wine. The contribution rates were 47.7% for the first principal component (PC1) and 33.1% for the second principal component (PC2). The cumulative variance contribution rate of the principal components reached 80.8%, while the information loss rate was only 19.2%. The information of the original indicators was mostly retained and used as the principal component to analyze the sterilized Petit Manseng wine. PC1 was mainly composed of alcohol and acid compounds, such as nerolidol and myristic acid, while PC2 primarily consisted of ester compounds providing volatile floral and fruity flavors and included ethyl phenylacetate, ethyl butyrate, isovalerate, and methyl apiate. EC1118 accumulated more aroma compounds, displaying the highest levels in the Petit Manseng wine treated with yeast. The specific types and content of the volatile ester compounds are shown in Table 5. The total relative content of the ester compounds in the YT13 group was 6,686.41 μg/L, which was significantly higher than in the control group. Ethyl phenylacetate, ethyl butyrate, phenethyl caproate, geranyl isovalerate, and ethyl decanoate accounted for a large proportion of the detected ester compounds. The H30 + YT13 group exhibited the most volatile ester compounds (15 types). In addition, the mixed fermentation group contained pearlitol, butyrolactone, and neryl propionate, which were not during single yeast fermentation, increasing the aroma complexity of the Petit Manseng wine exposed to the mixed fermentation process.

The interaction between the grape juice and other microorganisms in the environment and native yeast remains unclear, while the metabolite production may also affect the volatile compounds. Figure 2 shows the principal component analysis results for the volatile compounds in natural Petit Manseng wine. The contribution rates were 51.5% for PC1 is 51.5 and 33.2% for PC2. The cumulative variance contribution rate of the two principal components reached 84.7%, mostly retaining the information of the original indicators. Therefore, these two principal components can be used for two-dimensional plane analysis. In the Figure 2, YT13 was distributed in the third quadrant, while the H30 + EC1118 and H30 + YT13 mixed fermentation groups were distributed in the second quadrant. Furthermore, various aroma compounds were clustered together, including myristic acid, phenethyl

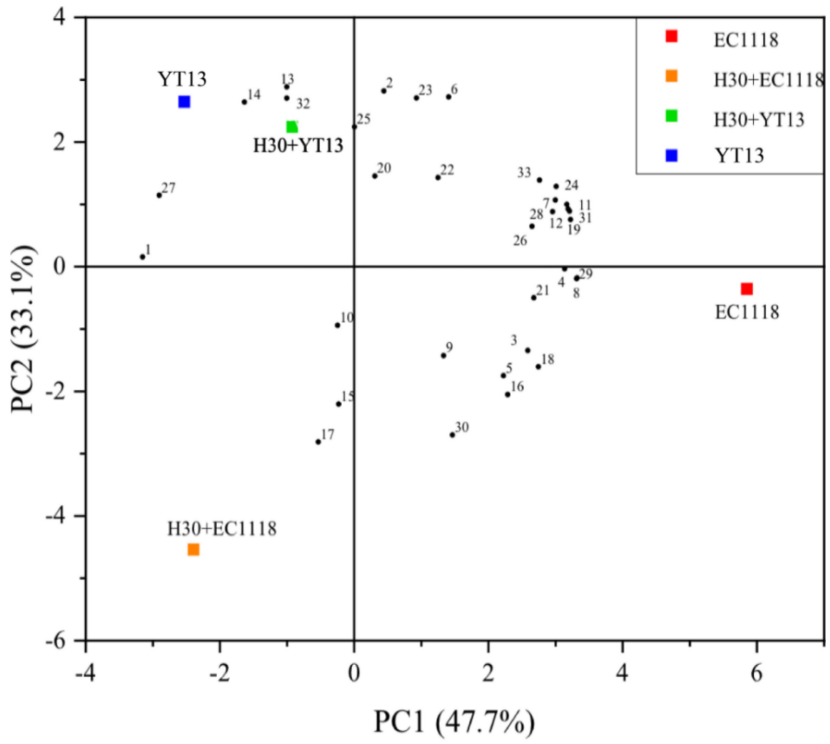

FIGURE 1
Principal component analysis diagram of the volatile compounds in wine fermented with sterilized Petit Manseng grape juice. The control group was inoculated with commercial *Saccharomyces cerevisiae* EC1118 (EC1118). YT13 refers to inoculation with YT13 *Saccharomyces cerevisiae*. H30 + EC1118 indicates that H30 and EC1118 are inoculated in sequence. H30 + YT13 indicates that H30 and YT13 are inoculated in sequence. PCA analysis is used to select the volatile compounds shared by the different yeast fermentation groups. The black dots with serial numbers in the figure represent volatile compounds: (1) 2-hexyn-1-ol, (2) cis-3-penten-1-ol, (3) 2-octyn-1-ol, (4) nerol, (5) 3,7,11-trimethyldodecanol, (6) 13-heptadene-1-ol, (7) 1-pentadecanol, (8) methyl myristelaidate, (9) 2-hydroxymyristic acid, (10) ethyl 2-non-ynoate, (11) 4-pentenoic acid, (12) 2-hydroxymyristic acid, (13) 9-hexadecenoic acid, ethyl ester, (14) traumatic acid, (15) ethyl phenylacetate, (16) 2-hydroxy-1-methyl propyl ester, (17) ethyl butanoate, (18) phenethyl caproate, (19) dodecyl acrylate, (20) geranyl isovalerate, (21) ethyl caprate, (22) γ-oryzanol, (23) methyl(9Z)-9-hexadecenoate, (24) methyl laurate, (25) methyl 6-octadecenoate, (26) 3-eicosanone, (27) cyclopentadecanone, (28) cyclohexadienone, (29) 1,2-epoxyheptane, (30) coumarin, (31) 3,4-diethylbiphenyl, and (32) 2,6-di-tert-butylhydroquinone, and (33) valerenic acid.

caproate, and ethyl caprate. These findings indicated that the mixed fermentation group was richer in aroma types and content and established a good aroma base. Furthermore, the results showed that the total relative content and types of ester compounds in the H30 + EC1118 group were the highest, yielding a total content value of 9,370.99 μg/L for 16 compounds, followed by the H30 + YT13 test group. In addition, similar to the sterilization system, both pearlitol and butyrolactone were detected in the mixed fermentation group, increasing the complexity of the volatile aroma.

Indigenous yeast enhances the fruity and floral characteristics of Petit Manseng dry white wine

Instrumental analysis and sensory appraisal were combined to evaluate the influence of different strains on the aroma of the dry white wine more comprehensively. Based on Gas Chromatography-Mass Spectrometer (GC-MS) instrumental analysis, seven professionals with extensive experience in wine tasting were invited to perform a sensory evaluation on the fermented Petit Manseng dry white wine, assessing the appearance (color and clarity), aroma (richness, coordination, freshness, and complexity), and taste (body, balance, and aftertaste). A total of 100 points was scored. As shown in Figure 3A, the H30 + YT13 group of sterilized Petit Manseng wine received the highest average sensory score of 76.4 points, which could be attributed to a lower content of higher alcohols, while the ester compounds displayed the most variety but little content, maintaining the balance and coordination of the wine. This was followed by the YT13 group with 74 points and the H30 + EC1118 treatment group with 73.4 points. However, the control group received the lowest score due to higher volatile acid content, displaying a boiled smell and sour taste. In addition, pearlitol, butyrolactone, and neryl propionate

TABLE 5 Relative content of volatile ester compounds in wine fermented from Petit Manseng grape juice.

Relative content (μg/L)	Sterilization group			Natural group		
	Control	YT13	H30 + EC1118	H30 + YT13	Control	YT13	H30 + EC1118	H30 + YT13
Ethyl cinnamate	N.D.	212.08 ± 2.08^{b}	20.46 ± 1.30^{c}	241.78 ± 13.47^{a}	N.D.	214.23 ± 0.23^{a}	175.78 ± 7.39^{b}	174.69 ± 13.40^{b}
Ethyl phenylacetate	238.54 ± 73.72^{ab}	157.19 ± 38.28^{b}	255.87 ± 68.59^{ab}	304.67 ± 12.24^{a}	402.25 ± 18.88^{a}	284.58 ± 0.36^{b}	308.01 ± 17.84^{ab}	394.34 ± 94.26^{a}
Ethyl caproate	40.33 ± 5.14^{a}	72.40 ± 35.58^{a}	N.D.	N.D.	86.16 ± 6.47^{a}	68.39 ± 9.43^{b}	N.D.	N.D.
Ethyl butyrate	2317.58 ± 215.99^{a}	2518.64 ± 231.79^{a}	2026.92 ± 218.02^{a}	2736.74 ± 580.95^{a}	3028.41 ± 360.42^{a}	2491.05 ± 40.00^{b}	3138.06 ± 91.35^{a}	3235.4 ± 83.98^{a}
Phenethyl caproate	117.90 ± 24.19^{b}	121.89 ± 19.65^{ab}	142.35 ± 8.49a^{b}	155.51 ± 14.99^{a}	333.35 ± 62.54^{a}	240.8 ± 29.57^{b}	310.09 ± 14.62^{ab}	358.05 ± 3.57^{a}
Geranyl isovalerate	1650.23 ± 79.97^{bc}	2257.39 ± 189.69^{a}	1290.54 ± 130.07^{c}	1984.11 ± 330.95^{ab}	3291.6 ± 421.80^{b}	2590.96 ± 127.07^{c}	3733.87 ± 128.14^{a}	3832.07 ± 77.43^{a}
Ethyl decanoate	13.88 ± 1.52^{ab}	15.65 ± 0.53^{a}	11.76 ± 1.70^{b}	15.76 ± 0.99^{a}	21.19 ± 0.16^{a}	20.45 ± 5.26^{a}	23.26 ± 0.27^{a}	24.77 ± 6.26^{a}
Methyl decanoate	123.25 ± 16.97^{b}	132.68 ± 13.83^{b}	161.02 ± 32.15^{b}	305.24 ± 20.87^{a}	73.85 ± 13.58a^{b}	56.85 ± 2.56^{b}	64.66 ± 0.20^{ab}	84.62 ± 17.85^{a}
Ethyl linoleate	24.50 ± 4.73^{b}	30.96 ± 3.40^{a}	11.59 ± 0.81^{c}	27.56 ± 1.02^{ab}	39.58 ± 0.25^{a}	38.31 ± 7.15^{a}	38.08 ± 0.06^{a}	40.47 ± 20.73^{a}
Ferulate	22.64 ± 1.90^{b}	30.88 ± 3.63^{a}	18.21 ± 7.11^{b}	19.75 ± 0.81^{b}	23.51 ± 2.60^{ab}	23.37 ± 2.90^{ab}	26.55 ± 0.97^{a}	21.17 ± 2.81^{b}
Hexyl acetate	14.62 ± 2.60^{ab}	18.33 ± 1.80^{ab}	20.86 ± 5.17^{a}	14.13 ± 0.13^{b}	22.26 ± 1.48^{a}	22.17 ± 3.94^{a}	21.88 ± 0.19^{a}	23.3 ± 9.31^{a}
Methyl laurate	26.78 ± 15.45^{a}	34.40 ± 25.10^{a}	18.43 ± 10.68^{a}	11.31 ± 4.62^{a}	35.49 ± 7.04^{bc}	18.39 ± 11.67^{c}	44.27 ± 13.08^{b}	100.43 ± 15.89^{a}
Total esters	4,590.25	5,602.49	3,978.01	5,815.78	7,357.65	6,069.55	7,884.51	8,289.31

The control group was inoculated with commercial *Saccharomyces cerevisiae* EC1118 (EC1118), while the test groups are treated as follows: YT13 *Saccharomyces cerevisiae* fermentation (YT13); H30 fermentation for 3 days, followed by inoculation with EC1118 for sequential fermentation (H30 + EC1118); H30 fermentation for 3 days, followed by inoculation with YT13 for sequential fermentation (H30 + YT13). In the table, N.D. means not detected. Different letters indicate significant differences at $p < 0.05$.

were only detected in the mixed fermentation group, providing enhanced floral, fruity, and fermented aromas. Therefore, the wines fermented with mixed bacteria received higher aroma scores.

Figure 3B shows the flavor radar chart of the smell evaluation of the sterilized Petit Manseng wine, displaying descriptive groups, such as "alcohol smell," "floral fragrance," "citrus fruits," "temperate fruits," and "fermented aroma." A significant difference was evident in attribute strength. The H30 + EC1118 group displayed the highest floral aroma (orange blossom) and temperate fruit aroma (peach and apricot), which was related to the high concentration of ethyl butyrate. Significant differences were apparent in the ferulate, palmitoleate, and neryl propionate levels of the H30 + YT13 group. Therefore, this group received the highest aroma evaluation score regarding citrus fruit (citrus and kumquat), tropical fruit (melon and pineapple), and fermented aromas (bread). Except for the undesirable and floral aromas, the other aroma scores of the control group were the lowest.

The natural wine was scored a total of 100 points according to appearance, aroma, and taste. The scores are shown in Figure 4A. The control group received the highest average score of 77.3 points, followed by the YT13 group with 76.6 points and the H30 + EC1118 group with 76.4 points. Since the YT13 group may contain higher decanoic acid levels, an undesirable fatty smell and abrasive taste may affect the final sensory score. Figure 4B shows the radar chart of the smell and flavor evaluations of the wine fermented with natural Petit Manseng grape juice. Due to its specific characteristics, the citrus fruit (lemon, citrus, and kumquat) and temperate fruit (apricot and peach) aromas provided by the Petit Manseng grape variety generally scored higher than other flavor properties. The YT13 group displayed the highest floral fragrance (neroli and honeysuckle), while the total alcohol and acid compound content was prominent. The YT13 group obtained the highest floral fragrance score due to the compound fragrance of higher alcohols. Since 2-hydroxymyristic acid and linalool showed significant differences, more intense sweet orange and cool lemon aromas were evident in the H30 + YT13 group.

Discussion

This study explored two indigenous yeast strains from Yantai. The results showed that the indigenous *Saccharomyces cerevisiae* YT13 displayed excellent fermentation performance, significantly increasing the gallic acid, protocatechuic acid, gentisic acid, and caffeic acid content in Petit Manseng wine and reducing the coumaric acid concentration. The lactic acid content, which most substantially improved the taste, also increased significantly. The ferulic acid content in the sequential fermentation group using the indigenous non-*Saccharomyces cerevisiae,* H30, was 1.4 times higher during mixed fermentation

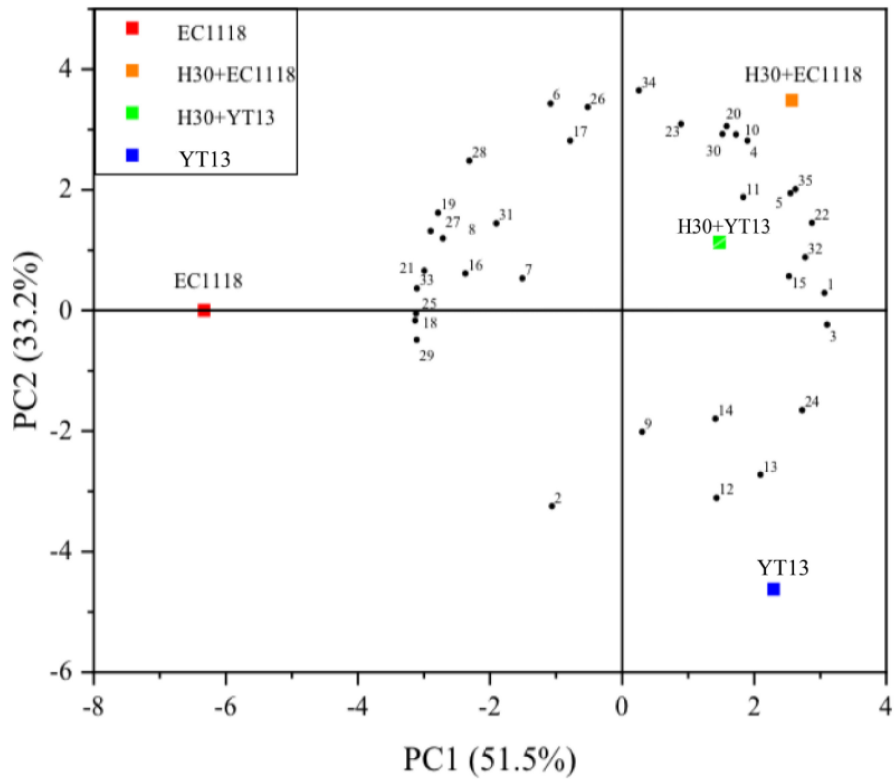

FIGURE 2
Principal component analysis diagram of the volatile compounds in wine fermented with Petit Manseng natural grape juice. The control group was inoculated with commercial *Saccharomyces cerevisiae* EC1118 (EC1118). YT13 refers to inoculation with YT13 *Saccharomyces cerevisiae*. H30 + EC1118 indicates that H30 and EC1118 are inoculated in sequence. H30 + YT13 indicates that H30 and YT13 are inoculated in sequence. PCA analysis is used to select the volatile compounds shared by the different yeast fermentation groups. The black dots with serial numbers in the figure represent volatile compounds: (1) 4-methylpentan-2-ol, (2) 2,4,5-trimethylbenzaldehyde, (3) cis-3-penten-1-ol, (4) cis-4-cyclopentene-1,3-diol, (5) nerolidol, (6) 2-octyn-1-ol, (7) linalool, (8) nerol, (9) 1-pentadecanol, (10) myristic acid, (11) 2-hydroxymyristic acid, (12) 2-decanoic acid, (13) 4-pentenoic acid, (14) 2-hydroxymyristic acid, (15)9-hexadecenoic acid,(16) traumatic acid, (17) ethyl phenylacetate, (18) 2-hydroxy-1-methyl propyl ester, (19) ethyl butanoate, (20) phenethyl caproate, (21) dodecyl acrylate, (22) geranyl isovalerate, (23) ethyl caprate, (24) γ-oryzanol, (25) methyl vaccenate, (26) methyl (9Z)-9-hexadecenoate, (27) methyl laurate, (28) neryl acetate, (29) methyl 6-octadecenoate (30) 5-Octadecanone, (31) 3-eicosanone, (32) cyclohexadienone, (33) 1,2-epoxyheptane, (34) coumarin, and (35) 3,4-diethylbiphenyl.

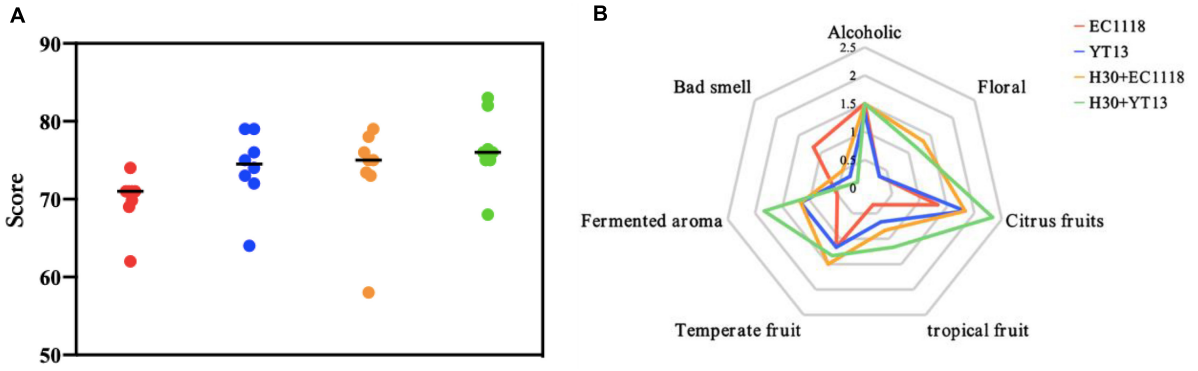

FIGURE 3
Sensory scoring map **(A)** and aroma evaluation radar map **(B)** of wine fermented with Petit Manseng sterilized grape juice. The control group was inoculated with commercial *Saccharomyces cerevisiae* EC1118 (EC1118); YT13 indicates inoculation with YT13 *Saccharomyces cerevisiae*; H30 + EC1118 indicates sequential inoculation with H30 and EC1118; H30 + YT13 indicates sequential inoculation with H30 and YT13.

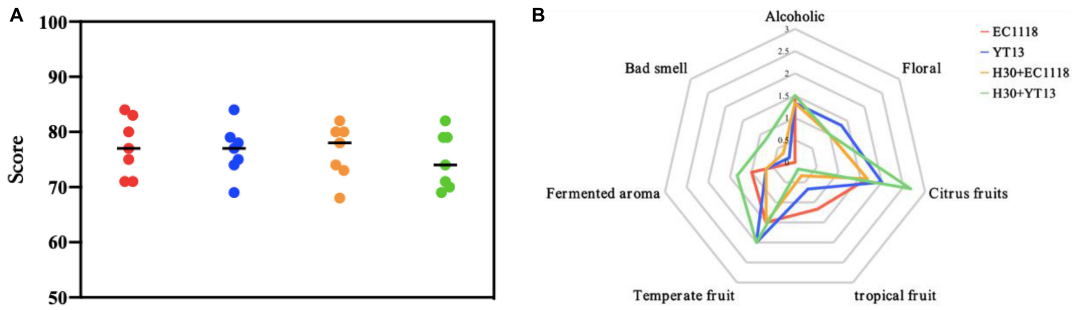

FIGURE 4
Sensory scoring map **(A)** and aroma evaluation radar map **(B)** of wine fermented with Petit Manseng natural grape juice. The control group was inoculated with commercial *Saccharomyces cerevisiae* EC1118 (EC1118); YT13 indicates inoculation with YT13 *Saccharomyces cerevisiae*; H30 + EC1118 indicates sequential inoculation with H30 and EC1118; H30 + YT13 indicates sequential inoculation with H30 and YT13.

than single yeast fermentation. In addition, due to the different metabolic pathways of different yeasts, obvious differences were evident between the types of trace aroma compounds and their respective contents (21). Pearlitol, butyrolactone, and neryl propionate were detected in the wine of the mixed fermentation group. These trace volatile compounds provided creamy, orange blossom, melon, and pineapple aromas.

The sharp acidity of a wine is reduced by malolactic fermentation (MLF). It is speculated that there may be a positive symbiotic relationship between lactic acid bacteria and indigenous yeast, which is also reflected in this research (22). The lactic acid content is used as a vital reference index to judge the taste of wine. The experiment revealed that the lactic acid content increased significantly during the alcohol fermentation stage when indigenous yeasts participated in fermentation. This phenomenon is also reflected in the mixed yeast fermentation, suggesting that it may be related to the non-*Saccharomyces cerevisiae* participating in the synergistic yeast interaction. The advantage of mixed fermentation is also reflected in the aroma of the wine. A study involving Syrah wine indicated that the interaction between *Oenococcus*, *Lactobacillus plantarum,* and yeast affected the mannoprotein content. Furthermore, the ethyl lactate level also increased significantly, enhancing the aroma of the wine (23–25).

Although the positive effect of phenolic acid compounds on the human body is currently attracting considerable research attention, minimal studies are available regarding the high-yield phenolic acid compounds in indigenous yeast. The indigenous yeast used in this study increased the levels of phenolic acid compounds, such as protocatechuic acid, gallic acid, and caffeic acid via fermentation. This is more pronounced during mixed fermentation and may be attributed to the interaction between the yeasts or between the yeast and phenolic acid (26). The metabolism in the digestive tract and the interaction between the intestinal flora and polyphenolic compounds, such as para-hydroxycinnamic acid, ferulic acid, *p*-Coumaric acid, and caffeic acid, have been proven effective against non-alcoholic fatty liver disease and obesity (27). In addition, the influence of phenolic compounds on the color strength and stability of wine has attracted significant attention. For example, caffeic acid can increase the color saturation of wine, while the chromaticity characteristics and phenolic composition of wine with exogenous ellagic acid are superior to wine with gallic acid (28, 29).

Regarding volatile ester compounds, pronounced differences were evident between the types of aroma compounds and their respective content due to the different metabolic yeast pathways (30). Previous research screened the indigenous *Hanseniaspora uvarum* H30 strain that caused the wine to release more terpene aroma substances. The H30 yeast displayed higher β-glucosidase activity, catalyzing glycosidic bond hydrolysis in the aroma substance molecule in a glycoside-bound state. Studies have shown that adding β-glucosidase BGL0224 during the fermentation process can increase the "tropical fruit" and "floral" scents of Cabernet Sauvignon (17, 31). However, the interaction between *Saccharomyces cerevisiae* and non-*Saccharomyces cerevisiae* may also lower the β-glucosidase activity, significantly reducing the nerol produced by β-glucosidase hydrolysis during mixed fermentation. This study detected no isoamyl lactate in the wine of the sterilization system, indicating to a certain extent that other microorganisms in the grape juice interact with *Saccharomyces cerevisiae*, modifying the aroma compound content (32). The competition for nitrogen source nutrients directly affects the fermentation performance of yeast. Due to the different metabolic yeast pathways to nitrogen sources, a two-pronged strategy using isotope labeling and RNA sequencing has been explored. Moreover, the metabolic network of nitrogen utilization in *Kluyveromyces marxianus* and its regulatory mechanism has been analyzed, showing the ultimate effect of the aroma compound content on key wine varieties (33–35). *Saccharomyces cerevisiae* can also act on the phenolic acid and norisoprene aroma precursors in grapes via specific enzyme

activity to effectively regulate the aroma of the variety and reduce the odor during the aging process (36).

Furthermore, differences were evident in the effect of indigenous yeast on the two different systems of the sterile and natural groups. During the fermentation process of the sterilized grape juice, the *Saccharomyces cerevisiae* and non-*Saccharomyces cerevisiae* used in the experiment displayed a competitive reproduction advantage, reflecting the influence of indigenous yeast on the quality of dry white wine. However, a large number of microorganisms are introduced into the environment during actual natural wine production. The interaction between these unknown microorganisms and the yeast may affect the metabolic pathways and enzyme activity. The difference between the two systems is particularly obvious during the fermentation process. Since the natural grape juice only required a short fermentation time, the fermentation rate was significantly higher than sterilized grape juice. The most important reason for this is that grape juice is a natural nutrient containing abundant microbial resources, such as indigenous yeast, lactic acid bacteria, acetic acid bacteria, hop bacteria, *Bacillus bitterus*, and molds. In addition to indigenous yeasts that provide wine with its unique flavor, hop bacteria can produce a strange acetaldehyde odor. Acetic acid bacteria produce a gray film on the surface of the wine during the fermentation process, causing a bad acetic acid taste (24, 37, 38). The phenolic acid results showed that the protocatechin and gentisic acid levels in the natural wine group were slightly higher than in the sterile wine group. The findings regarding the volatile aroma compounds indicated that the relative ester content in the wine fermented from natural grape juice was 2.3 times higher than wine fermented from sterile grape juice. However, the reasons and mechanisms regarding these effects required further exploration. In addition, whether a macromolecular nutrient loss occurs during the sterilization operation necessitates verification.

Water, soil, and terroir have cultivated relatively fixed microbial populations over an extended period. The characteristics of wine-producing areas are affected by the local climate, soil, and raw grape materials, as well as indigenous microorganisms, including *Saccharomyces cerevisiae*, non-*Saccharomyces cerevisiae*, and lactic acid bacteria (39, 40). For example, the Pinot Noir wines from various production areas in Australia are affected by the terroir, resulting in certain differences in mineral content (41). Furthermore, wine from different production areas shows unique regional sensory characteristics. "Mint" and "dark fruit" are important qualities of Coonawarra wines, while wine from the Margaret River region exhibit typical "floral" and "green pepper" flavors (42). In addition, a study involving Burgundy confirmed the uniqueness of the village-level production area (40). The microorganisms in different areas interact with the raw grape materials to produce metabolites that vary in type and content, including organic acids, phenolic acids, volatile compounds, and other products, affecting the sensory quality and characteristics of wines worldwide. Therefore, the impact of terroir and microorganisms requires further exploration.

Conclusion

The indigenous *Saccharomyces cerevisiae* YT13 can significantly enhance the lactic acid content in Petit Manseng dry white wine, increase the protocatechuic acid, caffeic acid, gallic acid, and ferulic acid concentrations in the phenolic acid, and promote the production of volatile ester compounds. Sequential inoculation and fermentation with indigenous non-*Saccharomyces cerevisiae* H30 and indigenous *Saccharomyces cerevisiae* YT13 can improve the quality of Petit Manseng dry white wine and promote the embodiment of the regional characteristics.

Data availability statement

The original contributions presented in this study are included in the article/supplementary material, further inquiries can be directed to the corresponding authors.

Ethics statement

The studies involving human participants were reviewed and approved by China Agricultural University, Tsinghua East Road 17, Haidian District, Beijing, 100083, China. Written informed consent for participation was not required for this study in accordance with the national legislation and the institutional requirements.

Author contributions

YY: guidance and supervision of whole experiments. YW and MW: participate in the whole experiment, data analysis, and manuscript writing. WL: participate in fermentation experiments. XW: participate in data analysis. WK: provide technical guidance. WH: provide experimental funding. JZ: provide experimental funding and supervise experiments. GX: guide the entire experiment and provide experimental raw materials. All authors contributed to the article and approved the submitted version.

Funding

This work was supported by the Science and Technology Project in Beijing (Z201100008920003) to YY, Basic Research on

Wine Industry Technology in Yantai Regions (50012305073) to GX, and the National "Thirteenth Five-Year" Plan for Science and Technology Support (2016YFD0400500) to WH.

Conflict of interest

YW, MW, WL, and GX were employed by Yantai Pula Valley Winery Management Co., Ltd.

The remaining authors declare that the research was conducted in the absence of any commercial or financial relationships that could be construed as a potential conflict of interest.

Publisher's note

All claims expressed in this article are solely those of the authors and do not necessarily represent those of their affiliated organizations, or those of the publisher, the editors and the reviewers. Any product that may be evaluated in this article, or claim that may be made by its manufacturer, is not guaranteed or endorsed by the publisher.

References

1. Borren E, Tian B. The important contribution of non-saccharomyces yeasts to the aroma complexity of wine: a review. *Foods.* (2021) 10:13. doi: 10.3390/foods10010013

2. Romano P, Ciani M, Fleet GH. *Yeasts in the Production of Wine*. Berlin: Springer (2019). doi: 10.1007/978-1-4939-9782-4

3. Strauss M, Jolly N, Lambrechts M, Van Rensburg P. Screening for the production of extracellular hydrolytic enzymes by non-Saccharomyces wine yeasts. *J Appl Microbiol.* (2001) 91:182–90.

4. Siebert TE, Solomon MR, Pollnitz AP, Jeffery DW. Selective determination of volatile sulfur compounds in wine by gas chromatography with sulfur chemiluminescence detection. *J Agric Food Chem.* (2010) 58:9454–62. doi: 10.1021/jf102008r

5. Jolly NP, Varela C, Pretorius IS. Not your ordinary yeast: non-*Saccharomyces* yeasts in wine production uncovered. *FEMS Yeast Res.* (2014) 14:215–37. doi: 10.1111/1567-1364.12111

6. Cuš F, Zabukovec P, Schroers HJ. Indigenous yeasts perform alcoholic fermentation and produce aroma compounds in wine. *Czech J Food Sci.* (2017) 35:339–45. doi: 10.17221/398/2016-CJFS

7. Ramírez M, López-Piñeiro A, Velázquez R, Muñoz A, Regodón JA. Analysing the vineyard soil as a natural reservoir for wine yeasts. *Food Res Int.* (2020) 129:108845. doi: 10.1016/j.foodres.2019.108845

8. Capece A, Siesto G, Romaniello R, Lagreca VM, Pietrafesa R, Calabretti A, et al. Assessment of competition in wine fermentation among wild *Saccharomyces cerevisiae* strains isolated from Sangiovese grapes in Tuscany region. *LWT Food Sci Technol.* (2013) 54:485–92. doi: 10.1016/j.lwt.2013.07.001

9. Williams MT, Khan W, Ntushelo N, Hart RS. An indigenous *Saccharomyces cerevisiae* yeast strain isolated from Paarl regional Shiraz grapes to enhance Shiraz wine typicity. *Oeno One.* (2021) 55:209–25. doi: 10.20870/oeno-one.2021.55.2.4552

10. Benito S, Morata A, Palomero F, González MC, Suárez-Lepe JA. Formation of vinylphenolic pyranoanthocyanins by *Saccharomyces cerevisiae* and *Pichia guillermondii* in red wines produced following different fermentation strategies. *Food Chem.* (2011) 124:15–23. doi: 10.1016/j.foodchem.2010.05.096

11. Morata A, Benito S, Loira I, Palomero F, González MC, Suárez-Lepe JA. Formation of pyranoanthocyanins by *Schizosaccharomyces pombe* during the fermentation of red must. *Int J Food Microbiol.* (2012) 159:47–53. doi: 10.1016/j.ijfoodmicro.2012.08.007

12. Chen K, Escott C, Loira I, del Fresno JM, Morata A, Tesfaye W, et al. Use of non-*Saccharomyces* yeasts and oenological tannin in red winemaking: influence on colour, aroma and sensorial properties of young wines. *Food Microbiol.* (2018) 69:51–63. doi: 10.1016/j.fm.2017.07.018

13. Castellari L, Ferruzzi M, Magrini A, Giudici P, Passarelli P, Zambonelli C. Unbalanced wine fermentation by cryotolerant vs. non-cryotolerant *Saccharomyces* strains. *Vitis.* (1994) 33:49–52.

14. Gamero A, Wesselink W, de Jong C. Comparison of the sensitivity of different aroma extraction techniques in combination with gas chromatography-mass spectrometry to detect minor aroma compounds in wine. *J Chromatogr A.* (2013) 1272:1–7. doi: 10.1016/j.chroma.2012.11.032

15. Magyar I, Tóth T. Comparative evaluation of some oenological properties in wine strains of *Candida stellata*, *Candida zemplinina*, *Saccharomyces uvarum* and *Saccharomyces cerevisiae*. *Food Microbiol.* (2011) 28:94–100. doi: 10.1016/j.fm.2010.08.011

16. Sipiczki M, Romano P, Lipani G, Miklos I, Antunovics Z. Analysis of yeasts derived from natural fermentation in a Tokaj winery. *Antonie Van Leeuwenhoek.* (2001) 79:97–105. doi: 10.1023/A:1010249408975

17. Han X, Qing X, Yang S, Li R, Zhan J, You Y, et al. Study on the diversity of non-*Saccharomyces* yeasts in Chinese wine regions and their potential in improving wine aroma by β-glucosidase activity analyses. *Food Chem.* (2021) 360:129886. doi: 10.1016/j.foodchem.2021.129886

18. Zhang X, Guo A, Han F, Zhang Y. Fast determination of phenolics and polyphenolics in wine by ultra performance liquid chromatography. *Food Sci.* (2016) 37:128–33. doi: 10.7506/spkx1002-6630-201610022

19. Chen J, Wen P, Zhan J, Li J, Pan Q, Kong W, et al. Studies on the determination of 11 phenolic acids in wines by rever se phase high per formance liquid chromatography. *J Chin Inst Food Sci Technol.* (2006) 6:133–8.

20. Li N, Wang QQ, Xu YH, Li AH, Tao YS. Increased glycosidase activities improved the production of wine varietal odorants in mixed fermentation of *P. fermentans* and high antagonistic *S. cerevisiae*. *Food Chem.* (2020) 332:127426.

21. Fairbairn S, Engelbrecht L, Setati ME, du Toit M, Bauer FF, Divol B, et al. Combinatorial analysis of population dynamics, metabolite levels and malolactic fermentation in *Saccharomyces cerevisiae*/ *Lachancea thermotolerans* mixed fermentations. *Food Microbiol.* (2021) 96:103712. doi: 10.1016/j.fm.2020.103712

22. Liu S, Laaksonen O, Kortesniemi M, Kalpio M, Yang B. Chemical composition of bilberry wine fermented with non-Saccharomyces yeasts (*Torulaspora delbrueckii* and *Schizosaccharomyces pombe*) and *Saccharomyces cerevisiae* in pure, sequential and mixed fermentations. *Food Chem.* (2018) 266:262–74. doi: 10.1016/j.foodchem.2018.06.003

23. Balmaseda A, Rozès N, Bordons A, Reguant C. Simulated lees of different yeast species modify the performance of malolactic fermentation by *Oenococcus oeni* in wine-like medium. *Food Microbiol.* (2021) 99:103839. doi: 10.1016/j.fm.2021.103839

24. Balmaseda A, Rozès N, Leal MÁ, Bordons A, Reguant C. Impact of changes in wine composition produced by non-Saccharomyces on malolactic fermentation. *Int J Food Microbiol.* (2021) 337:108954. doi: 10.1016/j.ijfoodmicro.2020.108954

25. Devi A, Konerira Aiyappaa AA, Waterhouse AL. Adsorption and biotransformation of anthocyanin glucosides and quercetin glycosides by *Oenococcus oeni* and *Lactobacillus plantarum* in model wine solution. *J Sci Food Agric.* (2020) 100:2110–20. doi: 10.1002/jsfa.10234

26. Pastorkova E, Zakova T, Landa P, Novakova J, Vadlejch J, Kokoska L. Growth inhibitory effect of grape phenolics against wine spoilage yeasts and acetic acid bacteria. *Int J Food Microbiol.* (2013) 161:209–13. doi: 10.1016/j.ijfoodmicro.2012.12.018

27. Leonard W, Zhang P, Ying D, Fang Z. Hydroxycinnamic acids on gut microbiota and health. *Compr Rev Food Sci Food Saf.* (2021) 20:710–37. doi: 10.1111/1541-4337.12663

28. Zhang B, Wang XQ, Yang B, Li NN, Niu JM, Shi X, et al. Copigmentation evidence of phenolic compound: the effect of caffeic and rosmarinic acids addition on the chromatic quality and phenolic composition of cabernet sauvignon red wine from the Hexi corridor region (China). *J Food Composit Anal.* (2021) 102:104037. doi: 10.1016/j.jfca.2021.104037

29. Zhang XK, He F, Zhang B, Reeves MJ, Liu Y, Zhao X, et al. The effect of prefermentative addition of gallic acid and ellagic acid on the red wine color, copigmentation and phenolic profiles during wine aging. *Food Res Int.* (2018) 106:568–79. doi: 10.1016/j.foodres.2017.12.054

30. Xi X, Xin A, You Y, Huang W, Zhan J. Increased varietal aroma diversity of marselan wine by mixed fermentation with indigenous non-saccharomyces yeasts. *Fermentation.* (2021) 7:133. doi: 10.3390/fermentation7030133

31. Zhang J, Wang T, Zhao N, Xu J, Qi Y, Wei X, et al. Performance of a novel β-glucosidase BGL0224 for aroma enhancement of cabernet sauvignon wines. *LWT.* (2021) 144:111244. doi: 10.1016/j.lwt.2021.111244

32. Gobert A, Tourdot-Maréchal R, Morge C, Sparrow C, Liu Y, Quintanilla-Casas B, et al. Non-*Saccharomyces* yeasts nitrogen source preferences: impact on sequential fermentation and wine volatile compounds profile. *Front Microbiol.* (2017) 8:2175. doi: 10.3389/fmicb.2017.02175

33. Rollero S, Bloem A, Ortiz-Julien A, Camarasa C, Divol B. Altered fermentation performances, growth, and metabolic footprints reveal competition for nutrients between yeast species inoculated in synthetic grape juice-like medium. *Front Microbiol.* (2018) 9:196. doi: 10.3389/fmicb.2018.00196

34. Rollero S, Bloem A, Ortiz-Julien A, Bauer FF, Camarasa C, Divol B. A comparison of the nitrogen metabolic networks of *Kluyveromyces marxianus* and *Saccharomyces cerevisiae*. *Environ Microbiol.* (2019) 21:4076–91. doi: 10.1111/1462-2920.14756

35. Seguinot P, Ortiz-Julien A, Camarasa C. Impact of nutrient availability on the fermentation and production of aroma compounds under sequential inoculation with *M. pulcherrima* and *S. cerevisiae*. *Front Microbiol.* (2020) 11:305. doi: 10.3389/fmicb.2020.00305

36. Denat M, Pérez D, Heras JM, Querol A, Ferreira V. The effects of *Saccharomyces cerevisiae* strains carrying alcoholic fermentation on the fermentative and varietal aroma profiles of young and aged Tempranillo wines. *Food Chem X.* (2021) 9:100116. doi: 10.1016/j.fochx.2021.100116

37. Su Y, Seguinot P, Sanchez I, Ortiz-Julien A, Heras JM, Querol A, et al. Nitrogen sources preferences of non-*Saccharomyces* yeasts to sustain growth and fermentation under winemaking conditions. *Food Microbiol.* (2020) 85:103287. doi: 10.1016/j.fm.2019.103287

38. Vendramini C, Beltran G, Nadai C, Giacomini A, Mas A, Corich V. The role of nitrogen uptake on the competition ability of three vineyard *Saccharomyces cerevisiae* strains. *Int J Food Microbiol.* (2017) 258:1–11. doi: 10.1016/j.ijfoodmicro.2017.07.006

39. Barham E. Translating terroir. *J Rural Stud.* (2003) 19:127–38. doi: 10.1016/S0743-0167(02)00052-9

40. Roullier-Gall C, Boutegrabet L, Gougeon RD, Schmitt-Kopplin P. A grape and wine chemodiversity comparison of different appellations in Burgundy: vintage vs terroir effects. *Food Chem.* (2014) 152:100–7. doi: 10.1016/j.foodchem.2013.11.056

41. Duley G, Dujourdy L, Klein S, Werwein A, Spartz C, Gougeon RD, et al. Regionality in Australian Pinot noir wines: a study on the use of NMR and ICP-MS on commercial wines. *Food Chem.* (2021) 340:127906. doi: 10.1016/j.foodchem.2020.127906

42. Souza Gonzaga L, Capone DL, Bastian SEP, Danner L, Jeffery DW. Sensory typicity of regional Australian cabernet sauvignon wines according to expert evaluations and descriptive analysis. *Food Res Int.* (2020) 138:109760. doi: 10.1016/j.foodres.2020.109760

frontiers | Frontiers in Nutrition

TYPE Original Research
PUBLISHED 19 December 2022
DOI 10.3389/fnut.2022.1092048

OPEN ACCESS

EDITED BY
Mingquan Huang,
Beijing Technology and Business University, China

REVIEWED BY
Yongqiang Zhao,
South China Sea Fisheries Research Institute (CAFS), China
Ya-Fang Shang,
Hefei University of Technology, China

*CORRESPONDENCE
Weijiang Sun
✉ 000q020007@fafu.edu.cn

†These authors have contributed equally to this work

SPECIALTY SECTION
This article was submitted to Food Chemistry, a section of the journal Frontiers in Nutrition

RECEIVED 07 November 2022
ACCEPTED 05 December 2022
PUBLISHED 19 December 2022

CITATION
Wang Z, Wang Z, Dai H, Wu S, Song B, Lin F, Huang Y, Lin X and Sun W (2022) Identification of characteristic aroma and bacteria related to aroma evolution during long-term storage of compressed white tea. *Front. Nutr.* 9:1092048. doi: 10.3389/fnut.2022.1092048

Identification of characteristic aroma and bacteria related to aroma evolution during long-term storage of compressed white tea

Zhihui Wang[1,2†], Zhihua Wang[1†], Haomin Dai[1,2], Shaoling Wu[1,2], Bo Song[1,2], Fuming Lin[1,2,3], Yan Huang[1,2,3], Xingchen Lin[4] and Weijiang Sun[1,2*]

[1]College of Horticulture, Fujian Agriculture and Forestry University, Fuzhou, China, [2]Ministerial and Provincial Joint Innovation Centre for Safety Production of Cross-Strait Crops, Fujian Agriculture and Forestry University, Fuzhou, China, [3]Anxi College of Tea Science, Fujian Agriculture and Forestry University, Quanzhou, China, [4]Fujian Ming Shan Tea Industry Co., Ltd., Fuding, China

Compressed white tea (CWT) is a reprocessed tea of white tea. Long-term storage has greatly changed its aroma characteristics, but the material basis and transformation mechanism of its unique aroma are still unclear. In this study, flavor wheel, headspace gas chromatography ion mobility spectroscopy, chemometrics, and microbiomics were applied to study the flavor evolution and important aroma components during long-term storage of CWT, and core functional bacteria were screened. During long-term storage, the aroma of CWT gradually changed from sweet, fruity and floral to stale flavor, woody and herbal. A total of 56 volatile organic compounds (VOCs) were identified, 54 of which were significantly differences during storage. The alcohols content was the highest during 1–5 years of storage, the esters content was the highest during 7–13 years of storage, and the aldehydes content was the highest during 16 years of storage. Twenty-nine VOCs were identified as important aroma components, which were significantly correlated with 6 aroma sub-attributes ($P < 0.05$). The functional prediction of bacterial community reminded that bacterial community could participate in the transformation of VOCs during storage of CWT. Twenty-four core functional bacteria were screened, which were significantly associated with 29 VOCs. Finally, 23 characteristic differential VOCs were excavated, which could be used to identify CWT in different storage years. Taken together, these findings provided new insights into the changes in aroma characteristics during storage of CWT and increased the understanding of the mechanism of characteristic aroma formation during storage.

KEYWORDS

compressed white tea, storage, volatile compounds, GC-IMS, aroma, bacteria

1. Introduction

White tea is a kind of slightly fermented tea (1). After a long aging period, white tea can get unique aroma characteristic and then is named aged white tea. It is similar with aging process of Pu-erh tea and red wine (2, 3). However, the traditional white tea is coarse and loose, which is inconvenient for transportation and storage, so the compressed white tea (CWT) has been developed (4). CWT is a reprocessed tea product manufacture from white tea by blending, weighing, steaming, shaping, and drying. Its appearance effectively solved the problem of inconvenient transportation and storage of traditional white tea (5). Previous studies have expounded that the process of steaming and shaping further destroys the bud and leaf tissue of white tea, and has a far-reaching impact on the type and content of aroma components of CWT, making the stale flavor of CWT more show, and the characteristic aroma types such as jujube scent and herbal more prominent, while the traditional white tea retains more floral and fruity (6).

Aroma is an important factor that determines the quality of tea and affects the choice of consumers (7). When white tea is not stored, its aroma characteristics are floral, sweet, clean and refreshing, and the high proportion of alcohols and aldehydes is the basis of these aroma characteristics. Phenylethyl alcohol, γ-nonalactone, *trans*-β-ionone, *trans*-linalool oxide (furanoid), α-ionone and *cis*-3-hexenyl butyrate are considered to be the key aroma components of different types of unstored white tea (8). In the long-term storage process of white tea, the aroma will change with the extension of time (9). In the sensory, the aroma of white tea will gradually transform from clean and refreshing and floral to stale flavor, jujube scent or herbal (10). In the volatile organic compounds (VOCs), the content of alcohols decreases, hydrocarbons' increases, and aldehydes' increases first and then decreases; the aroma components of floral and fruity, such as linalool, linalool oxide, geraniol, methyl salicylate, phenylethanol, nerolidol, and citral, decreased, which make white tea clean and refreshing and floral gradually decrease or even disappear. A variety of unsaturated alkenes, mainly dihydrokiriactone, 2-methylnaphthalene, cedrene, and β-cedrene, are increased, resulting in the formation of stale flavor. Meanwhile, under the coordination of benzaldehyde, α-ionone, β-ionone, and geranyl acetone, the characteristics of white tea during storage, namely stale flavor with jujube scent, plumy aroma are formed (8, 11). The aroma of CWT is very different from that of traditional white tea (6). So far, the changes of aroma characteristics, important aroma components and the chemical basis of special aroma during storage of CWT are still unclear.

Headspace gas chromatography-ion mobility spectrometry (HS-GC-IMS) is an emerging technology, which can visualize VOCs without pretreatment and high sensitivity, and can better separate isomers and polymers in tea (12, 13). Nevertheless, how to match valuable information on the chemicals with sensory descriptors is still challenging. Recently, chemometrics and quantitative descriptive analysis (QDA) have been widely used to reveal the relationship between the chemical data from instrumental analysis and sensory analysis, and to recognize those chemical components that contribute significantly to food flavor (14, 15). However, there are few reports on the relationship between aroma characteristics and VOCs during storage of CWT. In addition, microorganisms may play a key role in the changes of tea metabolites during storage (3), which has been confirmed in Fu Brick tea, Liupao tea, and Pu-erh tea (16–18), and it is found that the diversity of bacteria increases gradually during the storage process of tea, mainly involved in the decomposition, transformation and degradation of small molecule compounds (17). Previous study have identified bacterial communities during storage of white tea and CWT, and performed functional prediction. It is found that bacteria can participate in 246 kyoto encyclopedia of genes and genomes (KEGG) metabolic pathways, including the metabolism of some VOCs (19, 20). Whereas, the relationship between the changes of VOCs and bacterial communities during storage of CWT are also still unknown.

Therefore, the aims of the present study were to (a) elucidate the dynamic changes in aroma characteristics and VOCs during storage of CWT, (b) elucidate the correlation between VOCs and aroma sub-attributes, and (c) identify important aroma components and core functional bacteria that contribute to the formation of characteristic aroma of CWT. This study is of significant importance for providing information in-depth to enhance the understanding of the mechanisms on aroma formation during storage of CWT.

2. Materials and methods

2.1. Experimental materials

Samples of CWT (round cake) were collected from Fujian Ruida Tea Industry Co., LTD., named A1, A3, A5, A7, A9, A10, A13, and A16, respectively. The last numbers in the nomenclature indicated the years of storage, which corresponded to the production years of 2018, 2016, 2014, 2012, 2010, 2009, 2006, and 2003. All samples were manufactured by Fujian Ruida Tea Industry Co., Ltd. in the spring with the same tea plant cultivar, plantation, and processing technology. The processing technology of CWT was that Shoumei white tea → weighing (weight: 350.0 ± 5.0 g) → steam softening (steam temperature: 110°C; time: 30 s) → shaping (round cake; pressure: 40 KN; time: 7 min) → drying (temperature: 50°C; time: 48 h; water content ≤ 8%). All samples were stored in the same environment warehouse (dry and ventilated, temperature ≤ 35°C, relative humidity ≤ 50%). The samples of different batches prepared within 1 month each spring were regarded as biological repeats, and each sample was collected

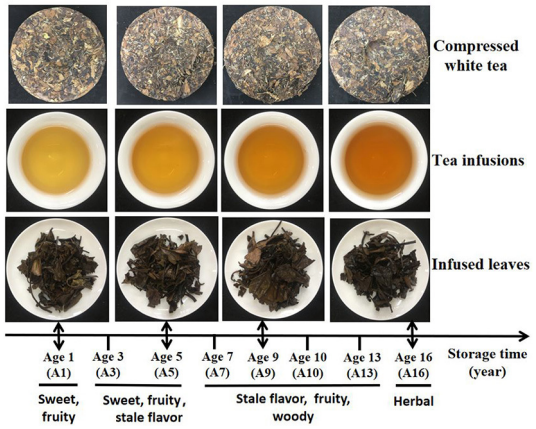

FIGURE 1
Photos of dry tea, tea infusions, and infused leaves during long-term storage of CWT.

with three biological repeats. The sample details are shown in Supplementary Table 1, and photos of dry tea, tea infusions and infused leaves of some CWT samples are shown in Figure 1.

2.2. Experimental method

2.2.1. Sensory evaluation of the aroma of CWT

Quantitative descriptive analysis (QDA) was performed by five well-trained panelists (two males and three females, aged 20–55 years) from the tea innovation team of Fujian Agriculture and Forestry University according to the Methodology for Sensory Evaluation of Tea (GB/T 23776-2018), with a little modification. Briefly, 3.0 g evenly mixed tea samples were weighed into a cylindrical cup of 150 mL, 150 mL boiling water was added, and soaked for 3 min. Then the tea infusion was poured into the evaluation bowl. After the initial evaluation of the aroma, the boiling water was added again, and the tea infusion was drained after 5 min for the second aroma evaluation. Aroma descriptors for each sample were recorded by each evaluator. After that, six descriptors with a usage rate of more than 80% were selected, namely sweet, floral, fruity, stale flavor, woody, and herbal. Descriptors were defined and their references were found based on published literature (Figure 2B) (21, 22). Finally, the tea samples were re-soaked according to the above method, and the 0–7 scale was used to evaluate the intensity of the six aroma sub-attributes of each sample, namely 0 = none, 4 = medium, and 7 = extremely. The aroma sub-attribute intensity value of each sample was the average value evaluated by the evaluation team. Each sample was evaluated in three biological replicates.

2.2.2. Qualitative and quantitative analysis of the VOCs by HS-GC-IMS

VOCs identification analysis was performed using HS-GC-IMS (FlavorSpec, G.A.S., Dortmund, Germany) (23). Briefly, 0.1 g of the ground CWT sample was weighed and placed into a 20 mL headspace injection bottle. The headspace injection conditions were as follows: incubation at 70°C for 15 min with revolving speed at 500 *r*/min, injection needle temperature at 90°C, and injection volume at 500 μL. Three biological replicates were performed.

GC condition: the chromatographic column was FS-SE-54-CB-1 (15 mL × 0.68 mm), and the carrier gas was N_2 (purity > 99.99%). The programmed flow rate was as follows: initially 2 mL/min holding for 10 min, linearly ramped up to 150 mL/min within 10 min, and then held for 30 min. IMS conditions: drift tube length and temperature were 98 mm and 45°C, drift gas flow rate was 150 mL/min. GC-IMS data were viewed through Laboratory Analytical Viewer (LAV), using the Reporter plug-in to directly compare 2D top view and 3D spectra, and the Gallery mapping plug-in to visualize fingerprint comparisons. Normal alkanes C9—C27 (Sigma Aldrich Corporation, Saint Louis, MO, USA) were served as external references to calculate the retention index (RI) of each compound. The calculation method of RI was referred to Mao et al. (24).

2.2.3. Identification of bacterial communities

Previously, the bacterial communities of samples A1, A3, A7, A9, A10, and A16 during storage of CWT were identified (20). Primers were designed according to the V3 and V4 conserved regions of bacterial 16S rDNA for polymerase chain reaction amplification. Two-end sequencing of 2 × 250 bp was performed by NovaSeq PE250 sequencer (Kapa Biosciences, Woburn, MA, USA). Three biological replicates were performed.

2.3. Data analysis

One-way analysis of variance (ANOVA) with least significant difference (LSD) was performed using SPSS (version 19.0; Chicago, IL, USA). Bacterial involvement in metabolic pathways was predicted by PICRUSt2 function prediction analysis software (https://www.omicstudio.cn/tool). Principal component analysis (PCA), orthonormal partial least-squares discriminant analysis (OPLS-DA), orthonormal partial least-square variable import of project (OPLS-VIP), and two way orthogonal partial least-squares analysis (O2PLS) were performed using SIMCA (version 14.0, Umetrics, Umea, Sweden). Heat maps and correlation analysis were generated using Hiplot (https://hiplot-academic.com). The correlation network diagrams were generated using Cytoscape (version 3.9.1; Beijing, China).

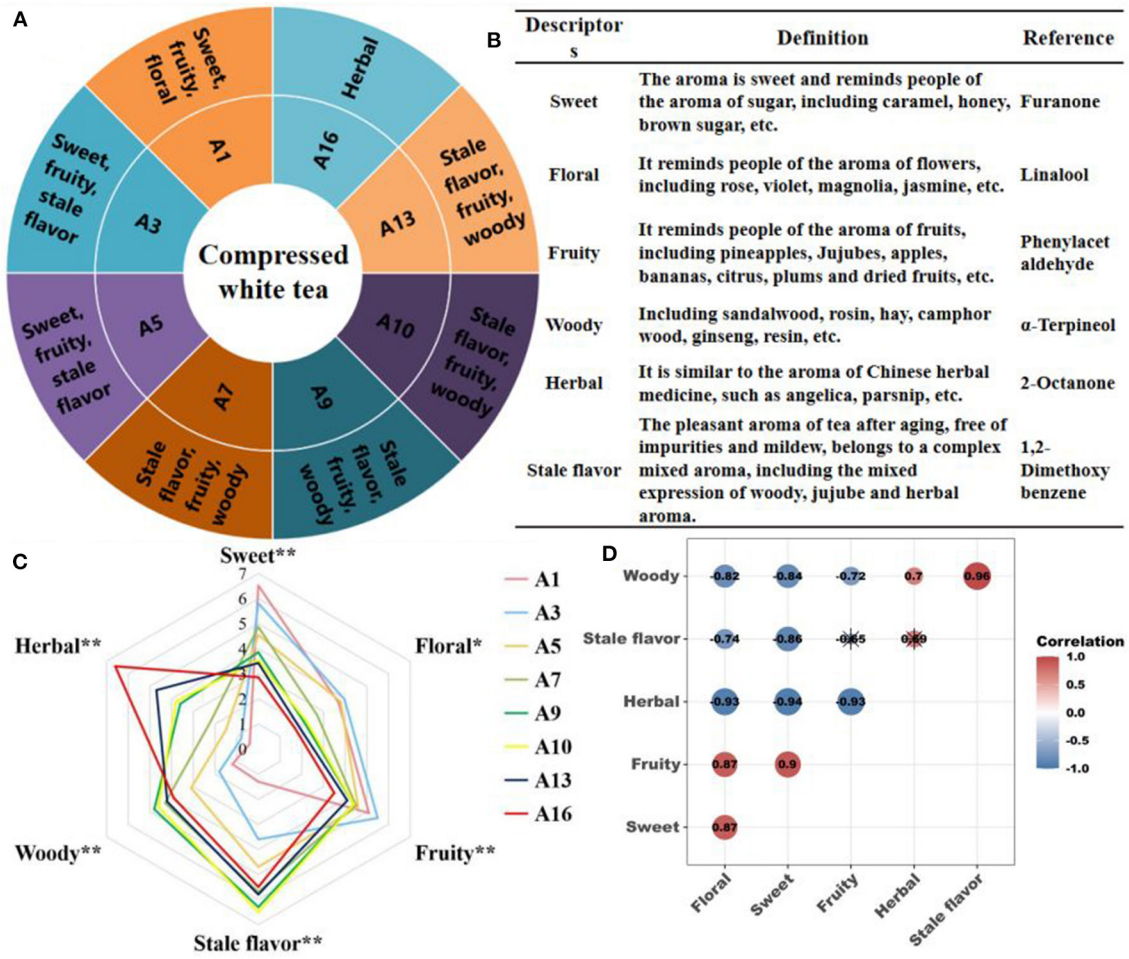

FIGURE 2
Sensory aroma characteristics of CWT. **(A)** Flavor wheel during storage of CWT. **(B)** Definition and reference of aroma descriptors. **(C)** Quantitative evaluation of aroma sub-attributes, $*P < 0.05$; $**P < 0.01$. **(D)** The intensity of the aroma sub-attribute correlation analysis, red and blue indicated positive and negative correlations, respectively. *meant that the difference was not significant ($P > 0.05$).

3. Results and Discussion

3.1. Flavor evolution during storage of CWT

QDA was used to construct the flavor wheel of CWT during storage (Figure 2A) and formed its aroma description system (Figure 2B). During the long-term storage of CWT, the characteristics of six typical aroma sub-attributes were happened significant ($P < 0.05$) or extremely significant changes ($P < 0.01$) (Figure 2C). The intensity of sweet, floral and fruity was significantly decreased with increasing storage years, while that of stale flavor, woody, and herbal emerged a significant increasing trend (Figure 2C). The aroma intensity of CWT in the first year of storage was dominated by sweet, fruity and floral, which were 6.5, 5.1, and 3.7, respectively. During 3–5 years of storage, the intensity of stale flavor gradually increased, and that of floral was gradually covered, with sweet, stale flavor and fruity as the dominant flavor. During 7–13 years of storage, the intensity of woody increased significantly, while that of sweet and floral decreased significantly. In this period, stale flavor, fruity and woody were the dominant flavor. After 16 years of storage, the intensity of herbal increased significantly and became the dominant flavor, with an aroma intensity of 6.6 (Figures 2A,C). In general, the change course of CWT aroma during long-term storage was as follows: sweet, fruity and floral → sweet, fruity and stale flavor → stale flavor, fruity and woody → herbal. The change trend was similar to the change of white tea aroma during storage (10). The difference was that CWT had no clean and refreshing at the beginning of the storage, and the floral was weaker. After 3 years of storage, CWT had shown obvious stale flavor, and the aging speed was faster than that of white tea.

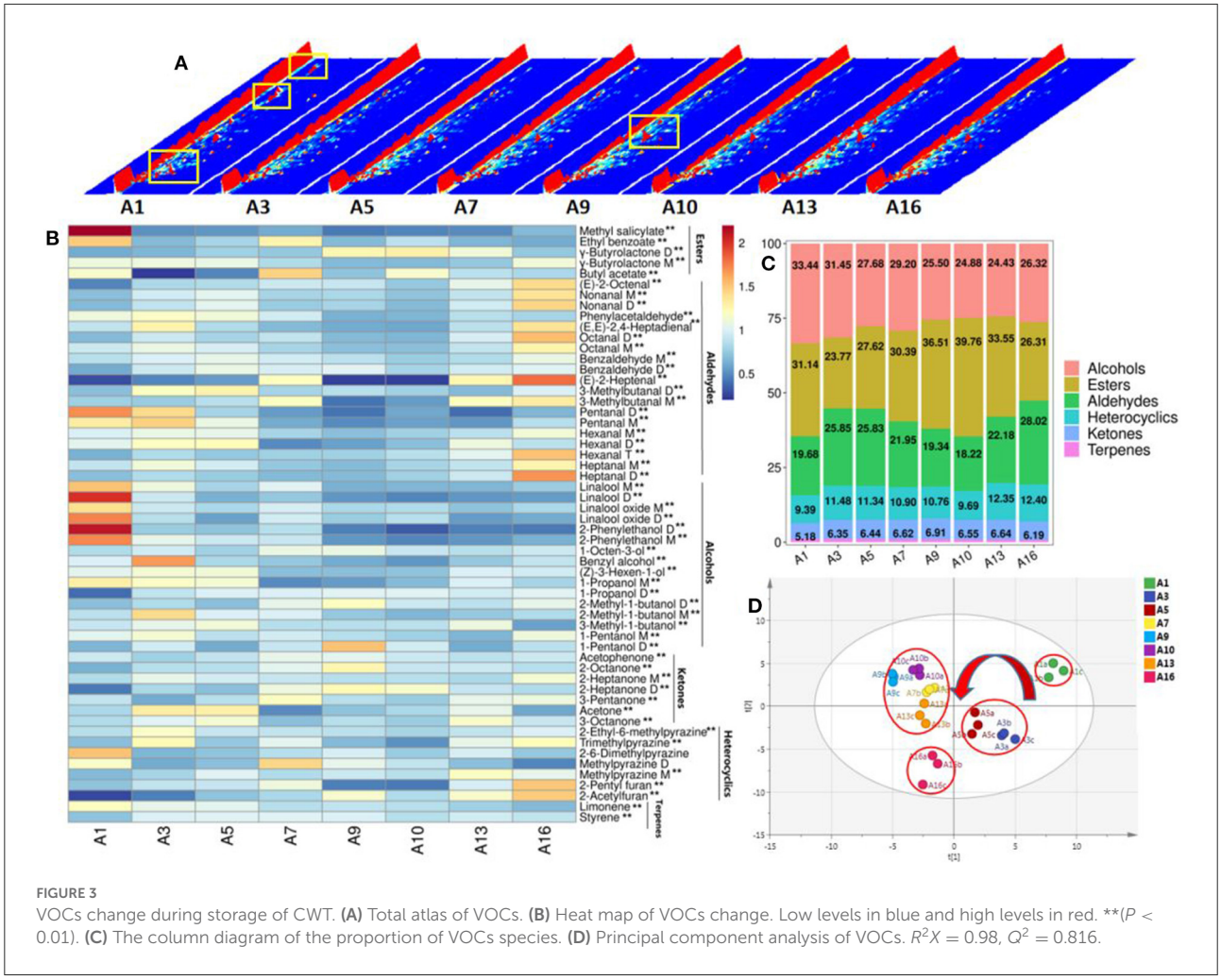

FIGURE 3
VOCs change during storage of CWT. **(A)** Total atlas of VOCs. **(B)** Heat map of VOCs change. Low levels in blue and high levels in red. **($P < 0.01$). **(C)** The column diagram of the proportion of VOCs species. **(D)** Principal component analysis of VOCs. $R^2X = 0.98$, $Q^2 = 0.816$.

There was a complex correlation between the six aroma sub-attributes ($P < 0.05$) (Figure 2D). Sweet, fruity and floral were significantly positively correlated with each other, and these three sub-attributes were significantly negatively correlated with woody and herbal, respectively, indicating that the aroma compounds contributing to the three sub-attributes might be similar. There was a significant positive correlation between woody and both stale flavor and herbal. There was a positive correlation between herbal and stale flavor, but the correlation did not reach a significant level ($P > 0.05$). Some studies have suggested that the biochemical basis of stale flavor in tea was aromatic compounds with pleasant woody and herbal (6, 25). This was similar to the conclusion of this study.

3.2. Changes of VOCs during storage of CWT

The general chromatogram of HS-GC-IMS showed that the relative abundance of VOCs in CWT during storage, and some VOCs increased and some decreased (yellow box) (Figure 3A). A total of 56 VOCs were identified, including 5 esters, 19 aldehydes, 16 alcohols, 7 ketones, 7 heterocycles, and 2 terpenes (Figure 3B). CAS, molecular formula, RI and relative content of all VOCs are shown in Supplementary Table 2. The most abundant VOCs in CWT were alcohols, esters and aldehydes. The dominant volatile components during long-term storage were constantly changing (Figure 3B). The alcohols content was the highest during 1–5 years of storage, the esters content was the highest during 7–13 years of storage, and the aldehydes content was the highest during 16 years of storage. The content of alcohols decreased gradually during long-term storage, ranging from 24.43 to 33.44%, and reached the highest level after 1 year of storage. During storage, esters first decreased, then increased, and then decreased, with the content ranging from 23.77 to 39.76%. The content was the highest after 10 years of storage. The variation trend of aldehydes was "N", and the content of aldehydes ranged from 18.22–28.02%, with the highest content after 16 years of storage. The contents of heterocycles, ketones and terpenes were relatively

low, and heterocycles' and ketones' gradually increased, while terpenes' gradually decreased. Previous study has claimed that the contents of alcohols, aldehydes and hydrocarbons in aged white tea are the highest (11). During storage of white tea, alcohols decrease continuously, hydrocarbons increase, and aldehydes increase first and then decrease (11). There were some differences with the conclusions of this study, which might be the difference between white tea and CWT. The content of esters in CWT was higher and further increased during storage, while aldehydes increased in a fluctuating manner. The increase of some esters and aldehydes might be caused by microbial metabolism, while the decreased of alcohols might be due to their own volatilization. Previous studies have shown that some alcohols gradually evaporate during tea storage (15). Some esters and aldehydes can be biosynthesized by microbial enzymes using precursors such as amino acids and fatty acids during tea fermentation (26).

The most abundant VOCs in CWT were γ-butyrolactone D (dimer) (13.79–29.44%), linalool M (3.99–9.54%), ethyl benzoate (3.89–9.51%), 1-propanol D (3.32–8.55%), linalool oxide M (3.27–6.39%), 2-ethyl-6-methylpyrazine (4.18–6.18%), and γ-butyrolactone M (monomer) (2.27–3.70%) (Supplementary Table 2). Linalool and its oxides have always been considered as VOCs with high content in white tea (27). This view was also similar in CWT. The high content of γ-butyrolactone in CWT was identified for the first time. γ-Lactone is the most common type of lactone, but less are identified by ordinary GC-MS (28). Xiao et al. (29) identified γ-butyrolactone in Fu brick tea from different producing areas by using GC-IMS, but failed to do so by using GC-MS. Therefore, it was speculated that GC-IMS have unique advantages in identifying γ-butyrolactone and its dimer. Zhu et al. (9) performed targeted identification of part of lactones in white tea with different storage times (unidentified γ-butyrolactone) through enantioselective gas sterics-mass spectrometry (Es-GC-MS), it was found that some lactones accumulated with the increase of white tea storage time. In the study of wine, the content of γ-lactone is also found to be related to the aging of wine (30, 31). Therefore, long-term storage of CWT might contribute to γ-butyrolactone accumulation. Among the 56 identified VOCs, 54 had significant differences in accumulation during storage ($P < 0.01$). Heat map analysis certified that γ-butyrolactone D increased significantly, γ-butyrolactone M rised first and then decreases, and some alcohols such as linalool M and linalool oxide M decreased significantly. Methyl salicylate and ethyl benzoate decreased significantly. Heterocycles such as 2-ethyl-6-methylpyrazine and methylpyrazine M increased significantly. Aldehyde such as benzaldehyde D and 3-methylbutanal D increased significantly (Figure 3C). The differential accumulation of these VOCs changed the flavor of CWT during storage, but not all VOCs contributed to the aroma. Therefore, chemometrics should be further combined to find the important aroma components.

PCA showed the similarities and differences of samples in CWT during storage. In terms of differences, there was no coincidence among samples, indicating that VOCs were different among samples (Figure 3D), which was consistent with the conclusion of heat map analysis (Figure 3B). From the perspective of similarity, the whole storage process was divided into four stages: stage 1: A1; stage 2: A3–A5; stage 3: A7–A13, stage 4: A16 (the closer the distance, the more similar) (Figure 3D). The four stages of the storage process divided by PCA were consistent with the changes of the sensory attributes of aroma mentioned above (Figure 2A). Based on the above analysis, it could be reasonably inferred that the flavor change of CWT during storage was due to the change of VOCs content, which might be related to the volatilization of compounds and the metabolism of microorganisms during storage.

3.3. Characteristic differential VOCs of CWT in different storage years

PCA confirmed differences between CWT samples from different storage years. In order to screen the differential VOCs of CWT in different years, OPLS-DA modeling analysis was performed. Samples were effectively distinguished in the score chart (Figure 4A), and cross-validation informed that the model was not overfitted (green points were below blue points) (Figure 4B). With VIP > 1, $P < 0.05$ as the criterion (32), 23 differential VOCs were screened. The screening of characteristic differential VOCs is based on the variable variation trend of differential VOCs in the heat map (Figure 3B). This method has been used accurately in the screening of characteristic differential metabolites of tea from different grades and different regions (33, 34). The differential VOCs with high content in the sample of this storage year but low content in other storage years were considered as the characteristic differential VOCs of CWT of this year. Therefore, the characteristic differential VOCs were screened as follows: 2 in A1, 5 in A3, 2 in A5, 3 in A7, 3 in A9, 1 in A10, 2 in A13, and 5 in A16 (Figure 4C). These characteristic differential VOCs were differential VOCs accumulated specifically by CWT in a certain year, which might contribute significantly to the formation of its unique flavor, and could also be used to trace and identify the origin of CWT in different storage years. However, the reasons for the unique accumulation of these VOCs in different storage years needed to be further studied.

3.4. Screening of important aroma components during storage of CWT

In order to find essential variables that are the most influential on the sensory attributes of tea aroma, especially

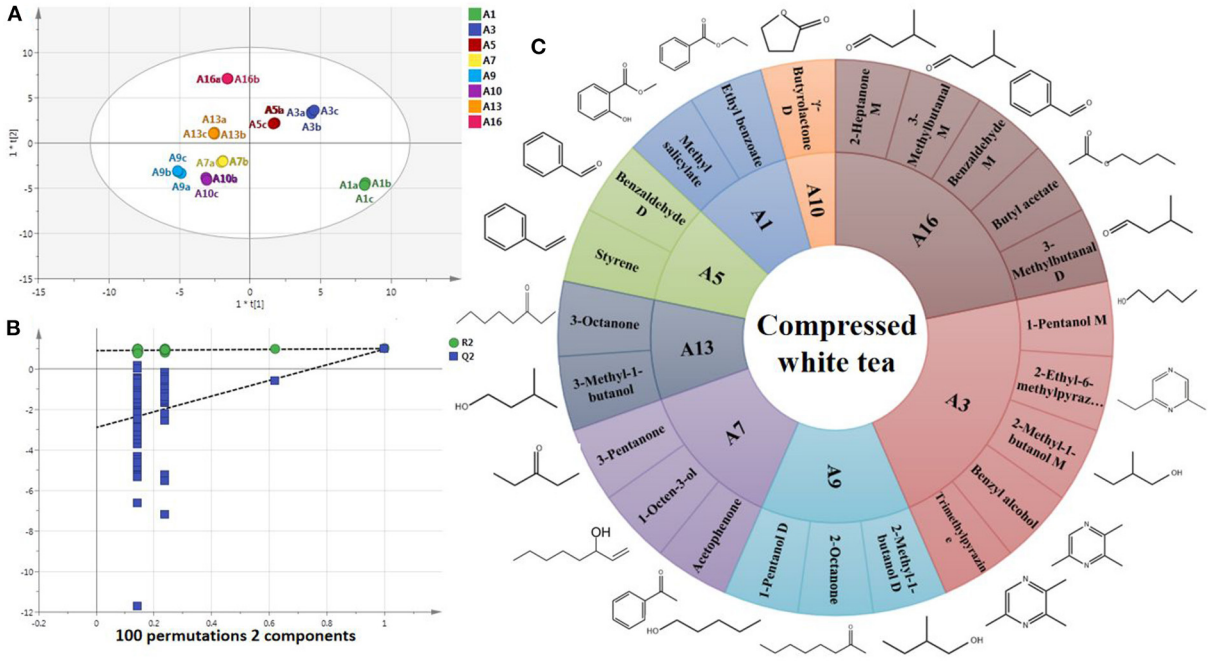

FIGURE 4
Characteristic differential VOCs of CWT in different storage years. **(A)** OPLS-DA model. $R^2X = 0.999$, $R^2Y = 0.998$, $Q^2 = 0.862$. **(B)** Cross validation of OPLS-DA model. **(C)** Rising sun chart and molecular formula of characteristic differential VOCs.

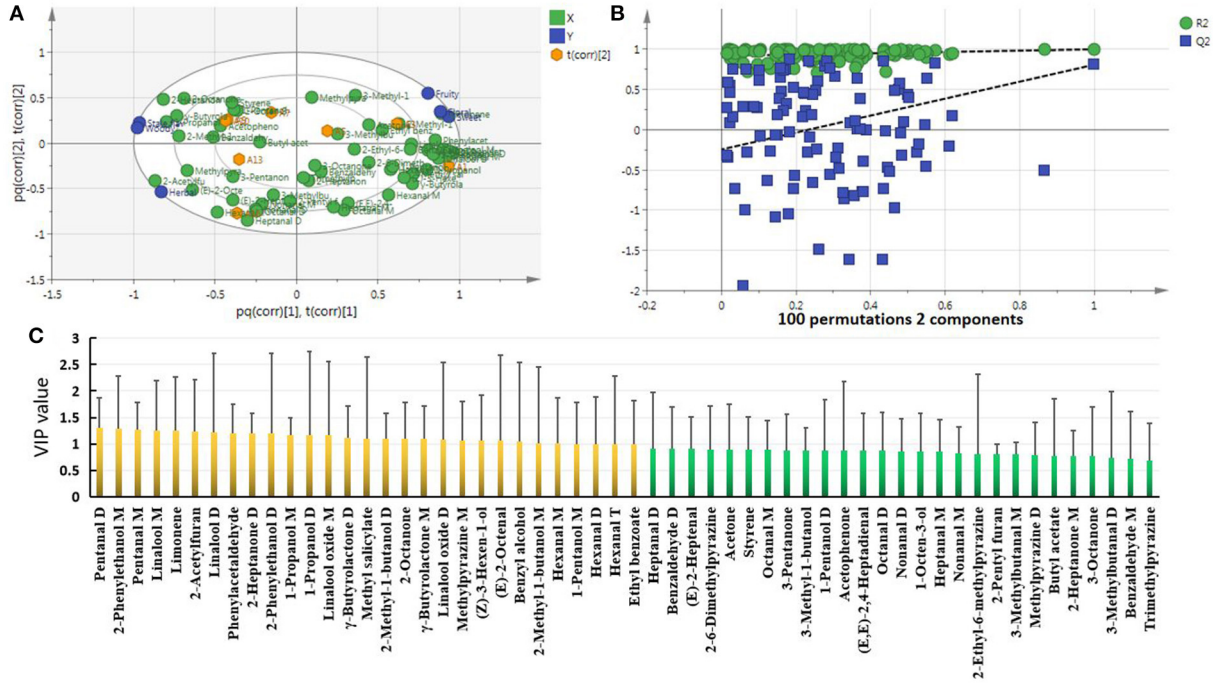

FIGURE 5
Screening of important aroma components during CWT storage. **(A)** OPLS-VIP model. $R^2X = 0.973$, $R^2Y = 0.976$, $Q^2 = 0.616$. **(B)** Cross validation of OPLS-VIP model. **(C)** VIP value of VOCs.

when multicollinearity exists among variables, a OPLS-VIP is conducted to explain sensory attribute intensities with volatile component content as the X variable and sensory attribute intensity as the Y variable, and the VIP value of each X variable is calculated (24). The variables whose VIP values are >1 are considered to be the important aromatic compounds (21).

The OPLS-VIP model had a high degree of interpretation ($R^2X = 0.973$, $R^2Y = 0.976$) (Figure 5A), and the closer the variables were, the greater the correlation was. Figure 5A showed that floral, fruity and sweet fragrance were the main aroma characteristics of A1, A3, and A5 (closer to each other), and stale flavor, woody and herbal were the main aroma characteristics of A7, A9, A10, A13, and A16 (closer to each other), which was consistent with the results of the above sensory analysis. Cross-validation informed that the model was not overfitted (Figure 5B). According to the principle of VIP value > 1.0, 29 volatile components were identified as aroma components that had important contributions to CWT sensory aroma (Figure 5C, yellow column). The aroma characteristics of these VOCs are relatively diversified, mainly including sweet, fruity, woody, caramel and fatty (Supplementary Table 2) (35, 36). These important aroma components acted as the aroma skeleton of CWT and interacted with other aroma components to form the unique aroma characteristics of CWT in different storage years. Linalool, linalool oxide, methyl salicylate, benzyl alcohol, 2-phenylethanol, and phenylacetaldehyde were closer to A1 and A3 (Figure 5A), and their aroma characteristics were fruit, sweet and floral (Supplementary Table 2) (35, 36). Many studies have verified that these VOCs are important aroma substances in fresh white tea (6, 11). In this study, chemometric methods were adopted to more accurately confirm the dominant contribution of these VOCs at the initial stage of CWT storage. γ-Butyrolactone D was closer to A7, A9, A10, A13, and A16 (Figure 5A). The thresholds of lactone compounds are extremely low, most of which have floral, fruity, milk flavor, and coconut, and are the important aroma substances of wine and fruit (9). There are also a variety of lactones in tea, which are mainly derived from γ(δ)-hydroxy carboxylic acid intramolecular esterification or carotene degradation during processing and storage. γ-Valerolactone, γ-heptanolactone, and γ(δ)-decanolactone have important contributions to tea quality (28). In this study, γ-butyrolactone was found to be a important aroma component in CWT storage process for the first time. It was likely that this is an important reason for the unique aroma of CWT.

3.5. Contribution of important aroma components to aroma sub-attributes

The correlation coefficient was used to determine the unique contribution of 29 important aroma components to six aroma sub-attributes. The 29 important aroma components were significantly correlated with six aroma sub-attributes ($P < 0.05$) (Figure 6). The correlation coefficient is shown in Supplementary Table 3, and the visual network diagram is shown in Figure 6.

Twelve VOCs were positively correlated with sweet, and six VOCs were negatively correlated with sweet. Six VOCs were positively correlated with fruity, and five VOCs were negatively correlated with fruity. There were nine VOCs positively correlated with floral, and six VOCs negatively correlated with floral ($P < 0.05$) (Figure 6). Linalool M, phenylacetaldehyde, pentanal D, pentanal M, and limonene were positively correlated with sweet, floral, and fruity. The aroma characteristics of these components are sweet, floral, fruit, citrus, lemon and cherry like (Supplementary Table 2) (35, 36). So they had a positive contribution to these aroma sub-attributes. The contents of these VOCs decreased significantly during storage (Figure 3B). (E)-2-Octenal and hexanal T were significantly negatively correlated with these three aroma sub-attributes, and the aroma characteristics of these two components are herbal, fatty and grass fragment (Supplementary Table 2) (35, 36). Therefore, it had a negative effect on sweet, floral and fruity. The contents of these two aroma components increased significantly during storage (Figure 3B). Sweet, floral and fruity had similar contribution components, which also verified the correlation analysis results among the above three (Figure 2B). The VOCs that had significant contribution to the aroma intensity of sweet, floral, and fruity also different. The VOCs with significant positive correlation with sweet also included methyl salicylate, ethyl benzoate, linalool D, linalool oxide M and linalool oxide D. The aroma characteristics of these components are mainly sweet, floral, fruity, honey-like and fresh (Supplementary Table 2). The VOCs with significant negative correlation with sweet were γ-butyrolactone D, 1-propanol D and methylpyrazine M, the aroma characteristics of these VOCs are caramel, cream, milk, fatty, ethanol-like, roasty, nutty and earthy (Supplementary Table 2). This hinted that the VOCs with caramel, fatty, roasty, and earthy were possible to reduce the sweet intensity of CWT. Benzyl alcohol (apple-like) had a significant positive correlation with fruity. γ-butyrolactone M (caramel) and 1-propanol M (pineapple) were significantly positively correlated with floral. The contents of these components of CWT decreased gradually during storage.

Six VOCs were positively correlated with stale flavor, and thirteen VOCs were negatively correlated with stale flavor. Six VOCs were positively correlated with woody, and eighteen VOCs were negatively correlated with woody. There were five VOCs positively correlated with herbal, and eight VOCs negatively correlated with herbal ($P < 0.05$) (Figure 6). γ-Butyrolactone D, 1-propanol D, and 2-heptanone D were positively correlated to the stale flavor and woody. The aroma characteristics of these three VOCs are carmel, cream, milk, fatty, herbal, and banana-like

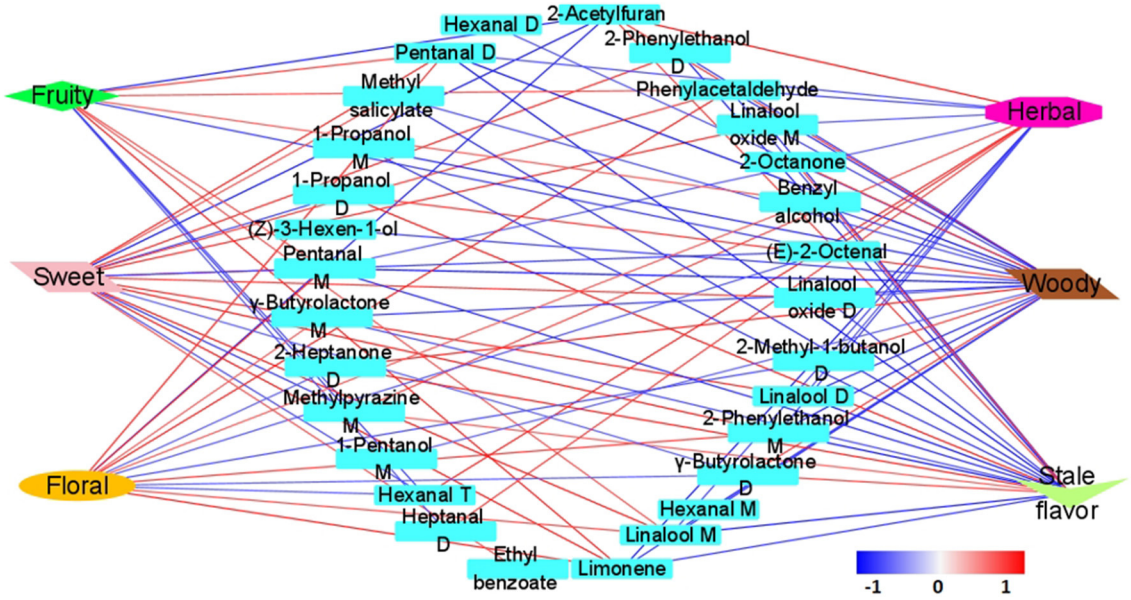

FIGURE 6
Correlation network diagram of aroma sub-attributes and key aroma components. Blue represented a significant negative correlation, red represented a significant positive correlation ($P < 0.05$), and the darker the color, the greater the correlation.

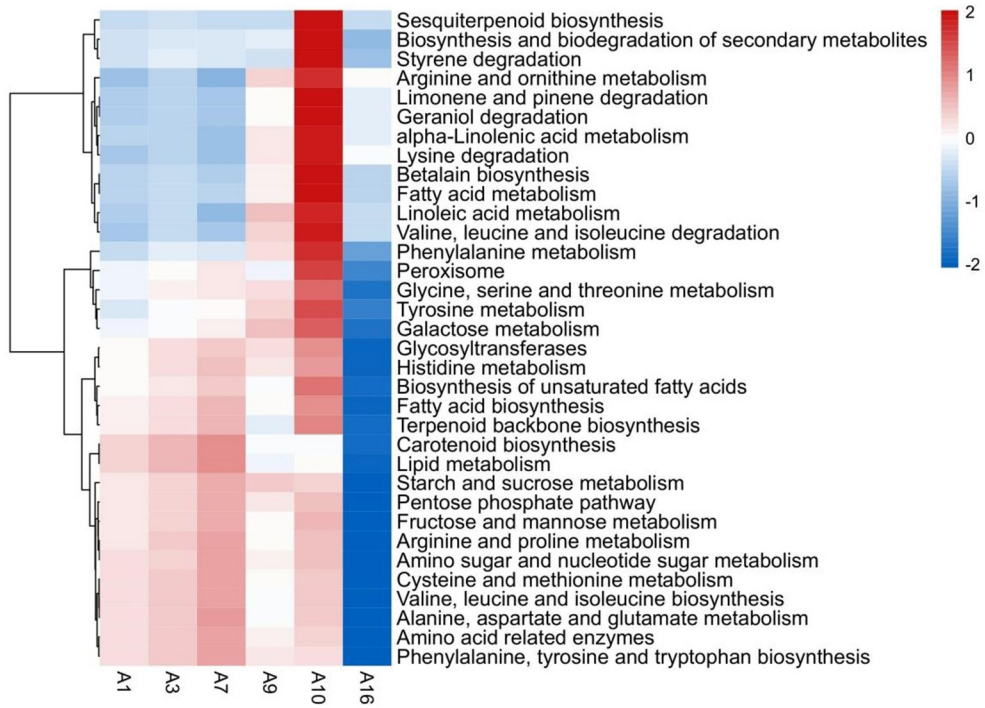

FIGURE 7
Intensity thermogram of KEGG pathway related to bacterial involvement in VOCs metabolism. Red indicated high intensity, while blue indicated low intensity.

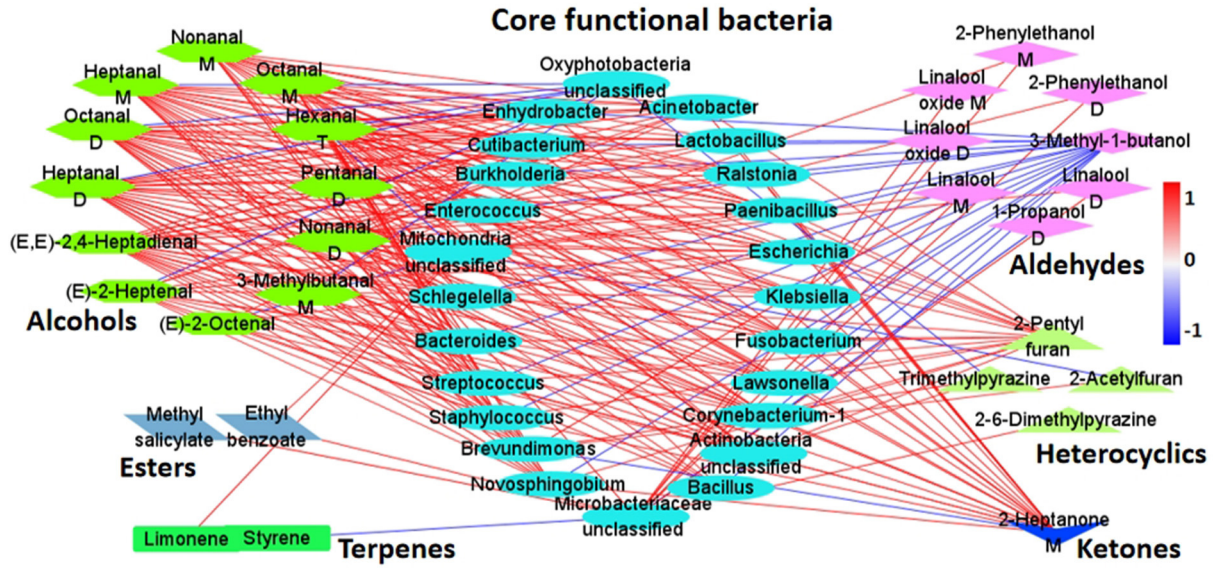

FIGURE 8
Correlation between core functional bacteria and VOCs. The red line indicated a significant positive correlation, and the blue line indicated a significant negative correlation, and the darker the color, the greater the correlation ($P < 0.05$).

(Supplementary Table 2) (35, 36). The contents of these three VOCs increased gradually during storage. γ-Butyrolactone M, phenylacetaldehyde, pentanal D, pentanal M, linalool M, linalool D, linalool oxide M, linalool oxide D, 1-propanol M, and limonene were negatively correlated with stale flavor and herbel. Their aroma characteristics are sweet, floral and fruity (Supplementary Table 2). The content of these VOCs decreased gradually during storage. Different with woody, methylpyrazine M showed significant positive correlations with the stale flavor. The aroma characteristic of methylpyrazine M is roasty, nutty, and earthy (Supplementary Table 2). This suggested that VOCs with roasty, earthy, nutty, and herbal might affect the strength of stale flavor. It has obvious stale flavor in the aged white tea, Pu-erh tea, and Liupao tea (19). However, there were differences in the VOCs identified to contribute to stale flavor in different tea types. In Pu-erh tea, which is methoxybenzenes (37); in Liupao tea, which is α-cedarol, β-linalool, dihydrokiristone, α-terpineol,, and β-ionone (38); in aged white tea, which is cedarol, α-cedarene, and β-cedarene (6). Deng et al. (25) believed that the material basis of stale flavor in tea was mainly aromatic substances with pleasant woody and herbal. The results of this study were similar to this conclusion. Therefore, it was hypothesized that the reason for the difference in VOCs contributing to stale flavor among different tea types was the result of the interaction between these components. Different from stale flavor and wood, the VOCs that were significantly positively correlated with herbal were mainly (E)-2-octenal, (E)-2-heptenal, hexanal T, heptanal D, and methylpyrazine M. The aroma characteristics of these VOCs are herbal, fatty, grassy, stale flavor, fruity and cilantro (Supplementary Table 2). The contents of these VOCs gradually increased during storage. The seven VOCs negatively correlated with the herbal are mainly floral, fruity, and sweet. Their contents decreased gradually during storage of CWT.

In general, during the storage process of CWT, the important VOCs that were positively correlated with sweet, fruity, and floral aroma gradually decreased, while the components that were negatively correlated with them gradually increased. However, the important VOCs that were positively correlated with stale flavor, woody, and herbal gradually increased, while those that were negatively correlated with them gradually decreased. This was the main reason why the aroma of the CWT changed from sweet, floral, and fruity to stale flavor, woody, and herbal during storage.

3.6. Functional prediction of bacterial community

Previous studies have found that microorganisms play an important role in the transformation of tea aroma during storage, among which bacteria may play a key role (17). Combined with the previous bacterial community data of CWT in different storage years (Supplementary Table 4) (20), PICRUSt2 was used to predict and analyze the function of bacteria, and acquire the information that bacteria in CWT storage process could participate in 264 KEGG metabolic pathways. Among them, 34 pathways were related to the

metabolic transformation of VOCs and aroma precursors (Figure 7). The formation of tea aroma is divided into four ways: degradation of carotenoids, oxidative degradation of lipids, maillard reaction of sugars and amino acids, and hydrolysis of glycosides (25). The 34 metabolic pathways screened by us were all related to the four pathways of tea aroma formation, mainly including amino acid and carbohydrate metabolism, fatty acid metabolism, glycosyltransferase synthesis, peroxidase synthesis, terpene degradation and secondary metabolite biosynthesis, and biodegradation. The styrene degradation, α-linolenic acid metabolism, limonene and pinene degradation participated by bacteria first increased and then decreased during storage of CWT (Figure 7). The styrene content first increased and then decreased during storage, and the limonene content gradually decreased during storage (Figure 3B). α-Linolenic acid metabolism could synthesize (Z)-3-hexen-1-ol (39), and that content decreased first and then increased during storage (Figure 3B). Moreover, bacteria could participate in the metabolism of amino acid related enzymes, glycosyltransferases and peroxisome (Figure 7). These enzymes can be involved in the synthesis or degradation of tea aroma (39). Previous studies have shown that bacteria can secrete extracellular enzymes during tea storage, thereby affecting the quality of tea (17). This study also verified this conclusion through the prediction of bacterial function. In conclusion, it was reasonable to speculate that bacteria could participate in the transformation of VOCs during storage of CWT and play an important role, but not all bacteria did this. Therefore, the core functional bacteria affecting VOCs were further screened.

3.7. Screening of core functional bacteria affecting the change of VOCs

Combined with the identified VOCs content and bacterial abundance data, an O2PLS model was established to study the association between bacteria and VOCs during storage of CWT. The O2PLS model had a high degree of interpretation ($R^2X = 0.791$, $R^2Y = 0.797$) (Supplementary Figure 1). Cross-validation showed no overfitting (Supplementary Figure 2). According to the principle of VIP value > 1.0, 116 bacterial genera were confirmed to have important influence on VOCs (Supplementary Table 5). Furthermore, three conditions were considered to identify the core functional bacteria that had an important contribution to the VOCs during storage of CWT: (a) VIP value > 1.0; (b) correlation coefficient $|r| > 0.8$ and $P < 0.05$; (c) the relative abundance of bacterial genera must be >1.0% (15, 16, 40, 41). Based on three criteria, 24 bacterial genera were identified as core functional bacteria. Core functional bacteria were significantly correlated with 29 VOCs (17 were important aroma components), including 12 aldehydes, 8 alcohols, 2 esters, 4 heterocycles, 2 terpenes, and 1 ketone (Figure 8). Correlation coefficients are shown in Supplementary Table 6. It could be seen from the network diagram that the core functional bacteria were the greatest correlation with 12 aldehydes, and these aldehydes tended to increase in the storage process (Figure 3B). The aroma precursors of hexanal, heptanal, and pentanal are lipids, and the aroma precursors of 3-methylbutanal M are amino acids (12, 42). Among the core functional bacteria, *Bacillus*, *Brevundimonas*, *Lactobacillus,* and *Enterococcus* can produce a large number of various types of extracellular enzymes (43, 44). In Liupao tea, Fu brick tea, and Pu-erh tea, microorganisms have been found to affect the aroma quality of tea by secreting extracellular enzymes (15, 16, 29). Therefore, it was speculated that these core functional bacteria promoted the degradation of amino acids and fatty acids by secreting extracellular enzymes, thus making the rise of these aldehydes aroma components. Similar to aldehydes were ketones. The precursor substances of 2-heptanone M are carotenoids (42). The content of alcohols such as linalool, 1-propanol and 2-phenylethanol decreased gradually during storage. Previous studies deem that the decline of alcohols during tea storage is related to its volatilization (15). This study found that *Mitochondria unclassified* and *Microbiaceae unclassified* were significantly correlated with content change of alcohols. Moreover, these two core functional bacteria were also significantly correlated with the content change of esters (methyl salicylate and ethyl benzoate) and terpenes (limonene). At present, there was no report on the functions of these two bacteria. So it was not clear how these two bacteria affected the decline of alcohols, esters and terpenes. *Oxyphotobacteria unclassified* was the dominant bacteria in CWT with the abundance range of 9.02–93.14%, which increased first and then decreased during storage (Supplementary Table 4). It was positively correlated with the content changes of most alcohols, and negatively correlated with the content changes of many aldehydes and heterocycles. *Oxyphotobacteria unclassified* exists in a large number of food fermentation processes, and its abundance gradually decreases with the increase of the degree of fermentation (45). However, the main function of this bacterium was still unclear, and further experiments needed to be designed and studied. These findings collectively indicated that core functional bacteria made a key contribution to the characteristic aroma formation during storage of CWT.

4. Conclusion

This study was the first report on the flavor evolution and dynamic changes of VOCs of CWT during long-term storage (1–16 years), and attempted to correlate them with bacterial communities. It was of great significance for us to further understand the flavor transformation and the formation mechanism of characteristic aroma of CWT during storage.

The flavor wheel and aroma description system for CWT during storage was constructed, and 29 VOCs were identified as important aroma components, among which the unique contribution of γ-butyrolactone to the aroma of CWT was first discovered. According to the flavor wheel and VOCs, the storage process of CWT was divided into four stages. The change process of aroma was sweet, fruity, and floral (1 year) → sweet, fruity, and stale flavor (3–5 years) → stale flavor, fruity, and woody (7–13 years) → herbal (16 years). The reason for the change of flavor was that the important aroma components which were positively correlated with sweet, fruity and floral gradually decrease, while the components that were positively correlated with stale flavor, woody and herbal gradually increased. The functional prediction of bacterial communities revealed that bacteria participated in 34 metabolic pathways related to VOCs transformation, and 24 bacterial genera were identified as core functional bacteria. In addition, 23 characteristic differential VOCs of CWT in different storage years were screened out, which could be used to distinguish CWT in different years. Since the standard of all VOCs could not be obtained, the absolute quantification of these VOCs was not carried out, and the aroma recombination or omission experiment was not used for verification. Therefore, only chemometrics was used in this study to screen VOCs that had an important contribution to the sensory aroma sub-attributes of CWT. Further studies should use molecular sensory science to explore the molecular sensory basis of a specific flavor of CWT.

Data availability statement

The data presented in the study are deposited in the OMIX, China National Center for Bioinformation/Beijing Institute of Genomics, Chinese Academy of Sciences, accession number OMIX002501, https://ngdc.cncb.ac.cn/omix/select-edit/OMIX002501.

Author contributions

WS, ZhihuiW, ZhihuaW, FL, YH, and XL conceived and designed the experiments. ZhihuiW, HD, and ZhihuaW performed the experiments. ZhihuiW analyzed the data and wrote the manscript. HD, SW, and BS revised the manuscript critically. WS administrated the project. All the authors read and approved the final manuscript.

Funding

This work was supported by Research and demonstration on quality evaluation of Fuding white tea (2020N3014), Key R&D plan of the Ministry of Science and Technology of China (2019YFD1001601), special project of China's central government to guide local science and technology development (2022L3071), and special fund for Science and Technology Innovation of Fujian Zhang Tianfu tea development foundation (FJZTF01).

Acknowledgments

We are particularly grateful to Fujian Ruida Tea Industry Co., Ltd., for providing us with experimental samples.

Conflict of interest

XL was employed by Fujian Ming Shan Tea Industry Co., Ltd.

The remaining authors declare that the research was conducted in the absence of any commercial or financial relationships that could be construed as a potential conflict of interest.

Publisher's note

Supplementary material

The Supplementary Material for this article can be found online at: https://www.frontiersin.org/articles/10.3389/fnut.2022.1092048/full#supplementary-material

References

1. Dai WD, Xie DC, Lu ML Li PL, Lv HP, Yang C, et al. Characterization of white tea metabolome: comparison against green and black tea by a nontargeted metabolomics approach. *Food Res Int.* (2017) 96:40–5. doi: 10.1016/j.foodres.2017.03.028

2. Lorenzo C, Garde-Cerdán T, Pedroza MA, Alonso GL, Salinas MR. Determination of fermentative volatile compounds in aged red wines by near infrared spectroscopy. *Food Res Int.* (2009) 42:1281–6. doi: 10.1016/j.foodres.2009.03.021

3. Xue J, Yang L, Yang Y, Yan J, Ye YT, Hu CY, et al. Contrasting microbiomes of raw and ripened Pu-erh tea associated with distinct chemical profiles. *LWT Food Sci Technol.* (2020) 124:109147. doi: 10.1016/j.lwt.2020.109147

4. Huang Y, Liu F, Sun WJ. Research progress of white tea products and processing technology. *China Tea Process*. (2015) 6:5–9 (in Chinese).

5. Weng GF. Quality and safety evaluation of compressed white tea. *Agric Eng.* (2020) 10:50–4 (in Chinese).

6. Chen ZD, Li P, Chen XH, Yang YJ, He PM, Tu YY. Effect of compressed processing on the aroma of aged white tea. *Food Ind Sci Technol.* (2020) 41:63–9 (in Chinese).

7. Wu HT, Chen YY, Feng WZ, Shen SS, Wei YM, Jia HY, et al. Effects of three different withering treatments on the aroma of white tea. *Foods.* (2022) 11:2502. doi: 10.3390/foods11162502

8. Chen QC, Zhu Y, Yan H, Chen M, Xie DC, Wang MQ, et al. Identification of aroma composition and key odorants contributing to aroma characteristics of white teas. *Molecules.* (2020) 25:6050. doi: 10.3390/molecules25246050

9. Zhu Y, Kang SY, Han Y, Lv HP, Zhang Y, Lin Z. Enantiomeric distributions of volatile lactones and terpenoids in white teas stored for different durations. *Food Chem.* (2020) 320:126632. doi: 10.1016/j.foodchem.2020.126632

10. Fu HF. *Study on Pressed Cake and Storage of Aged White Tea.* Fuzhou: Fujian Agriculture and Forestry University (2019) (in Chinese).

11. Liu LY. *Studies on the Quality Characteristics and Free Radical Scavenging Ability of Stored White Tea*. Fuzhou: Fujian Agriculture and Forestry University (2015) (in Chinese).

12. Liu HC, Xu YJ, Wu JJ, Wen J, Yu YS, An KJ, et al. GC-IMS and olfactometry analysis on the tea aroma of Yingde black teas harvested in different seasons. *Food Res Int.* (2021) 150:110784. doi: 10.1016/j.foodres.2021.110784

13. Sun P, Xu B, Wang Y, Lin X, Chen C, Zhu J, et al. Characterization of volatile constituents and odorous compounds in peach (*Prunus persica L*) fruits of different varieties by gas chromatography–ion mobility spectrometry, gas chromatography–mass spectrometry, and relative odor activity value. *Fron Nutr.* (2022) 9:965796. doi: 10.3389/fnut.2022.965796

14. Su D, He JJ, Zhou YZ Li YL, Zhou HJ. Aroma effects of key volatile compounds in Keemun black tea at different grades: HS-SPME-GC-MS, sensory evaluation, and chemometrics. *Food Chem.* (2022) 373:131587. doi: 10.1016/j.foodchem.2021.131587

15. Li Q, Li YD, Luo Y, Xiao LZ, Wang KB, Huang JA, et al. Characterization of the key aroma compounds and microorganisms during the manufacturing process of Fu brick tea. *LWT.* (2020) 127:109355. doi: 10.1016/j.lwt.2020.109355

16. Li Q, Hong X, Zheng XX, Xu YQ, Lai XM, Teng CQ, et al. Characterization of key aroma compounds and core functional microorganisms in different aroma types of Liupao tea. *Food Res Int.* (2022) 152:110925. doi: 10.1016/j.foodres.2021.110925

17. Li J, Wu J, Xu N, Yu Y, Wu X. Dynamic evolution and correlation between microorganisms and metabolites during manufacturing process and storage of pu-erh tea. *LWT.* (2022) 158:113128. doi: 10.1016/j.lwt.2022.113128

18. Li J, Xu R, Zong L, Brake J, Cheng L, Wu J, et al. Dynamic evolution and correlation between metabolites and microorganisms during manufacturing process and storage of Fu Brick tea. *Metabolites.* (2021) 11:703. doi: 10.3390/metabo11100703

19. Chen JJ, Hu YF, Shen SY, Wang ZH, Zhou Z, Tang Q, et al. Analysis of bacterial diversity on the surface of stored white peony based on high-throughput sequencing. *Tea Sci*. (2020) 40:519–27 (in Chinese).

20. Wang ZH. *Study on the Quality and Bacterial Community Changes of Compressed White Tea in Different Years*. Fuzhou: Fujian Agriculture and Forestry University (2021) (in Chinese).

21. Mao S. *Quality Analysis and Control of Congou Black Tea Based on Sensomics*. Chongqing: Southwest University (2018).

22. Yue CN, Yang PX, Qin DD, Cai HL, Wang ZH Li C, et al. Identification of volatile components and analysis of aroma characteristics of Jiangxi Congou black tea. *Int J Food Prop.* (2020) 23:2160–73. doi: 10.1080/10942912.2020.1844747

23. Wang ZH, Xue ZH, Zhu WW, Sun WJ. Analyses of volatile compounds in compressed white tea of different years based on GC-IMS. *J Food Sci Biotechnol.* (2021) 40:85–94 (in Chinese).

24. Mao S, Lu C, Li M, Ye Y, Wei X, Tong H. Identification of key aromatic compounds in Congou black tea by partial least-square regression with variable importance of projection scores and gas chromatography-mass spectrometry/gas chromatography-olfactometry. *J Sci Food Agric.* (2018) 98:5278–86. doi: 10.1002/jsfa.9066

25. Deng XJ, Huang GH, Tu Q, Zhou HJ Li YL, et al. Evolution analysis of flavor-active compounds during artificial fermentation of pu-erh tea. *Food Chem.* (2021) 357:129783. doi: 10.1016/j.foodchem.2021.129783

26. Stribny J, Gamero A, Perez-Torrado R, Querol A. Saccharomyces kudriavzevii and Saccharomyces uvarum differ from Saccharomyces cerevisiae during the production of aroma-active higher alcohols and acetate esters using their amino acidic precursors. *Int J Food Microbiol.* (2015) 205:41–6. doi: 10.1016/j.ijfoodmicro.2015.04.003

27. Qi DD, Miao AQ, Cao JX, Wang WW, Chen W, Pang S. Study on the effects of rapid aging technology on the aroma quality of white tea using GC-MS combined with chemometrics: in comparison with natural aged and fresh white tea. *Food Chem.* (2018) 265:189–99. doi: 10.1016/j.foodchem.2018.05.080

28. Yan H. *Study on the Enantiomers of Volatile Lactones and Terpenoids in Fuding White Tea*. Beijing: Chinese Academy of Agricultural Sciences (2019) (in Chinese).

29. Xiao Y, Huang Y, Chen Y, Xiao L, Zhang X, Yang C, et al. Discrimination and characterization of the volatile profiles of five Fu brick teas from different manufacturing regions by using HS–SPME/GC–MS and HS–GC–IMS. *Curr Res Food Sci.* (2022) 9:24. doi: 10.1016/j.crfs.2022.09.024

30. Stamatopoulos P, Brohan E, Prevost C, Siebert TE, Herderich M, Darriet P. Influence of chirality of lactones on the perception of some typical fruity notes through perceptual interaction phenomena in bordeaux dessert wines. *J Agric Food Chem.* (2016) 64:8160–7. doi: 10.1021/acs.jafc.6b03117

31. Cooke RC, Van Leeuwen KA, Capone DL, Gawel R, Elsey GM, Sefton MA. Odor detection thresholds and enantiomeric distributions of several 4-alkyl substituted γ-lactones in Australian red wine. *J Agric Food Chem.* (2009) 57:2462–7. doi: 10.1021/jf8026974

32. Yue CN, Peng H, Li WJ, Tong ZF, Wang ZH, Yang PX. Untargeted metabolomics and transcriptomics reveal the mechanism of metabolite differences in spring tender shoots of tea plants of different ages. *Foods.* (2022) 11:2303. doi: 10.3390/foods11152303

33. Wang ZH, Gan S, Sun WJ, Chen ZD. Widely targeted metabolomics analysis reveals the differences of nonvolatile compounds in Oolong tea in different production areas. *Foods.* (2022) 11:1057. doi: 10.3390/foods11071057

34. Han ZS, Wen MC, Zhang HW, Zhang L, Wan XC, Ho CT, et al. based metabolomics and sensory evaluation reveal the critical compounds of different grades of Huangshan Maofeng green tea. *Food Chem.* (2022) 374:131796. doi: 10.1016/j.foodchem.2021.131796

35. Wang J, Li MR, Wang H, Huang WJ Li F, Wang LL, et al. Decoding the specific roasty aroma Wuyi rock tea (*Camellia sinensis*: Dahongpao) by the sensomics approach. *J Agric Food Chem.* (2022) 70:10571–83. doi: 10.1021/acs.jafc.2c02249

36. Guo XY, Schwab W, Ho CT, Song CK, Wan XC. Characterization of the aroma profiles of oolong tea made from three tea cultivars by both GC–MS and GC-IMS. *Food Chem.* (2022) 376:131933. doi: 10.1016/j.foodchem.2021.131933

37. Xu YQ, Wang C, Li CW, Liu SH, Zhang CX Li LW, et al. Characterization of aroma-active compounds of pu-erh tea by headspace solid-phase microextraction (hs-spme) and simultaneous distillation-extraction (sde) coupled with gc-olfactometry and gc-ms. *Food Anal Methods.* (2016) 9:1188–98. doi: 10.1007/s12161-015-0303-7

38. Wen LX, Zhang F, He MZ, Huang SH, Peng JR, Lin JW, et al. Quality characteristics of stale flavor Liupao teas and establishment for evaluation method of aroma quality. *Food Ind Sci Technol.* (2021) 42:230–6 (in Chinese).

39. Qiao DH Mi XZ, An YL, Xie H, Cao KM, Chen HR, et al. Integrated metabolic phenotypes and gene expression profiles revealed the effect of spreading on aroma volatiles formation in postharvest leaves of green tea. *Food Res Int.* (2021) 149:110680. doi: 10.1016/j.foodres.2021.110680

40. Li Q, Chai S, Li YD, Huang JA, Luo Y, Xiao LZ, et al. Biochemical components associated with microbial community shift during the pile-fermentation of primary dark tea. *Front Microbiol.* (2018) 9:1509. doi: 10.3389/fmicb.2018.01509

41. Wang J, Zhang JW, Chen Y, Yu L, Teng JW, Xia N, et al. The relationship between microbial dynamics and dominant chemical components during liupao tea processing. *Food Biosci.* (2021) 2:101315. doi: 10.1016/j.fbio.2021.101315

42. Ho CT, Zheng X, Li SM. Tea aroma formation. *Food Sci Human Wellness.* (2015) 4:9–27. doi: 10.1016/j.fshw.2015.04.001

43. Parlapani FF, Ferrocino I, Michailidou S, Argiriou A, Boziaris IS. Microbiota and volatilome profile of fresh and chill-stored deepwater rose shrimp (*parapenaeus longirostris*). *Food Res Int.* (2020) 132:109057. doi: 10.1016/j.foodres.2020.109057

44. Li Y, Nishino N. Monitoring the bacterial community of maize silage stored in a bunker silo inoculated with *Enterococcus faecium*, *Lactobacillus plantarum* and *Lactobacillus buchneri*. *J Appl Microbiol.* (2011) 110:1561–70. doi: 10.1111/j.1365-2672.2011.05010.x

45. Liu YJ, Han YJ, Peng WJ, Niu QS, Fang XM, Zhao YZ, et al. Analysis of microbial community diversity in bee bread by high-throughput sequencing. *Food Sci.* (2020) 41:94–100 (in Chinese).

frontiers | Frontiers in Nutrition

TYPE Review
PUBLISHED 06 January 2023
DOI 10.3389/fnut.2022.1022977

OPEN ACCESS

EDITED BY
Mingquan Huang,
Beijing Technology and Business University, China

REVIEWED BY
Weizheng Sun,
South China University of Technology, China
Jiajia Song,
Southwest University, China

*CORRESPONDENCE
Zhiguo Huang
✉ hzgwww@126.com

†These authors have contributed equally to this work

SPECIALTY SECTION
This article was submitted to Food Chemistry, a section of the journal Frontiers in Nutrition

RECEIVED 19 August 2022
ACCEPTED 07 December 2022
PUBLISHED 06 January 2023

CITATION
Zhou Y, Hua J and Huang Z (2023) Effects of beer, wine, and baijiu consumption on non-alcoholic fatty liver disease: Potential implications of the flavor compounds in the alcoholic beverages. *Front. Nutr.* 9:1022977. doi: 10.3389/fnut.2022.1022977

Effects of beer, wine, and baijiu consumption on non-alcoholic fatty liver disease: Potential implications of the flavor compounds in the alcoholic beverages

Yabin Zhou[1,2,3†], Jin Hua[1,3†] and Zhiguo Huang[1,2*]

[1]School of Biological Engineering, Sichuan University of Science and Engineering (SUSE), Zigong, Sichuan, China, [2]Liquor-Making Biotechnology and Application Key Laboratory of Sichuan Province, Sichuan University of Science and Engineering (SUSE), Zigong, Sichuan, China, [3]College of Medicine and Public Health, Flinders University, Adelaide, SA, Australia

Non-alcoholic fatty liver disease (NAFLD) is one of the most common causes of chronic liver disease and its global incidence is estimated to be 24%. Beer, wine, and Chinese baijiu have been consumed worldwide including by the NAFLD population. A better understanding of the effects of these alcoholic beverages on NAFLD would potentially improve management of patients with NAFLD and reduce the risks for progression to fibrosis, cirrhosis, and hepatocellular carcinoma. There is evidence suggesting some positive effects, such as the antioxidative effects of bioactive flavor compounds in beer, wine, and baijiu. These effects could potentially counteract the oxidative stress caused by the metabolism of ethanol contained in the beverages. In the current review, the aim is to evaluate and discuss the current human-based and laboratory-based study evidence of effects on hepatic lipid metabolism and NAFLD from ingested ethanol, the polyphenols in beer and wine, and the bioactive flavor compounds in baijiu, and their potential mechanism. It is concluded that for the potential beneficial effects of wine and beer on NAFLD, inconsistence and contrasting data exist suggesting the need for further studies. There is insufficient baijiu specific human-based study for the effects on NAFLD. Although laboratory-based studies on baijiu showed the antioxidative effects of the bioactive flavor compounds on the liver, it remains elusive whether the antioxidative effect from the relatively low abundance of the bioactivate compounds could outweigh the oxidative stress and toxic effects from the ethanol component of the beverages.

KEYWORDS

non-alcoholic fatty liver disease, flavor compound, beer, wine, baijiu

1. Introduction

Alcoholic beverages not only have been consumed for thousands of years for social, ceremonial, behavioral, and ritual purposes but also are widely consumed. Around 43% of adults (aged 15 years or older) reported consuming alcohol globally in 2016 (1). The average global alcohol consumption was equivalent to approximately 6.43 L of pure ethanol per capita of the adult population in 2015 (2). In 2016, 46% of the total alcohol consumption was beers (34.3%) and wines (11.7%), and 44.8% was spirits (1). South-east Asia region consumed 87.9% of the total spirit globally (1). The major spirit consumed in China (one of the most populated areas of South-east Asia region) is baijiu. Despite its popularity, alcohol consumption ranks as the third most important preventable cause of the disease (3), the fifth-leading risk factor for premature death and disability globally (4), and accounted for 5.1% of the global burden of disease expressed in DALYs (disability-adjusted life years) (1). Excessive alcohol consumption, referring to daily consumption of greater than three drinks (one drink is equivalent to 14 g of pure ethanol), is associated with increased risk of various diseases (5–9), cancers (10–12), and all-cause mortality (13).

On the other hand, however, there are studies demonstrating that low alcohol consumption is not associated with an increased risk of some cancers (14–17). Moreover, some studies from recent years have indicated that low to moderate alcohol consumption, typically 2–3 drinks (approximately 28–42 g of ethanol) per day for men and 1–2 drinks (approximately 14–28 g of ethanol) per day for women, is associated with some beneficial health effects, such as lower risks for cardiovascular disease, dementia, and insulin resistance (18–21). Moderate alcohol consumption is also associated with reduced all-cause mortality (6, 10, 13), and the association is often formed a J-shape relationship (10, 13). Furthermore, some flavor compounds in alcoholic beverages, such as phenolic acids (in beers and wines), organic acids, esters, and terpenoids (22) (in baijiu), may also have additional impacts on health. For instance, the Copenhagen prospective population studies (23) have shown that wine intake is associated with better beneficial effects on all-cause mortality than those from purely alcohol consumption. It was hypothesized that the additional beneficial effects may have come from numerous phenolic compounds present in wine, such as phenolic acids, flavan-3-ols, and anthocyanins.

Non-alcoholic fatty liver disease (NAFLD), one of the most common causes of chronic liver disease worldwide, is clinically diagnosed with the presence of liver fat accumulation $\geq$5%, determined by radiological imaging techniques, in absence of other known causes (e.g., alcohol, drugs, and virus) (24). The prevalence of NAFLD is increasing constantly, and the current global incidence of NAFLD is estimated to be 24%, with Asia (27%) USA (24%), and Europe (23%) (25). Its prevalence is increasing at a fast pace. In the US alone, for instance, it was projected that the number of patients with NAFLD will increase from 83.1 million (in 2015) to around 100.9 million in 2030 (26). In addition, NAFLD is associated with metabolic syndrome, especially type 2 diabetes and enhances the comorbidities (24, 27). Furthermore, NAFLD, if left unmanaged/poorly managed, can progress to non-alcoholic steatohepatitis (NASH). Approximately 40–50% of the patients with NASH may further progress to hepatic fibrosis, with increased risks of cirrhosis and hepatocellular carcinoma (24). Thus, NAFLD is a growing burden for global healthcare systems. Having good strategies to manage and treat NAFLD, therefore, has become important. The diagnosis of NAFLD reveals NAFLD population consisted of either abstainers or low to moderate alcoholic beverage drinkers. A good understanding of the effects of common alcoholic beverage intake on NAFLD could improve daily NAFLD management and improve the condition of comorbidities.

In this review, the aim is to critically evaluate and discuss the current evidence of effects on liver and NAFLD from human-based and laboratory-based studies on beer, wine, and Chinese baijiu, with a focus on the effects and potential mechanism of ethanol in the beverages, the polyphenols in beer and wine, and the bioactive flavor compounds in baijiu.

2. The effects of ethanol on NAFLD

2.1. Evidence from studies

The consumption of equivalent to 50 g of ethanol per day has an estimated excess risk of 46% for liver cancer, the end stage of NAFLD progression, and the consumption of 100 g of ethanol per day has an excess risk of 66%. A meta-analysis of prospective studies by Turati et al. (12) has shown a positive association between heavy alcohol drinking and liver cancers. Moreover, excessive alcohol consumption is linked to an increased incidence of liver diseases (7). Consumption of alcohol equivalent to 30–50 g of ethanol/day for 5–10 years or longer is associated with an increased risk of alcoholic liver disease (ALD) (5). However, in NAFLD populations, alcohol consumption is either none or low to moderate. The effects of low to moderate alcohol consumption on NAFLD from studies are controversial. On the one side, Bagnardi et al. (28) found daily alcohol consumption no greater than 12.5 g showed no association with liver cancers. In addition, moderate alcohol drinking is associated with a reduced risk for NAFLD and NASH (29, 30). Some studies found low to moderate alcohol consumption could improve serum lipid profiles (31, 32), and alcohol consumption equal to or less than 25 g/day could significantly reduce cardiovascular risk in patients with diabetes (33). Animal studies showed a moderate baijiu (a type of spirit) consumption may potentially improve serum lipid profiles while having no significant damage to the liver (31). On the other side, however, there is evidence suggesting alcohol consumption has

no safe limit for NAFLD, even low alcohol consumption could still increase the risk of disease progression to advanced stages (34, 35). The putative mechanism of ethanol's effects on NAFLD, although not entirely clear, involves the impact of decreased NAD^+/NADH ratio, oxidation stress, and acetaldehyde on hepatic lipid metabolism. All three factors are the outcome of ethanol's metabolism in the liver (**Figure 1**; 36–38).

2.2. The mechanisms

After ingestion, approximately 94–98% of the ethanol is removed by two enzyme systems: alcohol dehydrogenase (ADH) (39, 40) and microsomal ethanol-oxidizing system (MEOS) (36, 41). Although ADH is expressed in the cytosol of both gastric mucosa and hepatocytes, the majority is presented in the liver. MEOS is presented predominantly in the endoplasmic reticulum of hepatocytes; it is also expressed in the intestinal mucosa. ADH is metabolizing the majority of the ingested ethanol, especially when consuming no more than three drinks. MEOS, however, plays an important role in removing ethanol after excessive alcohol consumption (such as binge drinking). It is because, in the presence of high blood alcohol concentration (BAC), the activity of MEOS is induced and increased.

After alcohol consumption, gastric ADH eliminates a small fraction of ingested ethanol before it is absorbed and delivered to the liver through the portal vein. The rate of ethanol elimination by Gastric ADH is affected by gender and age, polymorphisms between ethnic groups, rate of drink, and fed or fasted state. This may contribute to the variation and discrepancy of the results in studies. The majority of ingested ethanol is absorbed by the intestinal mucosa and transported to the liver for clearance. The ethanol oxidization catalyzed by ADH also reduces the coenzyme nicotinamide adenine dinucleotide (NAD^+) to NADH. After heavy drinking, ethanol oxidation by ADH decreases the ratio of NAD^+/NADH, which could enhance the synthesis of triglyceride and the accumulation of lipids in the liver. For patients with NAFLD, this may potential enhance disease progression. Moreover, the decrease in NAD^+/NADH ratio also inhibits the oxidation of acetaldehyde, the accumulation of which impairs mitochondria. Mitochondria impairment may lead to lipid accumulation in the liver.

MEOS (42) is predominantly found in the liver, whose main component is cytochrome P450 (CYP) isoform CYP2E1. CYP2E1 oxidizes ethanol to form acetaldehyde and converts nicotinamide adenine dinucleotide phosphate (NADPH) to $NADP^+$. MEOS has a higher Michaelis–Menten constant (K_m) for ethanol than ADH and activates with high BAC. It normally accounts for 20–25% of all alcohol metabolism. Ethanol metabolism facilitated by MEOS also results in the production of various reactive oxygen species (ROS), such as ethoxy radical $CH_3CH_2O\bullet$, hydroxyethyl radical $CH_3C(\bullet)HOH$, acetyl radical $CH_3CHO\bullet$, and singlet radical $^1O_2$. After heavy alcohol consumption, the elevated level of ROS generated undergoes covalent bonding to macromolecules on the membrane, subcellular organelles, and subsequently interferes with their biological function (43). In addition, the oxidative stress caused by the ROS on the one hand damages the mitochondria impairing fatty acid beta-oxidation and causing lipid accumulation. On the other hand, oxidative stress on the endoplasmic reticulum (ER) can activate its stress response and enhance fatty acid synthesis.

Acetaldehyde, the direct metabolite of ethanol, is not only IARC classified group 1 carcinogen but also toxic. It is oxidized to acetate by hepatic acetaldehyde dehydrogenase (ALDH), and acetate is further oxidized to CO_2. The generation of the elevated level of acetaldehyde and/or its slow removal is harmful. The main ALDH isozyme that metabolizes acetaldehyde in the liver is ALDH2. The polymorphism of ALDH2 results in a low-activity enzyme, which has been presented among the East Asian population (such as Han Chinese and Japanese). This polymorphism of ALDH2 may be a potential factor that causes study results discrepancy. Oxidation of acetaldehyde by ALDH requires the reduction of NAD^+ to NADH. Heavy alcohol consumption increases NADH levels and decreases the NAD^+/NADH ratio, which could inhibit acetaldehyde oxidation and cause its accumulation. Acetaldehyde can form adducts with DNA, lipids, and proteins; therefore, its accumulation could disrupt normal liver metabolism and may impose a negative impact on the NAFLD population.

3. The effects of beer on NAFLD

3.1. Evidence from clinical, epidemiological, and laboratory studies

Beer is a type of popular fermented beverage, and its consumption alone took 34.3% of total global alcohol consumption in 2016 (1). Low to moderate beer consumption has been shown to reduce the risk of cardiovascular disease compared to abstainers and heavy drinkers, suggesting the potential cardiovascular protection function of its polyphenols. However, its association with liver function is still inconclusive. The underline mechanism, although unclear, is thought to involve but not limited to the antioxidation, anti-inflammation, and lipid modulation properties of the polyphenolic and bitter acids.

There are limited epidemiological studies investigating beer consumption and liver health, and the outcome remains inconclusive. On the one hand, a positive and significant population-based association between beer consumption and liver disease-led mortality was demonstrated in 221 municipalities in the State of Louisiana in the US (44). In a Danish population–based study, 30,630 men and women with

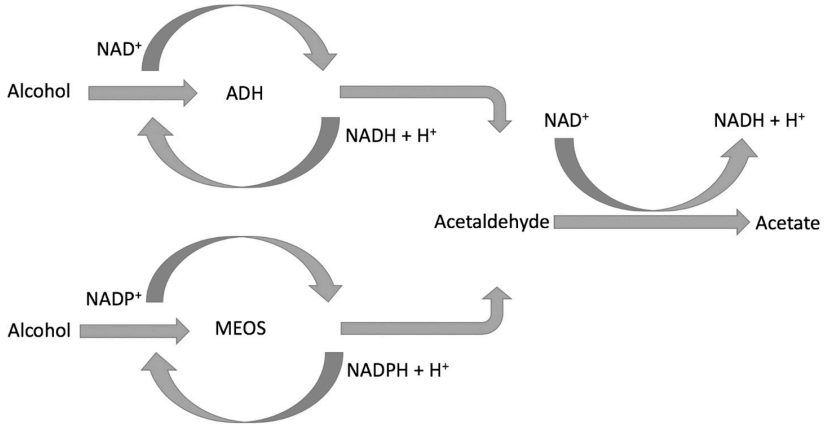

FIGURE 1
Schematic demonstration of alcohol metabolism.

more than five drinks/day of all three types of alcohol were associated with an increased risk for liver cirrhosis compared to abstainers or low alcohol drinkers. However, wine drinkers showed lower risk than beer and spirits drinkers (45). On the other hand, in an Eastern French population study, moderate beer consumption was not associated with increased mortality due to cirrhosis (46).

Various clinical studies and laboratory studies on human subjects have been carried out investigating the beneficial biological properties of polyphenols, bitter acids, and other non-alcoholic components in beer and their potential impact on health. In a randomized crossover trial involving 11 healthy middle-aged non-smoking men, beer consumption (equivalent to 40 g of ethanol per day) for 3 weeks did not increase the values of liver enzymes: gamma-glutamyltransferase (GGT), aspartate aminotransferase (AAT), and alanine aminotransferase (ALT) (47). Similar results were obtained from another crossover trial involving 60 healthy Spanish adults (31 men and 29 women), in which the levels of hepatic enzymes (GGT, GOT, and GPT) are unchanged after beer consumption (equivalent to 11 g/day for women and 22 g/day for men) for 1 month (48). However, in the crossover trial involving 10 middle-aged men and 10 post-menopausal women, the levels of both GGT and ALT showed a slight increase (but still within the normal clinical range) after beer consumption (equivalent to 40 g/day for men and 30 g/day for women) for 3 weeks. But interestingly, inflammation markers, C-reactive protein, and fibrinogen were decreased significantly, indicating anti-inflammatory action, after the 3-week beer consumption (49).

In a laboratory study, antioxidant melatonin was detected and measured in 18 brands of beer with different alcohol concentrations (50). In addition, serum samples from seven healthy human subjects were analyzed before and after beer consumption, which showed both melatonin and total antioxidant status increased after beer consumption. This suggests beer consumption may increase the antioxidative capability of human serum attributed to melatonin and other compounds beer contains. This coincides with the results from other studies, which found increased plasma polyphenolic contents and antioxidant capability (51, 52).

In vitro and *in vivo* studies also showed the beneficial biological effects of polyphenols, bitter acids, and other non-alcoholic components in beer. In a study using an aluminum-induced neurotoxicity murine model, the beer treatment group showed significant lower lipid peroxidation, higher expression of antioxidant enzymes (at mRNA levels), and lower expression (mRNA) of inflammation marker TNFα (53). The authors speculated polyphenols (such as resveratrol) and antioxidants (such as folic acid) in beer may have contributed a part to the antioxidation and anti-inflammation properties of the beer. These studies showed that beer-derived polyphenols may be absorbed and reach the blood circulation to exert biological functions. Two recent studies by Shafreen et al. and Tung et al. further demonstrate that serum polyphenols (come from beer) can bind and interact with serum proteins, such as human serum albumin, plasma circulation fibrinogen, and low-density lipoprotein to exert antioxidant functions (54, 55). In an *in vitro* study on peripheral blood mononuclear cells by Winkler et al., beer components were shown to increase neopterin production and tryptophan degradation and reduce ROS generation by inhibiting the production of pro-inflammatory cytokine interferon-γ (56).

3.2. The effects and putative mechanisms of the main flavor compounds in beer

Beer is fermented from cereals and hops (Humulus lupulus), consisting of over 90% of water, carbohydrates, ethanol,

(more than 50) polyphenolic compounds, bitter acids (e.g., humulones and lupulones), proteins, B-complex vitamins, and trace amounts of minerals (57, 58). The alcohol concentration of beer varied approximately from 3.5 to 10% (w/v) in different kinds of beers. The main non-alcoholic flavor compounds of beer thought to exert beneficial biological functions are (1) polyphenolic compounds: xanthohumol (around 0.2 mg/L), isoxanthohumol (around 0.6–3.4 mg/L), and phenolic acids (25–29 mg/L); (2) bitter acids: humulones (approximately up to 4 mg/L), lupulones (around 0.012–0.14 mg/L), and iso-humulones (around 10–100 mg/L) (57).

Among the non-alcoholic compounds in beer, the hop-derived phenolic compounds and bitter acids have been shown to modulate hepatic lipid metabolism and process anti-inflammatory, antioxidative, and anticarcinogenesis properties (**Table 1**). Xanthohumol, of which beer is the main human diet source, is a bioactive multifunctional prenylated flavonoid from the female inflorescence of the hop plant (59, 60). It has been shown with the capability to modulate hepatic lipid metabolism (61, 62). In type 1 diabetic rodent model, insulin deprivation led to down-regulation of fatty acid synthase (FAS), inactivation of Acetyl-CoA Carboxylase (ACC), and inhibition of lipogenesis (61). Xanthohumol was able to activate ACC, increase the expression of FAS, and restore some proportion of lipogenesis, through a mechanism not clearly understood. In mice fed with a high-fat diet, xanthohumol was able to reduce triglycerides and cholesterol content in the liver and skeletal muscle by inhibiting lipogenesis and lipid uptake and promoting β-oxidation (62). The putative mechanism involves xanthohumol activation of AMP-activated protein kinase (AMPK), which then inhibits the expression of sterol regulatory element-binding protein 1c (SREBP-1c), downstream ACC and FAS, down-regulation of the expression of lipid transporter CD36. In addition, xanthohumol was shown to inhibit liver fibrosis in type 1 diabetic rodent model (61). The mechanism, although not clear, is speculated to involve anti-inflammation and antioxidation actions as demonstrated in another study based on the same type 1 diabetic rodent model (63). Furthermore, xanthohumol was shown in a rodent model to protect the liver and the colon from DNA damage, and preneoplastic lesion caused by cooked food mutagen (64), indicating the capability to prevent liver cancer development from more general carcinogens, such as ethanol and acetaldehyde. Xanthohumol can be converted to isoxanthohumol during the brewing process and/or in the stomach. As one of the major flavonoids in normal beers, isoxanthohumol may also involve in modulating hepatic lipid metabolism, anti-inflammation, and antitumor (57, 61). Isoxanthohumol can be further converted to 8-prenylnaringenin by the microbiota in the intestine (57). 8-Prenylnaringenin not only exerts hormonal function as the strongest phytoestrogen but also involves modulating lipid metabolism (62, 65). Landmann et al. showed that normal beer (brewed with the hop) was able to attenuate hepatic lipid accumulation in a binge-drinking mouse model (66). The putative mechanism is shown to be the inhibition of hepatic iNOS induction and lipid peroxidation. The further study by the same group showed that iNOS and lipid peroxidation inhibition may be exerted by iso- α-acids (iso- humulones) from hop (67). The authors speculated the protection effects may also involve other compounds in the hop extracts, such as β-acids (lupulones).

TABLE 1 Bioactive flavor compounds in beer and their beneficial effects.

Compounds	Demonstrated beneficial effects	References
Xanthohumol	Modulate lipid metabolism; antioxidation; anti-inflammation; anticarcenogenesis	(59–64)
Isoxanthohumol	Modulate lipid metabolism; anti-inflammation; antitumor	(57, 61)
8-Prenylnaringenin	Hormonal function (Phytoesrongen); modulate lipid metabolism	(62, 65)
Bitter acids	Antioxidation; modulate lipid metabolism	(66, 67)
Other polyphenolic compounds	Antioxidation; anti-inflammation	(47–52)

The putative mechanisms that beer flavor compounds involved can be summarized as following three main areas (refer to **Figure 2**). (1) Modulate hepatic lipid metabolism: down-regulating hepatic lipogenesis, reducing hepatic lipid uptake from circulation, and enhancing β-oxidation; (2) antioxidation: as antioxidant removing ROS, increasing quantity and activity of antioxidant enzymes, and inhibition of lipid peroxidation; (3) anti-inflammation: preventing hepatic inflammation (through JNK/NF-κ B) caused by lipid accumulation induced endoplasmic reticulum stress in hepatocyte and lipid peroxidation. The exact process and how these are integrated remain elusive.

4. The effects of wine on NAFLD

4.1. Evidence from clinical and epidemiological studies

Wine is a type of popular alcoholic beverage fermented from grape vines. The term French paradox describes the observation of a lower incidence of coronary heart disease in France than in other Western countries, despite similar intake of high levels of saturated fat (68). This was based on epidemiological studies, which suggested the observation was attributed to the beneficial effects of red wine consumption, on the data collected

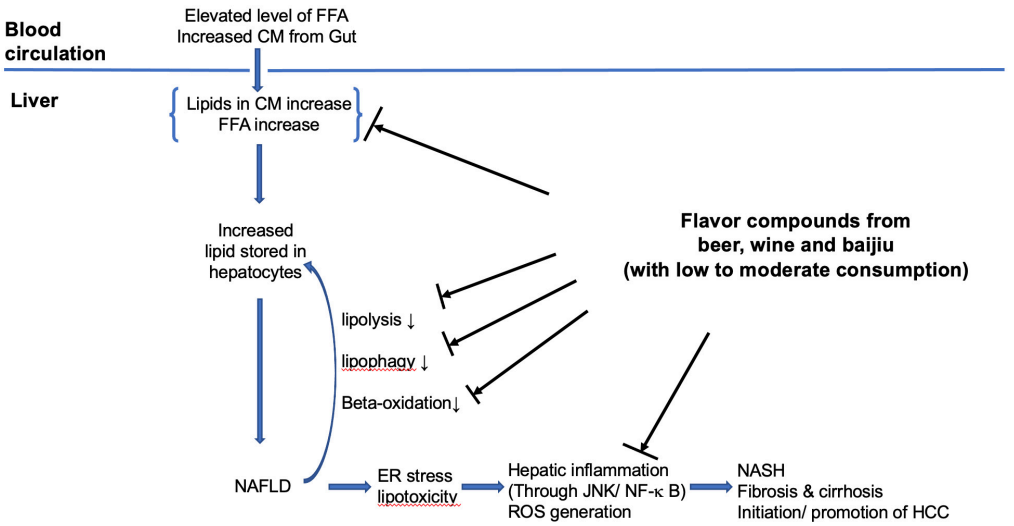

FIGURE 2
The putative mechanisms of flavor compounds on NAFLD. FFA, free fatty acids; CM, chylomicron remnants; ER, endoplasmic reticulum; HCC, hepatocellular carcinoma.

from the MONICA project organized by WHO. Since then, epidemiological studies and human trials have been carried out investigating the potential health benefit of wine. Among them, only limited studies directly investigated the effects of wine on NAFLD prevalence and progression with promising outcomes; however, more data are needed before any conclusion can be drawn. Dunn et al. performed the first epidemiological study investigating the association between modest consumption of wine and NAFLD (69). The study showed a lower NAFLD prevalence in participants who consumed up to four ounces of wine daily when compared to abstainers and participants whose daily consumption of up to 12 ounces of beer, 1 ounce of liquor, or 1 drink of mixed alcoholic drinks. The wine drinkers also demonstrated a lower prevalence of diabetics and other metabolic syndrome features in the study. However, this study did not demonstrate the safety of modest wine drinking in patients with NAFLD. A single-center cohort study by Mitchell et al. showed modest wine consumption (<70 g of ethanol per week without binge consumption) was associated with a significantly lower risk of advanced hepatic fibrosis compared to abstinence among patients with NAFLD (70). Some studies investigated the association between wine consumption and the risk of liver cirrhosis, the effects of wine drinking on hepatic lipid levels, functions, serum cholesterol profiles, and NAFLD co-exist metabolic syndrome. The outcome of the studies was inconsistent and inconclusive. In a prospective study in the Copenhagen area, Becker et al. found an increase in the risk of liver cirrhosis with increasing total alcohol intake for beer, wine, and spirit, but wine consumption showed a lower risk (45). In a large cohort prospective study including 1.3 million middle age UK women, with a mean of 15 years of following up of 401,806 women, the authors found that the risk of liver cirrhosis increased with the total amount of alcohol intake (event with moderate consumption), the increase of risk, in a given weekly intake of alcohol, was also associated with consumption without a meal or daily consumption, regardless whether drinking only wine or more than one type of alcoholic beverages (71). A randomized crossover trial by Beulens et al. showed 4 weeks of red wine consumption (40 g of ethanol per day) did not significantly increase liver fat compared to 4 weeks of consumption of de-alcoholized red wine (72). An interventional cohort study by Rajdl et al. showed, although there was an increase in liver enzymes AST (within the normal reference range) and ALT (slightly exceeded upper threshold), white wine consumption is associated with an increase in antioxidative effects (73). In a prospective randomized trial involving 44 healthy subjects (32 women and 12 men), Kechagias et al. showed an increase in ALT and AST (within an upper reference threshold), decrease in LDL cholesterol, and a trend of hepatic triglyceride content increase for subjects with moderate red wine consumption for 90 days (74). These changes in the red wine consumption group were significantly different when compared with the alcohol abstention group. Taborsky et al. carried out the prospective, multi-center, randomized In Vino Veritas study comparing the effects on healthy subjects between red and white wine consumption (75). The results showed that the changes in total cholesterol, HDL, LDL, triglyceride, liver function, and other markers during the 12-month wine consumption were not varied significantly between red and white wine groups, regardless of the significant difference in the polyphenolic compounds between the two wines. However, when comparing the baseline within each group, both groups

showed a significant reduction in LDL for time points at 6 months and 12 months, a significant total cholesterol reduction at 6 months, the red wine group showed a significant HDL reduction at 6 months and a significant total cholesterol reduction at 12 months. Type 2 diabetes is one of the most common metabolic syndromes that co-exist with NAFLD (24). In a 2-year randomized intervention trial, Gepner et al. demonstrated that red wine consumption significantly increased HDL-C levels and decreased the total cholesterol/HDL-C ratio (76). When compared to the non-drinking (water) group, the overall value of metabolic syndrome components was further significantly decreased in the red wine group.

4.2. The effects and putative mechanisms of the phenolic compounds in wine

Wine contains water, carbohydrates, organic acids, alcohol, polyphenols, minerals, and B vitamins. The rich phenolic compounds of wine (especially red wine) are thought to provide potential health benefit effects (**Table 2**). The main phenolic compounds in wine are stilbenes (resveratrol), phenolic acids, and flavonoids (flavan-3-ols, Anthocyanins, quercetin) (77–80). Although the mean level of resveratrol (a type of stilbenes) is 7 mg/L in red wine, the total stilbenes level could be up to 20 mg/L (80, 81). The levels of catechin and epicatechin, as main flavan-3-ols, are approximately 100 and 75 mg/L, respectively. The amount of anthocyanins and quercetin is up to 500 mg/L and around 16 mg/L, respectively (80, 81). Various mechanisms (concerning the polyphenolic compounds in wine) have been proposed for the potential beneficial effects of wine, especially red wine on liver metabolism and NAFLD. These include the antioxidation effects, anti-inflammatory effects, and modulation of lipid metabolism. Resveratrol, one of the most important phenolic compounds in wine, demonstrated the capability to ameliorate antioxidative stress and inflammation and modulated hepatic lipid metabolism (82, 83). Resveratrol is not only an antioxidant, scavenging ROS, HO, peroxyl radicals, and chelating metal ions interacting with ROS (84–86), but also capable of increasing the activity of hepatic antioxidation enzymes, such as superoxide dismutase, catalase, and glutathione peroxidase (87–90). Resveratrol has also been shown to be able to modulate hepatic lipid metabolism by activation of sirtuin 1 (SIRT 1)–AMPK signaling, which on the one hand promotes the fatty acid beta-oxidation by activating peroxisome proliferator-activated receptor α (PPARα), PPARγ co-activator 1α (PGC1α), and their target genes, on the other hand, down-regulates fatty acid synthesis through SREBP-1c inhibition (91). Additionally, resveratrol was shown to reduce intracellular lipid droplets possibly by promoting autophagy in HepG2 cells (92). Resveratrol has also been shown in studies to possess anti-inflammatory properties, such as inhibiting infiltration of macrophage and recruitment of Kupffer cells, reducing TNFα levels (93–95).

TABLE 2 Bioactive flavor compounds in wine and their beneficial effects.

Compounds	Demonstrated beneficial effects	References
Resveratrol	Antioxidation; anti-inflammation; reduce lipid accumulation	(82–95)
Quercetin	Antioxidation; anti-inflammation; antiapoptosis; hepatoprotective	(77, 78, 80)
Anthocyanins	Antioxidation; anticancer	(79, 80)
Total phenolic compounds	Antioxidation; anti-inflammation; modulate lipid metabolism; antifibrosis; improve serum lipid profile; improve metabolic syndrome condition	(68–76, 80)

The putative mechanisms that phenolic compounds in wine, such as resveratrol involved in can be summarized in three main areas (refer to **Figure 2**). (1) Antioxidation: as antioxidants scavenging ROS, HO, and peroxyl radicals, increasing quantity and activity of antioxidant enzymes and inhibition of lipid peroxidation; (2) modulating hepatic lipid metabolism: activation of SIRT 1–AMPK signaling leading to inhibition of hepatic lipogenesis and enhancing β-oxidation, promoting lipid autophagy; (3) anti-inflammation: through inhibition of NF-κ B pathways. The exact processing involved is not entirely clear, more studies are needed.

5. The effects of baijiu on NAFLD

5.1. Evidence from laboratory studies

Among the alcoholic beverages consumed globally, 44.8% are spirits. In China, alcohol consumption has been increasing since the 1960s with total recorded consumption reaching equivalent to 5.7 L of pure alcohol per capita in 2016 (**Figure 3A**). Spirits consumption is 67% of all alcoholic beverages in 2016 (**Figure 3B**; 1). Baijiu, the main category of spirits consumed in China, is produced by unique multi-strain and solid-state fermentation techniques.

A study (96) based on the human liver cell line, Hep3B, has shown a non-alcoholic residue of Maotai (a brand of baijiu), is able to up-regulate GST A1, an antioxidant-responsive element. This subsequently promotes antioxidative activity through an ERKs- and p38 K-dependent pathway, which may reduce oxidative stress caused by alcohol metabolism and provide protection to the liver. Subsequent animal studies (97, 98) on Maotai have shown that it has different effects on the liver than that of the same amount of alcohol.

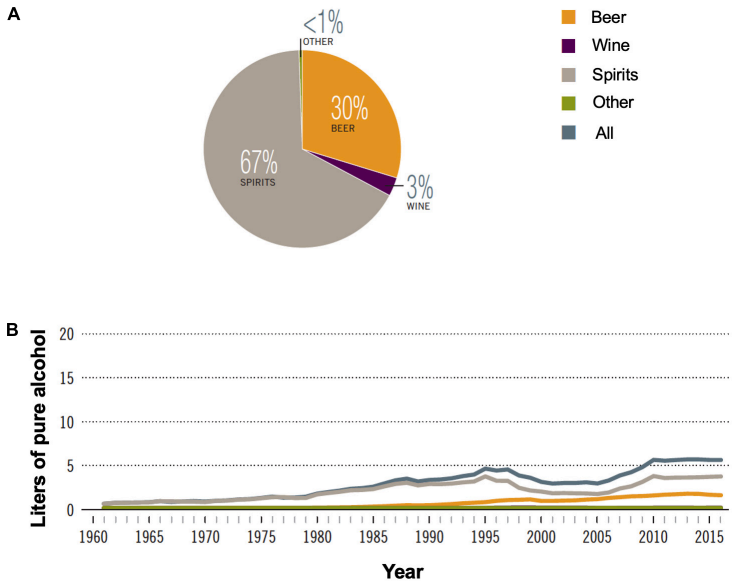

FIGURE 3
Alcohol consumption in China. **(A)** Proportion of different alcoholic beverages consumed in 2016; **(B)** recorded alcohol consumption per capita in adults (age > 15 years), 1961–2016. Adapted with permission from ref (1) under Creative Commons Attribution-Non-Commercial-ShareAlike 3.0 IGO license. (CC BY-NC SA 3.0 IGO; https://creativecommons.org/licenses/by-nc-sa/3.0/igo).

It significantly induced various antioxidation factors, heme oxygenase-l, metallothionein, Nrf2, and GCLC. A tetrapeptide from sesame flavor-type baijiu has been shown to promote hepatic antioxidation factors through various mechanisms to counteract the oxidative stress caused by alcohol metabolisms (99). A recent animal study (100) compared the effects of daily consumption of equivalent to approximately three drinks of baijiu or an equivalent amount of pure alcohol solution. Results showed that the baijiu treatment group has significantly less liver injury and steatosis. Further study on approximately 1.5 drinks of baijiu or equivalent pure alcohol solution showed pure alcohol solution treatment group induced significantly higher plasma ALT and hepatic triglyceride levels. The non-alcoholic flavor compounds in baijiu have been shown in an animal study, to be able to attenuate liver damage caused by ethanol potentially through differential impact on host gut microbiota (101).

Animal and *in vitro* studies have shown baijiu posts less injury to the liver than an equivalent amount of pure alcohol. This coincides with the speculation that the non-alcoholic components, especially biologically active compounds of baijiu may have additional effects on the liver that is apart from alcohol. However, due to the limited evidence, this hypothesis is still controversial. First, more laboratory studies are needed to demonstrate what are the main compounds that could convey these effects (either beneficial or harmful), the mechanisms, and potential interactions between the compounds and ethanol. Second, evidence is needed to show that the amount of compounds in baijiu is sufficient to convey the proposed effects. Moreover, the evidence from the epidemiology and clinical studies is insufficient and inconclusive (102, 103). Better controlled epidemiology and clinical studies, such as randomized controlled trials, would be needed (104).

5.2. The effects and putative mechanisms of the main flavor compounds in baijiu

It is proposed that the non-alcoholic components, such as polyphenols in alcoholic beverages, may have additional beneficial effects (83, 105). Baijiu, a type of distilled spirit produced through solid-state fermentation (106), has contained more than 1,874 kinds of identified flavor compounds (22, 106). Among these compounds, there are at least 138 kinds have been shown to be bioactive (22). It is speculated that the biologically active compounds in baijiu may have some protective effects on the liver from the injury caused by ethanol metabolism when baijiu consumption is low to moderate (**Table 3**; 22, 100).

The biological active volatile compounds include phenols, organic acids, esters, terpenes, pyrazines, sulfur compounds, and furan derivants. The non-volatile compounds include polyols, peptides, amino acids, vitamins, and minerals. Various phenols have been identified by techniques, such as GC-MS, HPLC-MS, and GC-TOF-MS. Five of them are shown to have beneficial effects. Ferulic acid, the main ingredient of several Chinese herbals, has been shown to have antioxidation and anti-inflammation effects and may be protective of the liver against the oxidative stress caused by alcohol metabolism (81,

TABLE 3 Bioactive flavor compounds in baijiu and their beneficial effects.

Compounds	Demonstrated beneficial effects	References
Ferulic acid (phenolic acid)	Antioxidation; anti-inflammation; liver protective;	(81, 107)
Acetic acid, butyric acid, linoleic acid, alpha-linolenic acid, lactic acid and L-Malic acid (organic acids)	Antibacterial; serum cholesterol and triglycerides reduction; anti-inflammation; Antioxidation; antiapoptosis; hepatoprotective	(110–114)
Tetramethylpyrazine (pyrazines)	Hepatoprotective; Antioxidation	(115, 116)
Ethyl linolenate and ethyl linoleate (ethyl esters)	Improve serum lipid profile	(119)
Terpenes	Antioxidation; antibacterial; potential hepatoprotective	(120)
5-hydroxymethyl furfural	Anti-inflammation; serum cholesterol reduction; antitumor	(121–123)
Lichenysin; tripeptide Pro-His-Pro	Antibacterial; antiviral; Antioxidation	(125–127)

TABLE 4 Abundant and bioactive compound in Luzhoulaojiao.

Compounds	Concentration (mg/L)
Ethyl hexanoate	2221 ± 12
Ethyl acetate	693 ± 8
Ethyl lactate	316 ± 4
Hexanoic acid	300 ± 111
Butanoic acid	109.7 ± 0.7
Ethyl butyrate	46.3 ± 0.8
Heptanoic acid	36 ± 1
Furfural	30.96 ± 0.05
Ethyl valerate	10.7 ± 0.1
Phenylethyl Alcohol	3.66 ± 0.03
Ethyl heptanoate	3.38 ± 0.04
1-Hexanol	2.76 ± 0.02
1-Butanol	1.784 ± 0.005

Adapted with permission from ref (109) under a Creative Commons Attribution 4.0 International License.

107). Baijiu contains 127 organic acids, which are important to the baijiu flavor. In the sesame-aroma type of baijiu, there are eight acids that have a quantity higher than 10 mg/L (108). In baijiu, Luzhoulaojiao, the quantity of the acid reaches as high as 300 mg/L (**Table 4**; 109). The acids may potentially have beneficial effects. To date, 16 acids have been reported to be health beneficial. Acetic acid, butyric acid, linoleic acid, alpha-linolenic acid, lactic acid, tartaric acid, and L-Malic acid are typical ones (110–114). The non-saturated acids, such as linoleic and linolenic acids, may improve lipid profiles. The acid may also help regulate liver lipid synthesis. SCFA, such as butyric acid (around 80 mg/L in baijiu), are known to involve in the regulation of energy homeostasis, obesity, immune system, brain function, and colorectal cancer prevention (113). Although the concentration of butyric acid in baijiu is low, it may serve as a source of dietary intake of butyrate to maintain its physiological concentration in the human body.

Pyrazines are a category of biologically active compounds in baijiu and may have health benefits. A pyrazine and its several derivants, such as tetramethylpyrazine, have been detected in Maotai, Laobaigan, Yanghe River Daqu, and Fenjiu. Tetramethylpyrazine is the main active ingredient of Rhizoma Ligustici Chuanxiong, a Chinese herbal that has long been used to treat liver disease and protect the liver from fibrosis (115, 116). It has antioxidation properties and enhances triglyceride degradation. Esters are the major flavor compounds in baijiu. To date, 510 esters have been identified in baijiu (117). For instance, lactic acid ethyl ester is approximately 900 mg/L in soy sauce aroma type baijiu (118). At least five of them have been reported to have beneficial effects. Fatty acid esters, such as ethyl linolenate and ethyl linoleate may have a regulatory property on cholesterol synthesis (119). Alpha-angelica lactone, an important ingredient of Chinese herbal Angelicae sinensis radix and Rhizoma Ligustici Chuanxiong, has been detected in Jiannanchun and Gujinggong. It is shown to protect and regulate the immune system, especially speeding the immune system recovery after chemotherapy. It may potentially regulate liver immune response upon oxidative stress caused by alcohol metabolism and prevent the progression of ALD. Terpenes are a category of important compounds in baijiu. Fifty-two of the seventy-six identified terpenes in baijiu have been reported to be health beneficial (106). They process antioxidation, antiviral, and antibacterial properties, which may potentially be liver protective (120). Its concentration in baijiu can be as high as 3,400–3,600 μg/L. Baijiu also contains sulfur compounds, to date, 73 compounds have been identified. At least six of the identified sulfur compounds have been reported to be beneficial to health. One of their properties is antioxidation, which protects cells from injury from oxidative stress. Furans have also been identified in baijiu, which have antitumor properties. In particular, 5-hydroxymethyl furfural has been shown to inhibit tumor progression and anti-inflammation and is capable to reduce the serum cholesterol level (121–123). Among the non-volatile compounds, peptides are recently identified as bioactive compounds in baijiu. Lichenysin is a lipopeptide identified in Dongjiu (124) with a concentration as high as 112 μg/L. One of its properties is antibacterial activity and antiviral activity (125, 126). Based on structural similarity to surfactin, it is speculated that lichenysin may process antitumor properties through tumor cell G2/M arrest; however, experimental confirmation is needed. A tripeptide Pro-His-Pro (PHP) has been identified in the sesame-aroma type of baijiu Gujinggong (127). An *in vitro* study on human liver cell line HepG2 cells has demonstrated its ability to up-regulate cellular antioxidation enzymes, such as superoxide dismutase,

catalase, and glutathione peroxidase through Nrf2/antioxidant response in the element signaling pathway. Therefore, PHP pre-treatment was able to prevent HepG2 cells from oxidative stress induced by 2,20-azobis (2-methylpropanimidamidine) dihydrochloride.

The proposed mechanisms of the flavor compounds in baijiu involved can be summarized as antioxidation, anti-inflammation, and lipid metabolism modulation (refer to **Figure 2**). For antioxidation mechanisms, the flavor compounds can act as antioxidants to remove ROS and to up-regulate cellular antioxidation enzyme quantity and activities. For the anti-inflammatory effects, the flavor compounds may alleviate hepatic inflammation by modulating NF-κB-regulated pathways. They can also reduce the hepatic inflammation induced by liver cell endoplasmic reticulum stress caused by intracellular oxidation stress (through antioxidation pathways). For hepatic lipid metabolism modulation, the flavor compounds enhance lipid degradation and β-oxidation and at the same time reduce lipogenesis.

Although the aforementioned compounds in baijiu have potential biological effects, many of them are in low concentrations. For moderate consumption of baijiu, therefore, it is less likely that the intake of each of those low-concentration compounds reaches a sufficient level to exert any effects. Therefore, it is important to identify the main compounds that possess the beneficial effects and potential combinational effects they impose as a whole and elucidate the mechanism underlining the combinational effects.

6. Discussion

It is commonly accepted that excessive alcohol consumption or binge drinking (128) leads to ALD as well as advanced stages of NAFLD. For low to moderate alcohol consumption, controversial evidence exists on ethanol effects on NAFLD from epidemiology and clinical studies, and the mechanism is not entirely clear. The genetic variance of ADH and ALDH among the study population could convey variation in effects on the liver.

In addition, the findings from epidemiology and clinical studies on the effect of the polyphenolic compounds from beer and wine on NAFLD are inconsistent and inconclusive. For epidemiological studies, for instance, there are variations in a range of factors that contribute to the resulting inconsistency. These factors include but are not limited to the drinking patterns (frequency and amount, binge drinking or not, with/without a meal, proportion of wine among total alcohol consumed), variation of wine consumed, biological variation of investigated subjects (ethnic, gender, age, health status, etc.), study duration, and population. Hence, more well-controlled, long-term, randomized trials are needed.

For baijiu, there are very limited epidemiology and clinical studies available, most of the evidence is from laboratory based *in vitro* and *in vivo* studies. Different from beer and wine, baijiu contains a much higher concentration of alcohol. One could speculate low to moderate baijiu consumption could result in a much lower intake of bio-activate non-alcoholic flavor compounds for any potential beneficial effects. However, laboratory studies demonstrate the significant effects between baijiu and pure ethanol (100, 102). More laboratory studies are needed to first verify this difference and then elucidate the reason/mechanisms behind it. In addition, more specifically designed, baijiu based epidemiology, and clinical studies are needed to further investigate the effects of baijiu on the liver and the mechanism.

7. Conclusion

The non-alcoholic bioactive flavor compounds in beer, wine, and baijiu have been shown beneficial to NAFLD. The underline mechanism for the beneficial effects is proposed to involve modulation of lipid metabolism, reduction of oxidative stress and damages, and alleviation of inflammation. However, it is inconclusive whether low to moderate consumption of these three types of beverages is beneficial to NAFLD. For patients with NAFLD, it is recommended to abstain, although a low level of alcohol consumption may be alright. For normal people, the recommendation is either abstaining or consuming low to moderate alcohol without binge drinking.

Author contributions

YZ: conceptualization and drafting of the manuscript. JH: manuscript writing. ZH: conceptualization, manuscript draft review, and modification. All authors contributed to the article and approved the submitted version.

Funding

This research was kindly supported by the Science and Technology Bureau of Sichuan Province (China) project grant (2019YJ0461), Sichuan Provincial Academician (Expert) Workstation (China) project grant (2018YSGZZ03), and Sichuan University of Science and Engineering (China) seeding grant (2017RCL72).

Conflict of interest

The authors declare that the research was conducted in the absence of any commercial or financial relationships that could be construed as a potential conflict of interest.

Publisher's note

References

1. WHO. *Global Status Report on Alcohol and Heatlh 2018*. Geneva: World Health Organization (2018).

2. WHO. *Global Information Sytem on Alcohol and Health (GISAH)*. Geneva: World Health Organization (2016).

3. Singal A, Anand B. Recent trends in the epidemiology of alcoholic liver disease. *Clin Liver Dis.* (2013) 2:53–6. doi: 10.1002/cld.168

4. Lim S, Vos T, Flaxman A, Danaei G, Shibuya K, Adair-Rohani H, et al. A comparative risk assessment of burden of disease and injury attributable to 67 risk factors and risk factor clusters in 21 regions, 1990–2010: a systematic analysis for the global burden of disease study 2010. *Lancet.* (2012) 380:2224–60. doi: 10.1016/S0140-6736(12)61766-8

5. Poli A, Marangoni F, Avogaro A, Barba G, Bellentani S, Bucci M, et al. Moderate alcohol use and health: a consensus document. *Nutr Metab Cardiovasc Dis.* (2013) 23:487–504. doi: 10.1016/j.numecd.2013.02.007

6. Wood A, Kaptoge S, Butterworth A, Willeit P, Warnakula S, Bolton T, et al. Risk thresholds for alcohol consumption: combined analysis of individual-participant data for 599 912 current drinkers in 83 prospective studies. *Lancet.* (2018) 391:1513–23. doi: 10.1016/S0140-6736(18)30134-X

7. French S. How to prevent alcoholic liver disease. *Exp Mol Pathol.* (2015) 98:304–7. doi: 10.1016/j.yexmp.2015.03.007

8. Molina P, Gardner J, Souza-Smith F, Whitaker A. Alcohol abuse: critical pathophysiological processes and contribution to disease burden. *Physiology.* (2014) 29:203–15. doi: 10.1152/physiol.00055.2013

9. Yoon S, Jung J, Lee S, Kim J, Ahn S, Shin E, et al. The protective effect of alcohol consumption on the incidence of cardiovascular diseases: is it real? A systematic review and meta-analysis of studies conducted in community settings. *BMC Public Health.* (2020) 20:90. doi: 10.1186/s12889-019-7820-z

10. Thun M, Peto R, Lopez A, Monaco J, Henley S, Heath C, et al. Alcohol consumption and mortality among middle-aged and elderly U.S. adults. *N Eng J Med.* (1997) 337:1705–14.

11. Scheideler J, Klein W. Awareness of the link between alcohol consumption and cancer across the world: a review. *Cancer Epidemiol Biomarkers Prev.* (2018) 27:429–37. doi: 10.1158/1055-9965.Epi-17-0645

12. Turati F, Galeone C, Rota M, Pelucchi C, Negri E, Bagnardi V, et al. Alcohol and liver cancer: a systematic review and meta-analysis of prospective studies. *Ann Oncol.* (2014) 25:1526–35. doi: 10.1093/annonc/mdu020

13. Di Castelnuovo A, Costanzo S, Bagnardi V, Donati M, Iacoviello L, de Gaetano G. Alcohol dosing and total mortality in men and women: an updated meta-analysis of 34 prospective studies. *Arch Intern Med.* (2006) 166:2437–45. doi: 10.1001/archinte.166.22.2437

14. Islami F, Tramacere I, Rota M, Bagnardi V, Fedirko V, Scotti L, et al. Alcohol drinking and laryngeal cancer: overall and dose–risk relation – A systematic review and meta-analysis. *Oral Oncol.* (2010) 46:802–10. doi: 10.1016/j.oraloncology.2010.07.015

15. Fedirko V, Tramacere I, Bagnardi V, Rota M, Scotti L, Islami F, et al. Alcohol drinking and colorectal cancer risk: an overall and dose–response meta-analysis of published studies. *Ann Oncol.* (2011) 22:1958–72. doi: 10.1093/annonc/mdq653

16. Tramacere I, Scotti L, Jenab M, Bagnardi V, Bellocco R, Rota M, et al. Alcohol drinking and pancreatic cancer risk: a meta-analysis of the dose-risk relation. *Int J Cancer.* (2010) 126:1474–86. doi: 10.1002/ijc.24936

17. Hamajima N, Hirose K, Tajima K, Rohan T, Calle E, Heath C Jr, et al. Alcohol, tobacco and breast cancer – Collaborative reanalysis of individual data from 53 epidemiological studies, including 58 515 women with breast cancer and 95 067 women without the disease. *Br J Cancer.* (2002) 87:1234–45. doi: 10.1038/sj.bjc.6600596

18. Ronksley P, Brien S, Turner B, Mukamal K, Ghali W. Association of alcohol consumption with selected cardiovascular disease outcomes: a systematic review and metaanalysis. *Br Med J.* (2011) 342:d671.

19. Anstey K, Mack H, Cherbuin N. Alcohol consumption as a risk factor for dementia and cognitive decline: meta-analysis of prospective studies. *Am J Geriatr Psychiatry.* (2009) 17:542–55.

20. Lazarus R, Sparrow D, Weiss S. Alcohol intake and insulin levels. The normative aging study. *Am J Epidemiol.* (1997) 145:909–16.

21. Kiechl S, Willeit J, Poewe W, Egger G, Oberhollenzer F, Muggeo M, et al. Insulin sensitivity and regular alcohol consumption: large, prospective, cross sectional population study (bruneck study). *Br Med J.* (1996) 313:1040–4. doi: 10.1136/bmj.313.7064.1040

22. Wu J, Huang M, Zheng F, Sun J, Sun X, Li H, et al. Research progress of healthy baijiu. *J Food Sci Technol.* (2019) 37:17–23.

23. Gronbaek M, Becker U, Johansen D, Gottschau A, Schnohr P, Hein H, et al. Type of alcohol consumed and mortality from all causes, coronary heart disease, and cancer. *Ann Intern Med.* (2000) 133:411–9.

24. Byrne C, Targher G. NAFLD: a multisystem disease. *J Hepatol.* (2015) 62(Suppl. 1):S47–64. doi: 10.1016/j.jhep.2014.12.012

25. Younossi Z, Koenig A, Abdelatif D, Fazel Y, Henry L, Wymer M. Global epidemiology of nonalcoholic fatty liver disease-meta-analytic assessment of prevalence, incidence, and outcomes. *Hepatology.* (2016) 64:73–84. doi: 10.1002/hep.28431

26. Estes C, Razavi H, Loomba R, Younossi Z, Sanyal A. Modeling the epidemic of nonalcoholic fatty liver disease demonstrates an exponential increase in burden of disease. *Hepatology.* (2018) 67:123–33. doi: 10.1002/hep.29466

27. Friedman S, Neuschwander-Tetri B, Rinella M, Sanyal A. Mechanisms of NAFLD development and therapeutic strategies. *Nat Med.* (2018) 24:908–22. doi: 10.1038/s41591-018-0104-9

28. Bagnardi V, Rota M, Botteri E, Tramacere I, Islami F, Fedirko V, et al. Light alcohol drinking and cancer: a meta-analysis. *Ann Oncol.* (2013) 24:301–8. doi: 10.1093/annonc/mds337

29. Ajmera V, Terrault N, Harrison S. Is moderate alcohol use in nonalcoholic fatty liver disease good or bad? A critical review. *Hepatology.* (2017) 65:2090–9. doi: 10.1002/hep.29055

30. Chhimwal J, Patial V, Padwad Y. Beverages and non-alcoholic fatty liver disease (NAFLD): think before you drink. *Clin Nutr.* (2021) 40:2508–19. doi: 10.1016/j.clnu.2021.04.011

31. Liu Y, Zhou L, Gr Y, Zhang H, Li Y, Tang X, et al. Effect of liquors on serum lipid and key enzymes in lipid metabolismof rats. *Mod Prev Med.* (2017) 44:4151–5.

32. Rs Z, Ping Z, Bai XQ, Shi J. The influence of drinking frequency to high-density lipoprotein cholesterol level. *Natl Med Front China.* (2012) 7:95–6.

33. Wu S, Zhang Q, Qi C, Qin T, Tian Q, Jing C, et al. Effect of alcohol consumption on cardio-cerebrovascular events in male diabetic population. *Chin J Hypertens.* (2011) 19:1065–9.

34. Di Ciaula A, Bonfrate L, Krawczyk M, Frühbeck G, Portincasa P. Synergistic and detrimental effects of alcohol intake on progression of liver steatosis. *Int J Mol Sci.* (2022) 23:2636. doi: 10.3390/ijms23052636

35. Idalsoaga F, Kulkarni A, Mousa O, Arrese M, Arab J. Non-alcoholic fatty liver disease and alcohol-related liver disease: two intertwined entities. *Front Med.* (2020) 7:448. doi: 10.3389/fmed.2020.00448

36. Teschke R. Alcoholic liver disease: current mechanistic aspects with focus on their clinical relevance. *Biomedicines.* (2019) 7:8. doi: 10.3390/biomedicines7030068

37. Teschke R. Alcoholic liver disease: alcohol metabolism, cascade of molecular mechanisms, cellular targets, and clinical aspects. *Biomedicines.* (2018) 6:106. doi: 10.3390/biomedicines6040106

38. Teschke R. Alcoholic steatohepatitis (ASH) and alcoholic hepatitis (AH): cascade of events, clinical aspects, and pharmacotherapy options. *Expert Opin Pharmacother.* (2018) 19:779–93. doi: 10.1080/14656566.2018.1465929

39. Ramchandani V. Genetics of alcohol metabolism. In: Watson RR editor. *Alcohol, Nutrition and Health Consequences*. New York, NY: Springer Science (2013) p. 15–25.

40. Chi Y, Lee S, Lai C, Lee Y, Lee S, Chiang C, et al. Ethanol oxidation and the inhibition by drugs in human liver, stomach and small intestine: quantitative assessment with numerical organ modeling of alcohol dehydrogenase isozymes. *Chem Biol Interact.* (2016) 258:134–41. doi: 10.1016/j.cbi.2016.08.014

41. Jones A. Alcohol, its absorption, distribution, metabolism, and excretion in the body and pharmacokinetic calculations. *WIREs Forensic Sci.* (2019) 1:e1340. doi: 10.1002/wfs2.1340

42. Lieber C, DeCarli L, Matsuzaki S, Ohnishi K, Teschke R. The microsomal ethanol oxidizing system (Meos). *Methods Enzyme.* (1978) 52:355–68.

43. Ceni E, Mello T, Galli A. Pathogenesis of alcoholic liver disease: role of oxidative metabolism. *World J Gastroenterol.* (2014) 20:17756–72.

44. Cohen D, Mason K, Farley T. Beer consumption and premature mortality in louisiana: an ecologic analysis. *J Stud Alcohol.* (2004) 65:398–403. doi: 10.15288/jsa.2004.65.398

45. Becker U, Gronbaek M, Johansen D, Sorensen T. Lower risk for alcohol-induced cirrhosis in wine drinkers. *Hepatology.* (2002) 35:868–75. doi: 10.1053/jhep.2002.32101

46. Renaud S, Guéguen R, Siest G, Salamon R. Wine, beer, and mortality in middle-aged men from Eastern France. *Arch Intern Med.* (1999) 159:1865–70. doi: 10.1001/archinte.159.16.1865

47. Sillanaukee P, van der Gaag M, Sierksma A, Hendriks H, Strid N, Pönniö M, et al. Effect of type of alcoholic beverages on carbohydrate-deficient transferrin, sialic acid, and liver enzymes. *Alcohol Clin Exp Res.* (2003) 27:57–60. doi: 10.1097/01.Alc.0000047302.67780.Fa

48. Romeo J, González-Gross M, Wärnberg J, Díaz L, Marcos A. Effects of moderate beer consumption on blood lipid profile in healthy Spanish adults. *Nutr Metab Cardiovasc Dis.* (2008) 18:365–72. doi: 10.1016/j.numecd.2007.03.007

49. Sierksma A, van der Gaag M, Kluft C, Hendriks H. Moderate alcohol consumption reduces plasma c-reactive protein and fibrinogen levels; a randomized, diet-controlled intervention study. *Eur J Clin Nutr.* (2002) 56:1130–6. doi: 10.1038/sj.ejcn.1601459

50. Maldonado M, Moreno H, Calvo J. Melatonin present in beer contributes to increase the levels of melatonin and antioxidant capacity of the human serum. *Clin Nutr.* (2009) 28:188–91. doi: 10.1016/j.clnu.2009.02.001

51. Gorinstein S, Caspi A, Libman I, Leontowicz H, Leontowicz M, Tashma Z, et al. Bioactivity of beer and its influence on human metabolism. *Int J Food Sci Nutr.* (2007) 58:94–107. doi: 10.1080/09637480601108661

52. Gasowski B, Leontowicz M, Leontowicz H, Katrich E, Lojek A, Ciz M, et al. The influence of beer with different antioxidant potential on plasma lipids, plasma antioxidant capacity, and bile excretion of rats fed cholesterol-containing and cholesterol-free diets. *J Nutr Biochem.* (2004) 15:527–33. doi: 10.1016/j.jnutbio.2004.03.004

53. Gonzalez-Munoz M, Meseguer I, Sanchez-Reus M, Schultz A, Olivero R, Benedi J, et al. Beer consumption reduces cerebral oxidation caused by aluminum toxicity by normalizing gene expression of tumor necrotic factor alpha and several antioxidant enzymes. *Food Chem Toxicol.* (2008) 46:1111–8. doi: 10.1016/j.fct.2007.11.006

54. Tung W, Rizzo B, Dabbagh Y, Saraswat S, Romanczyk M, Codorniu-Hernandez E, et al. Polyphenols bind to low density lipoprotein at biologically relevant concentrations that are protective for heart disease. *Arch Biochem Biophys.* (2020) 694:108589. doi: 10.1016/j.abb.2020.108589

55. Shafreen R, Lakshmi S, Pandian S, Park Y, Kim Y, Pasko P, et al. Unraveling the antioxidant, binding and health-protecting properties of phenolic compounds of beers with main human serum proteins: in vitro and in silico approaches. *Molecules.* (2020) 25:4962. doi: 10.3390/molecules25214962

56. Winkler C, Wirleitner B, Schroecksnadel K, Schennach H, Fuchs D. Beer down-regulates activated peripheral blood mononuclear cells in vitro. *Int Immunopharmacol.* (2006) 6:390–5. doi: 10.1016/j.intimp.2005.09.002

57. Osorio-Paz I, Brunauer R, Alavez S. Beer and its non-alcoholic compounds in health and disease. *Crit Rev Food Sci Nutr.* (2020) 60:3492–505. doi: 10.1080/10408398.2019.1696278

58. de Gaetano G, Costanzo S, Di Castelnuovo A, Badimon L, Bejko D, Alkerwi A, et al. Effects of moderate beer consumption on health and disease: a consensus document. *Nutr Metab Cardiovasc Dis.* (2016) 26:443–67. doi: 10.1016/j.numecd.2016.03.007

59. Liu M, Hansen P, Wang G, Qiu L, Dong J, Yin H, et al. Pharmacological profile of xanthohumol, a prenylated flavonoid from hops (*Humulus Lupulus*). *Molecules.* (2015) 20:754–79. doi: 10.3390/molecules20010754

60. Samuels J, Shashidharamurthy R, Rayalam S. Novel anti-obesity effects of beer hops compound xanthohumol: role of AMPK signaling pathway. *Nutr Metab.* (2018) 15:42. doi: 10.1186/s12986-018-0277-8

61. Lima-Fontes M, Costa R, Rodrigues I, Soares R. Xanthohumol restores hepatic glucolipid metabolism balance in type 1 diabetic wistar rats. *J Agric Food Chem.* (2017) 65:7433–9. doi: 10.1021/acs.jafc.7b02595

62. Costa R, Rodrigues I, Guardão L, Rocha-Rodrigues S, Silva C, Magalhães J, et al. Xanthohumol and 8-prenylnaringenin ameliorate diabetic-related metabolic dysfunctions in mice. *J Nutr Biochem.* (2017) 45:39–47. doi: 10.1016/j.jnutbio.2017.03.006

63. Costa R, Negrão R, Valente I, Castela Â, Duarte D, Guardão L, et al. Xanthohumol modulates inflammation, oxidative stress, and angiogenesis in type 1 diabetic rat skin wound healing. *J Nat Prod.* (2013) 76:2047–53. doi: 10.1021/np4002898

64. Ferk F, Huber W, Filipic M, Bichler J, Haslinger E, Misík M, et al. Xanthohumol, a prenylated flavonoid contained in beer, prevents the induction of preneoplastic lesions and DNA damage in liver and colon induced by the heterocyclic aromatic amine amino-3-methyl-imidazo[4,5-F]quinoline (Iq). *Mutat Res.* (2010) 691:17–22. doi: 10.1016/j.mrfmmm.2010.06.006

65. Trius-Soler M, Marhuenda-Munoz M, Laveriano-Santos E, Martinez-Huelamo M, Sasot G, Storniolo C, et al. Moderate consumption of beer (with and without Ethanol) and menopausal symptoms: results from a parallel clinical trial in postmenopausal women. *Nutrients.* (2021) 13:2278. doi: 10.3390/nu13072278

66. Landmann M, Sellmann C, Engstler A, Ziegenhardt D, Jung F, Brombach C, et al. Hops *(Humulus Lupulus*) content in beer modulates effects of beer on the liver after acute ingestion in female mice. *Alcohol Alcohol.* (2017) 52:48–55. doi: 10.1093/alcalc/agw060

67. Hege M, Jung F, Sellmann C, Jin C, Ziegenhardt D, Hellerbrand C, et al. An iso-α-acid-rich extract from hops (*Humulus Lupulus*) attenuates acute alcohol-induced liver steatosis in mice. *Nutrition.* (2018) 45:68–75. doi: 10.1016/j.nut.2017.07.010

68. Renaud S, de Lorgeril M. Wine, alcohol, platelets, and the French paradox for coronary heart disease. *Lancet.* (1992) 339:1523–6. doi: 10.1016/0140-6736(92)91277-f

69. Dunn W, Xu R, Schwimmer J. Modest wine drinking and decreased prevalence of suspected nonalcoholic fatty liver disease. *Hepatology.* (2008) 47:1947–54. doi: 10.1002/hep.22292

70. Mitchell T, Jeffrey G, de Boer B, MacQuillan G, Garas G, Ching H, et al. Type and pattern of alcohol consumption is associated with liver fibrosis in patients with non-alcoholic fatty liver disease. *Am J Gastroenterol.* (2018) 113:1484–93. doi: 10.1038/s41395-018-0133-5

71. Simpson R, Hermon C, Liu B, Green J, Reeves G, Beral V, et al. Alcohol drinking patterns and liver cirrhosis risk: analysis of the prospective UK million women study. *Lancet Public Health.* (2019) 4:e41–8. doi: 10.1016/s2468-2667(18)30230-5

72. Beulens J, van Beers R, Stolk R, Schaafsma G, Hendriks H. The effect of moderate alcohol consumption on fat distribution and adipocytokines. *Obesity.* (2006) 14:60–6. doi: 10.1038/oby.2006.8

73. Rajdl D, Racek J, Trefil L, Siala K. Effect of white wine consumption on oxidative stress markers and homocysteine levels. *Physiol Res.* (2007) 56:203–12. doi: 10.33549/physiolres.930936

74. Kechagias S, Zanjani S, Gjellan S, Leinhard O, Kihlberg J, Smedby O, et al. Effects of moderate red wine consumption on liver fat and blood lipids: a prospective randomized study. *Ann Med.* (2011) 43:545–54. doi: 10.3109/07853890.2011.588246

75. Taborsky M, Ostadal P, Adam T, Moravec O, Gloger V, Schee A, et al. Red or white wine consumption effect on atherosclerosis in healthy individuals (in vino veritas study). *Bratisl Lek Listy.* (2017) 118:292–8. doi: 10.4149/bll_2017_072

76. Gepner Y, Golan R, Harman-Boehm I, Henkin Y, Schwarzfuchs D, Shelef I, et al. Effects of initiating moderate alcohol intake on cardiometabolic risk in adults with type 2 diabetes: a 2-year randomized controlled trial. *Ann Intern Med.* (2015) 163:569–79. doi: 10.7326/m14-1650

77. Miltonprabu S, Tomczyk M, Skalicka-Woźniak K, Rastrelli L, Daglia M, Nabavi S, et al. Hepatoprotective effect of quercetin: from chemistry to medicine. *Food Chem Toxicol.* (2017) 108(Pt B):365–74. doi: 10.1016/j.fct.2016.08.034

78. Auger C, Teissedre P, Gérain P, Lequeux N, Bornet A, Serisier S, et al. Dietary wine phenolics catechin, quercetin, and resveratrol efficiently protect

hypercholesterolemic hamsters against aortic fatty streak accumulation. *J Agric Food Chem.* (2005) 53:2015–21. doi: 10.1021/jf048177q

79. Rivero-Pérez M, Muñiz P, González-Sanjosé M. Contribution of anthocyanin fraction to the antioxidant properties of wine. *Food Chem Toxicol.* (2008) 46:2815–22. doi: 10.1016/j.fct.2008.05.014

80. Forester S, Waterhouse A. Metabolites are key to understanding health effects of wine polyphenolics. *J Nutr.* (2009) 139:1824S–31S. doi: 10.3945/jn.109.107664

81. Di Lorenzo C, Colombo F, Biella S, Stockley C, Restani P. Polyphenols and human health: the role of bioavailability. *Nutrients.* (2021) 13:273. doi: 10.3390/nu13010273

82. Bedê T, de Jesus V, Rosse de Souza V, Mattoso V, Abreu J, Dias J, et al. Effect of grape juice, red wine and resveratrol solution on antioxidant, anti-inflammatory, hepactic function and lipid profile in rats feds with high-fat diet. *Nat Prod Res.* (2020) 35:5255–60. doi: 10.1080/14786419.2020.1747458

83. Silva P, Fernandes E, Carvalho F. Dual effect of red wine on liver redox status: a concise and mechanistic review. *Arch Toxicol.* (2015) 89:1681–93. doi: 10.1007/s00204-015-1538-1

84. López-Vélez M, Martínez-Martínez F, Del Valle-Ribes C. The study of phenolic compounds as natural antioxidants in wine. *Crit Rev Food Sci Nutr.* (2003) 43:233–44. doi: 10.1080/10408690390826509

85. Cai Y, Fang J, Ma L, Yang L, Liu Z. Inhibition of free radical-induced peroxidation of rat liver microsomes by resveratrol and its analogues. *Biochim Biophys Acta.* (2003) 1637:31–8. doi: 10.1016/S0925-4439(02)00174-6

86. Gülçin I. Antioxidant properties of resveratrol: a structure–activity insight. *Innov Food Sci Emerg Technol.* (2010) 11:210–8. doi: 10.1016/j.ifset.2009.07.002

87. Yang H, Lee M, Kim Y. Protective activities of stilbene glycosides from acer mono leaves against h2o2-induced oxidative damage in primary cultured rat hepatocytes. *J Agric Food Chem.* (2005) 53:4182–6. doi: 10.1021/jf050093

88. Kasdallah-Grissa A, Mornagui B, Aouani E, Hammami M, El May M, Gharbi N, et al. Resveratrol, a red wine polyphenol, attenuates ethanol-induced oxidative stress in rat liver. *Life Sci.* (2007) 80:1033–9. doi: 10.1016/j.lfs.2006.11.044

89. Bujanda L, Hijona E, Larzabal M, Beraza M, Aldazabal P, García-Urkia N, et al. Resveratrol inhibits nonalcoholic fatty liver disease in rats. *BMC Gastroenterol.* (2008) 8:40. doi: 10.1186/1471-230X-8-40

90. Hassan-Khabbar S, Vamy M, Cottart C, Wendum D, Vibert F, Savouret J, et al. Protective effect of post-ischemic treatment with trans-resveratrol on cytokine production and neutrophil recruitment by rat liver. *Biochimie.* (2010) 92:405–10. doi: 10.1016/j.biochi.2009.12.009

91. Ajmo J, Liang X, Rogers C, Pennock B, You M. Resveratrol alleviates alcoholic fatty liver in mice. *Am J Physiol Gastrointest Liver Physiol.* (2008) 295:G833–42. doi: 10.1152/ajpgi.90358.2008

92. Tang L, Yang F, Fang Z, Hu C. Resveratrol ameliorates alcoholic fatty liver by inducing autophagy. *Am J Chin Med.* (2016) 44:1207–20. doi: 10.1142/s0192415x16500671

93. Jeon B, Jeong E, Shin H, Lee Y, Lee D, Kim H, et al. Resveratrol attenuates obesity-associated peripheral and central inflammation and improves memory deficit in mice fed a high-fat diet. *Diabetes.* (2012) 61:1444–54. doi: 10.2337/db11-1498

94. Chan C, Lee K, Huang Y, Chou C, Lin H, Lee F. Regulation by resveratrol of the cellular factors mediating liver damage and regeneration after acute toxic liver injury. *J Gastroenterol Hepatol.* (2014) 29:603–13. doi: 10.1111/jgh.12366

95. Li L, Hai J, Li Z, Zhang Y, Peng H, Li K, et al. Resveratrol modulates autophagy and nf-κb activity in a murine model for treating non-alcoholic fatty liver disease. *Food Chem Toxicol.* (2014) 63:166–73. doi: 10.1016/j.fct.2013.08.036

96. Zhang D, Lu H, Li J, Shi X, Huang C. Essential roles of ERKS and P38k in up-regulation of GST A1 expression by maotai content in human hepatoma cell line Hep3b. *Mol Cell Biochem.* (2006) 293:161–71. doi: 10.1007/s11010-006-9238-z

97. Yi X, Long L, Yang C, Lu Y, Cheng M. Maotai ameliorates diethylnitrosamine-initiated hepatocellular carcinoma formation in mice. *PLoS One.* (2014) 9:e93599. doi: 10.1371/journal.pone.0093599

98. Liu J, Cheng M, Shi J, Yang Q, Wu J, Li C, et al. Differential effects between maotai and ethanol on hepatic geneexpression in mice: possible role of metallothionein and heme oxygenase-1 induction by maotai. *Exp Biol Med.* (2006) 231:1535–41. doi: 10.1177/153537020623100913

99. Wu J, Huo J, Huang M, Zhao M, Luo X, Sun B. Structural characterization of a tetrapeptide from sesame flavor-type baijiu and its preventive effects against aaph-induced oxidative stress in Hepg2 cells. *J Agric Food Chem.* (2017) 65:10495–504. doi: 10.1021/acs.jafc.7b04815

100. Fang C, Du H, Zheng X, Zhao A, Jia W, Xu Y. Solid-state fermented Chinese alcoholic beverage (baijiu) and ethanol resulted in distinct metabolic and microbiome responses. *FASEB J.* (2019) 33:7274–88. doi: 10.1096/fj.201802306R

101. Fang C, Zhou Q, Liu Q, Jia W, Xu Y. Crosstalk between gut microbiota and host lipid metabolism in a mouse model of alcoholic liver injury by chronic baijiu or ethanol feeding. *Food Funct.* (2022) 13:596–608. doi: 10.1039/d1fo02892h

102. Rehm J, Mathers C, Popova S, Thavorncharoensap M, Teerawattananon Y, Patra J. Global burden of disease and injury and economic cost attributable to alcohol use and alcohol-use disorders. *Lancet.* (2009) 373:2223–33.

103. Rimm E, Klatsky A, Grobbee D, Stampfer M. Review of moderate alcohol consumption and reduced risk of coronary heart disease: is the effect due to beer, wine, or spirits. *Br Med J.* (1996) 312:731–6.

104. Thelle D. Alcohol and heart health: the need for a randomized controlled trial. *Eur J Prev Cardiol.* (2020) 27:1964–6. doi: 10.1177/2047487320914433

105. Visioli F, Lastra C, Andres-Lacueva C, Aviram M, Calhau C, Cassano A, et al. Polyphenols and human health: a prospectus. *Crit Rev Food Sci Nutr.* (2011) 51:524–46.

106. Liu H, Sun B. Effect of fermentation processing on the flavor of baijiu. *J Agric Food Chem.* (2018) 66:5425–32. doi: 10.1021/acs.jafc.8b00692

107. Kumar N, Goel N. Phenolic acids: natural versatile molecules with promising therapeutic applications. *Biotechnol Rep.* (2019) 24:e00370. doi: 10.1016/j.btre.2019.e00370

108. Wu T, Zhu S, Sun X, Zhao W, Cui G. Analysis of health factors of meilanchun sesame-flavor liquor. *Liquor Making Sci Technol.* (2013) 8:125–30.

109. Yao F, Yi B, Shen C, Tao F, Liu Y, Lin Z, et al. Chemical analysis of the Chinese liquor luzhoulaojiao by comprehensive two-dimensional gas chromatography/time-of-flight mass spectrometry. *Sci Rep.* (2015) 5:9553. doi: 10.1038/srep09553

110. Budak N, Aykin E, Seydim A, Greene A, Guzel-Seydim Z. Functional properties of vinegar. *J Food Sci.* (2014) 79:R757–64. doi: 10.1111/1750-3841.12434

111. Saini R, Keum Y. Omega-3 and omega-6 polyunsaturated fatty acids: dietary sources, metabolism, and significance - A review. *Life Sci.* (2018) 203:255–67. doi: 10.1016/j.lfs.2018.04.049

112. Zhou H, Xin-Yan Y, Yu W, Liang X, Du X, Liu Z, et al. Lactic acid in macrophage polarization: the significant role in inflammation and cancer. *Int Rev Immunol.* (2022) 41:4–18. doi: 10.1080/08830185.2021.1955876

113. Stilling R, van de Wouw M, Clarke G, Stanton C, Dinan T, Cryan J. The neuropharmacology of butyrate: the bread and butter of the microbiota-gut-brain axis? *Neurochem Int.* (2016) 99:110–32. doi: 10.1016/j.neuint.2016.06.011

114. Chi Z, Wang Z, Wang G, Khan I, Chi Z. Microbial biosynthesis and secretion of l-malic acid and its applications. *Crit Rev Biotechnol.* (2016) 36:99–107. doi: 10.3109/07388551.2014.924474

115. Ge H, Lin P, Luo T, Yan Z, Xiao J, Miao S, et al. Fabrication of ligusticum chuanxiong polylactic acid microspheres: a promising way to enhance the hepatoprotective effect on bioactive ingredients. *Food Chem.* (2020) 317:126377. doi: 10.1016/j.foodchem.2020.126377

116. Mo Z, Liu Y, Li C, Xu L, Wen L, Xian Y, et al. Protective effect of SFE-Co2 of ligusticum chuanxiong hort against d-galactose-induced injury in the mouse liver and kidney. *Rejuvenation Res.* (2017) 20:231–43. doi: 10.1089/rej.2016.1870

117. Xu Y, Zhao J, Liu X, Zhang C, Zhao Z, Li X, et al. Flavor mystery of Chinese traditional fermented baijiu: the great contribution of ester compounds. *Food Chem.* (2022) 369:130920. doi: 10.1016/j.foodchem.2021.130920

118. Fang C, Du H, Jia W, Xu Y. Compositional differences and similarities between typical Chinese baijiu and western liquor as revealed by mass spectrometry-based metabolomics. *Metabolites.* (2018) 9:2. doi: 10.3390/metabo9010002

119. Spitalniak-Bajerska K, Szumny A, Pogoda-Sewerniak K, Kupczynski R. Effects of N-3 fatty acids on growth, antioxidant status, and immunity of preweaned dairy calves. *J Dairy Sci.* (2020) 103:2864–76. doi: 10.3168/jds.2019-17001

120. Kiyama R. Estrogenic terpenes and terpenoids: pathways, functions and applications. *Eur J Pharmacol.* (2017) 815:405–15. doi: 10.1016/j.ejphar.2017.09.049

121. Chow P, Kourghi M, Pei J, Nourmohammadi S, Yool A. 5-Hydroxymethyl-furfural and structurally related compounds block the ion conductance in human aquaporin-1 channels and slow cancer cell migration and invasion. *Mol Pharmacol.* (2020) 98:38–48. doi: 10.1124/mol.119.119172

122. Lin N, Liu T, Lin L, Lin S, Zang Q, He J, et al. Comparison of in vivo immunomodulatory effects of 5-hydroxymethylfurfural and 5, 5'-oxydimethylenebis (2-furfural). *Regul Toxicol Pharmacol.* (2016) 81:500–11. doi: 10.1016/j.yrtph.2016.10.008

123. Li W, Qu X, Han Y, Zheng S, Wang J, Wang Y. Ameliorative effects of 5-hydroxymethyl-2-furfural (5-hmf) from Schisandra chinensis on alcoholic liver oxidative injury in mice. *Int J Mol Sci.* (2015) 16:2446–57. doi: 10.3390/ijms16022446

124. Zhang R, Wu Q, Xu Y, Qian M. Isolation, identification, and quantification of lichenysin, a novel nonvolatile compound in Chinese distilled spirits. *J Food Sci.* (2014) 79:C1907–15. doi: 10.1111/1750-3841.12650

125. Grangemard I, Wallach J, Maget-Dana R, Peypoux F. Lichenysin: a more efficient cation chelator than surfactin. *Appl Biochem Biotechnol.* (2001) 90:199–210. doi: 10.1385/abab:90:3:199

126. Galie S, Garcia-Gutierrez C, Miguelez E, Villar C, Lombo F. Biofilms in the food industry: health aspects and control methods. *Front Microbiol.* (2018) 9:898. doi: 10.3389/fmicb.2018.00898

127. Wu J, Sun B, Luo X, Zhao M, Zheng F, Sun J, et al. Cytoprotective effects of a tripeptide from Chinese baijiu against aaph-induced oxidative stress in Hepg2 Cells Via NRF2 Signaling. *RSC Adv.* (2018) 8:10898–906. doi: 10.1039/c8ra01162a

128. Molina P, Nelson S. Binge drinking's effects on the body. *Alcohol Res.* (2018) 39:99–109.

frontiers | Frontiers in Nutrition

TYPE Original Research
PUBLISHED 25 January 2023
DOI 10.3389/fnut.2022.1035623

OPEN ACCESS

EDITED BY
Yanyan Zhang,
University of Hohenheim, Germany

REVIEWED BY
Pınar Kadiroğlu Kelebek,
Adana Alparslan Turkes Science and Technology University, Türkiye
Majid Mohammadhosseini,
Islamic Azad University, Shahrood, Iran

*CORRESPONDENCE
Fangzhou Yin
✉ yinfangzhou@njucm.edu.cn
Lin Li
✉ lilin@njucm.edu.cn
Wu Yin
✉ wyin@nju.edu.cn

SPECIALTY SECTION
This article was submitted to Food Chemistry, a section of the journal Frontiers in Nutrition

RECEIVED 03 September 2022
ACCEPTED 13 December 2022
PUBLISHED 25 January 2023

CITATION
Fei C, Xue Q, Li W, Xu Y, Mou L, Li W, Lu T, Yin W, Li L and Yin F (2023) Variations in volatile flavour compounds in *Crataegi* fructus roasting revealed by E-nose and HS-GC-MS. *Front. Nutr.* 9:1035623. doi: 10.3389/fnut.2022.1035623

Variations in volatile flavour compounds in *Crataegi* fructus roasting revealed by E-nose and HS-GC-MS

Chenghao Fei[1], Qianqian Xue[1], Wenjing Li[1], Yan Xu[1], Liyan Mou[1], Weidong Li[1], Tulin Lu[1], Wu Yin[2]*, Lin Li[1]* and Fangzhou Yin[1]*

[1]School of Pharmacy, Nanjing University of Chinese Medicine, Nanjing, China, [2]State Key Laboratory of Pharmaceutical Biotechnology, College of Life Sciences, Nanjing University, Nanjing, China

Introduction: *Crataegi* fructus (CF) is an edible and medicinal functional food used worldwide that enhances digestion if consumed in the roasted form. The odour of CF, as a measure of processing degree during roasting, significantly changes. However, the changes remain unclear, but are worth exploring.

Methods: Herein, the variations in volatile flavour compounds due to CF roasting were investigated using an electronic nose (E-nose) and headspace gas chromatography–mass spectrometry (HS-GC-MS).

Results: A total of 54 components were identified by GC-MS. Aldehydes, ketones, esters, and furans showed the most significant changes. The Maillard reaction, Strecker degradation, and fatty acid oxidation and degradation are the main reactions that occur during roasting. The results of grey relational analysis (GRA) showed that 25 volatile compounds were closely related to odour ($r > 0.9$). Finally, 9 volatile components [relative odour activity value, (ROAV) ≥ 1] were confirmed as key substances causing odour changes.

Discussion: This study not only achieves the objectification of odour evaluation during food processing, but also verifies the applicability and similarity of the E-nose and HS-GC-MS.

KEYWORDS

***Crataegi* fructus, E-nose, HS-GC-MS, roasting, volatile flavour compounds**

1. Introduction

Food processing converts normally inedible raw materials into edible, safe, and nutritious foods and plays an important role in food preservation and biotransformation (1). Food processing technology has evolved over thousands of years, from roasting meat over the fire approximately 1.8 million years ago, to current methods including cooking, preservation using heat, pickling, fermenting, freezing, and drying (2). In particular, roasting is widely used processing methods, wherein the temperature and time are critical factors (3). Many foods are processed by roasting, including coffee, tea, peanuts,

and barley (4, 5). Food processing by various methods induces changes in physical properties and is often accompanied by biochemical reactions (6). The complexity of food processing methods introduces new challenges for food quality evaluation.

Food flavours generally change during processing and the composition of volatile components is key to food flavour, actively affecting its overall evaluation (7). As an example, volatile components of fish (ammonia, indole, histamine, trimethylamine, and ammonia sulphide) can be used as indicators for detecting changes in freshness (8). It has been reported that the odour is directly related to the presence of volatile substances (9, 10). However, the judgment of food odour depends on human olfactory sensation, which is subjective and affected by the environment and the physical condition of the human, resulting in poor repeatability (11). With continuous technological developments, precise analytical instruments are gradually being developed for the study of food odour. The electronic nose (E-nose) is an odour detection technology that simulates the human olfactory system and provides low-cost and rapid sensory information for process monitoring and quality control during food production (12). Advantages of the E-nose include its rapid, sensitive, and non-destructive sample identification that objectively reflects the tested samples. Although the overall information regarding volatile flavour substances can be analysed by the E-nose, specific information on volatile components cannot be obtained. Headspace gas chromatography-mass spectrometry (HS-GC-MS) is commonly used for qualitative and quantitative analysis of volatile components (13, 14). It integrates the safety, accuracy, and high separation ability of GC with the superiority of MS for substance identification. Compared to the E-nose, GC-MS can provide detailed and accurate information regarding volatile flavour components (15). However, online sample monitoring is difficult due to high cost and long cycle for analysis. The E-nose and GC-MS can be used for quality control, fresh grading, and authenticity determination for fruits, vegetables, meat, cereals, beverages, and other products (16, 17). Although the combined use of the E-nose and GC-MS has been reported, odour characterisation by both methods is relatively independent, and their internal correlation has not been reported, meriting further exploration.

Crataegi fructus (CF) is harvested from plants of the genus *Crataegus*, belonging to the family Rosaceae. It is cultivated globally in regions including Asia, Europe, and North America (18). Previous studies have shown that CF has a variety of physiological functions, including digestion promotion, reducing blood lipid levels, and antibacterial activity (19, 20). CF has long been used as a traditional dual-purpose material for medicine and functional foods worldwide. Generally, fresh CF can be eaten, but it is often sliced and dried for preservation. In China, dried CF is further roasted to prevent gastrointestinal irritation caused by acidity, with three different processed products formed by roasting (21). Chao *Crataegi* fructus (CCF), whose fruity aroma decreases after roasting CF for a period of time, can promote digestion. Jiao *Crataegi* fructus (JCF), whose roasting time is longer than that for CCF and has a burnt aroma, promotes digestion and treats diarrhoea. Tan *Crataegi* fructus (TCF), whose roasting time is the longest and exhibits a charcoal-like odour, promotes haemostasis and treats diarrhoea. Therefore, during roasting, CF odours significantly change, and its sour flavour gradually diminishes, while the coke odour is enhanced. The odour changes, which are considered an intrinsic property of the fruit, indicates a change in its internal components. Previously, we established an odour detection method for CF based on the E-nose and identified differently processed CFs for the first time (22). Nevertheless, it only focused on the qualitative odour of the final products, as most of the related literature, and the detailed changes in volatile flavour substances remain unknown.

Hence, to comprehensively, reliably, and scientifically identify odour changes in CF during roasting, the E-nose and HS-GC-MS were used herein. Based on grey relational analysis (GRA) and the relative odour activity value (ROAV), a method that tracks and detects changes in volatile flavour compounds during CF roasting, was established. Taken together, these methods comprehensively and objectively reflect the changes in volatile flavour substances. The entire experimental flowchart is shown in **Supplementary Figure 1**.

2. Materials and methods

2.1. Sample collection and preparation

The dried CF slices were collected from Shandong of China, and the sample was roasted using CGD-750 drum roaster (Hangzhou Haishan Pharmaceutical Equipment Co., Ltd., Zhejiang, China). After the drum roaster was preheated to 200°C, the CF pieces were put into the drum roaster and roasted for 24 min. Samples were taken every 2 min. During roasting, the temperature of CF was controlled below 200°C, as monitored by infrared thermometer. Finally, 13 samples, including the original sample (S1) and 12 roasted samples (S2–S13) were obtained for further analysis. The profile of S1–13 sample are shown in **Supplementary Figure 2**. All the samples were pulverized and sieved (50 mesh), then the powder of the samples was sealed before analysis.

Abbreviations: CF, *Crataegi* fructus; E-nose, electronic nose; HS-GC-MS, headspace gas chromatography–mass spectrometry; GRA, grey relational analysis; CCF, Chao *Crataegi* fructus; JCF, Jiao *Crataegi* fructus; TCF, Tan *Crataegi* fructus; ROAV, relative odour activity value; TIC, total ion chromatogram; HCA, hierarchical cluster analysis; PCA, principal component analysis.

2.2. E-nose analysis

The E-nose analyses were conducted using a commercial Fox-4000 electronic nose (Alpha M.O.S., Toulouse, France). The structure of E-nose consists of HS-100 autosampler, sensor array units and pattern recognition system (Alpha Soft V11.0). The sensor array is composed of 18 metal oxide semiconductors as follows: LY2/LG, LY2/G, LY2/AA, LY2/GH, LY2/gCT, LY2/gCT, T30/1, P10/1, P10/2, P40/1, T70/2, PA/2, P30/1, P40/2, P30/2, T40/2, T40/1, and TA/2. The characteristics of sensors are described in **Supplementary Table 1**.

E-nose analysis was carried out by the method as we previously described (22). The CF samples (0.5 g) were accurately weighed and placed in 10-ml vials. Each sample was incubated at a temperature of 55°C for 600 s, then 1200 μl of the headspace air was injected into the testing chamber. The response curves were generated based on the response values acquired from 18 sensors within 120 s. Each sample was analysed in triplicate.

2.3. HS-GC-MS analysis

The GC-MS analysis was performed on an Agilent GC 7890B-MS 7000C (Agilent Technologies, Palo Alto, CA, USA) coupled with a 7697A headspace sampler. The sample (1.5 g) was put into 10-ml headspace vials for detection. The standard of C7–C30 saturated alkanes was provided by Sigma-Aldrich (St. Louis, MO, USA). The GC-MS analysis was referred to the published protocol with minor modifications (23).

(1) HS conditions: Equilibrium temperature and time were set at 80°C and 30 min, respectively. Loop temperature and transmission line were set at 95°C and 110°C, respectively. Oscillation frequency was set at 250 times/min. Filling pressure was set at 15 psi. Pressurization time and injection time was set at 0.1 and 0.5 min, respectively. The flow rate was maintained at 1.00 ml/min. The injection volume was 1,000 μl.

(2) GC conditions: The compounds were separated on a HP-INNOWAX capillary column (30 m × 250 μm, 0.25 μm). The injection port temperature was at 220°C in the split mode (5:1). Gasification chamber temperature was kept at 280°C. The oven temperature was programmed as follows: initial temperature was set at 40°C, ramped up to 65°C at 5°C/min, ramped up to 90°C at 10°C/min, ramped up to 110°C at 2°C/min, maintained isothermal for 10 min, then ramped up to 165°C at 5°C/min, ramped up to 260°C at 10°C/min, maintained isothermal for 5 min.

(3) MS conditions: EI source was selected. The ionization temperature was set at 230°C and mass spectra were obtained by electron energy at 70 eV. Temperature of quadrupole and detector interface were 270 and 150°C, respectively. Multiplier voltage was set at 1557.3 V and mass scan range was 45–500 amu.

The mass spectra of volatiles detected from samples were compared with those from NIST14 (National Institute of Standards and Technology, Gaithersburg, MD, USA). Based on the MS match factor (similarity > 750) and retention index (RI), each volatile compound was identified. Each sample was analysed in triplicate.

Relative odour activity value was calculated to measure the contribution of each volatile component to the aroma profile according to the method as previously described (24). The equation is as follows:

$$ROAV_i = 100 \times \frac{C_i}{C_{max}} \times \frac{T_{max}}{T_i}$$

where C_i and T_i indicate relative percentage content of each volatile component and the corresponding odour threshold (OT), respectively. C_{max} and T_{max} indicate relative percentage content of the volatile component that contributed the most to the flavor and the corresponding OT, respectively. The compounds with $0.1 \leq \text{ROAV} < 1$ modified the aroma profile, while the compounds with $\text{ROAV} \geq 1$ were regarded as the key volatile components.

2.4. Statistical analysis

Principal component analysis (PCA) was performed with SIMCA-P 14.1 (Umetrics AB, Umea, Sweden). The heatmap was conducted using TBtools.[1] Gray relational analysis was performed on DPS 7.05 software (Hangzhou Ruifeng Information Technology Co., Ltd., Zhejiang, China).

The basic idea of GRA is to investigate the correlation between two sets of variations (24). In this study, GRA was applied to find out the relationships between E-nose sensor responses of samples and their corresponding peak areas of volatile compounds gained by HS-GC-MS at different time-points during the processing. The specific method is as follows: Set $A_i = \{a_i(k) | k = 1, 2,..., n\} = (a_i(1), a_i(2),..., a_i(n))$ as the sequence of system behaviour characteristics. Set $P_i = \{p_i(k) | k = 1, 2,..., n\} = (p_i(1), p_i(2),..., p_i(n))$ as the sequence of system associated factors. In this study, A_i and P_i represents the data from E-nose and GC-MS, respectively. And k refers to the different time-point. Then, the correlation coefficient (ξ) is defined as follows:

$$\xi\left(a_i(k), p_i(k)\right) = \frac{\min\limits_i \min\limits_k \left|a_i(k) - p_i(k)\right| + \rho \max\limits_i \max\limits_k \left|a_i(k) - p_i(k)\right|}{\left|a_i(k) - p_i(k)\right| + \rho \max\limits_i \max\limits_k \left|a_i(k) - p_i(k)\right|}$$

1 http://www.tbtools.com/

ρ is the distinctive coefficient lying between 0 and 1, and it is generally set as 0.5.

The grey correlation degree (r_i) is the arithmetic mean of the correlation coefficient at different time-points, and is formulated as follows:

$$r_i = \xi(A_i, P_i) = \frac{1}{n}\sum_{k=1}^{n} \xi\left(a_i(k), p_i(k)\right)$$

The higher the value of r_i is, the closer the sequence of associate factors to the behaviour characteristics would be.

3. Results and discussion

3.1. Sensory evaluation of roasted CF

With extended heating time and increased CF temperature, the fruity aroma of CF gradually diminished, and a burnt aroma became increasingly dominant, resulting in only a charcoal-like odour remained. Based on colour and odour judgment by experienced personnel, among the 13 obtained samples, S4 and S5 (sample temperature of approximately 100°C after roasting for 6 min) were determined to be CCF, S7 and S8 (sample temperature of approximately 130°C after roasting for 12 min) were assigned to JCF, and S13 (sample temperature of approximately 170°C after roasting for 24 min) was determined to be TCF. Corresponding images of the products are shown in **Supplementary Figure 2**.

3.2. E-nose analysis

The volatile flavour characteristics of CF were comprehensively analysed using the E-nose. The sensor responses were influenced by the volatile component composition and their proportions. Representative E-nose sensor-intensity curves are shown in **Figure 1A**. Within 120 s, the sensor response values of LY2/G, LY2/AA, LY2/GH, LY2/gCTl, and LY2/gCT were negative due to gas oxidation on those sensors being the dominant reaction over reduction. In contrast, the response of the other sensors were positive because the gas reduction was dominant. Typically, a minimum relative standard deviation can be established for the peak or valley data in the same sample curve, allowing a maximum response value for each sensor to be extracted for further analysis. As shown in **Figure 1B**, the maximum response of most sensors when exposed to CF samples during roasting changed similarly, i.e., they initially increased and subsequently decreased. The highest response usually occurred at S10–S12. Notably, T40/1 and T40/2 were the only two sensors for which the maximum response decreased during this period. A total of 8 sensors showed higher response values (> 0.4), indicating higher sensitivity to the CF odour. In addition, as shown in **Figure 1C**, significant differences were observed for S1, S4–S5, S7–S8, and S13, indicating a noticeable alteration in the volatile compounds in CF during roasting. These differences can be attributed to the formation of novel or changes in existing volatile concentrations over time.

The above results suggest that the total concentration of volatile flavour substances during CF roasting initially increased and subsequently decreased. It was necessary to further analyse the changes of these substances during this period.

3.3. HS-GC-MS analysis

3.3.1. Sum of peak areas of volatile components

To explore the volatile flavour characteristics of CF at different roasting stages and their relationship with processing, HS-GC-MS was performed to analyse the volatile substances in the samples. The summed peak areas of the volatile components in CF at different roasting times are shown in **Supplementary Figure 3**. With prolonged roasting, the total amount of volatile components in the samples initially increased and subsequently decreased, as consistent with the sensor response trends obtained using the E-nose. When the roasting time was $\leq$ 4 min and the sample surface temperature was $<$ 100°C, the total amount of volatile components did not change significantly. However, when the surface temperature exceeded 100°C, the total amount of volatile components increased rapidly, indicating that the volatile components could only be completely released at $>$ 100°C. Furthermore, the sum of the peak areas of the volatile components reached a maximum in S9 and S10 (roasting times of 16–18 min), implying that numerous substances increased in content or formed during this stage.

3.3.2. Identification of volatile components in CF during roasting

The total ion chromatogram (TIC) curves of the volatile components during roasting are shown in **Figure 2A**. Overall, 57 chromatographic peaks were detected and marked in **Figure 2B**. A total of 54 volatile compounds were identified using the MS and RI database. Based on this analysis, 14 common compounds were found in 13 samples, which were hexanal, furfural, acetone, 2,3-butanedione, 4-methyl-2-pentanone, ethanol, acetic acid, methyl formate, dimethyl ether, limonene, 1-methyl-4-(1-methylethylidene)-cyclohexene, toluene, *o*-cymene, and 2-methyl-furan. In addition, compared to the original sample (S1), 19 novel compounds were produced during roasting, of which 12 were produced at 4 min and then disappeared at 22 min, and the other 9 compounds disappeared. The volatile compounds are listed in **Table 1** and the peak areas for the 13 samples are listed in **Supplementary Table 2**. Considering their chemical properties, the volatile compounds were divided into 9 categories that included 8 aldehydes, 14

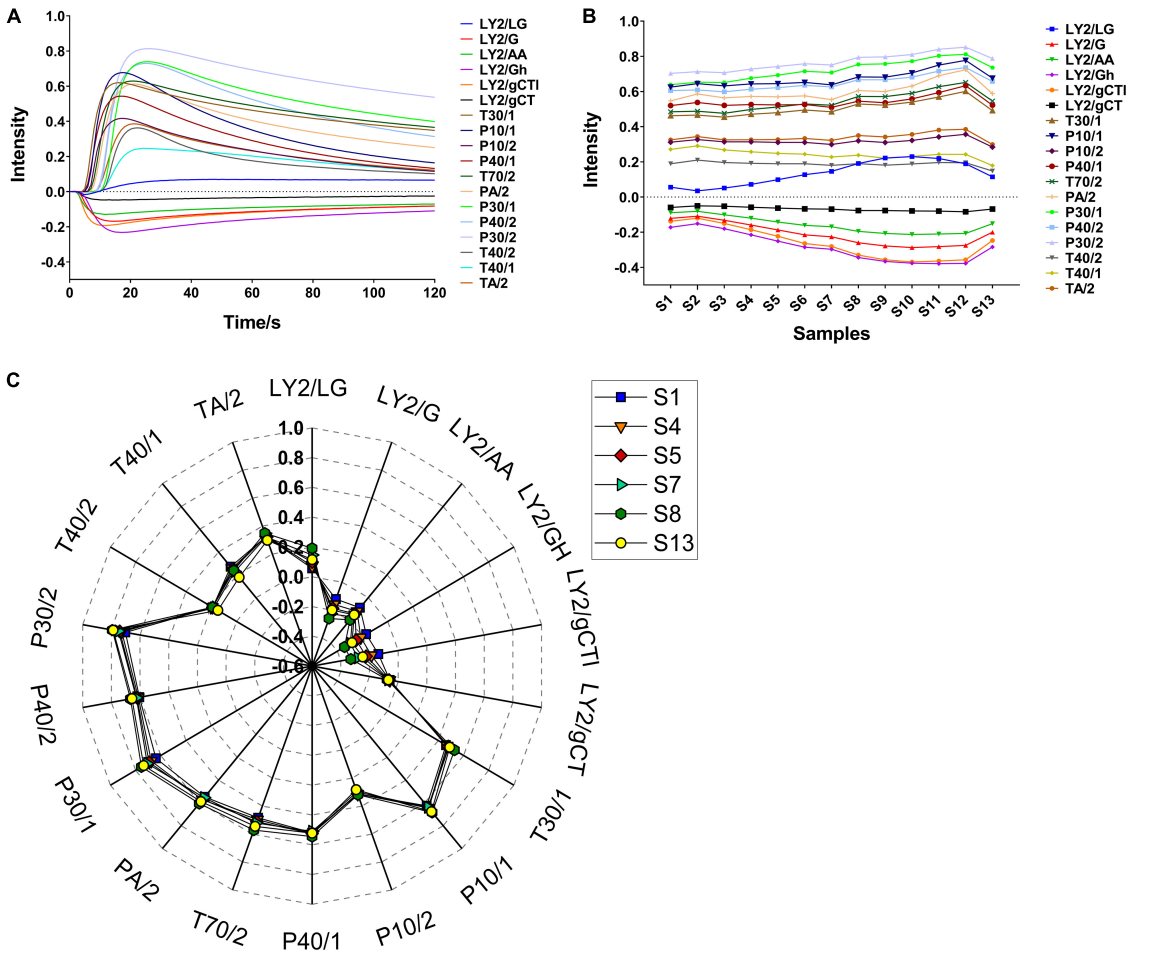

FIGURE 1
Typical plots of E-nose in CF roasting process. **(A)** Sensor intensity curves in S1; **(B)** the change of the maximum response value of all samples; **(C)** radar fingerprint chart of maximum sensor response on typical samples.

ketones, 6 alcohols, 3 acids, 6 esters, 2 ethers, 7 hydrocarbons, 4 arenes, and 4 furans. The relative percentage accumulation diagram is shown in Figure 2C. Aldehydes, ketones, esters, and furans accounted for a large proportion of the volatile components, and significantly contributed to the CF flavour.

To further examine the similarities and differences among the samples during different roasting stages, hierarchical cluster analysis (HCA) was performed using Ward's clustering method. As shown in Figure 2D, when the distance is 50, the 13 samples can be divided into Group I (S1 and S2), Group II (S3, S4, and S5), Group III (S6, S7, and S8), Group IV (S9, S10, S11, and S12), and Group V (S13). The samples in Group I were abundant in esters, accounting for ≥ 50% of the total volatiles. In addition, the proportion of volatile compounds changed considerably in the Group V samples, where the esters reduced to 4%, while furans, aldehydes, and ketones accounted for 36, 18, and 18%, respectively. Furthermore, the samples in Groups II, III, and IV contained similar volatile substance compositions, where aldehydes accounted for the highest proportion and reached≥ 70% in Groups III and IV.

3.3.3. Comprehensive analysis of volatile components

3.3.3.1. Aldehydes

The 8 aldehydes detected showed high contents and significant changes, and were considered to be the main components that caused flavour changes during CF roasting. 2-methyl-butanal, nonanal, 5-methyl-2-furancarboxaldehyde, 5-acetoxymethyl-2-furaldehyde, and 5-hydroxymethylfurfural are the newly produced aldehydes in this roasting process. With increasing roasting time, the contents of hexanal and benzaldehyde decreased sharply, while the content of other aldehydes initially increased and subsequently decreased. It was reported that CF could promote digestion after roasting due to the increased content of 2-methyl-butanal, 5-hydroxymethylfurfural and furfural (25–27), and our

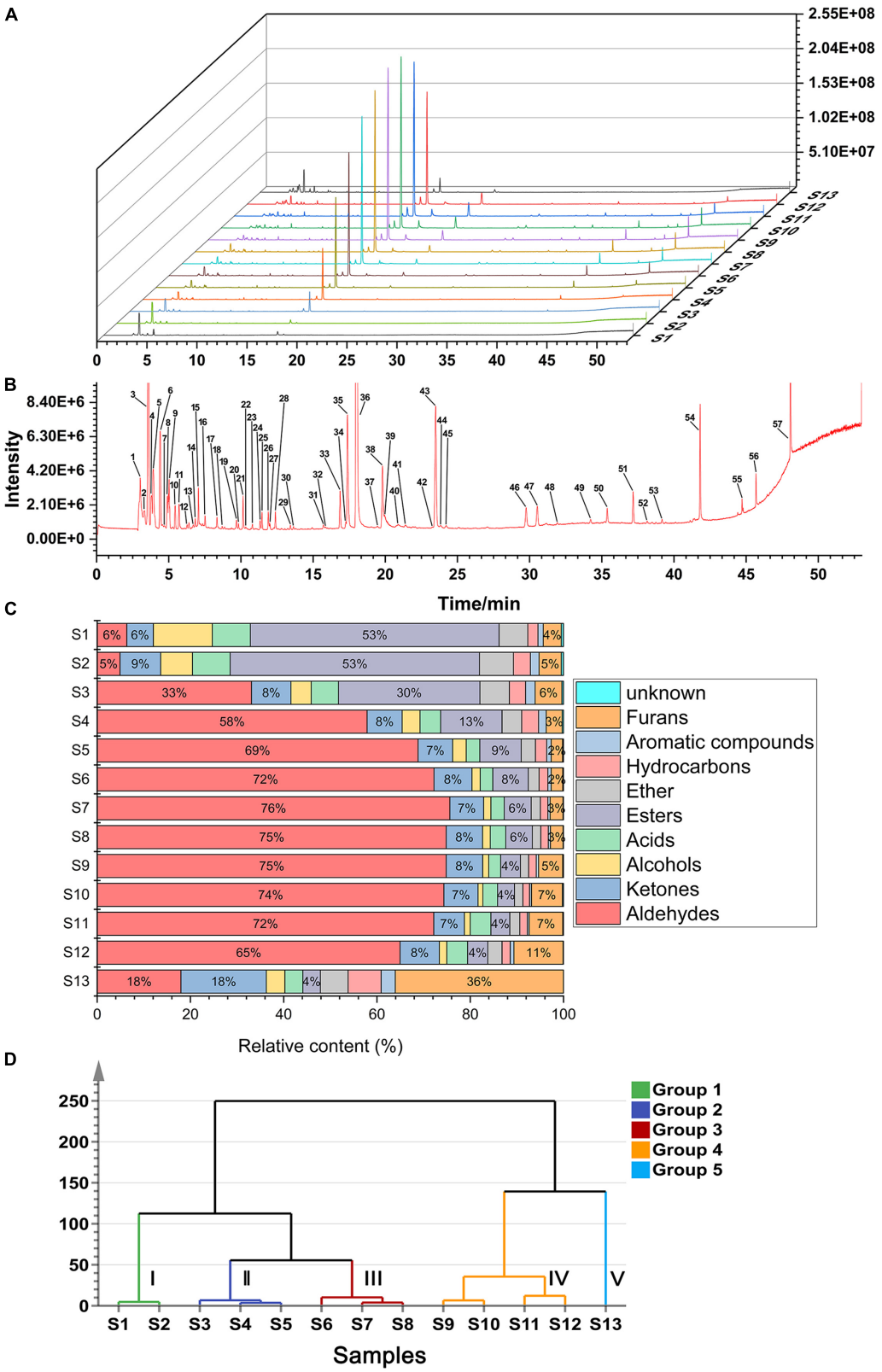

FIGURE 2
Analytical plots of CF samples in roasting process by HS-GC-MS. **(A)** Overlays of TICs of CF by HS-GC-MS; **(B)** typical TIC and distribution of volatile compounds in CF; **(C)** percentage chart of all kinds of volatile substances in CF; **(D)** HCA plot of CF by HS-GC-MS.

TABLE 1 Volatile compounds identified in CF during roasting by HS-GC-MS.

Peak No.	RT[a]	Compounds name	Formula	CAS	LRI[b]	MS match factor[c]
Aldehydes (8)						
8[d]	4.91	2-Methyl-butanal	$C_5H_{10}O$	96-17-3	869	892
16*	7.51	Hexanal	$C_6H_{12}O$	66-25-1	1039	898
31[d]	15.71	Nonanal	$C_9H_{18}O$	124-19-6	1335	813
36*	18.02	Furfural	$C_5H_4O_2$	98-01-1	1394	941
40[f]	20.75	Benzaldehyde	C_7H_6O	100-52-7	1443	828
43[d]	23.49	5-Methyl-2-furancarboxaldehyde	$C_6H_6O_2$	620-02-0	1490	915
55[e]	44.72	5-Acetoxymethyl-2-furaldehyde	$C_8H_8O_4$	10551-58-3	2136	889
57[d]	48.08	5-Hydroxymethylfurfural	$C_6H_6O_3$	67-47-0	2441	910
Ketones (14)						
5*	3.93	Acetone	C_3H_6O	67-64-1	781	948
7[d]	4.69	2-Butanone	C_4H_8O	78-93-3	849	900
11*	5.71	2,3-Butanedione	$C_4H_6O_2$	431-03-8	930	952
12*	6.27	4-Methyl-2-pentanone	$C_6H_{12}O$	108-10-1	967	835
15[d]	7.06	2,3-Pentanedione	$C_5H_8O_2$	600-14-6	1015	926
17[f]	8.34	3-Penten-2-one	C_5H_8O	625-33-2	1083	986
25[d]	11.46	Dihydro-2-methyl-3(2H)-furanone	$C_5H_8O_2$	3188-00-9	1209	950
27[f]	11.99	Acetoin	$C_4H_8O_2$	513-86-0	1225	972
30[f]	13.64	6-Methyl-5-hepten-2-one	$C_8H_{14}O$	110-93-0	1277	880
45[e]	24.22	4-Cyclopentene-1,3-dione	$C_5H_4O_2$	930-60-9	1502	838
47[e]	30.53	5-Methyl-2(5H)-Furanone	$C_5H_6O_2$	591-11-7	1590	921
49[e]	34.23	2(5H)-Furanone	$C_4H_4O_2$	497-23-4	1673	876
54[e]	41.81	1-(2-Furanyl)-2-hydroxy-ethanone	$C_6H_6O_3$	17678-19-2	1947	912
56[e]	45.69	2,3-Dihydro-3,5-dihydroxy-6-methyl-4H-pyran-4-one	$C_6H_8O_4$	28564-83-2	2214	890
Alcohols (6)						
9*	5.02	Ethanol	C_2H_6O	64-17-5	879	956
13[f]	6.69	2-Methyl-3-buten-2-ol	$C_5H_{10}O$	115-18-4	994	848
20[d]	9.83	2-Methyl-1-butanol	$C_5H_{12}O$	137-32-6	1146	895
46[e]	29.76	2-Furanmethanol	$C_5H_6O_2$	98-00-0	1579	868
48[e]	31.92	2-Methyl-5-(1-methylethenyl)-, $(1\alpha,2\beta,5\alpha)$-cyclohexanol	$C_{10}H_{18}O$	38049-26-2	1617	777
53[e]	39.18	3-acetoxy-7,8-Epoxylanostan-11-ol	$C_{32}H_{54}O_4$	917486-30-7	1823	796
Acids (3)						
35*	17.38	Acetic acid	$C_2H_4O_2$	64-19-7	1378	976
39[e]	19.97	Formic acid	CH_2O_2	64-18-6	1430	811
41[d]	21.40	Propanoic acid	$C_3H_6O_2$	79-09-4	1454	849
Esters (6)						
3*	3.58	Methyl formate	$C_2H_4O_2$	107-31-3	750	933
33[d]	16.87	5-Methyl-2(3H)-furanone	$C_5H_6O_2$	591-12-8	1365	881
37[e]	19.46	Furfuryl formate	$C_6H_6O_3$	13493-97-5	1421	818
42[d]	23.26	Pentanoic acid, 4- oxo-, methyl ester	$C_6H_{10}O_3$	624-45-3	1486	833
44[d]	23.84	Methyl 2-furoate	$C_6H_6O_3$	611-13-2	1496	885
51[d]	37.18	Dihydro-3-methylene-5-methyl-2-furanone	$C_6H_8O_2$	62873-16-9	1756	920

(Continued)

TABLE 1 (Continued)

Peak No.	RT[a]	Compounds name	Formula	CAS	LRI[b]	MS match factor[c]
Ether (1)						
1*	3.02	Dimethyl ether	C_2H_6O	115-10-6		927
Hydrocarbons (7)						
2[d]	3.33	1,4-Pentadiene	C_5H_8	591-93-5	727	938
19[f]	9.69	1-Methyl-4-(1-methylethyl)-1,3-cyclohexadiene	$C_{10}H_{16}$	554-61-0	1141	835
21*	10.15	Limonene	$C_{10}H_{16}$	138-86-3	1159	910
22[f]	10.34	β-Phellandrene	$C_{10}H_{16}$	555-10-2	1166	859
24[f]	11.33	γ -Terpinene	$C_{10}H_{16}$	99-85-4	1204	905
28*	12.39	1-Methyl-4-(1-methylethylidene)-cyclohexene	$C_{10}H_{16}$	586-62-9	1238	867
50[e]	35.38	1-Methyl-3-(1-methylethyl)-cyclohexene	$C_{10}H_{18}$	13828-31-4	1702	812
Arenes (4)						
14*	6.84	Toluene	C_7H_8	108-88-3	1003	861
18[d]	8.71	*p*-Xylene	C_8H_{10}	106-42-3	1102	901
26*	11.89	*o*-Cymene	$C_{10}H_{14}$	527-84-4	1222	906
34[f]	17.27	1-Methyl-4-(1-methylethenyl)-benzene	$C_{10}H_{12}$	1195-32-0	1375	892
Furans (5)						
4[d]	3.80	Furan	C_4H_4O	110-00-9	770	932
6*	4.41	2-Methyl-furan	C_5H_6O	534-22-5	824	933
10[d]	5.44	2,5-Dimethyl-furan	C_6H_8O	625-86-5	912	906
23[d]	10.80	2-(Methoxymethyl)-furan	$C_6H_8O_2$	13679-46-4	1185	912
38[d]	19.81	1-(2-furanyl)-ethanone	$C_6H_6O_2$	1192-62-7	1427	915
Unknown (3)						
29	13.43	Unknown			1271	
32	15.87	Unknown			1339	
52	38.15	Unknown			1785	

[a]RT: Retention time.
[b]LRI: Linear retention index on the HP-INNOWAX capillary column (Agilent Technologies), calculated *via* the C7-C30 n-alkanes.
[c]The maximum of MS match factor is 1,000.
[d]Compounds produced during roasting.
[e]Compounds produced at first and then disappeared during roasting.
[f]Compounds disappeared during roasting. *Common peaks.

experimental results are consistent with those reports. In addition, furfural and 5-hydroxymethylfurfural are typical thermal reaction products formed by the Maillard reaction (28). Meanwhile, the appearance of CF changed from red to black during roasting. In conclusion, the changes in colour and composition proved that the Maillard reaction was the main reaction during CF roasting. Previous research has shown that CF is rich in fatty acids such as linoleic acid and oleic acid, and hexanal and nonanal are typical oxidative volatile degradation products of these fatty acids. Therefore, it was speculated that aldehyde production during CF roasting was related to fatty acid oxidation and degradation (29). Furthermore, the 2-methyl-butanal and benzaldehyde produced during roasting were Strecker degradation reaction products (30). Because CF is rich in amino acids, it was speculated that significant production aldehydes during roasting was also related to the Strecker degradation reaction, a thermal reaction between amino acids and carbonyl compounds (31). Additionally, amino acids and fatty acids in CF are non-volatile, the changes in non-volatile components in CF samples during roasting must be further studied to confirm the contribution of Strecker degradation and fatty acid oxidation and degradation to overall flavour characteristics.

3.3.3.2. Ketones

The proportion of ketones (14 compounds) was relatively stable during CF roasting and reached a maximum in S13 (roasting time of 24 min). Among the identified ketones, acetone and 1-(2-furanyl)-2-hydroxy-ethanone accounted for

a relatively high proportion. Throughout roasting, the CF odour profile changed from fragrant to coke-like. The acetone content gradually increased, which contributed to the deterioration of flavour (32). Eight ketones were newly produced during roasting, while only three remained (2-butanone, 2,3-pentanedione and dihydro-2-methyl-3(2H)-furanone) after 24 min of roasting.

3.3.3.3. Alcohols, acids, esters, and others

The newly produced alcohols during CF roasting are 2-methyl-1-butanol, 2-furanmethanol, and 2-methyl-5-(1-methylethenyl)-, (1α, 2β, 5α)-cyclohexanol. Among these, only the 2-methyl-1-butanol contents continued to increase. 2-Furanmethanol is often produced during the Maillard reaction (33). Acetic acid accounted for a relatively high proportion of acids, and its change trend was the same as that of most components during the roasting period. Acetic acid is thought to be produced by the secondary decomposition of hexanal during heating (34). The increased composition of acetic acid not only stimulates the secretory function of the oxyntic glands in the stomach, accelerating gastric breakdown and transformation (35), but also dilates blood vessels and reduces blood pressure (36, 37). Five of the six ester compounds in CF were newly produced compounds, including furfuryl formate, pentanoic acid, 4- oxo-, methyl ester, methyl 2-furoate, and dihydro-3-methylene-5-methyl-2-furanone. The decreased content of methyl formate, the most abundant ester compound, was likely related to its thermal decomposition (38).

Prolonged roasting times and increased CF temperature of promoted the production of other components such as 1,4-pentadiene, 1-methyl-3-(1-methylethyl)-cyclohexene, *p*-xylene, furan, 2,5-dimethyl-furan, 1-(2-furanyl)-ethanone, and 2-(methoxymethyl)-furan. The production of hydrocarbons, arenes, and furans in CF was likely promoted by chemical reactions including the Maillard reaction and protein degradation (39).

In conclusion, volatile components were developed through three pathways during CF roasting: Maillard reaction, Strecker degradation, and fatty acid oxidation and degradation.

3.4. Relative odour activity value analysis

The significance of the volatile compound contribution to the overall aroma depends on two factors, namely, their concentration and OT. ROAV represent the above two factors, and were used to assess the contribution of each volatile compound to the overall aromatic characteristics (40). To determine the volatiles that contributed significantly to CF odour during roasting, the ROAVs of all volatiles were calculated using OT literature value (41). Because 2,3-butanedione had the lowest OT and a high relative content, it was considered as the volatile component with the greatest contribution to flavour. Its ROAV was defined as 100 for comparison with other compounds. Generally, compounds with ROAV $\geq$ 1 were considered to be key aromatic compounds. **Supplementary Table 3** shows 11 volatile compounds with ROAVs $\geq$ 1, namely, 2,3-butanedione, 2-methyl-butanal, 3-penten-2-one, hexanal, nonanal, limonene, 2,3-pentanedione, furfural, 5-methyl-2-furancarboxaldehyde, 1-methyl-4-(1-methylethenyl)-benzene, and 6-methyl-5-hepten-2-one (sorted by ROAV from large to small). These compounds were mainly aldehydes and ketones, which were inferred to be the main odour components in roasted CF. Generally, the sensory threshold of small-molecule aldehydes is lower and significantly contributes to the overall CF aroma. Based on the odour description of volatile components listed in **Supplementary Table 3**, aldehydes have aromatic characteristics including fruity, sour, and almond odours. Ketones have an important effect on fruit aroma. Its contribution to odour is less than that of aldehydes. The contribution of 2-methyl-butanal (ROAV 12.28–263.42) to the aroma was the second-greatest throughout CF roasting, although its content change was not significant. The ROAV of furfural showed a broad range from 0.28 to 12.27. Although the content of furfural varied the most, its contribution to aroma was not as high as that of 2-methyl-butanal. Furthermore, there were 5 components with ROAVs between 0 and 1, which are modifiable components of odour. Unfortunately, the OT values of 20 components have not been reported, requiring further studies to prove inference reliability.

3.5. Chemometric analysis

3.5.1. PCA

Principal component analysis is a common analysis method for visualising sample differences, reducing data dimensionality while retaining most information by studying all the variable relationships simultaneously (42). The results obtained using the E-nose and GC-MS were statistically analysed by PCA to highlight the differences in volatile flavour components.

The score plot of the E-nose response is presented in **Figure 3A**, where higher contributions more significantly contribute toward the principal components (PCs) that reflect the original multi-index information. The first two principal components (75.8 and 4.2% for PC1 and PC2, respectively) explained 80% of the total variance, indicating that the two components contributed most to the characteristic information of the original samples after dimensionality reduction. The sample spatial regions showed a clockwise rotation with prolonged roasting time. S1, S2, and S3 were close in dimensionality, indicating that negligible changes in volatile flavour substances within 4 min. A similar aggregation in the PCA was observed for S8 and S9. With increasing roasting time, the distance between the samples gradually increased with large

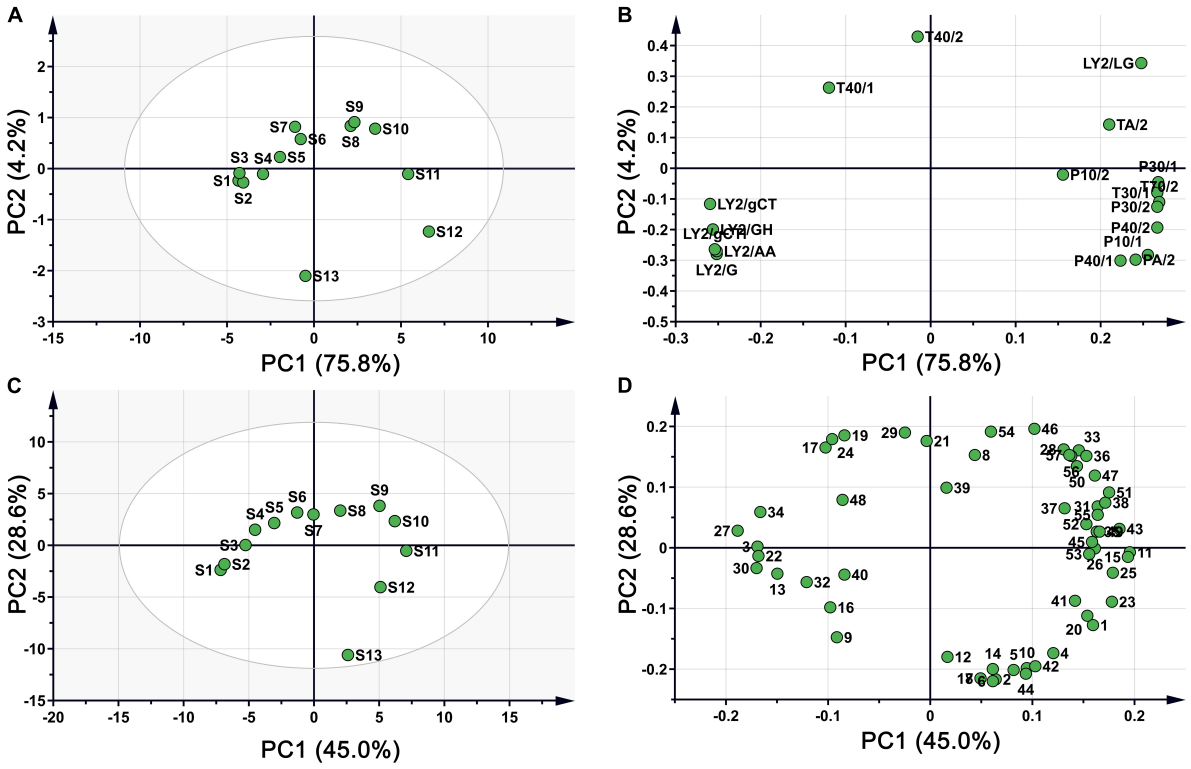

FIGURE 3
PCA plot of CF samples during roasting process. **(A)** Score plot based on E-nose; **(B)** loading plot based on E-nose; **(C)** score plot based on HS-GC-MS; **(D)** loading plot based on HS-GC-MS.

separation of S11, S12, and S13 from the previous samples. This indicated that roasting for 20 min at 150°C considerably impacted the volatile flavour substances in CF. Overall, the samples were distinguishable across PC1: S1–S7 and S13 had negative values on PC1, while S8–S12 occupied positive values on PC1. The loading plot in Figure 3B shows the influence of each sensor on sample differentiation.

The volatile components detected by HS-GC-MS were also analysed using PCA. From Figure 3C, the cumulative contribution rate of the two PCs exceeded 70%, and the spatial regions of the samples showed a clockwise rotation with prolonged roasting. The distance between samples at each time point gradually increased, similar to the PCA distribution of the E-nose data. These results further suggested that the E-nose and HS-GC-MS can be used to evaluate the quality of CF during processing, with consistent results across platforms. The loading plot in Figure 3D shows the influence of each compound on sample differentiation.

3.5.2. Grey relational analysis between the E-nose and HS-GC-MS

To further verify the correlation between the data obtained by the E-nose and GC-MS and explore the key components that cause odour changes during CF roasting, the grey relational method was used to calculate the correlation between each E-nose sensor response and volatile compound. The degree of correlation is shown in the two-colour gradient heatmap in Figure 4, where the *X*-axis represents sensors and the *Y*-axis represents volatile components. The last column represents the average of the correlation degree between each compound and sensor. In GRA, based on the criterion of the average correlation degree ($r > 0.9$) of 18 sensors (43), 25 known volatile components were screened, mainly aldehydes, ketones, and alcohols. They were dimethyl ether, *o*-cymene, 1-methyl-4-(1-methylethylidene)-cyclohexene, acetic acid, limonene, acetone, 1-methyl-4-(1-methylethyl)-1,3-cyclohexadiene, 2-methyl-1-butanol, toluene, 4-methyl-2-pentanone, nonanal, 2,3-butanedione, ethanol, γ-terpinene, furfural, hexanal, 5-methyl-2(3h)-furanone, dihydro-3-methylene-5-methyl-2-furanone, 2-furanmethanol, 3-penten-2-one, methyl formate, furan, 2-methyl-butanal, 2,3-pentanedione, and 5-methyl-2-furancarboxaldehyde (sorted by ROAV from large to small). By combining the ROAVs of the components in Supplementary Table 3, the key odour compounds were further screened (ROAV ≥ 1), which were limonene, 2,3-butanedione, nonanal, furfural, hexanal, 3-penten-2-one, 2-methyl-butanal, 2,3-pentanedione, and 5-methyl-2-furancarboxaldehyde. These compounds have special odour based on the odour description,

10.3389/fnut.2022.1035623

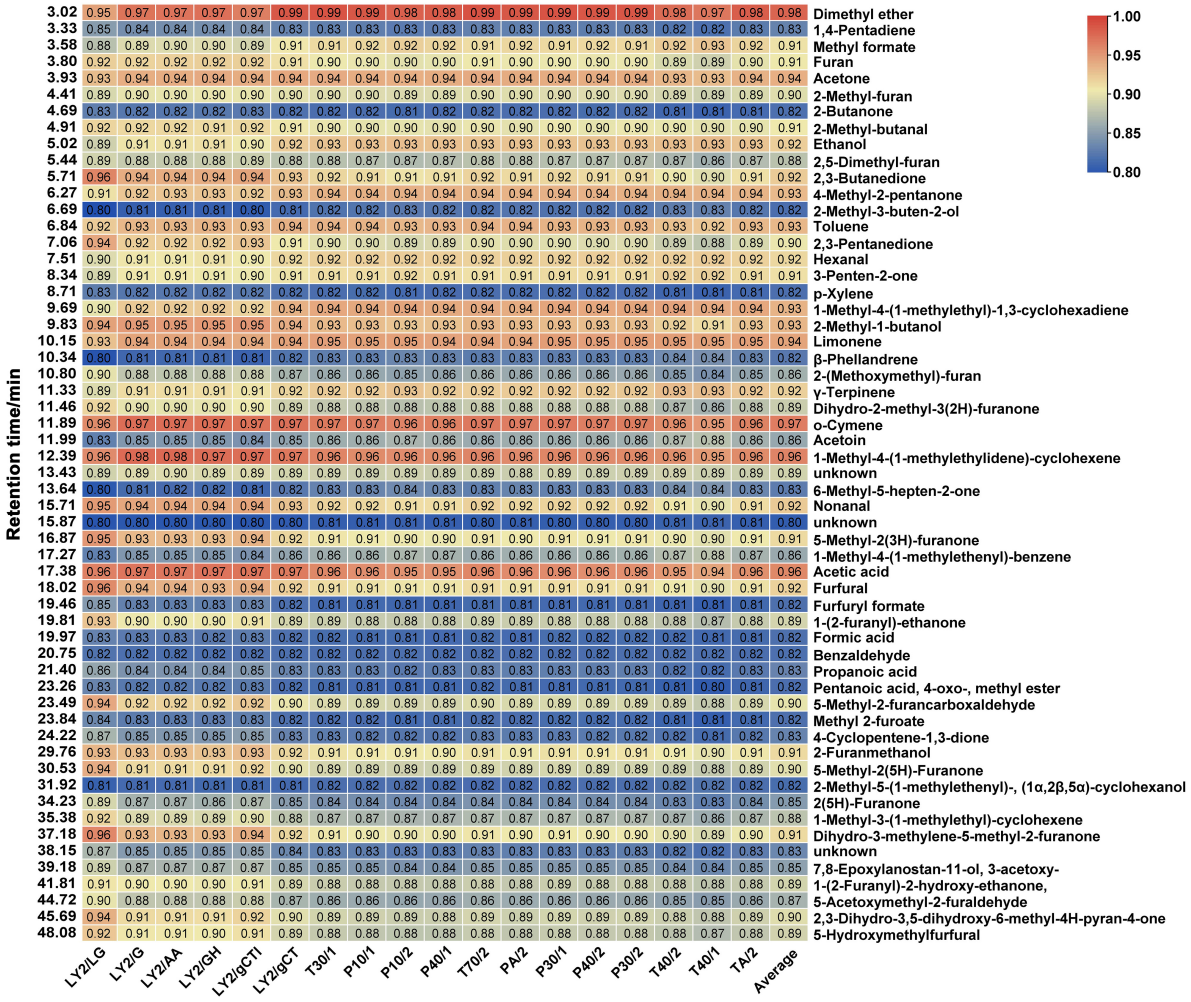

FIGURE 4
Heatmap of sensor response and volatile components based on grey relational analysis. GRA, a method to evaluate the correlation between two variables based on their change curves geometric shape similarity, is suitable for analyzing dynamically changing variables. Each row in the figure represents a volatile compound, and each column represents an E-nose sensor. The data values in the square represent the correlation degree. Red represents the correlation degree higher than 0.9 while blue represents the correlation degree lower than 0.9.

and most of them have biological activities. For instance, limonene, nonanal, hexanal, and 2,3-pentanedione have antimicrobial activity (44–47). GC-MS and the E-nose are different odour judgment technologies that characterise odours by different indicative values and the correlative components are related to the odour of the food. Therefore, the 9 volatile components are identified as the main substances driving odour changes during CF roasting.

4. Conclusion

Herein, the E-nose and HS-GC-MS were used to analyse the changes in volatile flavour substances during CF roasting. The results obtained by the E-nose were consistent with those obtained by HS-GC-MS, indicating that both methods can be used to track and detect the odour changes in CF. During CF roasting, 54 volatile components were detected and identified by HS-GC-MS, mostly aldehydes, ketones, acids, esters, and furans, which are the main substances contributing to the CF flavour. It was confirmed that the Maillard reaction, Strecker degradation, and fatty acid oxidation and degradation were the three main reactions during roasting. The correlation between the E-nose response and volatile components was analysed by GRA, and 25 volatile components closely related to odour changes were identified. Finally, 9 volatile components (ROAV $\geq$ 1), mostly aldehydes and ketones, were identified as key substances driving odour changes during CF roasting. In summary, our research not only provides a template for seeking flavour markers in food

processing, but also promotes the process of objectification and controllability of judgment of processing degree.

Data availability statement

The raw data supporting the conclusions of this article will be made available by the authors, without undue reservation.

Author contributions

CF performed the experiments and wrote the original draft. QX performed the GC-MS and E-nose data analysis. WJL carried out the mathematical analysis and validation. YX and LM applied the software and data visualization. WDL and TL collected the samples and edited the draft. LL and WY conceived the project and provided the guidance. FY conceived the project, provided the guidance, and edited the draft. All authors reviewed and approved the final version to be submitted.

Funding

This work was supported by Key Projects of Natural Science Foundation of Jiangsu Province for University (grant number 13KJA360003).

Acknowledgments

We would like to thank Editage (www.editage.cn) for English language editing.

Conflict of interest

The authors declare that the research was conducted in the absence of any commercial or financial relationships that could be construed as a potential conflict of interest.

Publisher's note

All claims expressed in this article are solely those of the authors and do not necessarily represent those of their affiliated organizations, or those of the publisher, the editors and the reviewers. Any product that may be evaluated in this article, or claim that may be made by its manufacturer, is not guaranteed or endorsed by the publisher.

Supplementary material

The Supplementary Material for this article can be found online at: https://www.frontiersin.org/articles/10.3389/fnut.2022.1035623/full#supplementary-material

References

1. Augustin M, Riley M, Stockmann R, Bennett L, Kahl A, Lockett T, et al. Role of food processing in food and nutrition security. *Trends Food Sci Technol.* (2016) 56:115–25. doi: 10.1016/j.tifs.2016.08.005

2. Dong W, Hu R, Long Y, Li H, Zhang Y, Zhu K, et al. Comparative evaluation of the volatile profiles and taste properties of roasted coffee beans as affected by drying method and detected by electronic nose, electronic tongue, and HS-SPME-GC-MS. *Food Chem.* (2019) 272:723–31. doi: 10.1016/j.foodchem.2018.08.068

3. Sruthi N, Premjit Y, Pandiselvam R, Kothakota A, Ramesh S. An overview of conventional and emerging techniques of roasting: effect on food bioactive signatures. *Food Chem.* (2021) 348:129088. doi: 10.1016/j.foodchem.2021.129088

4. Hamzalioglu A, Gokmen V. 5-Hydroxymethylfurfural accumulation plays a critical role on acrylamide formation in coffee during roasting as confirmed by multiresponse kinetic modelling. *Food Chem.* (2020) 318:126467. doi: 10.1016/j.foodchem.2020.126467

5. Zhu Y, Dong J, Jin J, Liu J, Zheng X, Lu J, et al. Roasting process shaping the chemical profile of roasted green tea and the association with aroma features. *Food Chem.* (2021) 353:129428. doi: 10.1016/j.foodchem.2021.129428

6. Choi Y, Yong S, Lee M, Park S, Yun Y, Park S, et al. Changes in volatile and non-volatile compounds of model kimchi through fermentation by lactic acid bacteria. *Lebensm Wiss Technol.* (2019) 105:118–26. doi: 10.1016/j.lwt.2019.02.001

7. Wang J, Chen Q, Hu K, Zeng L, Pan Y, Huang H. Change in aromatic components of banana during the preparation process of juice and microcapsule powder. *Int J Food Sci Technol.* (2011) 46:1398–405. doi: 10.1111/j.1365-2621.2011.02628.x

8. Wang H, Chen X, Zhang J, Wang X, Shi W. Postmortem changes in the freshness and volatile compounds of grass carp (*Ctenopharyngodon idella*). *J Food Meas Charact.* (2020) 14:584–96. doi: 10.1007/s11694-019-00337-8

9. Siró I, Kápolna E, Kápolna B, Lugasi A. Functional food, product development, marketing and consumer acceptance—A review. *Appetite.* (2008) 51:456–67. doi: 10.1016/j.appet.2008.05.060

10. Li Y, Fei C, Mao C, Ji D, Gong J, Qin Y, et al. Physicochemical parameters combined flash GC e-nose and artificial neural network for quality and volatile characterization of vinegar with different brewing techniques. *Food Chem.* (2022) 374:131658. doi: 10.1016/j.foodchem.2021.131658

11. Tan J, Xu J. Applications of electronic nose (e-nose) and electronic tongue (e-tongue) in food quality-related properties determination: a review. *Artif Intell Agric.* (2020) 4:104–15. doi: 10.1016/j.aiia.2020.06.003

12. Aparicio R, Rocha S, Delgadillo I, Morales M. Detection of rancid defect in virgin olive oil by the electronic nose. *J Agric Food Chem.* (2000) 48:853–60. doi: 10.1021/jf9814087

13. Mohammadhosseini, M, Akbarzadeh A, Flamini G. Profiling of compositions of essential oils and volatiles of *Salvia limbata* using traditional and advanced techniques and evaluation for biological activities of their extracts. *Chem Biodivers.* (2017) 14:e1600361. doi: 10.1002/cbdv.201600361

14. Nekoei M, Mohammadhosseini M. Chemical composition of the essential oils and volatiles of *Salvia leriifolia* by Three different extraction methods prior to gas chromatographic-mass spectrometric determination: comparison of HD with SFME and HS-SPME. *J Essent Oil Bear Plants.* (2017) 20:410–25. doi: 10.1080/0972060X.2017.1305918

15. Xiang X, Jin G, Gouda M, Jin Y, Ma M. Characterization and classification of volatiles from different breeds of eggs by SPME-GC–MS and chemometrics. *Food Res Int.* (2019) 116:767–77. doi: 10.1016/j.foodres.2018.09.010

16. Shi H, Zhang M, Adhikari B. Advances of electronic nose and its application in fresh foods: a review. *Crit Rev Food Sci Nutr.* (2018) 58:2700–10. doi: 10.1080/10408398.2017.1327419

17. Zhou H, Luo D, GholamHosseini H, Li Z, He J. Identification of Chinese herbal medicines with electronic nose technology: applications and challenges. *Sensors.* (2017) 17:1073. doi: 10.3390/s17051073

18. Li M, Chen X, Deng J, Ouyang D, Wang D, Liang Y, et al. Effect of thermal processing on free and bound phenolic compounds and antioxidant activities of hawthorn. *Food Chem.* (2020) 332:127429. doi: 10.1016/j.foodchem.2020.127429

19. Li T, Li S, Dong Y, Zhu R, Liu Y. Antioxidant activity of penta-oligogalacturonide, isolated from haw pectin, suppresses triglyceride synthesis in mice fed with a high-fat diet. *Food Chem.* (2014) 145:335–41. doi: 10.1016/j.foodchem.2013.08.036

20. Zhang L, Zhang L, Xu J. Chemical composition, antibacterial activity and action mechanism of different extracts from hawthorn (*Crataegus pinnatifida Bge.*). *Sci Rep.* (2020) 10:8876. doi: 10.1038/s41598-020-65802-7

21. Xue Q, Wang Y, Fei C, Ren C, Li W, Li W, et al. Profiling and analysis of multiple constituents in *Crataegi Fructus* before and after processing by ultrahigh-performance liquid chromatography quadrupole time-of-flight mass spectrometry. *Rapid Commun Mass Spectrom.* (2021) 35:e9033. doi: 10.1002/rcm.9033

22. Fei C, Ren C, Wang Y, Li L, Li W, Yin F, et al. Identification of the raw and processed *Crataegi Fructus* based on the electronic nose coupled with chemometric methods. *Sci Rep.* (2021) 11:1849. doi: 10.1038/s41598-020-79717-w

23. Liu T, Jiang H, Li S. Analysis of volatile components in *Crataegus pinnatifida* and its processed products by HS-SPME-GC-MS. *Modern Food Sci Technol.* (2021) 37:250–5. doi: 10.13982/j.mfst.1673-9078.2021.5.1026

24. Shen Y, Wu Y, Wang Y, Li L, Li C, Zhao Y, et al. Contribution of autochthonous microbiota succession to flavor formation during Chinese fermented mandarin fish (*Siniperca chuatsi*). *Food Chem.* (2021) 348:129107. doi: 10.1016/j.foodchem.2021.129107

25. Wang Y, Lv M, Wang T, Sun J, Wang Y, Xia M, et al. Research on mechanism of charred hawthorn on digestive through modulating "brain-gut" axis and gut flora. *J Ethnopharmacol.* (2019) 245:112166. doi: 10.1016/j.jep.2019.112166

26. Xu Y. *Study on the "Coke Aroma" Material Basis That Promote Digestion and the Synergistic Mechanism of "Jiao Sanxian" After Charred*. Sichuan: Southwest Jiaotong University (2018).

27. Zhou Y, He F, Yang Y, Shi J, Deng K, Tang Y, et al. Research situation of Maillard reaction and its influence on research methods for processing and preparation process of Chinese materia medica. *Chin Traditi Herb Drugs.* (2014) 45:125–30. doi: 10.7501/j.issn.0253-2670.2014.01.024

28. Gong R, Huo X, Lei Z, Liu C, Li S, Sun Y. Advances in effects and regulation of Maillard reaction on quality of Chinese materia medica. *Chin Tradit Herb Drugs.* (2019) 1:243–51. doi: 10.7501/j.issn.0253-2670.2019.01.035

29. Siegmund B, Murkovic M. Changes in chemical composition of pumpkin seeds during the roasting process for production of pumpkin seed oil (Part 2: volatile compounds). *Food Chem.* (2004) 84:367–74.

30. Pripis-Nicolau L, de Revel G, Bertrand A, Maujean A. Formation of flavor components by the reaction of amino acid and carbonyl compounds in mild conditions. *J Agric Food Chem.* (2000) 48:3761–6. doi: 10.1021/jf991024w

31. Delgado R, Hidalgo F, Zamora R. Antagonism between lipid-derived reactive carbonyls and phenolic compounds in the Strecker degradation of amino acids. *Food Chem.* (2016) 194:1143–8. doi: 10.1016/j.foodchem.2015.07.126

32. Didzbalis J, Ritter K, Trail A, Plog F. Identification of fruity/fermented odorants in high-temperature-cured roasted peanuts. *J Agric Food Chem.* (2004) 52:4828–33. doi: 10.1021/jf0355250

33. Ames J, Guy R, Kipping G. Effect of pH, temperature, and moisture on the formation of volatile compounds in glycine/glucose model systems. *J Agric Food Chem.* (2001) 49:4315–23. doi: 10.1021/jf010198m

34. Smuda M, Glomb M. Fragmentation pathways during Maillard-induced carbohydrate degradation. *J Agric Food Chem.* (2013) 61:10198–208. doi: 10.1021/jf305117s

35. Foster N, Lambert A. The effects of some organic acids on the secretion of gastric juice. *Proc Soc Exp Biol Med.* (1908) 5:108. doi: 10.3181/00379727-5-64

36. Li L, He M, Xiao H, Liu X, Wang K, Zhang Y. Acetic acid influences BRL-3A cell lipid metabolism via the AMPK signalling pathway. *Cell Physiol Biochem.* (2018) 45:2021–30. doi: 10.1159/000487980

37. Kondo S, Tayama K, Tsukamoto Y, Ikeda K, Yamori Y. Antihypertensive effects of acetic acid and vinegar on spontaneously hypertensive rats. *Biosci Biotechnol Biochem.* (2001) 65:2690–4. doi: 10.1271/bbb.65.2690

38. Rhoades J. Coffee volatiles, analysis of the volatile constituents of coffee. *J Agric Food Chem.* (1960) 8:136–41. doi: 10.1021/jf60108a019

39. Su G, Zheng L, Cui C, Yang B, Ren J, Zhao M. Characterization of antioxidant activity and volatile compounds of Maillard reaction products derived from different peptide fractions of peanut hydrolysate. *Food Res Int.* (2011) 44:3250–8. doi: 10.1016/j.foodres.2011.09.009

40. Zhang W, Cao J, Li Z, Li Q, Lai X, Sun L, et al. HS-SPME and GC/MS volatile component analysis of Yinghong No. 9 dark tea during the pile fermentation process. *Food Chem.* (2021) 357:129654. doi: 10.1016/j.foodchem.2021.129654

41. van Gemert L. *Odor Thresholds Compilations of Odor Threshold Values in Air, Water and other Media*. Utrecht: Oliemans Punter & Partners BV (2011).

42. Yang Y, Wang B, Fu Y, Shi Y, Chen F, Guan H, et al. HS-GC-IMS with PCA to analyze volatile flavor compounds across different production stages of fermented soybean whey tofu. *Food Chem.* (2021) 346:128880. doi: 10.1016/j.foodchem.2020.128880

43. Han Y, Cui S, Geng Z, Chu C, Chen K, Wang Y. Food quality and safety risk assessment using a novel HMM method based on GRA. *Food Control.* (2019) 105:180–9. doi: 10.1016/j.foodcont.2019.05.039

44. Zahi M, Liang H, Yuan Q. Improving the antimicrobial activity of d-limonene using a novel organogel-based nanoemulsion. *Food Control.* (2015) 50:554–9. doi: 10.1016/j.foodcont.2014.10.001

45. Zhang J, Sun H, Chen S, Zeng L, Wang T. Anti-fungal activity, mechanism studies on α-phellandrene and nonanal against *Penicillium cyclopium*. *Bot Stud.* (2017) 58:13. doi: 10.1186/s40529-017-0168-8

46. Gardini F, Lanciotti R, Caccioni D, Guerzoni M. Antifungal activity of hexanal as dependent on its vapor pressure. *J Agric Food Chem.* (1997) 45:4297–302. doi: 10.1021/jf970347u

47. Jay J, Rivers G. Antimicrobial activity of some food flavoring compounds. *J Food Saf.* (1984) 6:129–39. doi: 10.1111/j.1745-4565.1984.tb00609.x

Frontiers in Nutrition

Explores what and how we eat in the context of health, sustainability and 21st century food science

A multidisciplinary journal that integrates research on dietary behavior, agronomy and 21st century food science with a focus on human health.

Discover the latest Research Topics

See more →

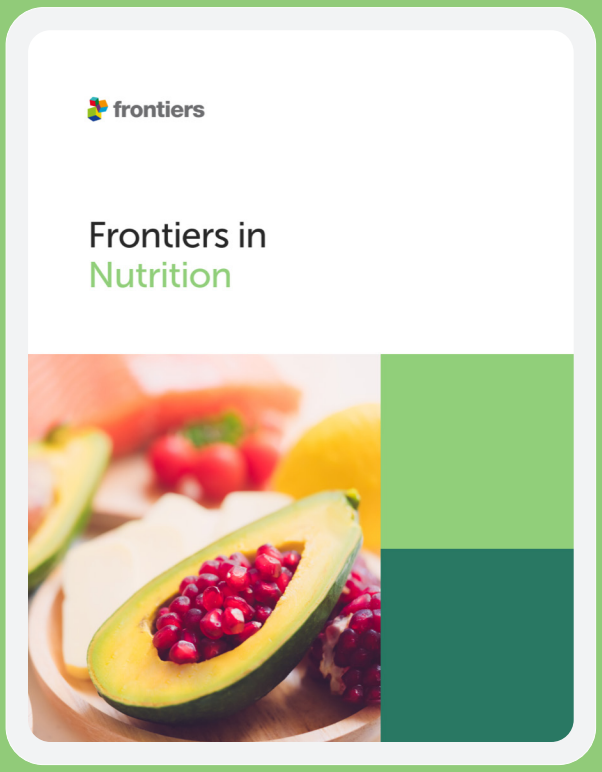

Frontiers

Avenue du Tribunal-Fédéral 34
1005 Lausanne, Switzerland
frontiersin.org

Contact us

+41 (0)21 510 17 00
frontiersin.org/about/contact